UNIVERSITAT DE VALÈNCIA

Facultad de Medicina y Odontología

Departamento de Farmacología

Estudio comparativo del efecto de diferentes fármacos antirretrovirales sobre la interacción leucocito-endotelio

Samuel Orden Ruiz

Valencia, 2016

UNIVERSITAT DE VALÈNCIA

Facultad de Medicina y Odontología

Departamento de Farmacología

Dña. Ángeles Álvarez Ribelles, Investigadora de la Fundación General de la Universidad de Valencia y Profesora Asociada del Departamento de Medicina de la Facultad de Ciencias de la Salud de la Universidad Jaume I de Castellón de la Plana,
D. Juan Vicente Esplugues Mota, Catedrático del Departamento de Farmacología de la Facultad de Medicina y Odontología de la Universidad de Valencia,

CERTIFICAN QUE:

El trabajo presentado por el Licenciado en Biología **D. Samuel Orden Ruiz** titulado **"Estudio comparativo del efecto de diferentes fármacos antirretrovirales sobre la interacción leucocito-endotelio"** ha sido realizado bajo nuestra dirección y asesoramiento en el Departamento de Farmacología de la Facultad de Medicina y Odontología de la Universidad de Valencia.

Concluido el trabajo experimental y bibliográfico, autorizamos la presentación y la defensa de esta Tesis Doctoral para que sea juzgada por el Tribunal correspondiente.

Para que así conste a los efectos oportunos, se expide la presente certificación en Valencia, a 13 de Mayo de 2016.

Fdo. Dra. Ángeles Álvarez Ribelles **Fdo. Dr. Juan Vicente Esplugues Mota**

Esta Tesis Doctoral ha sido realizada con la financiación de los siguientes proyectos y becas:

PROYECTOS:

- **SAF2007-60021** "*Efectos de los fármacos antirretrovirales sobre la interacción leucocito-endotelio*" del Ministerio de Educación y Ciencia. Investigador principal: Ángeles Álvarez Ribelles.
- **SAF2010-16030** "*Estudio de los mecanismos celulares y moleculares que median la toxicidad vascular inducida por la terapia antirretroviral*" del Ministerio de Ciencia e Innovación. Investigador principal: Ángeles Álvarez Ribelles.
- **PROMETEO/2010/060** "*Farmacología experimental del tracto digestivo*" de la Generalitat Valenciana. Investigador principal: Juan V. Esplugues Mota.
- **PI11/00327** "*Caracterización de nuevos mecanismos celulares de hepatotoxicidad por antirretrovirales*" del Instituto de Salud Carlos III. Investigador principal: Juan V. Esplugues Mota.

BECAS:

- **"Beca Predoctoral, en el marco del Subprograma Atracció de Talent de VLC-CAMPUS"** de la Universitat de València.
- "**Técnico Superior de Investigación Prometeo**" (PROMETEO/2010/060) de la Generalitat Valenciana. Beca con finalidad predoctoral.
- "**Beca de Actuación Local**" de la Fundación Juan Esplugues.

Dedicado a la gente que me quiere, y sobre todo, a mis padres

Agradecimientos

Hace ya casi 7 años que decidí venir a trabajar a Valencia a este laboratorio, recién terminada la carrera. La verdad es que en aquel momento no sabía si tenía intención o no de escribir la Tesis Doctoral, sino que era más bien el simple hecho, o el deseo, o la ambición, de tener mi primer trabajo y ser independiente de una vez, y más en uno que tenía buena pinta, estaba relacionado con "lo mío" y a primera vista parecía que me gustaba. Recuerdo que un par de meses antes de terminar de estudiar le decía a todo el mundo que había encontrado trabajo, y me daban la enhorabuena, sobre todo por haber encontrado algo para trabajar como biólogo, y más en los tiempos que corrían. Pero bueno, yo sabía que tampoco estaba tan relacionado con lo mío: yo había estudiado animalitos y plantitas, y en breve, me iba a meter en un laboratorio puro y duro.

He de reconocer que los inicios no fueron fáciles. Fui empalmando contratos de poco tiempo de duración, y mi situación no estaba para nada estabilizada. A lo que hay que sumar que cuando uno llega a un sitio nuevo, todo es desconocido, y tienes que estar aprendiendo constantemente, hasta que ya se coge una cierta soltura para poder hacer las cosas por uno mismo. A pesar de ello, no me costó mucho acostumbrarme al cambio radical en mi vida, quizá por mi capacidad para afrontar los problemas que surgen día a día, a lo que hay que sumar la ayuda incondicional de mis compañeros de trabajo.

Con el paso del tiempo, me he llegado a encontrar muy a gusto y cómodo, y he ido conociendo a gente que realmente ha aportado mucho a mi vida profesional, llegando muchas de ellas a jugar un papel muy importante en mi vida personal; no sin olvidar a las personas que están en mi vida desde que tengo uso de razón, o han ido apareciendo en ella aportando muchas cosas buenas. Es por este motivo, porque el que quiero escribirles estas palabras, tanto a mis compañeros de trabajo como a "los míos", para darles las gracias, y para demostrarles a muchas de ellos,

que sin su aportación, esta Tesis Doctoral nunca habría sido posible. Muchas gracias a todos vosotros.

En primer lugar quiero darles las gracias a Ángeles Álvarez Ribelles y a Juan Vicente Esplugues Mota, por haberme permitido realizar esta Tesis Doctoral bajo su dirección. Gracias Ángeles. Por brindarme la oportunidad de empezar a trabajar en este laboratorio, en el mini-grupo que formábamos Carmen, tu y yo cuando llegué. Por estar pendiente de mí en todo momento, solucionando los problemas que pudieran surgir. Por tu apoyo en lo profesional, y también en lo personal. Gracias Juan Vicente. Por haber confiado en mí y en mi trabajo, y por haberme brindado todo tu apoyo. También destacar a su padre, Juan Esplugues, y a la Fundación Juan Esplugues, por su apoyo en mis primeros momentos como investigador.

En segundo lugar, pero no menos importante, a mis compañeros de laboratorio, ya que sin ellos, los días de trabajo se hubieran hecho mucho más largos. Gracias Carmen, gracias "Carmela" por todo. Por todos esos momentos que hemos vivido tanto dentro como fuera del laboratorio. Porque aunque hemos trabajado juntos codo con codo, muchas tardes nos hemos llamado para contarnos cosas que no hemos podido o querido contarnos en persona. Por tu ayuda incondicional en el laboratorio. Por esas reuniones de grupo improvisadas para "exponer nuestros resultados". Por esas juergas que nos hemos pegado por Valencia y muchos otros lugares, con "bombas de humo" incluidas. Por saber entenderme en cosas que incluso yo no entendía. Por el apoyo mutuo que nos hemos dado siempre el uno al otro. Ya éramos amigos antes de conocernos, pero después de trabajar juntos, creo que ahora somos más que amigos, como la hermana mayor que nunca tuve. Porque aunque no estemos ya viviendo en la misma ciudad, seguimos muy en contacto. Muchas gracias por todo. Gracias César, gracias "Cesarito". Porque no puede haber mejor tío que tú, tan trabajador, siempre dispuesto a ayudar, no sólo dentro del laboratorio, sino fuera de él. Por las risas por los pasillos mientras nos limpiábamos la bata con la pared. Porque como muchas

veces te digo, no se puede ser tan bueno, que luego te tratan de … Porque quiero verte enfadado algún día (aunque últimamente lo estoy viendo). Porque necesito saber qué es eso que te tomabas, que te estaba sentando muy bien. Nepal!!!!! Porque espero que te vaya todo genial, y verte en poco tiempo como doctor de dos maneras. Gracias Nicole, gracias "Nicoleta", gracias "Cinquici". Por tu alegría, que hace que los días de trabajo se hagan muchísimo más amenos. Por los días de modelado con almidón de patata: ¡Un árbol!... Porque desde que llegaste al laboratorio, sienta mucho mejor venir a trabajar. Y por esos mensajes de wassap cuando me retraso un poco, para preguntar que dónde ando, y "para más inri", porque molas "mogolpón". Gracias Jesús, gracias "Cosinillos". Por tu optimismo en tu trabajo y fuera de él. Por los días de playa y fiesta. Porque compras guacamayos en la frutería. Por tu grado de inopia inconsciente, que más de una vez me ha hecho sacar una sonrisa. Porque espero que te vaya genial en tu nueva aventura suiza. Gracias Amelia, gracias "Amelita". Por tu espontaneidad y tu locura, que me han hecho reír en muchas ocasiones. Por tu ayuda al grupo y a mí en el trabajo, quitándonos la faena más pesada. Por los días de mercadillo juntos. Gracias Víctor. Por tu ayuda en el laboratorio, y ser de tu confianza al preguntarme dudas de trabajo. Gracias Fernando. Por tus ganas de aprender. Por estar siempre disponible para ayudar en cualquier cosa. Gracias Isa. Porque aunque hace poco que te uniste al grupo, ya estás trabajando conmigo mano a mano con los ratolines. Gracias Mariam, gracias Patri. Gracias Raquel, gracias "Raquelita". Por las historias que nos contabas que amenizaban las mañanas en cultivos. Por las confesiones en la rampa del Clínico. Por tu espontaneidad, que me han hecho soltar una carcajada en muchas ocasiones. Porque te echamos mucho de menos… Y en último lugar, gracias "Silvia", gracias "Tochi", gracias "Murciégala". Por los desayunos, por los arroces al horno y los pimientos rellenos, por la cenas en tu casa… Por las muchas veces que te hemos invitado a salir y no has "podido" venir. Por la largas conversaciones al teléfono por la tardes. Por ser una buena amiga de esas que se cuentan con los dedos de la mano. Y gracias a Toni y a los nanos, Raúl y Pablo, por esas cenas y veladas en vuestra casa, "ganándoles siempre" a la Wii. Y general, a

todos vosotros porque me habéis demostrado que hay vida más allá del laboratorio, y eso lo hemos exprimido al máximo posible siempre que hemos podido. Por esto, y por muchas cosas más, que sepáis que siempre os llevaré en mi corazón.

Gracias a todos los compañeros de laboratorio. Gracias Jorge. Gracias Miguel. Gracias Dulce. Gracias Pedro. Gracias Laura. Gracias Ana. Gracias Dolo. Gracias María. Gracias Miriam. Gracias Alberto. Gracias Susana. Gracias Rosa. Gracias Noelia. Gracias Sandra. Gracias Arancha. Y gracias también a la gente que ha pasado por el laboratorio. Gracias Lara. Gracias Miri. Gracias Irene. Gracias Jackie. Gracias Wil. Gracias Mario. Gracias Antonio. Gracias Sonia.

Gracias a l@s mayores. Gracias Loles. Gracias María Ángeles. Gracias Sara. Gracias Víctor. Gracias Carlos. Gracias Nade. Gracias Miguel. Gracias José Luis. Gracias Benjamín.

Gracias también a las compañeras del laboratorio de al lado. Gracias Cris. Por tu espontaneidad. Por nuestro intento de salir a correr, aunque yo fuera en bicicleta. Por nuestras quedadas cuando me dejo caer por Madrid. ¡Qué víva la novia! Gracias Paula. Por ser mi compañera de clases. Por las mañanas en el laboratorio intentando cuadrar las clases. Gracias Virginia. Por tu simpatía. Por hacer que compartir células para poder trabajar fuera una tarea demasiado fácil y cómoda. Y en extensión gracias a María Jesús. Por demostrarme lo que es amor a la ciencia. Por ser nuestra Presidenta de la SEF.

Gracias también a nuestros técnicos de laboratorio. Gracias Amparo. Por enseñarme en mis comienzos en el laboratorio, pero no sólo dentro de él, sino también fuera. Por demostrarme que eres una gran persona, con mucha sensatez, a la que se le puede contar cualquier cosa. Por darme consejos que me han servido en muchas ocasiones. Por esos debates tempranos en la cocina con Silvia y Maruja. Por la comida que tenemos que hacer en tu casa en Cullera. Gracias Maruja. Por esos

debates en el desayuno en los que intentábamos resolver el mundo. Por esos dulces que nos traías que nos endulzaban la mañana. Gracias Dora. Por tu sonrisa permanente en la cara. Por hacer de nuestras conversaciones una forma de alegrarnos las mañanas en cultivos. Por los caquis, por las calabazas, por las cocas, por los dulces, por los nísperos… Gracias Inés. Por tu simpatía y por tu alegría. Por las largas conversaciones mientras yo operaba ratas. Porque aunque tu estancia fue corta, conectamos desde el minuto uno. Por tus ganas de aprender cada día, aunque no tuviera que ver nada con lo que tú hacías. Gracias Raúl. Por tus buenos días a primera hora de la mañana. Por ser el más madrugador todos los días, eso sí, siempre después que yo…

Gracias a las secretarias del Departamento. Gracias Pepa. Por estar siempre dispuesta a organizar cosas por y para el laboratorio. Por ser la persona a la que preguntabas siempre que tenías una duda informática. Por esas risas viendo mensajes de wassap. Gracias Mamen. Por ayudarme en todo lo relacionado con el desarrollo de esta Tesis Doctoral. Por no mandarme a freir espárragos cuando te preguntaba las cosas muchas veces. Por hacerme muy fácil este proceso tan costoso. Por tu paciencia. Gracias María Ángeles. Por ayudarme en muchos temas relacionados con papeleo del Departamento.

También quería agradecer a mis amigas de Soria de toda la vida. Gracias Carmen. Por ser como eres. Porque espero que no cambies nunca. Porque ya te he agradecido mucho antes, no? Y por extensión, gracias Ricky. Porque aunque nos conocemos de hace poco tiempo, he vivido ya bastantes experiencias en tu compañía. Gracias Faty. Por tu sinceridad. Por ser tan extrovertida y decir las cosas como las piensas. Gracias Rebe. Por tu simpatía. Por tus bromas. Porque siempre estás en la parra, cosa que me hace mucha gracia. Y en extensión, gracias Remy. Por no tener sentido del ridículo disfrazado casi desnudo metido en una bañera. Y en general para vosotros, gracias, por nuestros viajes, por nuestras cenas en Soria, por nuestras salidas por Soria, por nuestras conversaciones sobre programas de

televisión en directo. Sabéis que sois de esos amigos con los que se puede contar para lo que sea, que aunque ahora estemos lejos físicamente, estamos siempre muy cerca. Gracias por todo de corazón.

Por supuesto, agradecer a mi gran grupo de amigos del pueblo. Gracias Fer. Por ser como eres, por ser el primo perfecto. Por esas charlas en el banco cuando estoy de vacaciones por Soria. Por preguntarme siempre que cómo iba la Tesis. Gracias Sara. Por ser la mejor "prima política". Por ser una de las personas a las que les puedo contar las cosas que me inquietan. Por atenderme al teléfono para solucionarme todos los problemas del banco. Y gracias a Elba, la pequeñaja del grupo. Gracias Laura. Por tu espontaneidad. Por tus bromas, por tus comentarios, que a todos nos hacen partirnos de risa. Porque aunque estando malita, esos comentarios siempre estaban. Porque espero que los problemillas se pasen y queden como una mera anécdota para que cuentes a tus nietos. Gracias Vicky. Por ser como eres, por ser la prima perfecta. Por estar dispuesta a cualquier plan. Porque me debes un jueves universitario por Soria. Gracias María. Por tu simpatía. Por esas noches de fiesta perfecta, llenas de risas. Por esas Fallas que pasamos llenas de risas. Gracias Noe. Gracias Roberto. Y gracias Iker. Gracias Marcos. Gracias Noelia. Gracias Rober. Gracias Encar. Gracias Tito. Y gracias Iván, hasta hace poco el más pequeño del grupo. Gracias Inés. Gracias Chus. Gracias Lorena. Gracias Mario. Gracias Dani. Gracias Soraya. Gracias Emilio. Gracias Cristina. Y en general, gracias a todos por esos momentos que hemos pasado en el pueblo, y por esos viajes que hemos hecho, incluso en algunas ocasiones todos juntos.

Gracias Nico. Por esas largas conversaciones hablando de "nuestras cosas". Por el 9 d'Octubre. Por ser mi confidente y yo el tuyo. Por esas quedadas para tomar algo y ver lo que se cuece por "Lotelito". Por los Gins entre semana. Por enseñarme que se puede conocer a gente de muchas formas. Por ser como eres. Gracias Enrico. Por las tardes que hemos pasado "tesisando" juntos. Porque fuiste un perfecto compañero de piso, y espero volver a verte muy pronto.

Agradecer también a mi vecina de toda la vida, Cristina. Gracias Cris. Por ser como eres, echada para adelante y sin que nada te frene. Por preguntarme siempre que nos juntamos como me va el trabajo por Valencia y como va la tesis. No cambies nunca.

También quiero darles las gracias a mis amigos de Salamanca. Gracias Adrián. Por ser un gran compañero de habitación y de piso durante la carrera. Por demostrarme que eres una gran persona. Gracias Sergio. Por darme consejos muy útiles durante mis tres últimos años de carrera. Por hacer que compartir piso fuera una terea muy fácil. Gracias Adrián, gracias "Canario". Por ser un gran amigo. Porque conectamos desde el primer momento que nos conocimos. Por mi visita a Canarias y tu visita a Soria. Porque te debo una visita a Zaragoza, más larga que la anterior, y tú me debes otra a Soria. Gracias Fany. Por tu simpatía. Por confiar en mí. Porque aunque estábamos lejos, y ahora más cerca, siempre hemos estado en contacto. Porque aunque nos vemos de Fallas a Fallas, estamos siempre en contacto. Gracias a mis compañeras de carrera. Gracias Sara. Gracias María. Gracias Elena. Gracias Jeza. Gracias Jenny. Por vuestra simpatía. Por vuestra sonrisa permanente en la cara. Por vuestras ganas de ayudar y por estar ahí siempre. Por vuestra locura, que me cautiva. Porque sois únicas. Porque creo que formamos un grupo de personas muy diferentes que encajamos perfectamente. Por llamarme Macho α del grupo, cosa que me provoca una gran sonrisa. Gracias a mi "Manada de Bicholog@s".

No me puedo olvidar de darte las gracias, Edu. Gracias "chaval". En realidad no puedo expresar el cariño que te tengo con palabras… Gracias por todo de corazón. Gracias por hacerme sentir una persona imporante en tu vida. Gracias por hacerme partícipe de muchas de tus cosas, tanto profesionales como personales. Gracias por invitarme al teatro tantas veces, al final me voy a tener que hacer crítico de teatro… Por que cuando estoy contigo, las horas se me hacen minutos, y los días se me hacen horas… Por hacerme parte de tu vida desde el primer minuto que nos

conocimos. Porque espero tenerte siempre cerca, para poder compartir momentos como este, tan bonitos, siempre a tu lado.

Y por último, pero no por ello menos importante, sino al contrario, gracias a mis padres. Gracias por estar ahí siempre. Por cuidarme y darme todo lo que habéis podido y más. Por hacerme ver la importancia de las cosas y valorar las cosas que realmente importan. Por ser como sois, aunque tenga que reconocer que en ocasiones no me guste. Porque sois lo más importante en mi vida y os quiero un montón, aunque no lo diga casi nunca. Porque juntos hemos superado situaciones difíciles, y eso me hace ver que sois y soy mucho más fuertes de lo que creía. ***Porque sois los mejores padres del mundo.***

ABREVIATURAS

ABC: Abacavir

ADN: Ácido desoxirribonucleico

ADNc: Ácido desoxirribonucleico complementario

ADP: Adenosina difosfato

Antagonistas CCR5: Antagonistas del co-receptor CCR5

APV: Amprenavir

ARN: Ácido ribonucleico

ARNm: Ácido ribonucleico mensajero

ATV: Atazanavir

AZT: Zidovudina

CCL3: "Chemokine C-C Ligand-3"

CCL4: "Chemokine C-C Ligand-4"

CCL5: "Chemokine C-C Ligand-5"

CCR5: "C-C Chemokine Receptor Type-5"

CD11d: "Integrin Alpha-D"

COBI: Cobicistat

CV: Carga Viral

CXCR4: "C-X-C Chemokine Receptor Type-4"

Da: Diámetro arteriolar

ddC: Zalcitabina

ddI: Didanosina

DLV: Delavirdina

DPBS: "Dulbecco's Phosphate Buffered Saline"

DMSO: "Dimethil sulfoxide"

DRV: Darunavir

DTG: Dolutegravir

Dv: Diámetro venular

d4T: Estavudina

EFV: Efavirenz

EGM-2: "Endothelial Growth Medium-2"

ELV: Elvitegravir

ESL-1: "E-Selectin Ligand-1"

ETR: Etravirina

EVG: Elvitegravir

FDA: "Food and Drug Administration"

fAPV: Fosamprenavir

FITC: Fluoresceína isotiocianato

FTC: Emtricitabina

gp120: "Glycoprotein 120"

gp150,95: "Integrin Alpha-X"

GP1bα: "Platelet Glycoprotein 1b Alpha"

gp41: "Glycoprotein 41"

HBSS: "Hanks Balanced Salt Solution"

HDL: "High-Density Lipoprotein"

HSA: "Human Serum Albumin"

HUVEC: "Human Umbilical Vein Endothelial Cell"

ICAM-1: "Intercellular Cell Adhesion Molecule-1"

ICAM-2: "Intercellular Cell Adhesion Molecule-2"

IDV: Indinavir

IF: Inhibidores de la fusión

InInt: Inhibidores de la integrasa

IP: Inhibidores de la proteasa

ITIAN: Inhibidores de la transcriptasa inversa análogos de nucleós(t)ido

ITINAN: Inhibidores de la transcriptasa inversa no análogos de nucleósido

LFA-1: "Lymphocyte-Function-Associated-1"

LPV: Lopinavir

Mac-1: "Macrophage 1 Antigen"

MAdCAM-1: "Mucosal Vascular Addressin Cell Adhesion Molecule-1"

MVC: Maraviroc

NFV: Nelfinavir

NVP: Nevirapina

PAF: "Platelet Activating Factor"

PAM: Presión arterial media

PBMC: "Peripheral Blood Mononuclear Cell"

PE: Ficoeritrina

PECAM-1: "Platelet-Endothelial Cell Adhesion Molecule-1"

PMN: "Polymorphonulear Cell"

PSGL-1: "P-Selectin Glycoprotein Ligand-1"

RAL: Raltegravir

RPV: Rilpivirina

RTV: Ritonavir

SIDA: Síndrome de la inmunodeficiencia adquirida

SQV: Saquinavir

TDF: Tenofovir

TNF-α: "Tumor Necrosis Factor-α"

TPV: Tipranavir

T-20: Enfuvirtida

VCAM-1: "Vascular Cell Adhesion Molecule-1

VIH: Virus de la inmunodeficiencia humana

VIS: Virus de la inmunodeficiencia en simios

VLA-4: "Very Late Antigen-4"

V_{mean}: Flujo de los eritrocitos

V_{rbc}: Velocidad de los eritrocitos

ZDV: Zidovudina

γ: "Shear Rate"

3TC: Lamivudina

RESUMEN

La "Terapia Antirretroviral Combinada", utilizada para el tratamiento de la infección por el VIH, se basa en la administración de al menos 3 fármacos: 2 ITIAN en combinación con 1 antagonista CCR5, 1 ITINAN, 1 InInt o 1 IP. Esta terapia se introdujo rápidamente debido a la gravedad de la enfermedad pero con su empleo han aparecido efectos adversos, teniendo las enfermedades cardiovasculares una incidencia del 15,7 % en estos pacientes. Se ha asociado la "Terapia Antirretroviral Combinada" con el desarrollo de enfermedades cardiovasculares; sin embargo, se desconoce el papel que tiene cada fármaco ya se administran en combinación.

El objetivo del presente estudio fue realizar un estudio sistemático de los efectos proinflamatorios de concentraciones clínicamente relevantes de MVC (antagonista CCR5), EFV, NVP y RPV (ITINAN), RAL (InInt), LPV, ATV y DRV (IP) sobre la interacción leucocito-endotelio como primer paso en el desarrollo de enfermedades cardiovasculares con componente inflamatorio utilizando modelos *in vivo* e *in vitro*. Asímismo, intentamos determinar el mecanismo responsable de este proceso para los fármacos que dieran resultados positivos.

Este estudio muestra que concentraciones plasmáticas de EFV, NVP y RPV, pero no de MVC, RAL, LPV, ATV y DRV, inducen interacciones leucocito-endotelio *in vivo*. En particular, EFV, NVP y RPV inducen rodamiento y adhesión de leucocitos sobre vénulas mesentéricas de rata, mientras que el parámetro de migración leucocitaria únicamente es producido por EFV y NVP, pero no por RPV. De nuevo EFV, NVP y RPV inducen interacciones leucocito (PMN y PBMC)-endotelio mientras que el resto de fármacos analizados (MVC, RAL, LPV, ATV y DRV) no inducen estas interacciones *in vitro*. EFV aumenta la expresión de Mac-1 (CD11b/CD18) y gp150,95 (CD11c/CD18) en neutrófilos y monocitos humanos, NVP no aumenta la expresión de ninguna de las moléculas analizadas y RPV aumenta la expresión de Mac-1 y gp150,95 en neutrófilos y únicamente CD11b en monocitos humanos. Ninguna de las moléculas de adhesión analizadas en linfocitos ni en células endoteliales ve modificada su expresión tras el tratamiento con EFV, NVP y RPV. El resto de fármacos analizados (MVC, RAL, LPV,

ATV y DRV) no aumentan la expresión de las moléculas de adhesión tanto leucocitarias como endoteliales analizadas *in vitro*.

Aunque la expresión de ICAM-1 no se ve modificada por los tratamientos con ninguno de los ITINAN, la acumulación leucocitaria inducida por EFV y RPV se debe a la interacción entre las moléculas de adhesión leucocitarias Mac-1 y gp150,95 con su ligando endotelial ICAM-1 ya que cuando se utilizan anticuerpos bloqueantes frente a estas moléculas se previenen los diferentes parámetros leucocitarios.

También hemos analizado el papel de las combinaciones más utilizadas en la terapéutica actual sobre el proceso inflamatorio. TDF/FTC/EFV, ABC/3TC/EFV, TDF/FTC/RPV, ABC/3TC/RPV, ABC/3TC/ATV y ABC/3TC/DRV inducen rodamiento y adhesión en vénulas mesentéricas de rata *in vivo*. Sin embargo, únicamente TDF/FTC/EFV, ABC/3TC/EFV y ABC/3TC/RPV inducen migración leucocitaria. Las combinaciones TDF/FTC/ATV y TDF/FTC/DRV no modifican la interacción leucocito-endotelio *in vivo. In vitro*, TDF/FTC/EFV, ABC/3TC/EFV, TDF/FTC/RPV, ABC/3TC/RPV, ABC/3TC/ATV y ABC/3TC/DRV inducen rodamiento y adhesión de leucocitos (PMN y PBMC) sobre células endoteliales humanas mientras que TDF/FTC/ATV y TDF/FTC/DRV no modifican estos parámetros.

Dado que las enfermedades cardiovasculares son una causa importante de muerte entre los pacientes que toman la "Terapia Antirretroviral Combinada", el pautar unos fármacos u otros es de gran relevancia. Aunque estos resultados deben ser interpretados con precaución y cautela, se muestran evidencias de que los antagonistas CCR5, los InInt o los IP, o incluso el ITINAN RPV tienen mejor perfil proinflamatorio que los ITINAN EFV y NVP. Teniendo en cuenta su parecida eficacia para suprimir la replicación del virus, la toxicidad vascular de estos fármacos debería tenerse en cuenta a la hora de establecer una pauta posológica a un paciente infectado por el VIH, enfermo de SIDA y con riesgo de sufrir enfermedad cardiovascular.

ÍNDICE

1. INTRODUCCIÓN

1.1. PROCESO INFLAMATORIO

El proceso inflamatorio es una respuesta biológicamente activa que ocurre en tejidos conectivos vascularizados y surge con el fin defensivo de aislar y destruir a un agente dañino así como de reparar el tejido u órgano dañado. Este proceso consiste, en su primera fase, en la interacción de las células leucocitarias que circulan por el torrente sanguíneo con las células endoteliales que rodean la zona luminal del vaso sanguíneo implicado (Galkina et al., 2009, Carlos et al., 1994). Por lo tanto, en este mecanismo juegan un papel importante dos tipos celulares distintos: las ***células endoteliales*** y las ***células leucocitarias***.

El ***endotelio vascular*** es un órgano altamente especializado y metabólicamente muy activo que regula multitud de funciones vasculares. Es una monocapa contínua de células que separa la sangre del tejido subendotelial. En el momento que se produzca un daño inflamatorio, las células sanguíneas van a tener que atravesar el endotelio, por tanto, tienen una importancia crucial en dicho proceso. Las células endoteliales son las encargadas de regular este tránsito leucocitario así como el tráfico de mediadores mediante la modificación de las propiedades adhesivas entre ellas.

Los ***leucocitos*** son las células implicadas en los mecanismos de defensa del organismo frente a sustancias patógenas, es decir, los efectores celulares de la respuesta inmunitaria. Estas células se mueven por la sangre libremente mediante pseudópodos y frente a un estímulo inflamatorio, pueden salir fuera de los vasos sanguíneos prolongando su contenido citoplasmático, proceso conocido como diapédesis. Esto les va a permitir tener contacto con diferentes tejidos u órganos donde van a ejercer sus funciones.

La inflamación es la forma de manifestarse de muchas enfermedades. Se trata de una respuesta inespecífica frente a las agresiones del medio, generada por

diferentes tipos de agentes inflamatorios. Se considera por tanto un mecanismo de inmunidad innata, en contraste con la reacción inmune adaptativa, específica para cada tipo de agente infeccioso. Se caracteriza por la aparición de tumefacción, calor, rubor, dolor y pérdida o disminución de la función del tejido u órgano dañado.

1.1.1. INTERACCIÓN LEUCOCITO-ENDOTELIO

El primer estadio del proceso inflamatorio lo constituye la interacción de las células leucocitarias con el endotelio vascular. Frente a un estímulo, células dendríticas, mastocitos y macrógafos van a segregar gran cantidad de mediadores inflamatorios que van a activar al endotelio vascular y a los leucocitos circulantes. Estos últimos van a ser rápidamente reclutados a los tejidos periféricos, siendo neutrófilos y monocitos el tipo celular leucocitario fundamental y mayoritario implicado en dicho proceso (Dimasi et al., 2013, Jaipersad et al., 2014). Esta etapa está mediada por la interacción entre moléculas de adhesión presentes en los leucocitos y sus correspondientes ligandos existentes en las células endoteliales. El resultado es la extravasación de las células leucocitarias hasta el foco inflamatorio (Van Buul et al., 2004, Rao et al., 2007, Carman et al., 2008, Mitroulis et al., 2015), proceso que puede ser producido por una gran variedad de estímulos (Galkina et al., 2009, Van Buul et al., 2004, McEver et al., 2010).

De este modo, tiene lugar una cascada secuencial de reacciones reversibles y transitorias entre ambos tipos celulares (Brown, 1997) entre las que se distinguen las siguientes fases: rodamiento, adhesión y migración leucocitaria (FIGURA 1).

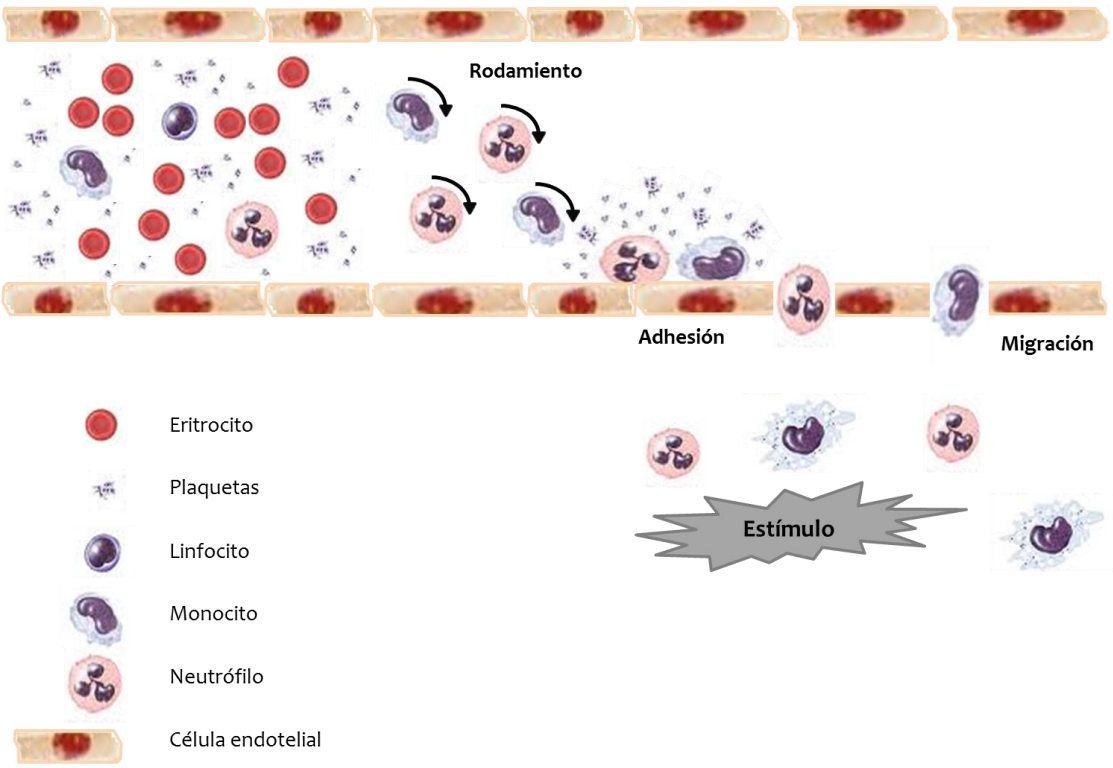

FIGURA 1. Etapas en el proceso de interacción leucocito-endotelio. En la figura se pueden observar las fases de rodamiento, adhesión y migración leucocitaria. Frente a un estímulo inflamatorio, los leucocitos se van a activar, interaccionando con el endotelio y finalmente migrando hacia el foco inflamatorio.

RODAMIENTO

Consiste en una deceleración en la velocidad de tránsito de los leucocitos (FIGURA 1). Como consecuencia, los leucocitos van a rodar por el endotelio en dirección al foco inflamatorio (Dimasi et al., 2013). Este proceso se inicia debido a la liberación de mediadores generados en respuesta a un daño producido (biológico, físico o químico, entre otros) que va a conllevar a una activación de los leucocitos, de las células endoteliales o de ambos tipos celulares. Esto va a producir un aumento de la expresión de las moléculas de adhesión pertenecientes a la familia de las selectinas (L-Selectina, E-Selectina y P-Selectina), de las integrinas α_4 ($\alpha_4\beta_1$ y $\alpha_4\beta_7$) y de las integrinas β_2 [LFA-1 ("Lymphocyte-Function-Associated-1") y Mac-1 ("Macrophage 1 Antigen")] (Ley et al., 2007) (FIGURA 2). La interacción entre estas moléculas de adhesión leucocitarias y endoteliales va a conducir al enlentecimiento de la velocidad de los leucocitos y por consiguiente, a un mayor contacto con el endotelio vascular (McEver et al., 2010, Brown, 1997, Ley et al., 2007).

Dentro de las selectinas, L-Selectina se expresa constitutivamente en los leucocitos e interacciona con sus ligandos que se encuentran en las células endoteliales, como es el caso de PSGL-1 ("P-Selectin Glycoprotein Ligand-1"), mucinas y otros ligandos glicosilados (Brown, 1997, Sriramarao et al., 1994, Alon et al., 1995, Dimasi et al., 2013). E-Selectina y P-Selectina, expresadas en el endotelio vascular, interaccionan con sus ligandos presentes en leucocitos, que pueden ser PSGL-1, CD44, ESL-1 ("E-Selectin Ligand-1") y otros ligandos glicosilados (Brown, 1997, Sriramarao et al., 1994, Alon et al., 1995, Dimasi et al., 2013). Existen evidencias de que la interacción entre E-Selectina y ESL-1 es necesaria para el paso a la siguiente etapa del proceso, la adhesión leucocitaria (Dimasi et al., 2013). Además P-Selectina también se expresa en gránulos intracitoplasmáticos de plaquetas, y al activarse, es traslocada a la membrana plasmática, permitiendo la interacción con sus ligandos tanto en los leucocitos como en el endotelio (Brown, 1997, Sriramarao et al., 1994, Alon et al., 1995).

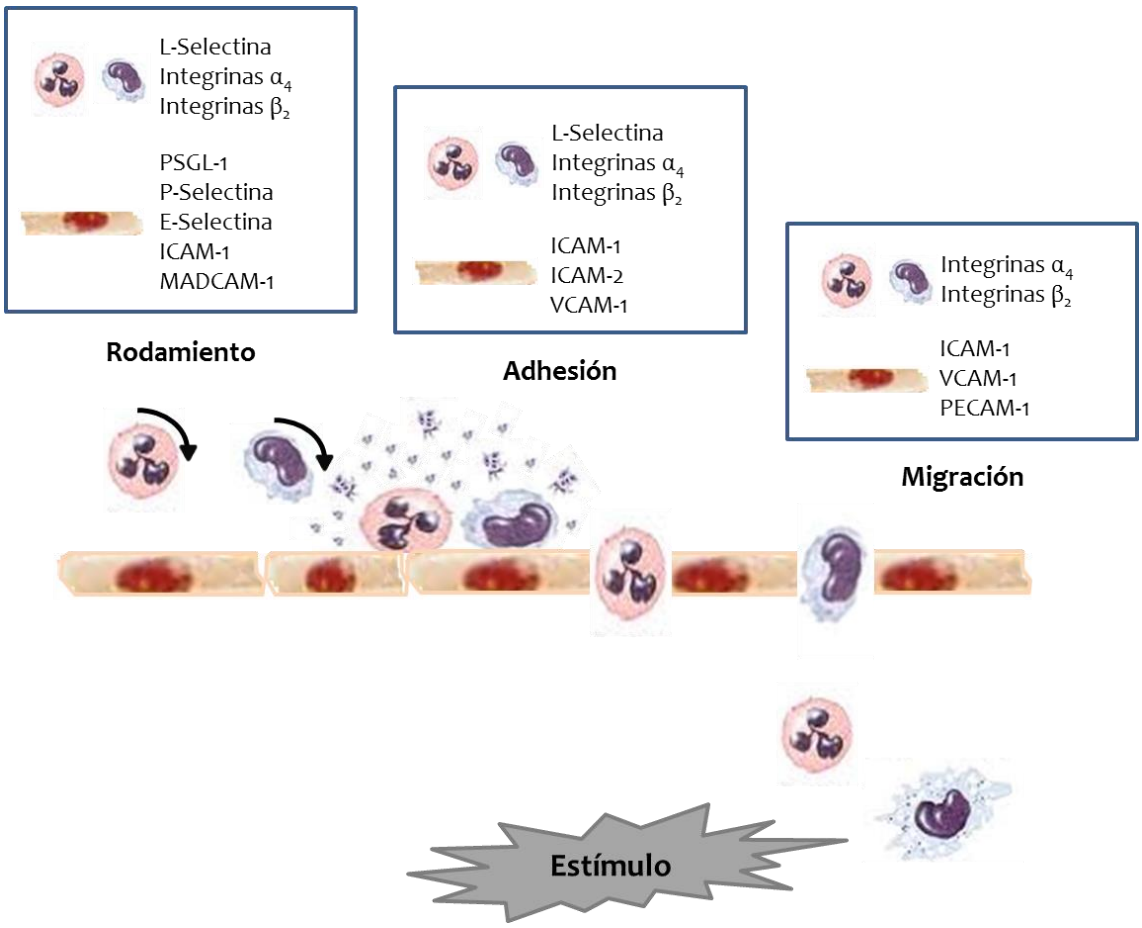

FIGURA 2. Etapas en el proceso de interacción leucocito-endotelio y principales moléculas de adhesión implicadas en cada una de ellas. En la figura se pueden observar las fases de rodamiento, adhesión y migración leucocitaria y las principales moléculas de adhesión leucocitarias y endoteliales implicadas en cada etapa del proceso.

En cuanto a las integrinas α_4, cabe destacar la implicación en el proceso de rodamiento de la integrina $\alpha_4\beta_1$ o VLA-4 ("Very Late Antigen-4") y de la integrina $\alpha_4\beta_7$, mediando en dicho proceso eosinófilos y linfocitos, respectivamente (Brown, 1997, Sriramarao et al., 1994, Alon et al., 1995). Estas moléculas de adhesión se expresan en las células leucocitarias e interaccionan con sus ligandos endoteliales, principalmente con VCAM-1 ("Vascular Cell Adhesion Molecule-1") y MAdCAM-1 ("Mucosal Vascular Addressin Cell Adhesion Molecule-1"). La integrinas son un tipo de receptores "susceptibles de ser activadas" que incrementan rápidamente su capacidad de unión a su ligando gracias a vías de señalización intracelulares (Dimasi et al., 2013). Existen en tres estados conformacionales, que condicionan su afinidad por sus diferentes ligandos: baja, media y alta afinidad (McEver et al., 2010, Ley et al., 2007).

- *Baja afinidad*: en este estado, las integrinas no van a interaccionar con sus ligandos aunque estos estén activados, ya que poseen una conformación cerrada con el casco cerrado.
- *Media afinidad*: tras la estimulación, las integrinas van a pasar a una conformación extendida, pero manteniendo el casco cerrado.
- *Alta afinidad*: si el estímulo persiste, la afinidad de las integrinas por sus ligandos va a aumentar, ya que se produce la apertura del casco manteniéndose la conformación extendida.

Últimamente, y cada vez con más fuerza, se está relacionando a las integrinas β_2 con el proceso de rodamiento leucocitario. Se ha descrito que LFA-1 y Mac-1 poseen un papel fundamental en dicho proceso (McEver et al., 2010, Ley et al., 2007). Existen evidencias que no sólo implican a E-Selectina en este proceso (Kunkel et al., 1996), sino que también se requiere la activación de LFA-1 y Mac-1 (Jung et al., 1998, Dunne et al., 2002). En esta etapa, las integrinas adoptan una conformación de baja-media afinidad, pudiendo interaccionar con ICAM-1

("Intercellular Cell Adhesion Molecule-1"), su principal ligando en el endotelio vascular (Dimasi et al., 2013).

ADHESIÓN

Consiste en la interacción firme de los leucocitos con el endotelio. Tras el estímulo inflamatorio, y si éste persiste, los leucocitos en fase de rodamiento se van a activar y a adherirse firmemente al endotelio vascular (FIGURA 1). En este proceso participan las integrinas leucocitarias α_4 y β_2 y las inmunoglobulinas endoteliales [ICAM-1, ICAM-2 ("Intercellular Cell Adhesion Molecule-2") y VCAM-1] (Ley et al., 2007, Lawrence et al., 1991) (FIGURA 2). Así, se va a producir la interacción específica entre las integrinas y las inmunoglobulinas, dando lugar a la adhesión célula-célula estable y próxima (Brown, 1997).

Las integrinas α_4 (VLA-4 y $\alpha_4\beta_7$) interaccionan principalmente con VCAM-1 y las integrinas β_2 (CD11/CD18) con LFA-1, Mac-1 y gp150,95 ("Integrin Alpha-X") que interaccionan, en mayor medida, con ICAM-1 (Ley et al., 2007, Mitroulis et al., 2015). Para que se produzca este proceso las integrinas leucocitarias deben estar activadas (en su conformación de máxima afinidad) (Dimasi et al., 2013).

Las integrinas β_2 son una familia de moléculas de adhesión leucocitarias que comparten la misma subunidad común β (CD18) y poseen una cadena α (CD11) diferente. La familia incluye 4 tipos conocidos de integrinas: αL (CD11a, LFA-1), αM (CD11b, Mac-1), αX (CD11c, gp150,95) y αD (CD11d, "Integrin Alpha-D") (Carlos et al., 1994). La expresión de CD11b y CD11c en linfocitos es limitada, pero estas moléculas son movilizadas de vesículas secretoras intracelulares a la superficie de neutrófilos y monocitos tras pocos minutos de estimulación (Carlos et al., 1994). Como ya se ha mencionado previamente, su principal ligando es ICAM-1, que está expresado constitutivamente en la superficie de las células del endotelio vascular (Carlos et al., 1994). Gp150,95 (CD11c/CD18)

también se ha relacionado con la fagocitosis, con la presentación de los antígenos por las células dendríticas y con la respuesta inflamatoria (Sadhu et al., 2007). Mac-1 (CD11b/CD18) ha sido propuesto como el nexo de unión entre la adhesión celular y la trombosis (Hirahashi et al., 2009) debido a su papel de mediar la adhesión de neutrófilos y monocitos a la pared de los vasos, mediando también en la agregación plaquetaria (Gawaz et al., 2005).

En el endotelio vascular, las inmunoglobulinas leucocitarias ICAM-1, ICAM-2 y VCAM-1 se encuentran expresadas de forma constitutiva. Frente a un estímulo van a aumentar su expresión, facilitando la interacción con sus ligandos leucocitarios, aunque estas moléculas pueden unirse a dichos ligandos sin que se produzca una activación endotelial previa (Dimasi et al., 2013). Estas inmunogobulinas son glicoproteínas transmembrana que pueden estar presentes en varias isoformas en el tejido vascular. Se expresan de manera constitutiva en este tejido, y se han relacionado con el inicio del proceso inflamatorio, ya que sus ligandos leucocitarios principales son LFA-1 y Mac-1 (Lyck et al, 2014).

Así, la activación de las integrinas va a conllevar a la interacción específica entre las integrinas en estado de alta afinidad y las inmunoglobulinas, dando lugar a la adhesión célula-célula estable y próxima (Brown, 1997). Las integrinas activadas y unidas a sus ligandos endoteliales van a generar multitud de señales intracelulares que van a iniciar gran cantidad de rutas de señalización celular, que conllevarán a una fase de post-adhesión y estabilización, llegando a la fase conocida como fortalecimiento de la adhesión (Ley et al., 2007).

MIGRACIÓN

Consiste en el paso de los leucocitos a través del endotelio vascular hasta el foco de la inflamación (FIGURA 1). Para que se llegue a este estadío, también es necesario que se produzca una activación leucocitaria. Las integrinas activadas van a emitir señales que hacen que las células leucocitarias, especialmente neutrófilos y monocitos, se aplanen y se concentren en ciertos lugares de los vasos sanguíneos para así poder migrar hacia el foco inflamatorio inmediatamente cuando se produzca el estímulo. Este proceso se denomina rastreo intravascular (Ley et al., 2007, Hynes, 1992). Los leucocitos van a atravesar los espacios intercelulares a través de las uniones presentes entre las células endoteliales y a través de la membrana basal perivascular, localizando los lugares más propicios para realizar este proceso (Hynes, 1992, Springer et al., 1994). Esta situación va a suponer una alteración mínima de la estructura de la pared vascular (Ley et al., 2007, Springer et al., 1994). En este proceso de extravasación leucocitaria va a tener mucha importancia el complejo formado por las integrinas β_2 (CD11/CD18)/ ICAM-1 (Carlos et al., 1994, Ley et al., 2007, Smith, 1993, Furie et al., 1991, Ebisawa et al., 1994, Luscinskas et al., 1991, Sadhu et al., 2007, Mitroulis et al., 2015) (FIGURA 2).

También es importante la molécula de adhesión PECAM-1 o CD31 ("Platelet-Endothelial Cell Adhesion Molecule-1"), que presenta niveles elevados en las uniones intercelulares (FIGURA 2). Además, esta molécula es capaz de producir la activación de las integrinas leucocitarias.

Las células endoteliales forman unos complejos denominados "docking structures" o "transmigratory cups", ricos en moléculas de adhesión como ICAM-1 y VCAM-1 entre otras, que ayudan a facilitar la migración de los leucocitos (Dimasi et al., 2013). Además, los leucocitos adheridos promueven la formación de microdominios pro-inflamatorios que expresan altas cantidades de ICAM-1 y VCAM-1 en estas estructuras (Dimasi et al., 2013). Frente a esta

situación, los leucocitos activados migran a través de la barrera endotelial y posteriormente atraviesan la matriz extracelular para así llegar al lugar donde se haya producido la inflamación, donde realizarán su función (Van Buul et al., 2004, Ley et al., 2007).

Los leucocitos también expresan otras integrinas β_1 y β_3, aunque en niveles mucho más bajos. Estas moléculas de adhesión se van a unir a proteínas de la matriz extracelular, como Laminina, Fribronectina o Vitronectina, promoviendo la llegada de los leucocitos hasta el foco inflamatorio (Brown, 1997, Ley et al., 2007).

DESARROLLO DE TROMBOSIS Y FORMACIÓN DE LA PLACA ATEROSCLERÓTICA

Si el estímulo proinflamatorio persiste, se podría llegar a la trombosis y a la formación de la placa aterosclerótica (Jackson, 2011). En este proceso, van a jugar un papel muy importante las plaquetas, uniéndose entre ellas, uniéndose a leucocitos y/o a células endoteliales, favoreciendo también la unión entre ambos tipos celulares (Projahn et al., 2012, Gawaz et al., 2005). Bajo un estímulo inflamatorio, las plaquetas se van a unir a los leucocitos mediante la interacción entre P-Selectina y su ligando leucocitario PSGL-1, unión que se estabiliza con la unión entre GPIbα ("Platelet Glycoprotein 1b Alpha") plaquetaria y Mac-1 leucocitaria (Projahn et al., 2012). Por otro lado, las plaquetas interaccionan con el endotelio vascular a través de P-Selectina y E-Selectina. Está demostrado que P-Selectina media la adhesión de las plaquetas al endotelio venular y arterial en procesos inflamatorios agudos (Gawaz et al., 2005).

Con todo ello, se llegaría a una fase inflamatoria irreversible, que conllevaría a la aterosclerosis, primera causa de infarto de miocardio en el mundo occidental (Jaipersad et al., 2014).

1.2. TERAPIA ANTIRRETROVIRAL

La "Terapia Antirretroviral Combinada" se utiliza para el tratamiento del Síndrome de la Inmunodeficiencia Adquirida (SIDA), enfermedad causada por el virus del Virus de la Inmunodeficiencia Humana (VIH). Esta Terapia permite suprimir la replicación del VIH, preservando o restaurando la función inmune, aumentando así la supervivencia de los pacientes infectados. Su principal inconveniente es que no permite erradicar el genoma viral de los tejidos reservorio, suponiendo un deterioro inmunológico y clínico de las personas infectadas y tratándose, por consiguiente, de un tratamiento de por vida.

Esta terapia se empezó a desarrollar en la década de los 80, cuando se reportaron los primeros casos de infección por el VIH y se diagnosticaron los primeros enfermos de SIDA, tras reportar una forma rara de neumonía en 5 personas homosexuales jóvenes (Barré-Sinoussi et al., 1983). Poco después, casos similares surgen por todo el mundo, describiéndose una enfermedad epidémica de la que se desconocía su etiología y su transmisión. Esta terapia se ha ido desarrollando hasta la actualidad intentando buscar fármacos que maximicen la supresión de la evolución del virus en el organismo y minimicen los efectos secundarios adversos que ésta produce. Existen más de 36 millones de personas infectadas actualmente por el VIH en todo el mundo, la mayoría de las cuales viven en países en vías de desarrollo del África sub-sahariana, Asia y América del Sur.

1.2.1. INFECCIÓN POR EL VIRUS DEL VIH

El VIH es un lentivirus (género *Lentivirus*) perteneciente a la familia *Retroviridae* agente causal del SIDA. El virus VIH-1 fue descubierto por el equipo del Doctor Luc Montagnier en Francia en 1983 (Barré-Sinoussi et al, 1983) y el VIH-2 se aisló en 1986 de pacientes con SIDA provenientes de África occidental por el equipo dei mismo doctor (Gallo et al, 1986). Su virión es esférico de un diámetro de 120-150 nm y está dotado de una envoltura y una cápside proteíca. Su genoma es de tipo cadena de ARN (Ácido ribonucleico) monocatenario que debe copiarse provisionalmente a ADN (Ácido desoxirribonucleico) para poder integrarse y multiplicarse en el genoma de la célula hospedadora a la cual infecta. Los antígenos específicos de su envoltura se acoplan perfectamente con las proteínas de la membrana de las células infectables, especialmente los linfocitos T CD4+.

Se conocen, hasta la fecha, dos tipos de VIH: el VIH-1 y el VIH-2. El VIH-1 y el VIH-2 poseen la misma estructura genética. Difieren entre ellos en las glicoproteínas de su envoltura proteíca y en su grado de virulencia. El tipo 1 es mucho más virulento e infeccioso, siendo el causante de la mayoría de la infecciones por el virus a nivel mundial, sin embargo, el tipo 2 es menos virulento y menos infeccioso, estando restringido únicamente a África occidental (Gilbert et al., 2003, Reeves et al., 2002).

Esta infección se asocia a una alta tasa de replicación viral en el organismo que tiene lugar principalmente en los linfocitos T CD4+, pudiendo ocurrir también en otros tipos celulares, como monocitos y macrófagos, células dendríticas, células de Langerhans y células de la microglía del cerebro. Un paciente infectado es capaz de neutralizar los nuevos viriones formados y regenerar las células inmunes que se han destruido. Así, se logra un equilibrio entre la cantidad de virus circulante, carga viral (CV), y el sistema inmunológico, medido como recuento de linfocitos T CD4+. De este modo, la persona infectada se mantiene asintomática. Con el tiempo se puede romper este equilibrio, aumentando la CV y disminuyendo bruscamente el recuento

de linfocitos T CD4+ (Ho et al., 1995, Wei, et al., 1995, Mellors et al., 1996). En este punto, se llega a lo que se conoce como fase de SIDA, produciéndose un deterioro inmunológico que permite la aparición de infecciones clásicas y oportunistas (Pantaleo et al., 1996). Si no se administra tratamiento, se podría llegar incluso a la muerte de la persona infectada. Actualmente, y gracias al desarrollo de la "Terapia Antirretroviral Combinada", la mortalidad no asociada al SIDA en regiones con acceso al tratamiento esta causada principalmente por cáncer (23,5 %), enfermedades cardiovasculares (15,7 %) y enfermedades hepáticas (14,1 %), siendo estas patologías más frecuentes respecto a la población sana de las mismas características.

Actualmente no existe una vacuna para el VIH, por lo que la prevención primaria sigue siendo el mecanismo más eficaz para combatir esta enfermedad. Aún así, se está investigando activamente en la búsqueda de una vacuna eficaz frente al SIDA. Los tratamientos en la actualidad se basan en la utilización de anticuerpos monoclonales, haciendo especial énfasis en situaciones en las que es probable que se transmita la enfermedad, como es el caso de la transmisión de la enfermedad madre-hijo (Hessell et al., 2013), aunque la profilaxis pre-exposición se considera eficaz a la hora de poder evitar el contagio de la enfermedad. Existen resultados prometedores en primates no humanos (en macacos Rhesus), en los cuales estos anticuerpos monoclonales son capaces de neutralizar la infección causada por VIS (Virus de la Inmunodeficiencia en Simios) (Hessell et al., 2013, Moldbt et al., 2016).

1.2.2. CICLO BIOLÓGICO DEL VIRUS

El principal lugar de replicación del virus se encuentra en los órganos linfoides, concretamente en los ganglios linfáticos aunque también se produce en diversos órganos como el cerebro, el timo o el intestino. El VIH también está presente en la sangre o en los fluídos genitales (Wei et al., 1995).

El ciclo biológico del VIH consta de las siguientes fases (FIGURA 3):

FIJACIÓN

Es la primera etapa en la infección de la célula. Se basa en el reconocimiento mutuo y en el acoplamiento de las proteínas de la envoltura del virión - las glicoproteínas gp120 ("Glycoprotein 120") y gp41 ("Glycoprotein 41") - con sus receptores presentes en los linfocitos T CD4, los CD4. Este reconocimiento no es posible sin ayuda de co-receptores propios de las células susceptibles de ser invadidas: en el caso de los macrófagos son los CCR5 ("C-C Chemokine Receptor Type-5") y en el caso de los linfocitos los CXCR4 ("C-X-C Chemokine Receptor Type-4") que interaccionan con las proteínas superficiales del virus. Únicamente van a ser sensibles a la infección aquellas células que expresen estos receptores, siendo este reconocimiento condición imprescindible para que el virus llegue a penetrar en la célula y continúe con el proceso de infección.

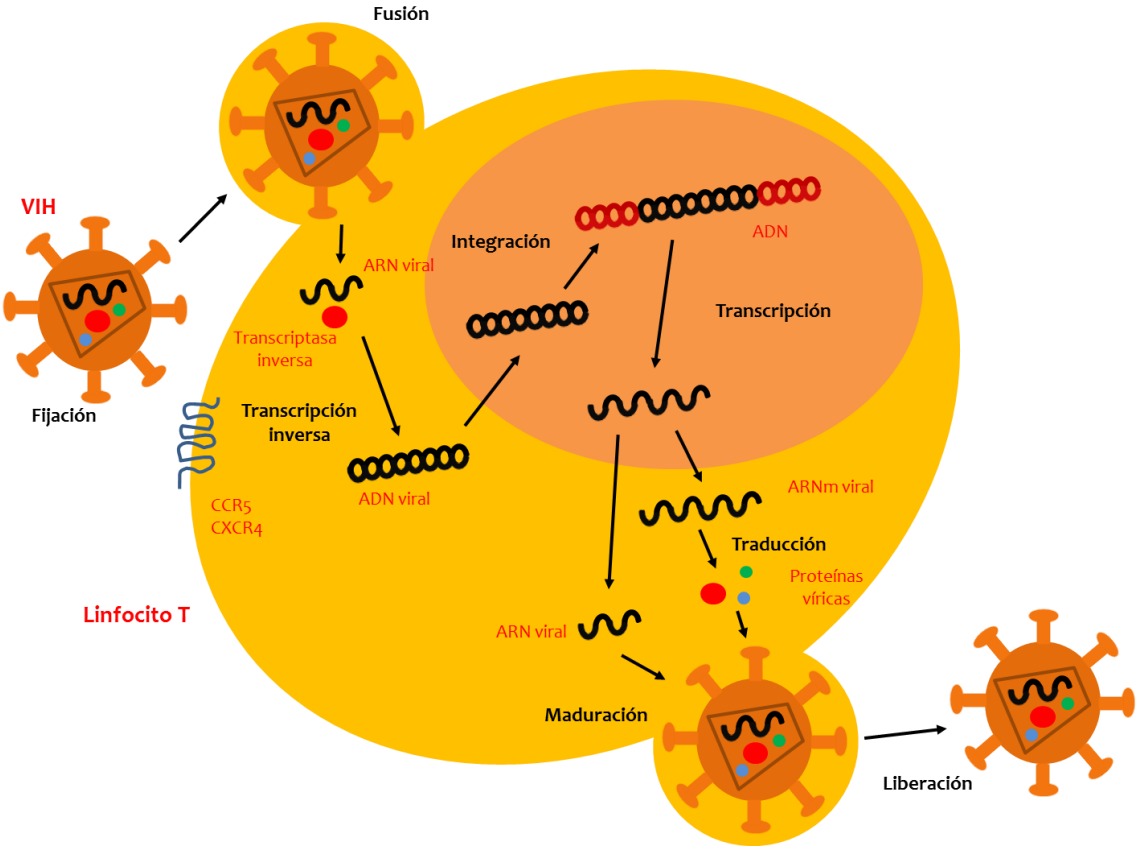

FIGURA 3. Esquema representativo del ciclo vital del VIH. En el esquema se pueden observar las distintas etapas del ciclo replicativo del ciclo biológico del virus: fijación, fusión, transcripción inversa, integración, transcripción, traducción, maduración y liberación de los nuevos viriones formados.

FUSIÓN

La envoltura lipídica del virus se va a fusionar con la membrana plasmática de la célula y se va a vaciar el contenido de la célula infectante en el interior de la célula hospedadora. Se eliminan las cubiertas proteicas, la cápside y la nucleocápside que protegen a las 2 copias de ARNm (Ácido ribonucleico mensajero, que forman el genoma viral) y sus proteínas asociadas. Así, el ARN viral queda libre en el citoplasma de la célula estando listo para ser procesado.

TRANSCRIPCIÓN INVERSA

Cada una de las 2 moléculas de ARNm llega asociada a una molécula de la enzima transcriptasa inversa, procedente del virión infectante, que se ocupa de dicho proceso. Esta transcripción inversa va a culminar con la formación de dos moléculas de ADNc (Ácido desoxirribonucleico complementario) monocatenario que posteriormente se asocian para formar una molécula de ADN.

INTEGRACIÓN

La cadena de ADN preformada va a penetrar en el núcleo de la célula hospedadora y gracias a la enzima integrasa, que también procede del virión infectante, se va a integrar en el ADN celular. En este punto, el ADN de la célula se puede replicar de manera masiva, hacerlo de forma controlada o permanecer latente.

TRANSCRIPCIÓN

Como resultado de la transcripción del ADN vírico se va a obtener un ARNm complejo que debe ser procesado antes de que la información que contiene pueda servir para producir las correspondientes proteínas virales. Este proceso se realiza a través de los mecanismos normales de la célula hospedadora. Una vez procesado, el ARNm puede salir del núcleo hacia el citoplasma a través de los poros nucleares.

TRADUCCIÓN

El ARNm proporciona la información para la traducción, es decir, para la síntesis de proteínas que se realiza a través de los ribosomas de la propia célula hospedadora. El resultado de la traducción no consiste inmediatamente en proteínas funcionales sino en poliproteínas que aún tienen que ser procesadas.

MADURACIÓN Y ENSAMBLAJE

Estas poliproteínas son cortadas en fragmentos y procesadas por la acción de las enzimas peptidasas específicas del VIH formando las proteínas constitutivas del virus. Estas proteínas se ensamblan, junto con el ARN proviral, para formar los constituyentes internos del virión que constituyen la cápside y su contenido.

LIBERACIÓN

Este último paso ocurre cuando los nucleoides víricos se aproximan a la membrana plasmática y se hacen envolver en una membrana que se acaba desprendiendo formando un nuevo virión o partícula infectante. En cada célula infectada se ensamblan varios millones de nuevos viriones, aunque muchos de ellos son incompletos y no tienen capacidad para infectar.

1.2.3. FÁRMACOS ANTIRRETROVIRALES

El tratamiento actual contra la infección por el VIH y contra el SIDA supone la actuación sobre alguno de los pasos del ciclo biológico del virus.

Existen en la actualidad gran cantidad de fármacos antirretrovirales. Estos fármacos surgen en la década de los años 80, como consecuencia de los primeros casos de infección por VIH reportados y su desarrollo se prolonga hasta la actualidad. La aparición de estos fármacos supuso un gran avance para el tratamiento de los pacientes infectados por el virus ya que, previo a su desarrollo, sólo existían medicamentos para paliar el deterioro immunológico y sintomatológico causado por la infección.

Inicialmente, estos fármacos se administraban en monoterapia o biterapia, lo que no suponía una mejora del estado de la infección ni de la sintomatología clínica asociada debido a su escasa eficacia inhibiendo la replicación viral. Es a partir de 1996, cuando se empiezan a administrar estos fármacos antirretrovirales en combinación de al menos 3 fármacos, cuando empieza la nueva era antirretroviral conocida como "Terapia Antirretroviral Combinada". Esta nueva etapa supone un gran avance en el tratamiento de la infección del VIH y el desarrollo de SIDA, ya que, con su empleo continuado permite reducir la CV y recuperar progresivamente el número de linfocitos T CD4+, restaurando con su empleo continuado y con el transcurso del tiempo el sistema inmune del paciente (Mocroft et al., 2003, Panos et al., 2008).

La Terapia Antirretroviral se basa en la inhibición de alguno de las fases del ciclo biológico replicativo del VIH, distinguiéndose así 6 grupos de fármacos (Imamichi, 2004, de Béthune, 2010) (FIGURA 4):

1. ***Antagonistas del co-receptor CCR5 (antagonistas CCR5).***
2. ***Inhibidores de la fusión (IF).***
3. ***Inhibidores de la transcriptasa inversa análogos de nucleós(t)ido (ITIAN).***
4. ***Inhibidores de la transcriptasa inversa no análogos de nucleósido (ITINAN).***
5. ***Inhibidores de la integrasa (InInt).***
6. ***Inhibidores de la proteasa (IP).***

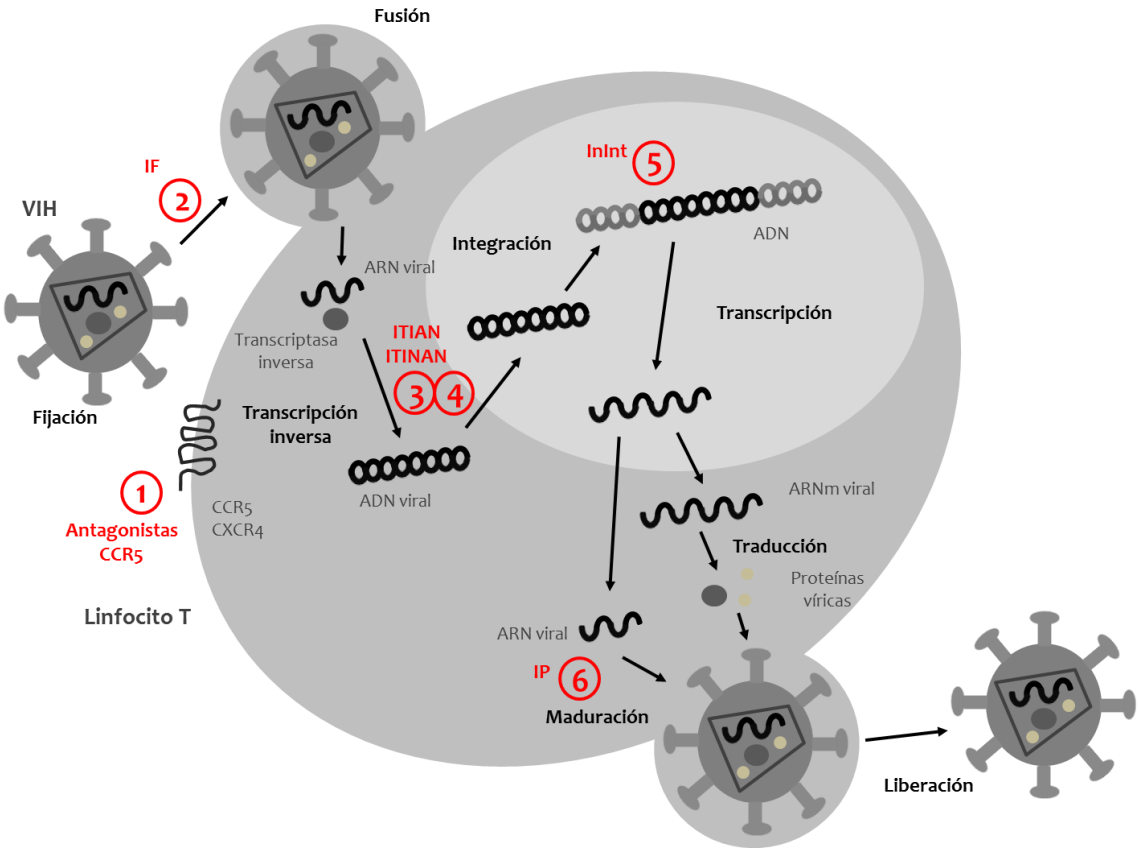

FIGURA 4. Esquema representativo del ciclo vital del VIH. En el esquema se pueden observar las distintas etapas que inhibe cada uno de los grupos de fármacos antirretrovirales que se usan en la terapéutica actual contra el VIH y el SIDA. Antagonistas del co-receptor CCR5 (Antagonistas CCR5), Inhibidores de la Fusión (IF), Inhibidores de la Transcriptasa Inversa Análogos de Nucleósi(t)ido (ITIAN), Inhibidores de la Transcriptasa Inversa no Análogos de Nucleósido (ITINAN), Inhibidores de la Integrasa (InInt) e Inhibidores de la Proteasa (IP).

ANTAGONISTAS DEL CO-RECEPTOR CCR5 (antagonistas CCR5)

Este grupo de fármacos actúa inhibiendo el co-receptor CCR5 propio de las células a infectar por el virus del VIH. Actualmente sólo existe un fármaco comercializado perteneciente a este grupo, ***Maraviroc (MVC)*** (FIGURA 5) (Günthard et al., 2014, Panel de expertos de GeSIDA, 2015, Ribera et al., 2011).

A pesar de ser un fármaco muy bien tolerado, MVC está indicado únicamente para el tratamiento de pacientes infectados por el VIH-1 que presenten un tropismo CCR5, y siempre en combinación con otros fármacos (Perry, 2010).

INHIBIDORES DE LA FUSIÓN (IF)

Estos fármacos inhiben la unión del virus a la célula hospedadora acoplándose a la glicoproteína gp41 presente en la cubierta del virus. Evitan así la fusión del virus con la membrana de las células a infectar y la entrada del material viral a esta célula. En la actualidad únicamente se encuentra comercializado ***Enfuvirtida (T-20)*** (FIGURA 5) (Günthard et al., 2014, Panel de expertos de GeSIDA, 2015, Ribera et al., 2011).

T-20 se administra por vía subcutánea. Su uso es reducido (Kilby et al., 1998) debido a que, cuando no se administra en combinación con otros antirretrovirales pueden aparecer mutaciones de resistencia (debido a que presenta una baja barrera genética) y de este modo hacer que pierda su eficacia.

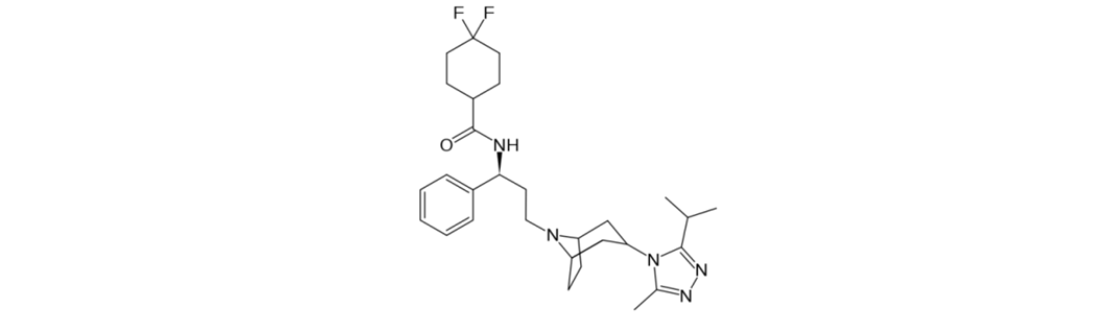

MVC

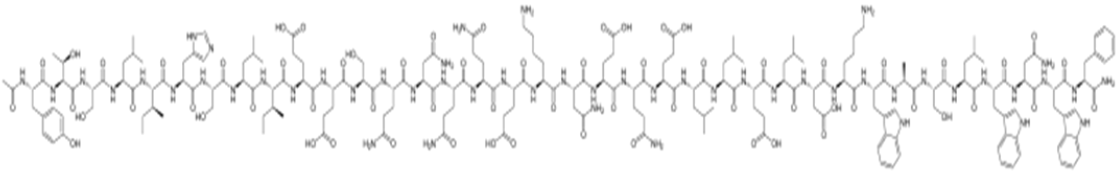

T-20

FIGURA 5. Fármacos antagonistas CCR5 e IF. La figura muestra las estructuras químicas de los distintos fármacos antagonistas ICCR5 e IF aprobados actualmente para el tratamiento del VIH. Maraviroc (MVC) y Enfuvirtida (T-20).

INHIBIDORES DE LA TRANSCRIPTASA INVERSA ANÁLOGOS DE NUCLEÓS(T)IDO (ITIAN)

Este grupo de fármacos fue el primero que se desarrolló dentro de la Terapia Antirretroviral, siendo Zidovudina (AZT) el primer fármaco aprobado por la FDA ("Food and Drug Administration") para el tratamiento del SIDA en 1987 (Ezzell, 1987).

Estos fármacos inhiben de forma competitiva la transcriptasa inversa del virus, inhibiendo la transcripción de ARNm viral a ADNc viral. Por lo tanto, los ITIAN actúan compitiendo con los nucleósidos fisiológicos impidiendo la elongación del ADN viral y la replicación viral. Se encuentran comercializados actualmente los siguientes fármacos: ***Abacavir (ABC)***, ***Didanosina (ddI)***, ***Tenofovir (TDF)***, ***AZT***, ***Estavudina (d4T)***, ***Lamivudina (3TC)*** y ***Emtricitabina (FTC)*** (FIGURA 6) (Günthard et al., 2014, Panel de expertos de GeSIDA, 2015, Ribera et al., 2011, Lewis et al., 2003).

Se subdividen en función de su estructura química: ABC, ddI y TDF son análogos de bases púricas y ZDV, d4T, 3TC y FTC son análogos de bases pirimidínicas (FIGURA 5). Todos ellos requieren tres fosforilaciones intracelulares para ser activos (son fármacos análogos de nucleósido), excepto TDF (es análogo del nucleótido adenina) que sólo requiere de dos fosforilaciones para convertirse en su metabolito activo (Piliero, 2004).

Los fármacos más utilizados de este grupo son las combinaciones TDF/FTC o ABC/3TC, formando la combinación de 2 ITIAN que se administran en la mayoría de las pautas posológicas (Günthard et al., 2014, Panel de expertos de GeSIDA, 2015). Las combinaciones ZDV/3TC y ddI/3TC también se recomiendan como pauta alternativa teniendo en cuenta los efectos adversos que tienen estos fármacos. Actualmente Zalcitabina (ddC) no se encuentra comercializado, debido a que fue retirado del mercado en 2006 debido a su toxicidad (principalmente neuropatía

periférica) y su complicada posología (ajuste de la dosis en función de la existencia de insuficiencia renal o hepática) (Ribera et al., 2011).

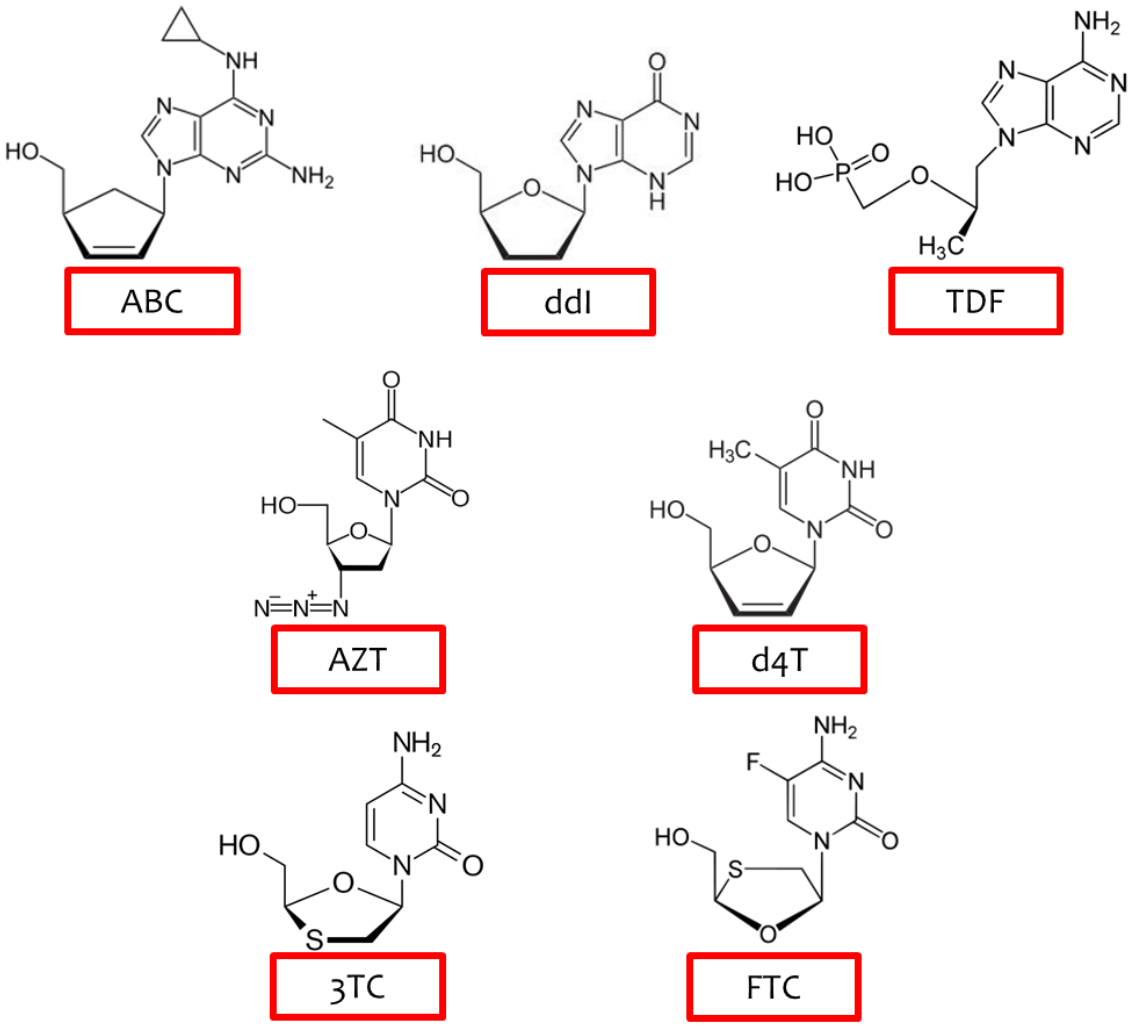

FIGURA 6. Fármacos ITIAN. La figura muestra las estructuras químicas de los distintos fármacos ITIAN aprobados actualmente para el tratamiento del VIH. Abacavir (ABC), Didanosina (ddI), Tenofovir (TDF), Zidovudina (AZT), Estavudina (d4T), Lamivudina (3TC) y Emtricitabina (FTC).

INHIBIDORES DE LA TRANSCRIPTASA INVERSA NO ANÁLOGOS DE NUCLEÓSIDO (ITINAN)

Dentro de este grupo se encuentran actualmente comercializados ***Efavirenz (EFV)***, ***Nevirapina (NVP)***, ***Etravirina (ETR)***, **Rilpivirina (RPV)** y ***Delavirdina (DLV)*** (FIGURA 7) (Günthard et al., 2014, Panel de expertos de GeSIDA, 2015, Ribera et al., 2011).

Estos fármacos también inhiben la transcriptasa inversa del virus, pero de manera diferente que los ITIAN. Lo hacen de forma no competitiva uniéndose a la enzima cerca de la zona de unión con su sustrato natural.

Se trata de un grupo de fármacos muy heterogéneo con estructuras químicas muy diferentes (FIGURA 6). No necesitan ser fosforilados para ser activos intracelularmente sino que bloquean la transcriptasa inversa directamente. Se unen al centro catalítico de la enzima o al bolsillo hidrofóbico de ésta; así, cambian conformacionalmente la enzima, inhibiendo su actividad ADN polimerasa y la replicación viral (Sluis-Cremer et al., 2004).

El fármaco más usado dentro de este grupo es EFV, aunque en la actualidad se está aumentando el empleo de RPV. Ambos forman parte de las dos terapias preferentes donde el tercer fármaco a administrar es un ITINAN. RPV se considera el fármaco más seguro de este grupo, únicamente cabe destacar que se tiene que administrar con comida para garantizar su correcta absorción. NVP sólo se usa en situaciones muy concretas, ya que es un fármaco inductor de la citocromo P450, por lo que puede reducir los niveles de los fármacos coadministrados (Günthard et al., 2014, Panel de expertos de GeSIDA, 2015). DLV no está comercializado en Europa debido a la falta de datos sobre su eficacia y su prescripción es muy rara debido a su posología, ya que se tiene tomar tres veces al día (Günthard et al., 2014, Panel de expertos de GeSIDA, 2015).

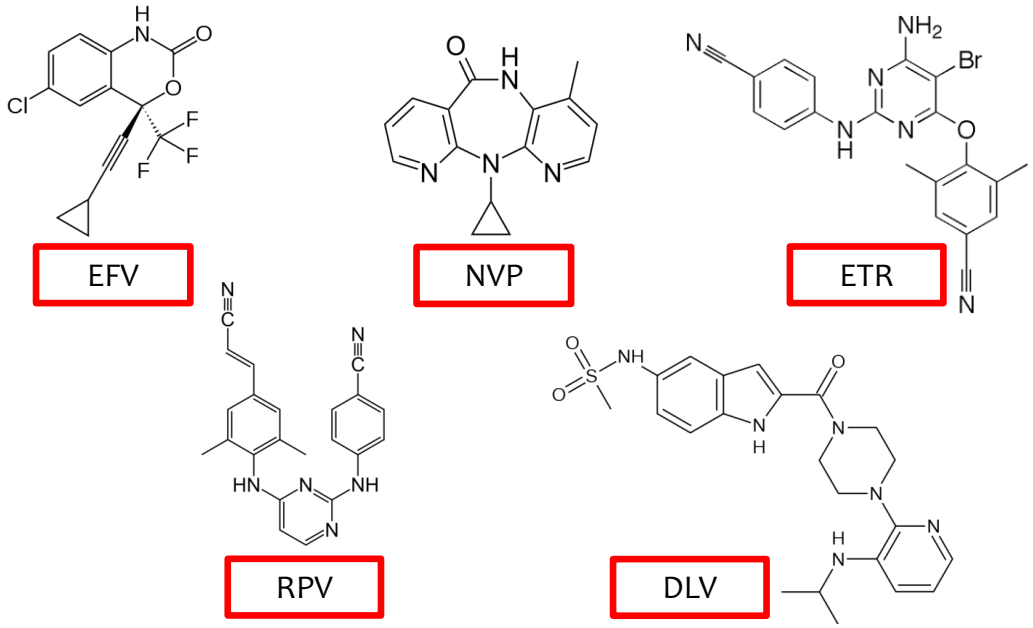

FIGURA 7. Fármacos ITINAN. La figura muestra las estructuras químicas de los distintos fármacos ITINAN aprobados actualmente para el tratamiento del VIH. Efavirenz (EFV), Nevirapina (NVP), Etravirina (ETR), Rilpivirina (RPV) y Delavirdina (DLV).

INHIBIDORES DE LA INTEGRASA (InInt)

Este grupo de fármacos antirretrovirales actúan inhibiendo la integración del ADN viral formado en el ADN de la célula hospedadora. Existen en la actualidad 3 fármacos pertenecientes a este grupo: ***Raltegravir (RAL)***, ***Elvitegravir (EVG)*** y ***Dolutegravir (DTG)*** (FIGURA 8) (Günthard et al., 2014, Panel de expertos de GeSIDA, 2015, Ribera et al., 2011, Hicks et al., 2009).

RAL es el compuesto de este grupo más utilizado actualmente en la Terapia Antirretroviral. Se recomienda el uso de EVG junto con Cobicistat (COBI), un potenciador farmacológico perteneciente al grupo de los IP para mejorar sus características farmacocinéticas, ya que actúa como inhibidor de la citocromo P450, que metaboliza otros antirretrovirales, con lo que aumenta la concentración del medicamento coadministrado en la sangre y su eficacia en el organismo. Ambos forman parte de las dos terapias preferentes donde el tercer fármaco a administrar es un InInt. Recientemente, se está recomendando también el uso de DTG, fármaco que no necesita ser administrado con un potenciador (Günthard et al., 2014, Panel de expertos de GeSIDA, 2015). Debido a que son fármacos de reciente comercialización no existen muchos datos a cerca de su toxicidad a largo plazo.

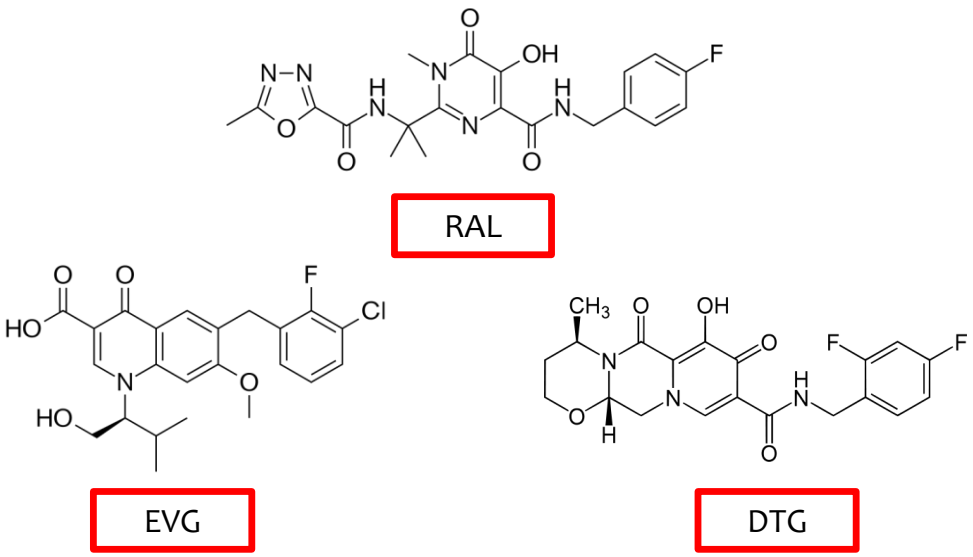

FIGURA 8. Fármacos InInt. La figura muestra la estructura química de los fármacos InInt aprobados actualmente para el tratamiento del VIH. Raltegravir (RAL), Elvitegravir (EVG) y Dolutegravir (DTG).

INHIBIDORES DE LA PROTEASA (IP)

Este grupo de fármacos actúa inhibiendo las peptidasas del VIH, impidiendo la maduración y el ensamblaje de las proteínas virales, no formándose así los nuevos viriones. Existe un gran número de fármacos pertenecientes a este grupo: ***Lopinavir (LPV)***, ***Ritonavir (RTV)***, ***Atazanavir (ATV)***, ***Indinavir (IDV)***, ***Darunavir (DRV)***, ***Saquinavir (SQV)***, ***Nelfinavir (NFV)***, ***Amprenavir (APV)***, ***Fosamprenavir (fAPV)***, ***Tipranavir (TPV)***, y ***COBI*** (FIGURA 9) (Günthard et al., 2014, Panel de expertos de GeSIDA, 2015, Ribera et al., 2011, Wensing et al., 2010).

Se trata de un grupo de fármacos bastante heterogéneo y directamente activos que no necesitan modificarse para actuar intracelularmente (Ribera et al., 2011). Tienen una estructura similar a los péptidos virales y poseen una gran afinidad por el centro activo de la proteasa. Así, cuando se unen a ésta, inhiben la enzima no permitiendo que ésta forme nuevas proteínas virales funcionales.

Fármacos como LPV, ATV, DRV, SQV, fAPV y TPV se administran en combinación con potenciadores farmacológicos como RTV y COBI. Estas dos sustancias se utilizan como potenciadores farmacocinéticos ya que inhiben el sistema citocromo P450 (metabolizador de fármacos). Además, debido a que no tienen efecto antiviral, no causan ningún tipo de resistencia. COBI se utiliza principalmente para potenciar ATV y DRV. Los fármacos más utilizados de este grupo son LPV, ATV y DRV, siendo ATV y DRV los fármacos a administrar en la Terapia Antirretroviral cuando el tercero es un IP. APV fue reemplazado por fAMP en 2004 y fue retirado del mercado. NFV ya no se comercializa en Europa debido a sus efectos adversos y contraindicaciones (Günthard et al., 2014, Panel de expertos de GeSIDA, 2015).

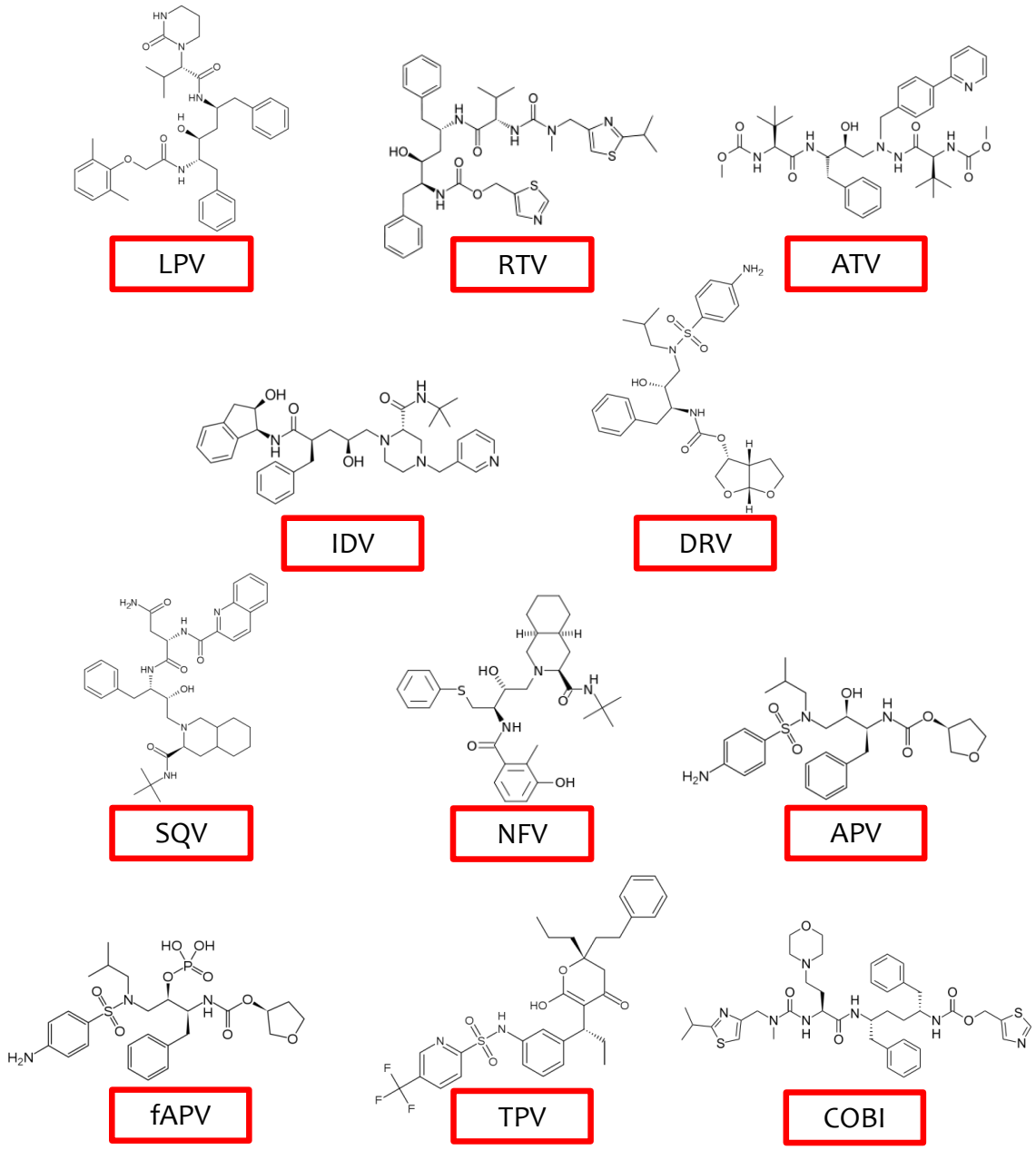

FIGURA 9. Fármacos IP. La figura muestra las estructuras químicas de los distintos fármacos IP aprobados actualmente para el tratamiento del VIH. Lopinavir (LPV), Ritonavir (RTV), Atazanavir (ATV), Indinavir (IDV), Darunavir (DRV), Saquinavir (SQV), Nelfinavir (NFV), Amprenavir (APV), Fosamprenavir (fAPV), Tipranavir (TPV) y Cobicistat (COBI).

1.2.4. TERAPEÚTICA ACTUAL

Los tratamientos con uno o dos fármacos están contraindicados, debido a su escasa eficacia inhibiendo la replicación viral y a la aparición de resistencias. Así, se recomienda la administración de al menos 3 fármacos, que es la que ha demostrado mayor eficacia y se denomina "Terapia Antirretroviral Combinada". La terapia estándar consiste generalemente en la administración de 2 ITIAN en combinación bien con un ITINAN, un IP, un InInt o un antagonista CCR5 (Günthard et al., 2014, Panel de expertos de GeSIDA, 2015).

Las combinaciones de fármacos antirretrovirales más usadas en la actualidad se indican en la TABLA 1. También existen otras combinaciones, pero menos usadas, en las que se co-administra un IP con un InInt (DRV/RTV + RAL o LPV/RTV + RAL) o un IP con un ITIAN (LPV/RTV + 3TC). Estas últimas sólo se utilizan en circunstancias especiales, cuando existen contraindicaciones en el uso de los fármacos incluidos en la terapia estádar o alternativa (Günthard et al., 2014, Panel de expertos de GeSIDA, 2015).

TABLA 1: Combinaciones de fármacos antirretrovirales recomendados en la actualidad.

PAUTA / COMBINACIONES	PREFERENTE	ALTERNATIVA
2 ITIAN + 1 ITINAN	TDF/FTC + EFV ABC/3TC + EFV TDF/FTC + RPV	ABC/3TC + RPV TDF/FTC + NVP ABC/3TC + NVP
2 ITIAN + 1 IP	TDF/FTC + ATV/RTV ABC/3TC + ATV/RTV TDF/FTC + DRV/RTV	ABC/3TC + DRV/RTV TDF/FTC + LPVRTV ABC/3TC + LPV/RTV TDF/FTC + ATV/COBI ABC/3TC + ATV/COBI TDF/FTC + DRV/COBI ABC/3TC + DRV/COBI
2 ITIAN + 1 InInt	TDF/FTC + RAL TDF/FTC + EVG/COBI TDF/FTC + DTG ABC/3TC + DTG	ABC/3TC + RAL
2 ITIAN + 1 a CCR5	TDF/FTC + MVC ABC/3TC + MVC	

Combinaciones de fármacos antirretrovirales empleados en la actualidad en pacientes que inician el tratamiento contra el VIH. Estas recomendaciones son una adaptación de dos guías terapeúticas: **Antiretroviral Treatment of Adult HIV Infection 2014 Recommendations of the International Antiviral Society–USA Panel** (Günthard et al., 2014) y **Documento de consenso de GeSIDA/Plan Nacional sobre el Sida respecto al tratamiento antirretroviral en adultos infectados por el virus de la inmunodeficiencia humana (Actualización enero 2015)** (Panel de expertos de GeSIDA, 2015). Tenofovir (TDF), Emtricitabina (FTC), Efavirenz (EFV), Abacavir (ABC), Lamivudina (3TC), Rilpivirina (RPV), Nevirapina (NVP), Atazanavir/Ritonavir (ATV/RTV), Darunavir/Ritonavir (DRV/RTV), Lopinavir/Ritonavir (LPV/RTV), Raltegravir (RAL), Elvitegravir/Cobicistat (EVG/COBI), Dolutegravir (DTG) y Maraviroc (MVC).

Aun así, el principal inconveniente de la "Terapia Antirretroviral Combinada" es que no permite erradicar el genoma viral de los tejidos reservorio tratándose, por consiguiente, de un tratamiento de por vida.

El desarrollo de esta terapia se produjo muy rápidamente, debido a la gravedad de la enfermedad. Debido a este factor, en combinación con otros (como el hecho de tratarse de una terapia crónica, la reducción de la tasa de mortalidad de pacientes tratados con esta terapia o el transcurso del tiempo en la utilización de estos fármacos), se ha observado la aparición de efectos adversos asociados a esta terapia. La Terapia Antirretroviral se sigue desarrollando actualmente, no siendo un tratamiento estanco; intentando sintetizar nuevos fármacos más eficaces y seguros. Exiten gran cantidad de fármacos antirretrovirales en fases avanzadas de ensayos clínicos que podrán ser comercializados en poco tiempo.

Como consecuencia, los objetivos actuales de la Farmacología de la "Terapia Antirretroviral Combinada" actual se encaminan hacia dos vertientes: por un lado, ***buscar las combinaciones de fármacos más eficaces contra la infección de VIH*** para así mejorar la vida de los pacientes con el virus y que han desarrollado SIDA; y por otro, ***determinar los efectos adversos así como los mecanismos toxicológicos de esta terapia*** para minimizar las comorbilidades asociadas a la administración de la terapia, buscando las combinaciones farmacológicas más inocuas para los pacientes.

1.2.5. EFECTOS ADVERSOS GENERALES DE LA TERAPIA ANTIRRRETROVIRAL

Se han descrito gran cantidad de efectos adversos asociados a la "Terapia Antirretroviral Combinada". En función de la cronología por la que aparecen estos efectos adversos se pueden clasificar en efectos adversos inmediatos o a corto plazo y efectos adversos tardíos o a largo plazo. Los primeros se producen en los primeros días o semanas de tratamiento, mientras que los últimos aparecen al cabo de meses o incluso años después del inicio de éste.

De forma general y a corto plazo, los pacientes bajo tratamiento antirretroviral manifiestan alteraciones cutáneas y ungueales, hipersensibilidad, transtornos gastrointestinales y efectos adversos neuropsiquiátricos (Santos Corraliza et al., 2006, Reust, 2011). Todos estos efectos adversos se manifiestan de forma transitoria asociados a la administración de la Terapia Antirretroviral.

A largo plazo, estos pacientes pueden presentar alteraciones metabólicas, anomalías en la distribución de la grasa corporal y lipodistrofia, daño mitocondrial, nefrotoxicidad e insuficiencia renal, osteopenia, osteoporosis y necrosis ósea aséptica (Santos Corraliza et al., 2006, Reust, 2011). Esta toxicidad se podría deber no sólo a procesos fisiológicos relacionados con la administración de esta terapia sino estar también asociada al envejecimiento de los pacientes, debido al aumento en el tiempo de vida de estos pacientes.

Si bien muchos de estos efectos adversos se dan de manera general con el uso de la "Terapia Antirretroviral Combinada", muchos de ellos son específicos para cada grupo de fármacos, incluso característicos de cada fármaco antirretroviral individual.

EFECTOS ADVERSOS ASOCIADOS AL USO DE ANTAGONISTAS CCR5

Con el uso de MVC no se han descrito efectos adversos graves, por lo que se considera un fármaco muy seguro (Panel de expertos de GeSIDA, 2015, Gulick et al., 2014).

EFECTOS ADVERSOS ASOCIADOS AL USO DE IF

Entre los efectos adversos que manifiestan más frecuentemente los pacientes bajo tratamiento antirretroviral con T-20 cabe destacar fatiga, insomnio, naúseas o diarrea, siendo las reacciones adversas en el lugar de inyección del fármaco (picor, inflamación, enrojecimiento, dolor o sensibilidad, endurecimiento y protuberancias en la piel) el efecto adverso más común (Panel de expertos de GeSIDA, 2015, Mirza et al., 2012). Además, se recomienda más de una inyección al día para mantener los niveles de CV indetectables. Debido a esto, su uso está relegado a pacientes que han fracasado con más de un tratamiento antirretroviral previo.

EFECTOS ADVERSOS ASOCIADOS AL USO DE ITIAN

Entre los efectos adversos que pueden desarrollar los pacientes bajo tratamiento con estos fármacos cabe destacar la toxicidad mitocondrial. También son muy importantes otros efectos adversos como la hiperlactatemia y acidosis láctica, pancreatitis, miopatía, neuropatía periférica, mielotoxicidad, hepatotoxicidad, dislipemia y lipodistrofia (Santos Corraliza et al., 2006, Panel de expertos de GeSIDA, 2015, Hawkins, 2010, Akanbi et al., 2012, Petit et al., 2005).

Los ITIAN con menos efectos secundarios son 3TC y FTC, y constituyen, por este motivo, la base de cualquier tratamiento nuevo en la mayoría de los casos en la actualidad.

En la TABLA 2 se detallan las toxicidades particulares descritas para los fármacos ITIAN.

TABLA 2: Toxicidad de los fármacos ITIAN.

Efectos adversos	ABC	ddI	TDF	ZDV	d4T	3TC	FTC
Acidosis láctica	x	x	x	x	x	x	x
Anemia				x			
Dislipemia	x	x		x	x	x	
Hepatotoxicidad		x		x	x		
Hiperlactatemia	x	x	x	x	x	x	x
Hipersensibilidad	x						
Hiperuricemia		x					
Leucopenia				x			
Lipodistrofia	x	x	x	x	x	x	x
Macrocitosis				x	x		
Mielotoxicidad				x			
Miopatía				x			
Naúseas				x			
Nefrotoxicidad			x				
Neuropatía perifférica		x			x		
Pancreatitis		x			x	x	
Pérdida de masa ósea			x				
Riesgo cardiovacular	x	x					
Trombocitopenia				x			

Efectos adversos individuales para cada uno de los fármacos pertenecientes al grupo de los ITIAN (Santos Corraliza et al., 2006, Panel de expertos de GeSIDA, 2015, Hawkins, 2010, Akanbi et al., 2012, Petit et al., 2005). Abacavir (ABC), Didanosina (ddI), Tenofovir (TDF), Zidovudina (ZDV), Estavudina (d4T), Lamivudina (3TC) y Emtricitabina (FTC).

EFECTOS ADVERSOS ASOCIADOS AL USO DE ITINAN

Entre los efectos adversos que manifiestan más frecuentemente los pacientes bajo tratamiento antirretroviral con este grupo de fármacos cabe destacar el exantema cutáneo por hipersensibilidad y las alteraciones del perfil hepático, apareciendo también otros de menos incidencia o importancia como es el caso de dislipemia, toxicidad en el Sistema Nervioso Central, teratogenicidad o alergia (Santos Corraliza et al., 2006, Panel de expertos de GeSIDA, 2015, Hawkins, 2010, Akanbi et al., 2012, Petit et al., 2005, Blas-García et al., 2010).

En la TABLA 3 se detallan las toxicidades particulares descritas para los fármacos ITINAN.

TABLA 3: Toxicidad de los fármacos ITINAN.

Efectos adversos	EFV	NVP	ETR	RPV	DLV
Alergia			x		
Dislipidemia	x	x			
Hepatotoxicidad	x	x			
Hipersensibilidad	x	x	x	x	x
Resistencia insulina	x				
Teratogenicidad	x				
Toxicidad en el SNC	x				

Efectos adversos individuales para cada uno de los fármacos pertenecientes al grupo de los ITINAN (Santos Corraliza et al., 2006, Panel de expertos de GeSIDA, 2015, Hawkins, 2010, Akanbi et al., 2012, Petit et al., 2005, Blas-García et al., 2010). Efavirenz (EFV), Nevirapina (NVP), Etravirina (ETR), RIlpivirina (RPV) y Delavirdina (DLV).

EFECTOS ADVERSOS ASOCIADOS AL USO DE InInt

Entre los efectos adversos que pueden desarrollar más frecuentemente los pacientes bajo tratamiento antirretroviral con los InInt destacan diarrea, reacciones cutáneas y rabdomiolisis (Panel de expertos de GeSIDA, 2015, Liedkte et al., 2014, Elion et al., 2013, Castagna et al., 2014). Es muy frecuente que en estos pacientes también aparezca dolor de cabeza y naúseas. En la TABLA 4 se detallan las toxicidades particulares descritas para los fármacos InInt.

TABLA 4: Toxicidad de los fármacos InInt.

Efectos adversos	RAL	EVG	DTG
Diarrea	x	x	x
Hipersensibilidad	x		x
Rabdomiolisis	x		

Efectos adversos individuales para cada uno de los fármacos pertenecientes al grupo de los InInt (Panel de expertos de GeSIDA, 2015, Liedkte et al., 2014, Elion et al., 2013, Castagna et al., 2014). Raltegravir (RAL), Elvitegravir (EVG) y Dolutegravir (DTG).

EFECTOS ADVERSOS ASOCIADOS AL USO DE IP

Los pacientes bajo tratamiento antirretroviral con este grupo de fármacos pueden desarrollar principalmente alteraciones en el metabolismo lipídico tales como dislipemia y lipodistrofia y del metabolismo hidrocarbonado como resistencia a la insulina o hiperglucemia. Cabe también destacar la aparición de diarrea, icteria, hepatotoxicidad, nefrotoxicidad e hiperbilirrubinemia (Santos Corraliza et al., 2006, Hawkins, 2010, Friis-Moller et al., 2007, Hull et al., 2011, Mulligan et al., 2000, Flint et al., 2009, Naggie et al., 2010, Gallant et al., 2013). También es común la aparición de naúseas, dolor de cabeza, arritmias y disfunción sexual.

En la TABLA 5 se detallan las toxicidades particulares descritas para los fármacos IP.

TABLA 5: Toxicidad de los fármacos IP.

Efectos adversos	LPV	RTV	ATV	IDV	DRV	SQV	NFV	APV	fAPV	TPV	COBI
Diarrea	x	x			x		x				x
Dislipemia	x	x	x	x	x	x	x	x	x	x	
Hepatotoxicidad		x									
Hiperbilirrubinemia			x	x							x
Hipersensibilidad					x			x			x
Icteria											x
Lipodistrofia	x	x		x		x	x	x	x	x	
Nefrotoxicidad			x	x							x
Resistencia insulina	x	x		x		x	x	x	x	x	

Efectos adversos individuales para cada uno de los fármacos pertenecientes al grupo de los IP (Santos Corraliza et al., 2006, Hawkins, 2010, Friis-Moller et al., 2007, Hull et al., 2011, Mulligan et al., 2000, Flint et al., 2009, Naggie et al., 2010, Gallant et al., 2013). Lopinavir (LPV), Ritonavir (RTV), Atazanavir (ATV), Indinavir (IDV), Darunavir (DRV), Saquinavir (SQV), Nelfinavir (NFV), Amprenavir (APV), Fosamprenavir (fAPV), Tipranavir (TPV) y Cobicistat (COBI).

1.2.6. ASOCIACIÓN DE LA TERAPIA ANTIRRETROVIRAL Y EL DESARROLLO DE ENFERMEDADES CARDIOVASCULARES CON COMPONENTE INFLAMATORIO

En los últimos años se está observando un aumento en la tasa de mortalidad de pacientes infectados por el VIH bajo tratamiento farmacológico debido a efectos adversos cardiovasculares. Concretamente, más de un 10 % de las muertes que se producen en los enfermos de SIDA se deben a este tipo de enfermedades (Sabin et al., 2008, Bonnet et al., 2002). Lo que se desconoce es si esta mayor incidencia de enfermedades cardiovasculares se debe a la infección en sí misma, al incremento en el tiempo de vida de los pacientes, al tratamiento con la Terapia Antirretroviral o a una combinación de todos estos factores.

Está ampliamente descrito que la infección por el VIH por sí misma está asociada con enfermedades cardiovasculares (Triant, 2012). Existen estudios clínicos que demuestran que pacientes infectados por el VIH poseen un mayor riesgo de padecer enfermedad prematura de arterias coronarias, aumento de la frecuencia de hipertensión pulmonar y accidentes cerebrovasculares isquémicos (Acevedo et al., 2002, Pellicelli et al., 2001, Chow et al., 2012), parámetros que se relacionan directamente con un mayor riesgo de sufrir eventos adversos cardiovasculares.

También está descrito que la infección por el VIH produce una respuesta inflamatoria a nivel del endotelio. Este virus puede atravesar el endotelio de arterias coronarias y cerebrales e iniciar una respuesta inflamatoria, provocando miocardiopatías y alteraciones de la barrera hematoencefálica (Gujuluva et al., 2001). También se han detectado alteraciones en la integridad del endotelio aórtico y una acumulación de leucocitos humanos en dicho endotelio en pacientes infectados por el VIH (Zietz et al., 1996), así como un incremento en los niveles de citocinas proinflamatorias y de moléculas de adhesión solubles en estos pacientes

(Puppo et al., 1993, Most et al., 1993, Sipsas et al., 1994, Galea et al., 1997, Seigneur et al., 1997, de Larranaga et al., 2003).

La relación entre Terapia Antirretroviral y enfermedades cardiovasculares se puso de manifiesto con estudios clínicos que correlacionaron la incidencia de sufrir enfermedades cardiovasculares con el periodo de exposición a esta terapia. La incidencia de sufrir infarto de miocardio en pacientes tratados con la Terapia Antirretroviral aumentó con el tiempo de tratamiento (Friis-Moller et al., 2003, Currier et al., 2003).

Además, como esta terapia se administra en combinación (probablemente las toxicidades individuales de cada fármaco se puedan ver potenciadas debido al uso simultáneo de varios fármacos), es difícil también dilucidar cuál es el grado de participación de cada grupo de fármacos en el desarrollo de estas enfermedades cardiovasculares.

Inicialmente, se había apuntado a los IP como los responsables de estos efectos adversos cardiovasculares ya que está ampliamente descrito que producen lipodistrofia e hiperlipidemia (Carr et al., 1999, Fontas et al., 2004) y su uso aumenta el riesgo de sufrir infarto de miocardio (Sabin et al., 2008). Sin embargo, no se puede descartar la participación del resto de los grupos de antirretrovirales: ni a los ITIAN (que siempre forman parte de la Terapia Antirretroviral actual), ni a los ITINAN, IP, InInt o antagonistas CCR5 que se administran en combinación con el primer grupo citado.

En los últimos años, se ha observado la correlación entre el uso de ITIAN (y más concretamente de ABC) y el desarrollo de enfermedades vasculares. En el año 2005 saltó la primera alarma, (Sanz, 2005) y desde entonces ha habido mucha controversia sobre el tema (Bavinger et al., 2013). Existen estudios clínicos que corroboran este hecho (Sabin et al., 2008, AIDS 2008 September 12, Obel et al.,

2010, Lang et al., 2010, Durand et al., 2011, Günthard et al., 2014) mientras que otros no (Cutrell et al., 2008, Brothers et al., 2009, RIbaudo et al., 2011, Bedimo et al., 2011, Cruciani et al., 2011). Por lo tanto, el impacto que el grupo de los ITIAN tiene sobre el desarrollo de enfermedades cardiovasculares no está claro.

Hay pocos estudios que relacionen a los antagonistas CCR5 con el riesgo cardiovascular, quizá porque su uso es muy limitado. Existen evidencias que apuntan al receptor CCR5 y sus ligandos CCL3 ("Chemokine C-C Ligand -3", MIP-1α), CCl4 ("Chemokine C-C Ligand-4", MIP-1β) y CCL5 ("Chemokine C-C Ligand-5, RANTES) como los responsables de la iniciación y la progresión de la aterosclerosis (Jones et al., 2011). Este dato implica un potencial uso de los antagonistas CCR5, en concreto MVC, como fármaco protector a nivel cardiovascular. De hecho, existe un estudio previo en ratones que muestra que MVC reduce la progresión de la placa aterosclerótica inducida por RTV (Cipriani et al., 2013). Este estudio apuntaría no sólo a un buen perfil toxicológico a nivel cardiovascular de MVC, sino a un efecto protector frente a la iniciación y progresión de la placa aterosclerótica.

No existen estudios sobre la relación de los IF, en concreto T-20 y el riesgo de padecer enfermedades cardiovasculares debido a que su uso está relegado a situaciones muy concretas (Mirza et al., 2012).

Dentro de los fármacos ITINAN, EFV es el fármaco que más se utiliza en la actualidad si bien RPV se está utilizando cada vez más debido a su similar eficacia combatiendo el virus con respecto a EFV, y su bajo índice de aparición de efectos adversos. NVP, el tercero de los fármacos más usados de este grupo, se utiliza sólo en situaciones muy concretas. Existen pocas evidencias que apuntan a que EFV podría ser uno de los fármacos responsables de las enfermedades cardiovasculares asociadas a la Terapia Antirretroviral. Un ensayo clínico realizado en pacientes VIH positivos bajo tratamiento antirretroviral lo ha relacionado directamente con un mayor riesgo de sufrir infarto agudo de miocardio (Durand et al., 2011), aunque cabe

destacar que en la gran mayoría de ellos, no se relaciona su uso con el aumento en el riesgo de padecer enfermedades cardiovasculares (Worm et al., 2010), o se sugiere, sin afirmarlo rotundamente, que con el incremento en el tiempo de exposición a EFV incrementa el riesgo de padecer este tipo de enfermedades (Friis-Moller et al., 2007). EFV produce hiperlipidemia, aumento de los niveles de radicales libres y de la permeabilidad endotelial. EFV es capaz de producir una alteración en el metabolismo de los lípidos, aumentando la relación Colesterol Total/Colesterol HDL ("High-dendity Lipoprotein"), (Tashima et al., 2003, Manfredi et al., 2005, Van Leth et al., 2004, Worm et al., 2010) y esto podría llevar a un incremento en el riesgo de padecer enfermedades cardiovasculares. La exposición de pacientes a EFV está asociada con disfunción endotelial (Gupta et al., 2012) y con aumento de la lipoproteína de baja densidad (Maggi et al., 2011), de isoprostano F2 y de proteína C-reactiva de alta sensibilidad (Gupta et al., 2012), que son marcadores de parámetros metabólicos, de estrés oxidativo y de inflamación vascular, respectivamente, factores de riesgo de sufrir enfermedades cardiovasculares en los tres casos. A nivel arterial endotelial EFV es capaz de aumentar la permeabilidad endotelial, reduciendo los niveles de proteínas que median la unión entre las células endoteliales y aumentando la producción de anión superóxido (Jamaluddin et al., 2010, Mondal et al., 2004). Todos estos indicios podrían situar a este fármaco como uno de los posibles responsables de la elevada incidencia de enfermedades cardiovasculares en personas infectadas con el virus del VIH. Los estudios con RPV a nivel cardiovascular son muchos más escasos ya que es un fármaco de segunda generación relativamente nuevo. Aun así, existen estudios que apuntarían a RPV como un fármaco con un mejor perfil en cuanto a incidencia de efectos adversos y su mayor uso estaría relacionado con una mejoría en cuanto a parámetro lipídicos y cálculo de riesgo cardiovascular, en pacientes que recibían IP y se cambiaron a RPV, siempre con un mantenimiento de la eficacia virológica (Casado et al., 2013). También existen dos estudios clínicos que correlacionan EFV y RPV en términos de parámetros lipídicos y de él se puede concluir que RPV produce un menor aumento de parámetros lipídicos y menor dislipidemia, aunque ambos contribuyeron a

producir cambios en los niveles de lípidos y en la distribución de la grasa corporal (Tebas et al., 2014). Por tanto, se puede deducir, que al menos a nivel cardiovascular, RPV parece un fármaco más seguro y con una eficacia virológica similar. NVP parece tener un mejor perfil a nivel cardiovascular cuando lo comparamos con EFV: un estudio ha revelado que el tratamiento con EFV produce una mayor liberación de citocinas proinflamatorias que NVP y que en algunos casos, este último fármaco disminuyó su liberación (Podzamczer, 2013). Otro estudio ha demostrado que NVP, con respecto a EFV y otros IP - como LPV - no produce una relajación del endotelio, (marcador de disfunción endotelial que precedería a la aparición de efectos adversos cardiovasculares) (Yeung et al., 2013). Así, se podría decir que NVP posee un mejor perfil a nivel cardiovascular que EFV.

Dentro del grupo de los IP, los fármacos que más se utilizan en la actualidad son ATV y DRV debido a la menor incidencia de efectos adversos con su uso. LPV se usa en menor medida porque se ha relacionado con la aparición de efectos adversos. Con respecto a los IP y al riesgo de toxicidad cardiovascular, siempre se ha tenido especial precaución (Friis-Moller et al., 2010, Friis-Moller et al., 2003). Sin embargo, estos fármacos no se relacionan directamente con el desarrollo de enfermedades cardiovasculares, sino que, probablemente su efecto negativo a este nivel se deba a la dislipidemia que producen. Se ha relacionado a LPV con la aparición de efectos adversos cardiovasculares: un estudio describe que LPV está asociado con cambios menos favorables en los niveles de lípidos con respecto a otros antirretrovirales (Shaffer et al., 2014). Este fármaco es capaz de producir una relajación del endotelio (Yeung et al., 2013). Sin embargo, ATV y DRV han demostrado tener un perfil lipídico más favorable que el resto de los IP (Overton et al., 2012) y con respecto a LPV. Otro estudio ha demostrado que el cambio en la terapia de LPV a DRV reduce el riesgo de sufrir enfermedades cardiovasculares, ya que DRV redujo los niveles de Cistatina C plasmática - marcador de riesgo cardiovascular - (Ucciferri et al., 2013). De hecho, un estudio previo realizado en células endoteliales coronarias arteriales humanas ha demostrado que DRV, mejor que ATV, y a su vez mejor que LPV, no afecta a la

función endotelial celular, al estrés oxidativo, ni modifica marcadores de inflamación o senescencia (Auclair et al., 2014).

Finalmente, RAL es el compuesto más utilizado actualmente en la "Terapia Antirretroviral Combinada" dentro del grupo de los InInt, si bien el uso de EVG y DTG se está haciendo mayor en los últimos tiempos, fomando los 3 parte de las pautas preferentes. Quizá el hecho de que son fármacos de reciente aparición justifique que existan muy pocos datos sobre el grupo de los InInt, y concretamente sobre RAL, y el riesgo cardiovascular. Dos estudios clínicos han demostrado que este compuesto no tiene un impacto significativo sobre la función endotelial (Gupta et al., 2013, Hatano et al., 2012). Incluso uno de ellos propone efectos beneficiosos de este fármaco en la activación de los monocitos (Gupta et al., 2013).

1.2.7. RELACIÓN ENTRE TERAPIA ANTIRRETROVIRAL E INTERACCIÓN LEUCOCITO-ENDOTELIO

En nuestro laboratorio esudiamos el efecto de los fármacos ITIAN sobre la interacción leucocito-endotelio como índice del primer paso en el desarrollo de enfermedades cardiovasculares. Así, demostramos que los análogos de purina ABC y ddI inducen interacciones leucocito-endotelio, tanto *in vivo* en vénulas y arteriolas del mesenterio de rata (de Pablo et al., 2013) (FIGURA 10), como *in vitro* utilizando leucocitos PMN ("Polymorphonuclear Cell) y PBMC ("Peripheral Blood Mononuclear Cell") extraídos de sangre humana y células endoteliales HUVEC ("Human Umbilical Vein Endothelial Cell") (de Pablo et al., 2010) (FIGURA 11), mientras que el resto de los fármacos del grupo (análogos de pirimidina o de nucleótido) no producen dicho efecto *in vivo* e *in vitro* (FIGURA 10 y 11).

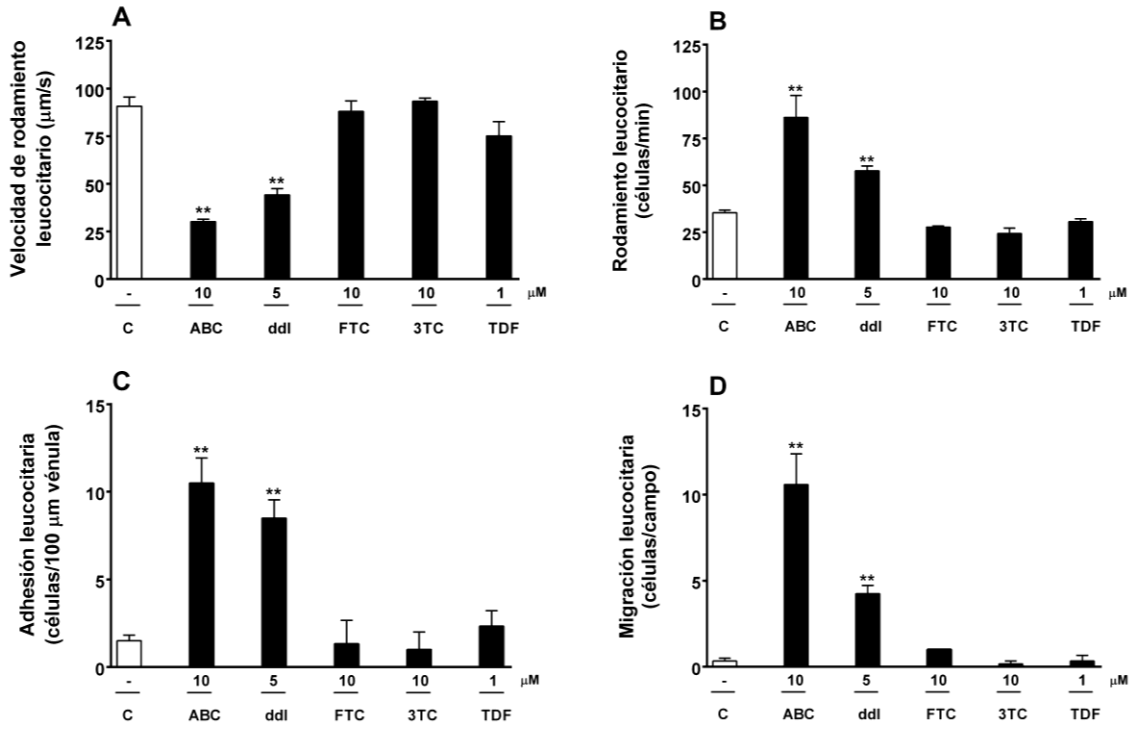

FIGURA 10. Interacción leucocito-endotelio inducida los fármacos ITIAN *in vivo*. La figura muestra la velocidad de rodamiento, el rodamiento, la adhesión y la migración leucocitaria en vénulas del mesenterio de rata. Adaptado de la publicación de Pablo et al., 2013 y de la Tesis Doctoral titulada "EFECTOS PROINFLAMATORIOS DE LOS FÁRMACOS ANTIRRETROVIRALES INHIBIDORES DE LA TRANSCRIPTASA INVERSA ANÁLOGOS DE NUCLEÓSIDO *IN VITRO* E *IN VIVO*" defendida por Carmen de Pablo Bernal en 2013. Abacavir (ABC), ddI (Didanosina), Emtricitabina (FTC), Lamivudina (3TC) y Tenofovir (TDF).

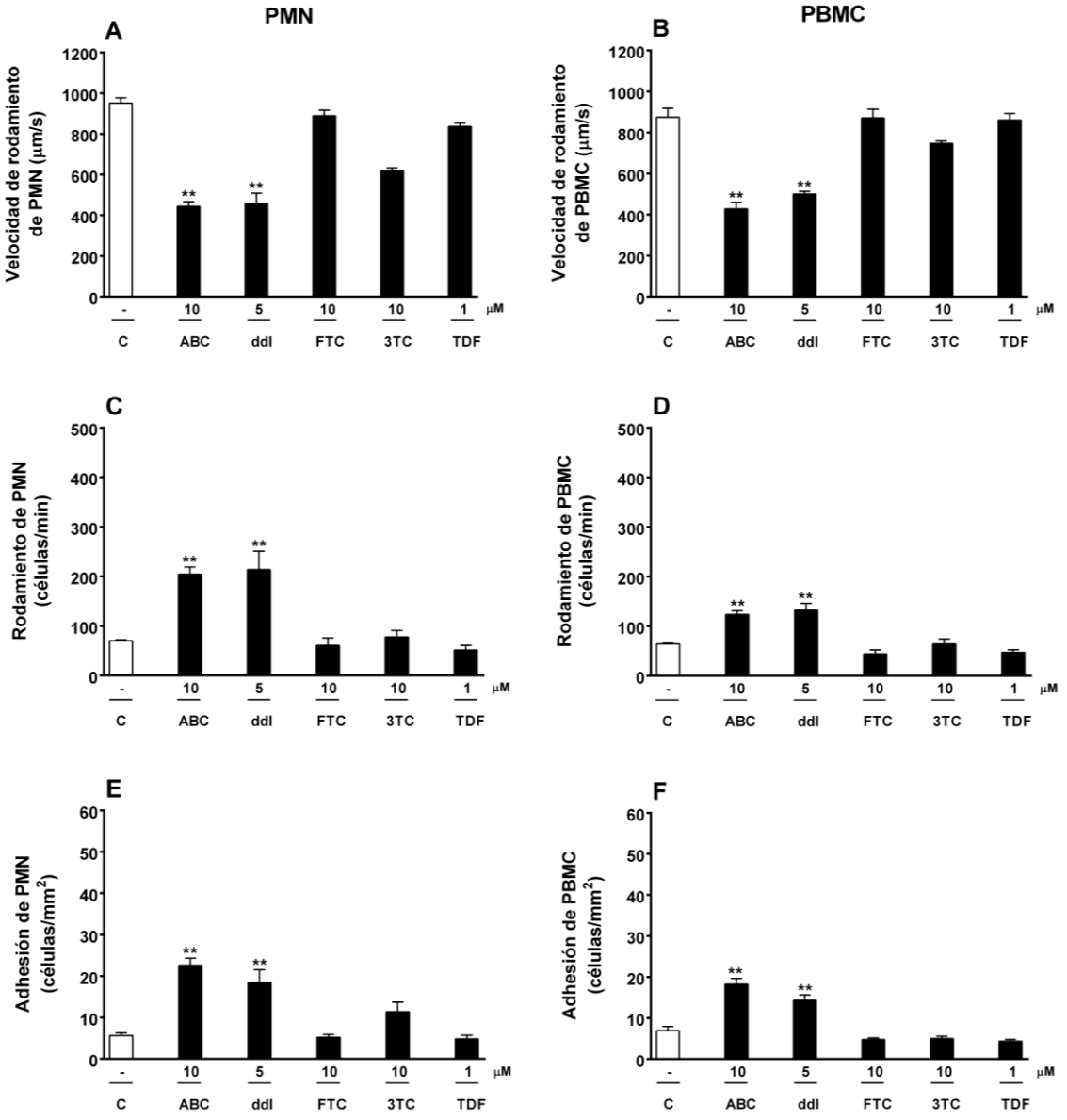

FIGURA 11. Interacción leucocito-endotelio inducida por los fármacos ITIAN *in vitro*. La figura muestra la velocidad de rodamiento, el rodamiento y la adhesión de PMN y PBMC sobre HUVEC, respectivamente. Adaptado de la publicación de Pablo et al., 2010 y de la Tesis Doctoral titulada "EFECTOS PROINFLAMATORIOS DE LOS FÁRMACOS ANTIRRETROVIRALES INHIBIDORES DE LA TRANSCRIPTASA INVERSA ANÁLOGOS DE NUCLEÓSIDO *IN VITRO* E *IN VIVO*" defendida por Carmen de Pablo Bernal en 2013. Abacavir (ABC), ddI (Didanosina), Emtricitabina (FTC), Lamivudina (3TC) y Tenofovir (TDF).

2. OBJETIVOS

El ***objetivo general*** de este trabajo fue caracterizar los efectos proinflamatorios de los diferentes fármacos más utilizados dentro de los distintos grupos de antirretrovirales. En particular, estudiar tanto *in vivo* como *in vitro* la acción de los fármacos ITINAN, antagonistas CCR5, InInt e IP sobre la acumulación leucocitaria como primer paso en el desarrollo de enfermedades cardiovasculares con componente inflamatorio. Para aquellos fármacos con actividad proinflamatoria (EFV, NVP y RPV), analizar el mecanismo responsable de este proceso fue también objetivo del presente estudio.

En particular, abordamos los siguientes ***objetivos específicos***:

1. Realizar un estudio sistemático del efecto de los distintos fármacos de los diferentes grupos de antirretrovirales (ITINAN, antagonistas CCR5, InInt e IP) sobre la interacción leucocito-endotelio *in vivo* (mesenterio de rata) e *in vitro* (células humanas).

2. Acercar nuestros resultados a la terapéutica actual, concretamente, evaluar los efectos de las combinaciones de fármacos más utilizados en la terapéutica sobre la interacción leucocito-endotelio *in vivo* (mesenterio de rata) e *in vitro* (células humanas).

3. Estudiar, para aquellos fármacos que promuevan la acumulación leucocitaria (EFV, NVP y RPV), el mecanismo de acción por el cual producen este proceso *in vivo* e *in vitro*: tipo celular y moléculas de adhesión implicadas.

3. MATERIAL Y MÉTODOS

MÉTODOS

3.1. ESTUDIOS IN VIVO

3.1.1. MICROSCOPÍA INTRAVITAL

Se utilizaron ratas Sprague Dawley macho (200-250 g), que se mantuvieron en condiciones de ayuno durante 8 horas (Álvarez et al., 2002, Álvarez et al., 2006) y se anestesiaron con pentobarbital sódico vía intraperitoneal (65 mg/kg, i.p.). Se realizó una traqueotomía (para facilitar la correcta ventilación pulmonar) así como la canulación de la vena yugular izquierda (para poder administrar más anestésico si fuera necesario) y de la arteria carótida derecha (para controlar los valores de presión arterial media - PAM - mediante un transductor de presión).

Posteriormente, se realizó una incisión abdominal longitudinal con un cauterio, se colocó el animal en posición supina y se exteriorizó una porción del yeyuno medio que fue extendida sobre un pedestal traslúcido que permite la transiluminación de una zona del mesenterio de 2 cm^2. El área seleccionada fue superfundida continuamente a una velocidad de flujo de 2 ml/min con una solución tampón bicarbonatada a pH 7.4 y a 37^{o}C de temperatura. Esta preparación se observó a través de un microscopio intravital ortostático (Nikon Optiphot-2, SMZ1) equipado con un objetivo 20x y un ocular 10x que proyecta las imágenes en color a un ordenador, grabándose éstas digitalmente para su posterior análisis (Álvarez et al., 2002, Álvarez et al., 2006) (FIGURA 12).

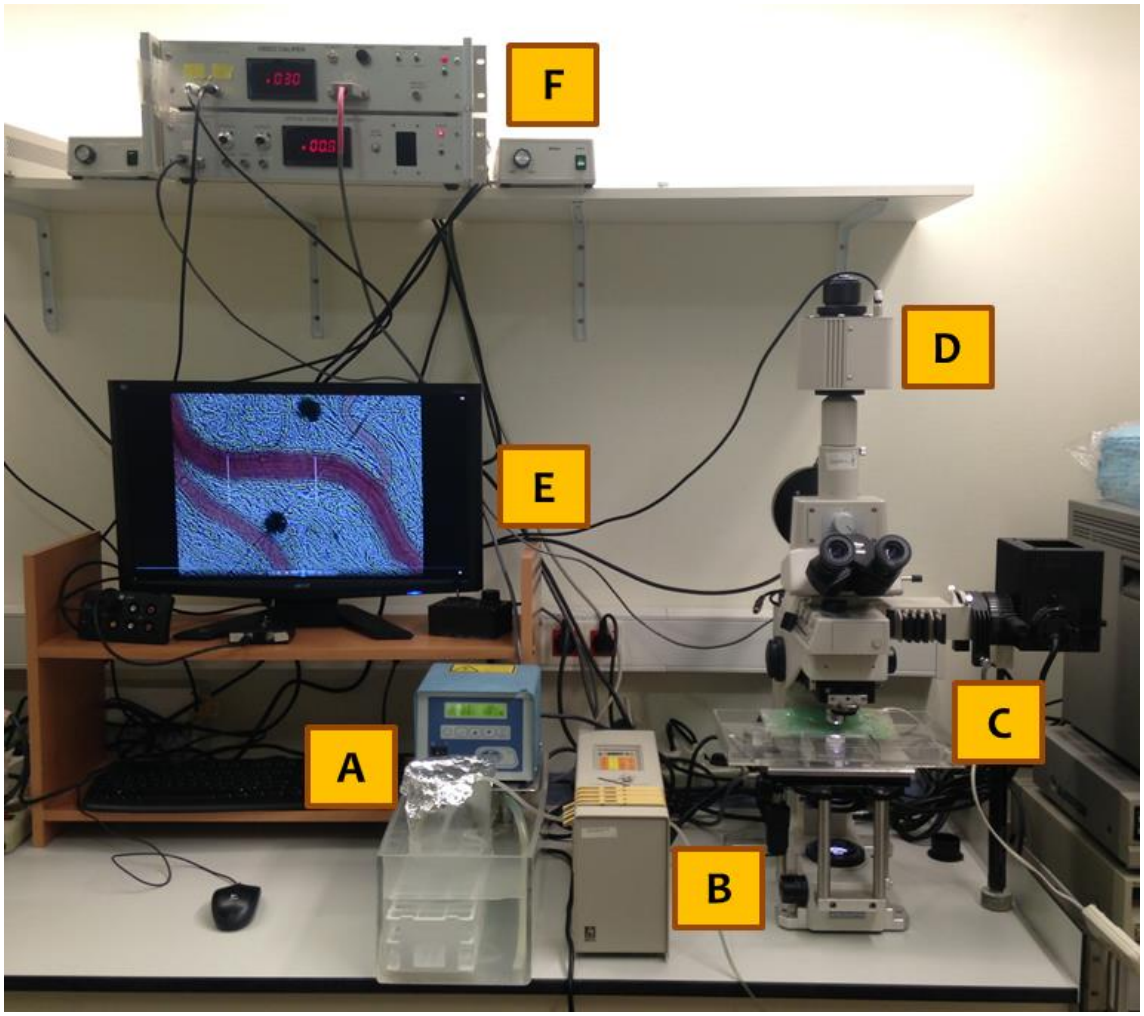

FIGURA 12. Sistema de microscopía intravital. Las imágenes muestran las diferentes partes que conforman dicho sistema. **A:** Baño termostático, **B:** Bomba de infusión, **C:** Pedestal traslúcido, **D:** Videocámara, **E:** Ordenador, **F:** "Video Caliper" y "Optical Doppler Velocimeter".

Para la realización de estos estudios, se seleccionaron vénulas mesentéricas de 25-40 µm de diámetro (FIGURA 13 y 14).

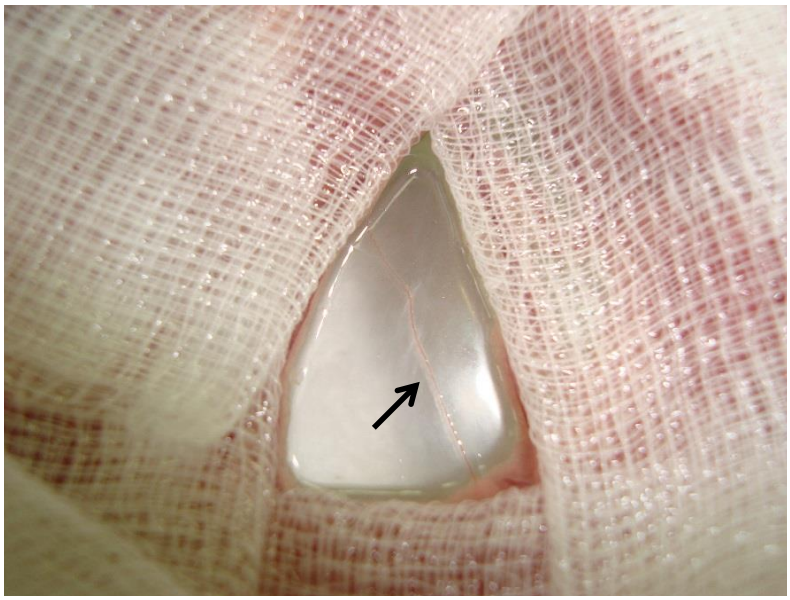

FIGURA 13. Zona del mesenterio seleccionada en la que se observan microvasos (↗).

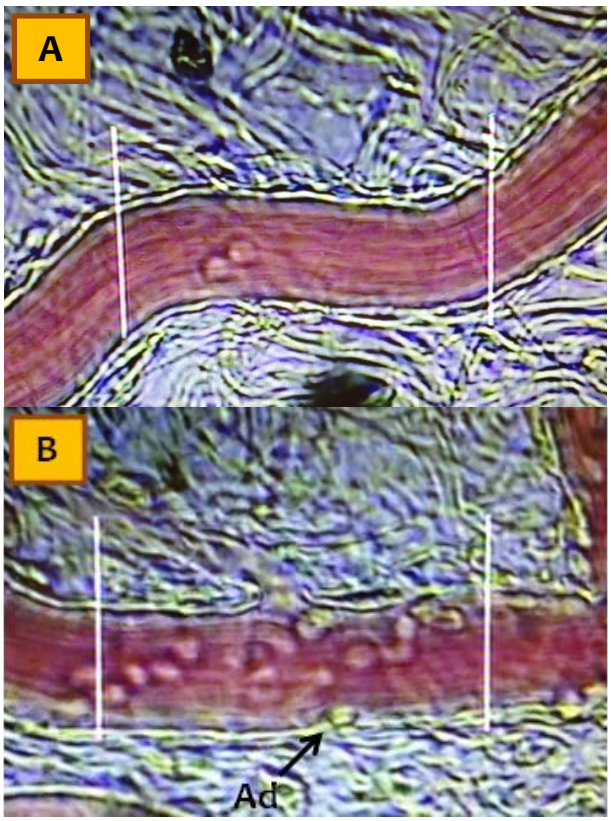

FIGURA 14. Imágenes representativas de vénulas mesentéricas. A: vénula de una rata control. **B:** vénula de una rata tratada con estímulo positivo proinflamatorio. En la imagen **B** podemos observar leucocitos adheridos (**Ad**) (↗).

Parámetros leucocitarios determinados

Se analizaron los siguientes parámetros leucocitarios (Orden et al., 2014): (FIGURA 15)

Rodamiento leucocitario: es el número de leucocitos que circulan a una velocidad inferior a la de los eritrocitos (ya que están interaccionando con el endotelio venular) y, por tanto, enlentecen su velocidad. Se determina contabilizando el número de leucocitos que pueden ser visualizados en un punto de referencia preestablecido de la vénula durante un periodo de 1 minuto. Se expresa en *células/min* (FIGURA 15).

Velocidad de rodamiento leucocitario: es el tiempo que tarda un leucocito en fase de rodamiento en recorrer 100 µm de vénula. Se determina promediando la velocidad de 10 leucocitos. Se expresa en µ*m/seg* (FIGURA 15).

Adhesión leucocitaria: es el número de leucocitos que permanecen estacionados o tienen contacto estable con el endotelio venular durante un periodo igual o superior a 30 segundos en 100 µm de vaso. Se expresa en *células adheridas/100* µ*m de vénula* (FIGURA 14 y 15).

Migración leucocitaria: es el número de leucocitos que se extravasan de la vénula al tejido circundante. Se determina contabilizando el número de leucocitos que pueden ser observados fuera de la vénula. Se expresa en *células/campo* (FIGURA 15).

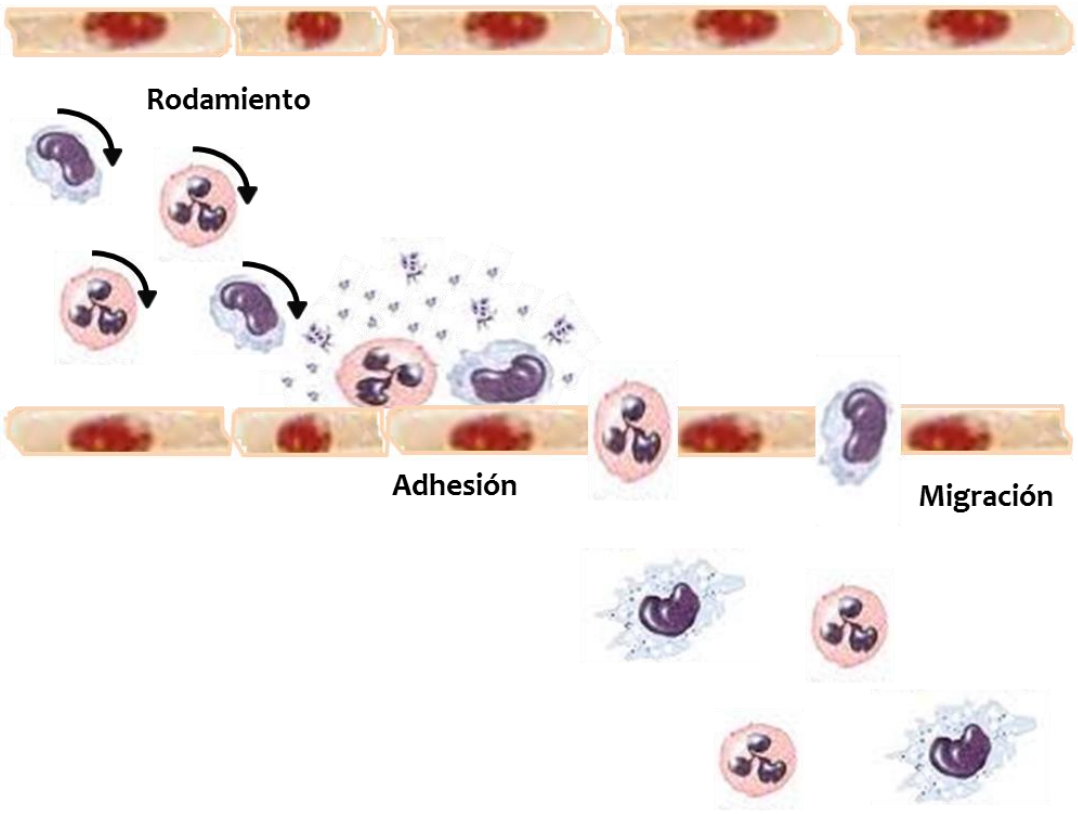

FIGURA 15. Parámetros leucocitarios determinados. La figura muestra los parámetros leucocitarios determinados tanto en la técnica de microscopía intravital, como en la técnica de adhesión dinámica en cámara paralela de flujo (Ver Adhesión Dinámica en Cámara Paralela de Flujo).

Parámetros hemodinámicos determinados

Se analizaron los siguientes parámetros hemodinámicos (House et al., 1987, Orden et al., 2014):

Diámetro venular (Dv): se mide con un "Video Caliper" (Microcirculation Research Institute). Se expresa en µ*m*.

"Shear rate" (γ): es la fuerza que ejerce la sangre sobre las paredes venulares. Se expresa en *segundos*$^{-1}$ y se calcula según la definicón newtoniana:

$$\gamma = 8\ (V_{mean}\ Dv^{-1})\ s^{-1}$$

Donde:

Dv: es el diámetro de la vénula.

$\mathbf{V_{mean}}$: es el flujo de los eritrocitos. Se calcula como el producto de la velocidad de los eritrocitos y el área seccional, asumiendo que el vaso es un cilindro geométrico ($V_{mean} = V_{rbc}\ 1.6^{-1}$). La velocidad de los eritrocitos en el torrente sanguíneo (V_{rbc}) se determina con la ayuda de un "Optical Doppler Velocimeter" (Microcirculation Research Institute).

PAM: es la presión que ejerce la sangre sobre la pared de las arterias. Se mide mediante un transductor de presión (Spectramed Stathan P-23XL) conectado a un polígrafo (GRASS RPS7C8B, Quincy). Se expresa en *mm Hg*.

Protocolo experimental

A los animales se les administraron, por vía intraperitoneal, concentraciones clínicas relevantes de fármacos representativos de los diferentes grupos de fármacos antirretrovirales: EFV (10-25 µM, equivalente a 40-100 µg/kg), NVP (10-50 µM, 35-165 µg/kg), RPV (0.25-1 µM, 1-5 µg/kg), MVC (5 µM, 35 µg/kg), RAL (5 µM, 30 µg/kg), LPV (25 µM, 200 µg/kg), ATV (25 µM, 250 µg/kg), DRV (25 µM, 190 µg/kg), sus correspondientes vehículos [metanol, agua ácida o DMSO ("Dimethil Sulfoxide")] o control (suero fisiológico). EFV, MVC y LPV se disolvieron en metanol, NVP en agua ácida y RPV, RAL, ATV y DRV en DMSO. Las dosis de los fármacos se seleccionaron de acuerdo con la literatura para mimetizar las concentraciones plasmáticas alcanzadas en pacientes (Waters et al., 2015, Burger et al., 2006, Cooper et al., 2007, Martinez-Rebollar et al., 2013, León et al., 2007, Boffito et al., 2011, Parks et al., 2007 Moyle et al., 2009, Usach et al., 2013, Blas-García et al., 2014, Jamaluddin et al., 2010) (FIGURA 16).

A otros animales se les administraron las siguientes combinaciones de fármacos antirretrovirales: TDF/FTC/EFV (1 µM/10 µM/15 µM), ABC/3TC/EFV (10 µM/10 µM/15 µM), TDF/FTC/RPV (1 µM/10 µM/0.5 µM), ABC/3TC/RPV (10 µM/10 µM/0.5 µM), TDF/FTC/ATV (1 µM/10 µM/25 µM), ABC/3TC/ATV (10 µM/10 µM/25 µM), TDF/FTC/DRV (1 µM/10 µM/25 µM), ABC/3TC/DRV (10 µM/10 µM/25 µM), sus correspondientes vehículos (metanol, DMSO) o control (suero fisiológico). TDF, FTC ABC y 3TC se disolvieron en agua de cultivo estéril (FIGURA 16).

Para analizar el papel de las moléculas de adhesión leucocitarias o endoteliales en la interacción leucocito-endotelio inducida por los diferentes fármacos antirretrovirales con efectos positivos, los animales fueron pretratados por vía intravenosa (i.v.) en la cola con anticuerpos bloqueantes frente a Mac-1 (CD11b, 2mg/Kg), frente a integrinas β_2 (CD18, 1 mg/Kg), frente a ICAM-1 (CD54, 1 mg/Kg), o

con los anticuerpos control (IgG1, 1 mg/Kg) e IgA (2 mg/Kg) 30 minutos antes del tratamiento con los diferentes antirretrovirales (Alvarez et al., 2004, Watanabe et al., 1997, Tamatani et al., 1990, Tamatani et al., 1991) (FIGURA 16).

3 horas después de los tratamientos con los antirretrovirales, los animales se anestesiaron y se realizó la técnica de microscopía intravital descrita anteriormente. Una vez concluida la cirugía y tras un periodo de estabilización (30 minutos), se determinaron los parámetros leucocitarios y hemodinámicos descritos previamente a las 4 horas (FIGURA 16).

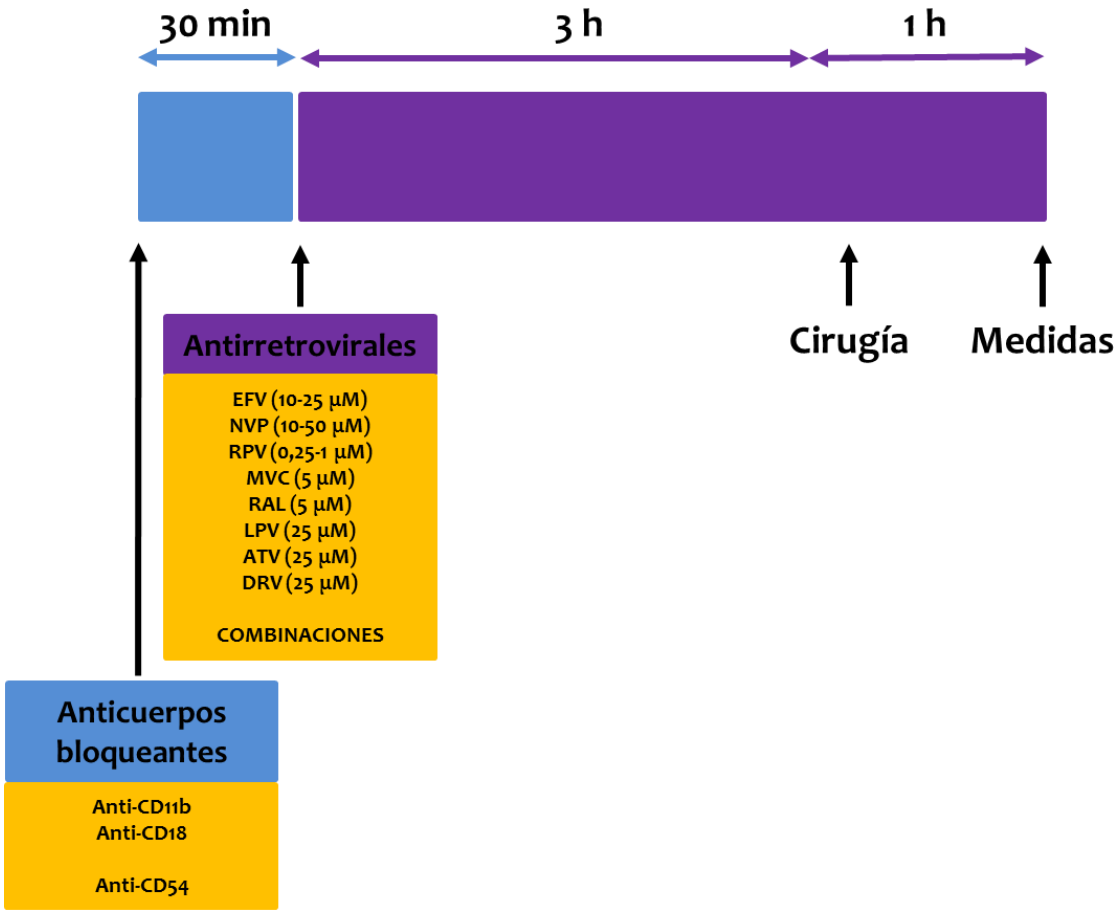

FIGURA 16. Protocolo experimental para la evaluación del efecto de diferentes fármacos antirretrovirales sobre la interacción leucocito-endotelio mediante microscopía intravital. A los animales se les administró intraperitonealmente (i.p.) distintos fármacos antirretrovirales: Efavirenz (EFV), Nevirapina (NVP), Rilpivirina (RPV), Maraviroc (MVC), Raltegravir (RAL), Lopinavir (LPV), Atazanavir (ATV) y Darunavir (DRV) o combinaciones de fármacos antirretrovirales: Tenofovir (TDF)/Emtricitabina (FTC)/EFV, Abacavir (ABC)/Lamivudina (3TC)/EFV, TDF/FTC/RPV, ABC/3TC/RPV, TDF/FTC/ATV, ABC/3TC/ATV, TDF/FTC/DRV y ABC/3TC/DRV. En algunos casos, los animales se pretrataron por vía intravenosa (i.v.) con anticuerpos bloqueantes frente a moléculas de adhesión leucocitarias (anti-CD11b, anti-CD18) o endoteliales (anti-CD54) 30 min antes del tratamiento intraperitoneal (i.p.) con EFV, NVP o RPV. 3 h después del tratamiento se realizó la cirugía y tras un periodo de estabilización, se determinaron los parámetros leucocitarios y hemodinámicos previamente descritos (4 h).

3.1.2. DETERMINACIÓN DEL TIPO CELULAR IMPLICADO

La determinación del tipo celular implicado se realizó en los mesenterios de rata aislados después de cada experimento de microscopía intravital. Estos mesenterios se fijaron con paraformaldehido al 4 % en PBS ("Phosphate Buffered Saline") a un pH de 7.4 y posteriormente se realizó una tinción con hematoxilina y eosina y una fijación con medio de montaje DPX (Alvarez et al., 2006). La preparación se observó bajo un microscopio de campo claro equipado con un objetivo 63x. Los leucocitos infiltrados (FIGURA 17) fueron clasificados en leucocitos polimorfonucleares (neutrófilos), macrófagos y linfocitos (FIGURA 18), expresándolos como *número de células*/2.5 x 10^{-4} cm^2.

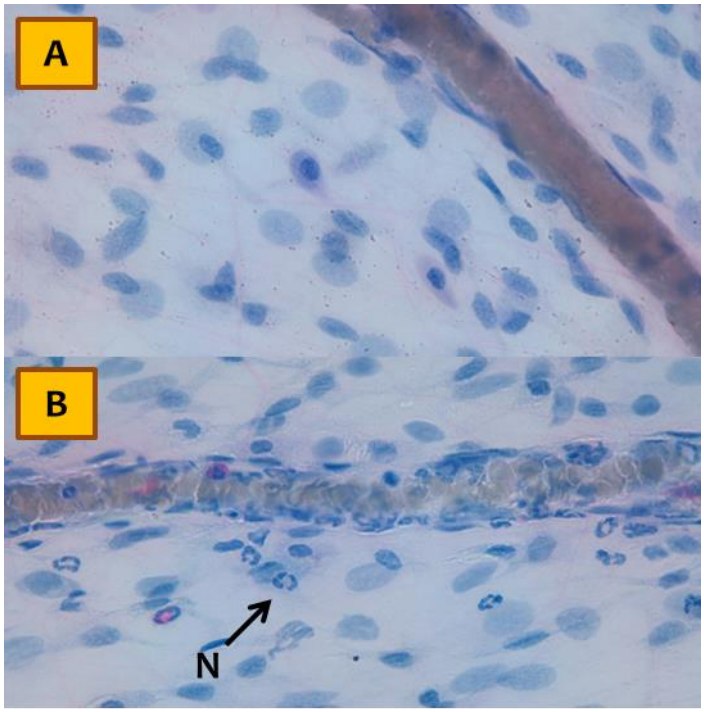

FIGURA 17. Imágenes representativas de vénulas mesentéricas tras la tinción hematoxilina-eosina. A: vénula de una rata control. **B:** vénula de una tratada con un estímulo positivo proinflamatorio. En la imagen **B** podemos observar neutrófilos (**N**) (↗) infiltrados.

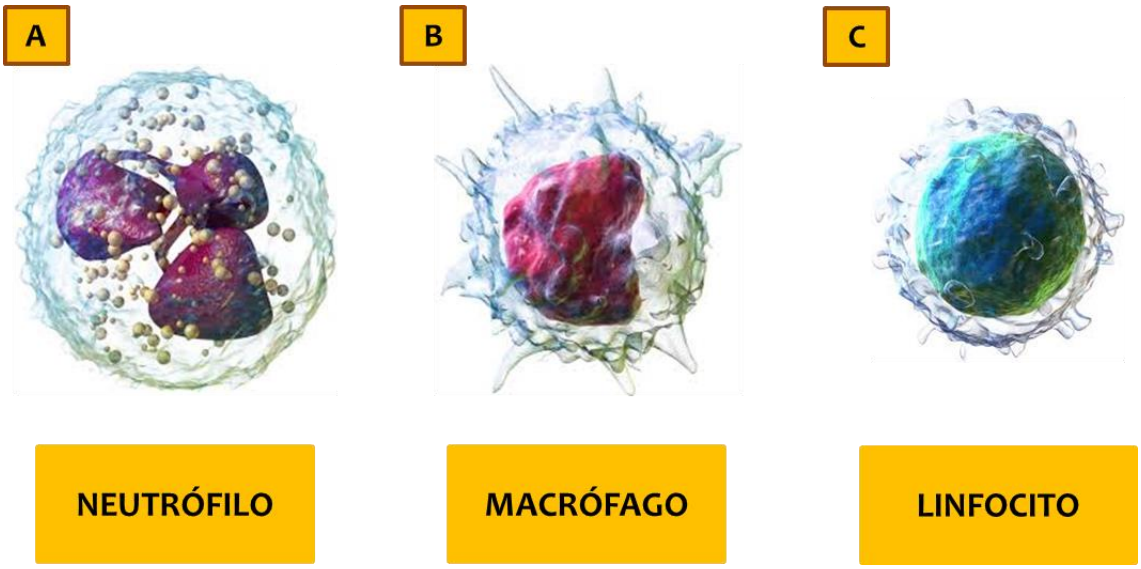

FIGURA 18. Morfología de los distintos tipos de leucocitos en función de las características de sus núcleos. A: neutrófilo. **B:** macrófago. **C:** linfocito. Figura adaptada de la página web www.leucocitos.org.

3.2. ESTUDIOS IN VITRO

3.2.1. AISLAMIENTO Y CULTIVO DE CÉLULAS ENDOTELIALES

Para la realización de los estudios que se detallan a continuación se utilizaron células HUVEC.

Estas células se extrajeron de la única vena presente en cordones umbilicales humanos frescos procedentes de donantes sanos y no infectados con el virus del VIH del Hospital Clínico Universitario de Valencia. Para ello se trabajó con el cordón umbilical completo sin disecar (FIGURA 19).

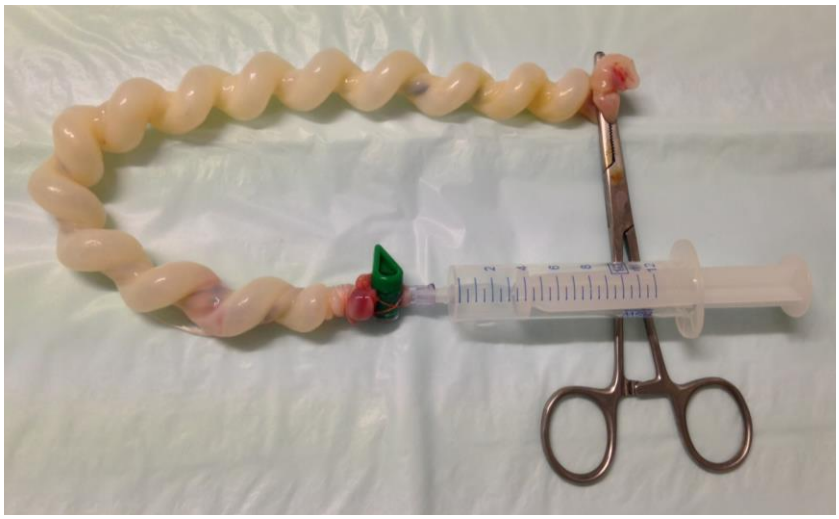

FIGURA 19. Cordón umbilical humano completo cuya vena se encuentra llena de colagenasa.

La vena del cordón umbilical humano se lavó con PBS a 37°C y a continuación, se llenó con colagenasa (1 mg/ml). El cordón umbilical se mantuvo en el incubador durante 17 minutos a 37°C (Jaffe et al., 1973, Ibiza et al., 2009). Transcurrido este tiempo, se realizó un masaje al cordón umbilical para asegurar la correcta separación de las células endoteliales de la pared del vaso, se recogió el contenido y se centrifugó a 259 xg. El precipitado obtenido se resuspendió en medio de cultivo EGM-2 ("Endothelial Growth Medium-2") suplementado con suero fetal bovino (2 % v/v), hidrocortisona (0.04 v/v), "Human Fibroblast Growth Factor-Basic" (hFGF-B, 0.4 % v/v), "Vascular Endothelial Growth Factor" (VEFG, 0.1 % v/v), "Recombinant Long R^3 Insulin-Like Growth Factor" (R^3-IGF-1, 0.1 % v/v), ácido ascórbico (0.1 % v/v), "Human Recombinant Epidermal Growth Factor" (rhEGF, 0.1 % v/v), "Gentamicine Sulfate Amphotericine B" (GA-1000, 0.1 % v/v), heparina (0.1 % v/v), penicilina (50 unidades/ml), estreptomicina (50 µg/ml) y fungizona (2.5 µg/ml). Todo el contenido celular se depositó en un frasco de cultivo celular T-25 donde las células de adhirieron y, tras varios días, alcanzaron el 100 % de confluencia. Las células endoteliales se mantuvieron en el incubador a 37°C en una atmósfera húmeda de 95 % de aire y 5 % de CO_2.

Posteriormente, los cultivos primarios se despegaron con tripsina y las células endoteliales se transfirieron a las placas de cultivo adecuadas. En todos los experimentos se utilizaron células del primer pase de los cultivos primarios de HUVEC.

3.2.2. AISLAMIENTO DE LEUCOCITOS

Para la extracción de células leucocitarias se utilizó sangre procedente de donantes sanos y no infectados con el virus del VIH del Centro de Transfusiones de la Comunidad Valenciana. Esta sangre se recogió en tubos que contienen citrato sódico como anticoagulante (de Pablo et al., 2010).

Leucocitos polimorfonucleares (PMN)

Todo el proceso de aislamiento se realizó a 4°C. 20 ml de sangre se incubaron durante 45 minutos en 10 ml de dextrano al 3 % (en suero fisiológico) consiguiendo con ello el depósito en la parte inferior de la mayor parte de los eritrocitos. Se recogió la parte superior, se depósito en Ficoll-Paque y por centrifugación a 259 xg y gradiente de densidad se obtuvieron los PMN en el precipitado. Éste se lisó y se centrifugó de nuevo a 259 xg durante 5 minutos. Los PMN se lavaron con HBSS ("Hanks Balanced Salt Solution") sin Ca^{2+} ni Mg^{2+} y se resuspendieron en medio RPMI completo [suplementado con suero fetal bovino inactivado (10 % v/v), penicilina/estreptomicina (1 % v/v), glutamina (1 % v/v) y piruvato sódico (1 % v/v)].

Leucocitos mononucleares (PBMC)

Todo el proceso de aislamiento se realizó a temperatura ambiente. 20 ml de sangre se incubaron durante 45 minutos en 10 ml de dextrano al 3 % (en suero fisiológico) consiguiendo con ello el depósito en la parte inferior de la mayor parte de los eritrocitos. Se recogió la parte superior, se depositó en Ficoll-Plaque y por centrifugación a 583 xg y gradiente de densidad se obtuvieron los PBMC en el anillo blanquecino. Se recogió esta fase y se centrifugó de nuevo a 583 xg durante 10 minutos. Los PBMC se lavaron con HBSS (sin Ca^{2+} ni Mg^{2+}) y se resuspendieron en medio RPMI completo [Ver Leucocitos Polimorfonucleares (PMN)].

3.2.3. ADHESIÓN DINÁMICA EN CÁMARA PARALELA DE FLUJO

Se utilizaron células endoteliales (HUVEC) y poblaciones leucocitarias aisladas (PMN y PBMC) provenientes de donantes sanos descritas previamente. Las células endoteliales se sembraron en cubre-objetos circulares de plástico de 25 mm de diámetro pretratados con Fibronectina (5 µg/ml).

Esta técnica de adhesión dinámica en cámara paralela de flujo ya ha sido descrita previamente (de Pablo et al., 2010). La cámara de flujo utilizada para la realización de estos experimentos posee una hendidura en la que se inserta el cubre-objetos circular que contiene la monocapa de células endoteliales confluentes (Goetz et al., 1999, Cai et al., 2006, Alvarez et al., 2004). Una vez montada la cámara, una porción de 5 x 25 mm fue expuesta al flujo (FIGURA 20). Todo el proceso se realizó a 37^{o}C ya que una de las placas que forma parte de esta cámara de flujo es calefactora.

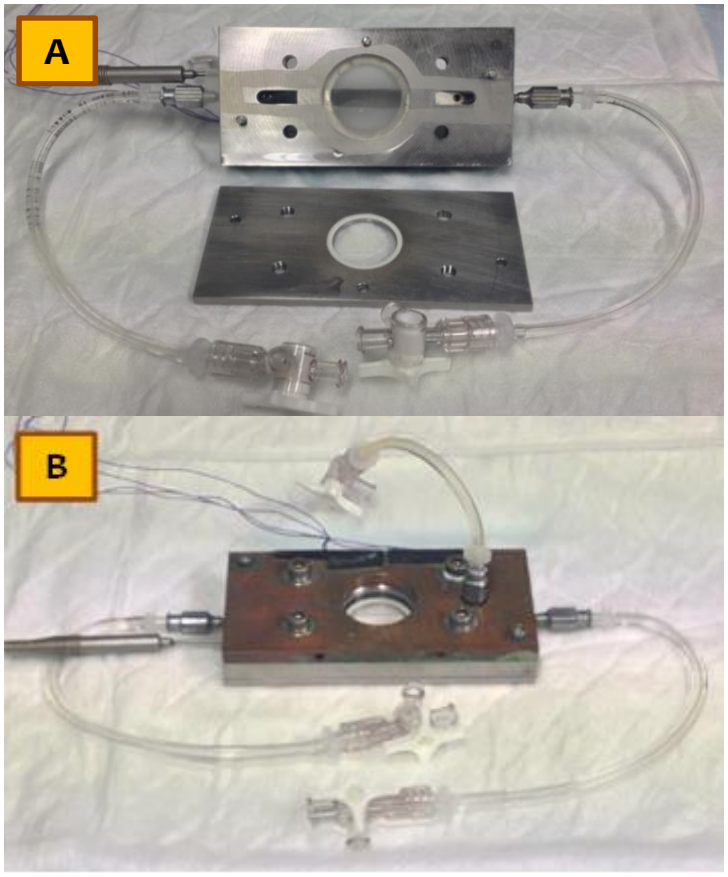

FIGURA 20. Montaje de la cámara paralela de flujo. A: cámara abierta. **B:** cámara cerrada. La cámara posee una hendidura circular en la que se inserta el cubre-objetos circular con las células endoteliales. Las conexiones permiten que se perfundan los leucocitos por la cámara de flujo.

Ambas poblaciones leucocitarias (PMN y PBMC) se resuspendieron en el tampón $DPBS^{+}$ ("Dulbecco's Phosphate Buffered Saline"), con Ca^{2+} y Mg^{2+} y con HSA ("Human Serum Albumin", 0.1 %) y se perfundieron 1 x 10^6 células/ml de PMN ó 0.5 x 10^6 células/ml de PBMC sobre la monocapa de células endoteliales a un flujo controlado de 0.36 ml/min (0.7 dinas/cm^2) gracias a una bomba de infusión.

Esta cámara se colocó sobre un microscopio invertido (Nikon Eclipse TE 2000-S) (FIGURA 21) conectado a una videocámara (Sony Exware HAD) que proyecta las imágenes a un ordenador donde se visualizaron y fueron grabadas (FIGURA 22).

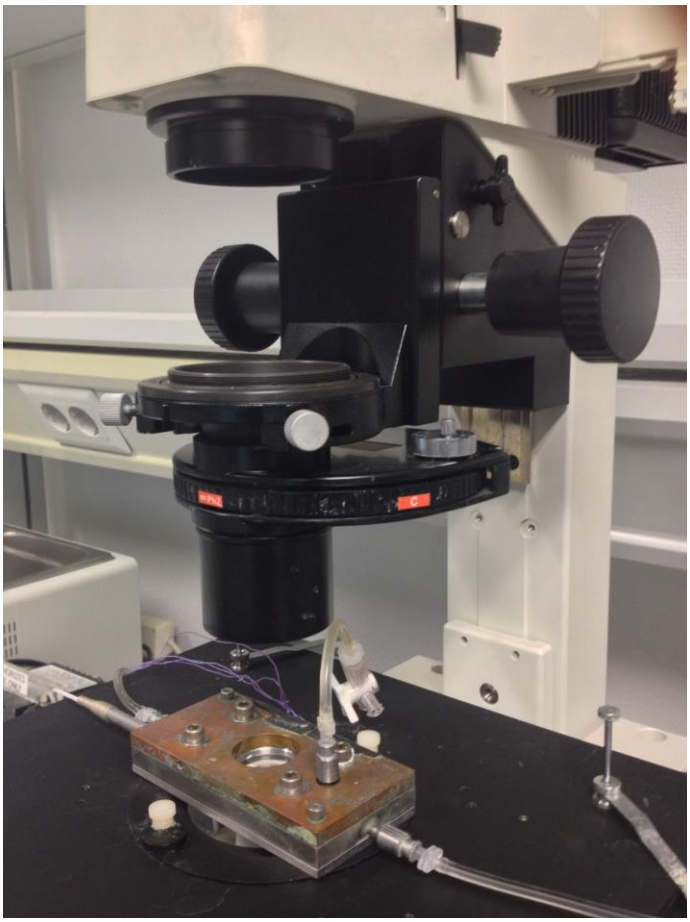

FIGURA 21. Sistema de cámara paralela de flujo situada en el microscopio.

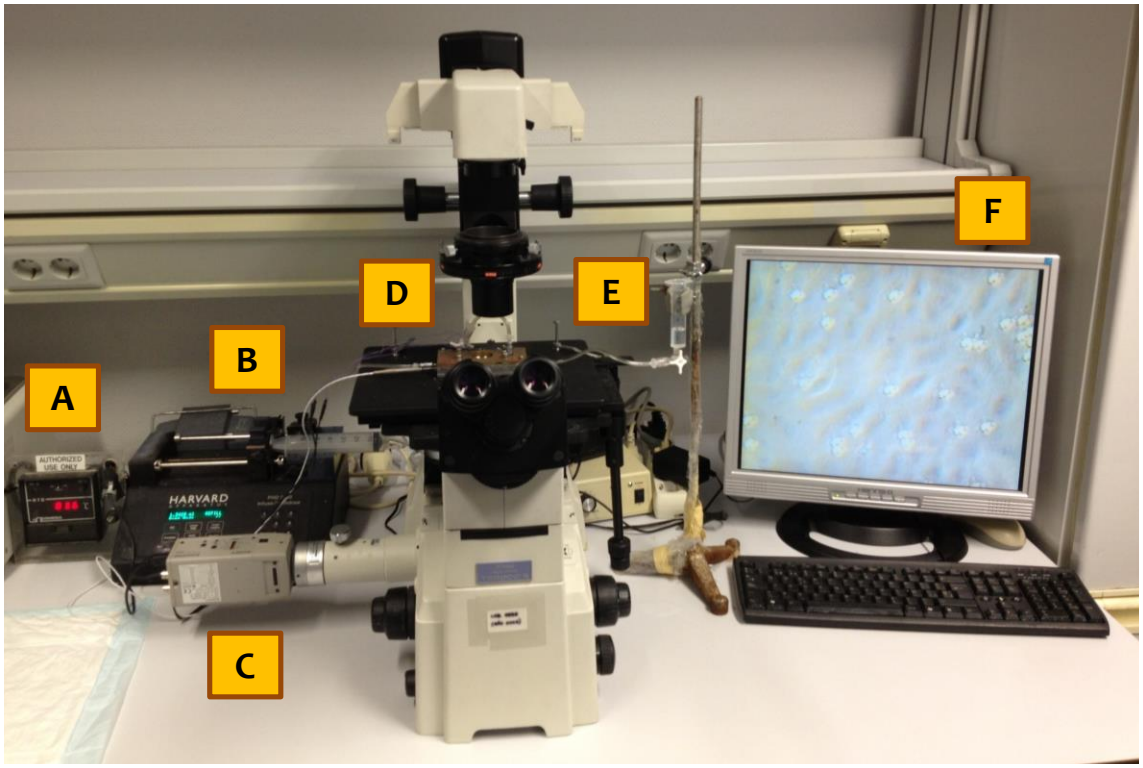

FIGURA 22. Sistema de cámara paralela de flujo en el microscopio. Las imágenes muestran las diferentes partes que conforman dicho sistema. **A:** Regulador de temperatura, **B:** Bomba de infusión, **C:** Videocámara, **D:** Cámara paralela de flujo, **E:** Jeringa invertida con una suspensión de leucocitos y **F:** Monitor de ordenador.

Para observar el flujo de leucocitos y su interacción con las células endoteliales se utilizó un objetivo 40x. La grabación se inició cuando se empezó a ver el paso de los leucocitos sobre la monocapa de células endoteliales y las imágenes fueron grabadas con el programa informático "Pinacle Studio". La grabación se realizó durante 5 minutos en el mismo campo donde se analizaron los parámetros de rodamiento y velocidad de rodamiento leucocitario. Posteriormente se grabaron 5 campos adicionales donde se analizó la adhesión leucocitaria al endotelio.

Parámetros leucocitarios determinados

Se analizaron los siguientes parámetros leucocitarios: (FIGURA 15)

Rodamiento leucocitario: es el número de leucocitos que circulan a una velocidad inferior a la de los eritrocitos ya que están interaccionando con el endotelio venular. Se expresa en *células/min* (FIGURA 15).

Velocidad de rodamiento leucocitario: es el tiempo que tarda un leucocito en fase de rodamiento en recorrer 100 µm de endotelio. Se expresa en µ*m/s* (FIGURA 15).

Adhesión leucocitaria: es el número de leucocitos que permanecen estacionados o tienen contacto estable con el endotelio venular durante un periodo igual a superior a 30 segundos en 100 µm de vaso. Se expresa en *células adheridas/mm*^{2} (FIGURA 15 y 23).

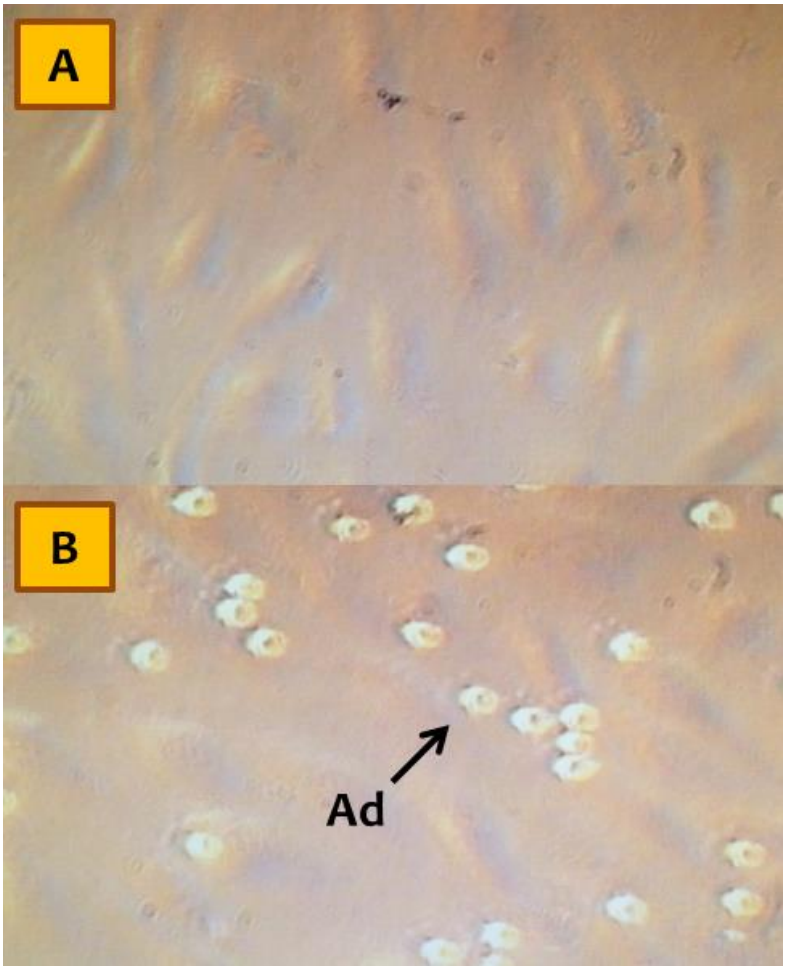

FIGURA 23. Imágenes representativas de monocapas de células endoteliales. A: monocapa control sobre la que se perfunden leucocitos control. **B:** monocapa estimulada con un estímulo positivo sobre la que se perfunden leucocitos tratados con un estímulo positivo proinflamatorio. En la imagen **B** podemos observar leucocitos adheridos (**Ad**) (↗).

Protocolo experimental

Tanto los leucocitos aislados (PMN y PBMC) como las células endoteliales (HUVEC) se trataron independientemente con concentraciones clínicas relevantes de fármacos representativos de los diferentes grupos de fármacos antirretrovirales o con las combinaciones de fármacos citadas previamente (Ver Protocolo experimental, Microcopía Intravital). PAF ("Platelet Activating Factor", 10 µM, 1 hora) y TNF-α ("Tumor Necrosis Factor-α", 25 ng/ml, 4 horas) se utilizaron como control positivo para leucocitos y células endoteliales, respectivamente. Transcurrido el periodo de incubación con los diferentes tratamientos se procedió a la realización de la técnica de adhesión dinámica en cámara paralela de flujo descrita anteriormente y se determinaron los parámetros leucocitarios y hemodinámicos descritos previamente (4 horas) (FIGURA 24).

Para analizar el papel de las moléculas de adhesión leucocitarias o endoteliales en la interacción leucocito-endotelio inducida por los diferentes fármacos antirretrovirales con efectos positivos, se pretrataron (antes del tratamiento con EFV y RPV) los leucocitos con los anticuerpos bloqueantes frente a LFA-1 (CD11a, 10 µg/ml), frente a Mac-1 (CD11b, 20 µg/ml), frente a gp150.95 (CD11c, 10 µg/ml), frente a integrinas β_2 (CD18, 10 µg/ml) o con el anticuerpo control (IgG1, 10 µg/ml) durante 20 minutos, en oscuridad y a 4°C o se pretrató la monocapa de células endoteliales con el anticuerpo bloqueante frente a ICAM-1 (CD54, 20 µg/ml) o con el anticuerpo control (IgG1, 10 µg/ml) durante 30 minutos, en oscuridad y a 37°C (Heit et al., 2005., Pluskota et al., 2008, Sadhu et al., 2007, Arndt et al., 2007) (FIGURA 24).

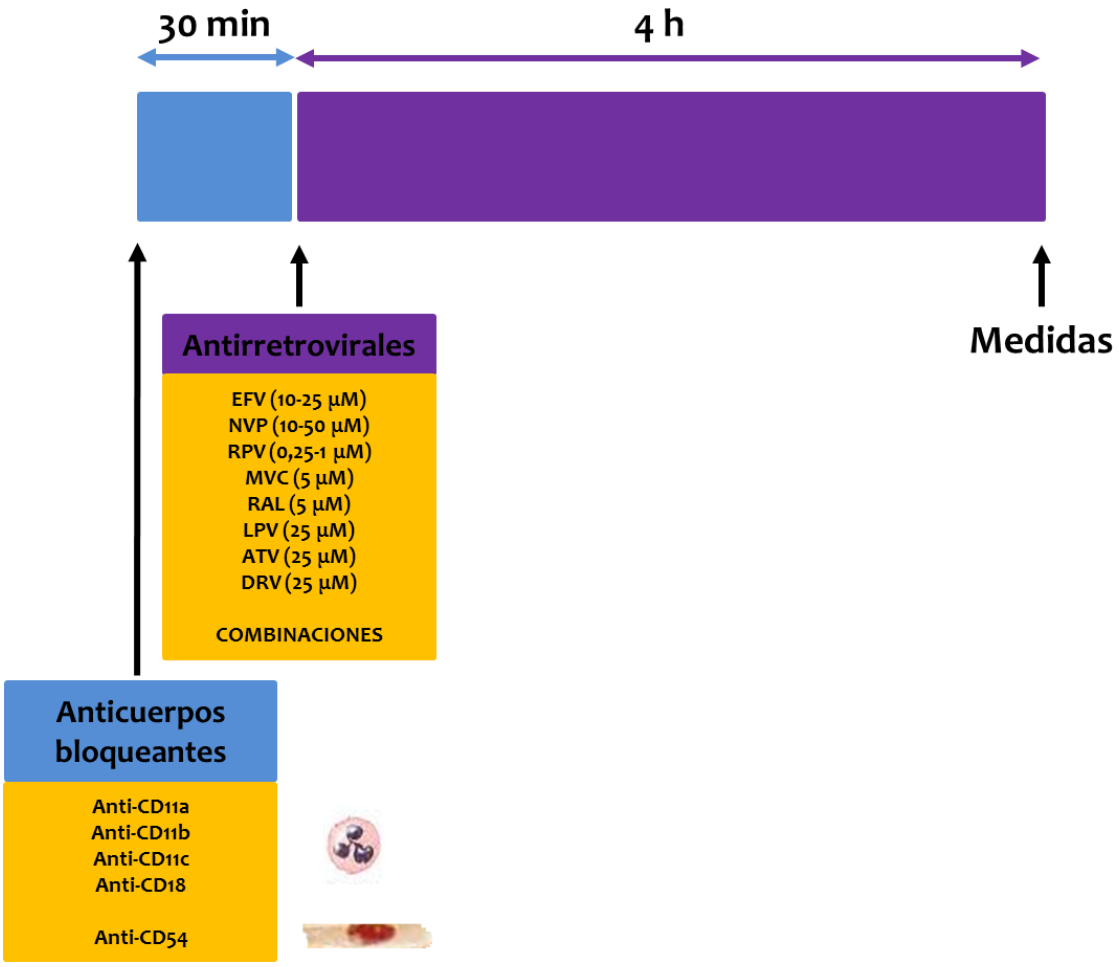

FIGURA 24. Protocolo experimental para la evaluación del efecto de diferentes fármacos antirretrovirales sobre la interacción leucocito-endotelio mediante adhesión dinámica en cámara paralela flujo. Las células endoteliales y los leucocitos se trataron con distintos fármacos antirretrovirales: Efavirenz (EFV), Nevirapina (NVP), Rilpivirina (RPV), Maraviroc (MVC), Raltegravir (RAL), Lopinavir (LPV), Atazanavir (ATV) y Darunavir (DRV) o con combinaciones de fármacos antirretroviral: Tenofovir (TDF)/Emtrivitabina (FTC)/EFV, Abacavir (ABC)/Lamivudina (3TC)/EFV, TDF/FTC/RPV, ABC/3TC/RPV, TDF/FTC/ATV, ABC/3TC/ATV, TDF/FTC/DRV y ABC/3TC/DRV. En algunos casos, se pretrataron los leucocitos con anticuerpos bloqueantes frente a sus moléculas de adhesión (anti-CD11a, anti-CD11b, anti-CD11c y anti-CD18) o las células endoteliales frente a su molécula de adhesión (anti-CD54) 20-30 min antes del tratamiento con EFV o RPV. A las 4 h se determinaron los parámetros leucocitarios previamente descritos.

3.2.4. ESTUDIO DE LA EXPRESIÓN DE LAS MOLÉCULAS DE ADHESIÓN POR CITOMETRÍA DE FLUJO

Para determinar la expresión de moléculas de adhesión leucocitarias o endoteliales se utilizó un citómetro de flujo (FACS Calibur, BD Biosciences) (FIGURA 25).

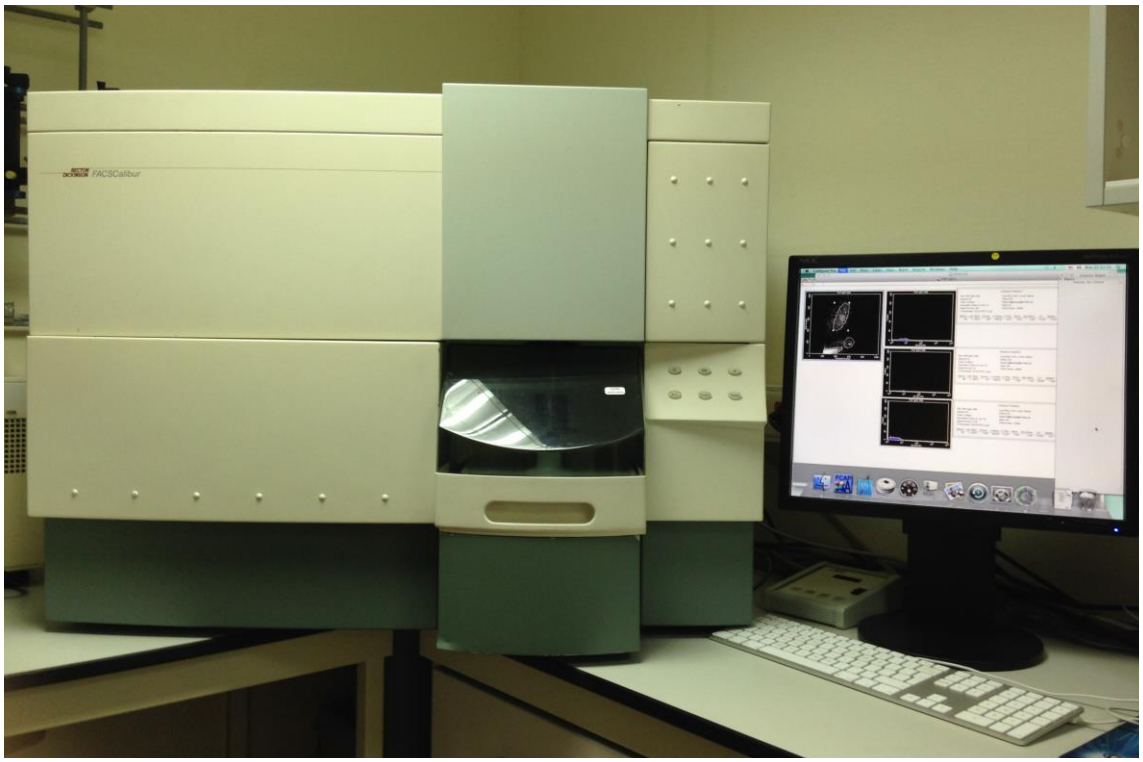

FIGURA 25. Citómetro de flujo FACS Calibur.

Las células se identificaron en función de sus características de tamaño y granulosidad ("forward scatter" -FS- and "side scatter" -SS-, respectivamente). Se utilizó la mediana de la intensidad de la fluorescencia como marcador de la expresión de las diferentes moléculas de adhesión analizadas. Se analizaron 10.000 eventos por muestra (Alvarez et al., 2004, Alvarez et al., 2007).

Expresión de moléculas de adhesión en leucocitos

Se utilizó sangre procedente de donantes sanos y no infectados con el virus del VIH del Centro de Transfusiones de la Comunidad Valenciana. Esta sangre se recogió en tubos que contienen Citrato Sódico como anticoagulante.

Protocolo experimental

La sangre (40 µL) se trató con concentraciones clínicas relevantes de fármacos representativos de los diferentes grupos de fármacos antirretrovirales (Ver Protocolo experimental, Adhesión Dinámica en Cámara Paralela de Flujo) (FIGURA 24). El PAF (10 µM, 1 hora) se utilizó como control positivo para leucocitos.

Una vez concluidos los tratamientos, la sangre se incubó con los correspondientes anticuerpos a saturación: LFA-1 (CD11a), Mac-1 (CD11b), gp150.95 (CD11c), integrina β_2 (CD18), VLA-4 (CD49d), L-Selectina (CD62L) o con el anticuerpo control (IgG1) conjugados con FITC (fluoresceína isotiocianato) o PE (Ficoeritrina) durante 20 minutos, en oscuridad y a 4°C. (FIGURA 24).

Posteriormente, las muestras se lisaron, lavaron y fijaron con solución de lisis ("FACS Lysing Solution", BD Biosciences) y se analizó la expresión de las moléculas de adhesión leucocitarias mediante el citómetro de flujo previamente citado donde neutrófilos, monocitos y linfocitos se separaron e identificaron por sus características específicas de tamaño y granulosidad (FIGURA 26).

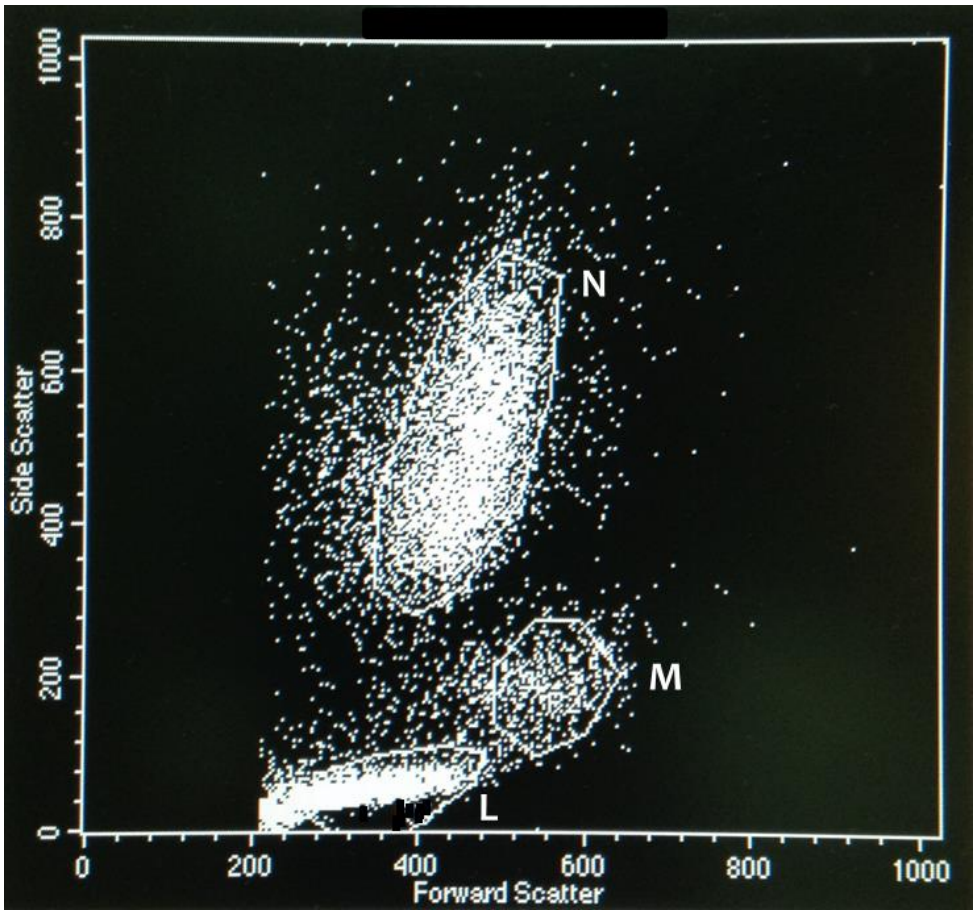

FIGURA 26. Identificación de las diferentes poblaciones leucocitarias a través del citómetro de flujo. Se muestra un histograma representativo de las diferentes poblaciones leucocitarias separadas e identificadas en función de sus características de tamaño ("forward scatter") y granulosidad ("side scatter") por el citómetro de flujo. **N**: neutrófilos. **M**: monocitos. **L**: linfocitos.

Expresión de moléculas de adhesión en células endoteliales

Las células endoteliales que se utilizaron en esta técnica se cultivaron en placas de 6 pocillos.

Protocolo experimental

Las células endoteliales (HUVEC) confluentes se trataron con concentraciones clínicas relevantes de fármacos representativos de los diferentes grupos de fármacos antirretrovirales (Ver Protocolo experimental, Adhesión Dinámica en Cámara Paralela de Flujo) (FIGURA 24). TNF-α (25 ng/ml, 4 horas) se utilizó como control positivo para HUVEC.

A las 4 horas, las HUVEC se despegaron con Tripsina y se neutralizó su efecto con medio EGM-2 completo. Esta suspensión de células se incubó con los correspondientes anticuerpos a saturación: ICAM-1 (CD54), VCAM-1 (CD106), E-Selectina (CD62E) o con el anticuerpo control (IgG1) conjugados con FITC o PE durante 20 minutos, en oscuridad y a 4°C (FIGURA 24).

Posteriormente las células se fijaron con formalina al 10 % y se analizó la expresión de las moléculas de adhesión endoteliales mediante el citómetro de flujo previamente citado donde las HUVEC se identificaron por sus características específicas de tamaño y granulosidad.

MATERIAL

En las TABLAS 6, 7, 8, 9 y 10 se muestran las casas comerciales de las cuales se obtuvieron los animales, fármacos antirretrovirales, anticuerpos frente a rata y frente a humano y reactivos utilizados, respectivamente.

TABLA 6: Animales.

ANIMALES	CASA COMERCIAL
Ratas Sprague-Dawley macho de 200-250 g	Charles River Laboratories

TABLA 7: Fármacos antirretrovirales.

FÁRMACOS ANTIRRETROVIRALES	CASA COMERCIAL
Efavirenz	Sequoia Research Products
Nevirapina	Sequoia Research Products
Rilpivirina	Sequoia Research Products
Maraviroc	Sequoia Research Products
Raltegravir	Sequoia Research Products
Lopinavir	Sequoia Research Products
Atazanavir	Sequoia Research Products
Darunavir	Sequoia Research Products
Tenofovir	Sequoia Research Products
Emtricitabina	Sequoia Research Products
Abacavir	Sequoia Research Products
Lamivudina	Sequoia Research Products

TABLA 8: Anticuerpos frente a rata.

ANTICUERPOS FRENTE A RATA	CASA COMERCIAL
Anticuerpo bloqueante IgG1κ Isotipo Control	BD Biosciences
Anticuerpo bloqueante IgA Isotipo Control	BD Biosciences
Anticuerpo bloqueante frente a CD11b (clon WT.5)	BD Biosciences
Anticuerpo bloqueante frente a CD18 (clon WT.3)	BD Biosciences
Anticuerpo bloqueante frente a CD54 (clon 1A29)	BD Biosciences

TABLA 9: Anticuerpos frente a humano.

ANTICUERPOS FRENTE A HUMANO	CASA COMERCIAL
Anticuerpo bloqueante IgG1 Isotipo Control	eBioscience
Anticuerpo bloqueante frente a CD11a (clon m38)	Calbiochem
Anticuerpo bloqueante frente a CD11b (clon ICRF44)	Calbiochem
Anticuerpo bloqueante frente a CD11c (clon CBR-p150/4G1)	AbD Serotec
Anticuerpo bloqueante frente a CD18 (clon IB4)	Calbiochem
Anticuerpo bloqueante frente a CD54	BD Biosciences
Anticuerpo frente a IgG1 κ Isotipo Control FITC	BD Biosciences
Anticuerpo frente a CD11a conjugado con FITC	BD Biosciences
Anticuerpo frente a CD11b conjugado con PE	BD Biosciences
Anticuerpo frente a CD11c conjugado con PE	BD Biosciences
Anticuerpo frente a CD18 conjugado con FITC	BD Biosciences
Anticuerpo frente a CD49d conjugado con PE	BD Biosciences
Anticuerpo frente a CD62L conjugado con FITC	BD Biosciences
Anticuerpo frente a CD54 conjugado con PE	BD Biosciences
Anticuerpo frente a CD106 conjugado con FITC	BD Biosciences
Anticuerpo frente a CD62E conjugado con PE	BD Biosciences

TABLA 10: Reactivos y material.

REACTIVOS	CASA COMERCIAL
ADP ("Adenosine di-Phosphate")	Sigma
Agua para cultivos	Sigma
Colagenasa	Gibco
Cubre de plástico de 25 mm de diámetro	Nunc
Dextrano	Sigma
DMSO ("Dimethil Sulfoxide")	Sigma
$DPBS^+$ ("Dulbecco's PBS con Ca^{2+} y Mg^{2+}")	Lonza
$DPBS^-$ ("Dulbecco's PBS sin Ca^{2+} y Mg^{2+}")	Lonza
EGM-2 ("Endothelial Growth Medium-2") completo	Lonza
Eosina	Panreac
Etanol	J. T. Baker
Fibronectina	Sigma
Ficoll-Paque TM Plus	GE Healthcare
Formalina 10 %	Sigma
Gases	AirLiquide
HBSS ("Hank`s Balanced Salt Solution")	Lonza
HCl	Fisher
Hematoxilina	Sigma
Heparina Sódica 5 %	Mayne Pharma
$NH4^+$, Hidróxido Amónico	Sigma
HSA ("Human Serum Albumin", "Albuminate 25 %")	Sigma
KCl, Cloruro Potásico	Panreac
Medio de Montaje DPX	Sigma
$MgSO_4$, Sulfato Magnésico	Panreac
NaCl, Cloruro Sódico	Panreac
$NaHCO_3$, Bicarbonato Sódico	Panreac
PAF ("Platelet Activating Factor")	Sigma
Paraformaldehído	Panreac
PBS ("Phosphate Buffered Saline")	Gibco
Pentobarbital Sódico	Guinama
RPMI 1640 suplementado con 20 mM HEPES	Sigma
Solución de lisis	BD Biosciences
Suero fetal bovino	Lonza
Suero fisiológico (NaCl 0.9 %)	Braun
TNF-α recombinante ("Tumor Necrosis Factor-α")	Sigma
Tripsina	Gibco
Tubos con Citrato sódico	BD Vacutainer
Xileno	Panreac

COMITÉS ÉTICOS

El Comité Ético del Hospital Clínico Universitario de Valencia aprobó el proyecto dentro del cual se enmarca este estudio con muestras de cordón umbilical humano y sangre humana. Todos los pacientes firmaron el correspondiente consentimiento informado y no se observaron diferencias significativas en cuanto al sexo, raza o etnia entre los diferentes grupos.

El Comité Ético de Experimentación Animal de la Universidad de Valencia así como de **la Conselleria de Agricultura, Medio Ambiente, Cambio Climático y Desarrollo Rural de la Generalitat Valenciana** aprobó los estudios con animales de experimentación realizados en este estudio. Además, estos estudios están en concordancia con las directrices institucionales para el cuidado y uso de animales de experimentación de laboratorio.

ANÁLISIS ESTADÍSTICO

Todos los resultados se expresaron como la media aritmética ± el error estándar de la media (E.E.M.). Se realizaron un número de experimentos ≥ 4. Los resultados obtenidos se analizaron con un análisis de varianza One-Way ANOVA, con la posterior corrección de Newman-Keuls, considerándose que la diferencia entre grupos es significativa cuando $p<0.05$. En algunos casos, los resultados se expresaron como porcentaje del control (%) considerando el control negativo como el 100 %.

4. RESULTADOS

4.1. ESTUDIOS *IN VIVO*

4.1.1. ESTUDIO DEL EFECTO DE LOS FÁRMACOS ANTIRRETROVIRALES SOBRE LA INTERACCIÓN LEUCOCITO-ENDOTELIO *IN VIVO*

4.1.1.1. EFECTO DE LOS FÁRMACOS ADMINISTRADOS INDIDUALMENTE

4.1.1.1.1. ITINAN

Se analizó el efecto de los fármacos más empleados dentro de este grupo (EFV, NVP y RPV) sobre la interacción leucocito-endotelio *in vivo* utilizando el modelo animal de microscopía intravital.

En vénulas mesentéricas, EFV, NVP y RPV produjeron una disminución significativa y dosis dependiente de la velocidad de rodamiento (FIGURA 27A, 28A y 29A), así como un aumento del rodamiento (FIGURA 27B, 28B y 29B) y la adhesión leucocitaria (FIGURA 27C, 28C y 29C). El parámetro de migración leucocitaria únicamente fue modificado por EFV y NVP (FIGURA 27D y 28D) pero no por RPV (FIGURA 29D) y además este efecto fue mayor para EFV que para NVP.

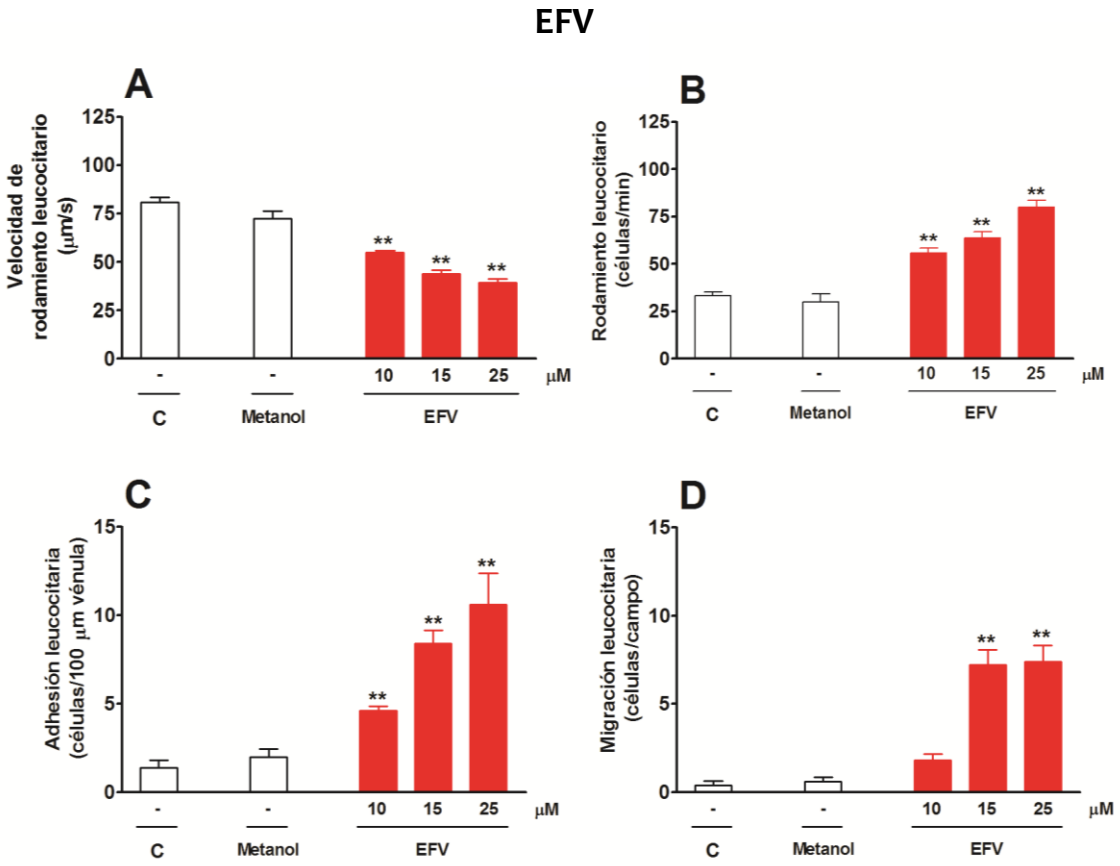

FIGURA 27. Efecto de Efavirenz sobre la interacción leucocito-endotelio en vénulas mesentéricas de rata. Se analizó la velocidad de rodamiento (A), el rodamiento (B), la adhesión (C) y la migración leucocitaria (D). Las ratas fueron tratadas intraperitonealmente (4 h) con Efavirenz (EFV, 10-25 µM), su correspondiente vehículo (metanol) o control (suero fisiológico). Los resultados fueron expresados como Media ± E.E.M. (n = 5). **p<0,01 respecto del valor correspondiente al grupo tratado con metanol. Análisis de varianza ANOVA seguido del post-test Newman-Keuls.

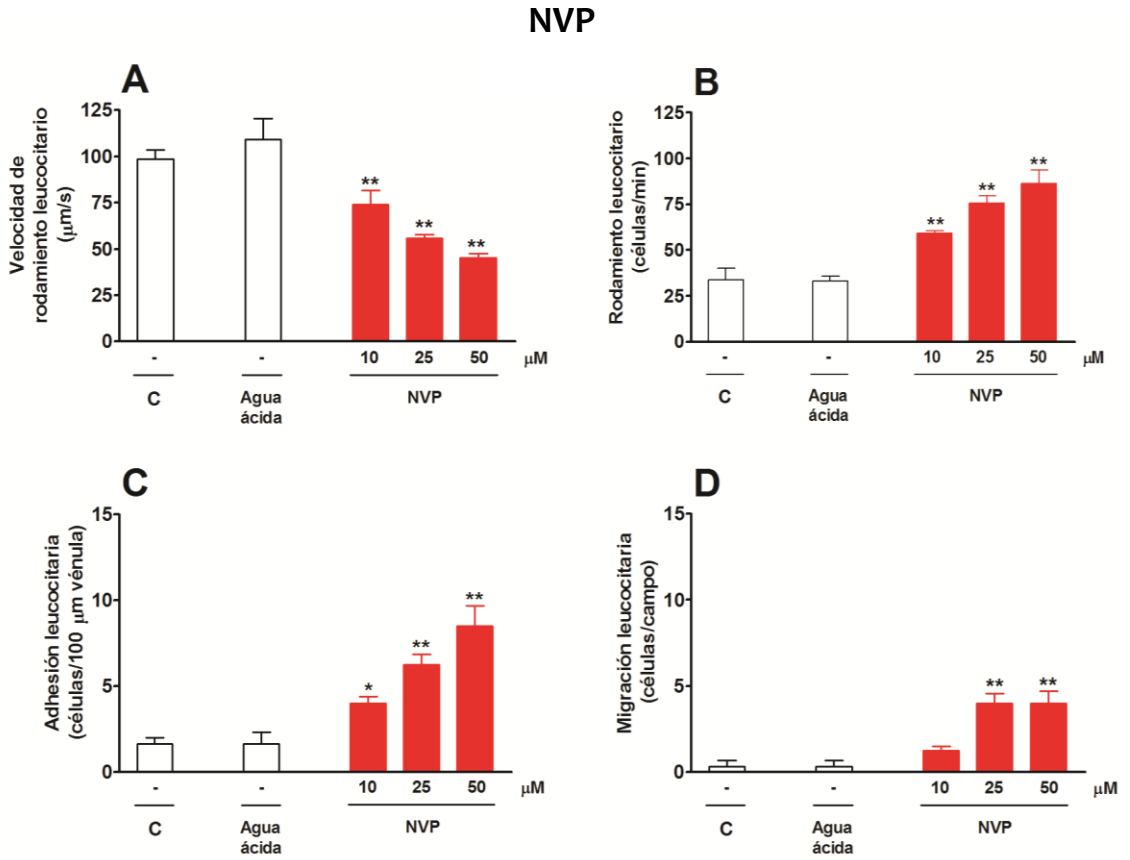

FIGURA 28. Efecto de Nevirapina sobre la interacción leucocito-endotelio en vénulas mesentéricas de rata. Se analizó la velocidad de rodamiento (A), el rodamiento (B), la adhesión (C) y la migración leucocitaria (D). Las ratas fueron tratadas intraperitonealmente (4 h) con Nevirapina (NVP, 10-50 µM), su correspondiente vehículo (agua ácida) o control (suero fisiológico). Los resultados fueron expresados como Media ± E.E.M. (n = 4). *p<0,05 ó **p<0,01 respecto del valor correspondiente al grupo tratado con agua ácida. Análisis de varianza ANOVA seguido del post-test Newman-Keuls.

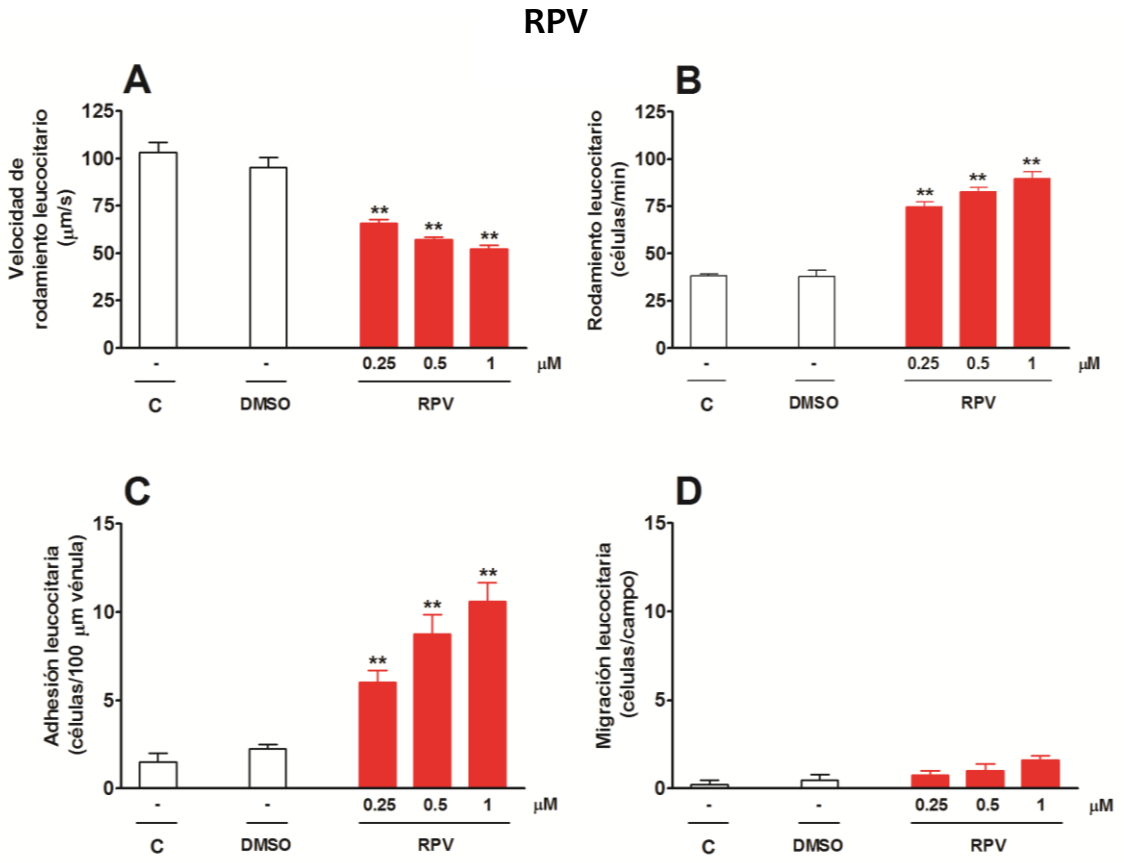

FIGURA 29. Efecto de Rilpivirina sobre la interacción leucocito-endotelio en vénulas mesentéricas de rata. Se analizó la velocidad de rodamiento (A), el rodamiento (B), la adhesión (C) y la migración leucocitaria (D). Las ratas fueron tratadas intraperitonealmente (4 h) con Rilpivirina (RPV, 0.25-1 µM), su correspondiente vehículo (DMSO) o control (suero fisiológico). Los resultados fueron expresados como Media ± E.E.M. (n = 4-5). ** p<0,01 respecto del valor correspondiente al grupo tratado con DMSO. Análisis de varianza ANOVA seguido del post-test Newman-Keuls.

4.1.1.1.2. ANTAGONISTAS CCR5, InInt E IP

Analizamos el efecto de los fármacos más empleados dentro de cada grupo: MVC (antagonista CCR5), RAL (InInt) y LPV, ATV y DRV (IP) sobre la interacción leucocito-endotelio *in vivo* mediante el modelo animal de microscopía intravital.

En vénulas mesentéricas, MVC, RAL, LPV, ATV y DRV no produjeron ninguna modificación en los parámetros leucocitarios analizados (FIGURA 30).

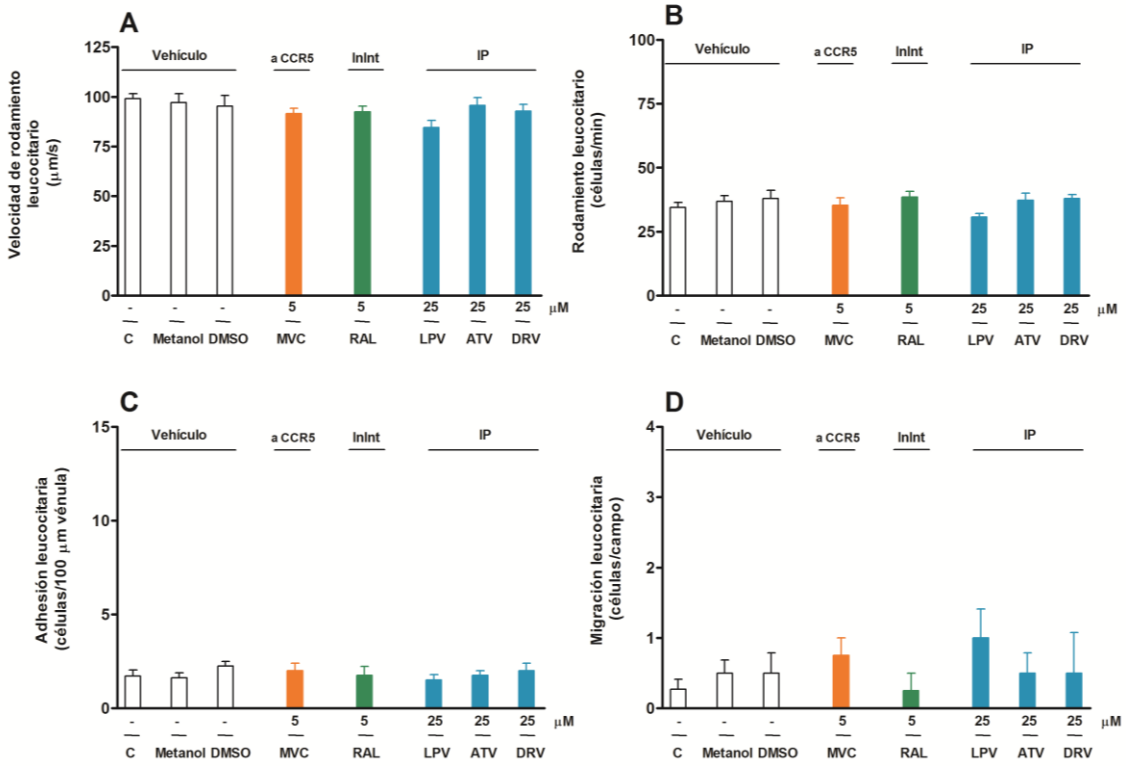

FIGURA 30. Efecto de de los fármacos antagonistas CCR5, InInt e IP sobre la interacción leucocito-endotelio en vénulas mesentéricas de rata. Se analizó la velocidad de rodamiento (A), el rodamiento (B), la adhesión (C) y la migración leucocitaria (D). Las ratas fueron tratadas intraperitonealmente (4 h) con Maraviroc (MVC, 5 µM), Raltegravir (RAL, 5 µM), Lopinavir (LPV, 25 µM), Atazanavir (ATV, 25 µM), Darunavir (DRV, 25 µM), sus correspondientes vehículos (metanol o DMSO) o control (suero fisiológico). Los resultados fueron expresados como Media ± E.E.M. (n = 4-8). Análisis de varianza ANOVA seguido del post-test Newman-Keuls.

4.1.1.2. EFECTO DE LAS COMBINACIONES DE LOS FÁRMACOS ANTIRRETROVIRALES MÁS EMPLEADAS EN LA TERAPEÚTICA ACTUAL

Se analizaron las combinaciones de fármacos más empleadas en la terapéutica actual: TDF/FTC/EFV, ABC/3TC/EFV, TDF/FTC/RPV, ABC/3TC/RPV, TDF/FTC/ATV, ABC/3TC/ATV, TDF/FTC/DRV, ABC/3TC/DRV sobre la interacción leucocito-endotelio *in vivo* mediante el modelo animal anteriomente citado.

En vénulas mesentéricas, únicamente las combinaciones TDF/FTC/EFV, ABC/3TC/EFV, TDF/FTC/RPV, ABC/3TC/RPV, produjeron una disminución significativa de la velocidad de rodamiento (FIGURA 31A), así como un aumento significativo del rodamiento (FIGURA 31B), la adhesión (FIGURA 31C) y la migración leucocitaria (FIGURA 31D). ABC/3TC/ATV y ABC/3TC/DRV produjeron una variación en los parámetros de velocidad de rodamiento, rodamiento y adhesión leucocitaria, pero no modificaron el de migración leucocitaria (FIGURA 31). Los demás tratamientos no produjeron ninguna variación en ninguno de los parámetros leucocitarios analizados (FIGURA 31).

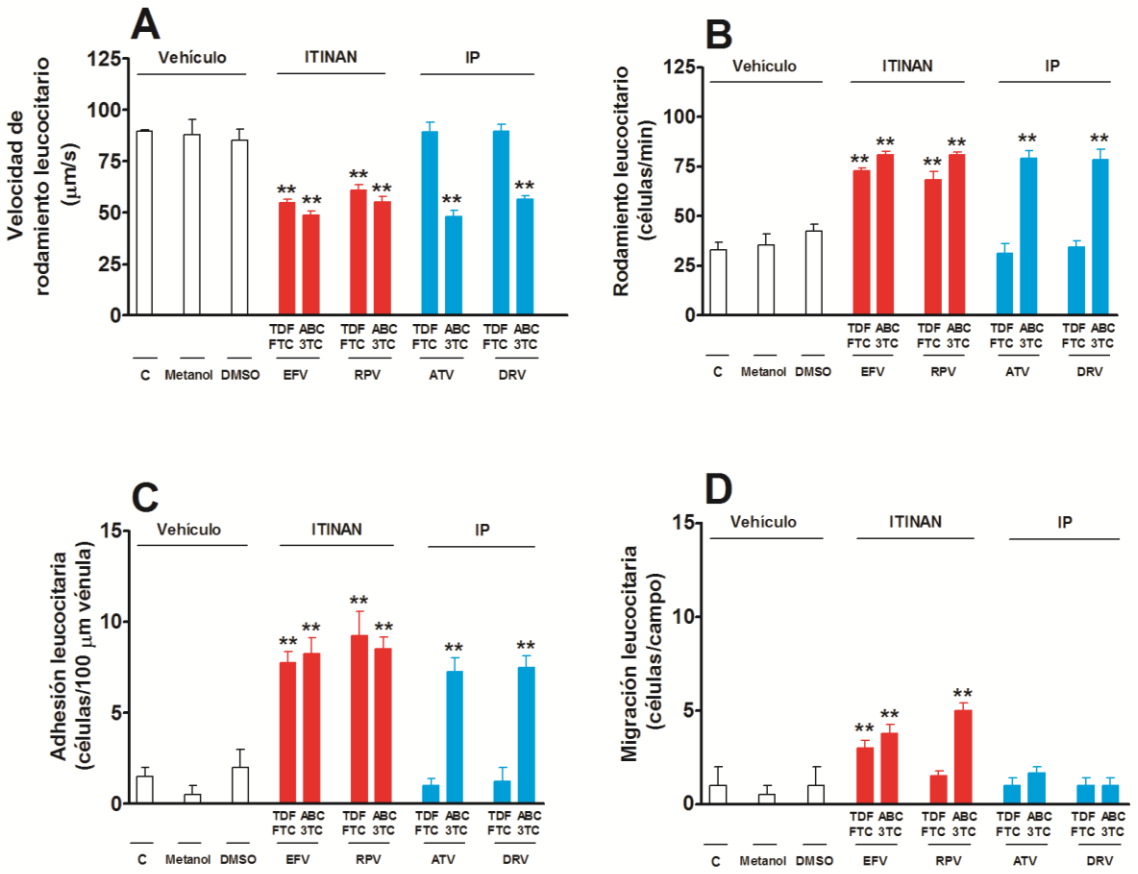

FIGURA 31. Efecto de las combinaciones de los fármacos antirretrovirales más utilizadas sobre la interacción leucocito-endotelio en vénulas mesentéricas de rata. Se analizó la velocidad de rodamiento (A), el rodamiento (B), la adhesión (C) y la migración leucocitaria (D). Las ratas fueron tratadas intraperitonealmente (4 h) con las combinaciones TDF/FTC/EFV, ABC/3TC/EFV, TDF/FTC/RPV, ABC/3TC/RPV, TDF/FTC/ATV, ABC/3TC/ATV, TDF/FTC/DRV, ABC/3TC/DRV, sus correspondientes vehículos (metanol o DMSO) o control (suero fisiológico). Las concentraciones utilizadas fueron TDF 1 µM, FTC 10 µM, EFV 15 µM, ABC 10 µM, 3TC 10 µM, RPV 0.5 µM, ATV 10 µM y DRV 10 µM. Los resultados fueron expresados como Media ± E.E.M. (n = 4). **p<0,01 respecto del valor correspondiente al grupo tratado con metanol o DMSO. Análisis de varianza ANOVA seguido del post-test Newman-Keuls.

4.1.2. ESTUDIO DEL EFECTO DE LOS FÁRMACOS ANTIRRETROVIRALES SOBRE LA INFILTRACIÓN LEUCOCITARIA EN MESENTERIO DE RATA

4.1.2.1. EFECTO DE LOS FÁRMACOS ADMINISTRADOS INDIVIDUALMENTE

4.1.2.1.1. ITINAN

Se analizó el efecto de EFV, NVP y RPV sobre la infiltración leucocitaria en mesenterio de rata.

EFV y NVP produjeron un aumento significativo en el número de leucocitos infiltrados con respecto a sus correspondientes vehículos (TABLA 11 y FIGURA 32) en el tejido mesentérico. Además, este parámetro fue significativamente mayor en animales tratados con EFV 15 µM (17,7 ± 3,3** vs. metanol: 1,0 ± 0,3 leucocitos/campo) que en aquellos tratados con NVP 25 µM (5,6 ± 0,4$^{\&\&}$ vs. agua ácida: 0,5 ± 0,3 leucocitos/campo). Además, en ambos casos, los PMN fueron los leucocitos predominantes. RPV 0.5 µM no tuvo efecto sobre la infiltración leucocitaria (0,9 ± 0,6 vs. DMSO: 0,9 ± 0,1 leucocitos/campo) (TABLA 11 y FIGURA 32). Estos resultados siguen el mismo patrón que los obtenidos mediante la técnica de microscopía intravital.

4.1.2.1.2. ANTAGONISTAS CCR5, InInt E IP

Analizamos el efecto de MVC, RAL, LPV, ATV y DRV sobre la infiltración leucocitaria en mesenterio de rata.

MRV, RAL, LPV, ATV y DRV no produjeron variaciones en la infiltración leucocitaria con respecto a sus correspondientes vehículos (TABLA 11 y FIGURA 32) en el tejido mesentérico.

TABLA 11: Infiltración de leucocitos producida por los fármacos ITINAN, antagonistas CCR5, InInt e IP en mesenterio de rata.

	Neutrófilos	Macrófagos
Control	0,5±0,3	0,5±0,4
Metanol	1,0±0,3	1,2±0,2
Agua ácida	0,7±0,3	0,5±0,2
DMSO	0,9±0,1	0,3±0,2
EFV 15 µM	17,7±3,3 **, ++	2,0±0,3
NVP 25 µM	5,6±0,4 &&	1,1±0,2
RPV 0.5 µM	0,9±0,6	0,2±0,1
MVC 5 µM	0,4±0,3	0,2±0,1
RAL 5 µM	0,2±0,1	0,2±0,1
LPV 25 µM	0,7±0,2	0,3±0,2
ATV 25 µM	0,6±0,1	0,2±0,1
DRV 25 µM	0,4±0,3	0,2±0,1

Las ratas fueron tratadas intraperitonealmente (4 h) con Efavirenz (EFV, 15 µM), Nevirapina (NVP, 25 µM), Rilpivirina (RPV, 0.5 µM), Maraviroc (MVC, 5 µM), Raltegravir (RAL, 5 µM), Lopinavir (LPV, 25 µM), Atazanavir (ATV, 25 µM), Darunavir (DRV, 25 µM), sus correspondientes vehículos (metanol, agua ácida o DMSO) o control (suero fisiológico). El mesenterio seleccionado para los experimentos de microscopía intravital fue retirado, fijado con paraformaldehido y teñido con Hematoxilina-Eosina y el número de leucocitos infiltrados (neutrófilos, macrófagos y linfocitos) fue analizado en un área de 2.5 x 10^{-4} cm^2. Los resultados fueron expresados como Media ± E.E.M. (n = 4-5). **p<0,01 respecto del valor correspondiente al grupo tratado con metanol, &&p<0,01 respecto del valor correspondiente al grupo tratado con agua ácida y ++p<0,01 respecto del valor correspondiente al grupo tratado con NVP 25 µM. Análisis de varianza ANOVA seguido del post-test Newman-Keuls.

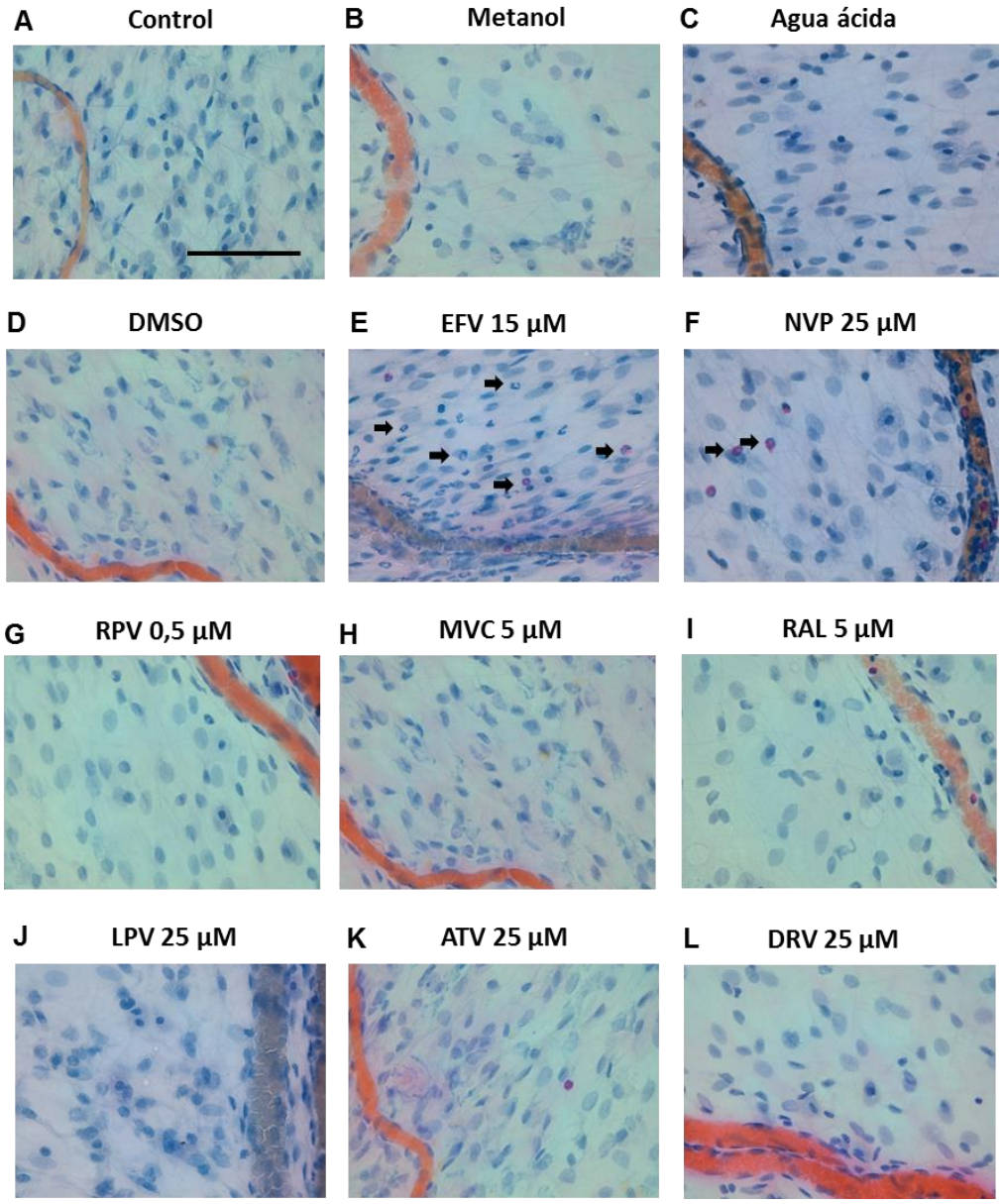

FIGURA 32. Imágenes representativas de la infiltración leucocitaria producida por los fármacos antagonistas CCR5, ITINAN, InInt e IP en mesenterio de rata. Las ratas fueron tratadas intraperitonealmente (4 h) con Efavirenz (EFV, 25 µM), Nevirapina (NVP, 25 µM), Rilpivirina (RPV, 0.5 µM), Maraviroc (MVC, 5 µM), Raltegravir (RAL, 5 µM), Lopinavir (LPV, 25 µM), Atazanavir (ATV, 25 µM), Darunavir (DRV, 25 µM), sus correspondientes vehículos (metanol, agua ácida o DMSO) o control (suero fisiológico). El mesenterio seleccionado para los experimentos de microscopía intravital fue recogido, fijado con paraformaldehido y teñido con Hematoxilina-Eosina, y el número de leucocitos infiltrados (neutrófilos y macrófagos) fue analizado en un área de 2.5 x 10^{-4} cm^2 en animales tratados con suero fisiológico (**A**), metanol (**B**), agua ácida (**C**), DMSO (**D**), EFV (**E**), NVP (**F**), RPV (**G**), MVC (**H**), RAL (**I**), LPV (**J**), ATV (**K**) y DRV (**L**). Las flechas (➡) indican ejemplos de neutrófilos infiltrados. Barra = 50 µm.

4.1.2.2. EFECTO DE LAS COMBINACIONES DE LOS FÁRMACOS ANTIRRETROVIRALES MÁS EMPLEADAS EN LA TERAPEÚTICA ACTUAL

Se analizaron las combinaciones de fármacos TDF/FTC/EFV, ABC/3TC/EFV, TDF/FTC/RPV, ABC/3TC/RPV, TDF/FTC/ATV, ABC/3TC/ATV, TDF/FTC/DRV, ABC/3TC/DRV sobre la infiltración leucocitaria en mesenterio de rata.

El análisis de las tinciones Hematoxilina-Eosina confirmó que las combinaciones TDF/FTC/EFV, ABC/3TC/EFV, ABC/3TC/RPV produjeron un mayor número de leucocitos infiltrados con respecto a sus correspondientes vehículos (TABLA 12 y FIGURA 33) y que en todos los casos, los PMN fueron los leucocitos predominantes. TDF/FTC/RPV, TDF/FTC/ATV, ABC/3TC/ATV, TDF/FTC/DRV y ABC/3TC/DRV no produjeron una mayor infiltración leucocitaria (TABLA 12 y FIGURA 33). Cabe destacar que los tratamientos ABC/3TC/ATV y ABC/3TC/DRV no produjeron dicha infiltración leucocitaria, si bien, resultados realizados anteriomente en nuestro laboratorio indican que ABC si que produce migración leucocitaria en mesenterio de rata (De Pablo et al., 2013). Los resultados obtenidos por esta técnica concuerdan en todos los casos con los obtenidos mediante de microscopía intravital.

TABLA 12: Infiltración de leucocitos producida por las combinaciones de los fármacos antirretrovirales más utilizadas en mesenterio de rata.

	Neutrófilos	Macrófagos
Control	0,7±0,2	0,7±0,2
Metanol	1,0±0,3	0,6±0,1
DMSO	0,8±0,1	0,6±0,1
TDF/FTC/EFV	19,4±4,1 **	1,2±0,5
ABC/3TC/EFV	10,7±2,3 **	1,8±0,4
TDF/FTC/RPV	0,7±0,3	0,4±0,1
ABC/3TC/RPV	7,6±3,2 ^^	0,5±0,1
TDF/FTC/ATV	1,2±0,2	0,7±0,1
ABC/3TC/ATV	0,2±0,1	0,3±0,2
TDF/FTC/DRV	0,9±0,2	0,4±0,1
ABC/3TC/DRV	0,3±0,2	0,4±0,1

Las ratas fueron tratadas intraperitonealmente (4 h) con las combinaciones TDF/FTC/EFV, ABC/3TC/EFV, TDF/FTC/RPV, ABC/3TC/RPV, TDF/FTC/ATV, ABC/3TC/ATV, TDF/FTC/DRV, ABC/3TC/DRV, sus correspondientes vehículos (metanol o DMSO) o control (suero fisiológico). Las concentraciones utilizadas fueron TDF 1 µM, FTC 10 µM, EFV 15 µM, ABC 10 µM, 3TC 10 µM, RPV 0.5 µM, ATV 10 µM y DRV 10 µM. El mesenterio seleccionado para los experimentos de microscopía intravital fue retirado, fijado con paraformaldehido y teñido con Hematoxilina-Eosina y el número de leucocitos infiltrados (neutrófilos, macrófagos y linfocitos) fue analizado en un área de 2.5×10^{-4} cm^2 en animales tratados. Los resultados fueron expresados como Media ± E.E.M. (n = 4-5). **$p<0.01$ respecto del valor correspondiente al grupo tratado con metanol y ^^$p<0.01$ respecto del valor correspondiente al grupo tratado con DMSO). Análisis de varianza ANOVA seguido del post-test Newman-Keuls.

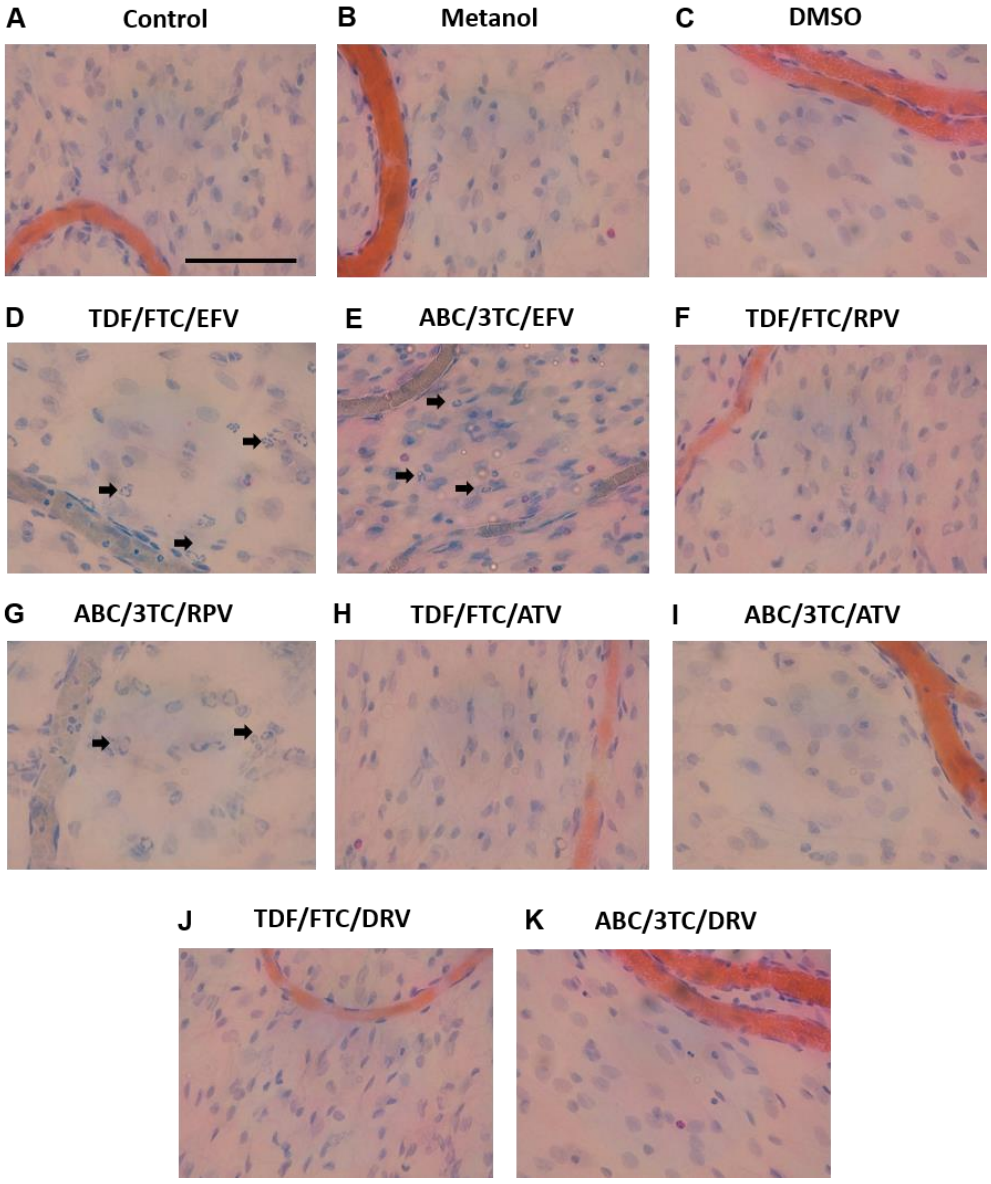

<u>FIGURA 33</u>. Imágenes representativas de la infiltración leucocitaria producida por las combinaciones de los fármacos antirretrovirales más utilizadas en mesenterio de rata. Las ratas fueron tratadas intraperitonealmente (4 h) con las combinaciones TDF/FTC/EFV, ABC/3TC/EFV, TDF/FTC/RPV, ABC/3TC/RPV, TDF/FTC/ATV, ABC/3TC/ATV, TDF/FTC/DRV, ABC/3TC/DRV, sus correspondientes vehículos (metanol o DMSO) o control (suero fisiológico). Las concentraciones utilizadas fueron TDF 1 µM, FTC 10 µM, EFV 15 µM, ABC 10 µM, 3TC 10 µM, RPV 0.5 µM, ATV 10 µM y DRV 10 µM. El mesenterio seleccionado para los experimentos de microscopía intravital fue retirado, fijado con paraformaldehido y teñido con Hematoxilina-Eosina, y el número de leucocitos infiltrados (neutrófilos, macrófagos y linfocitos) fue analizado en un área de 2.5 x 10^{-4} cm^2 en animales tratados con suero fisiológico (**A**), metanol (**B**), DMSO (**C**), TDF/FTC/EFV (**D**), ABC/3TC/EFV (**E**), TDF/FTC/RPV (**F**), ABC/3TC/RPV (**G**), TDF/FTC/ATV (**H**), ABC/3TC/ATV (**I**), TDF/FTC/DRV (**J**) y ABC/3TC/DRV (**K**). Las flechas (➡) indican ejemplos de neutrófilos infiltrados. Barra = 50 µm.

4.1.3. ESTUDIO DEL MECANISMO RESPONSABLE DE LA INTERACCIÓN LEUCOCITO-ENDOTELIO INDUCIDA POR LOS FÁRMACOS ITINAN *IN VIVO*

Con el fin de estudiar la posible implicación de las moléculas de adhesión en la interacción leucocito-endotelio inducida por los fármacos ITINAN, empleamos la técnica de microscopía intravital en mesenterio de rata administrando por vía intravenosa (i.v.) anticuerpos bloqueantes frente a distintas moléculas de adhesión (CD11b, CD18 e ICAM-1) 30 minutos antes del tratamiento de los animales con EFV, NVP o RPV.

Así, la interacción leucocito-endotelio inducida por EFV (FIGURA 34), y por RPV (FIGURA 36) fue completamente bloqueada mediante anticuerpos frente a CD11b, CD18 o ICAM-1. Las interacciones inducidas por NVP no fueron bloqueadas con el uso de los anticuerpos citados anteriormente (FIGURA 35), sugiriendo que habría otras moléculas implicadas en este proceso.

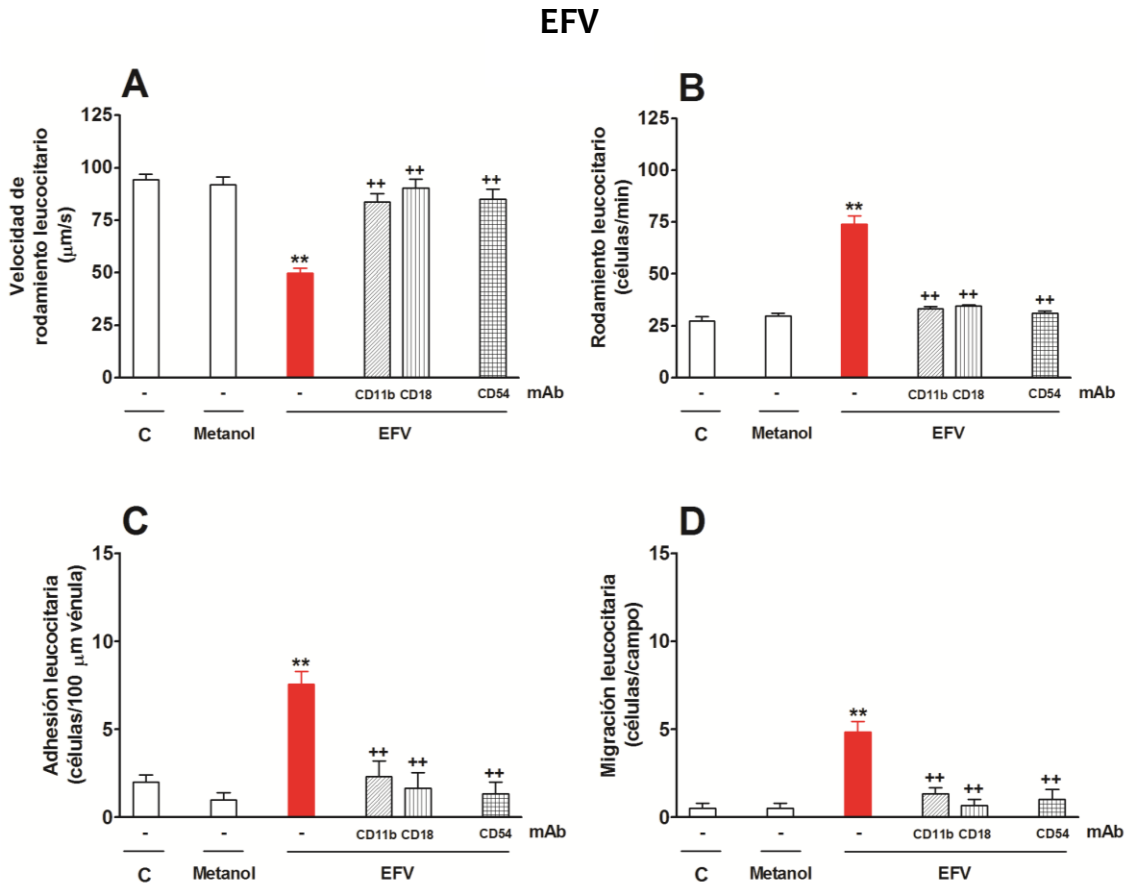

FIGURA 34. Estudio del mecanismo responsable de la interacción leucocito-endotelio inducida por Efavirenz *in vivo*. Se analizó la velocidad de rodamiento (A), el rodamiento (B), la adhesión (C) y la migración leucocitaria (D). Las ratas fueron pretratadas (i.v.) con los anticuerpos bloqueantes (anti-CD11b, anti-CD18, anti-CD54 o anticuerpo control) durante 30 min previo al tratamiento con Efavirenz (EFV, 15 µM), su correspondiente vehículo (metanol) o control (suero fisiológico) por vía intraperitoneal (4 h). Los resultados fueron expresados como Media ± E.E.M. (n = 4). **p<0,01 respecto del valor correspondiente al grupo tratado con metanol y $^{++}$p<0,01 respecto del valor correspondiente al grupo tratado con EFV 15 µM. Análisis de varianza ANOVA seguido del post-test Newman-Keuls.

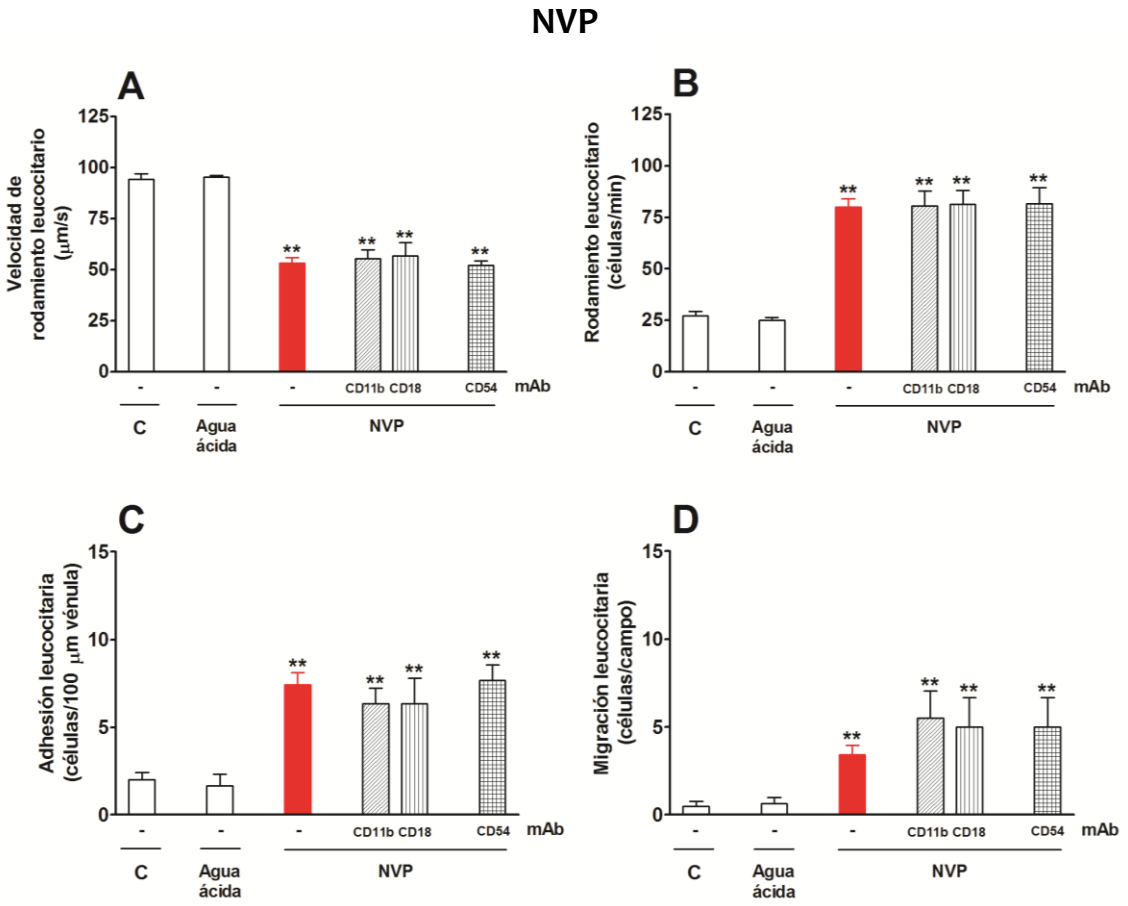

FIGURA 35. Estudio del mecanismo responsable de la interacción leucocito-endotelio inducida por Nevirapina *in vivo*. Se analizó la velocidad de rodamiento (A), el rodamiento (B), la adhesión (C) y la migración leucocitaria (D). Las ratas fueron pretratadas (i.v.) con los anticuerpos bloqueantes (anti-CD11b, anti-CD18, anti-CD54 o anticuerpo control) durante 30 min previo al tratamiento con Nevirapina (NVP, 25 µM), su correspondiente vehículo (agua ácida) o control (suero fisiológico) por vía intraperitoneal (4 h). Los resultados fueron expresados como Media ± E.E.M. (n = 4). **p<0,01 respecto del valor correspondiente al grupo tratado con agua ácida. Análisis de varianza ANOVA seguido del post-test Newman-Keuls.

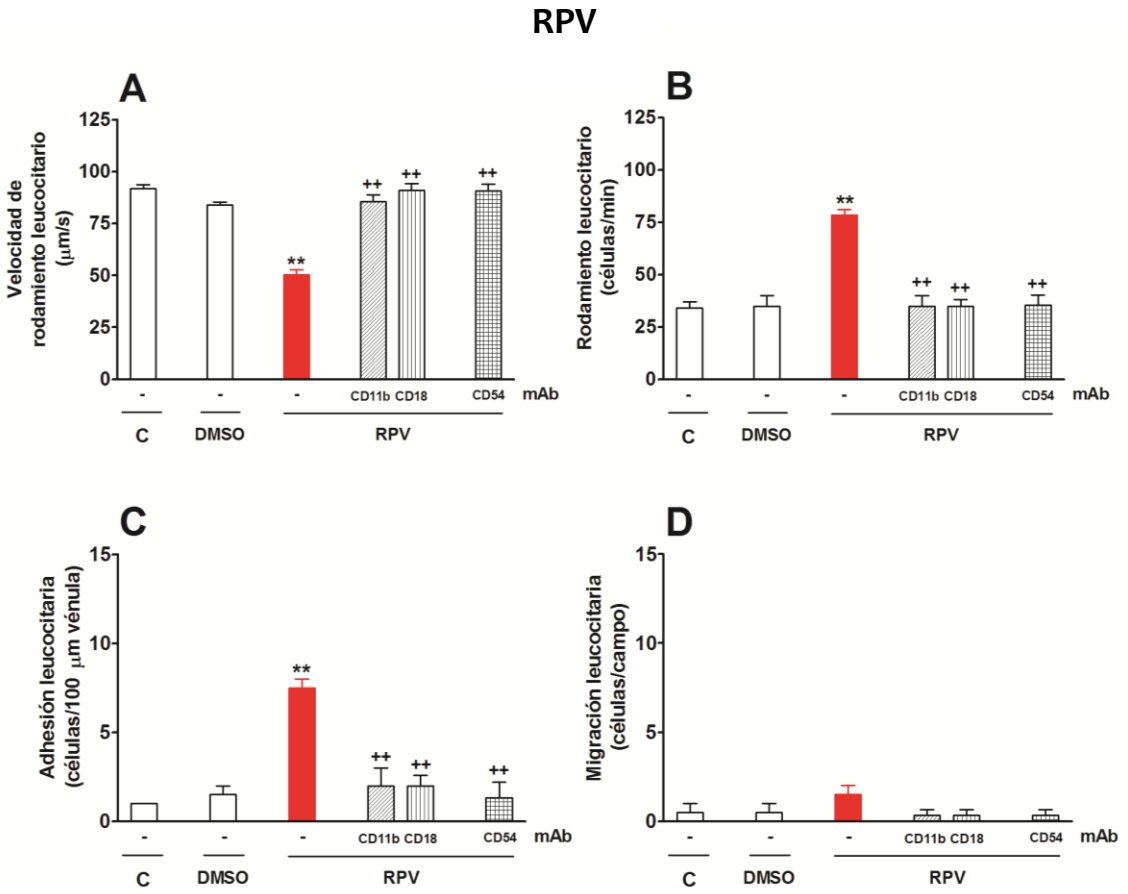

FIGURA 36. Estudio del mecanismo responsable de la interacción leucocito-endotelio inducida por Rilpivirina *in vivo*. Se analizó la velocidad de rodamiento (A), el rodamiento (B), la adhesión (C) y la migración leucocitaria (D). Las ratas fueron pretratadas (i.v.) con los anticuerpos bloqueantes (anti-CD11b, anti-CD18, anti-CD54 o anticuerpo control) durante 30 min previo al tratamiento con Rilpivirina (RPV, 0.5 µM), su correspondiente vehículo (DMSO) o control (suero fisiológico) por vía intraperitoneal (4 h). Los resultados fueron expresados como Media ± E.E.M. (n = 4). **p<0,01 respecto del valor correspondiente al grupo tratado con DMSO y $^{++}$p<0,01 respecto del valor correspondiente al grupo tratado con RPV 0.5 µM. Análisis de varianza ANOVA seguido del post-test Newman-Keuls.

4.2. ESTUDIOS *IN VITRO*

4.2.1. ESTUDIO DEL EFECTO DE LOS FÁRMACOS ANTIRRETROVIRALES SOBRE LA INTERACCIÓN LEUCOCITO-ENDOTELIO *IN VITRO*

4.2.1.1. EFECTO DE LOS FÁRMACOS ADMINISTRADOS INDIVIDUALMENTE

4.2.1.1.1. ITINAN

Se analizó el efecto de EFV, NVP y RPV sobre la interacción leucocito-endotelio *in vitro* utilizando el modelo de adhesión dinámica en cámara paralela de flujo.

En células humanas, EFV, NVP y RPV produjeron una disminución significativa y dosis dependiente de la velocidad de rodamiento (FIGURA 37A, 39A y 41A), así como un aumento del rodamiento (FIGURA 37B, 39B y 41B), y la adhesión de PMN (FIGURA 37C, 39C y 41C) a HUVEC. Resultados similares se obtuvieron cuando se analizó la interacción PBMC/HUVEC (FIGURA 38, 40 y 42).

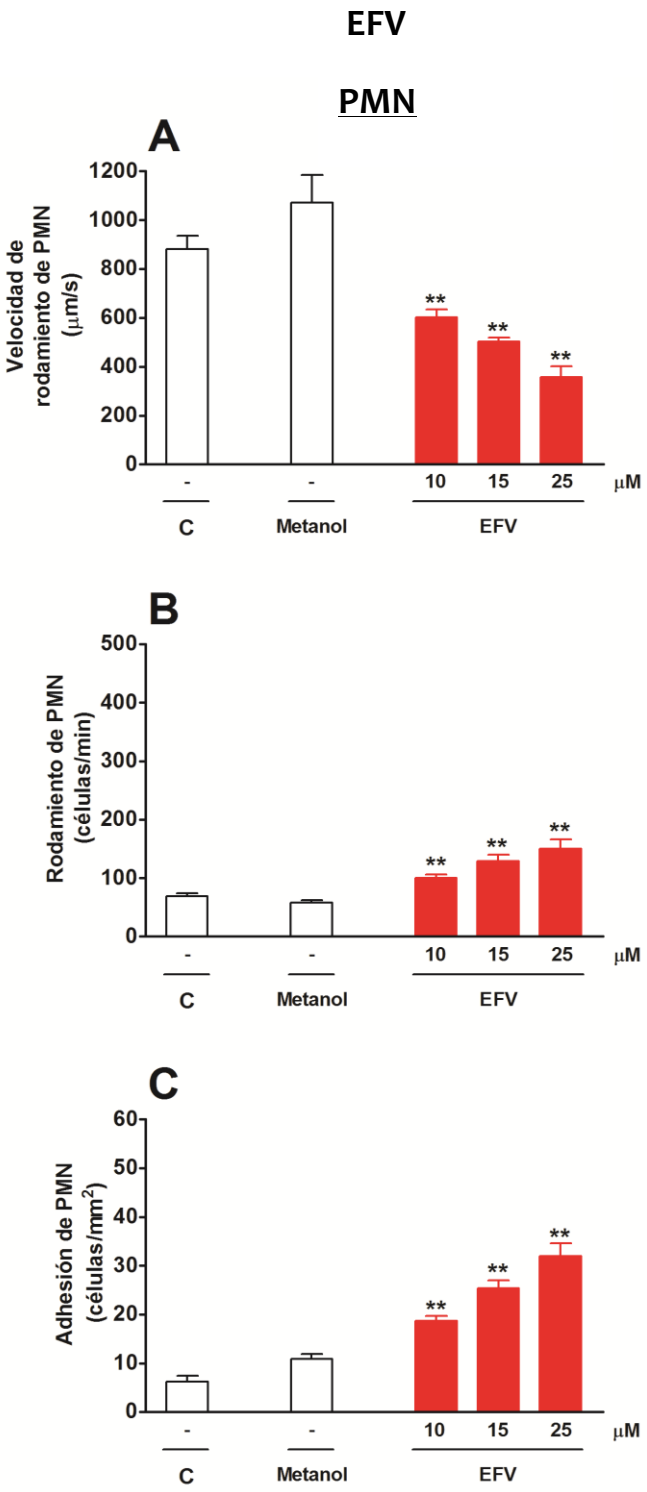

FIGURA 37. Efecto de Efavirenz sobre la interacción de PMN sobre el endotelio venular. Se analizó la velocidad de rodamiento (A), el rodamiento (B) y la adhesión leucocitaria (C). PMN y HUVEC fueron tratados independientemente (4 h) con Efavirenz (EFV, 10-25 μM), su correspondiente vehículo (metanol) o control (medio de cultivo o agua estéril). Los resultados fueron expresados como Media ± E.E.M. (n = 4-6). **p<0,01 respecto del valor correspondiente al grupo tratado con metanol. Análisis de varianza ANOVA seguido del post-test Newman-Keuls.

EFV

PBMC

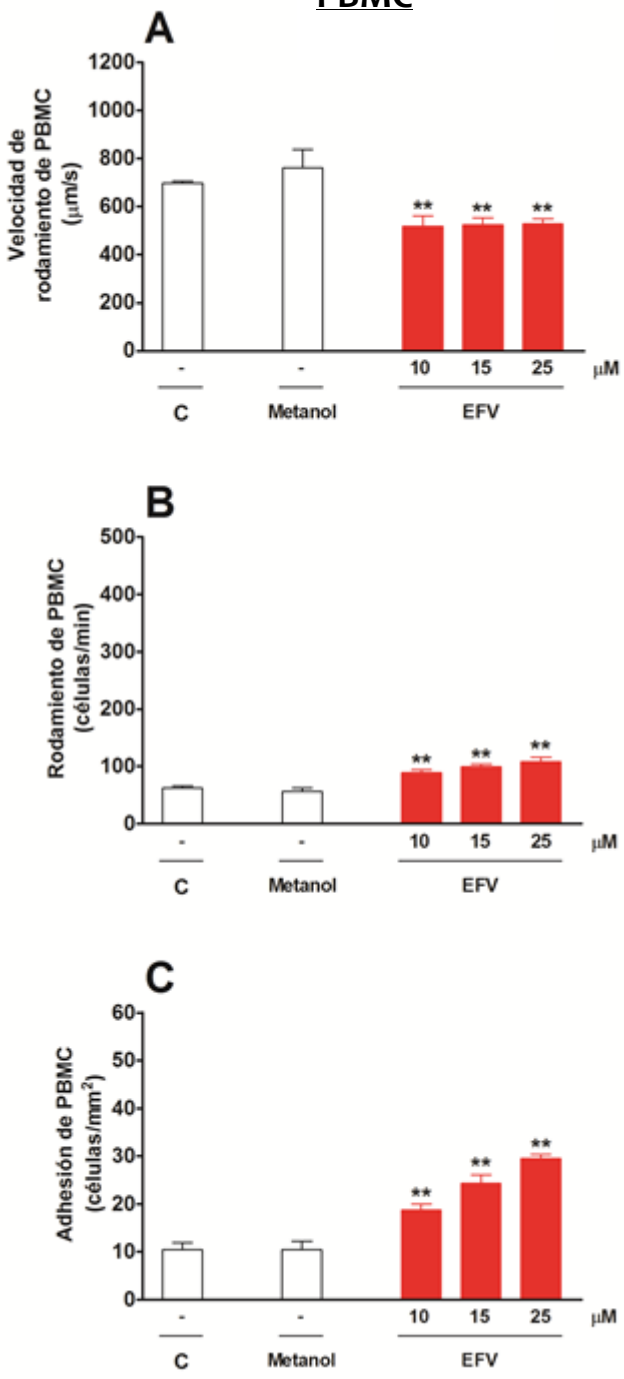

FIGURA 38. Efecto de Efavirenz sobre la interacción de PBMC sobre el endotelio venular. Se analizó la velocidad de rodamiento (A), el rodamiento (B) y la adhesión leucocitaria (C). PBMC y HUVEC fueron tratados independientemente (4 h) con Efavirenz (EFV, 10-25 μM), su correspondiente vehículo (metanol) o control (medio de cultivo o agua estéril). Los resultados fueron expresados como Media ± E.E.M. (n = 4). **p<0,01 respecto del valor correspondiente al grupo tratado con metanol. Análisis de varianza ANOVA seguido del post-test Newman-Keuls.

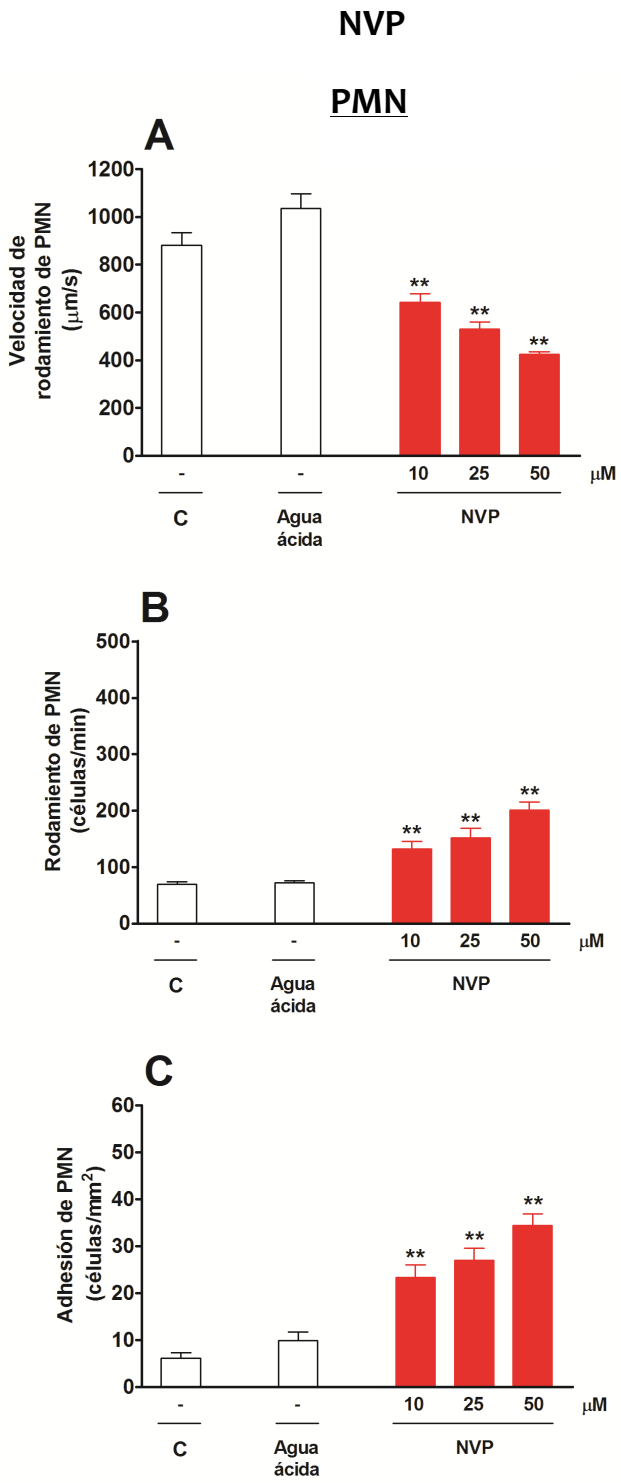

FIGURA 39. Efecto de Nevirapina sobre la interacción de PMN sobre el endotelio venular. Se analizó la velocidad de rodamiento (A), el rodamiento (B) y la adhesión leucocitaria (C). PMN y HUVEC fueron tratados independientemente (4 h) con Nevirapina (NVP, 10-50 μM), su correspondiente vehículo (agua ácida) o control (medio de cultivo o agua estéril). Los resultados fueron expresados como Media ± E.E.M. (n = 4-5). **p<0,01 respecto del valor correspondiente al grupo tratado con agua ácida. Análisis de varianza ANOVA seguido del post-test Newman-Keuls.

NVP

PBMC

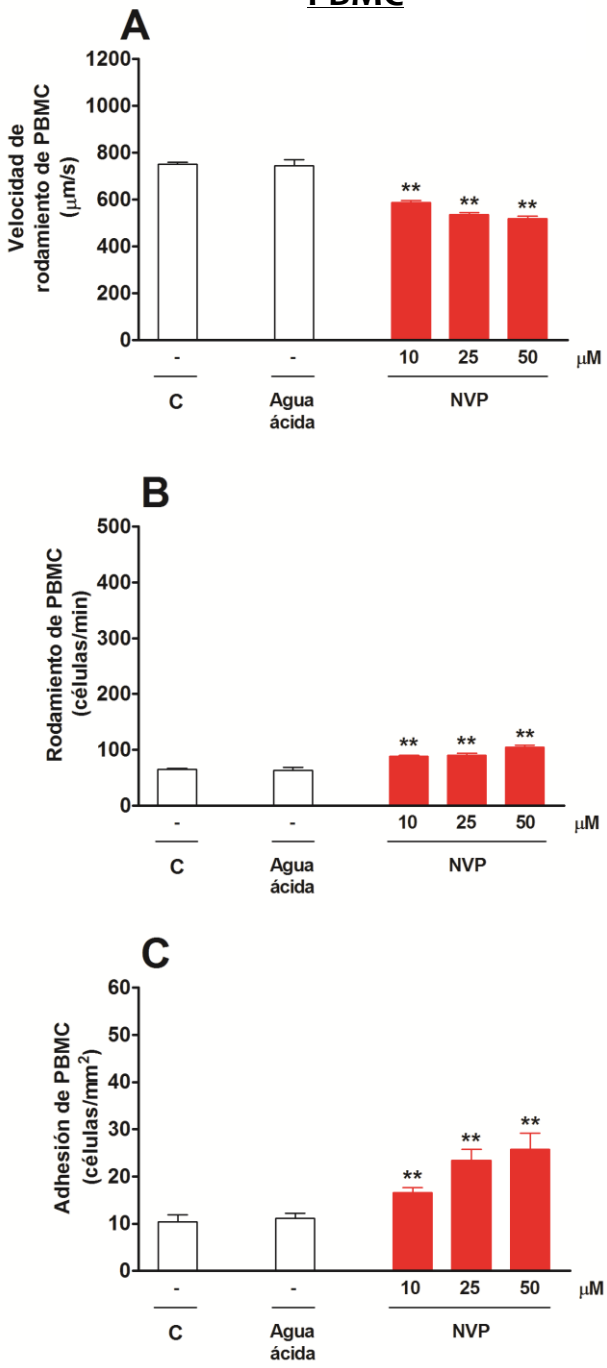

FIGURA 40. Efecto de Nevirapina sobre la interacción de PBMC sobre el endotelio venular. Se analizó la velocidad de rodamiento (A), el rodamiento (B) y la adhesión leucocitaria (C). PBMC y HUVEC fueron tratados independientemente (4 h) con Nevirapina (NVP, 10-50 μM), su correspondiente vehículo (agua ácida) o control (medio de cultivo o agua estéril). Los resultados fueron expresados como Media ± E.E.M. (n = 5). **p<0,01 respecto del valor correspondiente al grupo tratado con agua ácida. Análisis de varianza ANOVA seguido del post-test Newman-Keuls.

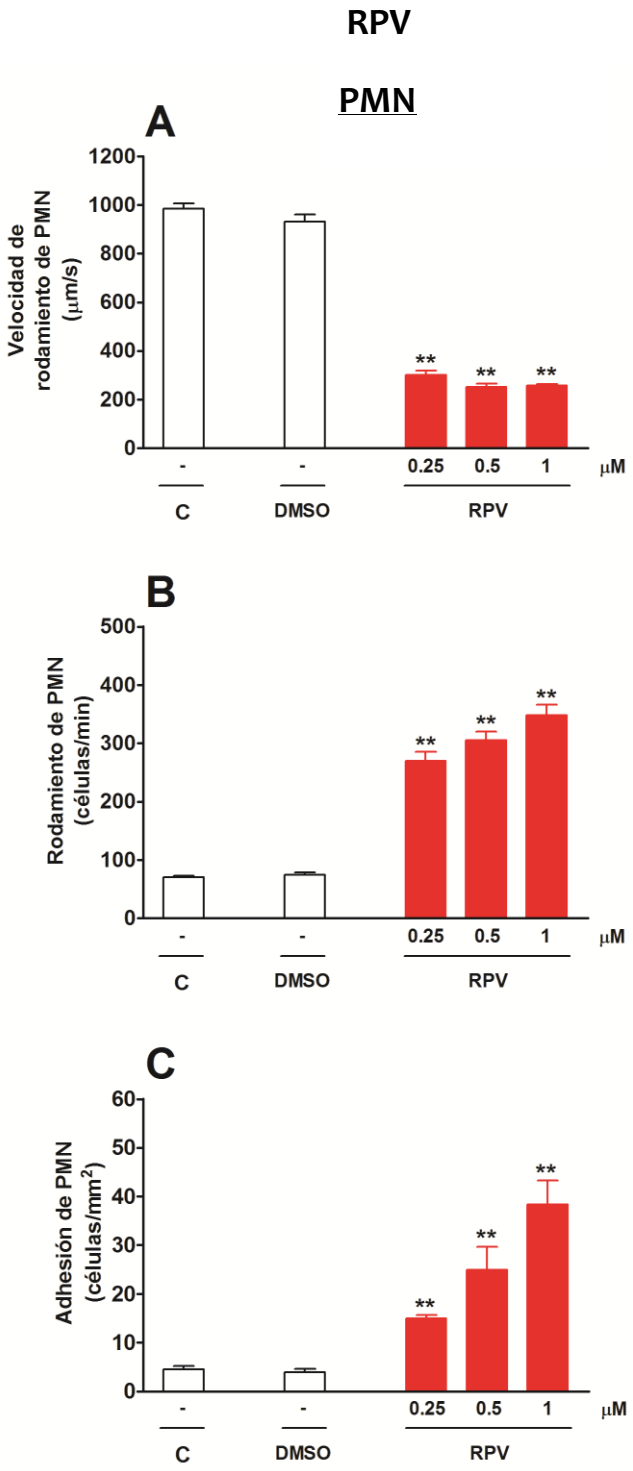

FIGURA 41. Efecto de Rilpivirina sobre la interacción de PMN sobre el endotelio venular. Se analizó la velocidad de rodamiento (A), el rodamiento (B) y la adhesión leucocitaria (C). PMN y HUVEC fueron tratados independientemente (4 h) con Rilpivirina (RPV, 0.25-1 µM), su correspondiente vehículo (DMSO) o control (medio de cultivo o agua estéril). Los resultados fueron expresados como Media ± E.E.M. (n = 4). **p<0,01 respecto del valor correspondiente al grupo tratado con DMSO. Análisis de varianza ANOVA seguido del post-test Newman-Keuls.

RPV

PBMC

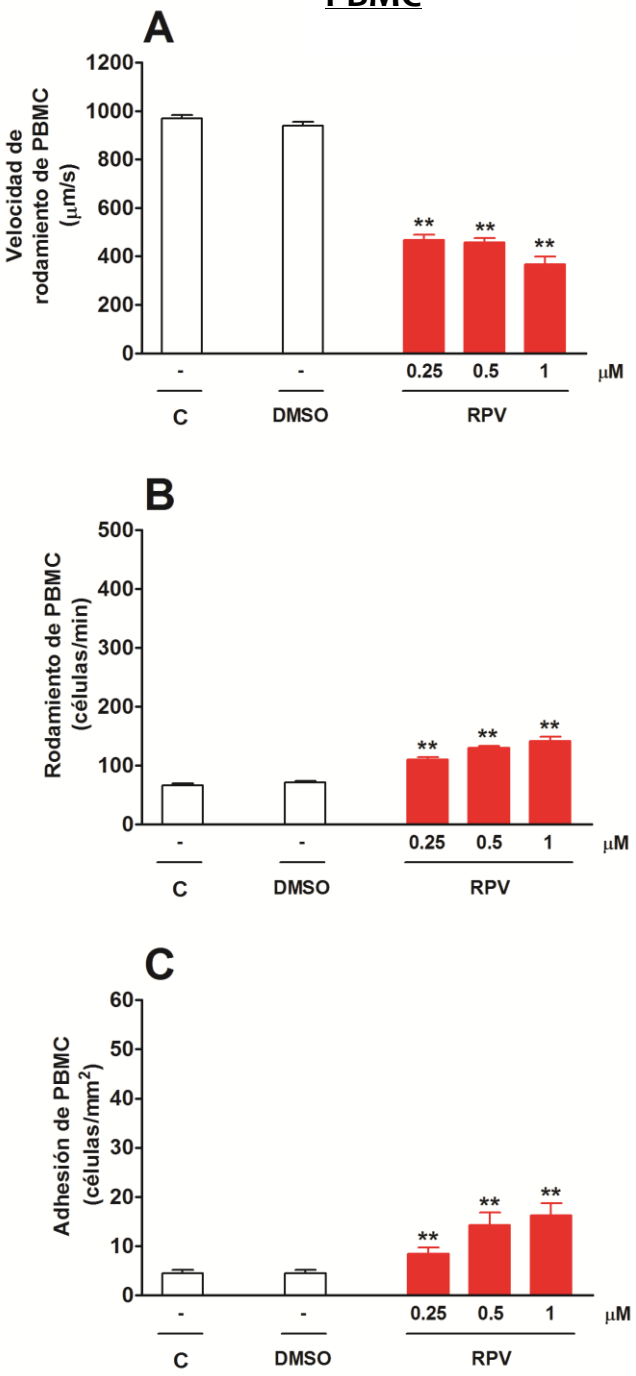

FIGURA 42. Efecto de Rilpivirina sobre la interacción de PMN sobre el endotelio venular. Se analizó la velocidad de rodamiento (A), el rodamiento (B) y la adhesión leucocitaria (C). PBMC y HUVEC fueron tratados independientemente (4 h) con Rilpivirina (RPV, 0.25-1 μM), su correspondiente vehículo (DMSO) o control (medio de cultivo o agua estéril). Los resultados fueron expresados como Media ± E.E.M. (n = 4). **p<0,01 respecto del valor correspondiente al grupo tratado con DMSO. Análisis de varianza ANOVA seguido del post-test Newman-Keuls.

4.2.1.1.2. ANTAGONISTAS CCR5, InInt E IP

Analizamos el efecto de MVC, RAL, LPV, ATV y DRV sobre la interacción leucocito-endotelio *in vitro* utilizando el modelo de adhesión dinámica en cámara paralela de flujo.

En células humanas, MVC, RAL, LPV, ATV y DRV no produjeron ninguna variación en los parámetros leucocitarios analizados utilizando PMN (FIGURA 43) o PBMC (FIGURA 44).

PMN

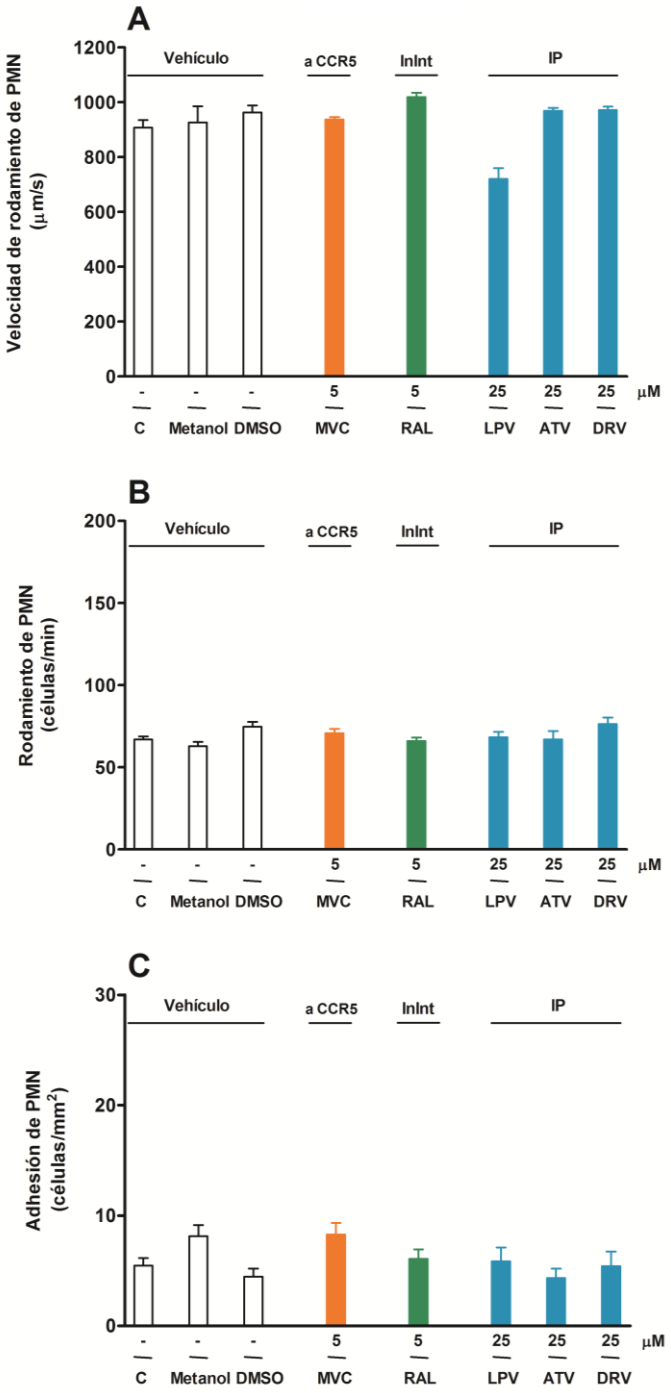

FIGURA 43. Efecto de los fármacos antagonistas CCR5, InInt e IP sobre la interacción de e PMN sobre el endotelio venular. Se analizó la velocidad de rodamiento (A), el rodamiento (B) y la adhesión leucocitaria (C). PMN y HUVEC fueron tratados independientemente (4 h) con Maraviroc (MVC, 5 µM), Raltegravir (RAL, 5 µM), Lopinavir (LPV, 25 µM), Atazanavir (ATV, 25 µM), Darunavir (DRV, 25 µM), sus correspondientes vehículos (metanol o DMSO) o control (medio de cultivo o agua estéril). Los resultados fueron expresados como Media ± E.E.M. (n = 4-8). Análisis de varianza ANOVA seguido del post-test Newman-Keuls.

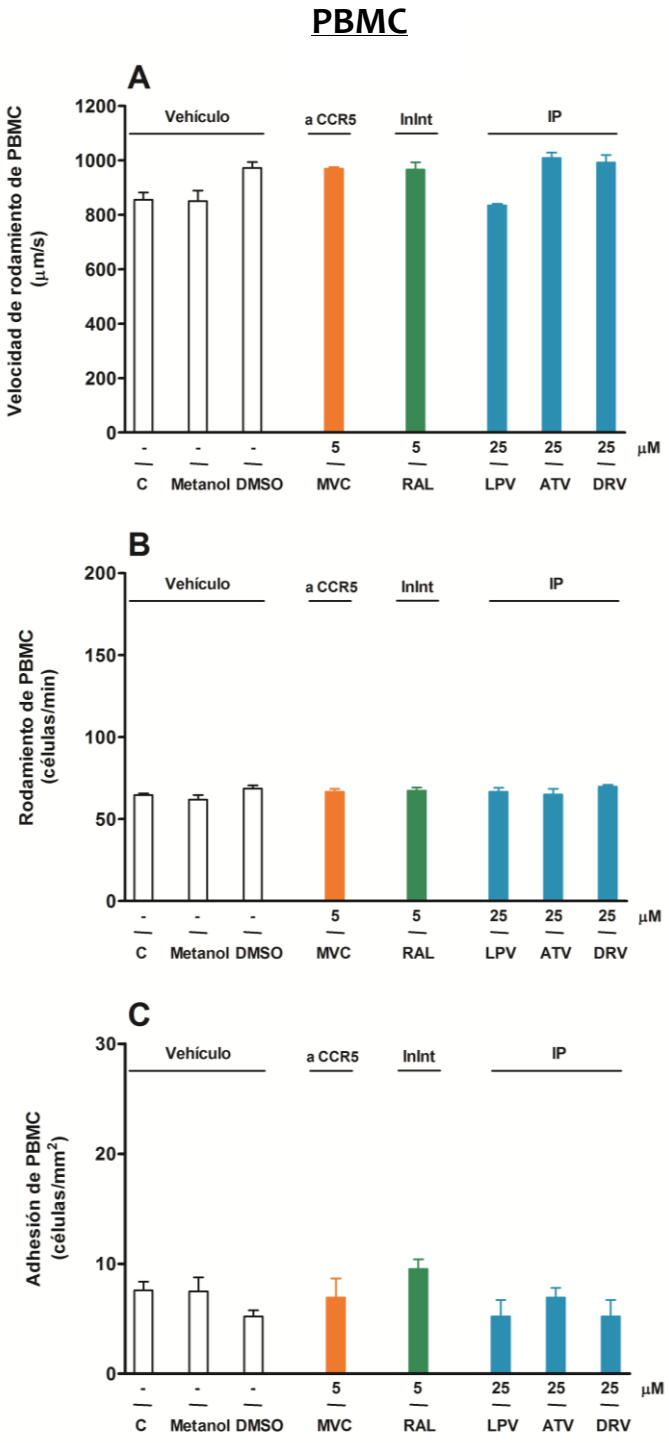

FIGURA 44. Efecto de los fármacos antagonistas CCR5, InInt e IP sobre la interacción de PBMC sobre el endotelio venular. Se analizó la velocidad de rodamiento (A), el rodamiento (B) y la adhesión leucocitaria (C). PBMC y HUVEC fueron tratados independientemente (4 h) con Maraviroc (MVC, 5 µM), Raltegravir (RAL, 5 µM), Lopinavir (LPV, 25 µM), Atazanavir (ATV, 25 µM), Darunavir (DRV, 25 µM), sus correspondientes vehículos (metanol o DMSO) o control (medio de cultivo o agua estéril). Los resultados fueron expresados como Media ± E.E.M. (n = 4-8). Análisis de varianza ANOVA seguido del post-test Newman-Keuls.

4.2.1.2. EFECTO DE LAS COMBINACIONES DE FÁRMACOS ANTIRRETROVIRALES MÁS EMPLEADAS EN LA TERAPEÚTICA ACTUAL

Se analizaron las combinaciones de fármacos TDF/FTC/EFV, ABC/3TC/EFV, TDF/FTC/RPV, ABC/3TC/RPV, TDF/FTC/ATV, ABC/3TC/ATV, TDF/FTC/DRV, ABC/3TC/DRV sobre la interacción leucocito-endotelio *in vitro* mediante el modelo anteriomente citado.

En células humanas, las combinaciones TDF/FTC/EFV, ABC/3TC/EFV, TDF/FTC/RPV, ABC/3TC/RPV, ABC/3TC/ATV y ABC/3TC/DRV produjeron una disminución significativa de la velocidad de rodamiento, así como un aumento significativo del rodamiento y la adhesión tanto de PMN (FIGURA 45) como de PBMC (FIGURA 46) sobre HUVEC. Las combinaciones TDF/FTC/ATV y TDF/FTC/DRV no produjeron ninguna variación en los parámetros anteriormente citados (FIGURA 45 y 46).

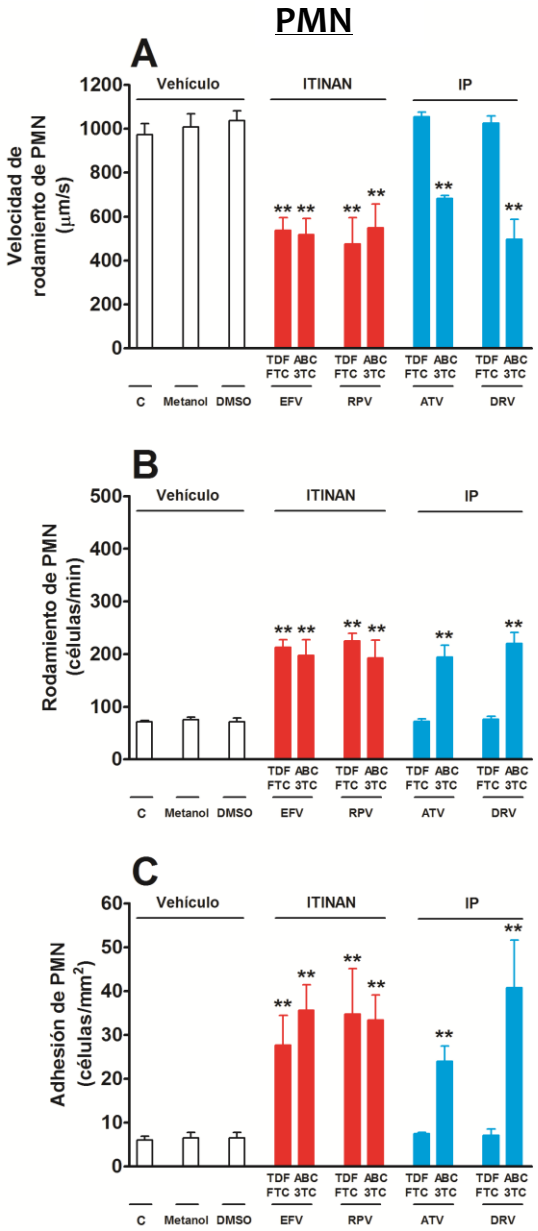

FIGURA 45. Efecto de las combinaciones de los fármacos antirretrovirales más utilizadas sobre la interacción de PMN sobre el endotelio venular. Se analizó la velocidad de rodamiento (A), el rodamiento (B) y la adhesión leucocitaria (C). PMN y HUVEC fueron tratados independientemente (4 h) con las combinaciones TDF/FTC/EFV, ABC/3TC/EFV, TDF/FTC/RPV, ABC/3TC/RPV, TDF/FTC/ATV, ABC/3TC/ATV, TDF/FTC/DRV, ABC/3TC/DRV, TDF/FTC/RAL, ABC/3TC/RAL, sus correspondientes vehículos (metanol o DMSO) o control (medio de cultivo o agua estéril). Las concentraciones utilizadas fueron TDF 1 µM, FTC 10 µM, EFV 15 µM, ABC 10 µM, 3TC 10 µM, RPV 0.5 µM, ATV 10 µM, DRV 10 µM y RAL 2 µM. Los resultados fueron expresados como Media ± E.E.M. (n = 4). **p<0,01 respecto del valor correspondiente al grupo tratado con metanol o DMSO. Análisis de varianza ANOVA seguido del post-test Newman-Keuls.

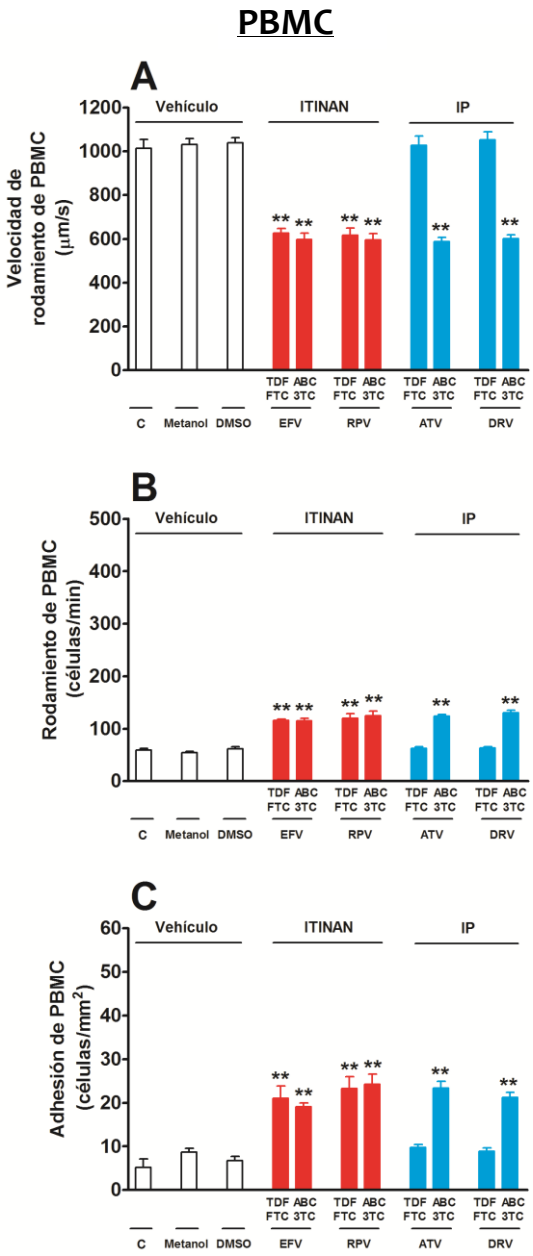

FIGURA 46. Efecto de las combinaciones de los fármacos antirretrovirales más utilizadas sobre la interacción de PBMC sobre el endotelio venular. Se analizó la velocidad de rodamiento (A), el rodamiento (B) y la adhesión leucocitaria (C). PBMC y HUVEC fueron tratados independientemente (4 h) con las combinaciones TDF/FTC/EFV, ABC/3TC/EFV, TDF/FTC/RPV, ABC/3TC/RPV, TDF/FTC/ATV, ABC/3TC/ATV, TDF/FTC/DRV, ABC/3TC/DRV, TDF/FTC/RAL, ABC/3TC/RAL, sus correspondientes vehículos (metanol o DMSO) o control (medio de cultivo o agua estéril). Las concentraciones utilizadas fueron TDF 1 µM, FTC 10 µM, EFV 15 µM, ABC 10 µM, 3TC 10 µM, RPV 0.5 µM, ATV 10 µM, DRV 10 µM y RAL 2 µM. Los resultados fueron expresados como Media ± E.E.M. (n = 4). **p<0,01 respecto del valor correspondiente al grupo tratado con metanol o DMSO. Análisis de varianza ANOVA seguido del post-test Newman-Keuls.

4.2.2. ESTUDIO DEL EFECTO DE LOS FÁRMACOS ANTIRRETROVIRALES SOBRE LA EXPRESIÓN DE MOLÉCULAS DE ADHESIÓN *IN VITRO*

4.2.2.1. EFECTO DE LOS FÁRMACOS ADMINISTRADOS INDIVIDUALMENTE

4.2.2.1.1. ITINAN

4.2.2.1.1.1. Células leucocitarias

Se analizó el efecto de EFV, NVP y RPV sobre la expresión de moléculas de adhesión leucocitarias *in vitro* utilizando la citometría de flujo.

EFV produjo el aumento en la expresión de CD11b, CD11c y CD18 en neutrófilos y monocitos (FIGURA 47 y 48), mientras que RPV aumentó la expresión de CD11b, CD11c y CD18 en neutrófilos, y únicamente CD11b en monocitos (FIGURA 51 y 52), no produciendo cambios en la expresión del resto de moléculas de adhesión analizadas en estas dos poblaciones leucocitarias, así como ningún cambio de expresión en las moléculas de adhesión analizadas en linfocitos (TABLA 13, 14 y 15). NVP, no modificó la expresión de las moléculas de adhesión analizadas en ninguna de las tres poblaciones leucocitarias (neutrófilos, monocitos y linfocitos) (FIGURA 49, 50 y TABLA 13, 14 y 15).

EFV

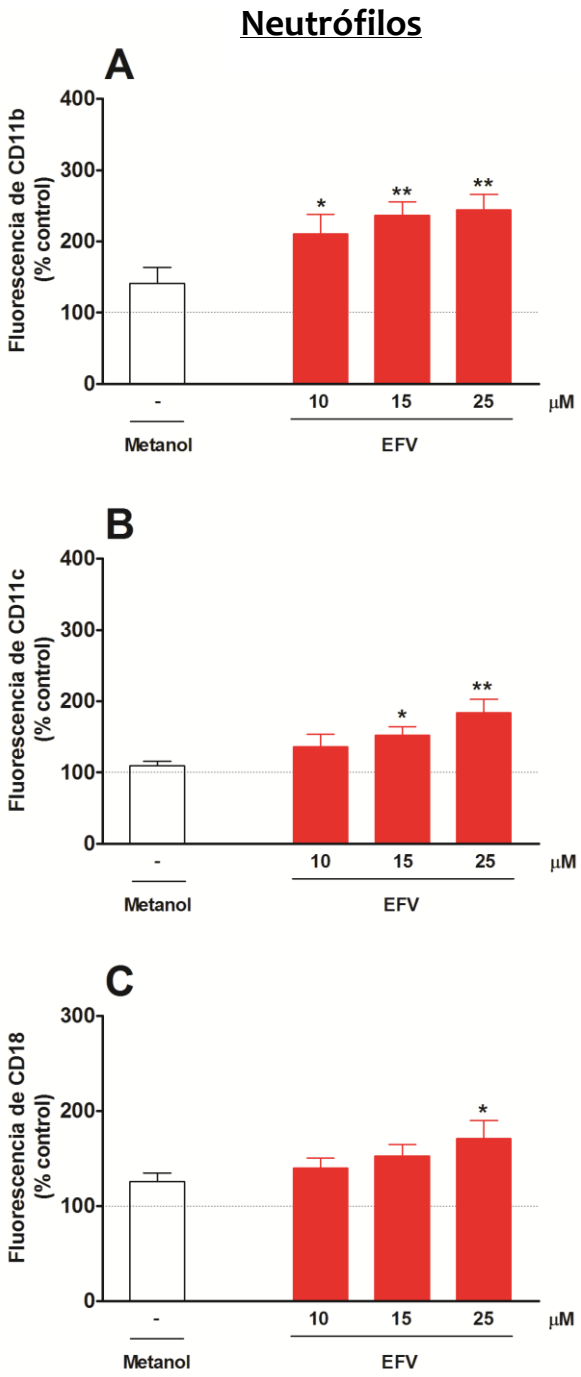

FIGURA 47. Efecto de Efavirenz sobre la expresión de moléculas de adhesión leucocitarias en neutrófilos de sangre humana. Se analizó la expresión de CD11b (A), CD11c (B) y CD18 (C). La sangre humana fue tratada con Efavirenz (EFV, 10-25 µM), su correspondiente vehículo (metanol) o control (agua estéril) (4 h). Los valores de fluorescencia (FITC o PE) representan el % de la mediana de la intensidad de la fluorescencia respecto del grupo control (agua estéril). Los resultados fueron expresados como Media ± E.E.M. (n = 5). *p<0,05 ó **p<0,01 respecto del valor correspondiente al grupo tratado con metanol. Análisis de varianza ANOVA seguido del post-test Newman-Keuls.

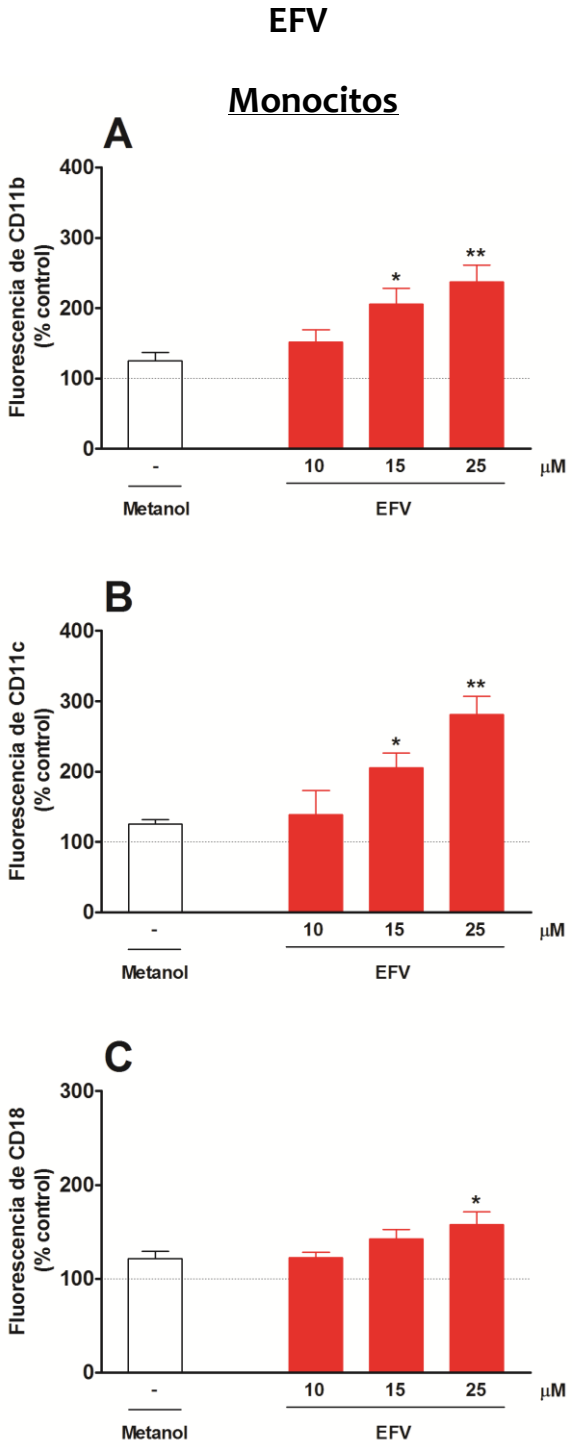

FIGURA 48. Efecto de Efavirenz sobre la expresión de moléculas de adhesión leucocitarias en monocitos de sangre humana. Se analizó la expresión de CD11b (A), CD11c (B) y CD18 (C). La sangre humana fue tratada con Efavirenz (EFV, 10-25 µM), su correspondiente vehículo (metanol) o control (agua estéril) (4 h). Los valores de fluorescencia (FITC o PE) representan el % de la mediana de la intensidad de la fluorescencia respecto del grupo control (agua estéril). Los resultados fueron expresados como Media ± E.E.M. (n = 4). *p<0,05 ó **p<0,01 respecto del valor correspondiente al grupo tratado con metanol. Análisis de varianza ANOVA seguido del post-test Newman-Keuls.

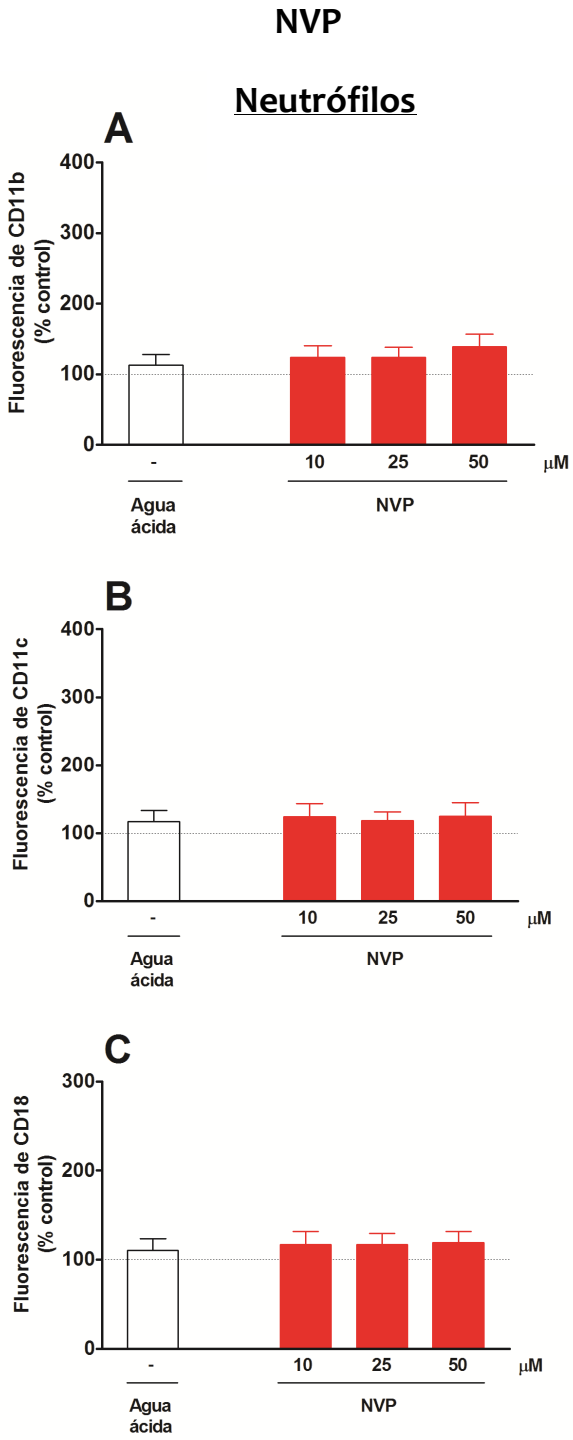

FIGURA 49. Efecto de Nevirapina sobre la expresión de moléculas de adhesión leucocitarias en neutrófilos de sangre humana. Se analizó la expresión de CD11b (A), CD11c (B) y CD18 (C). La sangre humana fue tratada con Nevirapina (NVP, 10-50 µM), su correspondiente vehículo (agua ácida) o control (agua estéril) (4 h). Los valores de fluorescencia (FITC o PE) representan el % de la mediana de la intensidad de la fluorescencia respecto del grupo control (agua estéril). Los resultados fueron expresados como Media ± E.E.M. (n = 5). Análisis de varianza ANOVA seguido del post-test Newman-Keuls.

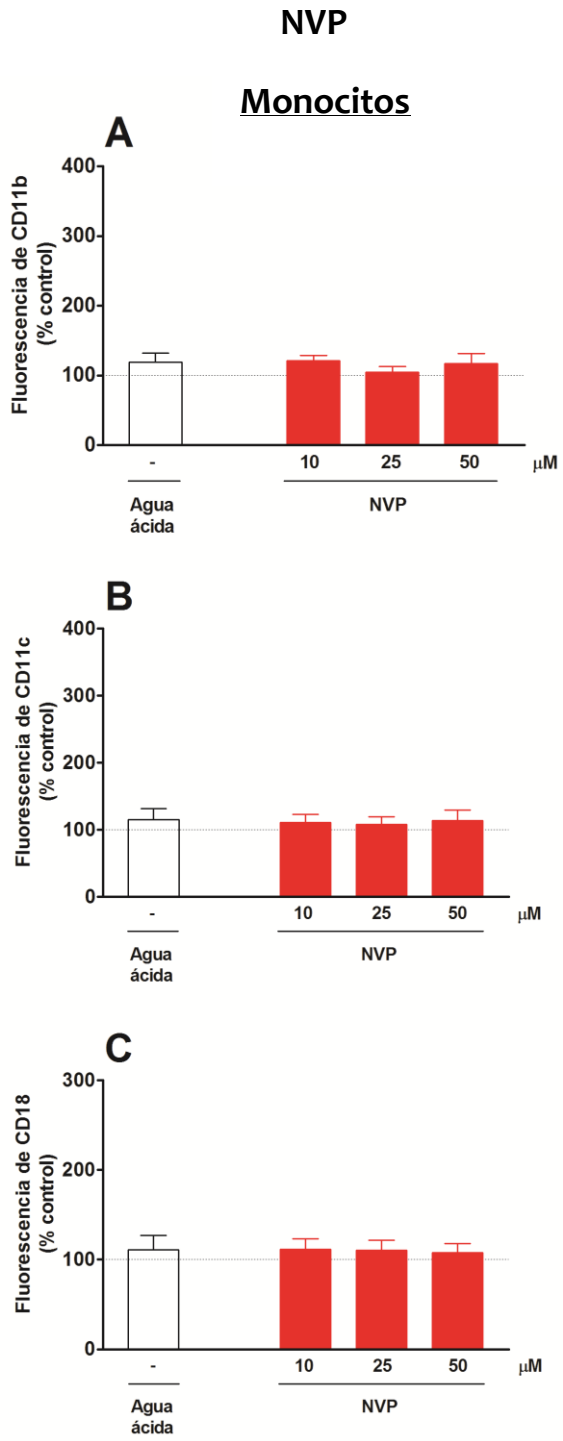

FIGURA 50. Efecto de Nevirapina sobre la expresión de moléculas de adhesión leucocitarias en monocitos de sangre humana. Se analizó la expresión de CD11b (A), CD11c (B) y CD18 (C). La sangre humana fue tratada con Nevirapina (NVP, 10-50 µM), su correspondiente vehículo (agua ácida) o control (agua estéril) (4 h). Los valores de fluorescencia (FITC o PE) representan el % de la mediana de la intensidad de la fluorescencia respecto del grupo control (agua estéril). Los resultados fueron expresados como Media ± E.E.M. (n = 5). Análisis de varianza ANOVA seguido del post-test Newman-Keuls.

RPV

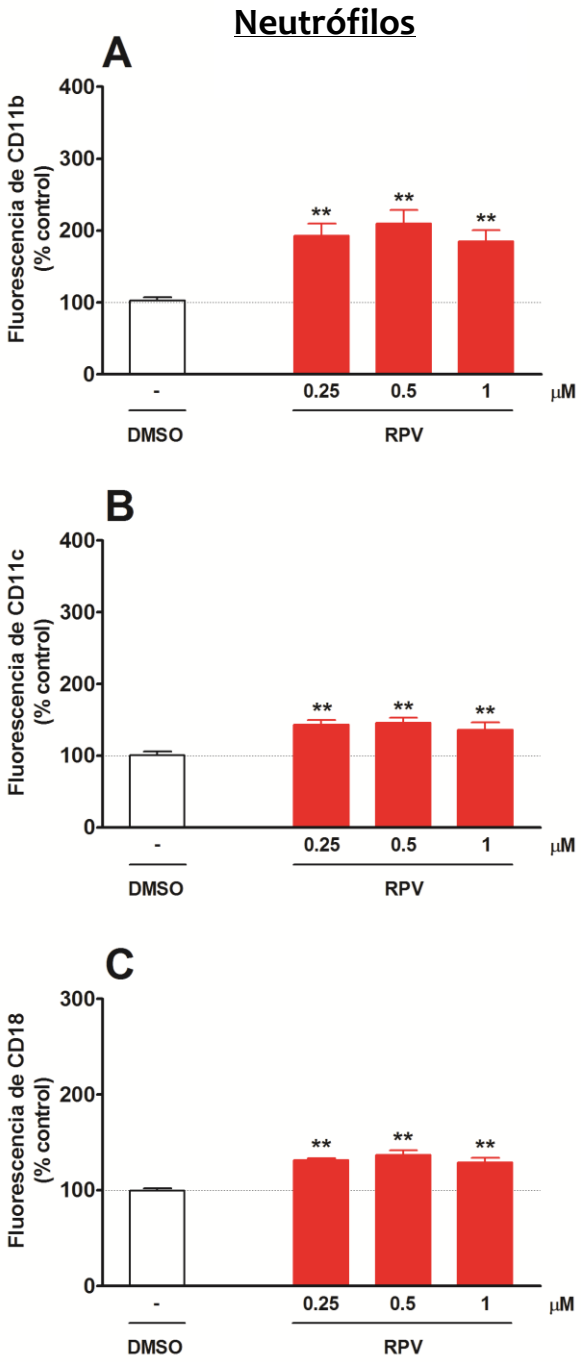

FIGURA 51. Efecto de Rilpivirina sobre la expresión de moléculas de adhesión leucocitarias en neutrófilos de sangre humana. Se analizó la expresión de CD11b (A), CD11c (B) y CD18 (C). La sangre humana fue tratada con Rilpivirina (RPV, 0.25-1 µM), su correspondiente vehículo (DMSO) o control (agua estéril) (4 h). Los valores de fluorescencia (FITC o PE) representan el % de la mediana de la intensidad de la fluorescencia respecto del grupo con control (agua estéril). Los resultados fueron expresados como Media ± E.E.M. (n = 8). **p<0,01 respecto del valor correspondiente al grupo tratado DMSO. Análisis de varianza ANOVA seguido del post-test Newman-Keuls.

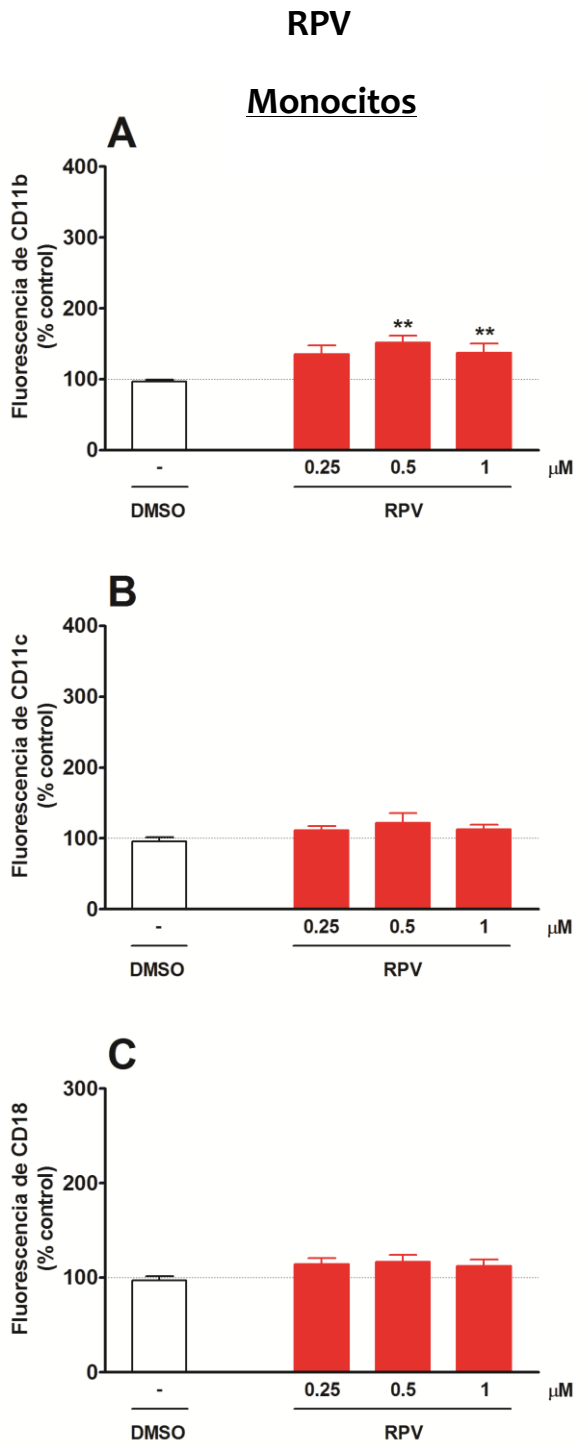

FIGURA 52. Efecto de Rilpivirina sobre la expresión de moléculas de adhesión leucocitarias en monocitos de sangre humana. Se analizó la expresión de CD11b (A), CD11c (B) y CD18 (C). La sangre humana fue tratada con Rilpivirina (RPV, 0.25-1 µM), su correspondiente vehículo (DMSO) o control (agua estéril) (4 h). Los valores de fluorescencia (FITC o PE) representan el % de la mediana de la intensidad de la fluorescencia respecto del grupo control (agua estéril). Los resultados fueron expresados como Media ± E.E.M. (n = 8). **p<0,01 respecto del valor correspondiente al grupo tratado con DMSO. Análisis de varianza ANOVA seguido del post-test Newman-Keuls.

TABLA 13: Efecto de los fármacos ITINAN sobre la expresión de moléculas de adhesión leucocitarias en neutrófilos de sangre humana.

	NEUTRÓFILOS		
	CD11a	**CD49d**	**CD62L**
Metanol	102,5±2,9	97,5±1,2	109,9±4,4
Agua ácida	96,2±3,7	97,0±3,4	98,8±2,4
DMSO	102,8±1,4	97,8±3,1	99,3±4,4
EFV 10 µM	114,0±5,5	100,3±0,3	110,8±4,2
EFV 15 µM	109,2±7,8	100,3±0,3	109,8±3,2
EFV 25 µM	111,5±8,7	100,3±0,3	119,8±6,3
NVP 10 µM	97,1±4,3	98,6±3,1	103,9±5,4
NVP 25 µM	96,3±6,6	101,4±3,4	101,1±5,6
NVP 50 µM	93,5±2,7	98,2±1,6	99,1±4,8
RPV 0.25 µM	110,9±0,6	105,4±6,5	99,4±0,9
RPV 0.5 µM	108,0±2,1	109,7±6,5	96,8±1,8
RPV 1 µM	107,2±2,5	106,7±7,5	93,5±2,8

Las sangre humana fue tratada con Efavirenz (EFV, 10-25 µM), Nevirapina (NVP, 10-50 µM), Rilpivirina (RPV, 0.25-1 µM), sus correspondientes vehículos (metanol, agua ácida o DMSO) o control (agua estéril) (4 h). Los valores de fluorescencia (FITC o PE) representan el % de la mediana de la intensidad de la fluorescencia respecto del grupo control (agua estéril). Los resultados fueron expresados como Media ± E.E.M. (n = 5-8). Análisis de varianza ANOVA seguido del post-test Newman-Keuls.

TABLA 14: Efecto de los fármacos ITINAN sobre la expresión de moléculas de adhesión leucocitarias en monocitos de sangre humana.

	MONOCITOS		
	CD11a	**CD49d**	**CD62L**
Metanol	108,1±4,5	106,2±5,3	104,0±5,4
Agua ácida	99,8±4,0	102,6±2,7	102,0±12,7
DMSO	104,7±5,3	99,7±2,6	82,9±10,1
EFV 10 µM	103,3±2,9	96,9±8,8	116,2±3,8
EFV 15 µM	106,8±4,4	97,2±11,6	109,4±6,5
EFV 25 µM	110,8±8,4	106,5±11,1	118,7±8,4
NVP 10 µM	98,8±3,3	100,9±1,4	102,4±12,4
NVP 25 µM	98,4±4,0	100,3±4,6	121,2±26,9
NVP 50 µM	97,5±3,2	102,8±1,6	106,0±10,5
RPV 0.25 µM	114,3±3,2	102,2±1,2	100,6±11,6
RPV 0.5 µM	114,8±5,1	105,6±4,5	106,6±11,1
RPV 1 µM	112,4±3,3	101,2±1,8	103,9±6,4

Las sangre humana fue tratada con Efavirenz (EFV, 10-25 µM), Nevirapina (NVP, 10-50 µM), Rilpivirina (RPV, 0.25-1 µM), sus correspondientes vehículos (metanol, agua ácida o DMSO) o control (agua estéril) (4 h). Los valores de fluorescencia (FITC o PE) representan el % de la mediana de la intensidad de la fluorescencia respecto del grupo control (agua estéril). Los resultados fueron expresados como Media ± E.E.M. (n = 4-8). Análisis de varianza ANOVA seguido del post-test Newman-Keuls.

TABLA 15: Efecto de los fármacos ITINAN sobre la expresión de moléculas de adhesión leucocitarias en linfocitos de sangre humana.

	LINFOCITOS					
	CD11a	**CD11b**	**CD11c**	**CD18**	**CD49d**	**CD62L**
Metanol	105,2±14,4	96,5±7,4	100,1±12,1	111,9±4,0	110,2±5,1	105,7±2,0
Agua ácida	98,8±3,2	94,7±15,7	107,5±4,0	97,4±4,2	98,0±2,9	93,1±4,1
DMSO	105,1±15,8	100,7±3,7	96,5±5,2	84,5±12,8	111,0±4,5	105,8±2,5
EFV 10 µM	100,2±5,1	98,8±5,3	110,0±11,2	96,5±4,3	95,9±8,1	114,6±6,5
EFV 15 µM	96,4±3,2	103,2±9,5	114,5±6,2	115,4±6,2	93,2±5,4	102,6±1,5
EFV 25 µM	102,4±7,7	98,7±6,4	100,4±5,1	96,4±6,2	88,2±15,1	115,5±7,5
NVP 10 µM	101,1±1,4	92,5±13,9	106,8±4,3	107,5±3,6	108,1±5,8	96,7±6,2
NVP 25 µM	94,3±1,6	90,8±12,6	98,5±3,9	111,0±4,2	96,0±2,7	99,2±2,2
NVP 50 µM	97,6±1,7	92,0±12,9	105,2±3,2	105,4±3,0	105,6±6,4	95,6±4,6
RPV 0.25 µM	101,9±21,9	99,9±5,2	103,8±6,9	136,4±32,0	102,8±8,7	123,7±19,6
RPV 0.5 µM	87,1±27,4	91,6±99,7	99,0±5,0	114,0±9,0	105,5±16,1	130,9±26,0
RPV 1 µM	118,2±25,8	105,9±13,1	95,0±5,7	92,4±6,8	114,9±10,3	115,7±17,1

Las sangre humana fue tratada con Efavirenz (EFV, 10-25 µM), Nevirapina (NVP, 10-50 µM), Rilpivirina (RPV, 0.25-1 µM), sus correspondientes vehículos (metanol, agua ácida o DMSO) o control (agua estéril) (4 h). Los valores de fluorescencia (FITC o PE) representan el % de la mediana de la intensidad de la fluorescencia respecto del grupo control (agua estéril). Los resultados fueron expresados como Media ± E.E.M. (n = 4-8). Análisis de varianza ANOVA seguido del post-test Newman-Keuls.

4.2.2.1.1.2. Células endoteliales

Analizamos el efecto de EFV, NVP y RPV sobre la expresión de moléculas de adhesión endoteliales *in vitro* utilizando la técnica anteriormente citada.

El análisis de la citometría de flujo desveló que ninguno de los tratamientos evaluados produjo variación alguna en la expresión de moléculas de adhesión endoteliales analizadas (TABLA 16).

TABLA 16: Efecto de los fármacos ITINAN sobre la expresión de moléculas de adhesión endoteliales en HUVEC.

	CÉLULAS ENDOTELIALES		
	ICAM-1	**VCAM-1**	**E-Selectina**
Metanol	100,3±5,8	101,4±4,7	93,1±5,7
Agua ácida	94,8±3,1	102,0±1,2	95,5±4,0
DMSO	109,5±4,2	102,1±1,3	91,0±10,5
EFV 10 µM	111,2±10,7	91,9±6,8	98,0±9,8
EFV 15 µM	96,2±8,8	91,2±8,7	90,2±11,0
EFV 25 µM	92,0±8,9	87,8±11,1	99,4±12,4
NVP 10 µM	95,5±2,5	97,8±2,3	99,6±7,0
NVP 25 µM	10,1±2,1	103,2±1,2	92,8±5,1
NVP 50 µM	100,3±2,2	101,8±4,1	90,3±5,1
RPV 0.25 µM	93,8±3,7	98,6±0,8	96,0±1,9
RPV 0.5 µM	95,0±2,6	100,4±3,0	105,7±6,4
RPV 1 µM	98,1±6,9	102,3±2,4	97,4±3,6

Las HUVEC fueron tratadas con Efavirenz (EFV, 10-25 µM), Nevirapina (NVP, 10-50 µM), Rilpivirina (RPV, 0.25-1 µM), sus correspondientes vehículos (metanol, agua ácida o DMSO) o control (medio de cultivo) (4 h). Los valores de fluorescencia (FITC o PE) representan el % de la mediana de la intensidad de la fluorescencia respecto del grupo control (medio de cultivo). Los resultados fueron expresados como Media ± E.E.M. (n = 4-8). Análisis de varianza ANOVA seguido del post-test Newman-Keuls.

4.2.2.1.2. ANTAGONISTAS CCR5, InInt E IP

4.2.2.1.2.1. Células leucocitarias

Se analizó el efecto de MVC, RAL, LPV, ATV y DRV sobre la expresión de moléculas de adhesión leucocitarias *in vitro* utilizando la citometría de flujo.

Ninguno de los tratamientos produjo una variación en la expresión de las moléculas de adhesión analizadas en ninguna de las tres poblaciones leucocitarias (neutrófilos, monocitos y linfocitos) (TABLA 17, 18 y 19).

TABLA 17: Efecto de los fármacos antagonistas CCR5, InInt e IP sobre la expresión de moléculas de adhesión leucocitarias en neutrófilos de sangre humana.

	NEUTRÓFILOS					
	CD11a	**CD11b**	**CD11c**	**CD18**	**CD49d**	**CD62L**
Metanol	102,5±2,9	111,2±13,0	101,5±3,3	107,6±8,2	97,5±1,2	109,9±4,4
DMSO	102,8±1,4	97,7±17,8	102,9±11,5	119,4±23,6	97,8±3,1	99,3±4,4
MVC 5 µM	97,1±1,5	105,3±8,4	109,1±8,8	91,4±5,2	97,4±8,0	97,9±3,6
RAL 5 µM	99,1±1,9	118,0±22,9	116, ±24,2	103,4±18,9	100,8±9,6	96,9±3,2
LPV 25 µM	98,4±2,1	108,2±20,4	101,2±7,9	103,0±5,2	96,9±3,0	105,2±12,3
ATV 25 µM	93,4±2,7	90,1±16,4	133,4±32,5	107,7±14,2	92,7±6,3	102,2±2,7
DRV 25 µM	91,8±5,7	103,1±21,4	110,1±16,2	107,4±22,4	87,9±7,8	100,0±0,9

Las sangre humana fue tratada con Maraviroc (MVC, 5 µM), Raltegravir (RAL, 5 µM), Lopinavir (LPV, 25 µM), Atazanavir (ATV, 25 µM), Darunavir (DRV, 25 µM), sus correspondientes vehículos (metanol o DMSO) o control (agua estéril) (4 h). Los valores de fluorescencia (FITC o PE) representan el % de la mediana de la intensidad de la fluorescencia respecto del grupo control (agua estéril). Los resultados fueron expresados como Media ± E.E.M. (n = 4-8). Análisis de varianza ANOVA seguido del post-test Newman-Keuls.

TABLA 18: Efecto de los fármacos antagonistas CCR5, InInt e IP sobre la expresión de moléculas de adhesión leucocitarias en monocitos de sangre humana.

	MONOCITOS					
	CD11a	**CD11b**	**CD11c**	**CD18**	**CD49d**	**CD62L**
Metanol	108,1±4,5	98,6±10,8	122,9±9,6	106,8±5,0	106,2±5,3	104,0±5,4
DMSO	104,7±5,3	119,5±19,6	121,2±17,6	101,6±10,2	99,7±2,6	82,9±10,1
MVC 5 µM	98,9±8,1	126,6±22,8	102,4±5,1	89,0±8,1	101,1±1,7	88,2±9,4
RAL 5 µM	101,3±2,2	97,8±18,3	101,3±18,1	83,2±15,0	99,9±7,0	91,7±10,8
LPV 25 µM	109,3±4,7	100,7±26,8	118,7±23,8	105,1±2,7	100,6±8,5	104,3±17,4
ATV 25 µM	91,5±4,5	103,7±9,8	104,6±5,9	93,2±4,8	100,3±6,6	114,4±21,7
DRV 25 µM	91,4±4,9	94,6±18,3	115,3±18,0	108,7±6,6	97,3±3,4	100,8±11,4

Las sangre humana fue tratada con Maraviroc (MVC, 5 µM), Raltegravir (RAL, 5 µM), Lopinavir (LPV, 25 µM), Atazanavir (ATV, 25 µM), Darunavir (DRV, 25 µM), sus correspondientes vehículos (metanol o DMSO) o control (agua estéril) (4 h). Los valores de fluorescencia (FITC o PE) representan el % de la mediana de la intensidad de la fluorescencia respecto del grupo control (agua estéril). Los resultados fueron expresados como Media ± E.E.M. (n = 4-8). Análisis de varianza ANOVA seguido del post-test Newman-Keuls.

TABLA 19: Efecto de los fármacos antagonistas CCR5, InInt e IP sobre la expresión de moléculas de adhesión leucocitarias en linfocitos de sangre humana.

	LINFOCITOS					
	CD11a	**CD11b**	**CD11c**	**CD18**	**CD49d**	**CD62L**
Metanol	105,2±14,4	96,5±7,4	100,1±12,1	111,9±4,0	110,2±5,1	105,7±2,0
DMSO	105,1±15,8	100,7±3,7	96,5±5,2	84,5±12,8	111,0±4,5	105,8±2,5
MVC 5 µM	88,3±25,1	94,1±7,1	91,4±4,7	88,8±19,4	116,0±13,8	101,5±10,0
RAL 5 µM	115,9±10,4	94,4±8,4	93,3±8,7	96,1±21,3	120,9±17,2	122,2±17,4
LPV 25 µM	72,8±19,7	103,6±10,7	103,9±11,3	120,8±18,4	92,1±5,3	111,3±14,6
ATV 25 µM	131,2±14,7	94,9±12,6	80,2±16,5	104,6±25,3	126,5±18,1	111,1±1,5
DRV 25 µM	115,7±11,5	101,4±13,4	99,4±7,5	101,9±22,4	116,0±11,5	120,0±16,6

Las sangre humana fue tratada con Maraviroc (MVC, 5 µM), Raltegravir (RAL, 5 µM), Lopinavir (LPV, 25 µM), Atazanavir (ATV, 25 µM), Darunavir (DRV, 25 µM), sus correspondientes vehículos (metanol o DMSO) o control (agua estéril) (4 h). Los valores de fluorescencia (FITC o PE) representan el % de la intensidad de la fluorescencia respecto del grupo control (agua estéril). Los resultados fueron expresados como Media ± E.E.M. (n = 4-8). Análisis de varianza ANOVA seguido del post-test Newman-Keuls.

4.2.2.1.2.2. Células endoteliales

Analizamos el efecto de MVC, RAL, LPV, ATV y DRV sobre la expresión de moléculas de adhesión endoteliales *in vitro* utilizando la técnica anteriormente citada.

El análisis de la citometría de flujo desveló que ninguno de los tratamientos evaluados produjo variación alguna en la expresión de moléculas de adhesión endoteliales analizadas (TABLA 20).

<u>TABLA 20</u>: Efecto de los fármacos antagonistas CCR5, InInt e IP sobre la expresión de moléculas de adhesión endoteliales en HUVEC.

	CÉLULAS ENDOTELIALES		
	ICAM-1	**VCAM-1**	**E-Selectina**
Metanol	100,3±5,8	101,4±4,7	93,1±5,7
DMSO	109,5±4,2	102,1±1,3	91,0±10,5
MVC 5 µM	102,9±3,6	101,2±2,7	93,8±6,3
RAL 5 µM	110,8±2,6	101,9±3,2	115,2±19,8
LPV 25 µM	101,6±10,8	99,4±4,7	113,6±11,1
ATV 25 µM	99,3±8,1	93,6±1,9	97,9±1,1
DRV 25 µM	89,8±15,8	95,3±4,2	96,6±3,8

Las HUVEC fueron tratadas con Maraviroc (MVC, 5 µM), Raltegravir (RAL, 5 µM), Lopinavir (LPV, 25 µM), Atazanavir (ATV, 25 µM), Darunavir (DRV, 25 µM), sus correspondientes vehículos (metanol o DMSO) o control (medio de cultivo) (4 h). Los valores de fluorescencia (FITC o PE) representan el % de la mediana de la intensidad de la fluorescencia respecto del grupo control (medio de cultivo). Los resultados fueron expresados como Media ± E.E.M. (n = 4-8). Análisis de varianza ANOVA seguido del post-test Newman-Keuls.

4.2.3. ESTUDIO DEL MECANISMO RESPONSABLE DE LA INTERACCIÓN LEUCOCITO-ENDOTELIO INDUCIDA POR LOS FÁRMACOS ITINAN *IN VITRO*

Con el fin de estudiar la posible implicación de las moléculas de adhesión en la interacción leucocito-endotelio inducida por los fármacos ITINAN, empleamos la técnica de adhesión dinámica en cámara paralela de flujo, pretratando PMN o PBMC y células endoteliales con anticuerpos bloqueantes frente a ciertas moléculas de adhesión (CD11b, CD11c, CD18 e ICAM-1) 30 minutos antes del tratamiento con EFV y RPV.

Así, la interacción PMN-HUVEC inducida por EFV (FIGURA 53), y por RPV (FIGURA 55) fue completamente bloqueada mediante anticuerpos frente a CD11b, CD11c, CD18 o ICAM-1. Resultados similares se obtuvieron cuando se analizó la interacción PBMC-HUVEC (FIGURA 54 y 56). Cabe destacar, que en el caso de RPV, cuando bloqueamos con el anticuerpo frente a CD11c usando PBMC, la reversión fue parcial aunque significativa, en los parámetros de velocidad de rodamiento, rodamiento y adhesión (FIGURA 56).

EFV

PMN

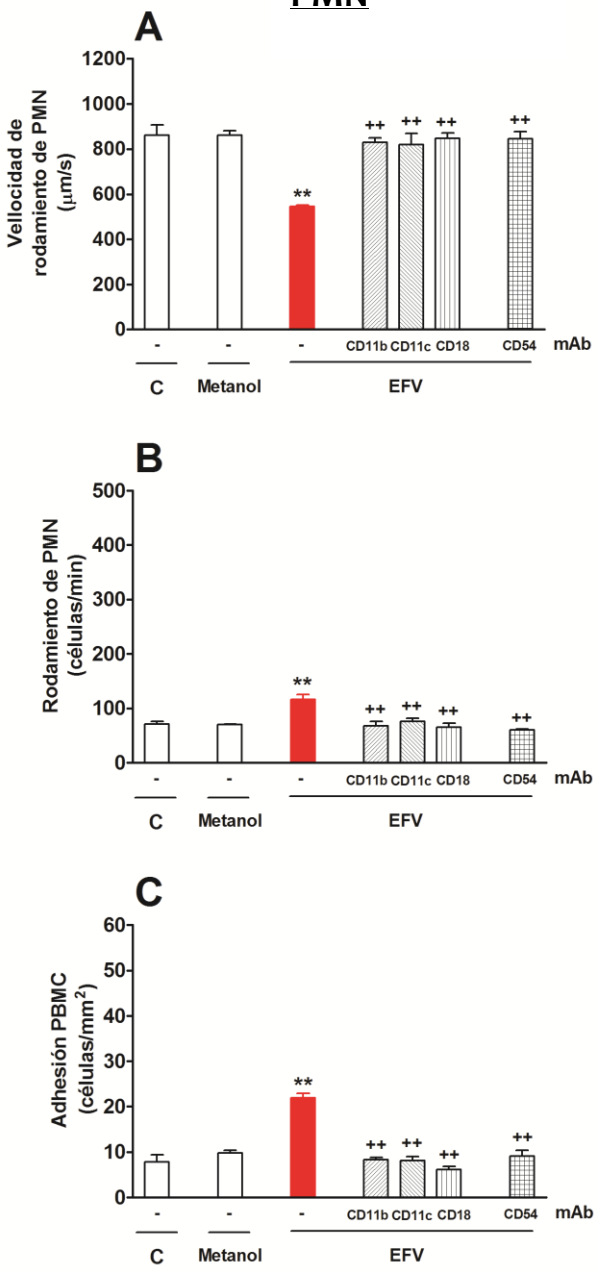

FIGURA 53. Estudio del mecanismo responsable de la interacción PMN-HUVEC inducida por Efavirenz. Se analizó la velocidad de rodamiento (A), el rodamiento (B) y la adhesión leucocitaria (C). Los PMN fueron pretratados con los anticuerpos bloqueantes (anti-CD11b, anti-CD11c, anti-CD18 o anticuerpo control) y las HUVEC fueron pretratadas con los anticuerpos bloqueantes (anti-CD54 o anticuerpo control) independientemente durante 30 min y posteriormente tratados ambos con Efavirenz (EFV, 15 µM), su correspondiente vehículo (metanol) o control (medio de cultivo o agua estéril) (4 h). Los resultados fueron expresados como Media ± E.E.M. (n = 4). **p<0,01 respecto del valor correspondiente al grupo tratado con metanol y $^{++}$p<0,01 respecto del valor correspondiente al grupo tratado con EFV 15 µM. Análisis de varianza ANOVA seguido del post-test Newman-Keuls.

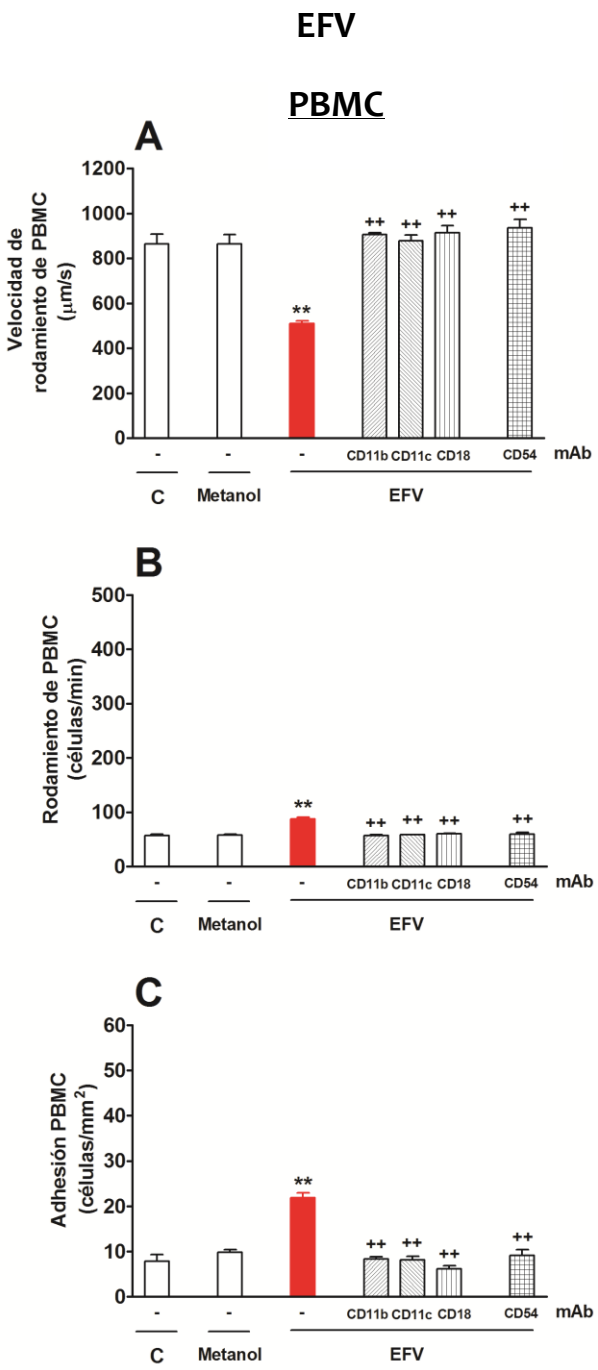

FIGURA 54. Estudio del mecanismo responsable de la interacción PBMC-HUVEC inducida por Efavirenz. Se analizó la velocidad de rodamiento (A), el rodamiento (B) y la adhesión leucocitaria (C). Los PBMC fueron pretratados con los anticuerpos bloqueantes (anti-CD11b, anti-CD11c, anti-CD18 o anticuerpo control) y las HUVEC fueron pretratadas con los anticuerpos bloqueantes (anti-CD54 o anticuerpo control) independientemente durante 30 min y posteriormente tratados ambos con Efavirenz (EFV, 15 μM), su correspondiente vehículo (metanol) o control (medio de cultivo o agua estéril) (4 h). Los resultados fueron expresados como Media ± E.E.M. (n = 4). **p<0,01 respecto del valor correspondiente al grupo tratado con metanol y $^{++}$p<0,01 respecto del valor correspondiente al grupo tratado con EFV 15 μM. Análisis de varianza ANOVA seguido del post-test Newman-Keuls.

RPV

PMN

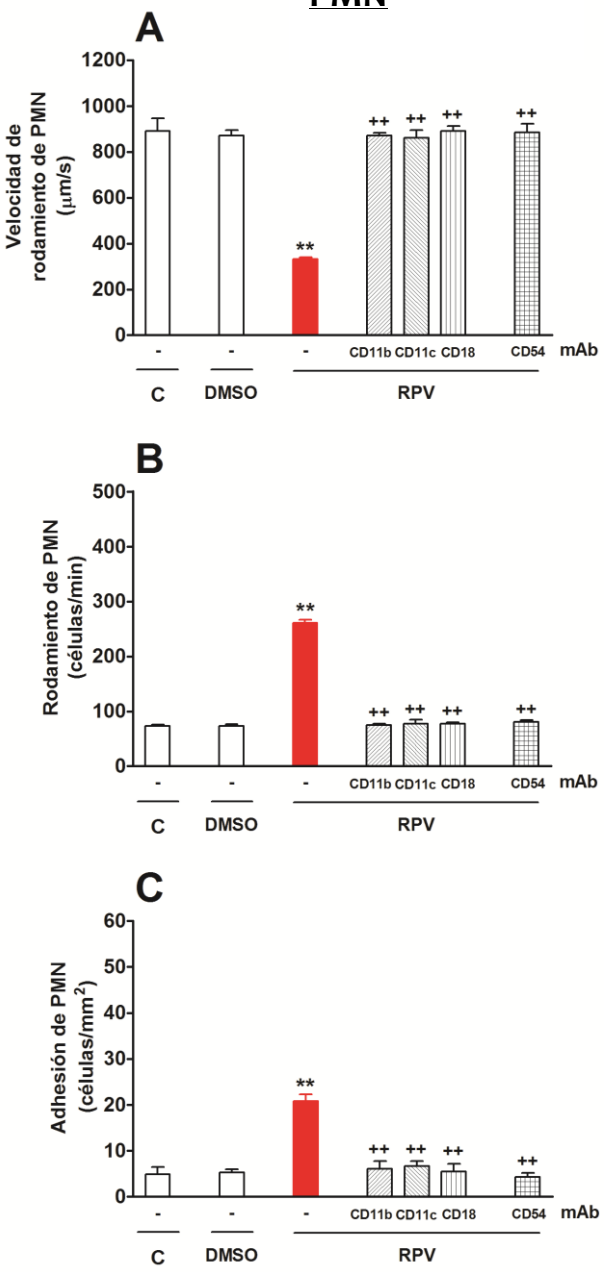

FIGURA 55. Estudio del mecanismo responsable de la interacción PMN-HUVEC inducida por Rilpivirina. Se analizó la velocidad de rodamiento (A), el rodamiento (B) y la adhesión leucocitaria (C). Los PMN fueron pretratados con los anticuerpos bloqueantes (anti-CD11b, anti-CD11c, anti-CD18 o anticuerpo control) y las HUVEC fueron pretratadas con los anticuerpos bloqueantes (anti-CD54 o anticuerpo control) independientemente durante 30 min y posteriormente tratados ambos con Rilpivirina (RPV, 0.5 µM), su correspondiente vehículo (DMSO) o control (medio de cultivo o agua estéril) (4 h). Los resultados fueron expresados como Media ± E.E.M. (n = 4). **p<0,01 respecto del valor correspondiente al grupo tratado con DMSO y $^{++}$p<0,01 respecto del valor correspondiente al grupo tratado con RPV 0.5 µM. Análisis de varianza ANOVA seguido del post-test Newman-Keuls.

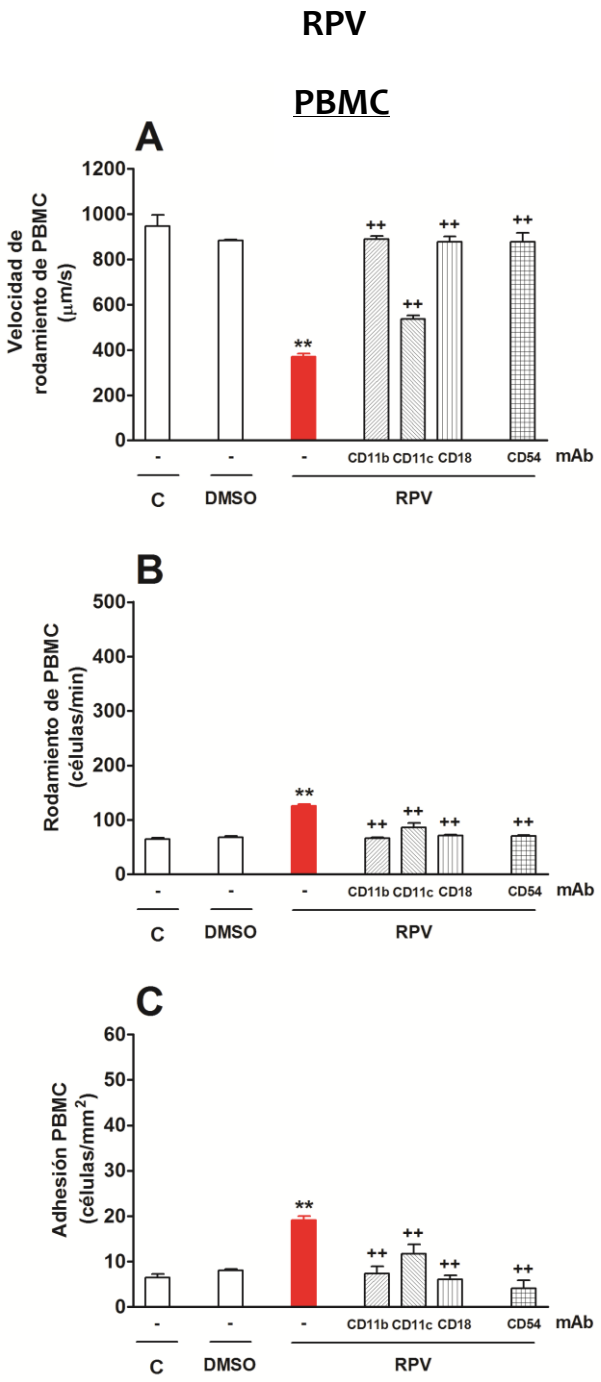

FIGURA 56. Estudio del mecanismo responsable de la interacción PBMC-HUVEC inducida por Rilpivirina. Se analizó la velocidad de rodamiento (A), el rodamiento (B) y la adhesión leucocitaria (C). Los PBMC fueron pretratados con los anticuerpos bloqueantes (anti-CD11b, anti-CD11c, anti-CD18 o anticuerpo control) y las HUVEC fueron pretratadas con los anticuerpos bloqueantes (anti-CD54 o anticuerpo control) independientemente durante 30 min y posteriormente tratados ambos con Rilpivirina (RPV, 0.5 μM), su correspondiente vehículo (metanol) o control (medio de cultivo o agua estéril) (4 h). Los resultados fueron expresados como Media ± E.E.M. (n = 4). **p<0,01 respecto del valor correspondiente al grupo tratado con DMSO y $^{++}$p<0,01 respecto del valor correspondiente al grupo tratado con RPV 0.5 μM. Análisis de varianza ANOVA seguido del post-test Newman-Keuls.

5. DISCUSIÓN

La "Terapia Antirretroviral Combinada" se desarrolló rápidamente a partir de que se notificaran los primeros casos de SIDA a principios de 1980, buscando los fármacos o combinaciones de fármacos más eficaces para este tratamiento. Una vez que la supervivencia de los pacientes de SIDA está superada, está cobrando mayor importancia la aparición de efectos adversos asociados al uso de estos fármacos. Así, se ha asociado la "Terapia Antirretroviral Combinada" con el desarrollo de efectos adversos.

La mortalidad no asociada a SIDA en regiones con acceso al tratamiento está causada principalmente por cáncer (23,5 %), enfermedades cardiovasculares (15,7 %) y enfermedades hepáticas (14,1 %) (Maartens et al., 2014). Respeto a la mayor incidencia de eventos adversos cardiovasculares (Sabin et al., 2008, Bonnet et al., 2002), se desconoce si se debe a la infección en sí misma, al incremento en el tiempo de vida de los pacientes, al tratamiento con la "Terapia Antirretroviral Combinada" o a una combinación de todos estos factores. Está ampliamente descrito que la infección por el VIH por sí misma está asociada con enfermedades cardiovasculares (Triant, 2012). Además, como la tasa de supervivencia es mayor, existe mayor probabilidad de desarrollar este tipo de efectos adversos. También se ha observado una correlación entre "Terapia Antirretroviral Combinada" y enfermedades cardiovasculares, existiendo estudios clínicos a este nivel (Friis-Moller et al., 2003, Currier et al., 2003), pero que no analizan de forma particular cada uno de los agentes que se administran en combinación.

En la actualidad, existen 6 grandes grupos de fármacos antirretrovirales comercializados. Desde que se instauró la triple terapia, los fármacos más utilizados han sido los ITIAN, los ITINAN y los IP. Pero con el paso del tiempo y el desarrollo de nuevos medicamentos, han ido apareciendo en el mercado nuevos fármacos con una similar eficacia antiviral pero con una menor incidencia de reacciones adversas a todos los niveles. Así, con cierta periodicidad, van apareciendo guías terapeúticas en las que se aconsejan las pautas preferentes y alternativas para mejorar la calidad de

vida de los pacientes infectados por el VIH (Günthard et al., 2014, Panel de expertos de GeSIDA, 2015). En la actualidad se recomienda como pauta preferente la administración de 2 ITIAN en combinación con un antagonista CCR5, un ITINAN, un InInt o un IP. La elección de una u otra pauta depende de las características del paciente a tratar tanto a nivel del tipo de virus VIH con el que esté infectado como de las características personales de cada individuo a nivel genético y patológico.

Respecto a los efectos adversos de la "Terapia Antirretroviral Combinada" a nivel cardiovascular, inicialmente se apuntó a los IP como los responsables ya que aumentan los niveles de lípidos (Friis-Moller et al., 2007), pero no podemos descartar al resto de grupos ya que esta terapia se administra generalmente en combinación de al menos 3 fármacos.

A partir del año 2005 se inició una de las mayores polémicas en este campo al relacionar a ABC (fármaco ITIAN) con el desarrollo de infarto de miocardio, apareciendo estudios que corroboraban esta afirmación (Sanz, 2005, Bavinger et al., 2013, Sabin et al., 2008, AIDS 2008 September 12, Obel et al., 2010, Lang et al., 2010, Durand et al., 2011) mientras que otros la contradecían (Cutrell et al., 2008, Brothers et al., 2009, Ribaudo et al., 2011, Bedimo et al., 2011). El primer paso en estas enfermedades cardiovasculares con componente inflamatorio lo constituye la interacción entre los leucocitos que circulan por el torrente sanguíneo con las células endoteliales que recubren el interior de los vasos sanguíneos a través de moléculas de adhesión expresadas en ambos tipos celulares (leucocitos y células endoteliales) y que permiten la interacción entre ellos. Así, en nuestro laboratorio nos planteamos analizar el efecto de este fármaco sobre este primer paso y demostramos que ciertos fármacos ITIAN, concretamente los análogos de purina ABC y ddI, inducen interacciones leucocito-endotelio (de Pablo et al., 2010, de Pablo et al., 2012, de Pablo et al., 2013) tanto *in vitro* como *in vivo*, mientras que los análogos de pirimidina FTC y 3TC y el análogo de nucleótido TDF no las producen. En

esta Tesis Doctoral nos planteamos extender el estudio al resto de grupos de fármacos antirretrovirales ya que se administran en combinación.

Así, analizamos los siguientes fármacos: MVC (antagonista CCR5), EFV, NVP y RPV (ITINAN), RAL (InInt) y LPV, ATV y DRV (IP). Hemos utilizado concentraciones similares, o incluso mayores, a aquellas que se han documentado en pacientes que toman esta terapia (Waters et al., 2015, Burger et al., 2006, Cooper et al., 2007, Martinez-Rebollar et al., 2013, León et al., 2007, Boffito et al., 2011, Parks et al., 2007 Moyle et al., 2009, Usach et al., 2013, Blas-García et al., 2014, Jamaluddin et al., 2010). Hemos usado dos aproximaciones experimentales comúnmente utilizadas para el análisis de la toxicidad vascular inducida por la administración de drogas: la microscopía intravital en mesenterio de rata (*in vivo*) y la adhesión dinámica en cámara paralela de flujo utilizando leucocitos y células endoteliales humanas (*in vitro*). La primera permite analizar con gran detalle el proceso inflamatorio evaluando la velocidad de rodamiento, el rodamiento, la adhesión y la migración de los leucocitos en vénulas de animales vivos anestesiados (Hughes et al., 2010, Masedunskas et al., 2012). En ella se utiliza la inyección intraperitoneal de drogas, una técnica usual en la microscopía intravital (Yamaki et al., 1998, Stalker et al., 2003, Nabah et al., 2005) porque permite tanto analizar el efecto de los fármacos administrados a nivel local como periodos de incubación mayores que la superfusión (Hughes et al., 2010). La segunda es una aproximación dinámica experimental en la cual utilizamos muestras humanas: los leucocitos humanos pasan a través de una capa de células endoteliales reproduciendo los procesos de rodamiento y adhesión que preceden a la formación del proceso aterosclerótico (Sundstrom et al., 2003, Gallego et al., 1996). Así, la combinación de estas dos técnicas experimentales nos permite hacer un análisis más exhaustivo de los efectos proinflamatorios producidos por la administración de diferentes drogas.

Este estudio muestra que concentraciones plasmáticas de los fármacos ITINAN (EFV, NVP y RPV), pero no del resto de fármacos analizados (MVC, RAL, LPV, ATV y

DRV), inducen interacciones leucocito-endotelio *in vivo.* En particular, EFV, NVP y RPV inducen rodamiento y adhesión de leucocitos sobre vénulas mesentéricas de rata en el modelo animal descrito, mientras que el parámetro de migración leucocitaria únicamente es producido por EFV y NVP, pero no por RPV. El nivel de migración inducido por EFV es significativamente superior al producido por NVP. Los resultados de migración leucocitaria obtenidos por microscopía intravital fueron corroborados por tinción hematoxilina-eosina determinando la infiltración leucocitaria. La migración leucocitaria es un parámetro de gran relevancia ya que el movimiento de los leucocitos al tejido inflamado es considerado un punto irreversible - de no retorno - en la cascada vascular inflamatoria mientras que las fases precedentes de rodamiento y adhesión son fases reversibles (Muller, 2009).

Respecto a los estudios *in vitro*, de nuevo EFV, NVP y RPV inducen interacciones leucocito (PMN y PBMC)-endotelio mientras que MVC, RAL, LPV, ATV y DRV no inducen estas interacciones. Debido a que estas interacciones se deben a la expresión de moléculas de adhesión, éstas fueron analizadas. Así, EFV aumenta la expresión de Mac-1 (CD11b/CD18) y gp150,95 (CD11c/CD18) en neutrófilos y monocitos humanos, NVP no aumenta la expresión de ninguna de las moléculas analizadas y RPV aumenta la expresión de Mac-1 y gp150,95 en neutrófilos y únicamente CD11b en monocitos humanos. La interacción PBMC-endotelio parece ser menor que la producida por los tres fármacos analizados sobre la interacción PMN-endotelio. Esta diferencia entre la adhesión de PMN y de PBMC al endotelio podría ser resultado del hecho de que en la población total de PBMC que se superfunden sobre la cámara de flujo, sólo aproximadamente el 10% son monocitos; con lo cual la acción de estos últimos se ve ocultada por el 90% de los linfocitos que no se pueden adherir al endotelio debido a que no pueden expresar CD11b ni CD11c (Carlos et al., 1994). Ninguna de las moléculas de adhesión analizadas en linfocitos ni en células endoteliales ve modificada su expresión tras el tratamiento con EFV, NVP y RPV. El resto de fármacos analizados (MVC, RAL, LPV, ATV y DRV) no aumentan la

expresión de las moléculas de adhesión tanto leucocitarias como endoteliales analizadas *in vitro*.

Cuando analizamos el papel funcional de las moléculas de adhesión sobre la interacción leucocito-endotelio inducida por los ITINAN, podemos ver que estas interacciones inducidas por EFV y RPV, pero no las inducidas por NVP, son revertidas completamente cuando usamos anticuerpos frente a CD11b, CD18 o ICAM-1 (CD54) *in vivo*. Una posible explicación para los resultados obtenidos para NVP es que este fármaco puede actúar a través de otras moléculas de adhesión - como P-Selectina - que están principalmente implicadas en el proceso de rodamiento leucocitario (Carlos et al., 1994). Nuestro análisis del papel de las moléculas de adhesión en el efecto de EFV y RPV sobre las interacciones leucocito-endotelio *in vitro* sugieren que Mac-1 (CD11b/CD18) y gp150,95 (CD11c/CD18) interactúan con su ligando endotelial ICAM-1 (CD54) debido a que el efecto de ambos fármacos sobre las interacciones leucocito-endotelio es completamente revertido cuando se usan anticuerpos frente a estas moléculas y además están también de acuerdo con los resultados de expresión de moléculas de adhesión obtenidos por citometría de flujo. El bloqueo de RPV en PBMC es parcial, aunque significativo, cuando se usa el anticuerpo bloqueante CD11c, hecho que está en concordancia con que RPV no aumenta la expresión de CD11c en monocitos humanos. Esta molécula se ha implicado en la migración de monocitos, hecho que también explica la disparidad en los resultados obtenidos con EFV y RPV sobre la migración leucocitaria (Sadhu et al., 2007). Además, aunque el papel de CD11b y CD11c en la adhesión y la migración era predecible, el rodamiento estaba establecido que estaba mediado por selectinas y/o VLA-4/VCAM-1 (Carlos et al., 2007). Sin embargo, hay una evidencia creciente de que las integrinas β_2 también pueden participar en el rodamiento leucocitario en función del estado conformacional en el que se encuentren (McEver et al., 2010, Ley et al., 2007).

Las integrinas β_2 son receptores de adhesión celular que comparten la misma cadena β CD18, pero que tienen una distinta cadena α. Se han descrito 4 tipos de esta familia: αL (CD11a, LFA-1), αM (CD11b, Mac-1), αX (CD11c, gp150,95) y αD (CD11d) (Carlos et al., 1994). La expresión de CD11b y CD11c es mayoritaria en neutrófilos y monocitos, donde son movilizadas de vesículas secretoras de la superficie celular de estos dos tipos celulares a los pocos minutos tras la estimulación (Carlos et al., 1994). La expresión de CD11c en linfocitos es limitada. El principal ligando de estas integrinas β_2 es ICAM-1, que se expresa de manera constitutiva en la superficie del endotelio vascular (Carlos et al., 1994). Gp150,95 (CD11c/CD18) se ha relacionado con la fagocitosis, la presentación de los antígenos por parte de las células dendríticas y la respuesta inflamatoria (que incluye la migración de los monocitos) (Sadhu et al., 2007). Mac-1 (CD11b/CD18) es la moléculas de adhesión que más se ha relacionado con la adhesión de neutrófilos y monocitos a las paredes vasculares, siendo también propuesta como el vínculo de unión entre adhesión celular y trombosis (Hirahashi et al., 2009). Mac-1 interacciona con ICAM-1 endotelial promoviendo la interacción entre los leucocitos circulantes y el endotelio (Ley et al., 2007). A su vez, Mac-1 también interacciona con GPIbα expresada en las plaquetas, propiciando que los leucocitos y las plaquetas se unan entre ellos (Projahn et al., 2012). Así, las plaquetas van a jugar un papel muy importante, uniéndose entre ellas, uniéndose a leucocitos y/o a células endoteliales, favoreciendo también la unión entre ambos tipos celulares (Projahn et al., 2012, Gawaz et al., 2005) pudiéndose llegar a la formación del trombo y de la placa aterosclerótica. Existen pocos estudios que analicen el efecto de estos fármacos sobre la función plaquetaria (agregación plaquetaria, interacción leucocito-endotelio-plaqueta), parámetros en los que nuestro grupo de investigación está centrando el interés.

EFV es uno de los fármacos del grupo de los ITINAN más empleados en la "Terapia Antirretroviral Combinada" y dentro de su grupo es el más utilizado. Inicialmente era considerado un fármaco muy seguro, pero con su uso han ido apareciendo toxicidades a distintos niveles principalmente a nivel hepático y en el

sistema nervioso. No existen apenas estudios concluyentes que correlacionen a EFV con la aparición de efectos adversos cardiovasculares (Worm et al., 2010) aunque un estudio sugiere que con el incremento en el tiempo de exposición a EFV aumenta el riesgo de padecer este tipo de enfermedades (Friis-Moller et al., 2007) y otro sí que lo relaciona directamente con un mayor riesgo de sufrir infarto agudo de miocardio (Durand et al., 2011). El hecho de que en este estudio se muestre que EFV induce interacciones leucocito-endotelio, no está en controversia con la casi total ausencia de estudios clínicos que afirmen taxativamente que el uso de EFV en pacientes infectados con VIH bajo tratamiento antirretroviral aumenta el riesgo de padecer enfermedades cardiovasculares. Por un lado, existen indicios que indicarían que este fármaco puede incrementar este riesgo como son el aumento en los niveles lipídicos, la permeabilidad vascular y la generación de radicales libres en pacientes bajo este tratamiento y un aumento de la relajación del endotelio vascular, fenómeno característico de disfunción vascular y por lo tanto de posibles afectaciones cardiovasculares (Tashima et al., 2003, Manfredi et al., 2005, Van Leth et al., 2004, Worm et al., 2010, Jammaludin et al., 2010, Mondal et al., 2004, Yeung et al., 2013). Por otro lado, este proyecto se analiza el posible efecto de EFV sobre el primer paso en el desarrollo de enfermedades cardiovasculares - efecto proinflamatorio - por sí sólo, mientras que en los estudios clínicos que existen se analiza dicho parámetro en pacientes enfermos infectados por el VIH, que se ha demostrado que por sí mismo está asociado con el desarrollo de enfermedades cardiovasculares (Triant, 2012). En este sentido hemos realizado estudios preliminares en nuestro laboratorio evaluando el efecto de EFV: 1) tras generar un sistema proinflamatorio en las células endoteliales y 2) tras generar un sistema proinflamatorio en las plaquetas. Hemos observado un papel antiinflamatorio de EFV, ya que el fármaco es capaz de revertir la expresión de ICAM-1, VCAM-1 y E-Selectina inducida en células endoteliales por TNF-α y de P-Selectina inducida en plaquetas por PAF. Estos hechos podrían explicar, en cierta medida, el carácter proinflamatorio de EFV por sí sólo, mientras que el fármaco en presencia de un estímulo proinflamatorio/protrombótico o en presencia de VIH,

tendría un cierto carácter antiinflamatorio, actuando como un fármaco protector en presencia de un estímulo previo. Este hecho no estaría en contradicción con que ICAM-1 participe en la interacción leucocito-endotelio inducida por EFV. Destacar que esta molécula de adhesión se puede expresar de forma constitutiva, con lo cual, que EFV revierta o inhiba su expresión en presencia de un estímulo proinflamatorio no va a impedir que a esta molécula se le unan sus ligandos leucocitarios Mac-1 o gp150,95 y que provoquen este proceso inflamatorio que produce EFV.

En cuanto a NVP, aunque en este estudio ha resultado un fármaco que induce interacciones leucocito-endotelio, siempre se ha considerado un fármaco seguro a nivel cardiovascular. Un estudio ha demostrado que NVP no produce relajación ni disfunción del endotelio vascular arterial en mesenterio de rata (Yeung et al., 2013). Además, este fármaco se ha correlacionado con altos niveles de colesterol HDL, factor protector contra el desarrollo de enfermedades cardiovasculares (Souza et al., 2013) en comparación con el resto de fármacos ITINAN (Souza et al., 2013). RPV se está convirtiendo en el mayor competidor de EFV en cuanto a su uso ya que ha demostrado tener una eficacia similar a este último fármaco exhibiendo un perfil toxicológico más seguro a nivel cardiovascular. Debido a que es un fármaco de uso muy reciente, no existen estudios que evalúen su posible efecto sobre el desarrollo de enfermedades cardiovasculares. Así, existe un estudio clínico que confirma que el tratamiento con RPV posee una menor incidencia de efectos adversos cardiovasculares así como una mejoría en los parámetros lipídicos al cambiar de IP a este fármaco (Casado et al., 2013).

Respecto al resto de fármacos analizados, existen evidencias que apuntan al receptor CCR5 y sus ligandos CCL3 (MIP-1α), CCl4 (MIP-1β) y CCL5 (RANTES) como los responsables de la iniciación y la progresión de la aterosclerosis (Jones et al., 2011). Este dato implica un potencial uso de los antagonistas CCR5 (como MVC) como fármacos protectores a nivel cardiovascular. De hecho, existe un estudio previo en ratones que muestra que MVC reduce la progresión de la placa

aterosclerótica inducida por RTV (Cipriani et al., 2013). Aunque en nuestro laboratorio no hemos evaluado el carácter antiinflamatorio de MVC, ambos resultados apuntarían a un mejor perfil toxicológico a nivel cardiovascular de MVC.

Con relación a los InInt, existen pocos estudios que analicen la relación entre RAL y el desarrollo de enfermedades cardiovasculares. En concreto, dos estudios clínicos han demostrado que este compuesto no tiene un impacto significativo sobre el riesgo cardiovascular, medido como disfunción endotelial (Gupta et al., 2013, Hatano et al., 2012). Incluso uno de ellos propone efectos beneficiosos de este fármaco sobre la activación de los monocitos (medido como sCD14) (Gupta et al., 2013) que está en corcondancia con nuestros datos.

Con respecto a los IP, siempre se ha tenido especial precaución ya que estos fármacos se han correlacionando con la aparición de efectos adversos a nivel cardiovascular (Friis-Moller et al., 2010, Friis-Moller et al., 2003). LPV ha sido el fármaco más utilizado del grupo hasta hace muy poco tiempo y se ha demostrado que su uso puede aumentar el riesgo de sufrir enfermedades cardiovasculares afectando a la función endotelial celular, al estrés oxidativo y modificando marcadores de inflamación o senescencia (Auclair et al., 2014). Además produce una relajación del endotelio mediado por óxido nítrico y una disfunción vascular que conllevaría a efectos adversos cardiovasculares (Yeung et al., 2013). En estudios con modelos animales y en pacientes se ha demostrado que este fármaco es capaz de aumentar el colesterol LDL y los niveles de triglicéridos (Reyskens et al., 2013, Souza et al., 2013). Sin embargo, ATV y DRV han demostrado tener un perfil lipídico más favorable que el resto de los IP (Overton et al., 2012). De hecho, un estudio previo realizado en células endoteliales coronarias arteriales humanas ha demostrado que DRV mejor que ATV y a su vez mejor que LPV, no afecta a la función endotelial celular, al estrés oxidativo, ni modifica marcadores de inflamación o senescencia (Auclair et al., 2014). Sin embargo, los resultados de nuestro estudio no van en esa línea. Así, no se observan efectos tóxicos a este nivel con LPV, ATV o DRV,

probablemente porque el efecto negativo de este grupo de fármacos se deba a la dislipidemia actuando sobre el perfil lipídico. Es por ello, que serían necesarios estudios a largo plazo para demostrar este hecho.

Por otro lado, también quisimos analizar el efecto de las combinaciones de fármacos antirretrovirales que más se utilizan en la actualidad en la práctica clínica, para observar como interactúan conjuntamente. Observamos que únicamente las combinaciones que contienen ABC, EFV y RPV inducen interacciones leucocito-endotelio *in vivo*. TDF/FTC/EFV, ABC/3TC/EFV, TDF/FTC/RPV, ABC/3TC/RPV, ABC/3TC/ATV y ABC/3TC/DRV inducen rodamiento y adhesión en vénulas mesentéricas de rata *in vivo*. Sin embargo, únicamente TDF/FTC/EFV, ABC/3TC/EFV y ABC/3TC/RPV inducen migración leucocitaria, mientras que las combinaciones que contienen ATV y DRV, en combinación con ABC/3TC no inducen migración leucocitaria, sugiriendo que estos 2 IP estarían impidiendo la última fase irreversible de la interacción leucocito-endotelio, la migración. Las combinaciones TDF/FTC/ATV y TDF/FTC/DRV no modifican la interacción leucocito-endotelio *in vivo*. Este hecho está en concordancia con los resultados obtenidos en las tinciones hematoxilina-eosina de los mesenterios de los animales analizados, donde únicamente las combinaciones TDF/FTC/EFV, ABC/3TC/EFV y ABC/3TC/RPV inducen extravasación leucocitaria. Con respecto a los experimentos *in vitro*, obtenemos resultados similares que indican que únicamente las combinaciones que contienen ABC, EFV y RPV inducen interacciones leucocito-endotelio. Es decir, las combinaciones formadas por TDF/FTC/EFV, ABC/3TC/EFV, TDF/FTC/RPV, ABC/3TC/RPV, ABC/3TC/ATV y ABC/3TC/DRV inducen rodamiento y adhesión de leucocitos (PMN y PBMC) sobre células endoteliales humanas mientras que TDF/FTC/ATV y TDF/FTC/DRV no modifican estos parámetros.

Dado que las enfermedades cardiovasculares son una causa importante de muerte entre los pacientes de edad normal que toman la "Terapia Antirretroviral Combinada", el pautar unos fármacos u otros es de gran relevancia. Aunque estos

resultados deben ser interpretados con precaución y cautela, se muestran evidencias de que los antagonistas CCR5, los InInt o los IP, o incluso el ITINAN RPV tienen mejor perfil proinflamatorio que los ITINAN EFV y NVP. Teniendo en cuenta su parecida eficacia para suprimir la replicación del virus, la toxicidad vascular de estos fármacos debería tenerse en cuenta a la hora de establecer una pauta posológica a un paciente infectado por el VIH, enfermo de SIDA y con riesgo de sufrir enfermedad cardiovascular.

6. CONCLUSIONES

1. EFV, NVP y RPV (ITINAN), pero no MVC (antagonista CCR5), RAL (InInt), LPV, ATV y DRV (IP) inducen interacción leucocito-endotelio a dosis clínicamente relevantes. *In vivo*, producen rodamiento, adhesión y migración leucocitaria en vénulas mesentéricas de rata, excepto RPV, que sólo induce rodamiento y adhesión leucocitaria. *In vitro*, estos tres fármacos producen rodamiento y adhesión de leucocitos (PMN y PBMC) sobre HUVEC.

2. EFV, pero no NVP, RAL MVC, LPV, ATV y DRV, provocan un aumento de la expresión de CD11b, CD11c y CD18 en neutrófilos y monocitos. RPV produce un aumento de la expresión de CD11b, CD11c y CD18 en neutrófilos, y únicamente CD11b en monocitos, no aumentando la expresión de CD11c y CD18 en este tipo celular. Ninguno de los fármacos analizados induce la expresión de otras moléculas de adhesión leucocitarias (LFA-1, CD49d o L-Selectina) o endoteliales (ICAM-1, VCAM-1 o E-Selectina), ni ninguna de las moléculas de adhesión leucocitarias en linfocitos.

3. El tipo celular implicado en la infiltración leucocitaria inducida por EFV y NVP *in vivo* es mayoritariamente el de los neutrófilos.

4. Los efectos proinflamatorios de EFV y RPV *in vivo* e *in vitro*, pero no los de NVP, se deben a la interacción entre las moléculas de adhesión leucocitarias Mac-1 y gp150,95 con su ligando endotelial ICAM-1.

5. Las combinaciones de antirretrovirales TDF/FTC/EFV, ABC/3TC/EFV, TDF/FTC/RPV, ABC/3TC/RPV, ABC/3TC/ATV y ABC/3TC/DRV, pero no TDF/FTC/ATV y TDF/FTC/DRV, inducen interacción leucocito-endotelio. *In vivo*, producen rodamiento, adhesión y migración leucocitaria en vénulas mesentéricas de rata, si bien las combinaciones TDF/FTC/RPV, ABC/3TC/ATV y ABC/3TC/DRV no modifican el parámetro de migración leucocitaria. *In vitro*, las combinaciones TDF/FTC/EFV, ABC/3TC/EFV, TDF/FTC/RPV, ABC/3TC/RPV,

ABC/3TC/ATV y ABC/3TC/DRV producen rodamiento y adhesión de leucocitos (PMN y PMBC) sobre HUVEC.

6. Como en el caso anterior, el tipo celular implicado en la infiltración leucocitaria producida por las citadas combinaciones *in vivo* es mayoritariamente el de los neutrófilos.

7. BIBLIOGRAFÍA

Acevedo M, Sprecher DL, Calabrese L, Pearce GL, Coyner DL, Halliburton SS, White RD, Sykora E, Kondos GT, Hoff JA. Pilot study of coronary atherosclerotic risk and plaque burden in HIV patients: 'a call for cardiovascular prevention'. **Atherosclerosis**. 2002; 163(2): 349-54.

Akanbi MO, Scarsi KK, Taiwo B, Murphy RL. Combination nucleoside/nucleotide reverse transcriptase inhibitors for treatment of HIV infection. **Expert Opin Pharmacother**. 2012; 13(1): 65-79.

Use of nucleoside reverse transcriptase inhibitors and risk of myocardial infarction in HIV-infected patients. **AIDS**. 2008; 22(14): F17-F24.

Alon R, Feizi T, Yuen CT, Fuhlbrigge RC, Springer TA. Glycolipid ligands for selectins support leukocyte tethering and rolling under physiologic flow conditions. **J Immunol**. 1995; 154(10): 5356-66.

Alvarez A, Hermenegildo C, Issekutz AC, Esplugues JV, Sanz MJ. Estrogens inhibit angiotensin II-induced leukocyte-endothelial cell interactions in vivo via rapid endothelial nitric oxide synthase and cyclooxygenase activation. **Circ Res**. 2002; 91(12): 1142-50.

Alvarez A, Cerdá-Nicolás M, Naim Abu Nabah Y, Mata M, Issekutz AC, Panés J, Lobb RR, Sanz MJ. Direct evidence of leukocyte adhesion in arterioles by angiotensin II. **Blood**. 2004; 104(2): 402-8.

Alvarez A, Ibiza S, Hernández C, Alvarez-Barrientos A, Esplugues JV, Calatayud S Gastrin induces leukocyte-endothelial cell interactions in vivo and contributes to the inflammation caused by Helicobacter pylori. **FASEB J**. 2006; 20(13): 2396-8.

Alvarez A, Ibiza MS, Andrade MM, Blas-García A, Calatayud S. Gastric antisecretory drugs induce leukocyte-endothelial cell interactions through gastrin release and activation of CCK-2 receptors. **J Pharmacol Exp Ther**. 2007; 323(1): 406-13.

Arndt S, Melle C, Mondal K, Klein G, von Eggeling F, Bosserhoff AK. Interactions of TANGO and leukocyte integrin CD11c/CD18 regulate the migration of human monocytes. **J Leukoc Biol**. 2007; 82(6): 1466-72.

Auclair M, Afonso P, Capel E, Caron-Debarle M, Capeau J. Impact of darunavir, atazanavir and lopinavir boosted with ritonavir on cultured human endothelial cells: beneficial effect of pravastatin. **Antivir Ther**. 2014; 19(8): 773-82.

Barré-Sinoussi F, Chermann JC, Rey F, Nugeyre MT, Chamaret S, Gruest J, Dauguet C, Axler-Blin C, Vézinet-Brun F, Rouzioux C, Rozenbaum W, Montagnier L. Isolation of a T-lymphotropic retrovirus from a patient at risk for acquired immune deficiency syndrome (AIDS). **Science**. 1983; 220(4599): 868-71.

Bavinger C, Bendavid E, Niehaus K, Olshen RA, Olkin I, Sundaram V, Wein N, Holodniy M, Hou N, Owens DK, Desai M. Risk of Cardiovascular Disease from Antiretroviral Therapy for HIV: A Systematic Review. **PLoS One**. 2013; 8(3): e59551.

Bedimo RJ, Westfall AO, Drechsler H, Vidiella G, Tebas P. Abacavir use and risk of acute myocardial infarction and cerebrovascular events in the highly active antiretroviral therapy era. **Clin Infect Dis**. 2011; 53(1): 84-91.

Blas-García A, Apostolova N, Ballesteros D, Monleón D, Morales JM, Rocha M, Victor VM, Esplugues JV. Inhibition of mitochondrial function by efavirenz increases lipid content in hepatic cells. **Hepatology**. 2010; 52(1): 115-25.

Blas-García A, Polo M, Alegre F, Funes HA, Martínez E, Apostolova N, Esplugues JV. Lack of mitochondrial toxicity of darunavir, raltegravir and rilpivirine in neurons and hepatocytes: a comparison with efavirenz. **J Antimicrob Chemother**. 2014; 69(11): 2995-3000.

Boffito M, Jackson A, Amara A, Back D, Khoo S, Higgs C, Seymour N, Gazzard B, Moyle G. Pharmacokinetics of once-daily darunavir-ritonavir and atazanavir-ritonavir over 72 hours following drug cessation. **Antimicrob Agents Chemother**. 2011; 55(9): 4218-23.

Bonnet F, Morlat P, Chêne G, Mercié P, Neau D, Chossat I, Decoin M, Djossou F, Beylot J, Dabis F; Groupe d'Epidémiologie Clinique du SIDA en Aquitaine (GECSA). Causes of death among HIV-infected patients in the era of highly active antiretroviral therapy, Bordeaux, France, 1998-1999. **HIV Med**. 2002; 3(3): 195-9.

Brothers CH, Hernandez JE, Cutrell AG, Curtis L, Ait-Khaled M, Bowlin SJ, Hughes SH, Yeo JM, Lapierre DH. Risk of myocardial infarction and abacavir therapy: no increased risk across 52 GlaxoSmithKline-sponsored clinical trials in adult subjects. **J Acquir Immune Defic Syndr**. 2009; 51(1): 20-8.

Brown E. Neutrophil adhesion and the therapy of inflammation. **Semin Hematol**. 1997; 34(4): 319-26.

Burger D, van der Heiden I, la Porte C, et al. Interpatient variability in the pharmacokinetics of the HIV non-nucleoside reverse transcriptase inhibitor efavirenz: the effect of gender, race, and CYP2B6 polymorphism. **Br J Clin Pharmacol**. 2006; 61: 148-54.

Cai YH, Alvarez A, Alcaide P, Duramad P, Lim YC, Jarolim P, Lowe JB, Luscinskas FW, Lichtman AH. Abrogation of functional selectin-ligand expression reduces migration of pathogenic CD8+ T cells into heart. **J Immunol**. 2006; 176(11): 6568-75.

Carlos TM, Harlan JM. Leukocyte-endothelial adhesion molecules. **Blood**. 1994; 84(7): 2068-101.

Carman CV, Springer TA. Trans-cellular migration: cell-cell contacts get intimate. **Curr Opin Cell Biol**. 2008; 20(5): 533-40.

Carr A, Samaras K, Thorisdottir A, Kaufmann GR, Chisholm DJ, Cooper DA. Diagnosis, prediction, and natural course of HIV-1 protease-inhibitorassociated lipodystrophy, hyperlipidaemia, and diabetes mellitus: a cohort study. **Lancet**. 1999; 353(9170): 2093-9.

Casado JL, Moreno S. Potential role of rilpivirine in simplification regimens. **Enferm Infecc Microbiol Clin**. 2013; 31 Suppl 2: 30-5.

Castagna A, Maggiolo F, Penco G, Wright D, Mills A, Grossberg R, Molina JM, Chas J, Durant J, Moreno S, Doroana M, Ait-Khaled M, Huang J, Min S, Song I, Vavro C, Nichols G, Yeo JM; VIKING-3 Study Group. Dolutegravir in antiretroviral-experienced patients with raltegravir- and/or elvitegravir-resistant HIV-1: 24-week results of the phase III VIKING-3 study. **J Infect Dis**. 2014; 210(3): 354-62.

Chow FC, Regan S, Feske S, Meigs JB, Grinspoon SK, Triant VA. Comparison of ischemic stroke incidence in HIV-infected and non-HIV-infected patients in a US health care system. **J Acquir Immune Defic Syndr**. 2012; 60(4): 351-8.

Cipriani S, Francisci D, Mencarelli A, Renga B, Schiaroli E, D'Amore C, Baldelli F, Fiorucci S. Efficacy of the CCR5 antagonist maraviroc in reducing early, ritonavir-induced atherogenesis and advanced plaque progression in mice. **Circulation**. 2013; 127(21): 2114-24.

Cooper CL, van Heeswijk RP. Once-daily nevirapine dosing: a pharmacokinetics, efficacy and safety review. **HIV Med**. 2007; 8(1): 1-7.

Currier JS, Taylor A, Boyd F, Dezii CM, Kawabata H, Burtcel B, Maa JF, Hodder S. Coronary heart disease in HIV-infected individuals. **J Acquir Immune Defic Syndr**. 2003; 33(4): 506-12.

Cutrell A, Brothers C, Yeo J, Hernandez J, Lapierre D. Abacavir and the potential risk of myocardial infarction. **Lancet**. 2008; 371(9622): 1413.

Cruciani M, Zanichelli V, Serpelloni G, Bosco O, Malena M, Mazzi R, Mengoli C, Parisi SG, Moyle G. Abacavir use and cardiovascular disease events: a meta-analysis of published and unpublished data. **AIDS**. 2011; 25(16): 1993-2004.

De Béthune MP. Non-nucleoside reverse transcriptase inhibitors (NNRTIs), their discovery, development, and use in the treatment of HIV-1 infection: a review of the last 20 years (1989-2009). **Antiviral Res**. 2010; 85(1): 75-90.

De Larranaga GF, Petroni A, Deluchi G, Alonso BS, Benetucci JA. Viral load and disease progression as responsible for endothelial activation and/or injury in human immunodeficiency virus-1-infected patients. **Blood Coagul Fibrinolysis**. 2003; 14(1): 15-8.

De Pablo C, Orden S, Apostolova N, Blanquer A, Esplugues JV, Alvarez A. Abacavir and didanosine induce the interaction between human leukocytes and endothelial cells through Mac-1 upregulation. **AIDS**. 2010; 24(9): 1259-66.

De Pablo C, Orden S, Calatayud S, Martí-Cabrera M, Esplugues JV, Alvarez A. Differential effects of tenofovir/emtricitabine and abacavir/lamivudine on human leukocyte recruitment. **Antivir Ther**. 2012; 17(8): 1615-9.

De Pablo C, Orden S, Peris JE, Barrachina MD, Esplugues JV, Alvarez A. Profile of leukocyte-endothelial cell interactions induced in venules and arterioles by nucleoside reverse-transcriptase inhibitors in vivo. **J Infect Dis**. 2013; 208(9): 1448-53.

Dimasi D, Sun WY, Bonder CS. Neutrophil interactions with the vascular endothelium. **Int Immunopharmacol**. 2013; 17(4): 1167-75.

Dunne JL, Ballantyne CM, Beaudet AL, Ley K. Control of leukocyte rolling velocity in TNF-alpha-induced inflammation by LFA-1 and Mac-1. **Blood**. 2002; 99(1): 336-41.

Durand M, Sheehy O, Baril JG, Lelorier J, Tremblay CL. Association between HIV infection, antiretroviral therapy, and risk of acute myocardial infarction: a cohort and nested case-control study using Quebec's public health insurance database. **J Acquir Immune Defic Syndr**. 2011;.57(3):.245-53.

Ebisawa M, Yamada T, Bickel C, Klunk D, Schleimer RP. Eosinophil transendothelial migration induced by cytokines. III. Effect of the chemokine RANTES. **J Immunol**. 1994; 153(5): 2153-60.

Elion R, Molina JM, Ramón Arribas López J, Cooper D, Maggiolo F, Wilkins E, Conway B, Liu YP, Margot N, Rhee M, Chuck SL, Szwarcberg J; Study 145 Team. A randomized phase 3 study comparing once-daily elvitegravir with twice-daily raltegravir in treatment-experienced subjects with HIV-1 infection: 96-week results. **J Acquir Immune Defic Syndr**. 2013; 63(4): 494-7.

Ezzell C. AZT given the green light for clinical treatment of AIDS. **Nature**. 1987; 326(6112): 430.

Flint OP, Noor MA, Hruz PW, Hylemon PB, Yarasheski K, Kotler DP, Parker RA, Bellamine A. The role of protease inhibitors in the pathogenesis of HIV-associated lipodystrophy: cellular mechanisms and clinical implications. **Toxicol Pathol**. 2009; 37(1): 65-77.

Fontas E, van LF, Sabin CA, Friis-Moller N, Rickenbach M, d'Arminio MA, Kirk O, Dupon M, Morfeldt L, Mateu S, Petoumenos K, El-Sadr W, De WS, Lundgren JD, Pradier C, Reiss P. Lipid profiles in HIV-infected patients receiving combination antiretroviral therapy: are different antiretroviral drugs associated with different lipid profiles? **J Infect Dis**. 2004; 189(6): 1056-74.

Friis-Moller N, Sabin CA, Weber R, d'Arminio MA, El-Sadr WM, Reiss P, Thiebaut R, Morfeldt L, De WS, Pradier C, Calvo G, Law MG, Kirk O, Phillips AN, Lundgren JD. Combination antiretroviral therapy and the risk of myocardial infarction. **N Engl J Med**. 2003; 349(21): 19932003

Friis-Møller N, Reiss P, Sabin CA, Weber R, Monforte Ad, El-Sadr W, Thiébaut R, De Wit S, Kirk O, Fontas E, Law MG, Phillips A, Lundgren JD, DAD Study Group. Class of antiretroviral drugs and the risk of myocardial infarction. **N Engl J Med**. 2007; 356(17): 1723-35.

Friis-Møller N, Thiébaut R, Reiss P, Weber R, Monforte AD, De Wit S, El-Sadr W, Fontas E, Worm S, Kirk O, Phillips A, Sabin CA, Lundgren JD, Law MG; DAD study group. Predicting the risk of cardiovascular disease in HIV-infected patients: the data collection on adverse effects of anti-HIV drugs study. **Eur J Cardiovasc Prev Rehabil**. 2010; 17(5): 491-501.

Furie MB, Tancinco MC, Smith CW. Monoclonal antibodies to leukocyte integrins CD11a/CD18 and CD11b/CD18 or intercellular adhesion molecule-1 inhibit chemoattractant-stimulated neutrophil transendothelial migration in vitro. **Blood**. 1991; 78(8): 2089-97.

Galea P, Vermot-Desroches C, Le CC, Wijdenes J, Chermann JC. Circulating cell adhesion molecules in HIV1-infected patients as indicator markers for AIDS progression. **Res Immunol**. 1997; 148(2): 109-17.

Galkina E, Ley K. Immune and inflammatory mechanisms of aterosclerosis. **Annu Rev Immunol**. 2009; 27: 165-97.

Gallant JE, Koenig E, Andrade-Villanueva J, Chetchotisakd P, DeJesus E, Antunes F, Arastéh K, Moyle G, Rizzardini G, Fehr J, Liu Y, Zhong L, Callebaut C, Szwarcberg J, Rhee MS, Cheng AK. Cobicistat versus ritonavir as a pharmacoenhancer of atazanavir plus emtricitabine/tenofovir disoproxil fumarate in treatment-naive HIV type 1-infected patients: week 48 results. **J Infect Dis**. 2013; 208(1): 32-9.

Gallego MJ, Zoja C, Morigi M, Micheletti G, Imberti B, Foppolo M, Remuzzi A, Remuzzi G. Cyclosporine enhances leukocyte adhesion to vascular endothelium under physiologic flow conditions. **Am J Kidney Dis**. 1996; 28(1): 23-31.

Gallo D, Diggs JL, Shell GR, Dailey PJ, Hoffman MN, Riggs JL. Comparison of detection of antibody to the acquired immune deficiency syndrome virus by enzyme immunoassay, immunofluorescence, and Western blot methods. **J Clin Microbiol**. 1986; 23(6): 1049-51.

Gawaz M, Langer H, May AE. Platelets in inflammation and atherogenesis. **J Clin Invest**. 2005; 115(12): 3378-84.

Gilbert PB, McKeague IW, Eisen G, Mullins C, Guéye-NDiaye A, Mboup S, Kanki PJ. Comparison of HIV-1 and HIV-2 infectivity from a prospective cohort study in Senegal. **Stat Med**. 2003; 22(4): 573-93.

Goetz DJ, Greif DM, Shen J, Luscinskas FW. Cell-cell adhesive interactions in an in vitro flow chamber. **Methods Mol Biol**. 1999; 96: 137-45.

Gujuluva C, Burns AR, Pushkarsky T, Popik W, Berger O, Bukrinsky M, Graves MC, Fiala M. HIV-1 penetrates coronary artery endothelial cells by transcytosis. **Mol Med**. 2001; 7(3): 169-76.

Gulick RM, Fatkenheuer G, Burnside R, Hardy WD, Nelson MR, Goodrich J, Mukwaya G, Portsmouth S, Heera JR. Five-year safety evaluation of maraviroc in HIV-1-infected treatment-experienced patients. **J Acquir Immune Defic Syndr**. 2014; 65(1): 78-81.

Günthard HF, Aberg JA2, Eron JJ3, Hoy JF4, Telenti A5, Benson CA6, Burger DM7, Cahn P8, Gallant JE9, Glesby MJ10, Reiss P11, Saag MS12, Thomas DL13, Jacobsen DM14, Volberding PA15; International Antiviral Society-USA Panel. Antiretroviral treatment of adult HIV infection: 2014 recommendations of the International Antiviral Society-USA Panel. **JAMA**. 2014; 23-30; 312(4):410-25.

Gupta SK, Shen C, Moe SM, Kamendulis LM, Goldman M, Dubé MP. Worsening endothelial function with efavirenz compared to protease inhibitors: a 12-month prospective study. **PLoS One**. 2012; 7(9): e45716.

Gupta SK, Mi D, Moe SM, Dubé MP, Liu Z. Effects of switching from efavirenz to raltegravir on endothelial function, bone mineral metabolism, inflammation, and renal function: a randomized, controlled trial. **J Acquir Immune Defic Syndr**. 2013; 64(3): 279-83.

Hatano H, Scherzer R, Wu Y, Harvill K, Maka K, Hoh R, Sinclair E, Palmer S, Martin JN, Busch MP, Deeks SG, Hsue PY. A randomized controlled trial assessing the effects of raltegravir intensification on endothelial function in treated HIV infection. **J Acquir Immune Defic Syndr**. 2012; 61(3): 317-25.

Hawkins T. Understanding and managing the adverse effects of antiretroviral therapy. **Antiviral Res**. 2010; 85(1): 201-9.

Heit B, Colarusso P, Kubes P. Fundamentally different roles for LFA-1, Mac-1 and alpha4-integrin in neutrophil chemotaxis. **J Cell Sci**. 2005; 118(Pt 22): 5205-20.

Hessell AJ, Jaworski JP, Epson E, Matsuda K, Pandey S, Kahl C, Reed J, Sutton WF, Hammond KB, Cheever TA, Barnette PT, Legasse AW, Planer S, Stanton JJ, Pegu A, Chen X, Wang K, Siess D, Burke D, Park BS, Axthelm MK, Lewis A, Hirsch VM, Graham BS, Mascola JR, Sacha JB, Haigwood NL. Early short-term treatment with neutralizing human monoclonal antibodies halts SHIV infection in infant macaques. **Nat Med**. 2013; 22(4): 362-68.

Hicks C, Gulick RM. Raltegravir: the first HIV type 1 integrase inhibitor. **Clin Infect Dis**. 2009; 48(7): 931-9.

Hirahashi J, Hishikawa K, Kaname S, Tsuboi N, Wang Y, Simon DI, Stavrakis G, Shimosawa T, Xiao L, Nagahama Y, Suzuki K, Fujita T, Mayadas TN. Mac-1 (CD11b/CD18) links inflammation and thrombosis after glomerular injury. **Circulation**. 2009; 120(13): 1255-65.

Ho DD, Neumann AU, Perelson AS, Chen W, Leonard JM, Markowitz M. Rapid turnover of plasma virions and CD4 lymphocytes in HIV-1 infection. **Nature**. 1995; 373(6510): 123-6.

House SD, Lipowsky HH. Leukocyte-endothelium adhesion: microhemodynamics in mesentery of the cat. **Microvasc Res**. 1987; 34(3): 363-79.

Hughes EL, Gavins FN. Troubleshooting methods: Using intravital microscopy in drug research. **J Pharmacol Toxicol Methods**. 2010; 61(2): 102-12.

Hull MW, Montaner JS. Ritonavir-boosted protease inhibitors in HIV therapy. **Ann Med**. 2011; 43(5): 375-88.

Hynes RO. Integrins: versatility, modulation, and signaling in cell adhesion. **Cell**. 1992; 69(1): 11-25.

Ibiza S, Alvarez A, Romero W, Barrachina MD, Esplugues JV, Calatayud S. Gastrin induces the interaction between human mononuclear leukocytes and endothelial cells through the endothelial expression of P-selectin and VCAM-1. **Am J Physiol Cell Physiol**. 2009; 297(6): C1588-95.

Imamichi T. Action of anti-HIV drugs and resistance: reverse transcriptase inhibitors and protease inhibitors. **Curr Pharm Des**. 2004; 10(32): 4039-53

Jackson SP. Arterial thrombosis--insidious, unpredictable and deadly. **Nat Med**. 2011; 17(11): 1423-36.

Jaffe EA, Nachman RL, Becker CG, Minick CR. Culture of human endothelial cells derived from umbilical veins. Identification by morphologic and immunologic criteria. **J Clin Invest**. 1973; 52(11): 2745-56.

Jaipersad AS, Lip GY, Silverman S, Shantsila E. The role of monocytes in angiogenesis and atherosclerosis. **J Am Coll Cardiol**. 2014; 63(1): 1-11.

Jamaluddin MS, Lin PH, Yao Q, Chen C. Non-nucleoside reverse transcriptase inhibitor efavirenz increases monolayer permeability of human coronary artery endothelial cells. **Atherosclerosis**. 2010; 208(1): 104-11.

Jones KL, Maguire JJ, Davenport AP. Chemokine receptor CCR5: from AIDS to atherosclerosis. **Br J Pharmacol**. 2011; 162(7): 1453-69.

Jung U, Norman KE, Scharffetter-Kochanek K, Beaudet AL, Ley K. Transit time of leukocytes rolling through venules controls cytokine-induced inflammatory cell recruitment in vivo. **J Clin Invest**. 1998; 102(8): 1526-33.

Kilby JM, Hopkins S, Venetta TM, DiMassimo B, Cloud GA, Lee JY, Alldredge L, Hunter E, Lambert D, Bolognesi D, Matthews T, Johnson MR, Nowak MA, Shaw GM, Saag MS. Potent suppression of HIV-1 replication in humans by T-20, a peptide inhibitor of gp41-mediated virus entry**. Nat Med**. 1998; 4(11): 1302-7.

Kunkel EJ, Ley K. Distinct phenotype of E-selectin-deficient mice. E-selectin is required for slow leukocyte rolling in vivo. **Circ Res**. 1996; 79(6): 1196-204.

Lang S, Mary-Krause M, Cotte L, Gilquin J, Partisani M, Simon A, Boccara F, Costagliola D. Impact of individual antiretroviral drugs on the risk of myocardial infarction in human immunodeficiency virus-infected patients: a case-control study nested within the French Hospital Database on HIV ANRS cohort CO4. **Arch Intern Med**. 2010; 170(14): 1228-38.

León A, Martinez E, Sarasa M, López Y, Mallolas J, De Lazzari E, Laguno M, Milincovic A, Blanco JL, Larrousse M, Lonca M, Gatell JM. Impact of steady-state lopinavir plasma levels on plasma lipids and body composition after 24 weeks of lopinavir/ritonavir-containing therapy free of thymidine analogues. **J Antimicrob Chemother**. 2007; 60(4): 824-30.

Lawrence MB, Springer TA. Leukocytes roll on a selectin at physiologic flow rates: distinction from and prerequisite for adhesion through integrins. **Cell**. 1991; 65(5): 859-73.

Lewis W, Day BJ, Copeland WC. Mitochondrial toxicity of NRTI antiviral drugs: an integrated cellular perspective. **Nat Rev Drug Discov**. 2003; 2(10): 812-22.

Ley K, Laudanna C, Cybulsky MI, Nourshargh S. Getting to the site of inflammation: the leukocyte adhesion cascade updated. **Nat Rev Immunol**. 2007; 7(9): 678-89.

Liedtke MD, Tomlin CR, Lockhart SM, Miller MM, Rathbun RC. Long-term efficacy and safety of raltegravir in the management of HIV infection. **Infect Drug Resist**. 2014; 7: 73-84.

Luscinskas FW, Cybulsky MI, Kiely JM, Peckins CS, Davis VM, Gimbrone MA Jr. Cytokine-activated human endothelial monolayers support enhanced neutrophil transmigration via a mechanism involving both endothelial-leukocyte adhesion molecule-1 and intercellular adhesion molecule-1. **J Immunol**. 1991; 146(5): 1617-25.

Lyck R, Enzmann G. The physiological roles of ICAM-1 and ICAM-2 in neutrophil migration into tissues. **Curr Opin Hematol**. 2015; 22(1): 53-9.

Maggi P, Bellacosa C, Carito V, Perilli F, Lillo A, Volpe A, Trillo G, Angiletta D, Regina G, Angarano G. Cardiovascular risk factors in patients on long-term treatment with nevirapine- or efavirenz-based regimens. **J Antimicrob Chemother**. 2011; 66(4): 896-900.

Manfredi R, Calza L, Chiodo F. An extremely different dysmetabolic profile between the two available nonnucleoside reverse transcriptase inhibitors: efavirenz and nevirapine. **J Acquir Immune Defic Syndr**. 2005; 38(2): 236-8.

Maartens G, Celum C, Lewis SR. HIV infection: Epidemiology, pathogenesis, treatment, and prevention. **Lancet.** 2014; 384(9939): 258-71.

Martínez-Rebollar M, Muñoz A, Pérez I, Hidalgo S, Brunet M, Laguno M, González A, Calvo M, Loncà M, Blanco JL, Martínez E, Gatell JM, Mallolas J. Pharmacokinetic study of dual therapy with raltegravir 400 mg twice daily and Darunavir/Ritonavir 800/100 mg once daily in HIV-1-infected patients. **Ther Drug Monit**. 2013; 35(4): 552-6.

Masedunskas A, Milberg O, Porat-Shliom N, Sramkova M, Wigand T, Amornphimoltham P, Weigert R. Intravital microscopy: a practical guide on imaging intracellular structures in live animals. **Bioarchitecture**. 2012; 2(5): 143-57.

Mellors JW, Rinaldo CR Jr, Gupta P, White RM, Todd JA, Kingsley LA. Prognosis in HIV-1 infection predicted by the quantity of virus in plasma. **Science**. 1996; 272(5265): 1167-70.

McEver RP, Zhu C. Rolling cell adhesion. **Annu Rev Cell Dev Biol**. 2010; 26: 363-96.

Mirza RA, Turiansky GW. Enfuvirtide and cutaneous injection-site reactions. **J Drugs Dermatol**. 2012; 11(10): e35-8.

Mitroulis I, Alexaki VI, Kourtzelis I, Ziogas A, Hajishengallis G, Chavakis T. Leukocyte integrins: role in leukocyte recruitment and as therapeutic targets in inflammatory disease. **Pharmacol Ther**. 2015; 147: 123-35.

Mocroft A, Ruiz L, Reiss P, Ledergerber B, Katlama C, Lazzarin A, Goebel FD, Phillips AN, Clotet B, Lundgren JD; EuroSIDA study group. Virological rebound after suppression on highly active antiretroviral therapy. **AIDS**. 2003; 17(12): 1741-51.

Moldbt B, Le K, Carnathan DG, Whitney JB, Schultz N, Lewis MG, Borducchi E, Smith K, Mackel JJ, Sweat SL, Hodges AP, Godzik A, Parren PW, SIlvestri G, Barouch DH, Burton DR. Neutralizing antibody affords comparable protection against vaginal and rectal SHIV challenge in macaques. **AIDS**. 2016. (Epub ahead of print).

Mondal D, Pradhan L, Ali M, Agrawal KC. HAART drugs induce oxidative stress in human endothelial cells and increase endothelial recruitment of mononuclear cells: exacerbation by inflammatory cytokines and amelioration by antioxidants. **Cardiovasc Toxicol**. 2004; 4(3): 287-302.

Most J, Zangerle R, Herold M, Fuchs D, Wachter H, Fritsch P, Dierich MP. Elevated concentrations of circulating intercellular adhesion molecule 1 (ICAM-1) in HIV-1 infection. **J Acquir Immune Defic Syndr**. 1993; 6(3): 221-6.

Moyle G, Boffito M, Fletcher C, Higgs C, Hay PE, Song IH, Lou Y, Yuen GJ, Min SS, Guerini EM. Steady-state pharmacokinetics of abacavir in plasma and intracellular carbovir triphosphate following administration of abacavir at 600 milligrams once daily and 300 milligrams twice daily in human immunodeficiency virus-infected subjects. **Antimicrob Agents Chemother**. 2009; 53(4): 1532-8.

Muller WA. Mechanisms of transendothelial migration of leukocytes. **Circ Res** 2009; 105(3): 223-30

Mulligan K, Grunfeld C, Tai VW, Algren H, Pang M, Chernoff DN, Lo JC, Schambelan M. Hyperlipidemia and insulin resistance are induced by protease inhibitors independent of changes in body composition in patients with HIV infection. **J Acquir Immune Defic Syndr**. 2000; 23(1): 35-43.

Nabah YN, Mateo T, Cerdá-Nicolás M, Alvarez A, Martinez M, Issekutz AC, Sanz MJ. L-NAME induces direct arteriolar leukocyte adhesion, which is mainly mediated by angiotensin-II. **Microcirculation**. 2005; 12(5): 443-53.

Naggie S, Hicks C. Protease inhibitor-based antiretroviral therapy in treatment-naive HIV-1-infected patients: the evidence behind the options. **J Antimicrob Chemother**. 2010; 65(6): 1094-9.

Obel N, Farkas DK, Kronborg G, Larsen CS, Pedersen G, Riis A, Pedersen C, Gerstoft J, Sorensen HT. Abacavir and risk of myocardial infarction in HIVinfected patients on highly active antiretroviral therapy: a populationbased nationwide cohort study. **HIV Med**. 2010; 11(2): 130-6.

Orden S, de Pablo C, Rios-Navarro C, Martinez-Cuesta MA, Peris JE, Barrachina MD, Esplugues JV, Alvarez A. Efavirenz induces interactions between leucocytes and endothelium through the activation of Mac-1 and gp150,95. **J Antimicrob Chemother**. 2014; 69(4): 995-1004.

Overton ET, Arathoon E, Baraldi E, Tomaka F. Effect of darunavir on lipid profile in HIV-infected patients. **HIV Clin Trials**. 2012; 13(5): 256-70.

[Panel de expertos de GeSIDA y Plan Nacional sobre el Sida. GESIDA/National AIDS Plan: Consensus document on antiretroviral therapy in adults infected by the human immunodeficiency virus (Updated January 2015)]. **Enferm Infecc Microbiol Clin**. 2015; 33(8): 543.e1-543.e43.

Panos G, Samonis G, Alexiou VG, Kavarnou GA, Charatsis G, Falagas ME. Mortality and morbidity of HIV infected patients receiving HAART: a cohort study. **Curr HIV Res**. 2008; 6(3): 257-60.

Pantaleo G, Fauci AS. Immunopathogenesis of HIV infection. **Annu Rev Microbiol**. 1996; 50: 825-54.

Parks DA, Jennings HC, Taylor CW, Acosta EP. Pharmacokinetics of once-daily tenofovir, emtricitabine, ritonavir and fosamprenavir in HIV-infected subjects. **AIDS**. 2007; 21(10): 1373-5.

Pellicelli AM, Palmieri F, Cicalini S, Petrosillo N. Pathogenesis of HIV-related pulmonary hypertension. **Ann N Y Acad Sci**. 2001; 946: 82-94.

Perry CM. Maraviroc: a review of its use in the management of CCR5-tropic HIV-1 infection. **Drugs**. 2010; 70(9): 1189-213.

Petit F, Fromenty B, Owen A, Estaquier J. Mitochondria are sensors for HIV drugs. **Trends Pharmacol Sci**. 2005; 26(5): 258-64.

Piliero PJ. Pharmacokinetic properties of nucleoside/nucleotide reverse transcriptase inhibitors**. J Acquir Immune Defic** Syndr. 2004; 37 Suppl 1: S2-S12.

Pluskota E, Woody NM, Szpak D, Ballantyne CM, Soloviev DA, Simon DI, Plow EF. Expression, activation, and function of integrin alphaMbeta2 (Mac-1) on neutrophil-derived microparticles. **Blood**. 2008; 112(6): 2327-35.

Projahn D, Koenen RR. Platelets: key players in vascular inflammation. **J Leukoc Biol**. 2012; 92(6): 1167-75.

Podzamczer D. Lipid metabolism and cardiovascular risk in HIV infection: new perspectives and the role of nevirapine. **AIDS Rev**. 2013; 15(4): 195-203.

Puppo F, Brenci S, Scudeletti M, Lanza L, Bosco O, Indiveri F. Elevated serum levels of circulating intercellular adhesion molecule-1 in HIV infection. **AIDS**. 1993; 7(4): 593-4.

Rao RM, Yang L, Garcia-Cardena G, Luscinskas FW. Endothelial-dependent mechanisms of leukocyte recruitment to the vascular wall. **Circ Res**. 2007; 101(3): 234-47.

Reeves JD, Doms RW. Human immunodeficiency virus type 2. **J Gen Virol**. 2002; 83(Pt 6): 1253-65.

Reust CE. Common adverse effects of antiretroviral therapy for HIV disease. **Am Fam Physician**. 2011; 83(12): 1443-51.

Reyskens KM, Fisher TL, Schisler JC, O'Connor WG, Rogers AB, Willis MS, Planesse C, Boyer F, Rondeau P, Bourdon E, Essop MF.Cardio-metabolic effectsof HIV protease inhibitors (lopinavir/ritonavir). **PLoS One**. 2013; 8(9): e73347.

Ribaudo HJ, Benson CA, Zheng Y, Koletar SL, Collier AC, Lok JJ, Smurzynski M, Bosch RJ, Bastow B, Schouten JT. No risk of myocardial infarction associated with initial antiretroviral treatment containing abacavir: short and long-term results from ACTG A5001/ALLRT. **Clin Infect Dis**. 2011; 52(7): 929-40.

Ribera E, Tuset M, Martín M, del Cacho E. Characteristics of antiretroviral drugs. **Enferm Infecc Microbiol Clin**. 2011; 29(5): 362-91.

Sabin CA, Worm SW, Weber R, Reiss P, El-Sadr W, Dabis F, De WS, Law M, d'Arminio MA, Friis-Moller N, Kirk O, Pradier C, Weller I, Phillips AN, Lundgren JD. Use of nucleoside reverse transcriptase inhibitors and risk of myocardial infarction in HIV-infected patients enrolled in the D:A:D study: a multi-cohort collaboration. **Lancet**. 2008; 371(9622): 1417-26.

Sadhu C, Ting HJ, Lipsky B, Hensley K, Garcia-Martinez LF, Simon SI, Staunton DE. CD11c/CD18: novel ligands and a role in delayed-type hypersensitivity. **J Leukoc Biol**. 2007; 81(6): 1395-403.

Santos Corraliza E, Fuertes Martín A. Side effects of antiretroviral therapy. Fisiopathology, clinical manifestations and treatment. **An Med Interna**. 2006; 23(7): 338-44.

Sanz E. Abacavir-myocardial infarction. **WHO Signal.** 5 A.D. May 4-6-2005.

Seigneur M, Constans J, Blann A, Renard M, Pellegrin JL, Amiral J, Boisseau M, Conri C. Soluble adhesion molecules and endothelial cell damage in HIV infected patients. **Thromb Haemost**. 1997; 77(4): 646-9.

Sadhu C, Ting HJ, Lipsky B, Hensley K, Garcia-Martinez LF, Simon SI, Staunton DE. CD11c/CD18: novel ligands and a role in delayed-type hypersensitivity. **J Leukoc Biol**. 2007; 81(6): 1395-403.

Shaffer D, Hughes MD, Sawe F, Bao Y, Moses A, Hogg E, Lockman S, Currier J. Cardiovascular disease risk factors in HIV-infected women after initiation of lopinavir/ritonavir- and nevirapine-based antiretroviral therapy in Sub-Saharan Africa: A5208 (OCTANE). **J Acquir Immune Defic Syndr**. 2014; 66(2): 155-63.

Sipsas N, Sfikakis PP, Sfikakis P, Choremi H, Kordossis T. Serum concentrations of soluble intercellular adhesion molecule-1 and progress towards disease in patients infected with HIV. **J Infect**. 1994; 29(3): 271-82.

Sluis-Cremer N, Temiz NA, Bahar I. Conformational changes in HIV-1 reverse transcriptase induced by nonnucleoside reverse transcriptase inhibitor binding. **Curr HIV Res**. 2004; 2(4): 323-32.

Smith CW. Endothelial adhesion molecules and their role in inflammation. **Can J Physiol Pharmacol**. 1993; 71(1): 76-87.

Souza SJ, Luzia LA, Santos SS, Rondó PH. Lipid profile of HIV-infected patients in relation to antiretroviral therapy: a review. **Rev Assoc Med Bras**. 2013; 59(2): 186-98.

Springer TA. Traffic signals for lymphocyte recirculation and leukocyte emigration: the multistep paradigm. **Cell**. 1994; 76(2): 301-14.

Sriramarao P1, von Andrian UH, Butcher EC, Bourdon MA, Broide DH. L-selectin and very late antigen-4 integrin promote eosinophil rolling at physiological shear rates in vivo. **J Immunol**. 1994; 153(9): 4238-46.

Stalker TJ, Skvarka CB, Scalia R. A novel role for calpains in the endothelial dysfunction of hyperglycemia. **FASEB J**. 2003; 17(11): 1511-3.

Sundstrom JB, Martinson DE, Mosunjac M, Bostik P, McMullan LK, Donahoe RM, Gravanis MB, Ansari AA. Norepinephrine enhances adhesion of HIV-1-infected leukocytes to cardiac microvascular endothelial cells. **Exp Biol Med (Maywood)**. 2003; 228(6): 730-40.

Tamatani T, Miyasaka M. Identification of monoclonal antibodies reactive with the rat homolog of ICAM-1, and evidence for a differential involvement of ICAM-1 in the adherence of resting versus activated lymphocytes to high endothelial cells. **Int Immunol**. 1990; 2(2): 165-71.

Tamatani T, Kotani M, Miyasaka M. Characterization of the rat leukocyte integrin, CD11/CD18, by the use of LFA-1 subunit-specific monoclonal antibodies. **Eur J Immunol**. 1991; 21(3): 627-33.

Tashima KT1, Bausserman L, Alt EN, Aznar E, Flanigan TP. Lipid changes in patients initiating efavirenz- and indinavir-based antiretroviral regimens. **HIV Clin Trials**. 2003; 4(1): 29-36.

Tebas P, Sension M, Arribas J, Duiculescu D, Florence E, Hung CC, Wilkin T, Vanveggel S, Stevens M, Deckx H; ECHO and THRIVE Study Groups. Lipid levels and changes in body fat distribution in treatment-naive, HIV-1-Infected adults treated with rilpivirine or Efavirenz for 96 weeks in the ECHO and THRIVE trials. **Clin Infect Dis**. 2014; 59(3): 425-34.

Triant VA. HIV infection and coronary heart disease: an intersection of epidemics. **J Infect Dis**. 2012; 205 Suppl 3: S355-61.

Ucciferri C, Falasca K, Vignale F, Di Nicola M, Pizzigallo E, Vecchiet J. Improved metabolic profile after switch to darunavir/ritonavir in HIV positive patients previously on protease inhibitor therapy. **J Med Virol**. 2013; 85(5): 755-9.

Usach I, Melis V, Peris JE. Non-nucleoside reverse transcriptase inhibitors: a review on pharmacokinetics, pharmacodynamics, safety and tolerability. **J Int AIDS Soc**. 2013; 16: 1-14.

van Buul JD, Hordijk PL. Signaling in leukocyte transendothelial migration. **Arterioscler Thromb Vasc Biol**. 2004; 24(5): 824-33.

van Leth F, Phanuphak P, Stroes E, Gazzard B, Cahn P, Raffi F, Wood R, Bloch M, Katlama C, Kastelein JJ, Schechter M, Murphy RL, Horban A, Hall DB, Lange JM, Reiss P. Nevirapine and efavirenz elicit different changes in lipid profiles in antiretroviral-therapy-naive patients infected with HIV-1. **PLoS Med**. 2004; 1(1): e19.

Watanabe T, Arakawa T, Fukuda T, Higuchi K, Kobayashi K. Role of neutrophils in a rat model of gastric ulcer recurrence caused by interleukin-1 beta. **Am J Pathol**. 1997; 150(3): 971-9.

Waters L, Jackson A, Else L, et al. Switching safely: pharmacokinetics, efficacy and safety of switching efavirenz to maraviroc twice-daily in patients on suppressive antiretroviral therapy. **Antivir Ther**. 2015; 20(2): 157-63

Wei X, Ghosh SK, Taylor ME, Johnson VA, Emini EA, Deutsch P, Lifson JD, Bonhoeffer S, Nowak MA, Hahn BH, et al. Viral dynamics in human immunodeficiency virus type 1 infection. **Nature**. 1995; 373(6510): 117-22.

Wensing AM, van Maarseveen NM, Nijhuis M. Fifteen years of HIV Protease Inhibitors: raising the barrier to resistance. **Antiviral Res**. 2010; 85(1): 59-74.

Worm SW, Sabin C, Weber R, Reiss P, El-Sadr W, Dabis F, De Wit S, Law M, Monforte AD, Friis-Møller N, Kirk O, Fontas E, Weller I, Phillips A, Lundgren J. Risk of myocardial infarction in patients with HIV infection exposed to specific individual antiretroviral drugs from the 3 major drug classes: the data collection on adverse events of anti-HIV drugs (D:A:D) study. **J Infect Dis**. 2010; 201(3): 318-30.

Yamaki K, Lindbom L, Thorlacius H, Hedqvist P, Raud J. An approach for studies of mediator-induced leukocyte rolling in the undisturbed microcirculation of the rat mesentery. **Br J Pharmacol**. 1998; 123(3): 381-9.

Yeung YY, Lee SS, Vanhoutte PM, Leung SW. Prolonged exposure to lopinavir impairs endothelium-dependent hyperpolarization-mediated relaxation in rat mesenteric arteries. **J Cardiovasc Pharmacol**. 2013; 62(4): 397-404.

Zietz C, Hotz B, Stürzl M, Rauch E, Penning R, Löhrs U. Aortic endothelium in HIV-1 infection: chronic injury, activation, and increased leukocyte adherence. **Am J Pathol**. 1996; 149(6): 1887-98.

8. PRODUCCIÓN BIBLIOGRÁFICA

PRODUCCIÓN BIBLIOGRÁFICA

1. De Pablo, **Orden S**, Apostolova N, Blanquer, Esplugues JV, Álvarez Á. Abacavir and didanosine induce the interaction between human leukocytes and endothelial cells through Mac-1 upregulation. ***AIDS*** 2010; 24: 1259-1266.

2. De Pablo C, **Orden S**, Calatayud S, Martí-Cabrera M, Esplugues JV, Álvarez Á. Differential effects of tenofovir/emtricitabine and abacavir/lamivudine on human leukocyte recruitment. ***Antiviral Therapy*** 2012; 17: 1615-1619.

3. De Pablo C, **Orden S**, Peris JE, Barrachina MD, Esplugues JV, Álvarez Á. Profile of leukocyte-endothelial cell interactions induced in venules and arterioles by nucleoside reverse-transcriptase inhibitors in vivo. ***The Journal of Infectious Diseases*** 2013; 208: 1448-1453

4. **Orden S**, de Pablo C, Ríos–Navarro, Martínez-Cuesta MA, Peris JE, Barrachina MD, Esplugues JV, Álvarez Á. Efavirenz induces interactions between leucocytes and endothelium through the activation of Mac-1 and gp150,95. ***Journal of Antimicrobial Chemotherapy*** 2014; 69: 995-1004.

5. Ríos-Navarro C, de Pablo C, Collado-Díaz V, **Orden S**, Blas-García A, Martínez-Cuesta MA, Esplugues JV and Álvarez Á. Differential effects of anti-TNF-α and anti-IL-12/23 agents on human leukocyte-endothelial cell interactions. ***European Journal of Pharmacology*** 2015; 765: 355-365.

6. Hernández-Mijares A, Bañuls C, Rovira-Llopis S, Álvarez Á, **Orden S**, Rubio-Puchol O, Víctor VM, Rocha M. Chronic consumption of an inositol-enriched beverage ameliorates endothelial dysfunction and oxidative stress in type 2 diabetic patients. ***Journal of Functional Foods*** 2015; 18: 598-607.

7. Esplugues JV, de Pablo C, Collado-Díaz V, Hernández C, **Orden S**, Álvarez Á. Interference of purinergic signalling: an explanation for the cardiovascular effect of Abacavir? ***AIDS*** 2016. En prensa.

8. Díaz-Morales N, Rovira-Llopis S, Bañuls C, Escribano-López I, Martínez de Marañón A, López-Domenech S, **Orden S**, Roldán-Torres I, Álvarez Á, Veses S, Jover A, Rocha M, Hernández-Mijares A, Víctor VM. Are mitochondrial fusion and fission impaired in leukocytes of type 2 diaberic patients? ***Antioxidants & Redox Signalling*** 2016. En prensa.

9. **Orden S**, De Pablo C, Calatayud S, Collado-Díaz V, Esplugues JV, Álvarez Á. Leucocyte-endothelial cell interactions of maraviroc, atazanavir, darunavir, raltegravir and rilpivirine: a comparison with abacavir. ***Antiviral Research*** 2016. En revisión.

ARTÍCULO 1

Abacavir and didanosine induce the interaction between leukocytes and endothelial cells through Mac-1 upregulation

De Pablo C, **Orden S,** Apostolova N, Blanquer A, Esplugues JV, Álvarez Á.

AIDS 2010; 24: 1259-1266

Abacavir and didanosine induce the interaction between human leukocytes and endothelial cells through Mac-1 upregulation

Carmen De Pablo[a], Samuel Orden[a], Nadezda Apostolova[a], Amando Blanquer[c], Juan V. Esplugues[a,b] and Angeles Alvarez[a]

Objective: Abacavir and didanosine are nucleoside reverse transcriptase inhibitors (NRTI) widely used in therapy for HIV-infection but which have been linked to cardiovascular complications. The objective of this study was to analyze the effects of clinically relevant doses of abacavir and didanosine on human leukocyte–endothelium interactions and to compare them with those of other NRTIs.

Design and methods: The interactions between human leukocytes – specifically peripheral blood polymorphonuclear (PMN) or mononuclear (PBMC) cells – and human umbilical vein endothelial cells were evaluated in a flow chamber system that reproduces conditions *in vivo*. The expression of adhesion molecules was analyzed by flow cytometry.

Results: Abacavir induced a dose-dependent increase in PMN and PBMC rolling and adhesion. This was reproduced by didanosine but not by lamivudine or zidovudine. Both abacavir and didanosine increased Mac-1 expression in neutrophils and monocytes, but produced no effects on either lymphocytes or the expression of endothelial adhesion molecules. The PMN/PBMC rolling and adhesion induced by abacavir or didanosine did not occur when antibodies against Mac-1 or its ligand ICAM-1 were blocked.

Conclusion: Abacavir induces significant human leukocyte accumulation through the activation of Mac-1, which in turn interacts with its endothelial ligand ICAM-1. The fact that didanosine exhibits similar effects and that lamivudine and zidovudine do not points to a relationship between the chemical structure of NRTIs and the induction of leukocyte/endothelial cell interactions. This mechanism may be especially relevant to the progression of the vascular damage associated with atherosclerosis and myocardial infarction in abacavir and didanosine-treated patients.

© 2010 Wolters Kluwer Health | Lippincott Williams & Wilkins

AIDS 2010, **24**:1259–1266

Keywords: abacavir, cardiovascular diseases, HIV, leukocyte–endothelium interactions, nucleoside reverse transcriptase inhibitor

Introduction

Continuous administration of 'highly active antiretroviral therapy' (HAART) has made AIDS a chronic illness. However, with the increased longevity of patients there is growing concern about the long-term adverse effects induced by this life-long pharmacological treatment, particularly its role in cardiovascular complications such as atherosclerosis and myocardial infarction [1]. HAART is a combination of at least three drugs: two nucleoside reverse transcriptase inhibitors (NRTI) plus a protease inhibitor and/or a nonnucleoside reverse transcriptase

[a]Departamento de Farmacología and CIBERehd, Facultad de Medicina, Universidad de Valencia, [b]Fundación Hospital Universitario Dr Peset, and [c]Centro de Transfusiones de la Comunidad Valenciana, Valencia, Spain.
Correspondence to Juan V. Esplugues, Departamento de Farmacología, Facultad de Medicina, Universidad de Valencia. Avda. Blasco Ibáñez 15-17, 46010 Valencia, Spain
Tel: +34 96 3864624; fax: +34 96 3983879; e-mail: Juan.V.Esplugues@uv.es
Received: 27 December 2009; revised: 12 March 2010; accepted: 23 March 2010.

DOI:10.1097/QAD.0b013e32833a2b02

De Pablo et al., 2010

inhibitor (NNRTI) [2]. Although protease inhibitors were originally considered responsible for these deleterious cardiovascular effects, there is recent evidence that also implicates NNRTIs and, particularly, NRTIs [1].

A potential link between abacavir (ABC), one of the most widely used NRTIs, and myocardial infarction was first highlighted in 2005 [3], and substantial controversy has surrounded the subject ever since. Recent studies have not only further implicated ABC as agent that raises the risk of myocardial infarction but also highlight a similar risk is, though to a lesser extent, with didanosine (ddI), another NRTI [4–7]. The reasons for these adverse effects are not clear as neither ABC nor ddI seem to exert a negative influence on major predisposing factors such as lipid and/or glucose metabolism. However, the fact that the potential to develop myocardial infarction exists as long as patients are receiving the drugs and decreases when therapy is discontinued points to the existence of a rapid mechanism involving vascular inflammation [4]. There is some evidence that ABC causes endothelial nitric oxide synthase (eNOS) downregulation and superoxide anion production in human endothelial cells [8], both of which situations can lead to vascular dysfunction and leukocyte accumulation [9,10]. In addition, ABC-treated patients exhibit elevated levels of the inflammatory markers C-reactive protein (CRP) and interleukin-6 [5].

The accumulation of leukocytes in the vessel wall is a hallmark of the early stages of atherosclerosis, acute myocardial infarction and other vascular diseases and is mediated by the interaction between the adhesion molecules expressed on white blood cells and/or endothelial cells. During this process, leukocytes roll along the wall of inflamed vessels before coming to a halt, after which they adhere and transmigrate [11]. In the present study, we demonstrate the capacity of both ABC and ddI to elicit such interactions and explore the molecular mechanisms involved. NRTIs can be classified as purine or pirimidine analogues. Purine analogues can be guanosine (ABC) or adenosine (ddI) derivates. Pirimidine analogues can be thymidine (zidovudine and stavudine) or cytosine (lamivudine, zalcitabine and emtricitabine) derivates [12,13]. Our primary hypothesis was based on the existing clinical evidence obtained with ABC and ddI; however for the sake of comparison, we extended our analysis to include the pirimidine analogues lamivudine and zidovudine.

Methods

Human umbilical vein endothelial cell culture

Human umbilical vein endothelial cells (HUVEC) were harvested from freshly obtained umbilical cords by collagenase treatment as previously described [14]. Briefly, umbilical cord veins were rinsed of blood products with warm PBS, after which the vein was filled with collagenase (1 mg/ml) for 17 min at 37°C. The cords were then gently massaged to ensure detachment of endothelial cells from the vessel wall. The digest was collected, centrifuged and pelleted once more. The pellet was resuspended in endothelial cell growth medium (EGM-2) inside T25 culture flasks where cells were cultured until confluence. After reaching confluence, primary cultures were detached with trypsin and transferred into appropriate culture dishes. Passage 1 from these primary cultures was subsequently employed. For adhesion studies, HUVEC were cultured on fibronectin (5 μg/ml)-coated 25-mm plastic coverslips until confluent (~48 h).

Leukocyte isolation

Human peripheral blood mononuclear (PBMC) or polymorphonuclear (PMN) cells were isolated from whole blood anticoagulated with sodium citrate drawn from healthy volunteers [14]. Samples were incubated with dextran (3%) for 45 min. PBMC and PMN in the supernatant were separated by gradient density centrifugation (250 g, 25 min) with Ficoll-Paque™ Plus. After red blood cell lysis, leukocytes were washed (HBSS without Ca^{2+} or Mg^{2+}) and resuspended in complete RPMI media.

The medical ethical committee of the Hospital Clínico Universitario de Valencia approved the study and all patients provided written informed consent.

Adhesion assay under flow conditions

The parallel plate flow chamber in-vitro model has been described previously in detail [14,15]. For adhesion assays, coverslips containing confluent HUVEC monolayers were inserted into a circular recess in the bottom plate of the flow chamber (maintained at 37°C), where a portion (5 × 25 mm) of the monolayer was exposed to the flow. The entire chamber was mounted on an inverted microscope (Nikon Eclipse TE 2000-S, Amstleveen, The Netherlands) connected to a video camera (Sony Exware HAD, Koeln, Germany). Experiments were conducted using a 40× objective lens. PMNs or PBMCs were resuspended in flow buffer ($DPBS^+$ containing 20 mmol/l HEPES and 0.1% HSA) at 1×10^6 or 0.5×10^6 cells/ml respectively and drawn across the HUVEC monolayer at a controlled flow rate of 0.36 ml/min (estimated shear stress of 0.7 dyne/cm^2). A circular glass window in the top plate of the chamber allowed direct live microscopic examination of the monolayer exposed to the flow. Images were recorded in a single field of view over a 5 min period during which leukocyte parameters were determined. Leukocyte rolling was calculated by counting the number of leukocytes rolling over 100 μm^2 of the endothelial monolayer during 1 min period. Velocities of 20

consecutive leukocytes in the field of focus were determined by measuring the time required to travel a distance of 100 μm. Leukocyte adhesion was determined by counting the number of leukocytes that maintained stable contact with the monolayer for 30 s.

Experimental protocol

In order to study the effects of NRTIs on leukocyte–endothelial cell interactions, we chose one of the analogues of each purine or pirimidine. In this way, leukocytes (PMNs or PBMCs) and HUVEC were treated for 4 h at 37°C with NRTI purine analogues [ABC (0.1–15 μmol/l) or ddI (5 μmol/l)] or NRTI pirimidine analogues [lamivudine (10 μmol/l) or zidovudine (5 μmol/l)] or with a control vehicle. Tumoral necrosis factor (TNF-α, 10 ng/ml, 4 h) and platelet-activating factor (PAF, 1 μmol/l, 1 h) were used as positive controls for HUVEC and leukocytes respectively. Doses were chosen in order to mimic clinical plasma concentrations of the drugs [8,16,17]. To study the effects of blocking antibodies on NRTI-induced leukocyte–endothelial cell interactions, PMN or PBMC were pretreated with anti-lymphocyte function-associated antigen 1 (LFA-1, 10 μg/ml), anti-macrophage 1 antigen (Mac-1, 20 μg/ml), anti-β_2 integrins (CD18, 10 μg/ml) or control antibodies (10 μg/ml) for 20 min (4°C, darkness) prior to NRTI administration or HUVEC monolayers were pretreated with anti-intercellular adhesion molecule-1 (ICAM-1, 20 μg/ml) or control antibodies for 30 min at 37°C prior to drug administration. The antibodies were assayed at the previously described doses [18,19].

Analysis of the expression of adhesion molecules in peripheral blood leukocytes and in human umbilical vein endothelial cells

Leukocyte adhesion molecules were analyzed in citrated blood samples from healthy donors (40 μl) as described previously [14,20]. These samples were treated for 4 h at 37°C with the NRTI agents and were then incubated for 20 min on ice in the dark with saturating amounts of the corresponding FITC-conjugated antibody. An automated lysing procedure to remove red blood cells and to fix leukocytes was carried out using the EPICS TQ-PREP system (Coulter Electronics, Hialeah, Florida, USA). Neutrophils, monocytes and lymphocytes were identified in the flow cytometer by their specific size (forward-angle light scatter) and granularity (side-angle light scatter). HUVEC were grown to confluence in six well plates as mentioned earlier. Cells were then stimulated for 4 h at 37°C with NRTI agents. Cells were detached with trypsin and placed in suspension and were then incubated with the corresponding antibody (20 min, ice, darkness), fixed (formaldehyde) and analyzed for protein expression according to forward and side scatter characteristics. For both leukocytes and HUVEC, the median of the specific fluorescence intensity was employed as a marker of the expression of the respective epitope, and all samples were compensated using the appropriate isotype-matched negative control. Ten thousand cells were analyzed in each case. Analysis was performed in an EPICS XL-MCL cytometer (Coulter Electronics).

Materials

Dulbecco's PBS with ($DPBS^+$) or without ($DPBS^-$) Ca^{2+} and Mg^{2+}, EGM-2 culture media and foetal bovine serum were provided by LONZA (Verviers, Belgium). Recombinant TNF-α, human serum albumine (HSA, Albuminate 25%), RPMI1640 supplemented with 20 mM HEPES, HBSS, fibronectin and dextran were purchased from Sigma Chemical Co (St Louis, Missouri, USA). Ficoll-Paque TM Plus was purchased from GE Healthcare (Little Chalfont, Buckinghamshire,UK). Plastic coverslips with a diameter of 25 mm were obtained from Nunc (supplied by Thermo Fisher Scientific). PBS, collagenase, and trypsin were obtained from Gibco Invitrogen. The Immunoprep reagent was acquired from Beckman Coulter. ABC, ddI, lamivudine and zidovudine were from Sequoia Research Products. The following mAb have been reported previously and were used as purified IgG: blocking antibodies against CD11a (clone m38), CD11b (clone ICRF44), β2-integrins and controls were purchased from Calbiochem (San Diego, California, USA). The blocking antibody against ICAM-1 was obtained from BD Bioscience. FITC or PE conjugated control antibodies and antibodies against E-selectin, ICAM-1, vascular cell adhesion molecule (VCAM)-1, CD18, CD11a, CD11b or CD11c were from BD Bioscience.

Data analysis and statistics

Data are mean ± SEM of n at least four experiments. Statistical significance was considered to be less than 0.05 by one-way ANOVA analysis of variance with Newman–Keuls post-test correction to compare multiple variances.

Results

Effects of nucleoside reverse transcriptase inhibitors on leukocyte–endothelium interactions

ABC induced a significant and dose-dependent increase in the rolling flux (Fig. 1a and 1c) and adhesion (Fig. 1b and 1d) of PMN and PBMC. Concomitantly, ABC induced a decrease in the rolling velocity of PMN (veh: 732 ± 104, ABC 5 μmol/l: 542 ± 58 μm/s, $P < 0.05$, $n = 5$) and PBMC (veh: 751 ± 69, ABC 5 μmol/l: 469 ± 120 μm/s, $P < 0.01$, $n = 6$). PBMC were more sensitive than PMN to the effects of ABC, and this difference reached significance with doses 10 times lower (1 μmol/l). Leukocyte–endothelium interactions were significantly increased by ddI but not by zidovudine or lamivudine (Fig. 2).

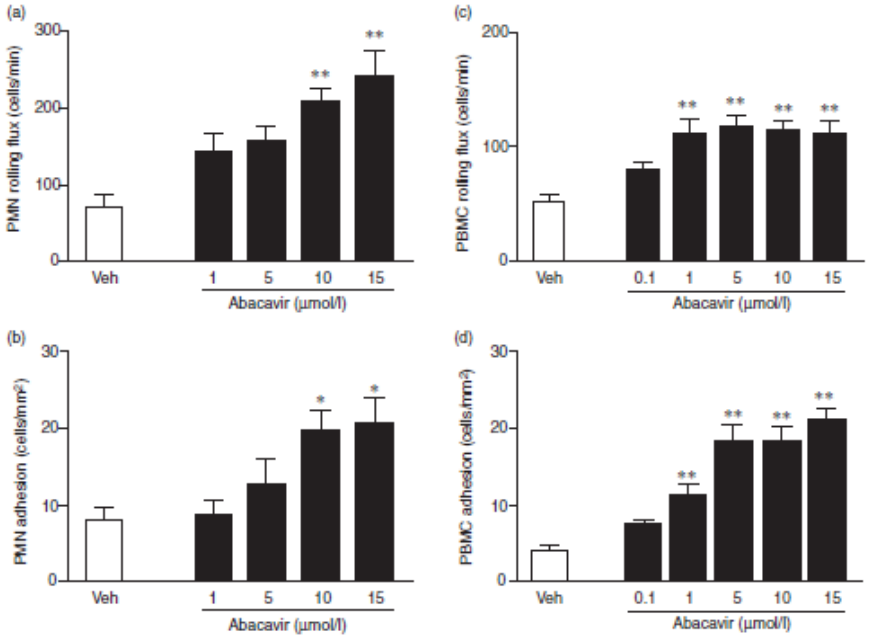

Fig. 1. Effects of ABC on PMN rolling (a) and adhesion (b), and PBMC rolling (c) and adhesion (d). HUVEC and leukocytes (PMNs or PBMCs) were treated (4 h) with ABC (0.1–15 μmol/l) or its vehicle. Results are mean ± SEM, $n = 4–6$. $^*P < 0.05$, $^{**}P < 0.01$ vs. corresponding value in vehicle-treated group (ANOVA followed by Newman–Keuls test).

Endothelial cells were not activated by ABC or ddI

In HUVECs, the highest concentrations of ABC (15 μmol/l, $n = 4$) or ddI (10 μmol/l, $n = 4$) had no effect on the expression (as % of control) of E-selectin (ABC: 103 ± 5%, ddI: 99 ± 2%), ICAM-1 (ABC: 99 ± 15, ddI: 93 ± 7%) or VCAM-1 (ABC: 98 ± 7%, ddI: 109 ± 18%).

Role of Mac-1 in the activation of leukocytes

Monocyte and neutrophil adhesion to the endothelium is generally mediated by the interaction of β_2-integrins LFA-1 and/or Mac-1 with their endothelial ligand ICAM-1. However, Mac-1 has other nonendothelial matrix ligands. β_2-integrins share a common β subunit (CD18) and have a specific α subunit (CD11a for LFA-1 and CD11b for Mac-1) [11]. Treatment of neutrophils and monocytes with ABC or ddI increased the expression of CD18 and CD11b (Fig. 3 and Supplemental Figure 1, http://links.lww.com/QAD/A33) but had no effect on the expression of CD11a, CD49d and L-selectin. Once again, monocytes were more sensitive than neutrophils to the effects of ABC. Neither ABC nor ddI had any effect on the adhesion molecules of lymphocytes (data not shown). The interactions induced by ABC or ddI were prevented by antibodies against CD11b, CD18 or ICAM-1, but not by antibodies against CD11a (Fig. 4 and Supplemental Figure 2, http://links.lww.com/QAD/A34), thus suggesting that a CD11b-CD18 (Mac-1) mechanism is responsible for the accumulation of leukocytes.

Discussion

This study demonstrates for the first time that both ABC and ddI induce the interaction between human leukocytes and endothelial cells by activating Mac-1 in neutrophils and monocytes, but not in lymphocytes, which in turn interacts with the ICAM-1 that is present on endothelial cells.

We used an in-vitro model in which human leukocytes flow over a monolayer of human endothelial cells with a shear stress similar to that observed *in vivo* [14]. This reproduces the processes that precede the formation of an inflammatory focus *in vivo* (rolling and adhesion) and

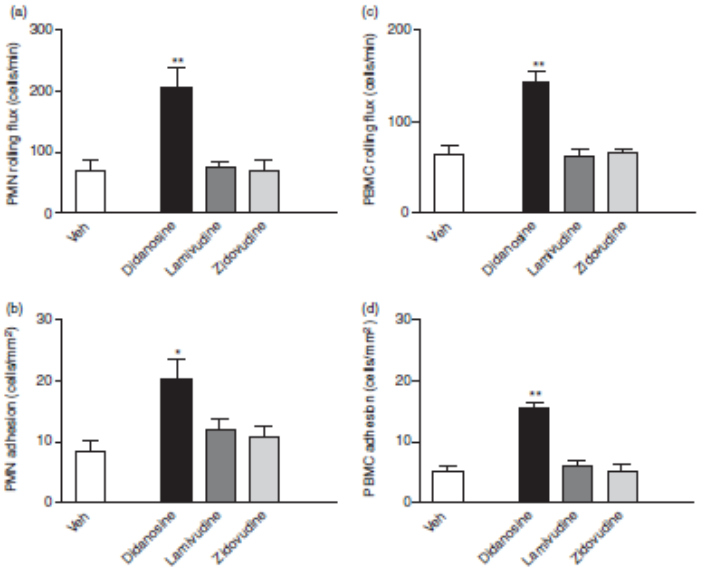

Fig. 2. Effects of NRTI on PMN rolling (a) and adhesion (b), and PBMC rolling (c) and adhesion (d). HUVEC and leukocytes were treated (4 h) with ddI (5 μmol/l), lamivudine (10 μmol/l), zidovudine (5 μmol/l) or vehicle. Results are mean ± SEM, $n = 4$. $^{*}P < 0.05$, $^{**}P < 0.01$ vs. corresponding value in vehicle-treated group (ANOVA followed by Newman–Keuls test).

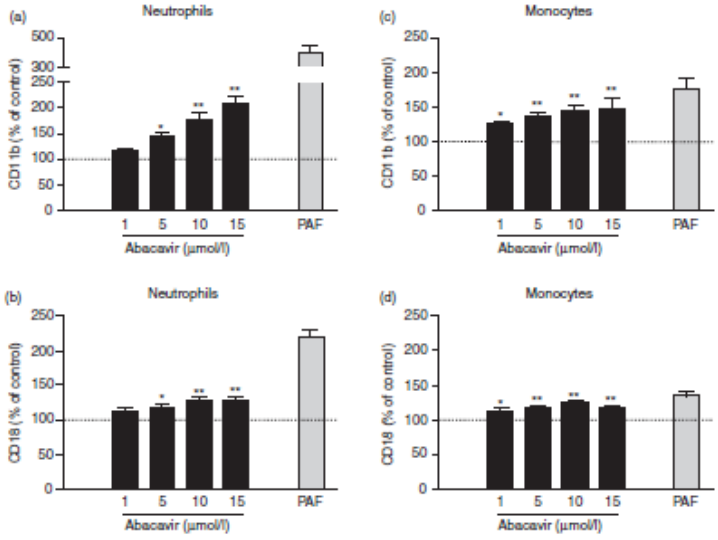

Fig. 3. Effects of ABC on the expression of CD11b (a, c) and CD18 (b, d) integrin subunits on the surface of neutrophils and monocytes. Whole blood was treated (4 h) with ABC (1–15 μmol/l) or vehicle. Fluorescence values are expressed as percentage of mean fluorescence intensities of control cells (dotted line). PAF (1 μmol/l, 1 h) was used as positive control. Results are mean ± SEM, $n = 4$–6. $^{*}P < 0.05$, $^{**}P < 0.01$ vs. corresponding value in vehicle-treated group (ANOVA followed by Newman–Keuls test).

De Pablo et al., 2010

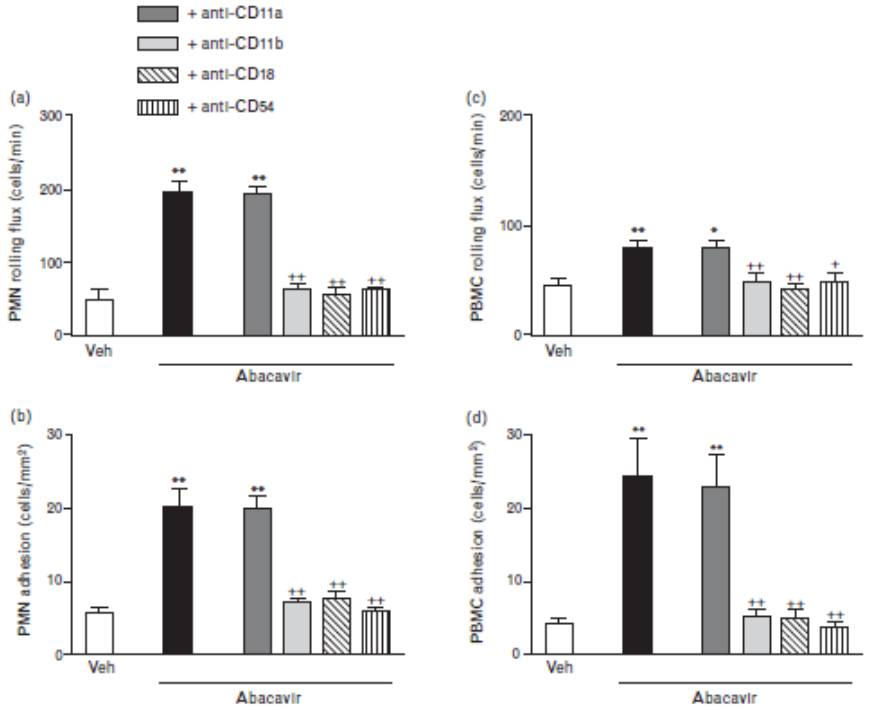

Fig. 4. Effects of blockade of CD11a, CD11b, CD18 or ICAM-1 (CD54) on PMN rolling (a) and adhesion (b), and PBMC rolling (c) and adhesion (d) induced by ABC. Leukocytes and HUVEC were treated (4 h) with ABC (15 μmol/l) or its vehicle. Results are mean ± SEM, $n = 4–6$. $^{*}P < 0.05$, $^{**}P < 0.01$ vs. corresponding value in vehicle-treated group and $^{+}P < 0.05$, $^{++}P < 0.01$ vs. corresponding value in ABC-treated group (ANOVA followed by Newman–Keuls test).

which are critical for hemostasis and vascular cell integrity. However, an exacerbation of these interactions contributes to the vascular dysfunction and injury associated with many vascular diseases (e.g., atherosclerosis, diabetic vasculopathy, hypercholesterolemia, hypertension, ischemia–reperfusion,...) [21]. Our dynamic experimental system has been widely used to visualize and analyze the multistep recruitment of leukocytes in these diseases; moreover, it allows the mechanisms of action implicated in this recruitment to be assessed [22,23].

In our experiments, concentrations of ABC (0.1–15 μmol/l) and ddI (5 μmol/l) that mimic those present in patients (1–8 and 3–10 μmol/l respectively) [8,24,25] induced leukocyte–endothelial cell interactions (rolling and adhesion). The magnitude of the increases obtained with both drugs was smaller than that observed after direct stimulation with proinflammatory agents such as TNF-α, interleukin-4 or RANTES [26,27]; however, it was substantially greater than that exhibited in unstimulated PMNs or PBMCs from patients with different vascular conditions [28–30]. Leukocyte accumulation induced by ABC or ddI occured simultaneously with the selective upregulation of Mac-1 on the surface of human neutrophils and monocytes. Nevertheless, the expression of other adhesion molecules in these leukocytes [CD11a/CD18 or very late antigen (VLA)-4] or in endothelial cells (E-selectin, ICAM-1 or VCAM-1) was not affected. Thus, our results suggest that ABC and ddI promote the recruitment of leukocytes before activating the endothelium, and thus before dysfunction appears which needs a much longer period of exposure (24 h) to develop [8].

HIV-infection itself is associated with a more pronounced adhesion of leukocytes to endothelial cells [31] and with an elevated cardiovascular risk [32]. Both situations could be related to the high levels of the endothelial dysfunction markers (ICAM-1, VCAM-1 and E-selectin) that are present in these patients [32]. Since ABC has been

specifically associated with an impaired endothelial function in HIV-infected patients [33] and given the difference between the activation profile of adhesion molecules observed in our experiments and that of HIV patients, the effects of antiretrovirals and those of the virus could feasibly be accumulative. In other words, the virus may cause endothelial activation [34] and antiretrovirals could activate leukocytes. This is an interesting hypothesis, but further clinical and experimental studies would be necessary before any solid conclusion can be drawn.

Mac-1 is mobilized from intracellular secretory vesicles to the cell surface within minutes of stimulating neutrophils and monocytes. Although it may interact with ICAM-2, iC3B, factor X or fibrinogen, its main ligand, ICAM-1 is constitutively expressed on the surface of the vascular endothelium [11]. Thus, the fact that blocking either Mac-1 or ICAM-1 significantly reduced the effects of ABC and ddI point to a role for both these molecules in the rolling and adhesion induced by these two antiretrovirals. Although their involvement in adhesion is to be expected, rolling is considered to be mediated by selectins and/or VLA-4/VCAM-1 [11]. However, there is growing evidence of the implication of Mac-1/ICAM-1 in rolling in both the activated and resting endothelium [35,36].

ABC and ddI specifically affect PMN and PBMC. This is of relevance given that there is a substantial increase in the levels of neutrophils and monocytes during acute myocardial infarction and in the expression of Mac-1 among the two cell populations [37]. In addition, it has been reported that Mac-1 induces the binding of neutrophils to activated cardiac myocytes [38], and recent evidence points to the mediation of the leukocyte engagement of platelets as the link between cellular adhesion and thrombosis by Mac-1 [36,39].

Finally, the fact that similar effects to those of ABC were observed with ddI but not with lamivudine or zidovudine suggests a relationship between the chemical structure of NRTIs and the induction of leukocyte/endothelial cell interactions. It is tempting to speculate that purine analogues such as ABC or ddI have the potential to interfere with purine-signaling pathways and to provoke cardiovascular complications with inflammatory components (such as atherosclerosis and myocardial infarction) by reducing the levels of adenosine and increasing those of proinflammatory ATP. However, it is necessary to evaluate the actions, on the one hand, of other NRTIs such as tenofovir and emtricitabine, both of which are potential alternatives to ABC for patients with an elevated risk of cardiovascular disease, and on the other hand, of NNRTIs and protease inhibitors in this and other experimental settings before a sound clinical conclusion can be established.

Acknowledgements

C.D.P. performed the research; S.O., N.A. and A.B. helped perform the research and J.V.E. and A.A. designed the research and wrote the paper. J.V.E. and A.A. contributed equally to this study.

This study has been supported by grants SAF2007-60021 from Ministerio de Educación y Cultura; GV/2007/074, GVACOMP2009-266, ACOMP2009-194 and CS2009-AP-030 from Generalitat Valenciana and CD06/04/0071 (CIBER ehd) and PI081325 from Ministerio de Sanidad y Consumo. C.D.P and S.O. have been supported by grants from Ministerio de Educación y Cultura and from Fundación Juan Esplugues respectively.

References

1. Friis-Moller N, Sabin CA, Weber R, D'Arminio MA, El Sadr WM, Reiss P, *et al.* **Combination antiretroviral therapy and the risk of myocardial infarction.** *N Engl J Med* 2003; **349**:1993–2003.
2. Hammer SM, Eron JJ Jr, Reiss P, Schooley RT, Thompson MA, Walmsley S, *et al.* **Antiretroviral treatment of adult HIV infection: 2008 recommendations of the International AIDS Society-USA panel.** *JAMA* 2008; **300**:555–570.
3. Sanz E. *Abacavir-myocardial infarction.* WHO Signal 5 A.D: 4–6. 2005.
4. Sabin CA, Worm SW, Weber R, Reiss P, El Sadr W, Dabis F, *et al.* **Use of nucleoside reverse transcriptase inhibitors and risk of myocardial infarction in HIV-infected patients enrolled in the D:A:D study: a multicohort collaboration.** *Lancet* 2008; **371**:1417–1426.
5. **Use of nucleoside reverse transcriptase inhibitors and risk of myocardial infarction in HIV-infected patients.** *AIDS* 2008; **22**:F17–F24.
6. Worm SW, Sabin C, Weber R, Reiss P, El Sadr W, Dabis F, *et al.* **Risk of myocardial infarction in patients with HIV infection exposed to specific individual antiretroviral drugs from the 3 major drug classes: the data collection on adverse events of anti-HIV drugs (D:A:D) study.** *J Infect Dis* 2010; **201**:318–330.
7. Obel N, Farkas DK, Kronborg G, Larsen CS, Pedersen G, Riis A, *et al.* **Abacavir and risk of myocardial infarction in HIV-infected patients on highly active antiretroviral therapy: a population-based nationwide cohort study.** *HIV Med* 2010; **11**:130–136.
8. Wang X, Chai H, Lin PH, Yao Q, Chen C. **Roles and mechanisms of human immunodeficiency virus protease inhibitor ritonavir and other antihuman immunodeficiency virus drugs in endothelial dysfunction of porcine pulmonary arteries and human pulmonary artery endothelial cells.** *Am J Pathol* 2009; **174**:771–781.
9. Alvarez A, Hermenegildo C, Issekutz AC, Esplugues JV, Sanz MJ. **Estrogens inhibit angiotensin II-induced leukocyte-endothelial cell interactions in vivo via rapid endothelial nitric oxide synthase and cyclooxygenase activation.** *Circ Res* 2002; **91**:1142–1150.
10. Alvarez A, Sanz MJ. **Reactive oxygen species mediate angiotensin II-induced leukocyte-endothelial cell interactions in vivo.** *J Leukoc Biol* 2001; **70**:199–206.
11. Carlos TM, Harlan JM. **Leukocyte-endothelial adhesion molecules.** *Blood* 1994; **84**:2068–2101.
12. Piliero PJ. **Pharmacokinetic properties of nucleoside/nucleotide reverse transcriptase inhibitors.** *J Acquir Immune Defic Syndr* 2004; **37 (Suppl 1)**:S2–S12.
13. De Clercq E. **The history of antiretrovirals: key discoveries over the past 25 years.** *Rev Med Virol* 2009; **19**:287–299.
14. Ibiza S, Alvarez A, Romero W, Barrachina MD, Esplugues JV, Calatayud S. **Gastrin induces the interaction between human mononuclear leukocytes and endothelial cells through the endothelial expression of P-selectin and VCAM-1.** *Am J Physiol Cell Physiol* 2009; **297**:C1588–C1595.

De Pablo et al., 2010

15. Ghandour H, Cullere X, Alvarez A, Luscinskas FW, Mayadas TN. **Essential role for Rap1 GTPase and its guanine exchange factor CalDAG-GEF1 in LFA-1 but not VLA-4 integrin mediated human T-cell adhesion.** *Blood* 2007; **110**:3682–3690.
16. Jiang B, Hebert VY, Li Y, Mathis JM, Alexander JS, Dugas TR. **HIV antiretroviral drug combination induces endothelial mitochondrial dysfunction and reactive oxygen species production, but not apoptosis.** *Toxicol Appl Pharmacol* 2007; **224**:60–71.
17. Caron M, Auclairt M, Vissian A, Vigouroux C, Capeau J. **Contribution of mitochondrial dysfunction and oxidative stress to cellular premature senescence induced by antiretroviral thymidine analogues.** *Antivir Ther* 2008; **13**:27–38.
18. Heit B, Colarusso P, Kubes P. **Fundamentally different roles for LFA-1, Mac-1 and alpha4-integrin in neutrophil chemotaxis.** *J Cell Sci* 2005; **118**:5205–5220.
19. Pluskota E, Woody NM, Szpak D, Ballantyne CM, Soloviev DA, Simon DI, *et al*. **Expression, activation, and function of integrin alphaMbeta2 (Mac-1) on neutrophil-derived microparticles.** *Blood* 2008; **112**:2327–2335.
20. Alvarez A, Cerda-Nicolas M, Naim Abu NY, Mata M, Issekutz AC, Panes J, *et al*. **Direct evidence of leukocyte adhesion in arterioles by angiotensin II.** *Blood* 2004; **104**:402–408.
21. Krieglstein CF, Granger DN. **Adhesion molecules and their role in vascular disease.** *Am J Hypertens* 2001; **14**:44S–54S.
22. Goetz DJ, Greif DM, Shen J, Luscinskas FW. **Cell-cell adhesive interactions in an in vitro flow chamber.** *Methods Mol Biol* 1999; **96**:137–145.
23. Rao RM, Yang L, Garcia-Cardena G, Luscinskas FW. **Endothelial-dependent mechanisms of leukocyte recruitment to the vascular wall.** *Circ Res* 2007; **101**:234–247.
24. Lagathu C, Eustace B, Prot M, Frantz D, Gu Y, Bastard JP, *et al*. **Some HIV antiretrovirals increase oxidative stress and alter chemokine, cytokine or adiponectin production in human adipocytes and macrophages.** *Antivir Ther* 2007; **12**:489–500.
25. Moyle G, Boffito M, Fletcher C, Higgs C, Hay PE, Song IH, *et al*. **Steady-state pharmacokinetics of abacavir in plasma and intracellular carbovir triphosphate following administration of abacavir at 600 milligrams once daily and 300 milligrams twice daily in human immunodeficiency virus-infected subjects.** *Antimicrob Agents Chemother* 2009; **53**:1532–1538.
26. Mateo T, Naim Abu NY, Losada M, Estelles R, Company C, Bedrina B, *et al*. **A critical role for TNFalpha in the selective attachment of mononuclear leukocytes to angiotensin-II-stimulated arterioles.** *Blood* 2007; **110**:1895–1902.
27. von Hundelshausen P, Weber KS, Huo Y, Proudfoot AE, Nelson PJ, Ley K, *et al*. **RANTES deposition by platelets triggers monocyte arrest on inflamed and atherosclerotic endothelium.** *Circulation* 2001; **103**:1772–1777.
28. Sundstrom JB, Martinson DE, Mosunjac M, Bostik P, McMullan LK, Donahoe RM, *et al*. **Norepinephrine enhances adhesion of HIV-1-infected leukocytes to cardiac microvascular endothelial cells.** *Exp Biol Med (Maywood)* 2003; **228**:730–740.
29. Luu NT, Madden J, Calder PC, Grimble RF, Shearman CP, Chan T, *et al*. **Comparison of the pro-inflammatory potential of monocytes from healthy adults and those with peripheral arterial disease using an in vitro culture model.** *Atherosclerosis* 2007; **193**:259–268.
30. Abu-Taha M, Rius C, Hermenegildo C, Noguera I, Cerda-Nicolas JM, Issekutz AC, *et al*. **Menopause and ovariectomy cause a low grade of systemic inflammation that may be prevented by chronic treatment with low doses of estrogen or losartan.** *J Immunol* 2009; **183**:1393–1402.
31. Zietz C, Hotz B, Sturzl M, Rauch E, Penning R, Lohrs U. **Aortic endothelium in HIV-1 infection: chronic injury, activation, and increased leukocyte adherence.** *Am J Pathol* 1996; **149**:1887–1898.
32. de Gaetano DK, Rabagliati R, Iacoviello L, Cauda R. **HIV infection, HAART, and endothelial adhesion molecules: current perspectives.** *Lancet Infect Dis* 2004; **4**:213–222.
33. Hsue PY, Hunt PW, Wu Y, Schnell A, Ho JE, Hatano H, *et al*. **Association of abacavir and impaired endothelial function in treated and suppressed HIV-infected patients.** *AIDS* 2009; **23**:2021–2027.
34. Francisci D, Giannini S, Baldelli F, Leone M, Belfiori B, Guglielmini G, *et al*. **HIV type 1 infection, and not short-term HAART, induces endothelial dysfunction.** *AIDS* 2009; **23**:589–596.
35. Dunne JL, Collins RG, Beaudet AL, Ballantyne CM, Ley K. **Mac-1, but not LFA-1, uses intercellular adhesion molecule-1 to mediate slow leukocyte rolling in TNF-alpha-induced inflammation.** *J Immunol* 2003; **171**:6105–6111.
36. Woollard KJ, Suhartoyo A, Harris EE, Eisenhardt SU, Jackson SP, Peter K, *et al*. **Pathophysiological levels of soluble P-selectin mediate adhesion of leukocytes to the endothelium through Mac-1 activation.** *Circ Res* 2008; **103**:1128–1138.
37. Meisel SR, Shapiro H, Radnay J, Neuman Y, Khaskia AR, Gruener N, *et al*. **Increased expression of neutrophil and monocyte adhesion molecules LFA-1 and Mac-1 and their ligand ICAM-1 and VLA-4 throughout the acute phase of myocardial infarction: possible implications for leukocyte aggregation and microvascular plugging.** *J Am Coll Cardiol* 1998; **31**:120–125.
38. Frangogiannis NG, Smith CW, Entman ML. **The inflammatory response in myocardial infarction.** *Cardiovasc Res* 2002; **53**:31–47.
39. Hirahashi J, Hishikawa K, Kaname S, Tsuboi N, Wang Y, Simon DI, *et al*. **Mac-1 (CD11b/CD18) links inflammation and thrombosis after glomerular injury.** *Circulation* 2009; **120**:1255–1265.

ARTÍCULO 2

Differential effects of tenofovir/emtricitabine and abacavir/lamivudine on human leukocyte recruitment

De Pablo C, **Orden S,** Calatayud S, Martí-Cabrera M, Esplugues JV, Álvarez Á.

Antiviral Therapy 2012; 17: 1615-1619

AntiViral Therapy 2012; 17:1615–1619 (doi: 10.3851/IMP2357)

Short communication

Differential effects of tenofovir/emtricitabine and abacavir/lamivudine on human leukocyte recruitment

*Carmen De Pablo[1], Samuel Orden[1], Sara Calatayud[1], Miguel Martí-Cabrera[1], Juan V Esplugues[1,2], Ángeles Álvarez[1,3]**

[1]Departamento de Farmacología and CIBERehd, Facultad de Medicina, Universidad de Valencia, Valencia, Spain
[2]Fundación Hospital Universitario Dr Peset, Valencia, Spain
[3]Fundación General Universidad de Valencia, Valencia, Spain

*Corresponding author e-mail: angeles.alvarez@uv.es

Background: The association of abacavir (ABC) with cardiovascular disease has led to HIV treatment guidelines favouring the combination of tenofovir/emtricitabine (TDF/FTC) over that of ABC/lamivudine (ABC/3TC). We have analysed the effects of plasma-relevant concentrations of TDF, FTC, ABC and 3TC, individually and in clinically employed combinations, on human leukocyte accumulation. The effects of ABC, 3TC, TDF and FTC on the expression of adhesion molecules were also evaluated.

Methods: Interactions between human leukocytes – specifically peripheral blood polymorphonuclear or mononuclear cells – and human umbilical vein endothelial cells were evaluated in a flow chamber reproducing *in vivo* conditions. The expression of adhesion molecules was analysed by flow cytometry.

Results: Concentrations of TDF, FTC or 3TC mimicking those in the plasma of patients did not have any effect on human leukocyte–endothelial cell interactions, while contrasting results were obtained with ABC. This distinct pattern was reproduced when the drugs were administered in combination; namely, ABC/3TC had a significant influence on rolling and adhesion while TDF/FTC did not. However, the effects produced by ABC alone did not differ when it was combined with 3TC, which suggests the former drug was responsible for the effects observed. ABC, 3TC, TDF and FTC did not modify the expression of endothelial adhesion molecules. Conversely, only ABC enhanced the expression of leukocyte CD11b/CD18 in neutrophils and monocytes.

Conclusions: Our results provide evidence that the combination TDF/FTC has a better vascular profile than ABC/3TC.

Introduction

Abacavir/lamivudine (ABC/3TC) and tenofovir/emtricitabine (TDF/FTC) are the most widely used nucleoside reverse transcriptase inhibitor (NRTI) associations in combined antiretroviral therapy [1]. Current clinical guidelines reflect a preference for the TDF/FTC combination due to the lower virological efficacy of ABC/3TC [1] and evidence, though not uniformly reproduced [2], that ABC (and not TDF) is associated with cardiovascular disease (CVD) [3,4]. This recommendation should however be viewed with caution, since a similar association between TDF/FTC and CVD may have gone undetected until now due to this combination having been commercialized for a shorter period of time.

The relationship between ABC and CVD cannot be explained by an effect on lipid and glucose metabolism. Indeed, the risk of CVD is reduced when therapy with this drug is discontinued, which points towards a direct and more acute mechanism such as vascular inflammation [3–5]. The role of vascular inflammation in CVD is widely acknowledged [5] and involves the accumulation in the vessel wall of both leukocytes and platelets as a consequence of interactions between adhesion molecules expressed on these cells and/or the endothelium [6,7]. In this circumstance, leukocytes roll along the wall of inflamed vessels before coming to a halt, after which they adhere and transmigrate. In a second phase, platelets bind to the endothelium and recruit other circulating platelets and leukocytes, thereby amplifying the thrombotic and atherosclerotic process.

©2012 International Medical Press 1359-6535 (print) 2040-2058 (online)

We have recently demonstrated the capacity of ABC and didanosine (ddI), another purine analogue, to elicit leukocyte accumulation, an effect that was not observed with the pyrimidine analogues 3TC and zidovudine [8]. In the present study, we compare TDF/FTC and ABC/3TC, individually and in combination, on leukocyte accumulation. The effects of FTC, TDF, ABC and 3TC on the expression of endothelial and leukocyte adhesion molecules are also analysed.

Methods

We employed passage 1 human umbilical vein endothelial cells (HUVECs) harvested from umbilical cords [8]. Peripheral blood mononuclear (PBMC) or polymorphonuclear (PMN) cells were isolated from whole blood of healthy volunteers [8]. Samples were obtained from Hospital Clínico Universitario (Valencia, Spain) following approval from its ethical committee.

Adhesion assay under flow conditions

The parallel plate flow chamber model was used for these assays [9,10]. Coverslips (fibronectin [5 μg/ml]-coated) containing confluent HUVEC monolayers were inserted in the chamber (37°C) so that a portion (5×25 mm) was exposed to the flow. The chamber was mounted on an inverted microscope (Nikon Eclipse TE 2000-S, ×40; Amstleveen, the Netherlands) with a video camera (Sony Exware HAD; Koeln, Germany). PMNs or PBMCs were re-suspended in buffer (Dulbecco's phosphate-buffered saline with Ca^{2+} and Mg^{2+} [DPBS$^+$] containing 20 mM HEPES and 0.1% HSA) at 1×10^6 or 0.5×10^6 cells/ml, respectively, and drawn across the monolayer (flow rate 0.36 ml/min, shear stress 0.7 dyne/cm^2). Images of a single field were recorded over 5 min and leukocyte parameters were determined. Rolling flux was calculated by counting the number of cells rolling across 100 μm^2 of the monolayer during 1 min [11]. Rolling leukocytes are easily visualized since they travel more slowly than free-flowing cells. Velocities of 20 consecutive leukocytes in the field of focus were determined by measuring the time required to travel 100 μm. Distances were calibrated using a Neubauer cell chamber. Adhesion was determined after 5 min of perfusion by analysis of 5–10 high power (40×) fields. Leukocytes were considered to be adherent after 30 s of stable contact with the monolayer [10].

Experimental protocol

Leukocytes and HUVECs were treated independently (4 h, 37°C) with TDF (0.5–1 μmol/l), FTC (5–10 μmol/l), ABC (10 μmol/l), 3TC (10 μmol/l), TDF/FTC (1/10 μmol/l), ABC/3TC (10/10 μmol/l) or control. These concentrations mimic clinically relevant plasma concentrations [12,13].

Expression of adhesion molecules

Leukocyte adhesion molecules were analysed in blood samples and endothelium molecules in confluent HUVECs [8]. Cells were treated with the NRTI (4 h, 37°C), incubated with saturating amounts of antibodies (20 min, 4°C, darkness), fixed and identified in a flow cytometer (EPICS XL-MCL cytometer; Coulter Electronics, Hialeah, FL, USA). Mean fluorescence intensity was employed as marker of expression of the respective epitope.

Materials

Dulbecco's PBS with (DPBS$^+$) or without (DPBS$^-$) Ca^{2+} and Mg^{2+}, endothelial cell growth media-2 culture media and fetal bovine serum (LONZA, Barcelona, Spain), human serum albumine (HSA, Albuminate 25%), RPMI1640 supplemented with 20 mM HEPES, HBSS, fibronectin and dextran (Sigma Chemical Co, Madrid, Spain); Ficoll-Paque TM Plus (GE Healthcare, Valencia, Spain), coverslips (Nunc, Thermo Fisher Scientific, Madrid, Spain), PBS, collagenase and trypsin (Gibco, Invitrogen, Barcelona, Spain), Immunoprep reagent (Beckman Coulter, Izasa, Barcelona, Spain), antiretrovirals (Sequoia Research Products, Pangbourne, UK) and fluorescein isothiocyanate- or phycoerythrin-conjugated antibodies (BD Bioscience, Madrid, Spain).

Statistics

One-way ANOVA with a Newman–Keuls post-test correction was employed for statistical analysis (mean ±SEM; $n\geq4$; $P<0.05$).

Results

Leukocyte–endothelial cell interactions

FTC, TDF, 3TC or TDF/FTC did not modify rolling velocity, rolling flux or adhesion of PMN and PBMC (Figure 1). ABC and ABC/3TC induced a significant increase in rolling flux and adhesion while decreasing the rolling velocity of PMN and PBMC (Figure 1).

Expression of adhesion molecules

FTC, TDF, ABC and 3TC had no effect on the expression of E-selectin, intercellular adhesion molecule-1 (ICAM-1) or vascular cell adhesion molecule-1 (VCAM-1) in HUVECs (Table 1). Treatment of whole blood with FTC, TDF or 3TC did not alter the expression of CD11a, CD11b, CD18 and CD49d in neutrophils or monocytes (Table 2). Incubation of whole blood with ABC significantly increased the expression of CD11b and CD18 in neutrophils and monocytes (Table 2) but had no effect on CD11a and CD49d. Lymphocyte adhesion molecules were not modified by any of the compounds.

©2012 International Medical Press

Figure 1. Effects of nucleoside reverse transcriptase inhibitors on leukocyte–endothelial cell interactions

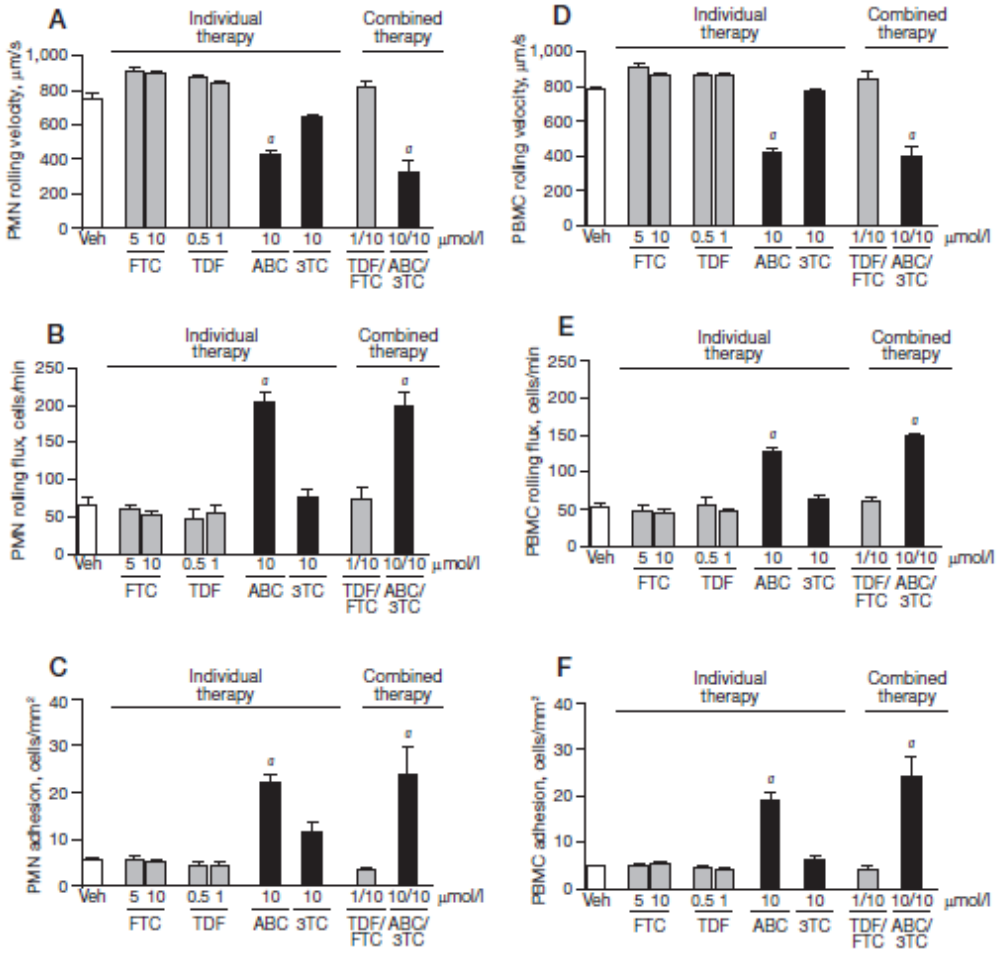

Comparison of the effects of emtricitabine (FTC), tenofovir (TDF), abacavir (ABC), lamivudine (3TC), TDF/FTC or ABC/3TC on **(A)** rolling velocity, **(B)** rolling flux and **(C)** adhesion of peripheral blood polymorphonuclear cells (PMN) and on **(D)** rolling velocity, **(E)** rolling flux and **(F)** adhesion of peripheral blood mononuclear cells (PBMC). Human umbilical vein endothelial cells and leukocytes (PMNs or PBMCs) were treated (4 h) with FTC (5–10 µmol/l), TDF (0.5–1 µmol/l), ABC (10 µmol/l), 3TC (10 µmol/l), TDF/FTC (1/10 µmol/l), ABC/3TC (10/10 µmol/l) or vehicle. Results are mean ±SEM, $n=4$. [a]$P<0.001$ versus corresponding value in vehicle-treated group (ANOVA followed by Newman–Keuls test).

Discussion

This is the first study to analyse the effects of the two most recommended NRTIs, TDF and FTC, on leukocyte accumulation. We evaluated the effects of both drugs individually and together, as they are administered in clinical practice, and compared them with those of the recommended alternative combination (ABC/3TC). Concentrations of TDF (0.5–1 µmol/l), FTC (5–10 µmol/l), ABC (10 µmol/l) or 3TC

Table 1. Expression of endothelial adhesion molecules E-selectin, ICAM-1 and VCAM-1 on HUVECs

	FTC	TDF	ABC	3TC
E-selectin	103.9 ±3.0	102.2 ±2.3	110.3 ±19.9	111.4 ±18.8
ICAM-1	102.9 ±5.7	105.7 ±7.4	104.4 ±16.8	89.3 ±9.7
VCAM-1	109.1 ±5.6	109.0 ±5.6	98.3 ±5.5	103.8 ±6.1

Data is adhesion molecules in human umbilical vein endothelial cells (HUVECs), percentage versus control. HUVECs were treated with emtricitabine (FTC; 10 μmol/l), tenofovir (TDF; 1 μmol/l), abacavir (ABC; 10 μmol/l), lamivudine (3TC; 10 μmol/l) or vehicle (4 h) and were analysed by flow cytometry as described in *Methods*. Fluorescein isothiocyanate- or phycoerythrin-fluorescence values are expressed as a percentage of the mean fluorescence intensities of control cells (100%). Results are mean ±s.e of n=4–6 experiments. ANOVA followed by Newman–Keuls test was performed. ICAM-1, intercellular adhesion molecule-1; VCAM-1, vascular cell adhesion molecule-1.

(10 μmol/l) mimicking those found in clinical contexts (0.5–1.3, 2.7–10.4, 3–10 and 1.5–8 μmol/l, respectively) were employed [12,13]. TDF, FTC and 3TC had no effect on human leukocyte–endothelial cell interactions. In contrast, ABC induced accumulation of white cells. This distinct pattern was reproduced when drugs were administered in combination; in other words, ABC/3TC significantly influenced rolling and adhesion while TDF/FTC did not. However, ABC exerted a similar action alone or in combination (ABC/3TC), which points to this drug as being responsible for the effects observed. The dynamic experimental system we have employed, in which leukocytes flow over a monolayer of HUVECs is widely acknowledged to accurately reproduce the rolling and adhesion processes that precede the formation of an inflammatory focus *in vivo*. It has provided valuable insight into leukocyte/endothelium interactions [9,10], and has been used to analyse leukocyte recruitment in patients with CVD [14] and to determine the vascular proinflammatory effects of drugs [15]. Furthermore, these *in vitro* conditions allow the actions of a specific agent or combination to be assessed, thereby overcoming the limitations of clinical studies.

We also evaluated effects of TDF, FTC and 3TC on key adhesion molecules and found that none of the three drugs altered the expression of CD11a, CD11b, CD18 or CD49d (present in leukocytes) or endothelial E-selectin, ICAM-1 or VCAM-1. In contrast, ABC induced CD11b and CD18 expression (Mac-1), while it had no effect on CD11a, CD49d or endothelial adhesion molecules.

Mac-1, an adhesion molecule, is thought to be the link between cellular adhesion and thrombosis [16]. Present in neutrophils and monocytes, it interacts with either its constitutive endothelial ligand ICAM-1, causing it to adhere to the endothelium [6], or with platelet ligands (GPIbα, $\alpha_{IIb}\beta_3$ and JAM-3) [7], thereby mediating leukocyte engagement of platelets [16].

The actions of ABC could be related to its chemical structure. Since leukocyte accumulation is induced only by cyclic purine analogues (ABC or ddI), and not by pyrimidine analogues (3TC, zidovudine, FTC) or the acyclic nucleotide TDF (current observations and [8]), we propose that ABC and ddI competitively inhibit the purine signalling cascade and increase levels of proinflammatory ATP. This would lead to augmentation of CD11b/CD18 and, consequently, of leukocyte–endothelial interactions. This mechanism is related to the one that seems to underlie activation of platelets by ABC, which involves inhibition of guanylyl cyclase, followed by a decrease in cGMP and increased expression of P-selectin [17].

Clinical studies suggested a relationship between ABC (but not TDF/FTC) and CVD [3,4] and have implicated the expression of metabolic, inflammatory, procoagulant or endothelial markers in said relationship [18,19]. For instance, patients switching from ABC/3TC to TDF/FTC show improvements in both arterial stiffness and CVD markers, including c-reactive protein, interleukin (IL)-6, D-dimer and cholesterol [20]. Indeed, two studies have concluded that TDF has anti-inflammatory potential. One reported a significant improvement in the endothelial dysfunction associated with HIV-infection and decreased levels of sVCAM-1 and monocyte chemoattractant protein-1 in patients receiving TDF, but not in those on ABC [21]. The second described the capacity of TDF to undermine the release of cardiovascular-related inflammatory cytokines (IL-8 and MIP-1α) from human primary cells and to produce a shift in the IL-10/IL-12 balance towards an anti-inflammatory profile [22].

Given that CVD is the most prevalent cause of death among the normal aged population, any hint of an association with the drugs used in combined antiretroviral therapy is of great relevance. Our results should be interpreted with caution, but they do confirm recent clinical evidence that the combination TDF/FTC has a better vascular profile than that of ABC/3TC and endorse recent guidelines favouring the use of TDF/FTC.

Acknowledgements

This study has been supported by grants SAF2007-60021 from Ministerio de Educación y Ciencia co-funded by FEDER; SAF2010-16030 from Ministerio de Ciencia e Innovación, CB06/04/0071 (CIBERehd), PI11/00327 from Ministerio de Sanidad y Consumo and PROMETEO/2010/060 from Generalitat Valenciana. CDP is funded by an FPI grant (BES-2008-004338) from Ministerio de Ciencia e Innovación and SO by a VLC-CAMPUS grant from Universidad de Valencia. AA was a beneficiary of Ramón y Cajal (RYC2005-002295) and I3 programmes from Ministerio de Ciencia e Innovación.

©2012 International Medical Press

Table 2. Expression of leukocyte adhesion molecules CD11a, CD11b, CD18 and CD49d integrin subunits on neutrophils and monocytes

Adhesion molecules in leukocytes		FTC	TDF	ABC	3TC
Adhesion molecules in neutrophils, % versus control	CD11a	96.8 ±2.4	96.2 ±2.6	102.9 ±2.6	97.9 ±3.1
	CD11b	96.3 ±10.3	103.3 ±13.4	160.8 ±18.5[a]	96.3 ±9.1
	CD18	96.8 ±4.1	96.3 ±5.7	122.4 ±7.0[a]	92.18 ±9.2
	CD49d	99.7 ±0.3	99.8 ±0.3	99.5 ±0.5	94.9 ±5.5
Adhesion molecules in monocytes, % versus control	CD11a	99.1 ±4.2	105.6 ±4.6	106.9 ±6.6	102.8 ±8.0
	CD11b	70.9 ±10.3	85.0 ±18.9	143.9 ±9.2[a]	87.5 ±17.7
	CD18	99.2 ±6.1	92.5 ±5.2	119.9 ±6.4[a]	92.0 ±5.3
	CD49d	102.4 ±3.2	97.8 ±3.5	100.1 ±5.1	102.6 ±0.4

Whole blood was treated with emtricitabine (FTC; 10 μmol/l), tenofovir (TDF; 1 μmol/l), abacavir (ABC; 10 μmol/l), lamivudine (3TC;10 μmol/l) or vehicle (4 h) and was analysed by flow cytometry, as described in Methods. Fluorescein isothiocyanate- or phycoerythrin-fluorescence values are expressed as a percentage of the mean fluorescence intensities of control cells (100%). Results are mean ±SEM of n=4–6 experiments. [a]P<0.01 versus corresponding value in vehicle-treated group (ANOVA followed by Newman–Keuls test).

CDP performed the research, and was assisted by SO, SC and MM-C. CDP and AA analysed the data. JVE and AA designed the research and wrote the manuscript.

Disclosure statement

The authors declare no competing interests.

References

1. Thompson MA, Aberg JA, Cahn P, *et al.* Antiretroviral treatment of adult HIV infection: 2010 recommendations of the International AIDS Society-USA panel. *JAMA* 2010; **304**:321–333.
2. Ribaudo HJ, Benson CA, Zheng Y, *et al.* No risk of myocardial infarction associated with initial antiretroviral treatment containing abacavir: short and long-term results from ACTG A5001/ALLRT. *Clin Infect Dis* 2011; **52**:929–940.
3. Sabin CA, Worm SW, Weber R, *et al.* Use of nucleoside reverse transcriptase inhibitors and risk of myocardial infarction in HIV-infected patients enrolled in the D:A:D study: a multi-cohort collaboration. *Lancet* 2008; **371**:1417–1426.
4. The SMART/INSIGHT and the D:A:D Study Groups. Use of nucleoside reverse transcriptase inhibitors and risk of myocardial infarction in HIV-infected patients. *AIDS* 2008; **22**:F17–F24.
5. Behrens GM, Reiss P. Abacavir and cardiovascular risk. *Curr Opin Infect Dis* 2010; **23**:9–14.
6. Carlos TM, Harlan JM. Leukocyte-endothelial adhesion molecules. *Blood* 1994; **84**:2068–2101.
7. Gawaz M, Langer H, May AE. Platelets in inflammation and atherogenesis. *J Clin Invest* 2005; **115**:3378–3384.
8. De Pablo C, Orden S, Apostolova N, Blanquer A, Esplugues JV, Alvarez A. Abacavir and didanosine induce the interaction between human leukocytes and endothelial cells through Mac-1 upregulation. *AIDS* 2010; **24**:1259–1266.
9. Goetz DJ, Greif DM, Shen J, Luscinskas FW. Cell-cell adhesive interactions in an *in vitro* flow chamber. *Methods Mol Biol* 1999; **96**:137–145.
10. Luscinskas FW, Kansas GS, Ding H, *et al.* Monocyte rolling, arrest and spreading on IL-4-activated vascular endothelium under flow is mediated via sequential action of L-selectin, beta 1-integrins, and beta 2-integrins. *J Cell Biol* 1994; **125**:1417–1427.
11. Gee DJ, Wright LK, Zimmermann J, Cole K, Soule K, Ubowski M. Dimethylsulfoxide exposure modulates HL-60 cell rolling interactions. *Biosci Rep* 2012; **32**:375–382.
12. Wang X, Chai H, Lin PH, Yao Q, Chen C. Roles and mechanisms of human immunodeficiency virus protease inhibitor ritonavir and other anti-human immunodeficiency virus drugs in endothelial dysfunction of porcine pulmonary arteries and human pulmonary artery endothelial cells. *Am J Pathol* 2009; **174**:771–781.
13. Parks DA, Jennings HC, Taylor CW, Acosta EP. Pharmacokinetics of once-daily tenofovir, emtricitabine, ritonavir and fosamprenavir in HIV-infected subjects. *AIDS* 2007; **21**:1373–1375.
14. Victor VM, Rocha M, Banuls C, *et al.* Induction of oxidative stress and human leukocyte/endothelial cell interactions in polycystic ovary syndrome patients with insulin resistance. *J Clin Endocrinol Metab* 2011; **96**:3115–3122.
15. Gallego MJ, Zoja C, Morigi M, *et al.* Cyclosporine enhances leukocyte adhesion to vascular endothelium under physiologic flow conditions. *Am J Kidney Dis* 1996; **28**:23–31.
16. Hirahashi J, Hishikawa K, Kaname S, *et al.* Mac-1 (CD11b/CD18) links inflammation and thrombosis after glomerular injury. *Circulation* 2009; **120**:1255–1265.
17. Baum PD, Sullam PM, Stoddart CA, McCune JM. Abacavir increases platelet reactivity via competitive inhibition of soluble guanylyl cyclase. *AIDS* 2011; **25**:2243–2248.
18. Rasmussen TA, Tolstrup M, Melchjorsen J, *et al.* Evaluation of cardiovascular biomarkers in HIV-infected patients switching to abacavir or tenofovir based therapy. *BMC Infect Dis* 2011; **11**:267.
19. Padilla S, Masia M, Garcia N, Jarrin I, Tormo C, Gutierrez F. Early changes in inflammatory and pro-thrombotic biomarkers in patients initiating antiretroviral therapy with abacavir or tenofovir. *BMC Infect Dis* 2011; **11**:40.
20. Sinn K, Richardson R, Carr A. Lower arterial stiffness and Framingham score after switching abacavir to tenofovir in men at high cardiovascular risk. *AIDS* 2010; **24**:2403–2405.
21. Francisci D, Falcinelli E, Belfiori B, *et al.* Impact of tenofovir versus abacavir on HIV-related endothelial dysfunction. *AIDS Patient Care STDS* 2011; **25**:567–569.
22. Melchjorsen J, Risor MW, Sogaard OS, *et al.* Tenofovir selectively regulates production of inflammatory cytokines and shifts the IL-12/IL-10 balance in human primary cells. *J Acquir Immune Defic Syndr* 2011; **57**:265–275.

Accepted 21 July 2012; published online 7 September 2012

ARTÍCULO 3

Profile of leukocyte-endothelial cell interactions induced in venules and arterioles by nucleoside reverse-transcriptase inhibitors in vivo

De Pablo C, **Orden S,** Peris JE, Barrachina MD, Esplugues JV, Álvarez Á.

The Journal of Infectious Diseases 2013; 208: 1448-1453

BRIEF REPORT

Profile of Leukocyte-Endothelial Cell Interactions Induced in Venules and Arterioles by Nucleoside Reverse-Transcriptase Inhibitors In Vivo

Carmen De Pablo,[1] Samuel Orden,[1] Jose E. Peris,[2] María D. Barrachina,[1] Juan V. Esplugues,[1,4] and Ángeles Álvarez[1,3]

[1]Departamento de Farmacología and CIBERehd, Facultad de Medicina, Universidad de Valencia; [2]Departamento de Farmacia y Tecnología Farmacéutica, Facultad de Farmacia, Universidad de Valencia; [3]Fundación General de la Universidad de Valencia; and [4]FISABIO–Fundación Hospital Universitario Doctor Peset, Valencia, Spain

Background. There is controversy regarding cardiovascular (CV) toxicity of the nucleoside reverse-transcriptase inhibitors used to treat human immunodeficiency virus infection.

Methods. We evaluated the effects of nucleoside reverse-transcriptase inhibitors on leukocyte-endothelium interactions, a hallmark of CV diseases, in rat mesenteric vessels using intravital microscopy and in human arterial cells using a flow chamber system.

Results. Abacavir and didanosine increased rolling, adhesion and emigration in rat vessels. These effects were reversed with antibodies against Macrophage-1 antigen (Mac-1) or intercellular adhesion molecule 1 and were reproduced in human cells. Lamivudine, zidovudine, emtricitabine, and tenofovir had no effects.

Conclusions. Our results support the association of abacavir and didanosine with CV diseases.

Keywords. Abacavir; didanosine; tenofovir; lamivudine; zidovudine; emtricitabine; leukocyte-endothelium interations; cardiovascular diseases.

Combined antiretroviral therapy has reduced the mortality rates associated with human immunodeficiency virus (HIV) infection. However, with the increased longevity of patients there is growing concern about the adverse effects generated by this life-long treatment. The association with cardiovascular (CV) diseases is especially worrying given that HIV-infected subjects are already at risk of developing such conditions because of the virus [1]. Combined antiretroviral therapy is a combination of at least 3 drugs: a nonnucleoside reverse-transcriptase inhibitor and/or a protease inhibitor plus 2 nucleoside reverse-transcriptase inhibitors (NRTIs), the latter of which always forms a part of this therapy. Despite the controversy surrounding the CV toxicity of abacavir (ABC) [2], recent guidelines continue to recommend an initial regimen of this NRTI with lamivudine (3TC) [3].

Evidence supports the implication of vascular inflammatory mechanisms in the association between ABC and CV, including enhanced platelet reactivity, T-cell activation, arterial stiffness, and endothelial dysfunction [1]. In addition, we have recently demonstrated in vitro the specific capacity of ABC and didanosine (ddI) to elicit leukocyte accumulation in venular endothelium [4, 5], a hallmark of vascular diseases characterized by inflammation such as atherosclerosis [2]. The endothelium is the principal controller of white cell traffic between the blood stream and extravascular space. This process involves a cascade of adhesive interactions between leukocytes and endothelial cells manifested in leukocyte rolling, leading to firm adhesion and subsequent endothelial transmigration. Although leukocyte recruitment via postcapillary venules is particularly important in many inflammatory diseases, despite being less common, the interaction with arteries is crucial to the mononuclear infiltration appearing in the genesis of atherosclerotic processes [6].

We have performed in vivo experiments, in venules and arterioles, to evaluate the relevance of and mechanisms implicated in the leukocyte-endothelium interactions induced by ABC and ddI. In addition, we have compared their actions with those of other NRTIs and assessed their effects on the interactions of leukocytes with human arterial cells in vitro.

METHODS

Intravital Microscopy

Leukocyte-endothelial cell interactions were evaluated in anesthetized Sprague-Dawley rats (200–250 g; anesthetized with sodium pentobarbital [65 mg/kg, administered intraperitoneally]) according to a standard technique [6]. A segment of the midjejunum was placed over an optically clear viewing pedestal at 37°C for tissue transillumination. The exposed mesentery was superfused with bicarbonate buffer saline (BBS; pH, 7.4; 37°C; 2 mL/min) and visualized using an orthostatic

Received 29 November 2012; accepted 12 April 2013; electronically published 1 August 2013.

Presented in part: 12th International Workshop on Adverse Drug Reactions and Co-Morbidities in HIV, London, United Kingdom, 4–6 November 2010 (abstract O03); 18th Conference on Retroviruses and Opportunistic Infections, Boston, Massachusetts, 27 February–2 March 2011 (abstract 815); Sixth European Congress of Pharmacology, Granada, Spain, 17–20 July 2012 (abstract P310).

Correspondence: Ángeles Álvarez, Departamento de Farmacología, Facultad de Medicina, Universidad de Valencia, Avda Blasco Ibáñez 15–17, 46010 Valencia, Spain (angeles.alvarez@uv.es).

The Journal of Infectious Diseases 2013;208:1448–53
© The Author 2013. Published by Oxford University Press on behalf of the Infectious Diseases Society of America. All rights reserved. For Permissions, please e-mail: journals.permissions@oup.com.
DOI: 10.1093/infdis/jit340

microscope (Nikon Optiphot-2, SMZ1; Nikon) coupled to a video camera (Sony SSC-C350P; Sony) to allow image capturing on videotape (Sony SVT-S3000P) for playback analysis. A video caliper (Microcirculation Research Institute, Texas A&M University) allowed the diameter of arterioles (15–30 μm) and single unbranched mesenteric venules (25–40 μm) to be measured online (during the acquisition of the images). Hemodynamic parameters were calculated as described elsewhere [6].

Experimental Protocol

Animals were injected (2.5 mL, administered intraperitoneally) with saline or 1 of the following NRTI solutions: ABC (1–10 μmol/L; equivalent to 8–80 μg/kg), ddI (5 μmol/L; 15 μg/kg), 3TC (10 μmol/L; 30 μg/kg), zidovudine (ZDV; 5 μmol/L; 17 μg/kg), emtricitabine (FTC; 10 μmol/L; 30 μg/kg), or tenofovir (TDF; 1–5 μmol/L; 4–18 μg/kg). All doses were representative of plasma concentrations in patients [7–9] and administered intraperitoneally, as is usual in intravital microscopy [6, 10]; ABC was also orally (100 mg/kg) administered [11]. Images were recorded 4 hours later (in some cases 24 or 48 hours later) during a 5-minute period and leukocyte parameters were evaluated offline (during a separate time period) by a blind observer.

Adhesion molecules were determined by pretreatment (30 minutes before NRTI) with blocking or with the corresponding control antibodies (monoclonal antibodies) injected through the tail vein in doses of 2 mg/kg for WT-5 (anti-rat macrophage-1 antigen [Mac-1]; CD11b) and 1 mg/kg for WT-3 (anti-rat β_2-integrins; CD18) and 1A29 (anti-rat intercellular adhesion molecule 1 [ICAM-1]; CD54), which have been shown to block the in vivo function of the adhesion molecules analyzed [6, 12].

Flow Cytometry

Portal blood samples were incubated (40 μL; 20 minutes; on ice and in darkness) with saturating amounts of the corresponding conjugated monoclonal antibody anti-rat fluorescein isothiocyanate and then lysed and fixed [6]. Expression of adhesion molecules in granulocytes, monocytes and lymphocytes was analyzed with a FACSCalibur flow cytometer (BD).

Cell Culture

Human umbilical arterial endothelial cells (HUAECs; passage 1) and peripheral blood mononuclear cells (PBMCs) from healthy volunteers were from Hospital Clínico Universitario, Valencia. Spain. The PBMCs and HUAECs were treated independently (4 hours; 37°C) with ABC (1–10 μmol/L), ddI (5 μmol/L), 3TC (10 μmol/L), ZDV (5 μmol/L), FTC (10 μmol/L), TDF (1 μmol/L), or control [4, 5].

Dynamic Adhesion Assay

The parallel plate flow chamber model used has been described elsewhere [5]. In brief, cover slips containing confluent HUAEC monolayers were inserted in a chamber (37°C), and a portion (5 × 25 mm) was exposed to flow. The chamber was mounted on an inverted microscope (Nikon Eclipse TE 2000-S; ×40) with a video-camera (Sony Exware HAD). The PBMCs were resuspended in buffer (Dulbecco phosphate-buffered saline [DPBS] with Ca^{2+} and Mg^{2+} containing 20 mmol/L HEPES and 0.1% human serum albumine [HSA]) at 0.5×10^6 cells/mL and drawn across the monolayer (flow rate, 0.36 mL/min; shear stress, 0.7 dyne/cm^2). Images of a single field were recorded (5 minutes), and parameters were determined.

Materials

Materials included Sprague-Dawley rats (Charles River Laboratories); pentobarbital (Guinama); antibodies and lysis solution (BD Bioscience); Dulbecco PBS, EGM-2 culture media and fetal bovine serum (Lonza); HSA (albuminate 25%), Roswell Park Memorial Institute 1640 medium supplemented with 20 mmol/L HEPES, Hank's balanced salt solution (HBSS), fibronectin, and dextran (Sigma Chemical); Ficoll-Paque Plus (GE Healthcare); cover slips (Nunc; Thermo Fisher Scientific); PBS, collagenase, and trypsin (Gibco; Invitrogen); and antiretrovirals (Sequoia Research Products).

Ethics and Statistics

Human (all donors provided informed consent) and animal procedures followed the Spanish laws and were approved by the respective hospital or faculty ethic committee. One-way analysis of variance with a Newman-Keuls correction was used (mean ± standard error of the mean; $n \geq 4$; $P < .05$).

RESULTS

Leukocyte-Endothelial Interactions in Venules and Arterioles

ABC induced a significant and dose-dependent decrease in leukocyte rolling velocity (Figure 1*A*), while increasing rolling flux (Figure 1*B*), adhesion (Figure 1*C*), and emigration (Figure 1*D*) in rat venules and adhesion in rat arterioles (Figure 1*E*). The effects of ABC (5 μmol/L, administered intraperitoneally) were reproduced after oral administration (100 mg/kg; data not shown). The effects of ABC (10 μmol/L, administered intraperitoneally) were acute and reversible, with values returning to levels similar to control levels 48 hours later (data not shown). The in vivo results obtained in rat arterioles were reproduced in vitro in human cells. ABC also induced a significant decrease in PBMC rolling velocity and an increase in rolling flux and adhesion (Supplementary Figure 1). ddI (Figure 1 and Supplementary Figure 1), but not ZDV, 3TC, FTC, or TDF (data not shown), triggered a response similar to that caused by ABC, both in vivo and in vitro.

Role of Mac-1 and ICAM-1

Flow cytometry revealed that both ABC and ddI induced a significant increase in CD11b and CD18 in rat neutrophils and monocytes, while having no effect on CD11a, CD49d, or

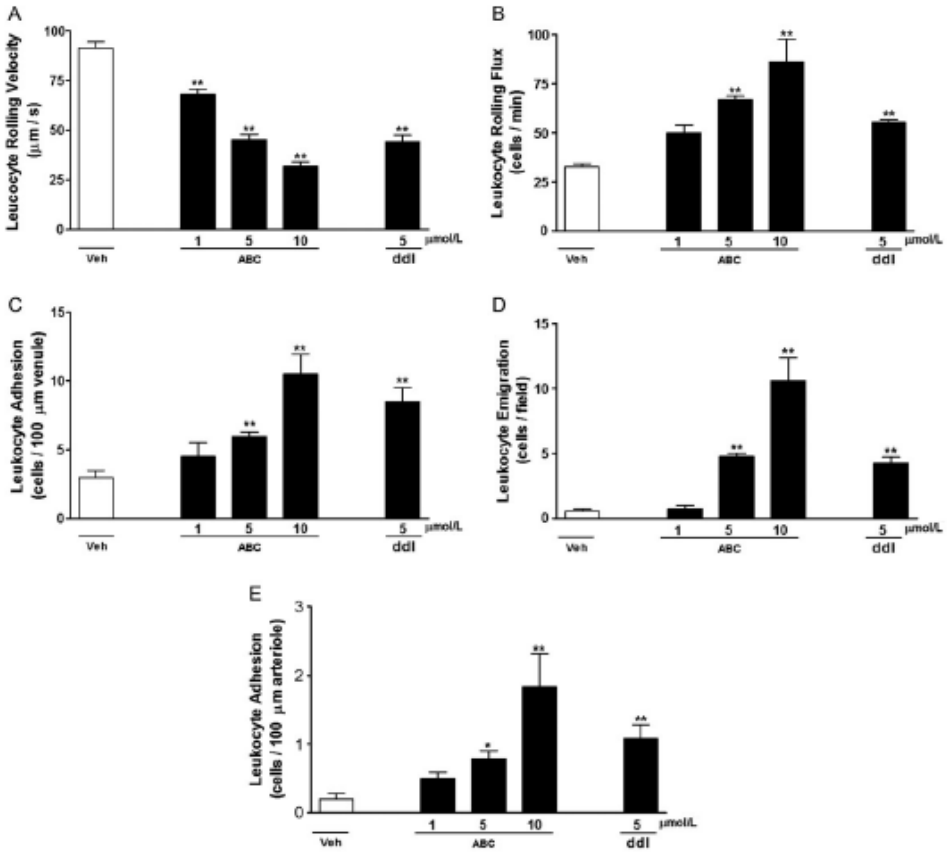

Figure 1. Effects of nucleoside reverse-transcriptase inhibitors on leukocyte responses in rat mesenteric postcapillary vessels. Rats were treated intraperitoneally with saline (vehicle), abacavir (ABC, 1–10 µmol/L), or didanosine (ddI, 5 µmol/L). Responses of leukocyte rolling velocity (*A*), rolling flux (*B*), adhesion (*C*), and emigration (*D*) in venules and adhesion (*E*) in arterioles were quantified 4 hours later. Rolling flux was assessed offline by counting the number of leukocytes passing a reference point in the vessel per minute. Leukocyte rolling velocity was calculated by measuring the time required for these cells to travel along 100 µm of the venule and expressed as micrometers per second. A leukocyte was considered to have adhered to the endothelium if it remained stationary for ≥30 seconds (cells per 100 µm of vessel), and emigration was expressed as the number of interstitial leukocytes per field. Results represent means ± standard errors of the mean (n = 4). **P* < .05 or ***P* < .01 for comparison with corresponding value in vehicle-treated group (analysis of variance followed by Newman-Keuls test).

CD62L (Supplementary Table 1). In animals treated with ddI, CD11b/c expression was enhanced in monocytes but not in neutrophils, whereas ABC had no bearing on either of these leukocyte populations. Neither ABC nor ddI exerted any influence on the adhesion molecules of lymphocytes (data not shown). The effects of ABC and ddI were reversed by pretreatment with antibodies against Mac-1 (CD11b/CD18) or its ligand ICAM-1 (CD54; Figure 2 and Supplementary Figure 2).

DISCUSSION

To our knowledge, this is the first study to analyze in vivo (in venules and arterioles) and in vitro (in arteries) the effects of the NRTIs most widely used to treat HIV infection (ABC, ddI, 3TC, ZDV, FTC, and TDF) on the trafficking of leukocytes from blood to tissue. Our in vivo results show that ABC and ddI induce inflammatory events through the interaction of the

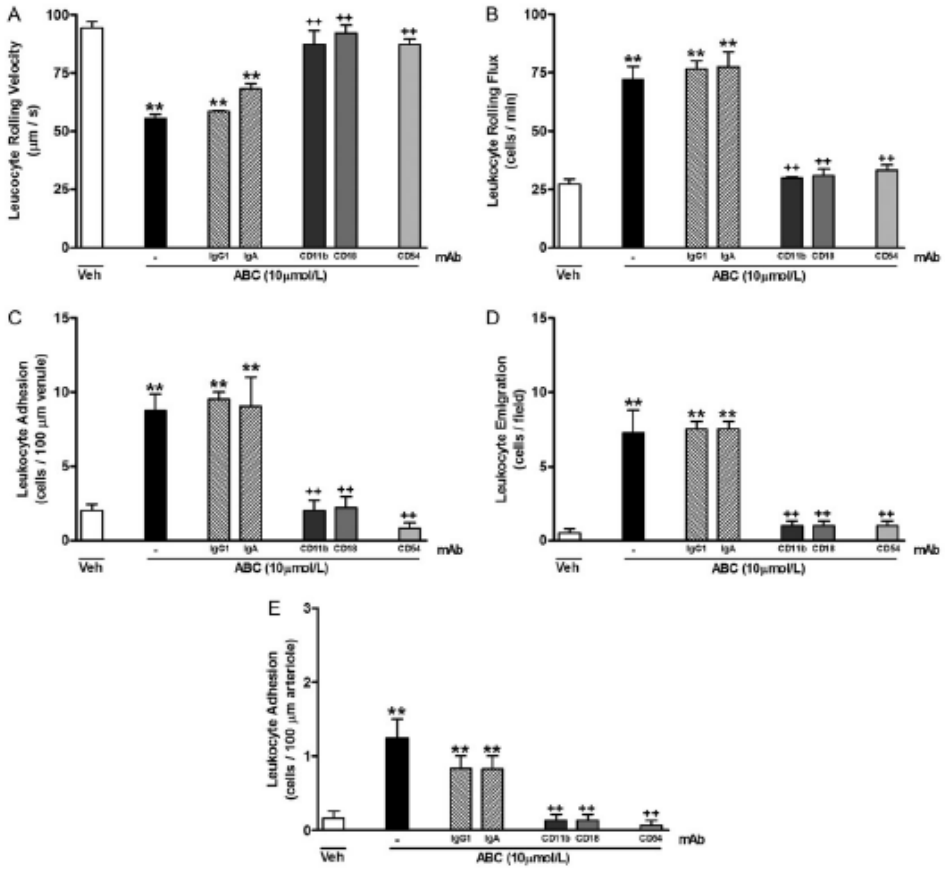

Figure 2. Role of Mac-1 and intercellular adhesion molecule 1 (ICAM-1) in abacavir (ABC)–induced leukocyte-endothelium interactions in rat mesenteric postcapillary vessels. Rats were treated intraperitoneally with saline (vehicle) or ABC (10 μmol/L). Some animals were treated intravenously with anti-CD11b monoclonal antibody (mAb), anti-CD18 mAb, anti–ICAM-1, or the corresponding control mAb 30 minutes before administration of ABC. Responses of leukocyte rolling velocity (*A*), rolling flux (*B*), adhesion (*C*), and emigration (*D*) in venules and adhesion (*E*) in arterioles were quantified 4 hours later. Rolling flux was assessed offline by counting the number of leukocytes passing a reference point in the vessel per minute. Leukocyte rolling velocity was calculated by measuring the time required for these cells to travel along 100 μm of the venule, expressed as micrometers per second. A leukocyte was considered to have adhered to the endothelium if it remained stationary for ≥30 seconds (cells per 100 μm of vessel), and emigration was expressed as the number of interstitial leukocytes per field. Results represent means ± standard errors of the mean (n = 4–5). $^{**}P < .01$ for comparison with corresponding value in vehicle-treated group; $^{++}P < .01$ for comparison with corresponding value in ABC-treated group (analysis of variance followed by Newman-Keuls test). Abbreviations: IgA, immunoglobulin A; IgG1, immunoglobulin G1.

leukocyte's Mac-1 with its endothelial ligand ICAM-1. These results expand preliminary in vitro data, which suggested that ABC and ddI elicit leukocyte accumulation in venular endothelial cells [4]. We have now performed an in-depth investigation with intravital microscopy, a technique that has been instrumental in understanding the inflammatory cascade associated with vascular diseases and its pharmacological modulation [10, 13], to analyze the nature and characteristics of the leukocyte-endothelial cell interplay induced by NRTIs.

In this setting, concentrations of ABC (1–10 μmol/L) and ddI (5 μmol/L) that mimicked those present in patients (1–8 and 3–10 μmol/L respectively) [7–9] not only induced

leukocyte rolling and adhesion in postcapillary venules—signs of which we have observed previously [4]—but also caused significant leukocyte emigration. The fact that similar results were obtained with oral and intraperitoneal ABC rules out a potential limitation of our intravital approach, that is, that the pharmacokinetics of intraperitoneal administration of the drug do not replicate the clinical reality. Furthermore, the effects of ABC were reversible, and although we did not measure the intracellular concentrations of its active metabolite, carbovir-triphosphate, the finding that these effects had a duration matching the longer intracellular half-life of the metabolite (12–21 hours) [9], but not that of plasmatic ABC (around 2 hours), suggests that carbovir-triphosphate was implicated.

The migratory effect evidences the high activation elicited by ABC and ddI, because white cells moving toward inflamed tissue represent the last and critical step of leukocyte-endothelium interactions. Indeed, emigration is the point of no return in inflammatory responses, because preceding phases—rolling and adhesion—are reversible, and most leukocytes that attach to postcapillary venules at the site of inflammation eventually reenter the circulation. In contrast, leukocytes that commit to diapedesis do not return, or at least not as the same cell type [14]. Importantly, we have appreciated that these 2 NRTIs also provoke leukocyte adhesion in arterioles. Although the level of adhesion was lower than in venules, and no rolling or emigration was apparent, these arterial effects are surprising, because few stimuli are capable of modifying the arteriolar-leukocyte parameters revealed by intravital microscopy, including perivascular laser injury, cigarette smoke, tumor necrosis factor α or angiotensin II [6]. Indeed, interaction with arteries is essential for mononuclear infiltration during genesis of the atherosclerotic process. Therefore, it is highly relevant that both drugs induced mononuclear (PBMC) rolling and adhesion in human arterial cells. This effect was evaluated in a dynamic flow adhesion assay, a well-established in vitro system used, for example, to analyze leukocyte recruitment in patients with CV diseases or the vascular pro- or anti-inflammatory effects of drugs [5].

Flow cytometry revealed that ABC and ddI induced selective up-regulation of Mac-1 (CD11b/CD18) on the surface of rat neutrophils and monocytes without influencing the expression of CD11a, CD49d, or CD62L. The only disparity between the 2 drugs was the augmentation of CD11b/c on rat monocytes by ddI. Furthermore, the in vivo interactions induced by ABC or ddI were prevented by antibodies against CD11b, CD18, or its endothelial ligand ICAM-1 (CD54). As a whole, these data clearly implicate Mac-1 (CD11b/CD18) and ICAM-1 (CD54) in the leukocyte-endothelial interactions induced by these 2 antiretrovirals. Interestingly, Mac-1 has been proposed as the link between cellular adhesion and thrombosis [15]. It is present in neutrophils and monocytes, where it interacts with ICAM-1, causing them to adhere to the endothelium [4]. It also interacts with platelet ligands [4] to mediate the leukocyte engagement of platelets, a fundamental step in the onset of the thrombotic process [15].

The effects of ABC and ddI in venules and arterioles were not reproduced (in vivo or in vitro) by the other NRTIs evaluated (data not shown [4, 5]). Remarkably, if the chemical structure of the compounds is taken into account, a pattern of activity emerges; changes were induced by cyclic purine analogues (ABC or ddI), but not by pyrimidine analogues (3TC, ZDV, and FTC) or the acyclic nucleotide TDF.

We must be cautious when extrapolating experimental data to the clinical human situation, particularly when complex pathological situations are involved. One potential limitation of this study could be that we have not used cells from HIV-infected patients to evaluate the effects of the drugs on their vascular responses. However, even if this is taken into account, the differences we observed in CV toxicity profiles support the recent clinical association of ABC and ddI with CV diseases.

Supplementary Data

Supplementary materials are available at *The Journal of Infectious Diseases* online (http://jid.oxfordjournals.org/). Supplementary materials consist of data provided by the author that are published to benefit the reader. The posted materials are not copyedited. The contents of all supplementary data are the sole responsibility of the authors. Questions or messages regarding errors should be addressed to the author.

Notes

Financial support. This work was supported by Ministerio de Ciencia e Innovación (grants SAF2010-16030 and SAF2010-20231, FPI grant BES-2008-004338 to C. D. P., and Ramón y Cajal program grant RYC2005-002295 and I3 program support to A. A.), Ministerio de Sanidad y Consumo (grant PI11/00327), CIBERehd (grant CB06/04/0071), Generalitat Valenciana (grant PROMETEO/2010/060), Fundación Juan Esplugues (C. D. P), and Universidad de Valencia (VLC-CAMPUS grant to S. O.).

Potential conflicts of interest. All authors: No reported conflicts.

All authors have submitted the ICMJE Form for Disclosure of Potential Conflicts of Interest. Conflicts that the editors consider relevant to the content of the manuscript have been disclosed.

References

1. Triant VA. HIV infection and coronary heart disease: an intersection of epidemics. J Infect Dis **2012**; 205(Suppl 3):S355–61.
2. Behrens GM, Reiss P. Abacavir and cardiovascular risk. Curr Opin Infect Dis **2010**; 23:9–14.
3. Thompson MA, Aberg JA, Hoy JF, et al. Antiretroviral treatment of adult HIV infection: 2012 recommendations of the International Antiviral Society-USA panel. JAMA **2012**; 308:387–402.
4. De Pablo C, Orden S, Apostolova N, Blanquer A, Esplugues JV, Alvarez A. Abacavir and didanosine induce the interaction between human leukocytes and endothelial cells through Mac-1 upregulation. AIDS **2010**; 24:1259–66.
5. De Pablo C, Orden S, Calatayud S, Marti-Cabrera M, Esplugues JV, Alvarez A. Differential effects of tenofovir/emtricitabine and abacavir/lamivudine on human leukocyte recruitment. Antivir Ther **2012**; 17:1615–19.
6. Alvarez A, Cerda-Nicolas M, Naim Abu NY, et al. Direct evidence of leukocyte adhesion in arterioles by angiotensin II. Blood **2004**; 104:402–8.

7. Wang X, Chai H, Lin PH, Yao Q, Chen C. Roles and mechanisms of human immunodeficiency virus protease inhibitor ritonavir and other anti-human immunodeficiency virus drugs in endothelial dysfunction of porcine pulmonary arteries and human pulmonary artery endothelial cells. Am J Pathol **2009**; 174:771–81.
8. Lagathu C, Eustace B, Prot M, et al. Some HIV antiretrovirals increase oxidative stress and alter chemokine, cytokine or adiponectin production in human adipocytes and macrophages. Antivir Ther **2007**; 12:489–500.
9. Moyle G, Boffito M, Fletcher C, et al. Steady-state pharmacokinetics of abacavir in plasma and intracellular carbovir triphosphate following administration of abacavir at 600 milligrams once daily and 300 milligrams twice daily in human immunodeficiency virus-infected subjects. Antimicrob Agents Chemother **2009**; 53:1532–8.
10. Hughes EL, Gavins FN. Troubleshooting methods: Using intravital microscopy in drug research. J Pharmacol Toxicol Methods **2010**; 61:102–12.
11. Sumpter LR, Inayat MS, Yost EE, et al. In vivo examination of hydroxyurea and the novel ribonucleotide reductase inhibitors trimidox and didox in combination with the reverse transcriptase inhibitor abacavir: suppression of retrovirus-induced immunodeficiency disease. Antiviral Res **2004**; 62:111–20.
12. Watanabe T, Arakawa T, Fukuda T, Higuchi K, Kobayashi K. Role of neutrophils in a rat model of gastric ulcer recurrence caused by interleukin-1 beta. Am J Pathol **1997**; 150:971–9.
13. Gavins FN. Intravital microscopy: new insights into cellular interactions. Curr Opin Pharmacol **2012**; 12:601–7.
14. Muller WA. Mechanisms of transendothelial migration of leukocytes. Circ Res **2009**; 105:223–30.
15. Hirahashi J, Hishikawa K, Kaname S, et al. Mac-1 (CD11b/CD18) links inflammation and thrombosis after glomerular injury. Circulation **2009**; 120:1255–65.

ARTÍCULO 4

Efavirenz induces interactions between leucocytes and endothelium through the activation of Mac-1 and gp150,95

Orden S, de Pablo C, Ríos-Navarro C, Martínez-Cuesta MA, Peris JE, Barrachina MD, Esplugues JV, Álvarez Á.

Journal of Antimicrobial Chemotherapy 2014; 69: 995-1004

J Antimicrob Chemother 2014; **69**: 995–1004
doi:10.1093/jac/dkt468 Advance Access publication 24 November 2013

Journal of Antimicrobial Chemotherapy

Efavirenz induces interactions between leucocytes and endothelium through the activation of Mac-1 and gp150,95

Samuel Orden[1], Carmen De Pablo[1], Cesar Rios-Navarro[1], Maria Angeles Martinez-Cuesta[1], Jose E. Peris[2], Maria D. Barrachina[1], Juan V. Esplugues[1,3] and Angeles Alvarez[1,4]*

[1]*Departamento de Farmacologia and CIBERehd, Facultad de Medicina, Universidad de Valencia, Valencia, Spain;* [2]*Departamento de Farmacia y Tecnologia Farmacéutica, Facultad de Farmacia, Universidad de Valencia, Valencia, Spain;* [3]*FISABIO-Fundación Hospital Universitario Dr. Peset, Valencia, Spain;* [4]*Fundación General Universidad de Valencia, Valencia, Spain*

*Corresponding author. Departamento de Farmacologia, Facultad de Medicina, Universidad de Valencia, Avda. Blasco Ibáñez 15–17, 46010 Valencia, Spain. Tel: +34-96-3864898; Fax: +34-96-3983879; E-mail: angeles.alvarez@uv.es

Received 23 May 2013; returned 19 July 2013; revised 1 October 2013; accepted 1 November 2013

Objectives: The potential cardiovascular (CV) toxicity associated with combined antiretroviral therapy (cART) has been attributed mainly to the nucleoside reverse transcriptase inhibitors abacavir and didanosine. However, the other two components of cART—non-nucleoside reverse transcriptase inhibitors (NNRTIs) and protease inhibitors (PIs)—may also be implicated, either directly or by influencing the action of the other drugs. This study evaluates the acute direct effects of the NNRTIs efavirenz and nevirapine and one of the most widely employed PIs, lopinavir, on leucocyte–endothelium interactions, a hallmark of CV disease.

Methods: Drugs were analysed *in vitro* in human cells (interactions of peripheral blood polymorphonuclear or mononuclear cells with human umbilical vein endothelial cells) using a flow chamber system, and *in vivo* in rat mesenteric vessels by means of intravital microscopy. The expression of adhesion molecules in leucocytes and endothelial cells was studied by flow cytometry, and the role of these molecules in white cell recruitment was evaluated by pre-treating human cells or rats with blocking antibodies.

Results: Efavirenz and nevirapine, but not lopinavir, increased the rolling flux and adhesion of leucocytes *in vitro* and *in vivo* while inducing emigration in rat venules. Efavirenz, but not nevirapine, augmented the levels of CD11b, CD11c and CD18 in neutrophils and monocytes. The actions of efavirenz, but not of nevirapine, were reversed by antibodies against Mac-1 (CD11b/CD18), gp150,95 (CD11c/CD18) or ICAM-1 (CD54).

Conclusions: NNRTIs, but not PIs, interfere with leucocyte–endothelial interactions. However, differences between efavirenz and nevirapine suggest a specific CV profile for each compound.

Keywords: nevirapine, lopinavir, leucocyte–endothelium interactions, cardiovascular

Introduction

There is growing awareness of the chronic toxic effects induced by the lifelong administration of combined antiretroviral therapy (cART) to HIV-infected patients, particularly in relation to the cardiovascular (CV) diseases that accompany ageing.[1] cART involves the administration of at least three drugs: typically, two nucleoside reverse transcriptase inhibitors (NRTIs) plus either a non-nucleoside reverse transcriptase inhibitor (NNRTI) or a protease inhibitor (PI).[2,3] Although CV toxicities have been attributed largely to the NRTI component of cART, in particular abacavir and didanosine,[4–6] a role has also been proposed for NNRTIs and, especially, PIs.[1,7,8]

Efavirenz is the most widely prescribed NNRTI; the majority of guidelines recommend its use in conjunction with tenofovir and emtricitabine or with abacavir and lamivudine as the initial treatment for HIV.[2,3] Although generally considered a safe drug, there is evidence that efavirenz could also be implicated in the onset of some CV disorders. The exposure of patients to efavirenz is associated with endothelial dysfunction[9] and with increases in low-density lipoprotein,[10] F2 isoprostane and high-sensitivity C-reactive protein,[9] which are markers of metabolic parameters, oxidative stress and vascular inflammation, respectively, and risk factors for CV conditions in all three cases. Furthermore, in isolated human cells, efavirenz has been shown to induce acute direct mitochondrial toxicity[11] and to increase superoxide anion and vascular permeability by reducing levels of the proteins that maintain endothelium–endothelium junctional structures.[12,13]

An increase in vascular permeability coupled with leucocyte infiltration is a hallmark of the inflammation that underlies vascular diseases and the HIV infection itself.[14] This recruitment of white

© *The Author 2013. Published by Oxford University Press on behalf of the British Society for Antimicrobial Chemotherapy. All rights reserved. For Permissions, please e-mail: journals.permissions@oup.com*

cells involves a sequential cascade of adhesive interactions between leucocytes and endothelial cells that begins with enhanced rolling and leads to the adhesion and subsequent endothelial transmigration of these white cells in a process mediated by the adhesion molecules present on both cell populations.[15,16] The aim of the present study was to evaluate the direct effect of efavirenz in the early phases of responses after exposure: leucocyte–endothelial cell interactions both *in vitro* and *in vivo*. We extended our analysis to include nevirapine, the other widely employed NNRTI, and lopinavir, a PI commonly used as an alternative to efavirenz in HIV therapy.

Materials and methods

Cell culture of human umbilical vein endothelial cells (HUVECs) and leucocyte isolation

HUVECs were harvested from freshly obtained umbilical cords as previously described,[17,18] and passage 1 cells were subsequently employed in the experiments. Human peripheral blood polymorphonuclear (PMN) cells or peripheral blood mononuclear cells (PBMCs) were isolated from whole blood drawn from healthy volunteers and anticoagulated with sodium citrate.[5] Leucocytes and HUVECs were treated independently (4 h, 37°C) with efavirenz (10–25 μM), nevirapine (10–50 μM), lopinavir (10–25 μM), control (without vehicle) or vehicle [efavirenz and lopinavir were dissolved in methanol and nevirapine in azide water (pH≤3)]. The aforementioned concentrations were employed because they mimic clinically relevant plasma levels.[12,19–21] The Medical Ethics Committee of the Hospital Clinico Universitario de Valencia approved the study, and the experiments were conducted in accordance with the Declaration of Helsinki after obtaining the written informed consent of each participant.

Dynamic adhesion assay under flow conditions

The characteristics of the parallel-plate flow chamber model used in this study have been described previously.[6,22] In brief, coverslips [coated with fibronectin (5 μg/mL)] containing confluent HUVEC monolayers were inserted in the chamber (37°C) and a portion (5×25 mm) was exposed to the flow. The chamber was mounted on an inverted microscope (Nikon Eclipse TE 2000-S, ×40, Amstelveen, The Netherlands) with a video camera (Sony Exwave HAD, Koeln, Germany). PMN cells or PBMCs were resuspended in Dulbecco's PBS with Ca^{2+} and Mg^{2+} buffer containing 20 mM HEPES and 0.1% human serum albumin at 1×10^6 or 0.5×10^6 cells/mL, respectively, and were drawn across the monolayer (flow rate 0.36 mL/min, shear stress 0.7 dyne/cm^2). Images of a single field were recorded for 5 min and leucocyte parameters were determined. Rolling flux was calculated by counting the number of cells rolling across 100 μm^2 of the monolayer during a 1 min period. The velocities of 20 consecutive leucocytes in the field of focus were determined by measuring the time required to travel 100 μm. Adhesion was determined after 5 min of perfusion by the analysis of 5–10 high-power (×40) fields. Leucocytes were considered to be adherent after 30 s of stable contact with the monolayer.

Flow cytometry

The expression of human leucocyte adhesion molecules was analysed in blood samples and that of endothelium molecules was quantified in confluent HUVECs. Blood samples and endothelial cells were treated (4 h, 37°C) with the different antiretroviral drugs and then incubated with saturating amounts of the antibodies (20 min, 4°C, in darkness). Subsequently, the samples were fixed and identified in a flow cytometer (FACScalibur Flow Cytometer, BD, Madrid, Spain).[23,24] Surface antigen expression [FITC or phycoerythrin (PE) fluorescence] was analysed in granulocytes, monocytes and lymphocytes, which were identified by their specific features of size [forward-angle light scatter (FS)] and granularity [side-angle light scatter (SS)]. HUVECs were also recognized by their FS and SS characteristics. Median fluorescence intensity (FITC or PE) was employed as a marker of the expression of the respective epitope.

Intravital microscopy

Leucocyte–endothelial cell interactions were evaluated in fasted male Sprague–Dawley rats (200–250 g) following a standard experimental technique.[25,26] In brief, rats were anaesthetized with sodium pentobarbital [65 mg/kg, intraperitoneally (ip)] and, following a midline abdominal incision, a segment of the mid-jejunum was exteriorized and placed on an optically clear viewing pedestal at 37°C for tissue transillumination. The exposed mesentery was visualized using an orthostatic microscope (Nikon Optiphot-2, SMZ1, Nikon, Badhoevedor, The Netherlands) equipped with a ×20 objective lens (Nikon SLDW) and ×10 eyepieces, during which time it was continuously superfused with bicarbonate buffer saline (pH 7.4, 37°C, 2 mL/min). A video camera (Sony SSC-C350P; Sony, Koeln, Germany) mounted on the microscope projected images onto a colour monitor (Sony Trinitron PVM-14N2E), and the images were captured on videotape (Sony SVT-S3000P) for playback analysis (final magnification of the video screen: ×1300). Single unbranched mesenteric venules were selected and their diameters (25–40 μm) measured online using a video caliper (Microcirculation Research Institute, Texas A&M University, College Station, TX, USA). Centerline red blood cell velocity (V_{rbc}) was quantified online with an optical Doppler velocimeter (Microcirculation Research Institute). Blood flow and wall shear rate (γ) were calculated as previously described,[27] and systemic arterial blood pressure was monitored. Numbers of rolling, adherent and emigrated leucocytes were determined offline during playback analysis of videotaped images. Rolling flux was assessed by counting the number of leucocytes passing a reference point in the vessel per minute. Leucocyte rolling velocity (V_{wbc}) was calculated by measuring the time required for these cells to travel along 100 μm of the venule and was expressed as μm/s. A leucocyte was considered to have adhered to the endothelium if it remained stationary for ≥30 s, and the numbers of these leucocytes were expressed per 100 μm of vessel. Leucocyte emigration was evaluated as the total number of interstitial leucocytes per field. In some cases, the area of the mesentery selected for the experiment was excised, fixed with paraformaldehyde (4% in PBS, pH 7.4) and stained with haematoxylin and eosin. The preparation was subsequently observed under a clear field microscope (×63), and the infiltrated leucocytes were counted (number per 2.5×10^{-4} cm^2) and classified morphologically as PMN leucocytes, macrophages and lymphocytes by an observer who was unaware of the treatment in question.[26] Animals were injected (2.5 mL, ip) with saline, vehicles (methanol or azide water) or one of the following antiretroviral drug solutions: efavirenz (10–25 μM, equivalent to 40–100 μg/kg), nevirapine (10–50 μM; 35–165 μg/kg) or lopinavir (10–25 μM; 80–200 μg/kg). Images (5 min period) were recorded 4 h later in order to allow enough time for the process of leucocyte emigration to initiate and were then evaluated by an observer who was blind to the treatment. The ip injection of drug solutions is a usual practice in intravital microscopy,[23,28–30] as it allows longer incubation periods than superfusion[31] and is, thus, more suited to lengthy time-course studies such as the present one. All doses were representative of plasma concentrations in patients.[12,19–21] Care was taken at each stage of the experiment to avoid any suffering of the animals. Procedures followed Spanish law concerning the use of experimental animals and were approved by the Ethics Committee of the Faculty of Medicine of the University of Valencia (Spain).

Functional role of adhesion molecules

This was assessed in both *in vitro* and *in vivo* settings by blocking the adhesion molecules with specific antibodies. For the *in vitro* experiments,

and prior to treatment with efavirenz, PMN cells and PBMCs were pre-treated with anti-lymphocyte function-associated antigen-1 (CD11a-LFA-1; 10 μg/mL), anti-macrophage-1 antigen (CD11b-Mac-1; 20 μg/mL), anti-alpha-X integrin (CD11c-gp150,95; 10 μg/mL), anti-β_2 integrins (CD18; 10 μg/mL) or control antibodies (IgG1; 10 μg/mL) for 20 min at 4°C in darkness. Prior to drug administration, HUVEC monolayers were pre-treated with anti-intercellular adhesion molecule-1 (ICAM-1-CD54; 20 μg/mL) or control antibodies (IgG1; 10 μg/mL) for 30 min at 37°C. The antibodies were assayed at previously described doses.[32–35] For the *in vivo* experiments, antibodies were injected through the tail vein 30 min before efavirenz or nevirapine administration, as previously described,[36,37] at doses that have been shown to block the *in vivo* function of the adhesion molecules analysed in the current study [2 mg/kg for WT-5 (anti-rat Mac-1, CD11b), and 1 mg/kg for WT-3 (anti-rat β_2 integrins, CD18) and for 1A29 (anti-rat ICAM-1, CD54)] or with control antibodies (2 mg/kg for IgA and 1 mg/kg for IgG1).[23,38] To rule out a direct effect of the monoclonal antibodies (MAbs) on circulating leucocytes, portal blood samples were obtained and their number evaluated after the intravital measurements.

Materials

Blocking antibodies, FITC-conjugated antibodies and lysis solution (BD Bioscience, Madrid, Spain); Dulbecco's PBS with or without Ca^{2+} and Mg^{2+}, EGM-2 culture media and fetal bovine serum (Lonza, Barcelona, Spain); human serum albumin (albuminate 25%), RPMI 1640 supplemented with 20 mM HEPES, HBSS, fibronectin, dextran and haematoxylin (Sigma Chemical Co., Madrid, Spain); eosin (Panreac, Barcelona, Spain); Ficoll-Paque™ Plus (GE Healthcare, Valencia, Spain); coverslips (Nunc, Thermo Fisher Scientific, Madrid, Spain); PBS, collagenase and trypsin (Gibco, Invitrogen, Barcelona, Spain); antiretroviral drugs (Sequoia Research Products, Pangbourne, UK); Sprague–Dawley rats (Charles River Laboratories, Barcelona, Spain); and pentobarbital (Guinama, Valencia, Spain).

Statistical analysis

One-way analysis of variance (ANOVA) with a Newman–Keuls post-test correction was employed for statistical analysis (mean ± SEM, $n \geq 4$, $P < 0.05$).

Results

Leucocyte–endothelial cell interactions

In human cells *in vitro*, efavirenz and nevirapine induced a decrease in rolling velocity (Figure 1a and b) and an increase in the rolling flux (Figure 1c and d) and adhesion (Figure 1e and f) of both PMN cells and PBMCs. None of these interactions was generated by any of the doses of lopinavir employed (Figure 1). These *in vitro* results were reproduced in rat post-capillary venules *in vivo*. Efavirenz and nevirapine (but not, once again, lopinavir) provoked a significant and dose-dependent decrease in leucocyte rolling velocity (Figure 2a), while increasing rolling flux (Figure 2b), adhesion (Figure 2c) and emigration (Figure 2d). Interestingly, the effects of efavirenz on emigration were significantly stronger than those of nevirapine. Analysis of the haematoxylin- and eosin-stained mesenteric tissue confirmed these observations, revealing a significantly higher number of infiltrated leucocytes in efavirenz-treated animals (17.7 ± 3.3 leucocytes per field versus 1.0 ± 0.3 leucocytes per field in methanol-treated animals, $P < 0.01$) than in the nevirapine group (6.0 ± 0.4 leucocytes per field versus 0.7 ± 0.3 leucocytes per field in azide water-treated animals, $P < 0.05$), which were predominantly PMN leucocytes in both cases (Figure 3). Systemic haemodynamic parameters were not affected by any of the compounds evaluated (data not shown).

Role of adhesion molecules in NNRTI-induced leucocyte–endothelium interactions

Flow cytometry revealed that treatment with efavirenz significantly and dose-dependently augmented the expression of CD11b, CD11c and CD18 on both neutrophils and monocytes in human blood, while that of CD11a, CD49d and CD62L (L-selectin) was not affected (Table S1, available as Supplementary data at *JAC* Online). Neither nevirapine nor lopinavir modified the expression of the adhesion molecules analysed on neutrophils or monocytes (Table S1, available as Supplementary data at *JAC* Online). None of the assayed doses of efavirenz, nevirapine or lopinavir had any effect on the adhesion molecules of lymphocytes (data not shown) or human endothelial cells (Table S1, available as Supplementary data at *JAC* Online).

The functional implication of adhesion molecules was assessed with specific antibodies. *In vitro*, the effects of efavirenz on interactions between human leucocytes (PMN cells or PBMCs) and the endothelium were completely reversed by blocking Mac-1 (CD11b), gp150,95 (CD11c), β_2 integrins (CD18) or their ligand ICAM-1 (CD54), but not by neutralizing LFA-1 (CD11a) (Figure 4). These *in vitro* results were confirmed in rat post-capillary venules *in vivo*; namely, the effects of efavirenz were not apparent when animals were pre-treated with antibodies against Mac-1 (CD11b), β_2 integrins (CD18) or ICAM-1 (CD54) (Figure 5). However, the responses induced by nevirapine were not modified when animals were pre-treated with any of the abovementioned antibodies. Neither haemodynamic parameters nor systemic leucocyte count was affected by any of the antibodies employed (data not shown).

Discussion

This study shows that efavirenz, the most commonly employed NNRTI in HIV therapy, induces leucocyte recruitment through the interaction of certain β_2 integrins with ICAM-1. We obtained our results in two experimental models: (i) human cells *in vitro*; and (ii) rat mesenteric venules *in vivo*. The former is a dynamic experimental setting in which human leucocytes flow over a monolayer of HUVECs in a way that reproduces the rolling and adhesion processes that precede the formation of an inflammatory focus.[39,40] The latter permits a more detailed analysis of the inflammatory outcome by evaluating the emigration of leucocytes from living vessels.[31,41] A combination of the two experimental approaches allows for a more comprehensive analysis of the potentially proinflammatory vascular effects of drugs.

Concentrations of efavirenz (10–25 μM) or nevirapine (10–50 μM) mimicking those found in patients (3–13 and 10–25 μM, respectively)[12,19,20] induced human leucocyte (PMN or PBMC)–endothelial cell interactions *in vitro*. Although the functional effect of efavirenz on PBMC–endothelial cell interactions seemed to be weak, the expression of CD11b and CD11c molecules was particularly evident on monocytes, while almost absent in lymphocytes.[42] In our opinion this discrepancy results from the fact that, of the total population of PBMCs superfused through the flow chamber, only a small proportion were monocytes (~10%); thus, their reactivity would be obscured by the 90% of lymphocytes that would not adhere to the endothelium due to their lack (both constitutively or after efavirenz incubation) of CD11b or CD11c.[42] Lopinavir (10–25 μM in our experiments; 7–17 μM in patients),[21] a PI, had no

Orden et al., 2014

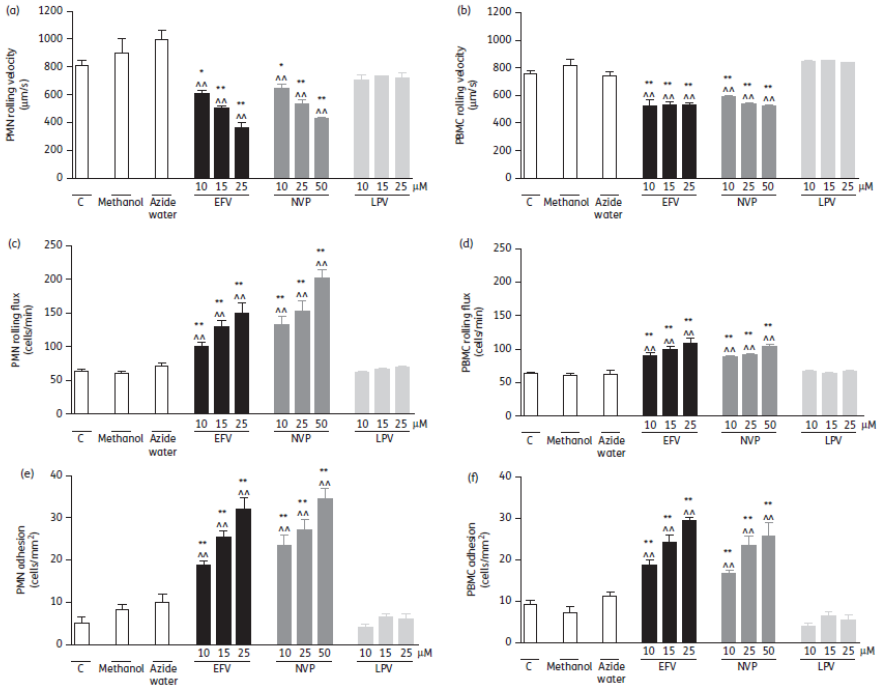

Figure 1. Effects of efavirenz, nevirapine and lopinavir on PMN–endothelial cell interactions and PBMC–endothelial cell interactions. HUVECs and leucocytes (PMN cells or PBMCs) were incubated (4 h) with efavirenz (10–25 μM), nevirapine (10–50 μM), lopinavir (10–25 μM) or the corresponding vehicles (efavirenz and lopinavir in methanol; nevirapine in azide water pH ≤ 3). After assembling the flow chamber, PMN rolling velocity (a), rolling flux (c) and adhesion (e) and PBMC rolling velocity (b), rolling flux (d) and adhesion (f) were quantified. Results are means ± SEM, $n = 4–6$. *$P < 0.05$ versus control (C) group, **$P < 0.01$ versus control group and ^^$P < 0.01$ versus methanol- or azide water-treated group (ANOVA followed by Newman–Keuls test). EFV, efavirenz; NVP, nevirapine; LPV, lopinavir.

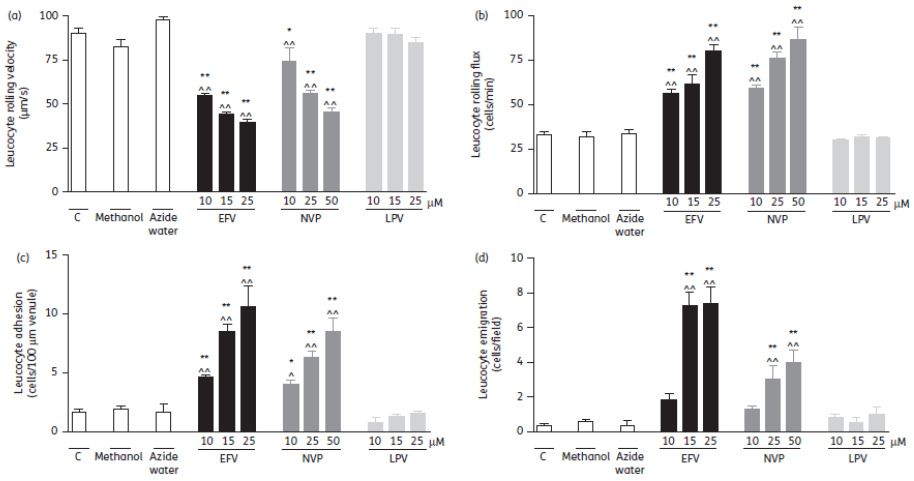

Figure 2. Effects of efavirenz, nevirapine and lopinavir on leucocyte responses in rat mesenteric post-capillary venules. Animals were treated (ip) with efavirenz (10–25 μM), nevirapine (10–50 μM), lopinavir (10–25 μM), control (saline) or the corresponding vehicles (efavirenz and lopinavir in methanol; nevirapine in azide water pH ≤ 3). Four hours later, responses of leucocyte rolling velocity (a), rolling flux (b), adhesion (c) and emigration (d) were quantified. Results are means ± SEM, $n = 4–5$. *$P < 0.05$ or **$P < 0.01$ versus corresponding value in saline-treated group and ^$P < 0.05$ or ^^$P < 0.01$ versus corresponding value in methanol- or azide water-treated group (ANOVA followed by Newman–Keuls test). EFV, efavirenz; NVP, nevirapine; LPV, lopinavir; C, control.

effect on any of the parameters evaluated. As a whole, these findings challenge previous perceptions of NNRTIs as relatively CV-friendly drugs and of PIs as potentially CV-toxic molecules.[7,43]

The results obtained *in vitro* were reproduced and expanded in the *in vivo* model; in addition to inducing leucocyte rolling and adhesion, both efavirenz and nevirapine (but not lopinavir) caused a significant emigration of white cells within post-capillary venules. This is of great relevance, as the movement of leucocytes towards inflamed tissue is considered the point of no return in the vascular inflammatory cascade, while the preceding phases (rolling and adhesion) are reversible.[44] The level of emigration induced by efavirenz was significantly higher than that produced by nevirapine (quantified by intravital microscopy and haematoxylin/eosin staining), which is compatible with the fact that nevirapine (and indeed lopinavir) had no effect on leucocytes or endothelial adhesion molecules. By contrast, efavirenz produced a selective up-regulation of the β_2 integrins Mac-1 (CD11b/CD18) and gp150,95 (CD11c/CD18) on neutrophils and monocytes, but not of the endothelial molecules E-selectin, ICAM-1 or VCAM-1.

When the functional implication of adhesion molecules was evaluated, the interactions induced by efavirenz were reversed by pre-treatment with antibodies against CD11b, CD18 or ICAM-1 (CD54), both *in vitro* and *in vivo*. The role of CD11c was evaluated in human cells only because of the unavailability of a commercially marketed rat antibody against this molecule. Our analysis of the role of adhesion molecules in the effects of efavirenz on the interplay between leucocytes and the endothelium strongly suggests that both β_2 integrins—gp150,95 (CD11c/CD18) and Mac-1 (CD11b/CD18)—interact with their endothelial ligand ICAM-1 (CD54). Although the involvement of CD11b and CD11c in adhesion and emigration would be expected, rolling was initially considered to be mediated by selectins and/or VLA-4/VCAM-1.[42] However, there is growing evidence that β_2 integrins also mediate leucocyte rolling in close dependence on their conformational state.[45,46]

β_2 Integrins (CD18) are cell adhesion receptors that share the same CD18 β chain but exhibit a distinctive α chain. The family includes four known types: αL (CD11a, LFA-1), αM (CD11b, Mac-1), αX (CD11c, gp95,150) and αD (CD11d).[42] The expression of CD11b and CD11c in lymphocytes is limited, but they are mobilized from intracellular secretory vesicles to the cell surface of neutrophils and monocytes within minutes of stimulation.[42] Their main ligand is ICAM-1, which is constitutively expressed on the surface of the vascular endothelium.[42] CD11c has already been implicated in phagocytosis, antigen presentation by dendritic cells and the inflammatory response.[34] In addition to its role in mediating the adherence of neutrophils and monocytes to the vessel wall, Mac-1 (CD11b) has been proposed as a key link between cellular adhesion and thrombosis[47] by mediating the engagement of platelets.[48]

The actions of nevirapine were not mediated by CD11b, CD11c or CD18, yet it did increase leucocyte rolling flux to a levels similar to that

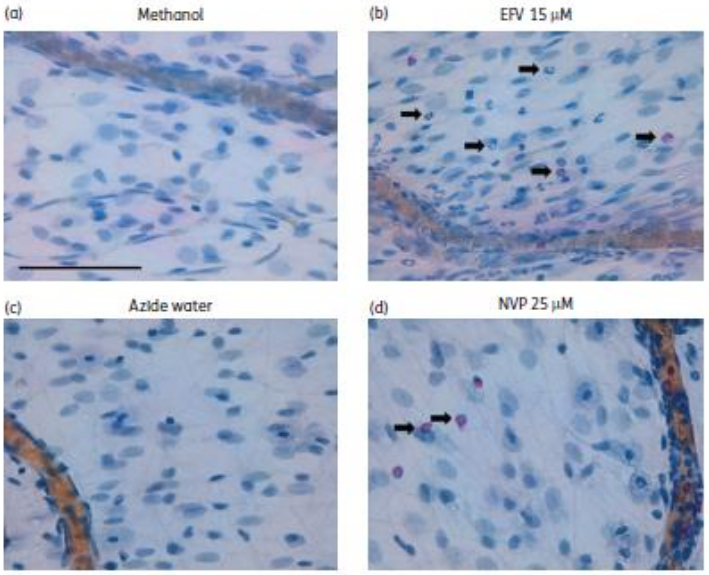

Figure 3. Leucocyte infiltration in the mesentery of rats treated with efavirenz or nevirapine. Animals were treated (ip) with efavirenz (15 μM), nevirapine (25 μM), control (saline) or the corresponding vehicles (efavirenz in methanol; nevirapine in azide water pH≤3) during the 4 h period. The mesentery selected for intravital experiments was excised, fixed with paraformaldehyde and stained with haematoxylin and eosin, and the number of infiltrated leucocytes (neutrophils, monocytes or lymphocytes) was counted in an area of 2.5×10^{-4} cm^2 in animals treated with methanol (a), 15 μM efavirenz (b), azide water (c) and 25 μM nevirapine (d). Arrows denote examples of infiltrated neutrophils. Bar= 50 μm. EFV, efavirenz; NVP, nevirapine.

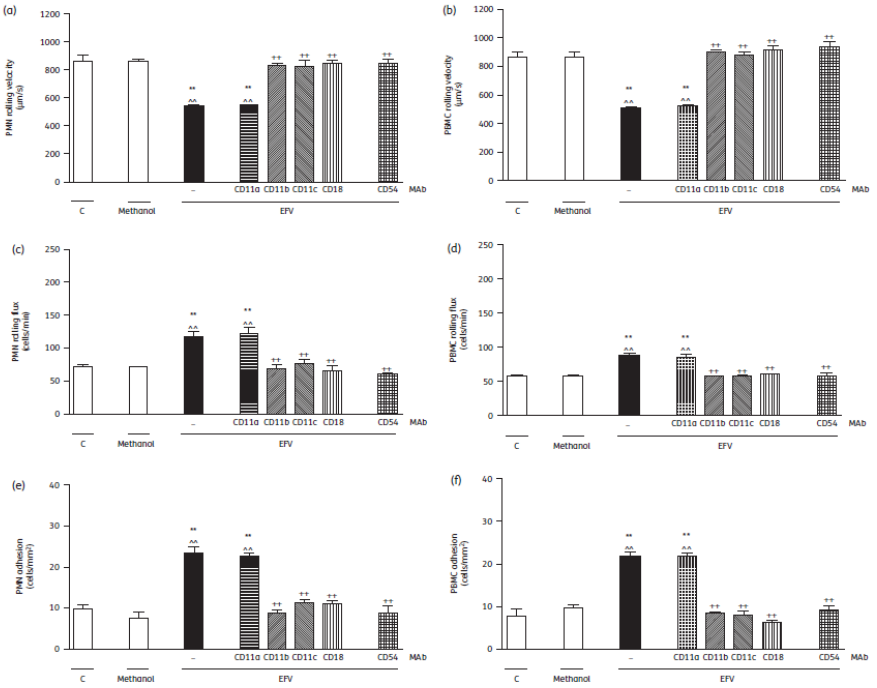

Figure 4. Role of Mac-1, gp150,95 and ICAM-1 in PMN–endothelial cell interactions and PBMC–endothelial cell interactions induced by efavirenz. HUVECs and leucocytes (PMN cells or PBMCs) were treated (4 h) with efavirenz (15 μM) or its vehicle (methanol). Some PMN cells or PBMCs were pre-treated with anti-CD11a MAb, anti-CD11b MAb, anti-CD11c MAb or anti-CD18 MAb, and some HUVECs were pre-treated with anti-ICAM-1 MAb 30 min before treatment with efavirenz. After assembling the flow chamber, PMN rolling velocity (a), rolling flux (c) and adhesion (e) and PBMC rolling velocity (b), rolling flux (d) and adhesion (f) were quantified. Results are means ± SEM, $n = 4–5$. $^{**}P < 0.01$ versus corresponding value in control (C) group, $^{\wedge\wedge}P < 0.01$ versus corresponding value in methanol-treated group and $^{++}P < 0.01$ versus corresponding value in efavirenz-treated group (ANOVA followed by Newman–Keuls test). EFV, efavirenz.

Orden et al., 2014

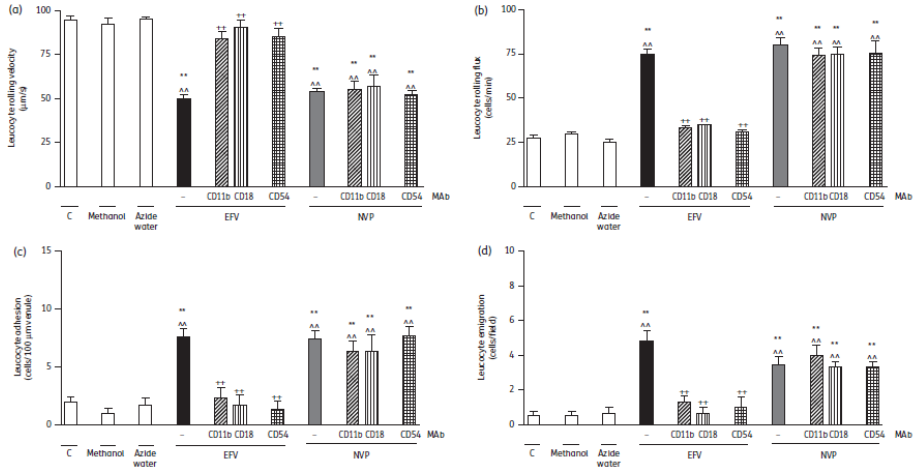

Figure 5. Role of Mac-1 and ICAM-1 in efavirenz- or nevirapine-induced leucocyte–endothelium interactions in rat mesenteric post-capillary venules. Rats were treated (ip) with efavirenz (15 μM), nevirapine (25 μM), control (saline) or the corresponding vehicles (efavirenz in methanol; nevirapine in azide water pH< 3). Some animals were pre-treated (intravenously) with anti-CD11b MAb, anti-CD18 MAb, anti-ICAM-1 or the corresponding control MAbs 30 min before administration of efavirenz or nevirapine. Four hours later, responses of leucocyte rolling velocity (a), rolling flux (b), adhesion (c) and emigration (d) were quantified. Results are means ± SEM, $n=4$. $^{**}P< 0.01$ versus corresponding value in saline-treated group, $^{\wedge\wedge}P< 0.01$ versus corresponding value in methanol- or azide water-treated group and $^{++}P< 0.01$ versus corresponding value in efavirenz-treated group (ANOVA followed by Newman–Keuls test). EFV, efavirenz; NVP, nevirapine; C, control.

induced by efavirenz while influencing less adhesion and particularly emigration. One possible explanation for this differential profile could be that nevirapine activates other families of adhesion molecules, such as P-selectin, which are implicated mainly in the rolling process.[42]

Although the clinical translation of our results should be contemplated with caution, we believe they provide strong evidence that NNRTIs, and in particular efavirenz, alter leucocyte–endothelial interactions. As a whole, our findings point to an effect by which efavirenz activates leucocytes but not endothelial cells. This contrasts with reports suggesting that efavirenz-containing regimens are responsible for impaired endothelial function in patients,[9] or that, *in vitro*, this drug induces an increase in the levels of superoxide anions responsible for the endothelial damage and altered endothelial junctions that restrict vascular permeability.[12] Nevertheless, it should be pointed out that the period of exposure to efavirenz was substantially shorter in the present study than in the reports in question. Furthermore, since HIV infection is itself characterized by an increase in endothelial adhesion molecules, the profile of which (ICAM-1, VCAM-1 and E-selectin)[49] differs from that induced by efavirenz in our experiments, it is feasible that the effects of efavirenz and those of the virus are cumulative in patients. In other words, the virus may cause endothelial activation whereas efavirenz stimulates white cells. Given the increasing longevity of HIV-infected patients, and taking into account that CV illnesses are the most frequent cause of death among the non-HIV-infected ageing population, a potential relationship between the compounds used in cART and CV toxicity is of considerable importance.

Funding

This work was supported by Ministerio de Ciencia e Innovación (grant numbers SAF2010-16030 and SAF2010-20231), Ministerio de Sanidad y Consumo (grant number PI11/00327), CIBERehd (grant number CB06/04/0071) and Generalitat Valenciana (grant numbers PROMETEO/2010/060, ACOMP/2013/147 and ACOMP/2013/236). S. O. was funded by Universidad de Valencia (VLC-CAMPUS grant) and C. d. P. by Ministerio de Ciencia e Innovación (FPI grant number BES-2008-004338) and by Fundación Juan Esplugues. A. A. was supported by Ministerio de Ciencia e Innovación (Ramón y Cajal program RYC2005-002295 and I3 program).

Transparency declarations

None to declare.

Author contributions

S. O. performed the research, C. d. P., C. R.-N., M. A. M.-C., J. E. P. and M. D. B. helped perform the research, S. O. and A. A. analysed the data, A. A. conceived the study and J. V. E. and A. A. designed the research and wrote the paper.

Supplementary data

Table S1 is available as Supplementary data at *JAC* Online (http://jac.oxfordjournals.org/).

References

1 Triant VA. HIV infection and coronary heart disease: an intersection of epidemics. *J Infect Dis* 2012; **205** Suppl 3: S355–61.

2 Thompson MA, Aberg JA, Hoy JF *et al.* Antiretroviral treatment of adult HIV infection: 2012 recommendations of the International Antiviral Society-USA panel. *JAMA* 2012; **308**: 387–402.

3 FDA notifications. DHHS panel releases new ART guidelines. *AIDS Alert* 2011; **26**: 34–5.

4 Behrens GM, Reiss P. Abacavir and cardiovascular risk. *Curr Opin Infect Dis* 2010; **23**: 9–14.

5 De Pablo C, Orden S, Apostolova N *et al.* Abacavir and didanosine induce the interaction between human leukocytes and endothelial cells through Mac-1 upregulation. *AIDS* 2010; **24**: 1259–66.

6 De Pablo C, Orden S, Calatayud S *et al.* Differential effects of tenofovir/emtricitabine and abacavir/lamivudine on human leukocyte recruitment. *Antivir Ther* 2012; **17**: 1615–9.

7 Friis-Moller N, Reiss P, Sabin CA *et al.* Class of antiretroviral drugs and the risk of myocardial infarction. *N Engl J Med* 2007; **356**: 1723–35.

8 Petoumenos K, Worm SW. HIV infection, aging and cardiovascular disease: epidemiology and prevention. *Sex Health* 2011; **8**: 465–73.

9 Gupta SK, Shen C, Moe SM *et al.* Worsening endothelial function with efavirenz compared to protease inhibitors: a 12-month prospective study. *PLoS One* 2012; **7**: e45716.

10 Maggi P, Bellacosa C, Carito V *et al.* Cardiovascular risk factors in patients on long-term treatment with nevirapine- or efavirenz-based regimens. *J Antimicrob Chemother* 2011; **66**: 896–900.

11 Apostolova N, Blas-Garcia A, Esplugues JV. Mitochondrial interference by anti-HIV drugs: mechanisms beyond Pol-γ inhibition. *Trends Pharmacol Sci* 2011; **32**: 715–25.

12 Jamaluddin MS, Lin PH, Yao Q *et al.* Non-nucleoside reverse transcriptase inhibitor efavirenz increases monolayer permeability of human coronary artery endothelial cells. *Atherosclerosis* 2010; **208**: 104–11.

13 Mondal D, Pradhan L, Ali M *et al.* HAART drugs induce oxidative stress in human endothelial cells and increase endothelial recruitment of mononuclear cells: exacerbation by inflammatory cytokines and amelioration by antioxidants. *Cardiovasc Toxicol* 2004; **4**: 287–302.

14 Zietz C, Hotz B, Sturzl M *et al.* Aortic endothelium in HIV-1 infection: chronic injury, activation, and increased leukocyte adherence. *Am J Pathol* 1996; **149**: 1887–98.

15 Rao RM, Yang L, Garcia-Cardena G *et al.* Endothelial-dependent mechanisms of leukocyte recruitment to the vascular wall. *Circ Res* 2007; **101**: 234–47.

16 Carman CV, Springer TA. Trans-cellular migration: cell-cell contacts get intimate. *Curr Opin Cell Biol* 2008; **20**: 533–40.

17 Jaffe EA, Nachman RL, Becker CG *et al.* Culture of human endothelial cells derived from umbilical veins. Identification by morphologic and immunologic criteria. *J Clin Invest* 1973; **52**: 2745–56.

18 Ibiza S, Alvarez A, Romero W *et al.* Gastrin induces the interaction between human mononuclear leukocytes and endothelial cells through the endothelial expression of P-selectin and VCAM-1. *Am J Physiol Cell Physiol* 2009; **297**: C1588–95.

19 Pilon AA, Lum JJ, Sanchez-Dardon J *et al.* Induction of apoptosis by a nonnucleoside human immunodeficiency virus type 1 reverse transcriptase inhibitor. *Antimicrob Agents Chemother* 2002; **46**: 2687–91.

20 Cooper CL, van Heeswijk RP. Once-daily nevirapine dosing: a pharmacokinetics, efficacy and safety review. *HIV Med* 2007; **8**: 1–7.

21 Leon A, Martinez E, Saraso M *et al*. Impact of steady-state lopinavir plasma levels on plasma lipids and body composition after 24 weeks of lopinavir/ritonavir-containing therapy free of thymidine analogues. *J Antimicrob Chemother* 2007; **60**: 824–30.

22 Goetz DJ, Greif DM, Shen J *et al*. Cell-cell adhesive interactions in an *in vitro* flow chamber. *Methods Mol Biol* 1999; **96**: 137–45.

23 Alvarez A, Cerda-Nicolas M, Naim Abu NY *et al*. Direct evidence of leukocyte adhesion in arterioles by angiotensin II. *Blood* 2004; **104**: 402–8.

24 Alvarez A, Ibiza MS, Andrade MM *et al*. Gastric antisecretory drugs induce leukocyte-endothelial cell interactions through gastrin release and activation of CCK-2 receptors. *J Pharmacol Exp Ther* 2007; **323**: 406–13.

25 Alvarez A, Hermenegildo C, Issekutz AC *et al*. Estrogens inhibit angiotensin II-induced leukocyte-endothelial cell interactions *in vivo* via rapid endothelial nitric oxide synthase and cyclooxygenase activation. *Circ Res* 2002; **91**: 1142–50.

26 Alvarez A, Ibiza S, Hernandez C *et al*. Gastrin induces leukocyte-endothelial cell interactions *in vivo* and contributes to the inflammation caused by *Helicobacter pylori*. *FASEB J* 2006; **20**: 2396–8.

27 House SD, Lipowsky HH. Leukocyte-endothelium adhesion: microhemodynamics in mesentery of the cat. *Microvasc Res* 1987; **34**: 363–79.

28 Yamaki K, Lindbom L, Thorlacius H *et al*. An approach for studies of mediator-induced leukocyte rolling in the undisturbed microcirculation of the rat mesentery. *Br J Pharmacol* 1998; **123**: 381–9.

29 Stalker TJ, Skvarka CB, Scalia R. A novel role for calpains in the endothelial dysfunction of hyperglycemia. *FASEB J* 2003; **17**: 1511–3.

30 Nabah YN, Mateo T, Cerda-Nicolas M *et al*. L-NAME induces direct arteriolar leukocyte adhesion, which is mainly mediated by angiotensin-II. *Microcirculation* 2005; **12**: 443–53.

31 Hughes EL, Gavins FN. Troubleshooting methods: using intravital microscopy in drug research. *J Pharmacol Toxicol Methods* 2010; **61**: 102–12.

32 Heit B, Colarusso P, Kubes P. Fundamentally different roles for LFA-1, Mac-1 and α_4-integrin in neutrophil chemotaxis. *J Cell Sci* 2005; **118**: 5205–20.

33 Pluskota E, Woody NM, Szpak D *et al*. Expression, activation, and function of integrin $\alpha_M\beta_2$ (Mac-1) on neutrophil-derived microparticles. *Blood* 2008; **112**: 2327–35.

34 Sadhu C, Ting HJ, Lipsky B *et al*. CD11c/CD18: novel ligands and a role in delayed-type hypersensitivity. *J Leukoc Biol* 2007; **81**: 1395–403.

35 Arndt S, Melle C, Mandal K *et al*. Interactions of TANGO and leukocyte integrin CD11c/CD18 regulate the migration of human monocytes. *J Leukoc Biol* 2007; **82**: 1466–72.

36 Tamatani T, Kotani M, Miyasaka M. Characterization of the rat leukocyte integrin, CD11/CD18, by the use of LFA-1 subunit-specific monoclonal antibodies. *Eur J Immunol* 1991; **21**: 627–33.

37 Tamatani T, Miyasaka M. Identification of monoclonal antibodies reactive with the rat homolog of ICAM-1, and evidence for a differential involvement of ICAM-1 in the adherence of resting versus activated lymphocytes to high endothelial cells. *Int Immunol* 1990; **2**: 165–71.

38 Watanabe T, Arakawa T, Fukuda T *et al*. Role of neutrophils in a rat model of gastric ulcer recurrence caused by interleukin-1β. *Am J Pathol* 1997; **150**: 971–9.

39 Sundstrom JB, Martinson DE, Masunjac M *et al*. Norepinephrine enhances adhesion of HIV-1-infected leukocytes to cardiac microvascular endothelial cells. *Exp Biol Med (Maywood)* 2003; **228**: 730–40.

40 Gallego MJ, Zoja C, Morigi M *et al*. Cyclosporine enhances leukocyte adhesion to vascular endothelium under physiologic flow conditions. *Am J Kidney Dis* 1996; **28**: 23–31.

41 Masedunskas A, Milberg O, Porat-Shliom N *et al*. Intravital microscopy: a practical guide on imaging intracellular structures in live animals. *Bioarchitecture* 2012; **2**: 143–57.

42 Carlos TM, Harlan JM. Leukocyte-endothelial adhesion molecules. *Blood* 1994; **84**: 2068–101.

43 Worm SW, Sabin C, Weber R *et al*. Risk of myocardial infarction in patients with HIV infection exposed to specific individual antiretroviral drugs from the 3 major drug classes: the data collection on adverse events of anti-HIV drugs (D:A:D) study. *J Infect Dis* 2010; **201**: 318–30.

44 Muller WA. Mechanisms of transendothelial migration of leukocytes. *Circ Res* 2009; **105**: 223–30.

45 McEver RP, Zhu C. Rolling cell adhesion. *Annu Rev Cell Dev Biol* 2010; **26**: 363–96.

46 Ley K, Laudanna C, Cybulsky MI *et al*. Getting to the site of inflammation: the leukocyte adhesion cascade updated. *Nat Rev Immunol* 2007; **7**: 678–89.

47 Hirahashi J, Hishikawa K, Kaname S *et al*. Mac-1 (CD11b/CD18) links inflammation and thrombosis after glomerular injury. *Circulation* 2009; **120**: 1255–65.

48 Gawaz M, Langer H, May AE. Platelets in inflammation and atherogenesis. *J Clin Invest* 2005; **115**: 3378–84.

49 de Gaetano DK, Rabagliati R, Iacoviello L *et al*. HIV infection, HAART, and endothelial adhesion molecules: current perspectives. *Lancet Infect Dis* 2004; **4**: 213–22.

ARTÍCULO 5

Differential effects of anti-TNF-α and anti-IL-12/23 agents on human leukocyte-endothelial cell interactions

Ríos-Navarro C, de Pablo C, Collado-Díaz V, **Orden S,**
Blas-García A, Martínez-Cuesta MA, Esplugues JV, Álvarez Á.

European Journal of Pharmacology 2015; 765: 355-365

European Journal of Pharmacology 765 (2015) 355–365

Contents lists available at ScienceDirect

European Journal of Pharmacology

journal homepage: www.elsevier.com/locate/ejphar

Immunopharmacology and inflammation

Differential effects of anti-TNF-α and anti-IL-12/23 agents on human leukocyte–endothelial cell interactions

Cesar Ríos-Navarro [a,b], Carmen de Pablo [a], Víctor Collado-Diaz [a,b], Samuel Orden [a,b], Ana Blas-Garcia [a,b], María Ángeles Martínez-Cuesta [a], Juan V. Esplugues [a,b,*,1], Angeles Alvarez [a,c,1]

[a] Departamento de Farmacología and CIBERehd, Facultad de Medicina, Universidad de Valencia, Valencia, Spain
[b] FISABIO- Hospital Universitario Dr. Peset, Valencia, Spain
[c] Fundación General Universidad de Valencia, Valencia, Spain

ARTICLE INFO

Article history:
Received 3 June 2015
Received in revised form
27 August 2015
Accepted 28 August 2015
Available online 4 September 2015

Keywords:
Rheumatic diseases
Biologics
Anti-TNF-α agents
Anti-IL-12/23 agents
Cardiovascular side effects
Leukocyte–endothelial cell interactions

ABSTRACT

Enhanced leukocyte recruitment is an inflammatory process that occurs during early phases of the vascular dysfunction that characterises atherosclerosis. We evaluated the impact of anti-TNF-α (adalimumab, infliximab and etanercept) and anti-IL-12/23 (ustekinumab) on interactions between human leukocytes and endothelial cells in a flow chamber that reproduced in vivo conditions. Clinical concentrations of anti-TNF-α were evaluated on the leukocyte recruitment induced by a variety of endothelial (TNF-α, interleukin-1β, lymphotoxin-α and angiotensin-II) and leukocyte (PAF, IL-12 and IL-23) stimuli related to inflammation and atherosclerosis. Treatment with anti-TNF-α, even before or after establishing the inflammatory situation induced by TNF-α, diminished leukocyte–endothelial cell interactions induced by this stimuli. Our results also implicated adhesion molecules (ICAM-1, VCAM-1 and E-selectin) in the actions of anti-TNF-α in terms of leukocyte adhesion to endothelium. However, anti-TNF-α drugs did not influence the actions of interleukin-1β, but prevented those of lymphotoxin-α and angiotensin-II. However, once established, inflammatory response elicited by the latter three stimuli could not be reversed. Pre-treatment with anti-TNF-α, also prevented leukocyte actions induced by IL-23 on PBMC rolling flux and rolling velocity and by IL-12 on PMN adhesion. Ustekinumab exhibited a more discreet profile, having no effect on leukocyte recruitment induced by any of the endothelial stimuli, while blocking the effects of IL-23 on leukocyte activation and those of IL-12 on PMN adhesion and PAF on PBMC rolling velocity. These findings endorse the idea that biological anti-inflammatory drugs, in particular anti-TNF-α, have the capacity to influence cardiovascular risk accompanying psoriasis and rheumatoid arthritis by ameliorating vascular inflammation.

© 2015 Published by Elsevier B.V.

1. Introduction

The increased risk of early cardiovascular disease (CVD) in patients with autoimmune diseases such as psoriasis (PS) and rheumatoid arthritis (RA) has been attributed to an acceleration of atherosclerosis produced by the systemic inflammation that characterizes said diseases (Roubille et al., 2015; Westlake et al., 2011; Spah, 2008; Alexandroff et al., 2009). Manifestations of vascular inflammation involving interaction between adhesion molecules on leukocytes and on the endothelium are one of the early hallmarks of plaque formation and lead to the accumulation of leukocytes in the vessel wall (Ley et al., 2007). Although all immunosuppressive therapies have the potential to interfere with such interactions, there is mounting evidence that anti-inflammatory biologic drugs used to treat PS and RA can ameliorate vascular systemic inflammation and reduce the risk of CVD (Westlake et al., 2011; Maki-Petaja et al., 2012; Ahlehoff et al., 2013; Tam et al., 2014; Ridker and Luscher, 2014; Nguyen and Wu, 2014; Roubille et al., 2015).

Evidence regarding anti-TNF-α therapies is particularly compelling, probably due to the widespread involvement of said

* Corresponding author at: Departamento de Farmacología, Facultad de Medicina, Universidad de Valencia, Avda. Blasco Ibáñez 15-17, 46010 Valencia, Spain. Fax: +34 96 3983879.
E-mail addresses: cesar.rios@uv.es (C. Ríos-Navarro), carmen.pablo@uv.es (C. de Pablo), victor.collado@uv.es (V. Collado-Diaz), samuel.orden@uv.es (S. Orden), ana.blas@uv.es (A. Blas-Garcia), angeles.martinez@uv.es (M.Á. Martínez-Cuesta), juan.v.esplugues@uv.es (J.V. Esplugues), angeles.alvarez@uv.es (A. Alvarez).
[1] Both authors contributed equally to this work.

http://dx.doi.org/10.1016/j.ejphar.2015.08.054
0014-2999/© 2015 Published by Elsevier B.V.

cytokine in a wide variety of vascular inflammatory responses (Elliott et al., 1994; Westlake et al., 2011; Roubille et al., 2015). However, theories concerning the mechanisms implicated are rather spurious, as these drugs have been related both, with heart failure and a reduction in inflammation and plaque formation. There is also a case for analyzing anti-IL-12/23 agents given the potential implication of both these cytokines in plaque formation and their frequent use in the treatment of PS as alternatives to anti-TNF-α; however, some reports have related them with an increase in adverse cardiovascular events, which calls into question their validity (Ahlehoff et al., 2013; Alexandroff et al., 2009).

The aim of the present study was to characterize the effects of the most widely used anti-TNF-α-adalimumab (ADA, fully human), infliximab (INF, chimeric origin with human constant and murine variable regions) and etanercept [ETA, human p75 region of tumor necrosis factor-α (TNF-α) receptor linked to the fragment crystallisable (Fc) region of human IgG1]-on leukocyte–endothelial cell interactions and endothelial adhesion molecules induced by various stimuli implicated in PS and RA, and to compare the effects with those of the anti-p40 subunit of IL-12/23 ustekinumab (UST) (Nestorov, 2005; Tracey et al., 2008; Koutruba et al., 2010; Price et al., 2007; Singh et al., 2011).

2. Materials and methods

2.1. Human umbilical vein endothelial cells (HUVEC) cell culture

HUVEC were harvested from freshly obtained umbilical cords by collagenase treatment, as previously described (De Pablo et al., 2010). In short, umbilical cord veins were rinsed of blood products with warm phosphate-buffered saline (PBS), after which the vein was filled with collagenase (1 mg/ml) for 17 min at 37 °C. The cords were then gently massaged to ensure detachment of endothelial cells from the vessel wall. The digest was collected, centrifuged and pelleted. The pellet was resuspended in endothelial cell growth medium (EGM-2) inside T25 culture flasks in which cells were cultured until confluence. After reaching confluence, primary cultures were detached with trypsin and transferred to 6-well plate culture dishes. Passage 1 of these primary cultures was subsequently employed. For adhesion studies, HUVEC were cultured on fibronectin (5 μg/ml)-coated 25-mm plastic coverslips until confluent (~48 h).

2.2. Leukocyte isolation

Polymorphonuclear (PMN) or peripheral blood mononuclear (PBMC) cells were isolated from whole blood drawn from healthy volunteers and anticoagulated with sodium citrate (De Pablo et al., 2010). Samples were incubated with dextran (3%) for 45 min. PBMC and PMN in the supernatant were separated by gradient density centrifugation (250 g, 25 min) with Ficoll-Paque™ Plus. After red blood cell lysis, leukocytes were washed (HBSS without Ca^{2+} or Mg^{2+}) and resuspended in complete RPMI media. The medical ethical committee of the Hospital Clínico Universitario de Valencia approved the study and all participating patients provided written informed consent.

2.3. Adhesion assay under flow conditions

The parallel plate flow chamber in vitro model has been described in detail previously (De Pablo et al., 2012; Cai et al., 2006). For adhesion assays, coverslips containing confluent HUVEC monolayers were placed in a circular recess in the bottom plate of the flow chamber (maintained at 37 °C), where a portion (5 mm × 25 mm) of the monolayer was exposed to the flow. The entire chamber was mounted on an inverted microscope (Nikon Eclipse TE 2000-S) connected to a video camera (Sony Exware HAD). Experiments were conducted using a 40× objective lens. PMN or PBMC were resuspended in flow buffer ($DPBS^{+}$ containing 20 mM HEPES and 0.1% HSA) at 1×10^6 or 0.5×10^6 cells/ml respectively and were drawn across the HUVEC monolayer at a controlled flow rate of 0.36 ml/min (estimated shear stress of 0.7 dyne/cm^2). A circular glass window in the top plate of the chamber allowed real-time microscopic examination of the monolayer exposed to the flow. Images in a single field of view were recorded over a 5-min period during which leukocyte parameters were determined. Leukocyte rolling was calculated by counting the number of leukocytes passing a reference point in the monolayer during a period of 1 min. The velocities of 20 consecutive leukocytes in the field of focus were determined by measuring the time required to travel a distance of 100 μm. Leukocyte adhesion was determined by counting the number of leukocytes that maintained stable contact with the monolayer for 30 s.

Two series of experiments were carried out in order to perform a comprehensive evaluation of the mechanisms and cell populations implicated and the pharmacological features of the drugs under assay. Initially, we focused on the role of the endothelium when activated by stimuli at doses that have been correlated with the onset of the inflammatory process in atherosclerosis (Libby, 2012; Alvarez et al., 2004): TNF-α (25 ng/ml, 4 h), IL-1β (interleukin-1β, 80 IU/ml, 4 h), LT-α (lymphotoxin-α, 3 ng/ml, 4 h) and Ang-II (angiotensin-II, 10 nM, 4 h) (Nakada et al., 1998; Yamagata et al., 2012; Suna et al., 2008; Mateo et al., 2006). When necessary, HUVEC were pre-treated (0.5 h before) or post-treated (0.5, 4 or 24 h after activation of the endothelium) with clinically relevant concentrations of ADA (3–11 μg/ml), INF (200 μg/ml), ETA (5 μg/ml) or UST (3–15 μg/ml) (Rigby, 2007; Nestorov, 2005; Furst et al., 2006; Gottlieb et al., 2007).

The second group of experiments was designed to explore the role of leukocytes. Hence, PMN or PBMC were stimulated with the general leukocyte activator Platelet-activating factor (PAF; 1-O-alkyl-2-acetyl-sn-glycero-3-phosphocholine, 10 μM, 1 h) (Montrucchio et al., 2000) or with stimuli specifically known to provoke leukocyte activation in psoriatic arthritis (Koutruba et al., 2010; Suzuki et al., 2014; Lowes et al., 2013): IL-12 (interleukin-12, 5 ng/ml, 1 h) and IL-23 (interleukin-23, 50 ng/ml, 1 h) (Allavena et al., 1994). When necessary, PMN or PBMC were pre-treated (0.5 h before activation of leukocytes) with clinically relevant concentrations of ADA and UST. Post-activation treatment could not be performed because of limits in the leukocytes' integrity.

2.4. Expression of adhesion molecules in HUVEC

Endothelial adhesion molecules [ICAM (intercellular adhesion molecule)-1, VCAM (vascular adhesion molecule)-1 and E-selectin] were analyzed as described previously (Alvarez et al., 2004; Ibiza et al., 2009). HUVEC were grown to confluence in 6-well plates and thereafter stimulated with TNF-α (25 ng/ml) for 4 h at 37 °C. Some cells were treated with ADA (0.01–11 μg/ml) 0.5 h before or 24 h after activation of the endothelium. Cells were detached with trypsin, placed in suspension, incubated with the corresponding antibody (20 min, on ice, in darkness), fixed (in formaline 10%) and analyzed for protein expression according to forward- and side-scatter characteristics in a FACS Calibur cytometer (BD, Franklin Lakes, NJ, USA). In each case, 10,000 cells were analyzed and the mean of the specific fluorescence intensity was employed as a marker of the expression of the respective epitope. All samples were compensated using the appropriate isotype-matched negative control.

2.5. Materials

Dulbecco's PBS, with ($DPBS^+$) or without ($DPBS^-$) Ca^{2+} and Mg^{2+}, EGM-2 culture media, HBSS and fetal bovine serum were acquired from LONZA (Verviers, Belgium). Recombinant TNF-α, human serum albumine (HSA, Albuminate 25%), RPMI1640 supplemented with 20 mM HEPES, fibronectin, formaline, dextran, IL-1β, IL-12, PAF and Ang-II were supplied by Sigma Chemical Co (St. Louis, MO, USA). LT-α and IL-23 were acquired from Prospecbio (supplied by Deltaclon, Madrid, Spain). Ficoll-Paque TM Plus was supplied by GE Healthcare Life Sciences (Amersham, UK). Plastic coverslips with a diameter of 25 mm were obtained from Nunc, supplied by Thermo Fisher Scientific (Walthman, MA, USA). PBS, collagenase, and trypsin were acquired from Gibco Invitrogen, Life Technologies (Carlsbad, CA, USA). Fluorescein isothyocianate (FITC) and phycoerithrin (PE) conjugated control antibodies and antibodies against E-selectin, ICAM-1 or VCAM-1 were purchased from BD Bioscience (Franklin Lakes, NJ, USA). Adalimumab (Humira®), infliximab (Remicade®), etanercept (Enbrel®) and ustekinumab (Stelara®) were used in the form of their clinically available preparations.

2.6. Data analysis and statistics

Data are mean ± S.E.M of 3–6 experiments. Statistical significance was considered to be <0.05 by one-way ANOVA analysis

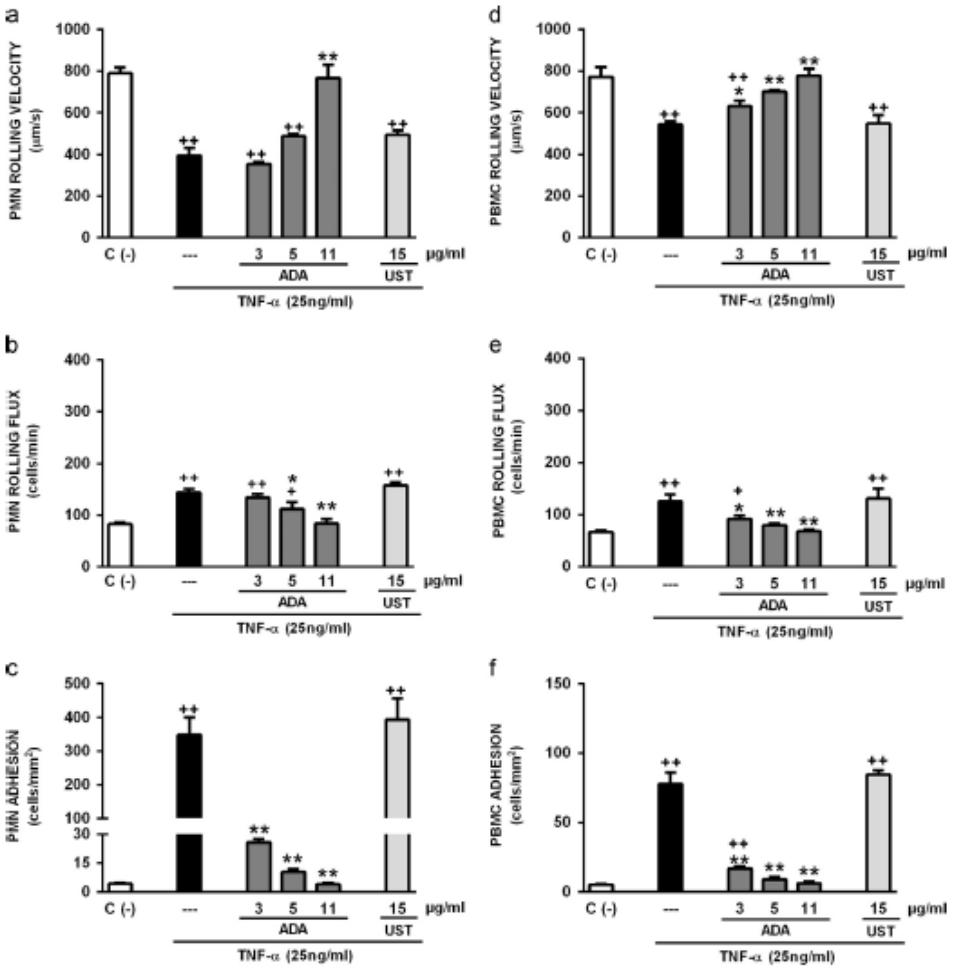

Fig. 1. Effects of pre-treatment with adalimumab or ustekinumab on PMN- or PBMC-endothelial cell interactions induced by TNF-α. HUVEC were pre-treated (0.5 h) with adalimumab (ADA, 3–11 μg/ml) or ustekinumab (UST, 15 μg/ml) before stimulation (4 h) with tumor necrosis factor-α (TNF-α, 25 ng/ml) or medium (control). Polymorphonuclear (PMN) cells rolling velocity (a), rolling flux (b) and adhesion (c) and peripheral blood mononuclear cells (PBMC) rolling velocity (d), rolling flux (e) and adhesion (f) were quantified after assembling the flow chamber. Results are mean ± S.E.M., $n \geq 4$. $^{+}P<0.05$ or $^{++}P<0.01$ vs. corresponding value in control group and $^{*}P<0.05$ or $^{**}P<0.01$ vs. corresponding value in TNF-α-treated group (ANOVA followed by Newman–Keuls test).

of variance, with Newman–Keuls post-test correction to compare multiple variances.

3. Results

3.1. Effects on cell interactions induced by endothelial stimuli

As expected, only a small number of PMN or PBMC cells adhered to unstimulated HUVEC (Figs. 1, 2, 4, 5 and 6), thus reproducing the conditions of a normal non-inflamed vessel (Supplementary material S1). In order to mimic the typical scenario of the development of the atherosclerotic plaque, HUVEC were stimulated with TNF-α, IL-1β, LT-α or Ang-II.

TNF-α (Supplementary material S2) induced a significant decrease in the rolling velocity and an increase in the rolling flux and adhesion of both PMN and PBMC (Figs. 1 and 2). ADA prevented leukocyte (PMN and PBMC)–endothelial cell interactions induced by TNF-α in a dose-dependent manner (Supplementary movies S3, S4 and S5). The actions of the anti-TNF-α on adhesion were more pronounced than those on rolling, and this pattern was particularly obvious in PMN, in which the lowest concentration employed (3 μg/ml) significantly reduced adhesion while having no effect on rolling velocity or flux (Fig. 1). Of note, 24 h treatment with

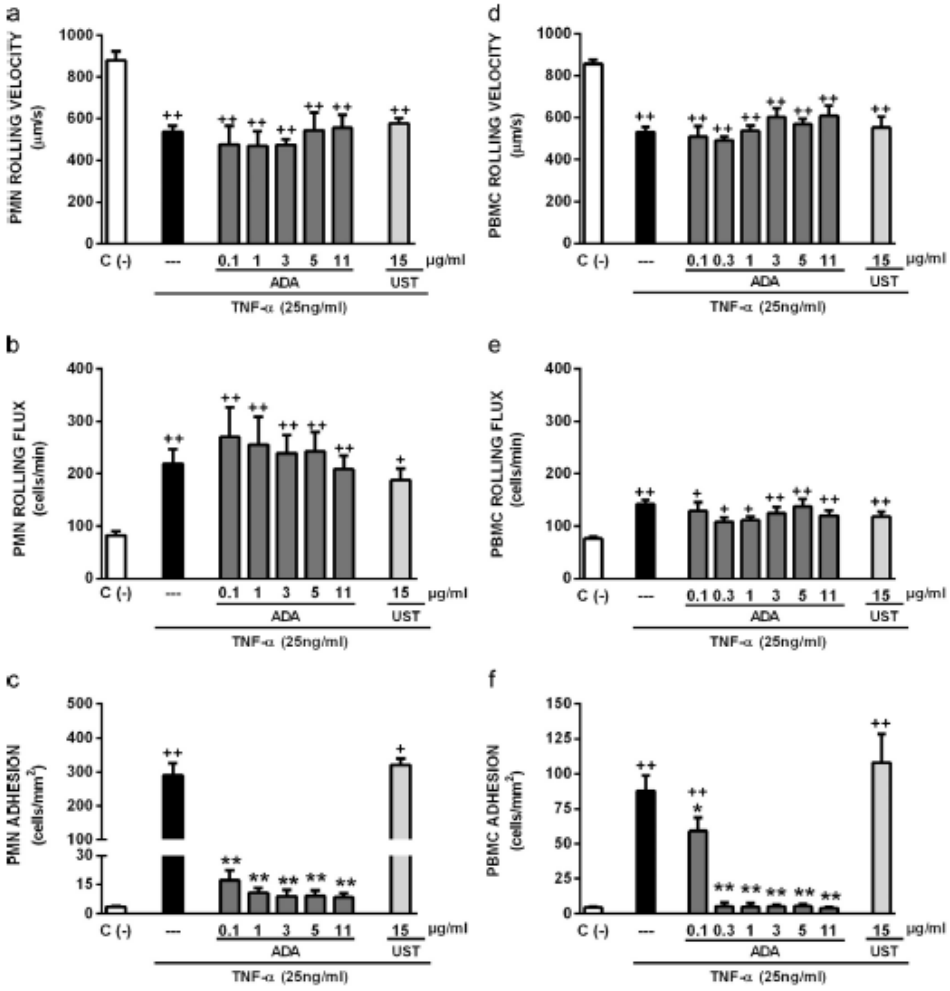

Fig. 2. Capacity of adalimumab and ustekinumab to reverse PMN- or PBMC-endothelial cell interactions induced by TNF-α. HUVEC were treated (4 h) with tumor necrosis factor-α (TNF-α, 25 ng/ml) or medium (control) before incubation with adalimumab (ADA, 0.1–11 μg/ml) or ustekinumab (UST, 15 μg/ml) for a further 24 h period. Polymorphonuclear (PMN) cells rolling velocity (a), rolling flux (b) and adhesion (c) and peripheral blood mononuclear cells (PBMC) rolling velocity (d), rolling flux (e) and adhesion (f) were quantified after assembling the flow chamber. Results are mean ± S.E.M., $n \geq 4$. $^{+}P < 0.05$ or $^{++}P < 0.01$ vs. corresponding value in control group and $^{*}P < 0.05$ or $^{**}P < 0.01$ vs. corresponding value in TNF-α-treated group (ANOVA followed by Newman–Keuls test).

Table 1
Capacity of adalimumab, infliximab and etanercept to reverse PMN- or PBMC-endothelial cell interactions induced by TNF-α.

		Vehicle	TNF-α	TNF-α+ADA	TNF-α+INF	TNF-α+ETA
PMN	Rolling velocity (μm/seg)	898,81 ± 26,7	546,33 ± 24,8[bb]	557,87 ± 61,9[bb]	563,25 ± 70,6[bb]	651,33 ± 75,7[bb]
	Rolling flux (cells/min)	65,04 ± 5,7	218,75 ± 28,3[bb]	209,25 ± 25,3[bb]	176,57 ± 14,5[bb]	166,08 ± 23,1[bb]
	Adhesion (cells/mm²)	2,62 ± 0,3	290,32 ± 35,1[bb]	8,46 ± 2,2[bb]	11,25 ± 7,6[bb]	10,73 ± 6,1[bb]
PBMC	Rolling velocity (μm/seg)	875,72 ± 22,8	531,38 ± 25,1[bb]	609,33 ± 49,8[bb]	667,10 ± 28,9[bb]	659,23 ± 28,9[bb]
	Rolling flux (cells/min)	65,31 ± 5,9	142,33 ± 7,5[bb]	120,5 ± 9,3[bb]	106,67 ± 8,8[bb]	108,67 ± 14,5[bb]
	Adhesion (cells/mm²)	3,22 ± 0,4	87,72 ± 11,1[bb]	3,93 ± 1,2[bb]	1,95 ± 0,7[bb]	4,94 ± 0,8[bb]

HUVEC were treated (4 h) with tumor necrosis factor-α (TNF-α, 25 ng/ml) or medium (control) before incubation with adalimumab (ADA, 11 μg/ml), infliximab (INF, 200 μg/ml) or etanercept (ETA, 5 μg/ml) for a further 24 h period. Polymorphonuclear (PMN) cells rolling velocity, rolling flux and adhesion and peripheral blood mononuclear cells (PBMC) rolling velocity, rolling flux and adhesion were quantified after assembling the flow chamber. Results are mean ± S.E.M., $n \geq 3$.

[a] $P < 0.01$ vs. corresponding value in control group.

[bb] $P < 0.01$ vs. corresponding value in TNF-α-treated group (ANOVA followed by Newman–Keuls test).

concentrations of ADA lower than 0.1 μg/ml specifically reversed the adhesion of leukocytes following endothelium activation (4 h) by TNF-α without affecting earlier steps of the vascular inflammatory process, such as leukocyte rolling velocity and flux (Fig. 2). Shorter periods of incubation with ADA (i.e., 0.5 h or 4 h) had no effect on the changes in leukocyte parameters induced by 4 h incubation with TNF-α (data not shown). 24 h incubation with INF and ETA produced a similar profile to ADA in terms of reversing leukocyte recruitment induced by 4 h TNF-α; i.e., leukocyte adhesion was reversed without disturbing rolling velocity or flux (Table 1). UST, whether used pre- or post-TNF-α, had no effect on any of the leukocyte–endothelial cell interactions induced by this inflammatory cytokine.

Supplementary material related to this article can be found online at http://dx.doi.org/10.1016/j.ejphar.2015.08.054.

TNF-α (25 ng/ml) increased the expression of VCAM-1, ICAM-1 and E-selectin (Fig. 3, Supplementary Fig. S1) in HUVEC. ADA both prevented and reversed the induction of these adhesion molecules, even at very low concentrations (0.3 μg/ml).

IL-1β and LT-α also induced a significant decrease in the rolling velocity and an increase in the rolling flux and adhesion of both PMN and PBMC (Figs. 4 and 5). In the case of Ang-II, there was a similar and significant decrease of rolling velocity and an increase in rolling flux both in PMN and PBMC, while only PMN adhesion was increased by this peptide (Figs. 4 and 5). TNF-α evidently had no bearing on the effects of IL-1β on leukocyte recruitment, since pre-treatment with ADA did not alter the response of PMN or PBMC to this stimulus. On the contrary, some TNF-α-activated receptors seemed to be implicated in the inflammatory actions of LT-α, as all parameters of PMN- and PBMC-endothelial interactions elicited by this cytokine were significantly prevented by the highest dose of ADA employed (11 μg/ml). Once again, ADA had a greater impact on adhesion (a complete return to control levels) than on rolling velocity and flux, which were only partially prevented (Fig. 4). ADA's effect on the actions of Ang-II on PMN were similar to those on LT-α, while Ang-II has no bearing on PBMC (Fig. 4). Finally, pre-incubation with UST had no effect on leukocyte–endothelial cell interactions induced by IL-1β, LT-α or Ang-II (Fig. 4).

In a scenario where the endothelium had previously been activated by IL-1β, LT-α or Ang-II (4 h), 24 h post-treatment with either ADA or UST did not reverse the leukocyte–endothelial cell interactions elicited by all three stimuli (Fig. 5).

3.2. Effects on cell interactions induced by leukocyte stimuli

Leukocytes were stimulated with three mediators that have been correlated with inflammation in atherosclerosis or PS. PAF, a broad and unspecific leukocyte activator, induced a significant decrease in rolling velocity and an increase in rolling flux and adhesion of both PMN and PBMC (Fig. 6). ADA had no effect on these actions, and, while UST also lacked an influence on any of the effects of PAF on PMN, it specifically reduced PBMC rolling flux. IL-23 induced a reduction in PMN and PBMC rolling velocity and increased rolling flux. While ADA reversed the effects of IL-23 on PBMC only, UST blocked these effects on both leukocyte populations. IL-12 had no effect at physiological doses and affected only PMN at very high doses (50-fold), reducing their rolling velocity and increasing their rolling flux and adhesion. Both ADA and UST reversed the effects of IL-12 on adhesion, but not on rolling velocity or rolling flux (Fig. 6).

4. Discussion

The exacerbation of leukocyte–endothelial interactions is an inflammatory process associated with the early phases of the vascular dysfunction that characterises important cardiovascular diseases (Krieglstein and Granger, 2001). The aim of the present study was to compare the actions of two of the most potent anti-inflammatory treatments for PS – anti-TNF-α and anti-IL-12/23 agents – on a variety of endothelial (TNF-α, IL-1β, LT-α and Ang-II) and leukocyte (PAF, IL-12 and IL-23) stimuli implicated in endothelial dysfunction and/or PS pathogenesis (Tracey et al., 2008; Koutruba et al., 2010; Price et al., 2007; Singh et al., 2011). We employed a dynamic in vitro model that is widely used to analyze the multistep recruitment of leukocytes and the vascular anti-inflammatory actions of drugs (Victor et al., 2011; Luu et al., 2007). In this system, human leukocytes (PMN and PBMC) flow over a monolayer of human endothelial cells in a way that closely resembles processes (rolling and adhesion) that are critical for hemostasis and vascular cell integrity and which precede the formation of an atherosclerotic plaque in vivo (Goetz et al., 1999; De Pablo et al., 2013). Our results demonstrate that clinically relevant concentrations of the three anti-TNF-α drugs tested, but not of UST, significantly undermine leukocyte recruitment when the endothelium is activated. However, when leukocytes are activated, UST reduces some, but not all, of these interactions, while, surprisingly, ADA also exerts a significant effect.

Pre-incubation with concentrations of ADA (3–11 μg/ml) that mimicked those present in patients (Rigby, 2007; Nestorov, 2005; Furst et al., 2006) prevented all the effects induced by subsequent administration of TNF-α, one of the most potent stimuli of leukocyte–endothelial interplay (Griffin et al., 2012). On the other hand, when an inflammatory response to TNF-α had been established – a scenario that resembles clinical conditions more closely – subsequent treatment with any of three anti-TNF-α evaluated (ADA, INF or ETA) also reversed the effects of this mediator on adhesion, while having no influence on its effects on rolling velocity and flux, despite the on-going presence of the cytokine.

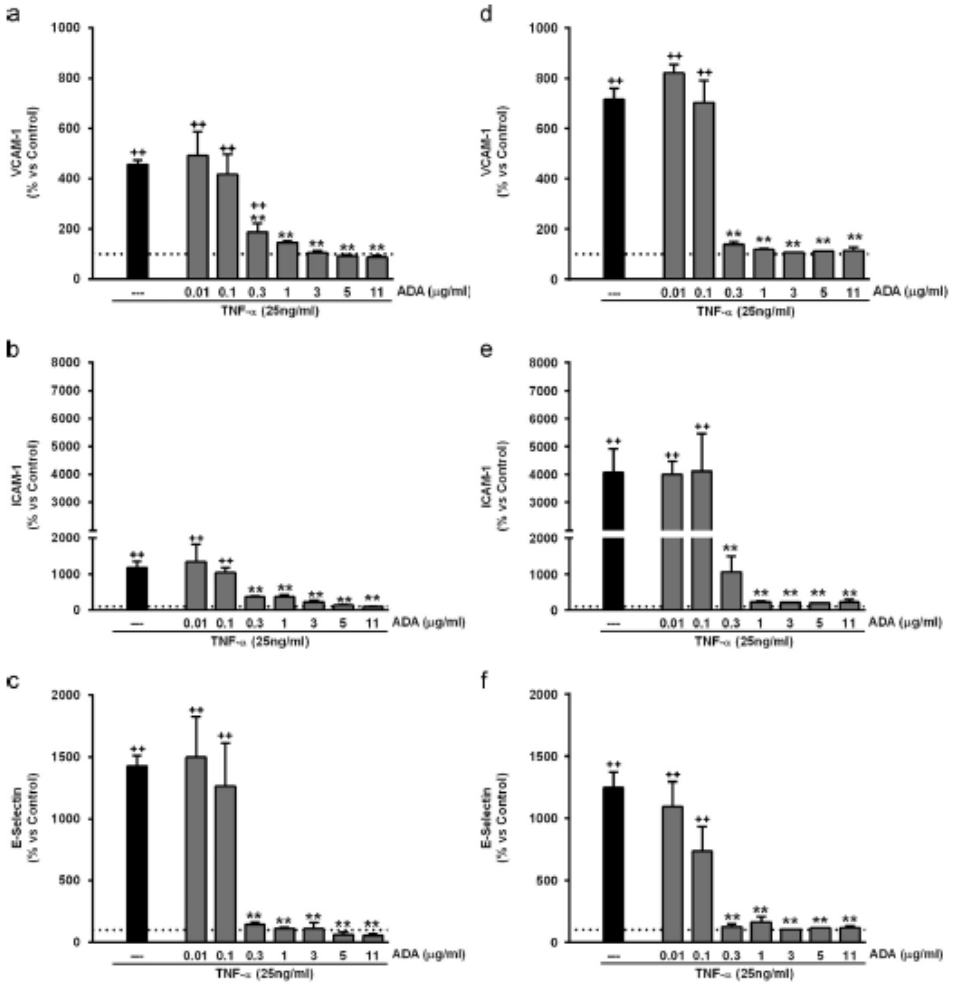

Fig. 3. Effects of adalimumab on the expression of endothelial adhesion molecules induced by TNF-α. HUVEC were treated with adalimumab (ADA, 0.01–11 μg/ml) 0.5 h before (a–c) or 24 h after (d–f) stimulation (4 h) with tumor necrosis factor-α (TNF-α, 25 ng/ml) or medium (control). Expression of vascular cell adhesion molecule-1 (VCAM-1) (a and d), intracellular adhesion molecule-1 (ICAM-1) (b and e) and E-selectin (c and f) was analyzed by flow cytometry. Fluorescein isothyocianate (FITC) or phycoerithrin (PE)-fluorescence values are expressed as a percentage of the mean fluorescence intensities of control cells (100%). Results are mean ± S.E.M., $n \geq 3$. $^{+}P < 0.05$ or $^{++}P < 0.01$ vs. corresponding values in control group and $^{**}P < 0.01$ vs. corresponding value in TNF-α-treated group (ANOVA followed by Newman–Keuls test).

Furthermore, the effects arising from deferred blockade of TNF receptors were not noticeable after short periods (0.5 h or 4 h) of anti-TNF-α incubation and reached significance only after 24 h, which is evidence of the multiple inflammatory pathways triggered following administration of the cytokine and its reduced role in subsequent responses. In addition, ADA had no influence on the actions of IL-1β, but prevented the actions of LT-α and Ang-II when pre-administered. However, ADA failed to reverse the inflammatory response elicited by the latter two stimuli once it had been established. The effects described with ADA, which binds to TNF-α and avoids the interaction of this cytokine with its two receptors (TNF receptor 1 and TNF receptor 2) (Van et al., 2011), are generally in line with published evidence implicating TNF-α in the actions of the stimuli we have evaluated in this study. Thus, whereas IL-1β exerts its action through receptors unrelated to TNF-α (Dinarello, 2011), LT-α exhibits certain similarity with the tertiary and quaternary structure of TNF-α (Buhrmann et al., 2013), which probably explains its susceptibility to TNF-α blockade. Indeed, its actions are a result of its binding to a variety of receptors, including TNF receptor 1 and TNF receptor 2 and the more specific LT-β receptor (Etemadi et al., 2013). Lastly, Ang-II binds to angiotensin-II receptor type I, which activates signal pathways shown to upregulate TNF-α production (Abadir et al., 2011).

The interaction of leukocytes with endothelial cells is

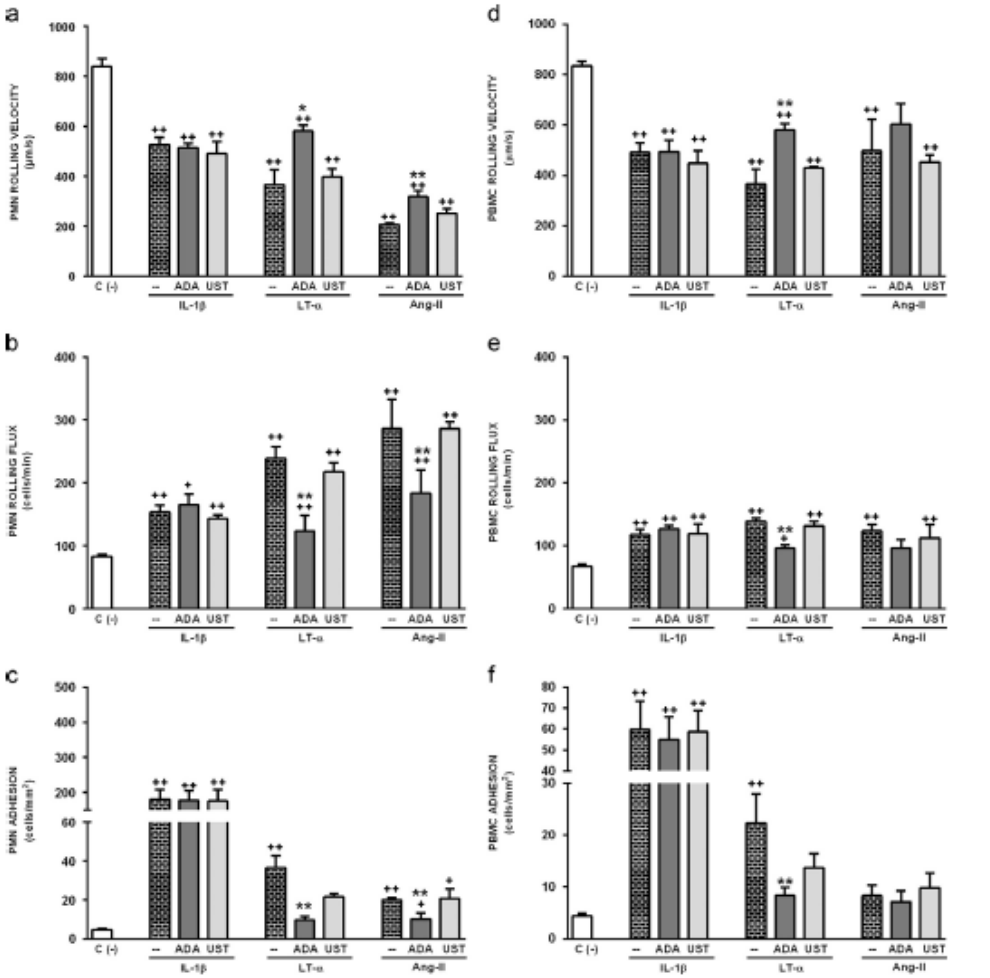

Fig. 4. Effects of pre-treatment with adalimumab or ustekinumab on PMN- or PBMC-endothelial cell interactions induced by IL-1β, LT-α or Ang-II. HUVEC were pre-treated (0.5 h) with adalimumab (ADA, 11 μg/ml) or ustekinumab (UST, 15 μg/ml) before stimulation (4 h) with interleukin-1β (IL-1β, 80 IU), lymphotoxin-α (LT-α, 3 ng/ml), angiotensin II (Ang-II, 10 nM) or medium (control). Polymorphonuclear (PMN) cells rolling velocity (a), rolling flux (b) and adhesion (c) and peripheral blood mononuclear cells (PBMC) rolling velocity (d), rolling flux (e) and adhesion (f) were quantified after assembling the flow chamber. Results are mean ± S.E.M., $n \geq 3$. $^{+}P < 0.05$ or $^{++}P < 0.01$ vs. corresponding value in control group and $^{*}P < 0.05$ or $^{**}P < 0.01$ vs. corresponding value in IL-1β, LT-α or Ang-II-treated group (ANOVA followed by Newman–Keuls test).

controlled by the interplay of adhesion molecules present in both cell groups (Ley et al., 2007; Muller, 2009). However, until now, there has been very little evidence of the implication of these molecules in the protective cardiovascular actions of anti-TNF-α, and the few existing reports have assessed non-functional soluble forms of adhesion molecules in plasma (Gonzalez-Gay et al., 2006; den Broeder et al., 2002; Klimiuk et al., 2004). In addition, most studies have been performed with INF and ETA, and so very little data has been obtained regarding newer, "non-chimeric" anti-TNF-α. Our results clearly endorse a role for adhesion molecules in the actions of anti-TNF-α, particularly as we have measured the expression of functional molecules – not just soluble ones – in the very same endothelial cell monolayer in which the flow chamber studies were performed. We can confirm previous evidence that TNF-α induces the expression of ICAM-1, VCAM-1 and E-selectin (Zhang et al., 2002), and we demonstrate that this enhancement is prevented and reversed by concentrations of ADA well below clinical levels. The fact that ICAM-1, VCAM-1 and E-selectin are responsible for leukocyte adhesion would explain why ADA reverses this specific parameter and not rolling velocity and flux, which would seem to implicate other molecules (Muller, 2009; Ley et al., 2007). This profile of the actions of anti-TNF-α is of special

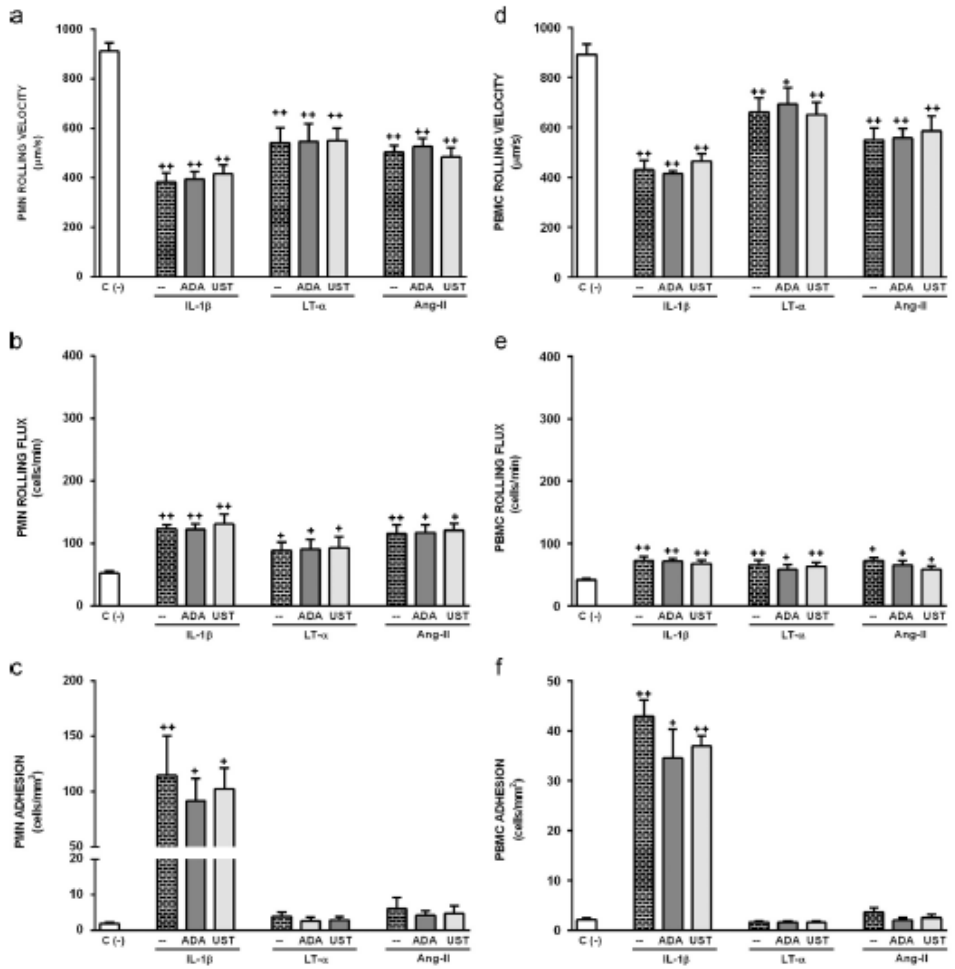

Fig. 5. Capacity of adalimumab and ustekinumab to reverse PMN- or PBMC-endothelial cell interactions induced by IL-1β, LT-α or Ang-II. HUVEC were treated (4 h) with interleukin-1β (IL-1β, 80 IU), lymphotoxin-α (LT-α, 3 ng/ml), angiotensin II (Ang-II, 10 nM) or medium (control) before incubation with adalimumab (ADA, 11 μg/ml) or ustekinumab (UST, 15 μg/ml) for a further 24 h period. Polymorphonuclear (PMN) cells rolling velocity (a), rolling flux (b) and adhesion (c) and peripheral blood mononuclear cells (PBMC) rolling velocity (d), rolling flux (e) and adhesion (f) were quantified after assembling the flow chamber. Results are mean ± S.E.M., $n \geq 4$. $^{+}P < 0.05$ or $^{++}P < 0.01$ vs. corresponding value in control group (ANOVA followed by Newman-Keuls test).

relevance, since adhesion represents a stable interaction of white cells with the endothelium and occurs immediately prior to dyapedesis/emigration, the "point of no return" in leukocyte inflammatory vascular enrollment (Muller, 2009). Of note, this response is in keeping with that of drugs such as natalizumab (anti-α_4 integrin antibody) and roquinimix, which also abolish leukocyte adhesion, but not rolling, under TNF-α-stimulating conditions (Coisne et al., 2009; Zhang et al., 2000).

UST had no effect on the leukocyte recruitment induced by any of the four stimuli used to activate the endothelium, as was expected given the limited evidence of the implication of IL-12 and IL-23, whose p40 subunit is blocked by UST, in the inflammatory responses of HUVEC. However, UST prevented the effects of IL-23 on leukocyte activation and the PMN adhesion induced by IL-12. UST would seem to block both cytokines, thus avoiding their binding to the IL-12 β1 receptor chain of both IL-12 (IL-12 β1/β2) and IL-23 (IL-12β1/IL-23) receptor complexes (Suzuki et al., 2014; Lowes et al., 2013; Benson et al., 2011). IL-12 exerted a differential profile on both leukocyte subpopulations in terms of leukocyte–endothelial cells interactions by inducing them only on PMN but not on PBMC. Similar results were observed by Allavena et al. (1994) when evaluated the chemotactic response of PMN and PBMC to the cytokine IL-12. However, the effects of IL-12 on PMN rolling were not blocked by UST, but this result needs to be interpreted with caution given the clinical concentration of IL-12 on psoriatic patients (36.6 ± 17.93 pg/ml, Arican et al., 2005) is much

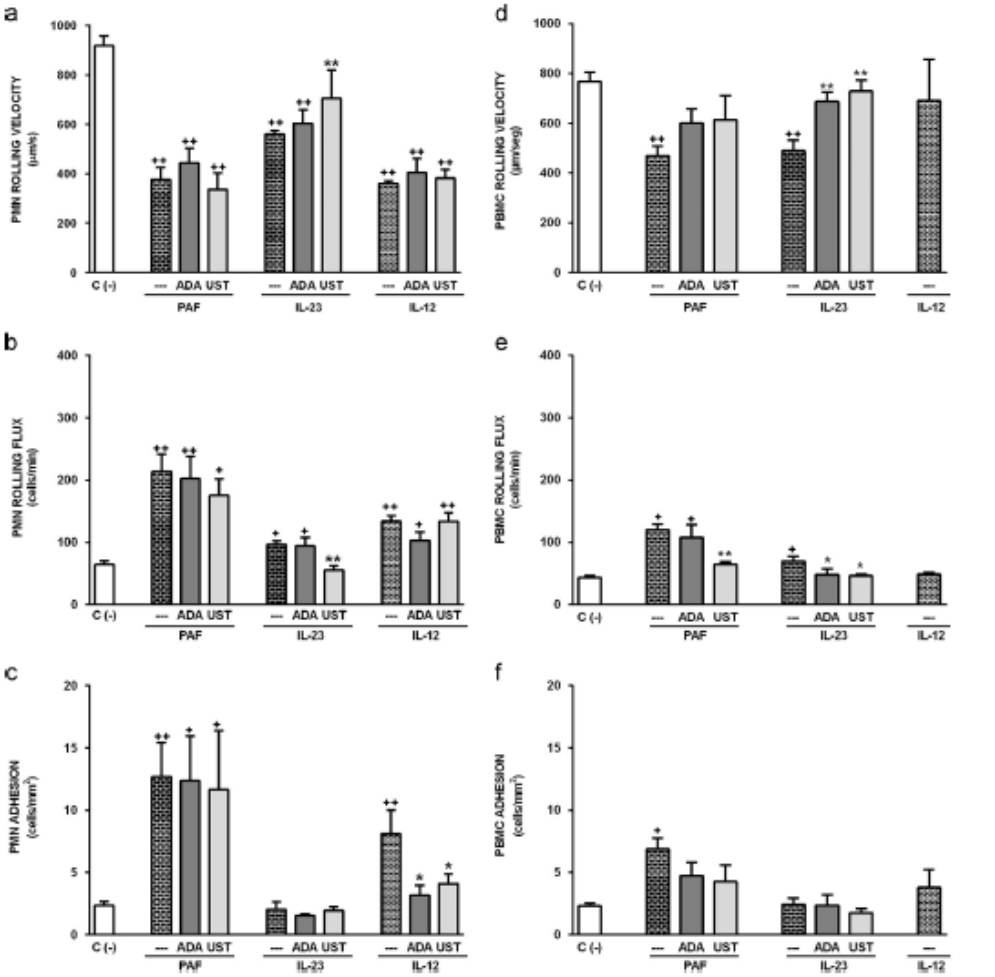

Fig. 6. Effects of pre-treatment with adalimumab or ustekinumab on PMN- or PBMC-endothelial cell interactions induced by PAF, IL-23 or IL-12. PMN and PBMC were pre-treated with adalimumab (ADA, 11 μg/ml) or ustekinumab (UST, 15 μg/ml) for 0.5 h before stimulation (1 h) with platelet-activating factor (PAF, 10 μM), interleukin-23 (IL-23, 50 pg/ml), interleukin-12 (IL-12, 5 ng/ml) or medium (control). Polymorphonuclear (PMN) cells rolling velocity (a), rolling flux (b) and adhesion (c) and peripheral blood mononuclear cells (PBMC) rolling velocity (d), rolling flux (e) and adhesion (f) were quantified after assembling the chamber. Results are mean ± S.E.M., $n \geq 4$. $^{+}P < 0.05$ or $^{++}P < 0.01$ vs. corresponding value in control and $^{*}P < 0.05$ or $^{**}P < 0.01$ vs. corresponding value in PAF or IL-23 or IL-12-treated group (ANOVA followed by Newman–Keuls test).

lower than the concentration necessary to induce in vitro leukocyte–endothelial cell interactions (5000 pg/ml; Allavena et al., 1994) in our experimental model.

ADA prevented rolling velocity and rolling flux triggered by IL-23 in PBMC, but not in PMN. This was not expected, as there is no previous functional evidence of such an action. This could have been the result of the blockade of the TNF-α produced, in conjunction with other cytokines (interferon-γ, interleukin-17, interleukin-22…), by PBMC (Lowes et al., 2013) – but not by PMN (Allavena et al., 1994; Suzuki et al., 2014) – in response to IL-12 and IL-23 stimulation.

5. Conclusions

In summary, our results demonstrate that clinically relevant concentrations of three distinct and widely used anti-TNF-α drugs inhibit the leukocyte recruitment induced by a wide variety of stimuli that act on both the endothelium and leukocytes. UST exhibits a more discreet profile, blocking the actions of IL-23 and IL-12 on leukocyte activation without modifying those arising from endothelial stimuli activation. These findings endorse the idea that treatment with currently prescribed biological anti-inflammatory drugs can have a positive impact on CVD risk by reducing the vascular systemic inflammation associated with PS and

RA. However, the degree of such effects varies considerably; in light of our in vitro results obtained in human cells, the wider profile of actions of anti-TNF-α – owing to the ubiquity of the mediator in the inflammatory cascade – seems to promise a more potent, and thus more clinically relevant effect. Importantly, this potential CV effect is in addition to these drugs' ability to counteract the inflammatory conditions that characterize the dermatologic and rheumatic diseases for whose treatment they were designed, and obviously requires clinical corroboration.

Conflict of interest

JVE has given conferences and/or participated in advisory boards for AstraZeneca, Gilead, Abbvie, MSD and Pfizer. JVE and AA have received research funding from Gilead and Abbvie. None of the other authors report any potential conflicts.

Acknowledgments

CRN and CDP performed the research, MAMC, ABG, VCD and SO helped perform the research, CRN, CDP and AA analyzed the data and JVE and AA designed the research and wrote the paper. We would like to thank Nicole Roupain, Dora Martí and Fernando Sabater for their technical support to perform the experiments of this manuscript. This work was supported by Ministerio de Ciencia e Innovación [Grant SAF2010-16030], Ministerio de Sanidad y Consumo [Grant PI11/00327 and PI14/00312], CIBERehd [Grant CB06/04/0071] and Generalitat Valenciana [Grant PROMETEOII/2014/035, PROMETEO/2010/060, ACOMP2013/147, ACOMP2013/236 and Gerónimo Forteza FPA/2013/A/051]. CDP was funded by Ministerio de Ciencia e Innovación [FPI Grant BES-2008-004338] and by Fundación Juan Esplugues. SO was funded by Universidad de Valencia [VLC CAMPUS Grant] and Fundación Fisabio Grant 2015/01. CRN and VCD were funded by Fundación Fisabio. Grants 2014/22 and 2014/23 respectively. ABG is recipient of a Juan de la Cierva contract (ref. JCI-2012-15124, Ministerio de Economía y Competitividad). AA was supported by Ministerio de Ciencia e Innovación [Ramón y Cajal program RYC2005-002295 and I3 program].

Appendix A. Supplementary information

Supplementary data associated with this article can be found in the online version at http://dx.doi.org/10.1016/j.ejphar.2015.08.054.

References

Abadir, P.M., Walston, J.D., Carey, R.M., Siragy, H.M., 2011. Angiotensin II type-2 receptors modulate inflammation through signal transducer and activator of transcription protein-3 phosphorylation and TNFalpha production. J. Interferon Cytokine Res. 31, 471–474.

Ahlehoff, O., Skov, L., Gislason, G., Lindhardsen, J., Kristensen, S.L., Iversen, L., Lasthein, S., Gniadecki, R., Dam, T.N., Torp-Pedersen, C., Hansen, P.R., 2013. Cardiovascular disease event rates in patients with severe psoriasis treated with systemic anti-inflammatory drugs: a Danish real-world cohort study. J. Intern. Med. 273, 197–204.

Alexandroff, A.B., Pauriah, M., Camp, R.D., Lang, C.C., Struthers, A.D., Armstrong, D.J., 2009. More than skin deep: atherosclerosis as a systemic manifestation of psoriasis. Br. J. Dermatol. 161, 1–7.

Allavena, P., Paganin, C., Zhou, D., Bianchi, G., Sozzani, S., Mantovani, A., 1994. Interleukin-12 is chemotactic for natural killer cells and stimulates their interaction with vascular endothelium. Blood 84, 2261–2268.

Alvarez, A., Cerda-Nicolas, M., Naim Abu, N.Y., Mata, M., Issekutz, A.C., Panes, J., Lobb, R.R., Sanz, M.J., 2004. Direct evidence of leukocyte adhesion in arterioles by angiotensin II. Blood 104, 402–408.

Arican, O., Aral, M., Sasmaz, S., Ciragil, P., 2005. Serum levels of TNF-α, IFN-γ, IL-6, IL-8, IL-12, IL-17 and IL-18 in patients with active psoriasis and correlation with disease severity. Mediat. Inflamm. 5, 273–279.

Benson, J.M., Peritt, D., Scallon, B.J., Heavner, G.A., Shealy, D.J., Giles-Komar, J.M., Mascelli, M.A., 2011. Discovery and mechanism of ustekinumab: a human monoclonal antibody targeting interleukin-12 and interleukin-23 for treatment of immune-mediated disorders. MAbs 3, 535–545.

Buhrmann, C., Shayan, P., Aggarwal, B.B., Shakibaei, M., 2013. Evidence that TNF-beta (lymphotoxin alpha) can activate the inflammatory environment in human chondrocytes. Arthritis Res. Ther. 15, R202.

Cai, Y.H., Alvarez, A., Alcaide, P., Durrmad, P., Lim, Y.C., Jarolim, P., Lowe, J.B., Luscinskas, F.W., Lichtman, A.H., 2006. Abrogation of functional selectin-ligand expression reduces migration of pathogenic CD8+ T cells into heart. J. Immunol. 176, 6568–6575.

Coisne, C., Mao, W., Engelhardt, B., 2009. Cutting edge: natalizumab blocks adhesion but not initial contact of human T cells to the blood-brain barrier in vivo in an animal model of multiple sclerosis. J. Immunol. 182, 5909–5913.

De Pablo, C., Orden, S., Apostolova, N., Blanquer, A., Esplugues, J.V., Alvarez, A., 2010. Abacavir and didanosine induce the interaction between human leukocytes and endothelial cells through Mac-1 upregulation. AIDS 24, 1259–1266.

De Pablo, C., Orden, S., Calatayud, S., Marti-Cabrera, M., Esplugues, J.V., Alvarez, A., 2012. Differential effects of Tenofovir/Emtricitabine and Abacavir/Lamivudine on human leukocyte recruitment. Antivir. Ther. 17, 1615–1619.

De Pablo, C., Orden, S., Peris, J.E., Barrachina, M.D., Esplugues, J.V., Alvarez, A., 2013. Profile of leukocyte–endothelial cell interactions induced in venules and arterioles by nucleoside reverse-transcriptase inhibitors in vivo. J. Infect. Dis. 208, 1448–1453.

den Broeder, A.A., Joosten, L.A., Saxne, T., Heinegard, D., Fenner, H., Miltenburg, A. M., Frasa, W.L., van Tits, L.J., Buurman, W.A., van Riel, P.L., van de Putte, L.B., Barrera, P., 2002. Long term anti-tumour necrosis factor alpha monotherapy in rheumatoid arthritis: effect on radiological course and prognostic value of markers of cartilage turnover and endothelial activation. Ann. Rheum. Dis. 61, 311–318.

Dinarello, C.A., 2011. Interleukin-1 in the pathogenesis and treatment of inflammatory diseases. Blood 117, 3720–3732.

Elliott, M.J., Maini, R.N., Feldmann, M., Kalden, J.R., Antoni, C., Smolen, J.S., Leeb, B., Breedveld, F.C., Macfarlane, J.D., Bijl, H., 1994. Randomised double-blind comparison of chimeric monoclonal antibody to tumour necrosis factor alpha (cA2) versus placebo in rheumatoid arthritis. Lancet 344, 1105–1110.

Etemadi, N., Holien, J.K., Chau, D., Dewson, G., Murphy, J.M., Alexander, W.S., Parker, M.W., Silke, J., Nachbur, U., 2013. Lymphotoxin alpha induces apoptosis, necroptosis and inflammatory signals with the same potency as tumour necrosis factor. FEBS J. 280, 5283–5297.

Furst, D.E., Wallis, R., Broder, M., Beenhouwer, D.O., 2006. Tumor necrosis factor antagonists: different kinetics and/or mechanisms of action may explain differences in the risk for developing granulomatous infection. Semin. Arthritis Rheum. 36, 159–167.

Goetz, D.J., Greif, D.M., Shen, J., Luscinskas, F.W., 1999. Cell–cell adhesive interactions in an in vitro flow chamber. Methods Mol. Biol. 96, 137–145.

Gonzalez-Gay, M.A., Garcia-Unzueta, M.T., de Matias, J.M., Gonzalez-Juanatey, C., Garcia-Porrua, C., Sanchez-Andrade, A., Martin, J., Llorca, J., 2006. Influence of anti-TNF-alpha infliximab therapy on adhesion molecules associated with atherogenesis in patients with rheumatoid arthritis. Clin. Exp. Rheumatol. 24, 373–379.

Gottlieb, A.B., Cooper, K.D., McCormick, T.S., Toichi, E., Everitt, D.E., Frederick, B., Zhu, Y., Pendley, C.E., Graham, M.A., Mascelli, M.A., 2007. A phase 1, double-blind, placebo-controlled study evaluating single subcutaneous administrations of a human interleukin-12/23 monoclonal antibody in subjects with plaque psoriasis. Curr. Med. Res. Opin. 23, 1081–1092.

Griffin, G.K., Newton, G., Tarrio, M.L., Bu, D.X., Maganto-Garcia, E., Azcutia, V., Alcaide, P., Grabie, N., Luscinskas, F.W., Croce, K.J., Lichtman, A.H., 2012. IL-17 and TNF-alpha sustain neutrophil recruitment during inflammation through synergistic effects on endothelial activation. J. Immunol. 188, 6287–6299.

Ibiza, S., Alvarez, A., Romero, W., Barrachina, M.D., Esplugues, J.V., Calatayud, S., 2009. Gastrin induces the interaction between human mononuclear leukocytes and endothelial cells through the endothelial expression of P-selectin and VCAM-1. Am. J. Physiol.: Cell Physiol. 297, C1588–C1595.

Klimiuk, P.A., Sierakowski, S., Domyslawska, I., Fiedorczyk, M., Chwiecko, J., 2004. Reduction of soluble adhesion molecules (sICAM-1, sVCAM-1, and sE-selectin) and vascular endothelial growth factor levels in serum of rheumatoid arthritis patients following multiple intravenous infusions of infliximab. Arch. Immunol. Ther. Exp. (Warsz.) 52, 36–42.

Koutruba, N., Emer, J., Lebwohl, M., 2010. Review of ustekinumab, an interleukin-12 and interleukin-23 inhibitor used for the treatment of plaque psoriasis. Ther. Clin. Risk Manag. 6, 123–141.

Krieglstein, C.F., Granger, D.N., 2001. Adhesion molecules and their role in vascular disease. Am. J. Hypertens. 14, 44S–54S.

Ley, K., Laudanna, C., Cybulsky, M.I., Nourshargh, S., 2007. Getting to the site of inflammation: the leukocyte adhesion cascade updated. Nat. Rev. Immunol. 7, 678–689.

Libby, P., 2012. Inflammation in atherosclerosis. Arterioscler. Thromb. Vasc. Biol. 32, 2045–2051.

Lowes, M.A., Russell, C.B., Martin, D.A., Towne, J.E., Krueger, J.G., 2013. The IL-23/T17 pathogenic axis in psoriasis is amplified by keratinocyte responses. Trends Immunol. 34, 174–181.

Luu, N.T., Madden, J., Calder, P.C., Grimble, R.F., Shearman, C.P., Chan, T., Tull, S.P., Dastur, N., Rainger, G.E., Nash, G.B., 2007. Comparison of the pro-inflammatory

potential of monocytes from healthy adults and those with peripheral arterial disease using an in vitro culture model. Atherosclerosis 193, 259–268.
Maki-Petaja, K.M., Elkhawad, M., Cheriyan, J., Joshi, F.R., Ostor, A.J., Hall, F.C., Rudd, J. H., Wilkinson, I.B., 2012. Anti-tumor necrosis factor-alpha therapy reduces aortic inflammation and stiffness in patients with rheumatoid arthritis. Circulation 126, 2473–2480.
Mateo, T., Abu Nabah, Y.N., Abu, T.M., Mata, M., Cerda-Nicolas, M., Proudfoot, A.E., Stahl, R.A., Issekutz, A.C., Cortijo, J., Morcillo, E.J., Jose, P.J., Sanz, M.J., 2006. Angiotensin II-induced mononuclear leukocyte interactions with arteriolar and venular endothelium are mediated by the release of different CC chemokines. J. Immunol. 176, 5577–5586.
Montrucchio, G., Alloatti, G., Camussi, G., 2000. Role of platelet-activating factor in cardiovascular pathophysiology. Physiol. Rev. 80, 1669–1699.
Muller, W.A., 2009. Mechanisms of transendothelial migration of leukocytes. Circ. Res. 105, 223–230.
Nakada, M.T., Tam, S.H., Woulfe, D.S., Casper, K.A., Swerlick, R.A., Ghrayeb, J., 1998. Neutralization of TNF by the antibody cA2 reveals differential regulation of adhesion molecule expression on TNF-activated endothelial cells. Cell Adhes. Commun. 5, 491–503.
Nestorov, I., 2005. Clinical pharmacokinetics of TNF antagonists: how do they differ? Semin. Arthritis Rheum. 34, 12–18.
Nguyen, T., Wu, J.J., 2014. Relationship between tumor necrosis factor-alpha inhibitors and cardiovascular disease in psoriasis: a review. Perm. J. 18, 49–54.
Price, A., Lockhart, J.C., Ferrell, W.R., Gsell, W., McLean, S., Sturrock, R.D., 2007. Angiotensin II type 1 receptor as a novel therapeutic target in rheumatoid arthritis: in vivo analyses in rodent models of arthritis and ex vivo analyses in human inflammatory synovitis. Arthritis Rheum. 56, 441–447.
Ridker, P.M., Luscher, T.F., 2014. Anti-inflammatory therapies for cardiovascular disease. Eur. Heart J. 35, 1782–1791.
Rigby, W.F., 2007. Drug insight: different mechanisms of action of tumor necrosis factor antagonists-passive-aggressive behavior? Nat. Clin. Pract. Rheumatol. 3, 227–233.
Roubille, C., Richer, V., Starnino, T., McCourt, C., McFarlane, A., Fleming, P., Siu, S., Kraft, J., Lynde, C., Pope, J., Gulliver, W., Keeling, S., Dutz, J., Bessette, L., Bissonnette, R., Haraoui, B., 2015. The effects of tumour necrosis factor inhibitors, methotrexate, non-steroidal anti-inflammatory drugs and corticosteroids on cardiovascular events in rheumatoid arthritis, psoriasis and psoriatic arthritis: a systematic review and meta-analysis. Ann. Rheum. Dis. 74, 480–489.
Singh, T.P., Huettner, B., Koefeler, H., Mayer, G., Bambach, I., Wallbrecht, K., Schon, M.P., Wolf, P., 2011. Platelet-activating factor blockade inhibits the T-helper type 17 cell pathway and suppresses psoriasis-like skin disease in K5.hTGF-beta1 transgenic mice. Am. J. Pathol. 178, 699–708.
Spah, F., 2008. Inflammation in atherosclerosis and psoriasis: common pathogenic mechanisms and the potential for an integrated treatment approach. Br. J. Dermatol. 159 (Suppl. 2), 510–517.
Suna, S., Sakata, Y., Sato, H., Mizuno, H., Nakatani, D., Shimizu, M., Usami, M., Takashima, S., Takeda, H., Hori, M., 2008. Up-regulation of cell adhesion molecule genes in human endothelial cells stimulated by lymphotoxin alpha: DNA microarray analysis. J. Atheroscler. Thromb. 15, 160–165.
Suzuki, E., Mellins, E.D., Gershwin, M.E., Nestle, F.O., Adamopoulos, I.E., 2014. The IL-23/IL-17 axis in psoriatic arthritis. Autoimmun. Rev. 13, 496–502.
Tam, L.S., Kitas, G.D., Gonzalez-Gay, M.A., 2014. Can suppression of inflammation by anti-TNF prevent progression of subclinical atherosclerosis in inflammatory arthritis? Rheumatol.: Oxf. 53, 1108–1119.
Tracey, D., Klareskog, L., Sasso, E.H., Salfeld, J.G., Tak, P.P., 2008. Tumor necrosis factor antagonist mechanisms of action: a comprehensive review. Pharmacol. Ther. 117, 244–279.
Van, H.F., Vandenbroucke, R.E., Libert, C., 2011. Treatment of TNF mediated diseases by selective inhibition of soluble TNF or TNFR1. Cytokine Growth Factor Rev. 22, 311–319.
Victor, V.M., Rocha, M., Banuls, C., Alvarez, A., De Pablo, C., Sanchez-Serrano, M., Gomez, M., Hernandez-Mijares, A., 2011. Induction of oxidative stress and human leukocyte/endothelial cell interactions in polycystic ovary syndrome patients with insulin resistance. J. Clin. Endocrinol. Metab. 96, 3115–3122.
Westlake, S.L., Colebatch, A.N., Baird, J., Curzen, N., Kiely, P., Quinn, M., Choy, E., Ostor, A.J., Edwards, C.J., 2011. Tumour necrosis factor antagonists and the risk of cardiovascular disease in patients with rheumatoid arthritis: a systematic literature review. Rheumatol.: Oxf. 50, 518–531.
Yamagata, K., Tanaka, N., Matsufuji, H., Chino, M., 2012. Beta-carotene reverses the IL-1beta-mediated reduction in paraoxonase-1 expression via induction of the CaMKKII pathway in human endothelial cells. Microvasc. Res. 84, 297–305.
Zhang, F., Yu, W., Hargrove, J.L., Greenspan, P., Dean, R.G., Taylor, E.W., Hartle, D.K., 2002. Inhibition of TNF-alpha induced ICAM-1, VCAM-1 and E-selectin expression by selenium. Atherosclerosis 161, 381–386.
Zhang, X.W., Hedlund, G., Borgstrom, P., Arfors, K.E., Thorlacius, H., 2000. Linomide abolishes leukocyte adhesion and extravascular recruitment induced by tumor necrosis factor alpha in vivo. J. Leukoc. Biol. 68, 621–626.

ARTÍCULO 6

Chronical consumption of an inositol-enriched beverage ameliorates endothelial dysfunction and oxidative stress in type 2 diabetes

Hernández-Mijares A, Bañuls C, Rovira-Llopis S, Álvarez Á, **Orden S,** Rubio-Puchol O, Víctor VM, Rocha M.

Journal of Functional Foods 2015; 18: 598-607

Journal of Functional Foods 18 (2015) 598–607

Available online at www.sciencedirect.com

ScienceDirect

journal homepage: www.elsevier.com/locate/jff

Chronic consumption of an inositol-enriched beverage ameliorates endothelial dysfunction and oxidative stress in type 2 diabetes

Antonio Hernández-Mijares [a,b,c,d,*], Celia Bañuls [a,b,c], Susana Rovira-Llopis [a,b,c], Ángeles Álvarez [e,f], Samuel Orden [e,f], Olalla Rubio-Puchol [b], Víctor M. Víctor [a,b,c,e,g,*], Milagros Rocha [a,b,c,e,*]

[a] Foundation for the Promotion of Healthcare and Biomedical Research in the Valencian Community (FISABIO), Avda Cataluña 21, 46020 Valencia, Spain
[b] Service of Endocrinology, University Hospital Dr. Peset, Av Gaspar Aguilar 90, 46017 Valencia, Spain
[c] Institute of Health Research INCLIVA, Av Blasco Ibáñez 17, 46010 Valencia, Spain
[d] Department of Medicine, Faculty of Medicine, University of Valencia, Av Blasco Ibáñez 13, 46010 Valencia, Spain
[e] CIBER CB06/04/0071 Research Group, CIBER Hepatic and Digestive Diseases, University of Valencia, Av Blasco Ibáñez 13, 46010 Valencia, Spain
[f] Department of Pharmacology, Faculty of Medicine, University of Valencia, Av Blasco Ibáñez 13, 46010 Valencia, Spain
[g] Department of Physiology, Faculty of Medicine, University of Valencia, Av Blasco Ibáñez 13, 46010 Valencia, Spain

ARTICLE INFO

Article history:
Received 5 March 2015
Received in revised form 24 August 2015
Accepted 27 August 2015
Available online

Keywords:
Type 2 diabetes
Inositol
Inflammation
Endothelial function
Oxidative stress

ABSTRACT

The anti-diabetic properties of an inositol-enriched beverage (IEB) on the endothelial function and redox status in diabetic subjects were assessed. This was a 12-week, double-blind randomized controlled trial employing thirty-eight diabetic subjects that were divided into two intervention groups: one receiving an IEB and the other a sucrose-enriched beverage. Subjects consuming IEB exhibited a significant decrease in triacylglycerol (8.82%) and HbA1c (4.53%) levels. Continuous glucose monitoring revealed a significant net reduction of 2.51 and 7.11% during postprandial and overnight fasting periods after consumption of IEB, respectively. Moreover, IEB improved endothelial function by reducing P-selectin levels and leucocyte–endothelium interactions, as there was an increase in rolling velocity and a reduction in polymorphonuclear leucocyte adhesion and induced a significant diminution in the generation of ROS. The present results show that IEB supplementation induces a significant improvement in glycaemic control in diabetic subjects by improving endothelial function and intracellular redox status.

© 2015 Elsevier Ltd. All rights reserved.

Trial registration: This trial was registered on clinicaltrials.gov under study number NCT01754792.

* *Corresponding authors.* FISABIO-University Hospital Dr. Peset, Av. Gaspar Aguilar 90, 46017 Valencia, Spain. Tel.: +34 961622492; fax: +34 961622492.
E-mail addresses: hernandez_antmij@gva.es (A. Hernández-Mijares); victor.victor@uv.es (V.M. Víctor); milagros.rocha@uv.es (M. Rocha).

Abbreviations: Apo, apolipoprotein; BMI, body mass index; CGMS, control glucose monitoring system; CMFDA, 5-chloromethyl fluorescein diacetate; CVD, cardiovascular disease; DCFH-DA, 2′,7′-dichlorodihydrofluorescein diacetate; DPBS, Dulbecco's phosphate buffered saline; EGM-2, endothelial cell growth medium; GSH, reduced glutathione; HbA1c, glycated haemoglobin; HBSS, Hank's balanced salt solution; HDLc, high density lipoprotein cholesterol; HOMA-IR, homeostasis model assessment of insulin resistance; HSA, human serum albumin; HUVEC, Human umbilical vein endothelial cells; ICAM-1, intercellular adhesion molecule-1; IEB, Inositol-enriched beverage; IL-6, interleukin 6; LDLc, low density lipoprotein cholesterol; PAF, platelet activating factor; PMN, polymorphonuclear leucocytes; ROS, reactive oxygen species; SB, sucrose-sweetened beverage; TG, triacylglycerols; TNF-α, tumoural necrosis factor alpha; VCAM-1, vascular adhesion molecule-1

http://dx.doi.org/10.1016/j.jff.2015.08.025
1756-4646/© 2015 Elsevier Ltd. All rights reserved.

Hernández-Mijares et al., 2015

1. Introduction

Atherosclerosis and cardiovascular diseases (CVDs) are a major cause of mortality among diabetic patients. In recent years, accumulating evidence has demonstrated that endothelial function is impaired (Johnstone et al., 1993) and is an independent predictor for future cardiovascular events in patients with type 2 diabetes (Beckman, Creager, & Libby, 2002). Hyperglycaemia and hyperlipidaemia are risk factors for endothelial impairment and can induce endothelial dysfunction (Brownlee, 2001; Steinberg et al., 1997). In fact, the risk of vascular complications is strongly associated with previous hyperglycaemia in type 2 diabetic patients, in whom the reduction of glycated haemoglobin (HbA1c) reduces the risk of complications (Stratton et al., 2000).

Endothelial damage is heralded by the movement and accumulation of leucocytes in the vessel wall. These processes are mediated by interaction between the adhesion molecules expressed on leucocytes and/or endothelial cells. Different cellular adhesion molecules have been implicated in atherogenesis, including vascular cell adhesion molecule-1 (VCAM-1), intercellular adhesion molecule-1 (ICAM-1) and selectins (Jude, Douglas, Anderson, Young, & Boulton, 2002). A known underlying mechanism of endothelial dysfunction is the enhanced generation of endothelial mitochondrial superoxide (Brownlee, 2001). We have previously shown that oxidative stress occurs in polymorphonuclear leucocytes (PMNs) of type 2 diabetic patients and is related to an impairment of mitochondrial function and enhanced leucocyte–endothelium interaction (Hernández-Mijares et al., 2011; Rovira-Llopis et al., 2013).

Evidence indicates the great potential of herbal constituents for the treatment of type 2 diabetes, with extracts of numerous plants having been reported to reduce blood glucose levels. For example, in traditional medicine, carob pods have been used as hypoglycaemic agent for treating diabetes (Yaniv, Dafni, Friedman, & Palevitch, 1987). Recently, we have published data showing that the acute consumption of a carob pod extract containing bioactive carbohydrates (16.0%), pinitol (3-O-methyl-D-chiro-inositol) (11.04%) and other minor compounds (myoinositol and D-chiro-inositol (1.06%)), and soluble fibre (3.90%) influences parameters of whole-body glucose tolerance and insulin sensitivity in healthy subjects (Hernández-Mijares et al., 2013). These bioactive carbohydrates, most of which are polyols, appear to be mediators of the insulin signalling pathway and to be involved in glycosylphosphatidyl-inositol protein anchors (Larner et al., 1998; Larner, Brautigan, & Thorner, 2010).

Pinitol, D-chiro-inositol and myoinositol are reported to act as insulin mimetics to improve hyperglycaemia in both rodents and humans (Bates, Jones, & Bailey, 2000; Cheang et al., 2008; Dang, Mukai, Yoshida, & Ashida, 2010; Kim et al., 2005, 2007, 2012). However, there is little evidence that inositols improve endothelial function and intracellular redox status (Nascimento et al., 2006; Sivakumar, Palsamy, & Subramanian, 2010a, 2010b; Sivakumar & Subramanian, 2009), and even less from studies in humans. Therefore, the primary aim of the present study was to assess the anti-diabetic properties of a carob pod extract enriched in inositol derivatives on glycaemic control. A secondary aim was to investigate how this extract influences the inflammatory state and/or endothelial function and/or intracellular redox status of type 2 diabetic subjects.

2. Subjects and methods

2.1. Subjects

Forty type 2 diabetic patients were recruited at the Outpatient's Department of the Endocrinology Service of the University Hospital Dr. Peset between March 2012 and December 2013. The inclusion criteria for all subjects were age range of 40–73 years, body mass index of 20–40 kg/m^2 and clinically normal kidney, liver and heart functions, protein status and haematological profile. Type 2 diabetes was defined according to the American Diabetes Association guidelines (American Diabetes Association, 2012): fasting glycaemia ≥126 mg/dl on at least two occasions, or glycaemia 2 h after 75 g glucose oral load of ≥200 mg/dl, or HbA1c ≥ 6.5%. Exclusion criteria were type 1 diabetes, malignant neoplasm, triacylglycerols (TG) >400 mg/dl, macrovascular complications, patients with poorly controlled type 2 diabetes (HbA1c ≥ 8%) or who were being treated with insulin or intestinal disaccharidase inhibitors.

The study was conducted according to the guidelines laid down in the Declaration of Helsinki, and all procedures involving human subjects were approved by the hospital's Ethics Committee. Written informed consent was obtained from all patients. Two subjects dropped out of the study for personal reasons, because of an inability or unwillingness to comply with the protocol.

2.2. Study design

This study was a randomized, double-blind, controlled study. Before dietary therapy was initiated, subjects underwent a 1-month run-up period during which they followed a normocaloric diet in order to stabilize dietary patterns prior to intervention. After this adaptation period, subjects were randomly assigned to two groups which received either an inositol-enriched beverage (IEB) (n = 19) or a matching beverage based on sucrose (SB) (n = 19) for 12 weeks. We have recently reported that a maximum bloodstream concentration of pinitol is reached 3–4 hours after consuming a single dose of the IEB (Hernández-Mijares et al., 2013). Therefore, subjects were recommended to consume the beverage twice a day, during their mid-morning and mid-afternoon snacks, in order to ensure the maximum concentration of pinitol at main mealtimes. IEB consists of a complex mixture of naturally occurring soluble carbohydrates including mono-, di-, oligo-saccharides and polyols – mainly pinitol myoinositol plus D-chiro-inositol – soluble fibre and minor compounds (in trace contents: organic acids, minerals, amino-acids) derived from carob pods. The SB contained very similar amounts of non-polyol soluble sucrose-based carbohydrates, macronutrient composition and total number of calories to the IEB, but obviously excluding inositols. Sugars and sugar-alcohols were determined by ion exchange chromatography in a Dionex IC System 3000 (Thermo Fisher Scientific Inc., Sunnyvale, CA, USA) by an External & Accredited Laboratory (Global Analytical Services Heidelberg,

Table 1 – Nutritional composition per day (in 500 ml) of the main soluble carbohydrates contained in the inositol-enriched beverage (IEB) and the sucrose-sweetened beverage (SB) administered in the study.

	IEB	SB
Pinitol (g)	4.00	–
Myoinositol + D-chiro-inositol (g)	0.45	–
Other polyols (g)	0.13	–
Sugars (g)	34.90	42.5
Glucose	6.23	–
Fructose	4.83	–
Sucrose	23.26	42.5
Other sugars	0.58	–
Oligosaccharides (g)	0.05	–
Soluble fibre (g)	1.65	–
Arabinoxylan	1.31	
Other soluble fibres	0.34	
Total carbohydrates (g)	41.18	42.50
Total available carbohydrates (g)	39.12	42.50

Inositol-enriched beverage (IEB) or sucrose-sweetened beverage (SB) was consumed twice daily (250 ml on each occasion), during mid-morning and mid-afternoon snacks.

Eppelheim, Germany). In addition to this, total fibre and soluble fibre were determined based upon the principles of AOAC 2010 Official Methods 985.29 and 993.19, respectively. The nutritional composition of the IEB with respect to SB is provided in Table 1. The IEB (prepared with the commercial natural food ingredient Fruit Up®) and SB (prepared with sucrose syrup) were produced by Wild-Valencia SAU (Spain) and prepared as follows: 123.0 g of Fruit Up® 70°Brix (IEB) and 126.7 g of liquid sucrose syrup 67°Brix (SB) per litre. In addition, both drinks contained 2.3 g per litre of citric acid monohydrate (E-330), 1.3 g per litre of sodium citrate dehydrate (E-331), 0.35 g per litre of black carrot colour extract (natural colour E-163), 0.5 g per litre of strawberry flavouring (natural flavour) and 0.2 g per litre of potassium sorbate (E-202). The mixture was packaged in cans of 250 ml. Each can contained 2.29 g of inositols (2.00 g of pinitol, 0.23g of myoinositols plus D-chiro-inositol and 0.06 g of other polyols).

Aside from this, they were encouraged to follow a normocaloric diet and their normal pattern of activity throughout the period of the trial. Depending on daily caloric expenditure, an average daily energy intake of 7118–9630 kJ (1700–2300 kcal) was recommended as follows: 15–20% protein, 50–55% carbohydrate and 28–33% fat. In reference to type of carbohydrate, patients were recommended to eat vegetables, fruits and whole grains, and to avoid foods naturally enriched in inositols, such as legumes. Diets were determined taking into account that sugars (mono- and disaccharides) were included within the total amount of carbohydrate and should not be higher than 20% of the total caloric content of carbohydrates. Thus, the drinks under assay provided roughly 15% of this 20 and 5% left were provided by fruits and dairy products (skimmed milk or yoghurts). Adherence to the diet was monitored by means of 3-day food records, which were designed to provide an accurate description of daily diet (compiled on two weekdays and one day at the weekend). The information contained in the questionnaire was analysed by software NutriBer v1.1.3 (FUNIBER, Barcelona, Spain), which estimates average daily intake of calories, carbohydrate, protein, fat and cholesterol. Food records were obtained before the adaptation period, at baseline, at 6 weeks and at the end of the study (12 weeks).

Anthropometrical parameters were evaluated as follows: weight was determined using electronic scales with an approximation of 0.1 kg; height was measured with a stadiometer with an approximation of 0.5 cm; BMI was calculated by dividing the subject's weight in kilograms by the square of his/her height in metres; blood pressure was measured twice consecutively using a sphygmomanometer.

2.3. *Blood sampling*

Venous blood samples were collected from patients at 8–10 am after 12 h overnight fasting at baseline (t = 0) and at the end of the study (t = 12 weeks). Serum and plasma were obtained after centrifugation at 2000 *g* for 15 min at 4 °C. Freshly separated samples were employed for determination of lipid profile and hydrocarbonated metabolism parameters, and the remaining aliquots were stored at −80 °C for subsequent measurement of inflammatory parameters and adhesion molecules.

2.4. *Biochemical determinations*

Glucose concentrations were measured with a Beckman LX-20 autoanalyzer (Beckman Coulter, La Brea, CA, USA) by means of enzymatic assay. The intraseries coefficient of variation was <3.5% for all determinations. Insulin was measured by an enzymatic luminescence technique. Insulin resistance was calculated by homeostasis model assessment (HOMA-IR = (fasting insulin (μU/ml) × fasting glucose (mg/dl))/405).

Total cholesterol and triacylglycerols were measured by means of enzymatic assays, and HDLc concentrations were recorded with a Beckman LX-20 autoanalyzer (Beckman Coulter) using a direct method. The intraserial variation coefficient was <3.5% for all determinations. LDLc concentration was calculated using the method of Friedewald. Apolipoprotein (Apo) AI and B were determined by immunonephelometry (Dade Behring BNII, Marburg, Germany) with an intra-assay variation coefficient of <5.5%.

2.5. *Continuous glucose monitoring system*

Blood glucose levels were measured in 8 subjects from each group using "Dexcom SEVEN Plus" (Dexcom, Inc., San Diego, CA, USA), a CGMS that records glucose levels every 5 minutes. In this way, a total of 288 blood glucose readings were recorded every 24 hours over a 3-day period at baseline and at the end of the study. To do this, the sensor of the CGMS was inserted under the skin of the patient's abdominal region at 10:00 am the day before the study and removed at 10:00 am on the third day of the study. Each patient was supplied with a glucometer (BG Star, Sanofi-Aventis, S.A. Barcelona, Spain), which uses the glucose oxidase principle for measuring capillary blood glucose, and was instructed to measure glucose levels before meals and snacks and to record the values in the CGMS for internal calibration. During this period, subjects

adhered to a specific diet containing 2000 kcal, of which 15.5% was protein, 56.0% was carbohydrate and 28.5% was fat.

2.6. Endothelial and inflammatory parameters

2.6.1. Leucocyte isolation

Human PMNs were isolated from citrated blood samples and incubated with dextran (3%) for 45 min. The supernatant was released over Ficoll-Hypaque and centrifuged at 250 *g* for 25 min. The pellet was resuspended in lysis buffer, and, after centrifugation at room temperature (100 *g*, 5 min), PMNs were counted by a ScepterTM 2.0 Cell Counter (Millipore Corporation, Billerica, MA, USA), and were then washed and resuspended in Hank's buffered salt solution (HBSS).

2.6.2. Human umbilical vein endothelial cell culture

Human umbilical vein endothelial cells (HUVEC) were harvested from recently obtained umbilical cords by collagenase treatment. In short, umbilical cord veins were rinsed of blood products with warm PBS, after which the vein was filled with collagenase (1 mg/ml) at 37 °C for 17 min. The cords were then gently massaged to ensure detachment of endothelial cells from the vessel wall. The digest was collected, centrifuged and pelleted. The pellet was resuspended in endothelial cell growth medium (EGM-2) and cells were cultured in T25 culture flasks until confluence was reached. Primary cultures were then detached with trypsin and transferred into culture dishes. Passage 1 from these primary cultures was subsequently employed. For adhesion studies, HUVEC were cultured on fibronectin (5 mg/ml)-coated 25-mm plastic coverslips until confluent (~48 h).

2.6.3. Adhesion assay under flow conditions

The parallel plate flow chamber in-vitro model has been described in detail previously (De Pablo et al., 2010). For adhesion assays, coverslips containing confluent HUVEC monolayers were inserted into a circular recess in the bottom plate of the flow chamber (maintained at 37 °C), where a portion (5 × 25 mm) of the monolayer was exposed to the flow. The entire chamber was mounted on an inverted microscope (Nikon Eclipse TE 2000-S, Amstelveen, The Netherlands) connected to a video camera (Sony Exware HAD, Koeln, Germany). Experiments were conducted using a 40× objective lens. PMNs were resuspended in Dulbecco's Phosphate-Buffered Saline (DPBS) containing 20×10^{-3} mol/l HEPES and 0.1% HSA at 1×10^{6} cells/ml, and were drawn across the HUVEC monolayer at a controlled flow rate of 0.36 ml/min (estimated shear stress of 0.7 dyne/cm^2). A circular glass window in the top plate of the chamber allowed microscopic examination of the monolayer exposed to the flow in real time. Images in a single field of view were recorded over a 5-min period during which leucocyte parameters were determined. The velocity of 20 consecutive leucocytes was determined by measuring the time required to travel a distance of 100 μm. Leucocyte rolling flux was calculated by counting the number of leucocytes rolling over 100 μm^2 of the endothelial monolayer during a 1-min period. Leucocyte adhesion was determined by counting the number of leucocytes that maintained stable contact with the monolayer for 30 s. Tumoural necrosis factor (TNF-α, 10 ng/ml, 4 h) and platelet activating factor (PAF, 1 μmol/l, 1 h) were used as positive controls for HUVEC and leucocytes, respectively.

Serum levels of proinflammatory cytokines – IL-6 and TNF-α – and soluble adhesion molecules VCAM-1, ICAM-1 and P-selectin were analysed with a Luminex 200 flow analyser system (Austin, TX, USA).

2.7. Oxidative stress parameters

Total ROS production and GSH content were assessed by fluorimetry using a fluorescence microscope (IX81; Olympus) coupled with the static cytometry software "ScanR" version 2.03.2 (Olympus). PMNs from each subject were seeded in 48-well plates and incubated (30 min) with the fluorescent probe: 2′,7′-dichlorodihydrofluorescein diacetate (DCFH-DA, 5×10^{-6} mol/l) and 5-chloromethyl fluorescein diacetate (CMFDA, 2.5×10^{-6} mol/l) for total ROS and GSH content, respectively. Experiments were performed in triplicate and 16 images per well were recorded and analysed.

2.8. Statistical analyses

Our sample consisted of 19 subjects per group in order to achieve 80% statistical power and, thus, detect differences between the two paired groups in values of the primary efficacy criterion (HbA1c variation) equal to or greater than 0.30%, assuming a common standard deviation of 0.45%.

Statistical analysis was carried out with the statistics program SPSS version 17.0. Data are expressed as mean and standard deviation (SD) in tables and standard error of the mean (SEM) in figures. Differences between groups were analysed by an unpaired or paired Student's t-test and Mann–Whitney U test or Wilcoxon test for parametric or non-parametric data, respectively. The Chi-Square test was employed to compare proportions between the subject groups. All tests used a confidence interval of 95% and differences were considered significant when $p < 0.05$.

3. Results

3.1. Patients, anthropometric parameters and biochemical determinations

The present study analysed a total of 38 type 2 diabetic patients – 19 men and 19 women – with a mean age of 60.0 ± 7.3 years and whose diabetes had been diagnosed for 5.2 ± 3.3 years. Men and women were distributed similarly between the two intervention groups. The disease was well controlled by oral antidiabetic medication in all the patients, and no differences were detected between the SB and IEB intervention groups with respect to treatment with metformin (100% vs 89.5%, $p = 0.146$) and DPP4 inhibitors (26.3% vs 31.6%, $p = 0.721$) or hypolipidaemic drugs such as statins (63.2% vs 68.4%, $p = 0.732$) or fibrate (15.8% vs 21.1%, $p = 0.676$), respectively. Subjects receiving the IEB showed a significant decrease in BMI (Table 2) despite their appropriate and not changing caloric intake during the course of the experimental period (Table 3). However, no significant differences were observed in terms of fasting lipid

Table 2 – Anthropometric and fasting metabolic parameters in type 2 diabetic subjects at baseline and after 12 weeks following a normocaloric diet plus sucrose-sweetened beverage (SB) or inositol-enriched beverage (IEB).

	Group	Baseline	12 weeks
Male/Female (n)	SB	10/9	–
	IEB	9/10	–
Duration of diabetes (years)	SB	5.8 ± 3.2	
	IEB	4.5 ± 3.4	
Age (years)	SB	61.2 ± 7.6	–
	IEB	58.8 ± 7.0	–
BMI (kg/m²)	SB	31.5 ± 5.0	31.5 ± 5.3
	IEB	32.2 ± 5.2	31.7 ± 5.0*
Systolic BP (mmHg)	SB	140 ± 12	137 ± 12
	IEB	133 ± 12	130 ± 12
Diastolic BP (mmHg)	SB	83 ± 8	83 ± 8
	IEB	83 ± 8	80 ± 8
Glucose (mg/dl)	SB	125.5 ± 23.01	127.9 ± 28.5
	IEB	120.1 ± 26.6	120.5 ± 27.0
HbA1c (%)	SB	6.19 ± 0.42	6.10 ± 0.47
	IEB	6.52 ± 0.85	6.22 ± 0.77***
Insulin (μIU/ml)	SB	14.4 ± 6.4	13.6 ± 8.1
	IEB	13.0 ± 5.6	12.0 ± 5.9
HOMA-IR index	SB	4.48 ± 2.22	4.21 ± 2.66
	IEB	4.31 ± 2.56	3.78 ± 1.93
Total cholesterol (mg/dl)	SB	172 ± 32	170 ± 30
	IEB	179 ± 34	181 ± 41
LDLc (mg/dl)	SB	98.7 ± 24.7	97.1 ± 22.5
	IEB	105.1 ± 27.6	109.6 ± 36.1
HDLc (mg/dl)	SB	46.7 ± 13.3	46.4 ± 14.6
	IEB	44.6 ± 10.1	45.1 ± 11.0
Triacylglycerol (mg/dl)	SB	112 (92,158)	107 (87,189)
	IEB	144 (102,172)	124 (102,142)*
Apo AI (mg/dl)	SB	145 ± 27	153 ± 39
	IEB	148 ± 18	148 ± 21
Apo B (mg/dl)	SB	87.6 ± 27.2	87.2 ± 2.9
	IEB	93.2 ± 20.6	94.6 ± 26.5
hsCRP (mg/l)	SB	3.21 ± 2.53	3.50 ± 3.15
	IEB	4.00 ± 3.60	4.27 ± 3.29
IL-6 (pg/ml)	SB	3.33 ± 2.32	4.81 ± 4.09*
	IEB	3.82 ± 3.54	3.95 ± 3.45
TNF-α (pg/ml)	SB	5.05 ± 1.52	6.11 ± 3.49
	IEB	5.55 ± 2.49	5.35 ± 1.96

Data are expressed as mean ± SD for parametric data or as median (25th and 75th percentiles) for non-parametric data. *$p < 0.05$, ***$p < 0.001$ when compared by a paired Student's t-test for parametric or Wilcoxon test for non-parametric data, respectively. No significant differences were found at baseline between SB and IEB when compared by an unpaired Student's t-test or Mann–Whitney U test. The Chi-Square test was used to compare proportions between groups.

BP, systolic blood pressure; DPP4: Dipeptidyl peptidase-4, HbA1c: glycated haemoglobin, HOMA-IR: homeostasis model assessment, hsCRP, high-sensitivity C-reactive protein; IL-6, interleukin 6, TNF-α, tumour necrosis factor alpha.

parameters, with the exception of a reduction in triacylglycerol levels after 12 weeks of IEB consumption ($p = 0.012$; Table 2). Surprisingly, although no change was observed in fasting hydrocarbonated metabolism parameters, the IEB induced an improvement in HbA1c over the 12-week intervention period (Table 2), with a significant percentage of change detected with respect to the SB group (–4.5% vs –1.6%, respectively $p = 0.028$) (Fig. 1A).

Table 3 – Nutrient composition of a normocaloric diet for diabetic subjects receiving sucrose-sweetened beverage (SB) or inositol-enriched beverage (IEB).

	Group	Baseline	12 weeks
Carbohydrates (%)	SB	50.3 ± 0.7	50.9 ± 1.0
	IEB	50.5 ± 0.8	50.9 ± 0.7
Protein (%)	SB	18.2 ± 1.1	17.3 ± 0.8
	IEB	17.7 ± 1.1	17.4 ± 1.0
Fat (%)	SB	31.6 ± 0.8	31.8 ± 0.9
	IEB	31.8 ± 1.0	31.7 ± 0.7
Saturated	SB	7.5 ± 0.8	7.9 ± 1.2
	IEB	8.0 ± 2.0	7.3 ± 1.0
Polyunsaturated	SB	4.9 ± 1.4	4.4 ± 1.1
	IEB	4.6 ± 1.3	4.5 ± 1.1
Monounsaturated	SB	19.2 ± 1.3	19.5 ± 1.5
	IEB	19.1 ± 2.3	19.9 ± 1.4
Cholesterol (mg)	SB	164 ± 51	164 ± 37
	IEB	158 ± 33	174 ± 48
kcal	SB	1944 ± 239	1962 ± 231
	IEB	1880 ± 208	1933 ± 227

Data are expressed as mean ± SD. No significant differences were detected between groups ($p < 0.05$) when compared by a paired Student's t-test. Average daily nutrient intake as a percentage of total dietary caloric intake; 3-day food records (data collected on two weekdays and one day at the weekend). Food intake was converted into energy and nutrients with the help of the software Nutrîber v1.1.3 (FUNIBER, Barcelona, Spain).

3.2. *Continuous glucose monitoring system*

Postprandial glycaemia was assessed by CGMS over a 3 h period following breakfast, lunch and dinner, both at the beginning and end of the study. Chronic consumption of the IEB markedly reduced postprandial glycaemia as a whole with respect to values in subjects consuming the SB. In fact, after postprandial periods, a net decrease in glucose levels of –2.97% and –0.46% was detected in the inositol-enriched group and SB group, respectively (Fig. 1B). In addition, chronic consumption of IEB reduced glycaemia over a 6-h fasting nocturnal period, with a reduction of mean nocturnal glucose levels from 107.3 ± 5.6 at the beginning of the experimental period to 102.1 ± 3.9 mg/dl at the end ($p < 0.001$). However, subjects receiving the SB showed a significant increase from 111.4 ± 2.5 at the beginning of the intervention to 115.9 ± 9.6 mg/dl ($p < 0.001$) at the end. Consequently, a net decrease of 7.11% was detected among subjects receiving IEB (Fig. 1C).

3.3. *Endothelial and inflammation parameters*

Inflammatory markers were enhanced after chronic consumption of the SB; a significant increase in IL-6 ($p < 0.05$) and a trend rise in TNF-α levels were detected ($p = 0.077$) (Table 2). These alterations indicated an underlying inflammatory state. In line with this, soluble adhesion molecule levels showed a moderate rise after consumption of the SB, which was evident in P-selectin (Fig. 2A) and ICAM-1 values (Fig. 2B) ($p = 0.061$ and $p = 0.055$, respectively). In contrast, the IEB prevented this increase in inflammatory markers (Table 2) and induced a significant decrease in P-selectin levels (Fig. 2A) ($p = 0.040$), with

Hernández-Mijares et al., 2015

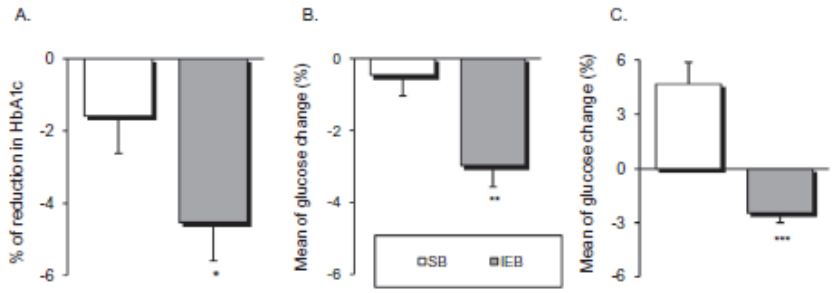

Fig. 1 – Glycaemic control in type 2 diabetic patients after consuming sucrose-sweetened beverage (SB) or inositol-enriched beverage (IEB) for 12 weeks. A: Percentage of reduction in HbA1c. B: Mean of glucose change (percentage) after main meals (breakfast, lunch and dinner). C: Mean of glucose change (percentage) after overnight fasting. Data are represented as mean ± standard error. *p < 0.05, **p < 0.01 and ***p < 0.001 when compared by an unpaired Student's t-test. HbA1c: glycated haemoglobin.

a significant percentage of change detected between IEB and SB (–9.6% vs 33.3%, respectively p = 0.014). This later was associated with an improvement in adhesion assay under flow conditions; i.e. an increase in rolling velocity (Fig. 2D) and a reduction in PMN adhesion (Fig. 2F). Comparison of percentage of change from baseline for each of the intervention groups revealed a net increase of 32.7% (p > 0.05) in rolling velocity and a significant reduction of 69.0% (p = 0.039) in subjects consuming IEB. These data suggest that inositols prevent the inflammation induced by chronic consumption of a SB and improve endothelial function in well-controlled type 2 diabetic subjects.

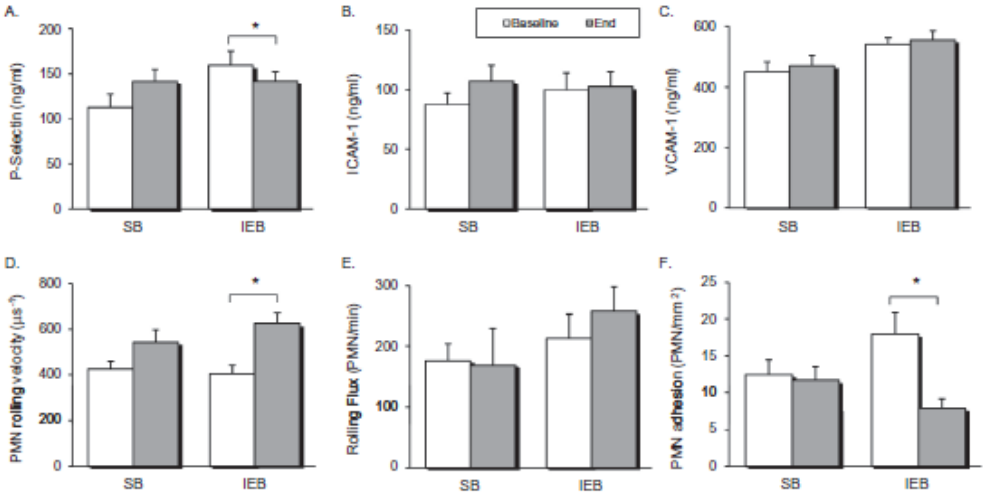

Fig. 2 – Endothelial function determined by cellular adhesion molecules and leucocyte–endothelial interactions in type 2 diabetic patients after consuming sucrose-sweetened beverage (SB) or inositol-enriched beverage (IEB) for 12 weeks. Levels of cellular adhesion molecules represented by P-selectin (A), ICAM-1 (B) and VCAM-1 (C) at the beginning of treatment (white bars) and at the end of the experimental period (solid bars). Leucocyte–endothelial interactions were evaluated by leucocyte rolling velocity (D), leucocyte rolling flux (E) and leucocyte adhesion (F), at the beginning of treatment (white bars) and at the end of the experimental period (solid bars). Data are represented as mean ± standard error of 7–8 patients. *p < 0.05 when compared by a paired Student's t-test. No significant differences were found at end-point between SB and IEB when compared by an unpaired Student's t-test. ICAM: intercellular adhesion molecule, VCAM: vascular cell adhesion molecule, PMN: polymorphonuclear leucocytes.

3.4. Oxidative stress parameters

To investigate whether inositols improve endothelial function by reducing oxidative stress, we employed static cytometry to determine total ROS production and glutathione levels in PMNs. As shown in Fig. 3, chronic consumption of IEB induced a reduction in total ROS ($p = 0.002$) (Fig. 3A and B), with a significant percentage of change detected between IEB and SB (−35.6% vs 1.7%, respectively $p = 0.036$), whereas glutathione levels were unchanged throughout the experimental period in both intervention groups (Fig. 3C and D). Therefore, inositols themselves would appear to be effective scavengers of ROS.

3.5. Safety

No adverse reactions – hypoglycaemic episodes, diarrhoea, constipation, nausea, belching, flatulence, indigestion and bloating – were observed in subjects consuming the IEB. Only two diabetic patients reported "heaviness" after rapid intake of the preparation, which was solved by a slower ingestion, although this effect could not be correlated with the consumption

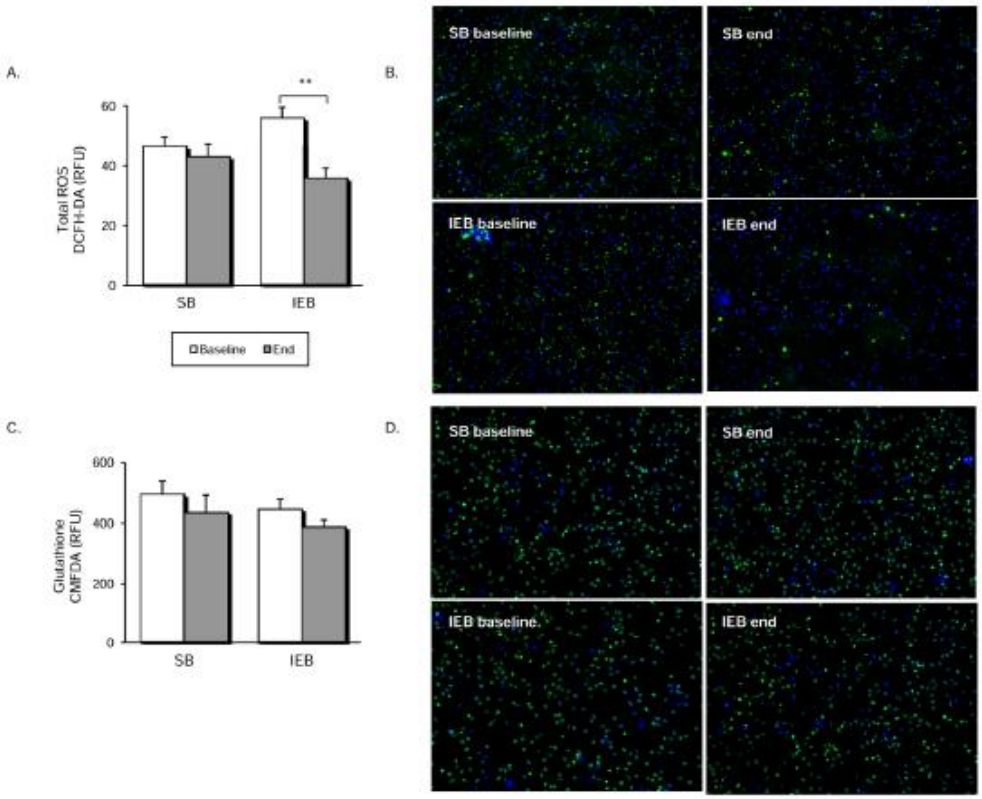

Fig. 3 – Oxidative stress parameters determined by total ROS production and intracellular glutathione in type 2 diabetic patients after consuming sucrose-sweetened beverage (SB) or inositol-enriched beverage (IEB) for 12 weeks. Mean of fluorescence intensity of DCFH-DA (A) and CMFDA (B) at the beginning of treatment (white bars) and at the end of the experimental period (solid bars). Representative fluorescent images depicting DCFH-DA and CMFDA intensities (green signals) are shown in panels C and D, respectively. The nuclei were visualized by using the specific nuclear stain Hoechst 33342 (blue). Data are represented as mean ± standard error. "$p < 0.01$ when compared by a paired Student's t-test. No significant differences were found at end-point between SB and IEB when compared by an unpaired Student's t-test. DCFH-DA: 2′,7′-dichlorodihydrofluorescein diacetate, CMFDA: 5-chloromethyl fluorescein diacetate, RFU: relative fluorescent units.

(For interpretation of the references to colour in this figure legend, the reader is referred to the web version of this article.)

of IEB, since one of the patients in question ingested the SB and the other patient ingested the IEB.

4. Discussion

The results of the present study demonstrate that chronic consumption of an inositol-enriched beverage induces a moderate reduction in triacylglycerol levels and improves metabolic control in well-controlled type 2 diabetic patients. In addition, we have observed an anti-inflammatory effect of inositol, as it prevented the enhancement of inflammatory mediators associated with consumption of a sucrose-enriched beverage and improved endothelial function by reducing soluble P-selectin, which was accompanied by an increase in rolling velocity and a reduction in cellular adhesion of PMNs. The underlying mechanism involved in this response could be mediated by a reduction in the generation of ROS.

The importance of tight glycaemic control in the prevention of complications produced by diabetes has been demonstrated in several trials, including the Diabetes Control and Complications Trial (The Diabetes Control and Complications Trial Research Group, 1993) and The United Kingdom Prospective Diabetes Study (Stratton et al., 2000). The CGMS is one of the first commercially available devices to monitor glucose levels on a continuous basis for up to 72 hours. Although the accuracy of this sensor has been questioned and discrepancies are occasionally seen between interstitial tissue and blood glucose levels, it is generally considered a reliable method for assessing patterns of glycaemic excursions (McDonnell, Donath, Vidmar, Werther, & Cameron, 2005). In the present study, we demonstrate that chronic consumption of IEB, which contains bioactive carbohydrates – mainly pinitol enriched with myo-inositol and D-chiro-inositol, improves the metabolic control of type 2 diabetic patients, since HbA1c levels were significantly reduced and glycaemia was decreased after meals and during fasting nocturnal period in our subjects. These results are in accordance with those of previous studies (Kim et al., 2005, 2007), but contrast with those of others (Davis et al., 2000). We should point out that our patients were well-controlled by oral antidiabetic drugs at initiation of the trial; consequently, the effect of inositols on glycaemic control would be expected to be moderate in comparison with that seen in studies in which type 2 diabetic patients were uncontrolled or who were not responding adequately to hypoglycaemic drugs (Kim et al., 2005, 2007, 2012). Davis et al. (2000) reported that insulin sensitivity did not increase in obese individuals with mild type 2 diabetes after pinitol treatment, although the dose administered was lower and the treatment period was shorter than that of our study. These differences could explain the discrepancies between Davis's study and ours.

Although the exact mechanism by which carob extract lowers glucose is unclear, it may involve metabolism of inositol phosphoglycan and enhanced action of insulin on peripheral target tissues, as carob pods are enriched in inositol derivatives. Myo-inositol and D-chiro-Inositol have been shown to increase the action of insulin in patients with insulin resistance and reduced triacylglycerol concentrations (Giordano et al., 2011; Minozzi, Nordio, & Pajalich, 2013; Nestler, Jakubowicz, Reamer, Gunn, & Allan, 1999), whereas reduction of triacylglycerols after pinitol treatment has been reported only in animal models of diabetes (Geethan & Prince, 2008; Nascimento et al., 2006). These past reports are in accordance with the reduction in fasting triacylglycerol concentrations we have observed in the present study. Its action could be similar to that of thiazolidinediones, which have been shown to improve insulin-stimulated glucose uptake and reduce triacylglycerol and free fatty acids (Kumar et al., 1996; Saltiel & Olefsky, 1996).

Oxidative stress has been identified as a major pathogenic mechanism in the development of atherosclerosis, and hyperglycaemia and hyperlipidaemia are risk factors for endothelial impairment and can induce endothelial dysfunction (Brownlee, 2001; Steinberg et al., 1997). Hyperglycaemia per se induces increased production of ROS derived from mitochondrial respiration of endothelial cells; in this sense, mitochondrial dysfunction plays a key role in the development of atherogenesis (Victor et al., 2009). There is also evidence that triacylglycerol accumulation in macrophages activates production of ROS (Rosenblat, Volkova, Paland, & Aviram, 2012), and that triacylglycerol-rich lipoprotein lipolysis elicits proinflammatory responses, thereby inducing TNFα, adhesion molecule expression and ROS production in human endothelial cells (Wang et al., 2009; Wang, Sapuri-Butti, Aung, Parikh, & Rutledge, 2008). As far as we know, this is the first study to address the effect of an IEB on oxidative stress and endothelial function in type 2 diabetic patients. To date, the effects of inositols on proinflammatory cytokines, endothelial function and oxidative stress have been evaluated only in diabetic rats and rabbits, in which they were found to have mostly beneficial protective effects (Kim et al., 2005; Nascimento et al., 2006; Sivakumar et al., 2010a, 2010b). Our results show that IEB has an anti-inflammatory effect by preventing the enhancement in inflammatory mediators associated with SB. This seems to occur through a reduction of IL-6 and TNFα and improvement of endothelial function through a reduction of soluble P-selectin, which is accompanied by an increase in rolling velocity of PMNs and a decrease in cellular adhesion of PMNs. It has been shown that pinitol acts as an antioxidant to protect against hepatocyte and renal injury by attenuating hyperglycaemia-mediated pro-inflammatory cytokines and oxidative stress in streptozotocin-induced diabetic rats (Sivakumar et al., 2010a, 2010b). In addition, inositols have been shown to prevent and reverse endothelial dysfunction in diabetic rodent vasculature, both metabolically and by scavenging superoxide (Nascimento et al., 2006), which is in accordance with the reduction in total ROS and the improvement in endothelial function we report in the present study. Thus, a potential mechanism through which inositols improve endothelial dysfunction is a decrease in ROS; in this way, they would act as an antioxidant per se, since glutathione levels remain unaltered throughout the intervention.

One of this study's strong points is its randomized, double-blind, controlled design. Also in its favour is that the patients' diet was monitored by an experienced dietician and their type 2 diabetes was well controlled by oral antidiabetic medication in all cases. On the other hand, the main limitation of the present trial was that SB contained almost 20 g more sucrose. However, we designed the SB so that it contained similar

quantities of total carbohydrates, total available carbohydrates and total calories. In addition to this, the SB contained 7.6 g more of sugars in order to compensate the 4.58 g of inositols and 1.65 g of fibre in the interventional drink. We have also assessed the effect of a combination of functional bioactive carbohydrates from carob pod extract, and therefore cannot affirm that the response of carbohydrate metabolism was due only to inositols (major components, 75%). Indeed, our IEB contained other minor bioactive components (e.g. arabinoxylan) and other soluble fibres that may be active and/or enhance effects on glycaemic response, although such effects have been reported at higher doses than those contained in our beverage (Lu, Walker, Muir, Mascara, & O'Dea, 2000; Lu, Walker, Muir, & O'Dea, 2004).

In light of the present evidence, dietary supplementation with an inositol-enriched beverage can mediate insulin action and thus improve glycaemic control in diabetic patients by significantly lowering HbA1c, postprandial and nocturnal glycaemia. In addition to this, it prevents the increase of proinflammatory cytokine IL-6 associated with the consumption of sucrose-sweetened beverages and improves intracellular redox status by reducing total ROS production, which, in turn, could be responsible for an improvement in endothelial function brought about by a reduction in soluble P-selectin and leucocyte-endothelium interactions. In this context, this dietary intervention could be an effective strategy in the prevention of atherosclerosis and cardiovascular complications in diabetic patients, reducing cardiovascular events independently of oral antidiabetic therapy.

Conflict of interest

Authors declare no conflicts of interest.

Acknowledgements

The authors acknowledge the editorial assistance of Brian Normanly (CIBERehd), the extraction of the biological samples by Isabel Soria-Cuenca from University Hospital Dr. Peset, and the supply of the Fruit Up® and sucrose-sweetened beverages used in the study to R Salom and R García-Bou by WILD-Valencia SAU (Spain).

The study has been supported by grants HENUFOOD from the University of Valencia, PI12/01984, PI13/1025 and PI13/0073 from Fund for Health Research (FIS), SAF2010-16030 from the Ministry of Economy and Competitiveness and has been co-funded by the European Regional Development Fund of the European Union (ERDF "A way to build Europe"), PROMETEO 2010/060 from the Regional Ministry of Education of Valencian Community and UGP-14-93, UGP-14-95 from FISABIO. SR-L is the recipient of a predoctoral fellowship from Institute of Health Carlos III (FI11/00637). C.B. is the recipient of a postdoctoral contract from Institute of Health Carlos III (CD14/00043). AA is the recipient of a Ramón y Cajal contract (RYC2005-002295 and I3 program) from the Ministry of Economy and Competitiveness. SO is funded by Universidad de Valencia (VLC-CAMPUS grant). VMV is the recipient of a contract from the Valencian Regional Ministry of Health and Institute of Health Carlos III (CES10/030). MR is the recipient of a Miguel Servet contract from FIS (CP10/00360).

REFERENCES

American Diabetes Association (2012). Diagnosis and classification of diabetes mellitus. *Diabetes Care*, 35, S64–S71.

Bates, S. H., Jones, R. B., & Bailey, C. J. (2000). Insulin-like effect of pinitol. *British Journal of Pharmacology*, 130, 1944–1948.

Beckman, J. A., Creager, M. A., & Libby, P. (2002). Diabetes and atherosclerosis: Epidemiology, pathophysiology, and management. *JAMA: The Journal of the American Medical Association*, 287, 2570–2581.

Brownlee, M. (2001). Biochemistry and molecular cell biology of diabetic complications. *Nature*, 414, 813–820.

Cheang, K. I., Baillargeon, J. P., Essah, P. A., Ostlund, R. E., Jr., Apridonize, T., Islam, L., & Nestler, J. E. (2008). Insulin-stimulated release of D-chiro-inositol-containing inositolphosphoglycan mediator correlates with insulin sensitivity in women with polycystic ovary syndrome. *Metabolism: Clinical and Experimental*, 57, 1390–1397.

Dang, N. T., Mukai, R., Yoshida, K., & Ashida, H. (2010). D-pinitol and myo-inositol stimulate translocation of glucose transporter 4 in skeletal muscle of C57BL/6 mice. *Bioscience, Biotechnology, and Biochemistry*, 74, 1062–1067.

Davis, A., Christiansen, M., Horowitz, J. F., Klein, S., Hellerstein, M. K., & Ostlund, R. E., Jr. (2000). Effect of pinitol treatment on insulin action in subjects with insulin resistance. *Diabetes Care*, 23, 1000–1005.

De Pablo, C., Orden, S., Apostolova, N., Blanquer, A., Esplugues, J. V., & Alvarez, A. (2010). Abacavir and didanosine induce the interaction between human leukocytes and endothelial cells through Mac-1 upregulation. *AIDS (London, England)*, 24, 1259–1266.

Geethan, P. K., & Prince, P. S. (2008). Antihyperlipidemic effect of D-pinitol on streptozotocin-induced diabetic Wistar rats. *Journal of Biochemical and Molecular Toxicology*, 22, 220–224.

Giordano, D., Corrado, F., Santamaria, A., Quattrone, S., Pintaudi, B., & D'Anna, R. (2011). Effects of myo-inositol supplementation in postmenopausal women with metabolic syndrome: A perspective, randomized, placebo-controlled study. *Menopause (New York, N.Y.)*, 18, 102–104.

Hernández-Mijares, A., Bañuls, C., Peris, J. E., Monzó, N., Jover, A., Bellod, L., Victor, V. M., & Rocha, M. (2013). A single acute dose of pinitol from a naturally-occurring food ingredient decreases hyperglycaemia and circulating insulin levels in healthy subjects. *Food Chemistry*, 141, 1267–1272.

Hernández-Mijares, A., Rocha, M., Apostolova, N., Borras, C., Jover, A., Bañuls, C., Sola, E., & Victor, V. M. (2011). Mitochondrial complex I impairment in leukocytes from type 2 diabetic patients. *Free Radical Biology & Medicine*, 50, 1215–1221.

Johnstone, M. T., Creager, S. J., Scales, K. M., Cusco, J. A., Lee, B. K., & Creager, M. A. (1993). Impaired endothelium-dependent vasodilation in patients with insulin-dependent diabetes mellitus. *Circulation*, 88, 2510–2516.

Jude, E. B., Douglas, J. T., Anderson, S. G., Young, M. J., & Boulton, A. J. (2002). Circulating cellular adhesion molecules ICAM-1, VCAM-1, P- and E-selectin in the prediction of cardiovascular disease in diabetes mellitus. *European Journal of Internal Medicine*, 13, 185–189.

Kim, H. J., Park, K. S., Lee, S. K., Min, K. W., Han, K. A., Kim, Y. K., & Ku, B. J. (2012). Effects of pinitol on glycemic control, insulin resistance and adipocytokine levels in patients with type 2 diabetes mellitus. *Annals of Nutrition & Metabolism*, 60, 1–5.

Hernández-Mijares et al., 2015

Kim, J. I., Kim, J. C., Kang, M. J., Lee, M. S., Kim, J. J., & Cha, I. J. (2005). Effects of pinitol isolated from soybeans on glycaemic control and cardiovascular risk factors in Korean patients with type II diabetes mellitus: A randomized controlled study. *European Journal of Clinical Nutrition*, 59, 456–458.

Kim, M. J., Yoo, K. H., Kim, J. H., Seo, Y. T., Ha, B. W., Kho, J. H., Shin, Y. G., & Chung, C. H. (2007). Effect of pinitol on glucose metabolism and adipocytokines in uncontrolled type 2 diabetes. *Diabetes Research and Clinical Practice*, 77, S247–S251.

Kumar, S., Boulton, A. J., Beck-Nielsen, H., Berthezene, F., Muggeo, M., Persson, B., Spinas, G. A., Donoghue, S., Lettis, S., & Stewart-Long, P. (1996). Troglitazone, an insulin action enhancer, improves metabolic control in NIDDM patients. Troglitazone Study Group. *Diabetologia*, 39, 701–709.

Larner, J., Allan, G., Kessler, C., Reamer, P., Gunn, R., & Huang, L. C. (1998). Phosphoinositol glycan derived mediators and insulin resistance. Prospects for diagnosis and therapy. *Journal of Basic and Clinical Physiology and Pharmacology*, 9, 127–137.

Larner, J., Brautigan, D. L., & Thorner, M. O. (2010). D-chiro-inositol glycans in insulin signaling and insulin resistance. *Molecular Medicine*, 16, 543–552.

Lu, Z. X., Walker, K. Z., Muir, J. G., Mascara, T., & O'Dea, K. (2000). Arabinoxylan fiber, a byproduct of wheat flour processing, reduces the postprandial glucose response in normoglycemic subjects. *American Journal of Clinical Nutrition*, 71, 1123–1128.

Lu, Z. X., Walker, K. Z., Muir, J. G., & O'Dea, K. (2004). Arabinoxylan fibre improves metabolic control in people with type II diabetes. *European Journal of Clinical Nutrition*, 58, 621–628.

McDonnell, C. M., Donath, S. M., Vidmar, S. I., Werther, G. A., & Cameron, F. J. (2005). A novel approach to continuous glucose analysis utilizing glycemic variation. *Diabetes Technology & Therapeutics*, 7, 253–263.

Minozzi, M., Nordio, M., & Pajalich, R. (2013). The combined therapy myo-inositol plus D-Chiro-inositol, in a physiological ratio, reduces the cardiovascular risk by improving the lipid profile in PCOS patients. *European Review for Medical and Pharmacological Sciences*, 17, 537–540.

Nascimento, N. R., Lessa, L. M., Kerntopf, M. R., Sousa, C. M., Alves, R. S., Queiroz, M. G., Price, J., Heimark, D. B., Larner, J., Du, X., Brownlee, M., Gow, A., Davis, C., & Fonteles, M. C. (2006). Inositols prevent and reverse endothelial dysfunction in diabetic rat and rabbit vasculature metabolically and by scavenging superoxide. *Proceedings of the National Academy of Sciences of the United States of America*, 103, 218–223.

Nestler, J. E., Jakubowicz, D. J., Reamer, P., Gunn, R. D., & Allan, G. (1999). Ovulatory and metabolic effects of D-chiro-inositol in the polycystic ovary syndrome. *The New England Journal of Medicine*, 340, 1314–1320.

Rosenblat, M., Volkova, N., Paland, N., & Aviram, M. (2012). Triglyceride accumulation in macrophages upregulates paraoxonase 2 (PON2) expression via ROS-mediated JNK/c-Jun signaling pathway activation. *Biofactors (Oxford, England)*, 38, 458–469.

Rovira-Llopis, S., Rocha, M., Falcon, R., de Pablo, C., Alvarez, A., Jover, A., Hernandez-Mijares, A., & Victor, V. M. (2013). Is myeloperoxidase a key component in the ROS-induced vascular damage related to nephropathy in type 2 diabetes? *Antioxidants & Redox Signaling*, 19, 1452–1458.

Saltiel, A. R., & Olefsky, J. M. (1996). Thiazolidinediones in the treatment of insulin resistance and type II diabetes. *Diabetes*, 45, 1661–1669.

Sivakumar, S., Palsamy, P., & Subramanian, S. P. (2010a). Attenuation of oxidative stress and alteration of hepatic tissue ultrastructure by D-pinitol in streptozotocin-induced diabetic rats. *Free Radical Research*, 44, 668–678.

Sivakumar, S., Palsamy, P., & Subramanian, S. P. (2010b). Impact of D-pinitol on the attenuation of proinflammatory cytokines, hyperglycemia-mediated oxidative stress and protection of kidney tissue ultrastructure in streptozotocin-induced diabetic rats. *Chemico-Biological Interactions*, 188, 237–245.

Sivakumar, S., & Subramanian, S. P. (2009). Pancreatic tissue protective nature of D-Pinitol studied in streptozotocin-mediated oxidative stress in experimental diabetic rats. *European Journal of Pharmacology*, 622, 65–70.

Steinberg, H. O., Tarshoby, M., Monestel, R., Hook, G., Cronin, J., Johnson, A., Bayazeed, B., & Baron, A. D. (1997). Elevated circulating free fatty acid levels impair endothelium-dependent vasodilation. *The Journal of Clinical Investigation*, 100, 1230–1239.

Stratton, I. M., Adler, A. I., Neil, H. A., Matthews, D. R., Manley, S. E., Cull, C. A., Hadden, D., Turner, R. C., & Holman, R. R. (2000). Association of glycaemia with macrovascular and microvascular complications of type 2 diabetes (UKPDS 35): Prospective observational study. *BMJ (Clinical Research Ed.)*, 321, 405–412.

The Diabetes Control and Complications Trial Research Group (1993). The effect of intensive treatment of diabetes on the development and progression of long-term complications in insulin-dependent diabetes mellitus. *The New England Journal of Medicine*, 329, 977–986.

Victor, V. M., Rocha, M., Solá, E., Bañuls, C., Garcia-Malpartida, K., & Hernández-Mijares, A. (2009). Oxidative stress, endothelial dysfunction and atherosclerosis. *Current Pharmaceutical Design*, 15, 2988–3002.

Wang, L., Gill, R., Pedersen, T. L., Higgins, L. J., Newman, J. W., & Rutledge, J. C. (2009). Triglyceride-rich lipoprotein lipolysis releases neutral and oxidized FFAs that induce endothelial cell inflammation. *Journal of Lipid Research*, 50, 204–213.

Wang, L., Sapuri-Butti, A. R., Aung, H. H., Parikh, A. N., & Rutledge, J. C. (2008). Triglyceride-rich lipoprotein lipolysis increases aggregation of endothelial cell membrane microdomains and produces reactive oxygen species. *American Journal of Physiology, Heart and Circulatory Physiology*, 295, H237–H244.

Yaniv, Z., Dafni, A., Friedman, J., & Palevitch, D. (1987). Plants used for the treatment of diabetes in Israel. *Journal of Ethnopharmacology*, 19, 145–151.

ARTÍCULO 7

Interference of purinergic signalling: an explanation for the cardiovascular effect of Abacavir?

Esplugues JV, de Pablo C, Collado-Díaz V, Hernández C, **Orden S**, Álvarez Á.

AIDS 2016, en prensa

Interference with purinergic signalling: an explanation for the cardiovascular effect of abacavir?

Juan V. Esplugues[a,b,*], Carmen De Pablo[a,*], Víctor Collado-Díaz[a,b], Carlos Hernández[a,b], Samuel Orden[a,b] and Ángeles Álvarez[a,c]

Objective: The association of abacavir (ABC), a guanosine analogue, with cardiovascular toxicity is a long-lasting matter of controversy engendered by the lack of a mechanism of action. Clinical data point to an acute mechanism of vascular inflammation. Previous studies have shown that ABC induces leukocyte–endothelial cell interactions, an indicator of vascular inflammation. These effects are reproduced by another purine analogue, didanosine, but not by pyrimidine or acyclic nucleotide analogues, hinting at an interference with the purinergic system. The aim of the present study was to assess the role of ATP-receptors in leukocyte accumulation induced by ABC.

Design and methods: Clinical concentrations of ABC were analysed in an animal model *in vivo* (intravital microscopy using male C57BL/6 wild-type or P2rx7 knockout mice), in human endothelial cells and leukocytes *in vitro* (flow chamber), or in leukocyte Mac-1 expression (flow cytometry).

Results: ABC reduced leukocyte rolling velocity and increased rolling flux and adhesion both *in vivo* and *in vitro*. These effects were absent in P2rx7 knockout mice and following the specific blockade of ATP-P2X_7 receptors in wild-type animals. Further pharmacological characterization in flow chamber experiments confirmed the role of ATP-P2X_7 receptors and suggested that those located on leukocytes were particularly implicated. Activation of ATP-P2X_7 receptors is needed for expression of leukocytic Mac-1. Similar effects were obtained with didanosine.

Conclusion: ABC induces leukocyte–endothelial cell interactions through a mechanism involving interference with purine-signalling pathways via ATP-P2X_7 receptors located mainly on leukocytes. Our data are compatible with existing clinical data revealing an increased cardiovascular risk in ABC-treated patients.

Copyright © 2016 Wolters Kluwer Health, Inc. All rights reserved.

AIDS 2016, **30**:000–000

Keywords: abacavir, ATP, cardiovascular diseases, HIV, leukocyte-endothelium interactions, P2X7 receptors, purinergic

Introduction

The high risk of cardiovascular diseases among HIV patients [1–3] has generally been attributed to classical cardiovascular risk factors and the vascular inflammatory condition associated with the infection [4–6]. However, given that the administration of combined antiretroviral therapy is for life, cardiovascular comorbidities in these patients are on the rise, and the patient population is ageing, there is increasing interest in clarifying the impact of said therapy on the cardiovascular system.

[a]Departamento de Farmacología and CIBERehd, Facultad de Medicina, Universidad de Valencia, [b]FISABIO-Fundación Hospital Universitario Dr Peset, and [c]Fundación General Universidad de Valencia; all in Valencia, Spain.

Correspondence to Juan V. Esplugues, PhD, MD, Departamento de Farmacología, Facultad de Medicina, Universidad de Valencia, Avda. Blasco Ibáñez 15-17, 46010 Valencia, Spain.

Tel: +34 96 3864624; fax: +34 96 3983879; e-mail: juan.v.esplugues@uv.es

*Juan V. Esplugues and Carmen De Pablo contributed equally.

Received: 30 September 2015; revised: 18 January 2016; accepted: 4 March 2016.

DOI:10.1097/QAD.0000000000001088

ISSN 0269-9370 Copyright © 2016 Wolters Kluwer Health, Inc. All rights reserved.

Esplugues et al., 2016

Abacavir (ABC), a guanosine analogue belonging to the nucleoside reverse transcriptase inhibitor family, is widely prescribed to treat HIV. Although generally considered well tolerated, there is evidence that associates this drug with adverse cardiovascular effects. The first warning appeared in 2005 [7], but it was only after the publication of the results of 'The Data collection and Adverse events of anti-HIV Drugs study group' (D:A:D) in 2008 that the risk was acknowledged and expanded to include didanosine (ddI), another nucleoside reverse transcriptase inhibitor analogue of purine with which ABC shares a close structural analogy [8]. This report correlated current or recent (≤6 months) exposure to ABC with a two-fold increase in the risk of myocardial infarction [8]. Later studies confirmed this relationship [9–11], whereas others did not [12–14], thus engendering one of the most long-lasting controversies in the area of HIV treatment. However, despite the lack of a consensus, major clinical guidelines now recommend limited use of ABC when there is a risk of cardiovascular disease [15,16].

Regardless of methodological discrepancies among the published clinical trials, the aforementioned debate has been fuelled particularly by the lack of a credible mechanism of action to justify the cardiovascular toxicity of ABC. Nonetheless, there are data pointing to an acute vascular inflammatory response, as the cardiovascular risk subsides following discontinuation of the drug and has not been related to traditional predisposing factors (lipids, glucose metabolism, etc.) or to past or cumulative exposure [8]. Vascular inflammation involves the accumulation of both leukocytes and platelets in the vessel wall. In the first stages of this process, leukocytes roll along the endothelium of inflamed vessels before coming to a halt, after which they eventually adhere and transmigrate. In a subsequent phase, platelets bind to this endothelium and recruit other circulating platelets and leukocytes, thus generating thrombi and promoting the atherosclerotic process [17–19]. There is mounting experimental data linking ABC with these early steps of vascular inflammation. Thus, there is some evidence of platelet dysfunction produced by ABC [20–22]. Additionally, we have previously described the ability of clinical concentrations of ABC to induce leukocyte–endothelial cell interactions. They were first demonstrated *in vitro* using human cells in a flow chamber system, and were found to be mediated by an interplay between adhesion molecules in leukocytes (Mac-1) and endothelial cells (ICAM-1). These responses appeared rapidly and seemed related to the chemical structure of ABC, as they were specifically reproduced by ddI but not by analogues of pyrimidine (lamivudine, zidovudine, or emtricitabine) or by an acyclic nucleotide (tenofovir) [23,24]. The effects of ABC and ddI were reproduced in rats *in vivo* employing the intravital microscopy approach, and corroborated the potential of both purine analogues to induce responses considered hallmarks of vascular inflammation [25]. However, the specifics of the mechanism behind such actions remained unclear, and so their identification became the main objective of the present study.

Purinergic mediators, such as ATP and some of its metabolites (ADP, AMP, etc.), are major paracrine signalling molecules capable of triggering prothrombotic and proinflammatory vascular programmes implicating leukocyte traffic, platelet activation and formation of the atherosclerotic plaque by interacting with P2-nucleotide receptors located on endothelial cells, leukocytes and platelets [26–28]. Given the structural similarity of ABC and ddI with endogenous purines, we hypothesized that interference with the purinergic signalling pathway underlies a deleterious effect of ABC or ddI on the cardiovascular system. Thus, the present study focused on exploring the role of ATP receptors in the leukocyte–endothelial cell interactions induced by ABC.

Methods

Intravital microscopy

Male wild-type C57BL/6 (Charles River Laboratories, Barcelona, Spain) or knockout mice were compared. The knockout animals employed were homozygous P2rx7 knockout mice (B6.129P2-*P2rx7*^{tm1Gab}/J) (Jackson Laboratory, Bar Harbor, Maine, USA), which have been reported to be viable, fertile, normal in size and do not display any physical or behavioural abnormalities [29]. Mice (22–30 g) were anaesthetized (xylacine hydrochloride 10 mg/kg and ketamine hydrochloride 200 mg/kg, intraperitoneally). The cremaster muscle was exteriorized onto an optical clear viewing pedestal for tissue transillumination and continuously superfused with bicarbonate-buffered saline (pH 7.4, 37°C, 2 ml/min). It was visualized using an orthostatic microscope (Nikon Optiphot-2, SMZ1; Nikon, Badhoevedor, The Netherlands) onto which a video camera (Sony SSC-C350P; Sony, Koeln, Germany) was incorporated. Images (5 min period, x1300) of single unbranched cremasteric venules [30], diameter 25–40 μm, measured with a video caliper (Microcirculation Research Institute, Texas A&M University, College Station, Texas, USA), were captured digitally using the Pinacle studio program. Centreline red blood cell velocity was quantified with an optical Doppler velocimeter (Microcirculation Research Institute, USA). Systemic arterial blood pressure was monitored and blood flow and wall shear rate calculated as previously described [31]. Numbers of rolling, adherent and emigrated leukocytes were determined offline during playback analysis of digital images by an observer who was unaware of the treatments administered. Rolling flux was assessed by counting the number of leukocytes passing a reference point in the vessel per minute. Leukocyte rolling velocity was calculated by measuring the time required for these cells to travel along 100 μm of venule and was expressed as μm/s. A leukocyte was considered to have adhered to the

endothelium if it remained stationary for 30 s or more, and numbers were expressed per 100 μm of vessel. Leukocyte emigration was evaluated as the total number of interstitial leukocytes per field.

Clinically relevant concentrations of ABC (2.5–7.5 μg/ml) or ddI (1 μg/ml) [32,33] were injected intrascrotally (100 μl) 4 h before measurements. This route was chosen as it allows the stimulus solution to directly bath the cremaster tissue. Mice were pretreated (intraperitoneally) before ABC (5 μg/ml) or ddI (1 μg/ml) with antagonists for the following ATP receptors at doses described to block leukocyte parameters [34–38]: nonspecific P2 (suramin 400 mg/kg, 60 min), specific for $P2X_7$ [A804598 1 μg/kg, 30 min or Brilliant Blue G (BBG) 45 mg/kg, 30 min] or $P2X_{2/3}$ (A317491 0.1 μg/kg, 30 min).

In-vitro leukocyte adhesion

We employed passage one of human umbilical vein endothelial cells (HUVECs) harvested from human umbilical cords [23]. Peripheral blood polymorphonuclear (PMN) or mononuclear cells (PBMCs) were isolated from whole blood of healthy volunteers [23] from Hospital Clínico Universitario (Valencia). To perform a thorough analysis of white cells, we evaluated both PMN (the first leukocyte population to be recruited by a proinflammatory stimulus) and PBMC (lymphocytes and monocytes are generally considered more important in the formation of atherosclerosis and thrombi).

The adhesion assay was performed under flow conditions using the parallel plate flow chamber model [23,24]. Coverslips [fibronectin (5 μg/ml) coated] containing confluent HUVEC monolayers were inserted in the chamber (37°C) and a portion (5 × 25 mm) was exposed to the flow. The chamber was mounted on an inverted microscope (Nikon Eclipse TE 2000-S, x40) fitted with a video camera (Sony Exware HAD). PMN or PBMC were resuspended in buffer (Dulbecco's PBS, $DPBS^+$, containing 20 mmol/l HEPES and 0.1% human serum albumin) at 1×10^6 or 0.5×10^6 cells/ml, respectively, and were drawn across the monolayer (flow rate 0.36 ml/min, shear stress 0.7 dyne/cm^2). Images of a single field were recorded over a 5-min period and leukocyte parameters determined. Rolling flux was the number of cells rolling across 100 μm^2 of the monolayer during a 1-min period. Velocities of 20 consecutive leukocytes in the field of focus were determined by measuring the time required to travel 100 μm. Adhesion was determined after 5 min of perfusion by analysis of 5–10 high power (40×) fields. Leukocytes were considered to be adherent after 30 s of stable contact with the monolayer.

Prior to exposure (4 h at 37°C) to ABC (5 μg/ml) or ddI (1 μg/ml), we pretreated either HUVEC or leukocytes (either PMN or PBMC), or both HUVEC and leukocytes, with the following [34–46]: a Ca^{2+} Chelator [Ethylene glycol tetraacetic acid (EGTA) 2 mmol/l; 30 min]; antagonists for the following ATP receptors: nonselective P2 (suramin 100 μmol/l, 60 min), $P2X_1$ (MRS2159 10 μmol/l, 30 min), $P2X_{1-4}$ (NF023 10 μmol/l, 30 min), $P2X_{2-3}$ (A317491 25 nmol/l, 30 min), $P2X_7$ (A804598 1 μmol/l or BBG 5 μmol/l, 30 min), $P2Y_2$ (AR-C 118925XX 10 μmol/l, 30 min), $P2Y_6$ (MRS2578 10 μmol/l, 30 min) or $P2Y_{11}$ (NF340 10 μmol/l, 30 min); an ATP-ase (apyrase 1 UI/ml, 30 min) or a selective A_{2A} adenosine receptor agonist (CGS-21680 10 μmol/l, 60 min).

Effects of apyrase on abacavir degradation

HPLC was used to perform a time course (3, 5 and 10 min; 1 and 4 h) to evaluate the effects of apyrase (1 UI/ml) on known concentrations of ABC (5 μg/ml) or ATP (10 μg/ml) in endothelial growth media-2 without cells.

Flow cytometry

The expression of the two subunits of the human leukocyte adhesion molecule Mac-1 (CD11b and CD18) was analysed in blood samples treated (4 h, 37°C) with ABC (5 μg/ml) and then incubated with saturating amounts of the antibodies against CD11b and CD18 (20 min, 4°C, in darkness). In some cases, prior to exposure to ABC, blood was pretreated with suramin (100 μmol/l, 60 min), A804598 (1 μmol/l, 30 min) or A317491 (25 nmol/l, 30 min). Subsequently, the samples were fixed and identified in a flow cytometer (FACScalibur Flow Cytometer; BD, Madrid, Spain) [23,24]. Surface antigen expression (Fluorescein isothiocyanate or phycoerythrin-fluorescence) was analysed in neutrophils, monocytes and lymphocytes, which were identified by their specific features of size (forward-angle light scatter) and granularity (side-angle light scatter). Median fluorescence intensity was employed as a marker of the expression of the respective epitope.

Materials

Ketamine (Merial, Spain); physiological serum (Braun, Spain); Dulbecco's PBS, endothelial growth media-2 culture and fetal bovine serum (Lonza, Spain); xylazine, human serum albumin (albuminate 25%), RPMI1640 supplemented with 20 mmol/l HEPES, HBSS, fibronectin, dextran, EGTA, ATP antagonists (Sigma Chemical Co, Spain); Ficoll-Paque TM Plus (GE Healthcare, Spain); PBS, collagenase, and trypsin (Gibco; Invitrogen, Spain) and ABC and ddI (Sequoia Research Products, UK).

Ethics and statistics

Human and animal procedures complied with Spanish law and were approved by the respective Hospital or Faculty Ethics Committee. One-way ANOVA with a Newmann–Keuls correction was employed for statistical analysis (mean ± SEM, $n \geq 4$, $P < 0.05$).

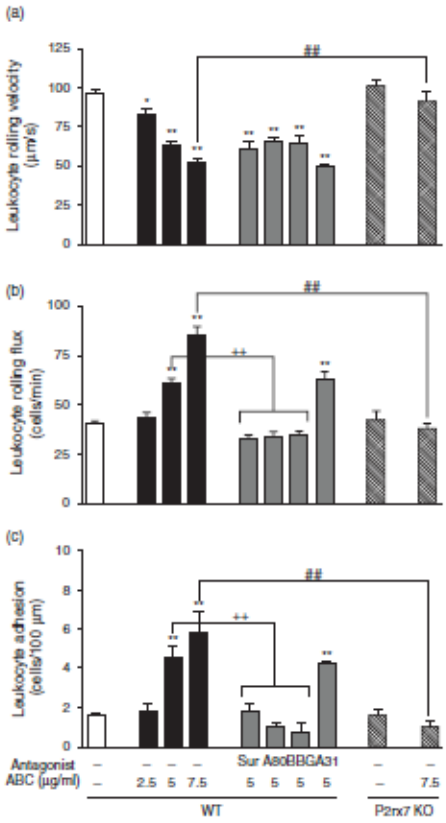

Fig. 1. Leukocyte responses induced by abacavir (ABC) in cremasteric venules of wild-type and P2rx7 knockout mice. Animals were treated (intrascrotally) with saline (vehicle) or ABC (2.5–7.5 μg/ml). Some animals were pretreated with suramin (nonselective P2 antagonist, 400 mg/kg, 60 min, Sur), A804598 ($P2X_7$ antagonist, 1 μg/kg, 30 min, A80), BBG ($P2X_7$ antagonist, 45 mg/kg, 30 min) or A317491 ($P2X_{2-3}$ antagonist, 1 μg/ml 30 min, A31) prior to ABC, and leukocyte rolling velocity (a), rolling flux (b) and adhesion (c) were quantified (4 h). Results are mean ± SEM, $n \geq 5$. $^{*}P < 0.05$ or $^{**}P < 0.01$ vs. corresponding value in wild-type vehicle-treated group, $^{++}P < 0.01$ vs. corresponding value in wild-type ABC 5 μg/ml-treated group, $^{\#\#}P < 0.01$ vs. corresponding value in wild-type ABC 7.5 μg/ml-treated group (ANOVA followed by Newman–Keuls test).

Results

In vivo

In wild-type mice, ABC and ddI promoted a significant decrease in leukocyte rolling velocity while increasing rolling flux and adhesion (Figs. 1 and 2a–c). Emigration was not affected (data not shown). The actions of ABC and ddI on leukocyte rolling flux and adhesion were absent following pretreatment with suramin or either of the two selective ATP-$P2X_7$ receptor antagonists evaluated (A804598 and BBG), while A317491 had no influence (Figs. 1 and 2a–c). The effects on leukocyte parameters of the highest dose of ABC evaluated were nonexistent in P2rx7 knockout mice (Fig. 1).

In vitro

ABC (5 μg/ml) and ddI (1 μg/ml) induced a significant decrease in human leukocyte (PMN and PBMC) rolling velocity while augmenting leukocyte rolling flux and adhesion (Figs. 3 and 2d–i; Supplementary videos 1 and 2, http://links.lww.com/QAD/A899 and http://links.lww.com/QAD/A900). ABC actions were prevented by pretreatment of both cell types (endothelium and leukocytes) with suramin, EGTA or the selective ATP-$P2X_7$ receptor antagonists A804598 (Supplementary video 3, http://links.lww.com/QAD/A901) or BBG (Fig. 3). Blockade of the other P2X or P2Y receptors evaluated did not prevent the leukocyte responses stimulated by ABC (Fig. 3). The effects of ABC were absent following pretreatment with an enzyme that degrades ATP (apyrase) or activation of adenosine-A_{2A} receptors (Fig. 3). Likewise, the actions of ddI were prevented by pretreatment of endothelium and leukocytes with suramin or A804598, but not by A317491 (Fig. 2d–i).

To determine the cell type in which the ATP-$P2X_7$ response was most pronounced, we replicated the ABC experiments, but this time incubated independently either leukocytes (PMN or PBMC) or endothelial cells with various ATP receptor antagonists before exposure of both cell types to ABC. As shown in Fig. 4, incubation of both leukocytes and endothelial cells with suramin or A804598 abolished the effect of ABC. Incubation of only leukocytes (either PMN or PBMC), but not HUVEC, with any one of the two agents also substantially reduced the effects of ABC to values that, though generally slightly lower, did not differ in a statistically significant way from those obtained following exposure of both cell types to the drug. Incubation of HUVEC alone with any of the two agents also diminished the effects of ABC. However, the degree of inhibition was generally lower than that observed following the combined (HUVEC and leukocytes) or specific incubation of leukocytes.

Effects of apyrase on abacavir degradation

Apyrase did not modify ABC concentrations during the 4-h period evaluated (ABC: 5.4 ± 0.2 vs. ABC + apyrase: 5.6 ± 0.3 μg/ml). As expected, it completely degraded ATP, for which no signal was detected at the first time

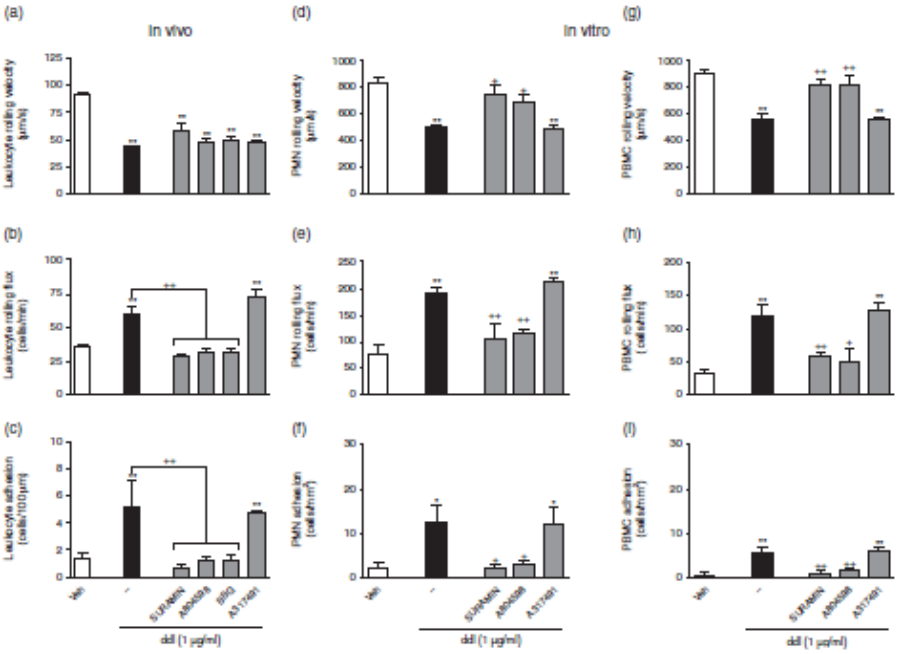

Fig. 2. Leukocyte responses induced by didanosine (ddI) *in vivo* (in cremasteric venules of mice) and *in vitro* (in human cells). Animals were treated (intrascrotally) with saline (vehicle) or ddI (1 μg/ml). Some animals were pretreated with suramin (nonselective P2 antagonist, 400 mg/kg, 60 min), A804598 ($P2X_7$ antagonist, 1 μg/kg, 30 min), BBG ($P2X_7$ antagonist, 45 mg/kg, 30 min) or A317491 ($P2X_{2-3}$ antagonist, 1 μg/ml, 30 min) prior to ddI and leukocyte rolling velocity (a), rolling flux (b) and adhesion (c) were quantified (4 h). HUVECs and leukocytes (either human PMN or PBMCs) were incubated (4 h) with ddI (1 μg/ml) or vehicle (Veh). In some cases, both cell types (HUVEC and leukocytes) were pretreated with suramin (nonselective P2 antagonist, 100 μmol/l, 60 min), A804598 ($P2X_7$ antagonist, 1 μmol/l, 30 min) or A317491 ($P2X_{2-3}$ antagonist, 25 nmol/l, 30 min) prior to ddI. After assembling the flow chamber, PMN rolling velocity (d), PMN rolling flux (e), PMN adhesion (f) and PBMC rolling velocity (g), PBMC rolling flux (h) and PBMC adhesion (i) were quantified. Results are mean ± SEM, $n \geq 4$. $^{*}P < 0.05$ or $^{**}P < 0.01$ vs. corresponding value in vehicle-treated group. $^{+}P < 0.05$ or $^{++}P < 0.01$ vs. corresponding value in ddI-treated group (ANOVA followed by Newman–Keuls test).

point assessed (3 min; ATP: 10.7 ± 0.1 vs. ATP + apyrase: 0.0 ± 0.0 μg/ml).

Flow cytometry

ABC (5 μg/ml) induced a significant increase in the two subunits of the β_2-integrin Mac-1 (CD11b and CD18) in both neutrophils (Fig. 5a and b) and monocytes (Fig. 5c and d), as we have previously published [23]. The fact that the actions of ABC increasing this integrin were prevented by pretreatment of blood with suramin or A804598, but not by A317491 (Fig. 5), suggest that ATP-$P2X_7$ receptors mediated the activation of leukocytes, expressed by an increase in Mac-1.

Discussion

Our results confirm that clinically relevant concentrations of ABC induce leukocyte–endothelial interactions, in particular rolling and adhesion, and demonstrate that these actions involve interference with the purinergic signalling system in a mechanism involving ATP-P2 receptors, specifically $P2X_7$. Our data have been obtained using procedures that have been instrumental in understanding the inflammatory cascade associated with vascular diseases and its pharmacological modulation – intravital microscopy *in vivo* and the flow chamber system *in vitro* [47–54] – whereas the receptors implicated have

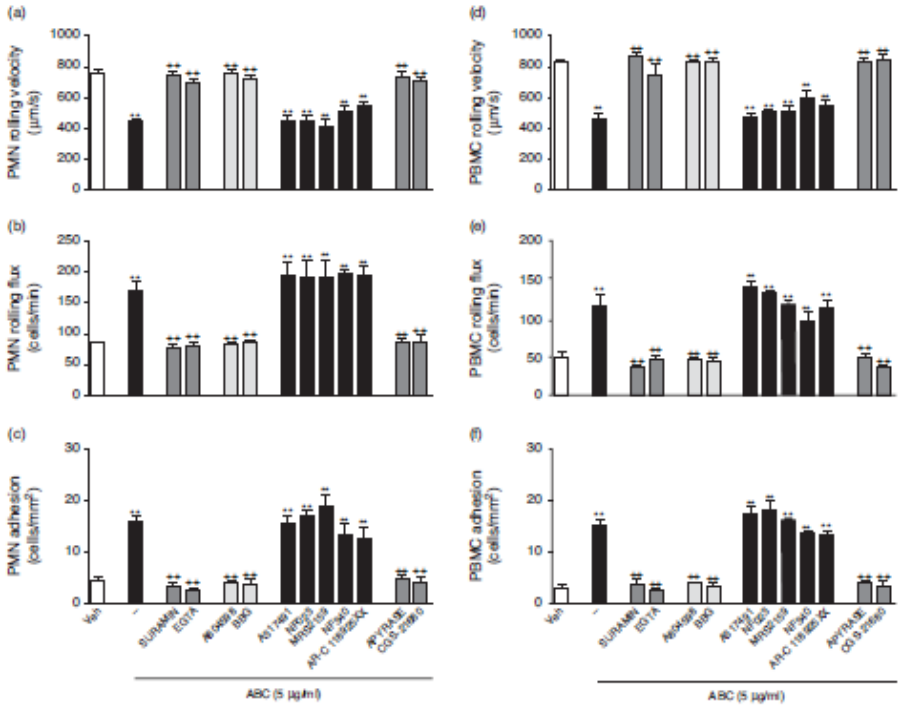

Fig. 3. ATP-P2 receptors and leukocyte responses induced by abacavir (ABC). HUVEC and leukocytes [either human PMN or mononuclear cells (PBMC)] were incubated (4 h) with ABC (5 μg/ml) or vehicle (Veh). In some cases, both cell types (HUVEC and leukocytes) were pretreated with suramin (nonselective P2 antagonist, 100 μmol/l, 60 min), EGTA (a Ca^{2+} Chelator, 2 nmol/l, 30 min), A804598 ($P2X_7$ antagonist, 1 μmol/l, 30 min), Brilliant Blue G ($P2X_7$ antagonist, 5 μmol/l, 30 min, BBG), A317491 ($P2X_{2-3}$ antagonist, 25 nmol/l, 30 min), NF023 ($P2X_{1-4}$ antagonist, 10 μmol/l, 30 min), MRS2159 ($P2X_1$ antagonist, 10 μmol/l, 30 min), NF340 ($P2Y_{11}$ antagonist, 10 μmol/l, 30 min), AR-C118925XX ($P2Y_2$ antagonist, 10 μmol/l, 30 min), apyrase (an ATP-ase, 1 U/ml, 30 min) or CGS-21680 (selective A_{2A} adenosine receptor agonist, 10 μmol/l, 60 min) prior to ABC. After assembling the flow chamber, PMN rolling velocity (a), PMN rolling flux (b), PMN adhesion (c) and PBMC rolling velocity (d), PBMC rolling flux (e) and PBMC adhesion (f) were quantified. Results are mean ± SEM, $n \geq 4$. $^{**}P < 0.01$ vs. corresponding value in vehicle-treated group. $^{++}P < 0.01$ vs. corresponding value in ABC-treated group (ANOVA followed by Newman–Keuls test).

been characterized using both a broad variety of pharmacological agents and genetically deficient animals.

The effects of ABC on rolling flux and adhesion *in vivo* (mice cremaster) were prevented by suramin, an antagonist of both P2X and P2Y receptor subtypes, and by two specific antagonists of the $P2X_7$ receptor, but not by blockade of other subtypes of P2X receptors. The lack of induction of leukocyte emigration by ABC contrasts with the results of our previous studies in rats using intravital microscopy of mesenteric venules [25]. We have no suitable explanation for this, other than the singularity of each preparation. Importantly, the actions of ABC on rolling velocity, rolling flux and adhesion were also absent in P2rx7 knockout mice, which emphasises the crucial role of these particular receptors.

The in-vitro experiments with human cells bolstered our hypothesis further and allowed for the determination of the cellular types implicated. Again, suramin prevented the actions of ABC on PMN/PBMC rolling velocity, rolling flux and adhesion. The fact that this action was reproduced by a calcium chelator such as EGTA confirms the involvement of a subtype of P2X receptors, which are all coupled to calcium channels and are thus sensitive to this type of drug, whereas it excludes the P2Y variety, which is a G-protein coupled receptor and would not be responsive to this rapid interference with extracellular calcium. The

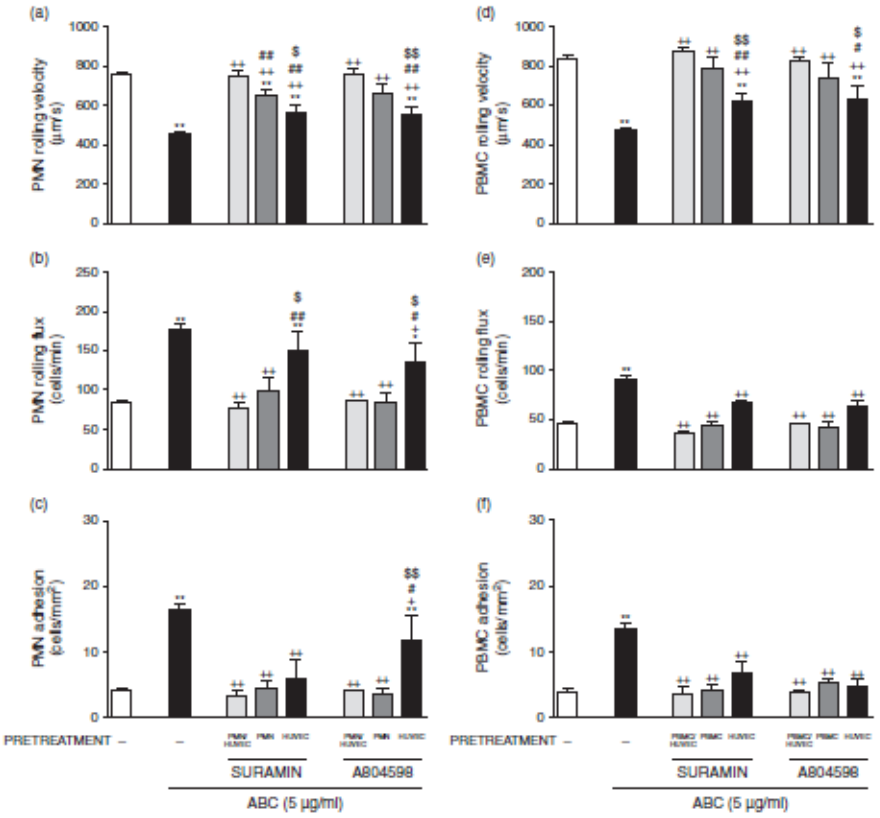

Fig. 4. Relevance of leukocytes or human umbilical vein endothelial cell (HUVEC) in the blockade of abacavir (ABC) response. HUVECs and leukocytes (either PMN or PBMCs) were incubated (4 h) with ABC (5 μg/ml) after pretreatment of either HUVEC or leukocytes, or both, with suramin (nonselective P2 antagonist, 100 μmol/l, 60 min) and A804598 ($P2X_7$ antagonist, 1 μmol/l, 30 min). After assembling the flow chamber, PMN rolling velocity (a), PMN rolling flux (b), PMN adhesion (c) and PBMC rolling velocity (d), PBMC rolling flux (e) and PBMC adhesion (f) were quantified. Results are mean ± SEM, $n = 5$. $^{**}P < 0.01$ vs. corresponding value in vehicle-treated group. $^{+}P < 0.05$ or $^{++}P < 0.01$ vs. corresponding value in ABC-treated group. $^{\#}P < 0.05$ or $^{\#\#}P < 0.01$ vs. corresponding value in both cell type-pretreated group. $^{\$}P < 0.05$ or $^{\$\$}P < 0.01$ vs. corresponding value in only leukocyte-pretreated group (ANOVA followed by Newman–Keuls test).

lack of P2Y receptor implication is also substantiated by the fact that their pharmacological blockade had no effect on ABC leukocyte responses. The specific blockade of $P2X_7$ receptors with two different antagonists impeded the response to ABC, whereas blockade of other important P2X receptor subtypes, such as $P2X_1$, $P2X_{2/3}$ and $P2X_{1/4}$, had no effect. Likewise, given the similarity in chemical structure between both purine analogues and purinergic mediators, the fact that ddI reproduced the actions of ABC *in vivo* and *in vitro* bolsters our previous findings [23,24] and endorses the hypothesis that interference with purinergic signalling, in which ATP–$P2X_7$ receptors are implicated, mediates the aforementioned leukocyte–endothelial cell interactions.

The actions of apyrase are particularly enlightening in outlining how ABC works. This ATP-ase prevented the effects of the antiretroviral without degradating its molecule, thus pointing to an indirect action mediated by metabolites of ABC and/or by changes in the levels of endogenous purines sensitive to the metabolizing effects of the enzyme and capable of prompting the activation of ATP-sensitive $P2X_7$ receptors [55].

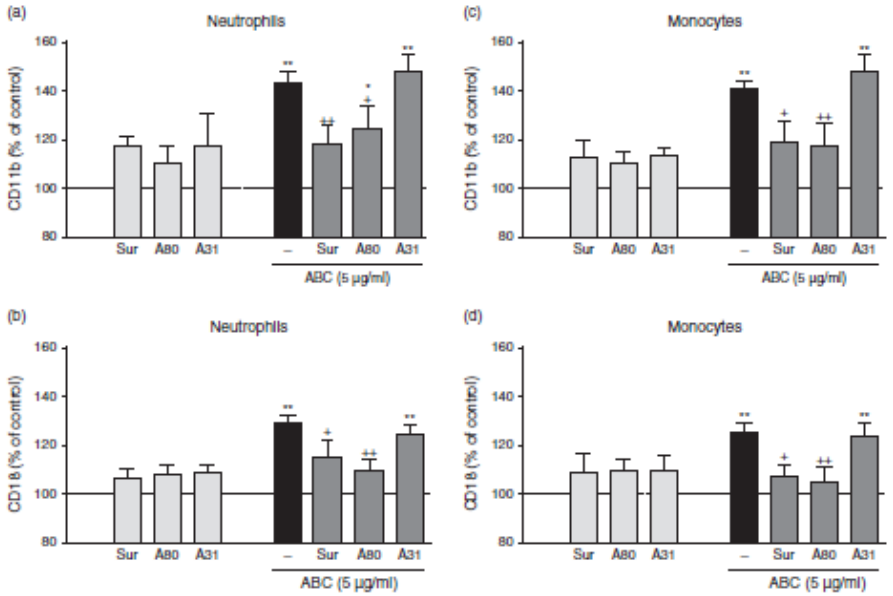

Fig. 5. ATP-P2 receptors and Mac-1 expression induced by abacavir (ABC). Whole blood was treated with ABC (5 µg/ml, 4 h) and the surface expression of the two subunits of Mac-1 CD11b (a, c) and CD18 (b, d) on neutrophils and monocytes, respectively, was quantified. In some cases, blood was pretreated with suramin (nonselective P2 antagonist, 100 µmol/l, 60 min), A804598 ($P2X_7$ antagonist, 1 µmol/l, 30 min) or A317491 ($P2X_{2-3}$ antagonist, 25 nmol/l, 30 min) prior to ABC. Fluorescence values are expressed as percentage of mean fluorescence intensities of control cells (dotted line). Results are mean ± SEM, $n \geq 4$. $^{*}P < 0.05$ or $^{**}P < 0.01$ vs. corresponding value in vehicle-treated group. $^{+}P < 0.05$ or $^{++}P < 0.01$ vs. corresponding value in ABC-treated group (ANOVA followed by Newman–Keuls test).

ATP-$P2X_7$ receptors have been described on both leukocytes and endothelial cells [28,56,57]. Our results, with the exception of those regarding PBMC and adhesion, strongly suggest that ABC targets predominantly receptors on leukocytes, as the preincubation of either type of leukocyte (PMN or PBMC) with suramin or A804598 inhibited the action of ABC in the same way as when both leukocytes and endothelial cells underwent the same treatment. Endothelial ATP-$P2X_7$ receptors also played a role, but seemingly to a lesser extent than those present on leukocytes.

There are many reports linking the activation of $P2X_7$ receptors to the genesis of vascular inflammation. Thus, their stimulation by ATP triggers a cascade implicating the NALP3-inflammasomme, caspase-1 and, among others, the proinflammatory cytokine interleukin-1β. Furthermore, it induces reactive oxygen species production and nuclear factor-κB translocation, and, eventually, the expression of a variety of endothelial and leukocytic adhesion molecules [26,27,58,59]. We have previously demonstrated that the recruitment of white cells induced by ABC is mediated by an interaction between two adhesion molecules: endothelial ICAM-1 and leukocytic Mac-1 [23]. The present findings expand this concept by suggesting that the ATP-$P2X_7$ receptors involved in the actions of the drug are largely located on leukocytes, and that their activation is needed for the expression of Mac-1.

The functioning of purinergic homeostasis in vessels requires a cascade of extracellular ectonucleotidases that preserve the equilibrium between the levels of ATP/ADP/AMP and the anti-inflammatory molecule adenosine. Accordingly, the progressive breakdown of ATP to adenosine is counteracted by its continuous resynthesis through opposite reactions and/or the release of ATP from intracellular stores, through a miscellany of channels and transporting mechanisms. There is evidence relating a variety of pathologic conditions to alterations in these enzymes that subsequently induce changes in the proportions of nucleotides and promote the accumulation of proinflammatory nucleotides, thus leading to leukocyte recruitment and platelet aggregation [26,55,60–62]. In light of this evidence, the fact that the in-vitro actions of ABC were counteracted by an agonist of adenosine A_2

receptors in our experiments further supports the involvement of purinergic activation in the actions of ABC.

Pharmacological interference of cardiovascular regulatory pathways in clinical settings tends to potentiate ongoing vascular processes, and are largely visualized during treatment and reduced following cessation. Our data is compatible with the reversibility of the cardiovascular effects of ABC described in patients, as we have already shown that its acute effects on leukocytes disappear within 48h [25]. However, we must be cautious when extrapolating experimental data to clinical human conditions, particularly when involving pathological situations as complex as those underlying the onset of cardiovascular disorders. A potential limitation of this study is that we have not confirmed our hypothesis in cells infected with HIV. In addition, the interaction with platelets is an important step in the induction of the atherosclerotic plaque and/or thrombi that we have not explored. Although both points need to be evaluated in future studies, we do not feel that either one compromises the main achievements of the present study; that is evidence that ABC induces leukocyte–endothelial cell interactions – an initial and important aspect of the inflammatory cascade associated with vascular diseases – through an indirect mechanism involving ATP-$P2X_7$ receptors located mainly on leukocytes. Our data point to a mechanism that could underlie the increased cardiovascular risk in patients treated with ABC, which may be a step towards resolving the long-standing controversy surrounding this antiretroviral.

Acknowledgements

Contribution: C.D.P., V.C.D. and S.O. performed the research, C.H. helped perform the research, A.A. conceived the study and J.V.E. and A.A. designed the research and wrote the manuscript. We would like to thank Brian Normanly for his English language editing and assistance with the preparation of the manuscript and Nicole Roupain, Dora Martí and Fernando Sabater for their technical support with the experiments described in this article.

Funding support: this work was supported by SAF2010-16030 (Ministerio de Ciencia e Innovación); PI14/00312 and CB06/04/0071-CIBERehd (Ministerio de Sanidad y Consumo) and PROMETEOII/2014/035 (Generalitat Valenciana), along with an unrestricted grant from Gilead Sciences SL. Funding received by individual researchers: Cd.P. (Ministerio de Ciencia e Innovación FPI grant BES-2008-004338); V.C.D. (Fundación Fisabio); S.O. (Universidad de Valencia VLC CAMPUS); C.H. and A.A. (Ministerio de Ciencia e Innovación Ramón y Cajal program RYC2011-09571 and RYC2005-002295, respectively).

Conflicts of interest

J.V.E. has received funds for speaking at symposia organized on behalf of Abbvie, Pfizer, Janssen, AstraZeneca and Gilead Sciences. All other authors have nothing to declare. There are no conflicts of interest.

This study was presented in part at the XXXIV Congreso de la Sociedad Española de Farmacología, San Pedro del Pinatar, Spain, 16–19 September 2013 (abstract O19-03); 21st Conference on Retroviruses and Opportunistic Infections, Boston, EEUU, 3–6 March 2014 (abstract 774); VI Congreso Nacional GESIDA (Grupo de Estudio de SIDA-SEIMC), Málaga, Spain, 25–28 November 2014 (abstract P-060).

References

1. Durand M, Sheehy O, Baril JG, LeLorier J, Tremblay CL. **Association between HIV infection, antiretroviral therapy, and risk of acute myocardial infarction: a cohort and nested case-control study using Quebec's public health insurance database.** *J Acquir Immune Defic Syndr* 2011; **57**:245–253.
2. Lang S, Mary-Krause M, Cotte L, Gilquin J, Partisani M, Simon A, *et al.* **Impact of individual antiretroviral drugs on the risk of myocardial infarction in human immunodeficiency virus-infected patients: a case-control study nested within the French Hospital Database on HIV ANRS cohort CO4.** *Arch Intern Med* 2010; **170**:1228–1238.
3. Triant VA. **HIV infection and coronary heart disease: an intersection of epidemics.** *J Infect Dis* 2012; **205 (Suppl 3)**:S355–S361.
4. Friis-Moller N, Sabin CA, Weber R, D'Arminio MA, El Sadr WM, Reiss P, *et al.* **Combination antiretroviral therapy and the risk of myocardial infarction.** *N Engl J Med* 2003; **349**:1993–2003.
5. Phillips AN, Carr A, Neuhaus J, Visnegarwala F, Prineas R, Burman WJ, *et al.* **Interruption of antiretroviral therapy and risk of cardiovascular disease in persons with HIV-1 infection: exploratory analyses from the SMART trial.** *Antivir Ther* 2008; **13**:177–187.
6. Masia M, Padilla S, Garcia N, Jarrin I, Bernal E, Lopez N, *et al.* **Endothelial function is impaired in HIV-infected patients with lipodystrophy.** *Antivir Ther* 2010; **15**:101–110.
7. Sanz E. Abacavir-myocardial infarction. *WHO Signal* 5 A.D. May 4–6 2005.
8. Sabin CA, Worm SW, Weber R, Reiss P, El Sadr W, Dabis F, *et al.* **Use of nucleoside reverse transcriptase inhibitors and risk of myocardial infarction in HIV-infected patients enrolled in the D:A:D study: a multicohort collaboration.** *Lancet* 2008; **371**:1417–1426.
9. Strategies for Management of Anti-Retroviral Therapy/INSIGHT; DAD Study Groups. **Use of nucleoside reverse transcriptase inhibitors and risk of myocardial infarction in HIV-infected patients.** *AIDS* 2008; **22**:F17–F24.
10. Worm SW, Sabin C, Weber R, Reiss P, El Sadr W, Dabis F, *et al.* **Risk of myocardial infarction in patients with HIV infection exposed to specific individual antiretroviral drugs from the 3 major drug classes: the data collection on adverse events of anti-HIV drugs (D:A:D) study.** *J Infect Dis* 2010; **201**:318–330.
11. Obel N, Farkas DK, Kronborg G, Larsen CS, Pedersen G, Riis A, *et al.* **Abacavir and risk of myocardial infarction in HIV-infected patients on highly active antiretroviral therapy: a population-based nationwide cohort study.** *HIV Med* 2010; **11**:130–136.

12. Brothers CH, Hernandez JE, Cutrell AG, Curtis L, Ait-Khaled M, Bowlin SJ, *et al.* **Risk of myocardial infarction and abacavir therapy: no increased risk across 52 GlaxoSmithKline-sponsored clinical trials in adult subjects.** *J Acquir Immune Defic Syndr* 2009; **51**:20–28.
13. Bedimo RJ, Westfall AO, Drechsler H, Vidiella G, Tebas P. **Abacavir use and risk of acute myocardial infarction and cerebrovascular events in the highly active antiretroviral therapy era.** *Clin Infect Dis* 2011; **53**:84–91.
14. Ribaudo HJ, Benson CA, Zheng Y, Koletar SL, Collier AC, Lok JJ, *et al.* **No risk of myocardial infarction associated with initial antiretroviral treatment containing abacavir: short and long-term results from ACTG A5001/ALLRT.** *Clin Infect Dis* 2011; **52**:929–940.
15. Gunthard HF, Aberg JA, Eron JJ, Hoy JF, Telenti A, Benson CA, *et al.* **Antiretroviral treatment of adult HIV infection: 2014 recommendations of the International Antiviral Society-USA Panel.** *JAMA* 2014; **312**:410–425.
16. **GESIDA/National AIDS Plan: Consensus document on antiretroviral therapy in adults infected by the human immunodeficiency virus (Updated January 2015).** *Enferm Infecc Microbiol Clin* 2015; **33**:543.e1–543.e43.
17. Ley K, Laudanna C, Cybulsky MI, Nourshargh S. **Getting to the site of inflammation: the leukocyte adhesion cascade updated.** *Nat Rev Immunol* 2007; **7**:678–689.
18. Jackson SP. **Arterial thrombosis–insidious, unpredictable and deadly.** *Nat Med* 2011; **17**:1423–1436.
19. Offermanns S. **Activation of platelet function through G protein-coupled receptors.** *Circ Res* 2006; **99**:1293–1304.
20. Falcinelli E, Francisci D, Belfiori B, Petito E, Guglielmini G, Malincarne L, *et al.* **In vivo platelet activation and platelet hyperreactivity in abacavir-treated HIV-infected patients.** *Thromb Haemost* 2013; **110**:349–357.
21. Satchell CS, O'Halloran JA, Cotter AG, Peace AJ, O'Connor EF, Tedesco AF, *et al.* **Increased platelet reactivity in HIV-1-infected patients receiving abacavir-containing antiretroviral therapy.** *J Infect Dis* 2011; **204**:1202–1210.
22. Baum PD, Sullam PM, Stoddart CA, McCune JM. **Abacavir increases platelet reactivity via competitive inhibition of soluble guanylyl cyclase.** *AIDS* 2011; **25**:2243–2248.
23. De Pablo C, Orden S, Apostolova N, Blanquer A, Esplugues JV, Alvarez A. **Abacavir and didanosine induce the interaction between human leukocytes and endothelial cells through Mac-1 upregulation.** *AIDS* 2010; **24**:1259–1266.
24. De Pablo C, Orden S, Calatayud S, Marti-Cabrera M, Esplugues JV, Alvarez A. **Differential effects of Tenofovir/Emtricitabine and Abacavir/Lamivudine on human leukocyte recruitment.** *Antivir Ther* 2012; **17**:1615–1619.
25. De Pablo C, Orden S, Peris JE, Barrachina MD, Esplugues JV, Alvarez A. **Profile of leukocyte-endothelial cell interactions induced in venules and arterioles by nucleoside reverse-transcriptase inhibitors *in vivo*.** *J Infect Dis* 2013; **208**:1448–1453.
26. Yegutkin GG. **Nucleotide- and nucleoside-converting ectoenzymes: important modulators of purinergic signalling cascade.** *Biochim Biophys Acta* 2008; **1783**:673–694.
27. Idzko M, Ferrari D, Eltzschig HK. **Nucleotide signalling during inflammation.** *Nature* 2014; **509**:310–317.
28. Burnstock G, Ralevic V. **Purinergic signaling and blood vessels in health and disease.** *Pharmacol Rev* 2014; **66**:102–192.
29. Solle M, Labasi J, Perregaux DG, Stam E, Petrushova N, Koller BH, *et al.* **Altered cytokine production in mice lacking P2X(7) receptors.** *J Biol Chem* 2001; **276**:125–132.
30. Hickey MJ, Granger DN, Kubes P. **Molecular mechanisms underlying IL-4-induced leukocyte recruitment in vivo: a critical role for the alpha 4 integrin.** *J Immunol* 1999; **163**:3441–3448.
31. House SD, Lipowsky HH. **Leukocyte-endothelium adhesion: microhemodynamics in mesentery of the cat.** *Microvasc Res* 1987; **34**:363–379.
32. Wang X, Chai H, Lin PH, Yao Q, Chen C. **Roles and mechanisms of human immunodeficiency virus protease inhibitor ritonavir and other antihuman immunodeficiency virus drugs in endothelial dysfunction of porcine pulmonary arteries and human pulmonary artery endothelial cells.** *Am J Pathol* 2009; **174**:771–781.
33. Moyle G, Boffito M, Fletcher C, Higgs C, Hay PE, Song IH, *et al.* **Steady-state pharmacokinetics of abacavir in plasma and intracellular carbovir triphosphate following administration of abacavir at 600 milligrams once daily and 300 milligrams twice daily in human immunodeficiency virus-infected subjects.** *Antimicrob Agents Chemother* 2009; **53**:1532–1538.
34. Coddou C, Yan Z, Obsil T, Huidobro-Toro JP, Stojilkovic SS. **Activation and regulation of purinergic P2X receptor channels.** *Pharmacol Rev* 2011; **63**:641–683.
35. Donnelly-Roberts DL, Namovic MT, Surber B, Vaidyanathan SX, Perez-Medrano A, Wang Y, *et al.* **[3H]A-804598 ([3H]2-cyano-1-[(1S)-1-phenylethyl]-3-quinolin-5-ylguanidine) is a novel, potent, and selective antagonist radioligand for P2X7 receptors.** *Neuropharmacology* 2009; **56**:223–229.
36. Neelands TR, Burgard EC, Uchic ME, McDonald HA, Niforatos W, Faltynek CR, *et al.* **2′, 3′-O-(2,4,6,trinitrophenyl)-ATP and A-317491 are competitive antagonists at a slowly desensitizing chimeric human P2X3 receptor.** *Br J Pharmacol* 2003; **140**:202–210.
37. Brandely M, Lagrange PH, Huttrel B. **Effects of suramin on the in vivo antimicrobial resistance against Listeria monocytogenes and Mycobacterium bovis (BCG) in mice.** *Clin Exp Immunol* 1986; **63**:118–126.
38. Diaz-Hernandez M, Diez-Zaera M, Sanchez-Nogueiro J, Gomez-Villafuertes R, Canals JM, Alberch J, *et al.* **Altered P2X7-receptor level and function in mouse models of Huntington's disease and therapeutic efficacy of antagonist administration.** *FASEB J* 2009; **23**:1893–1906.
39. Soto F, Lambrecht G, Nickel P, Stuhmer W, Busch AE. **Antagonistic properties of the suramin analogue NF023 at heterologously expressed P2X receptors.** *Neuropharmacology* 1999; **38**:141–149.
40. Henriquez M, Herrera-Molina R, Valdivia A, Alvarez A, Kong M, Munoz N, *et al.* **ATP release due to Thy-1-integrin binding induces P2X7-mediated calcium entry required for focal adhesion formation.** *J Cell Sci* 2011; **124 (Pt 9)**:1581–1588.
41. Prior HM, Yates MS, Beech DJ. **Role of K+ channels in A2A adenosine receptor-mediated dilation of the pressurized renal arcuate artery.** *Br J Pharmacol* 1999; **126**:494–500.
42. Clementi E, Brown GC, Foxwell N, Moncada S. **On the mechanism by which vascular endothelial cells regulate their oxygen consumption.** *Proc Natl Acad Sci U S A* 1999; **96**:1559–1562.
43. Badrnya S, Schrottmaier WC, Kral JB, Yaiw KC, Volf I, Schabhauer G, *et al.* **Platelets mediate oxidized low-density lipoprotein-induced monocyte extravasation and foam cell formation.** *Arterioscler Thromb Vasc Biol* 2014; **34**:571–580.
44. Kukulski F, Ben YF, Lefebvre J, Warny M, Tessier PA, Sevigny J. **Extracellular nucleotides mediate LPS-induced neutrophil migration in vitro and in vivo.** *J Leukoc Biol* 2007; **81**:1269–1275.
45. Meis S, Hamacher A, Hongwiset D, Marzian C, Wiese M, Eckstein N, *et al.* **NF546 [4,4′-(carbonylbis(imino-3,1-phenylene-carbonylimino-3,1-(4-methyl-phenylene)-carbonylimino))-bis(1,3-xylene-alpha,alpha′-diphosphonic acid) tetra sodium salt] is a non-nucleotide P2Y11 agonist and stimulates release of interleukin-8 from human monocyte-derived dendritic cells.** *J Pharmacol Exp Ther* 2010; **332**:238–247.
46. Kemp PA, Sugar RA, Jackson AD. **Nucleotide-mediated mucin secretion from differentiated human bronchial epithelial cells.** *Am J Respir Cell Mol Biol* 2004; **31**:446–455.
47. Gavins FN. **Intravital microscopy: new insights into cellular interactions.** *Curr Opin Pharmacol* 2012; **12**:601–607.
48. Hughes EL, Gavins FN. **Troubleshooting methods: Using intravital microscopy in drug research.** *J Pharmacol Toxicol Methods* 2010; **61**:102–112.
49. Goetz DJ, Greif DM, Shen J, Luscinskas FW. **Cell-cell adhesive interactions in an in vitro flow chamber.** *Methods Mol Biol* 1999; **96**:137–145.
50. Gee DJ, Wright LK, Zimmermann J, Cole K, Soule K, Ubowski M. **Dimethylsulfoxide exposure modulates HL-60 cell rolling interactions.** *Biosci Rep* 2012; **32**:375–382.
51. Victor VM, Rocha M, Banuls C, Alvarez A, De Pablo C, Sanchez-Serrano M, *et al.* **Induction of oxidative stress and human leukocyte/endothelial cell interactions in polycystic ovary syndrome patients with insulin resistance.** *J Clin Endocrinol Metab* 2011; **96**:3115–3122.

52. Luu NT, Madden J, Calder PC, Grimble RF, Sheaman CP, Chan T, *et al.* **Comparison of the pro-inflammatory potential of monocytes from healthy adults and those with peripheral arterial disease using an in vitro culture model.** *Atherosclerosis* 2007; **193**:259–268.
53. Gallego MJ, Zoja C, Morigi M, Micheletti G, Imberti B, Foppolo M, *et al.* **Cyclosporine enhances leukocyte adhesion to vascular endothelium under physiologic flow conditions.** *Am J Kidney Dis* 1996; **28**:23–31.
54. Guba M, Steinbauer M, Buchner M, Frolich D, Farkas S, Jauch KW, *et al.* **Differential effects of short-term ace- and AT1-receptor inhibition on postischemic injury and leukocyte adherence in vivo and in vitro.** *Shock* 2000; **13**:190–196.
55. Bours MJ, Dagnelie PC, Giuliani AL, Wesselius A, Di VF. **P2 receptors and extracellular ATP: a novel homeostatic pathway in inflammation.** *Front Biosci (Schol Ed)* 2011; **3**:1443–1456.
56. Mehta N, Kaur M, Singh M, Chand S, Vyas B, Silakari P, *et al.* **Purinergic receptor P2X(7): a novel target for anti-inflammatory therapy.** *Bioorg Med Chem* 2014; **22**:54–88.
57. Suh BC, Kim JS, Namgung U, Ha H, Kim KT. **P2X7 nucleotide receptor mediation of membrane pore formation and superoxide generation in human promyelocytes and neutrophils.** *J Immunol* 2001; **166**:6754–6763.
58. Martinon F, Mayor A, Tschopp J. **The inflammasomes: guardians of the body.** *Annu Rev Immunol* 2009; **27**:229–265.
59. Lohman AW, Billaud M, Isakson BE. **Mechanisms of ATP release and signalling in the blood vessel wall.** *Cardiovasc Res* 2012; **95**:269–280.
60. Bours MJ, Swennen EL, Di Virgilio F, Cronstein BN, Dagnelie PC. **Adenosine 5′-triphosphate and adenosine as endogenous signaling molecules in immunity and inflammation.** *Pharmacol Ther* 2006; **112**:358–404.
61. Shryock JC, Belardinelli L. **Adenosine and adenosine receptors in the cardiovascular system: biochemistry, physiology, and pharmacology.** *Am J Cardiol* 1997; **79 (12A)**:2–10.
62. Zernecke A, Bidzhekov K, Ozuyaman B, Fraemohs L, Liehn EA, Luscher-Firzlaff JM, *et al.* **CD73/ecto-5′-nucleotidase protects against vascular inflammation and neointima formation.** *Circulation* 2006; **113**:2120–2127.

ARTÍCULO 8

Are mitochondrial fusion and fission impaired in leukocytes of type 2 diaberic patients?

Díaz-Morales N, Rovira-Llopis S, Bañuls C, Escribano-López I, Martínez de Marañón A, López-Domenech S, **Orden S**, Roldán-Torres I, Álvarez Á, Veses S, Jover A, Rocha M, Hernández-Mijares A, Víctor VM.

Antioxidants & Redox Signalling 2016, en prensa

ARS-2016-6707-ver9-DiazMorales_1P
Type: news

ANTIOXIDANTS & REDOX SIGNALING
Volume 00, Number 00, 2016
© Mary Ann Liebert, Inc.
DOI: 10.1089/ars.2016.6707

NEWS & VIEWS

Are Mitochondrial Fusion and Fission Impaired in Leukocytes of Type 2 Diabetic Patients?

Noelia Diaz-Morales,[1] Susana Rovira-Llopis,[1,2] Celia Bañuls,[1,2] Irene Escribano-Lopez,[1] Arantxa Martinez de Marañon,[1] Sandra Lopez-Domenech,[1] Samuel Orden,[3] Ildefonso Roldan-Torres,[4] Angeles Alvarez,[3] Silvia Veses,[1] Ana Jover,[1] Milagros Rocha,[1–3] Antonio Hernandez-Mijares,[1,2,3,5] and Victor M. Victor[1–3]

Abstract

Mitochondrial fusion/fission alterations have been evaluated in different tissues of type 2 diabetic (T2D) patients. However, it is not known whether mitochondrial dynamics is disturbed in the leukocytes of T2D patients and whether glycemic control affects its regulation. Anthropometric and metabolic parameters in 91 T2D patients (48 with glycated hemoglobin [HbA1c] <6.5% and 43 with HbA1c >6.5%) were characteristic of the disease when compared with 78 control subjects. We observed increased reactive oxygen species production in leukocytes from diabetic patients, together with a reduced mitochondrial oxygen consumption rate, especially in poorly controlled patients. Mitochondrial fusion was reduced and fission was increased in diabetic patients, and both features were accentuated in patients with poor glycemic control. Furthermore, leukocyte rolling flux rose in parallel to HbA1c levels. The induction of leukocyte–endothelial interactions in diabetic patients was related to reduced mitochondrial fusion and higher mitochondrial fission. Our findings suggest that mitochondrial dynamics could be influenced by glycemic control in leukocytes of diabetic patients, in which there is decreased mitochondrial fusion and elevated fission related to enhanced leukocyte–endothelial interactions. These findings lead to the hypothesis that poor glycemic control during T2D may alter mitochondrial dynamics and could eventually promote leukocyte–endothelial interactions and the onset of cardiovascular diseases. *Antioxid. Redox Signal.* 00, 000–000.

Introduction

ADEQUATE GLYCEMIC CONTROL is the key for preventing the cardiovascular complications associated with type 2 diabetes (T2D). Numerous studies suggest that T2D is closely related to mitochondrial dysfunction and oxidative stress (5). Mitochondria form a complex and dynamic network that undergoes continuous cycles of fusion and fission events. This phenomenon, known as mitochondrial dynamics, is a quality control system that is crucial in maintaining a healthy mitochondrial population and also a mechanism of adaptation to cellular energetic demands. The core machinery for mitochondrial fusion and fission processes consists of several dynamin-related GTPases. Proteins involved in mitochondrial fusion include optic atrophy 1 (OPA1) and mitofusins, 1 (MFN1) and 2 (MFN2), and mitochondrial fission is mainly orchestrated by fission protein 1 (FIS1) and dynamin-related protein 1 (DRP1). The fusion process begins when mitofusins anchored to the outer mitochondrial membranes on opposing mitochondria interact with each other, then the outer membranes fuse. Afterward, OPA1 induces inner membrane tethering and fusion. During the fission process, DRP1 forms

[1]Service of Endocrinology, Foundation for the Promotion of Health and Biomedical Research in the Valencian Region (FISABIO), University Hospital Doctor Peset, Valencia, Spain.
[2]Institute of Health Research INCLIVA, University of Valencia, Valencia, Spain.
[3]CIBERehd—Department of Pharmacology and Physiology, University of Valencia, Valencia, Spain.
[4]Service of Cardiology, University Hospital Doctor Peset, Foundation for the Promotion of Health and Biomedical Research in the Valencian Region (FISABIO), Valencia, Spain.
[5]Department of Medicine, University of Valencia, Valencia, Spain.

Innovation

Mitochondrial function is altered in type 2 diabetes (T2D), in part, due to altered mitochondrial dynamics. Glycemic control is essential for preventing the T2D-associated cardiovascular complications. However, there are no studies that question whether glycemic control influences mitochondrial dynamics or the impact of these disturbances on the increased leukocyte–endothelium interactions observed in T2D patients. Our results suggest that poor glycemic control may inhibit mitochondrial fusion and enhance mitochondrial fission, highlighting glycemic control in T2D as crucial to maintain a healthy mitochondrial network. These changes in mitochondrial dynamics may promote leukocyte–endothelium contact, favoring the onset of cardiovascular disease.

rings around mitochondria at fission sites, which are favored after FIS1 and DRP1 interaction (9).

Alterations in the mitochondrial fission and fusion machinery are directly associated with mitochondrial dysfunction as fusion is necessary to allow functional mitochondria to complement dysfunctional mitochondria. Furthermore, mitochondrial networks have been reported to permit the transmission of membrane potential from areas of high oxygen availability to those with low oxygen levels to increase ATP production (9). As metabolic diseases are associated with defects in energy production and utilization, and mitochondria are the powerhouses of the cell, altered mitochondrial function represents a key pathophysiological feature of metabolic diseases. In this sense, alterations in mitochondrial fusion and fission processes have been detected in different tissues during T2D (3).

The onset of atherosclerosis involves the recruitment of leukocytes to the endothelium that begins when these cells roll over the endothelial cells until coming to a halt, after which they finally adhere firmly. In T2D, a potential role of mitochondrial dynamics in the maintenance of endothelial cell function has been postulated (8). However, leukocyte mitochondrial dynamics has not been evaluated in T2D, nor the influence of glycemic control on this process.

The aim of the current study was to evaluate mitochondrial function and mitochondrial dynamics in leukocytes of T2D patients, considering the degree of glycemic control and comparing it with that in control subjects. In addition, the potential regulation of leukocyte–endothelial interactions by mitochondrial dynamics was evaluated.

Metabolic Parameters

We evaluated 91 T2D patients, divided into two groups according to glycated hemoglobin (HbA1c) levels below and higher than 6.5% ($n=48$, $n=43$, respectively), and compared them with 78 control subjects (Table 1). Diabetic patients exhibited greater weight, body–mass index (BMI), waist circumference, waist-to-hip ratio (WHR), fasting glucose, insulin, homeostasis model assessment of insulin resistance (HOMA-IR), and HbA1c ($p<0.001$) than controls. Blood

◀T1

TABLE 1. ANTHROPOMETRIC PARAMETERS, HYDROCARBONATED METABOLISM PARAMETERS, LIPID PROFILE, AND INFLAMMATORY MARKERS OF THE STUDY POPULATION

	Control	*T2D HbA1c <6.5*	*T2D HbA1c >6.5*
n	78	48	43
Male %	44.4	50.0	62.8
Age (years)	57.6 ± 16.0	58.5 ± 8.2	57.8 ± 8.1
Weight (kg)	67.7 ± 12.7	84.7 ± 16.3***	87.0 ± 18.4***
BMI (kg/m^2)	25.3 ± 3.9	31.8 ± 5.6***	30.8 ± 5.6***
Waist (cm)	87.0 ± 15.2	105.5 ± 12.9***	107.2 ± 13.0***
WHR	0.86 ± 0.11	0.96 ± 0.08***	0.98 ± 0.07***
SBP (mmHg)	123.9 ± 15.6	140.1 ± 14.6***	134.9 ± 16.9**
DBP (mmHg)	73.1 ± 8.8	82.7 ± 8.2***	79.0 ± 7.7**
Glucose (mg/dl)	92.5 ± 13.2	114.7 ± 27.4**	168.2 ± 55.2***-†††
Insulin (μUI/ml)	8.65 ± 4.16	12.21 ± 5.66*	16.98 ± 9.70***-††
HOMA-IR	2.06 ± 1.28	3.57 ± 2.05**	6.94 ± 4.11***-†††
HbA1c (%)	5.30 ± 0.30	6.07 ± 0.43***	8.14 ± 1.32***-†††
(mmol/mol)	34.4 ± 3.3	42.8 ± 4.7***	65.4 ± 14.5***-†††
Total cholesterol (mg/dl)	202.1 ± 31.9	177.1 ± 32.5***	168.9 ± 42.8***
HDL-c (mg/dl)	52.9 ± 13.0	45.5 ± 11.2**	41.5 ± 8.9***
LDL-c (mg/dl)	129.8 ± 29.3	106.0 ± 31.2***	93.9 ± 34.5***
Triglycerides (mg/dl)	83.5 (63.8; 122.5)	120 (94.0; 167.0)**	134.5 (91.5; 234.0)***
hs-CRP (mg/l)	1.91 (0.56; 3.55)	2.46 (1.35; 7.94)*	3.24 (1.56; 5.36)*

Data are expressed as mean ± standard deviation for parametric data or as median (25th and 75th percentiles) for nonparametric data. Nonparametric data were log transformed for statistic analysis. One-way ANOVA with Tukey's HSD *post hoc* test was used to compare means of normally distributed samples. The chi-square test was used to compare proportions among groups.

HOMA-IR = fasting insulin (mU/ml) · fasting glucose (m*M*)/22.5.

*$p<0.05$, **$p<0.01$, and ***$p<0.001$ with regard to controls and $^{\dagger\dagger}p<0.01$ and $^{\dagger\dagger\dagger}p<0.001$ with respect to HbA1c <6.5% group using one-way ANOVA with Tukey's HSD *post hoc* test.

T2D, type 2 diabetes; BMI, body–mass index; WHR, waist-to-hip ratio; SBP, systolic blood pressure; DBP, diastolic blood pressure; HOMA-IR, homeostasis model assessment of insulin resistance; HbA1c, glycated hemoglobin; HDL-c, high-density lipoprotein cholesterol; LDL-c, low-density lipoprotein cholesterol; hs-CRP, high-sensitive C-reactive protein; ANOVA, analysis of variance; HSD, honestly significant difference.

pressure was also higher in T2D patients than in controls ($p<0.01$). T2D patients with poor glycemic control (HbA1c >6.5%) showed increased glucose and insulin levels with respect to well-controlled T2D patients (HbA1c <6.5%) ($p<0.001$ and $p<0.01$, respectively) and therefore higher HOMA-IR ($p<0.001$). The lipid profile of diabetic subjects was characterized by higher triglyceride and lower high-density lipoprotein cholesterol (HDL-c) levels with respect to controls ($p<0.001$). However, due to the lipid-lowering treatment received by most of the T2D patients (62.5% were taking statins and 5.8% ezetimibe), levels of total cholesterol and low-density lipoprotein cholesterol (LDL-c) were reduced ($p<0.001$). Inflammation, measured as high-sensitive C-reactive protein (hs-CRP) levels, was also more pronounced in diabetic patients *versus* controls ($p<0.05$).

Mitochondrial Function and Oxidative Stress

F1 ► T2D patients exhibited lower leukocyte O_2 consumption rates than healthy subjects (Fig. 1A, $p<0.05$). Leukocytes from diabetic patients displayed enhanced levels of mitochondrial reactive oxygen species (ROS) (Fig. 1B, $p<0.01$) and total ROS (Fig. 1C, $p<0.05$).

When evaluated separately according to HbA1c levels below and higher than 6.5%, significant differences were specifically found in the O_2 consumption rates of T2D patients with HbA1c >6.5% (Fig. 1D, $p<0.01$ with respect to controls, $p<0.05$ between HbA1c <6.5% and HbA1c >6.5% groups), suggesting that impaired mitochondrial respiration is related to poor glycemic control. Indeed, we found a negative correlation between O_2 consumption and HbA1c levels ($r=-0.317$; $p<0.05$). However, mitochondrial and total ROS levels increased similarly in both groups of T2D patients regardless of their glycemic control status (Fig. 1E, F).

Fusion and Fission Protein Expression

The expression of MFN1, MFN2, and OPA1, which are implicated in mitochondrial fusion, was downregulated in T2D patients when compared with the control group (Fig. 2A, ◄F2 MFN1 $p<0.05$; Fig. 2B, MFN2 $p<0.01$; and Fig. 2C, OPA1 $p<0.01$).

When data were split by HbA1c, we observed that MFN1 expression was specifically reduced in well-controlled diabetic patients (Fig. 2D, $p<0.05$), whereas MFN2 levels were specifically reduced in patients with HbA1c >6.5% (Fig. 2E, $p<0.05$). Decreases in the expression of OPA1 were observed in both groups of diabetic patients, being more pronounced in those presenting HbA1c values over 6.5% (Fig. 2F, $p<0.05$ in patients with HbA1c <6.5%, and $p<0.01$ when HbA1c >6.5%).

Regarding fission proteins, we found higher expression of FIS1 when T2D patients were compared with controls and a similar expression of DRP1 in T2D and control subjects (Fig. 3A, FIS1 $p<0.05$; and Fig. 3B, DRP1). The differences ◄F3 found in FIS1 seemed to be due to an increase in its expression in the patients with HbA1c >6.5% (Fig. 3C, $p<0.05$). Although DRP1 protein levels were increased in patients with HbA1c >6.5%, there were no statistical differences between groups (Fig. 3D).

Leukocyte–Endothelium Interactions

When leukocyte–endothelium interactions were assessed in controls and T2D patients, we observed a decrease in

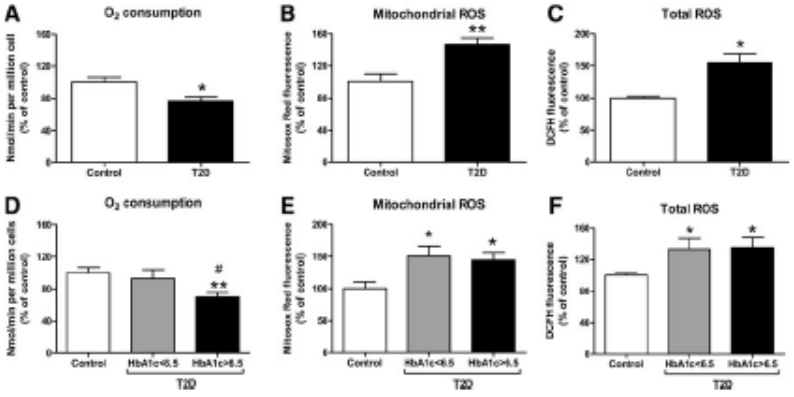

FIG. 1. Mitochondrial function and oxidative stress in T2D patients compared with healthy subjects. $n=20$ subjects per group. **(A)** Leukocyte O_2 consumption rates (measured as nmol/min per million cell and expressed as percentage of control). **(B)** Mitochondrial ROS production (measured as Mitosox Red fluorescence and expressed as percentage of control). **(C)** Total ROS production (measured as DCFH fluorescence and expressed as percentage of control). Effects of HbA1c levels on **(D)** O_2 consumption, **(E)** mitochondrial ROS, and **(F)** total ROS in well-controlled T2D patients (HbA1c <6.5%), poorly controlled T2D patients (HbA1c >6.5%), and healthy subjects. $^*p<0.05$ and $^{**}p<0.01$ with regard to controls and $^\#p<0.05$ with regard to HbA1c <6.5% T2D patients using Student's *t*-test or one-way ANOVA with Tukey's HSD *post hoc* test. ANOVA, analysis of variance; DCFH, dichlorodihydrofluorescein; HSD, honestly significant difference; ROS, reactive oxygen species; T2D, type 2 diabetes.

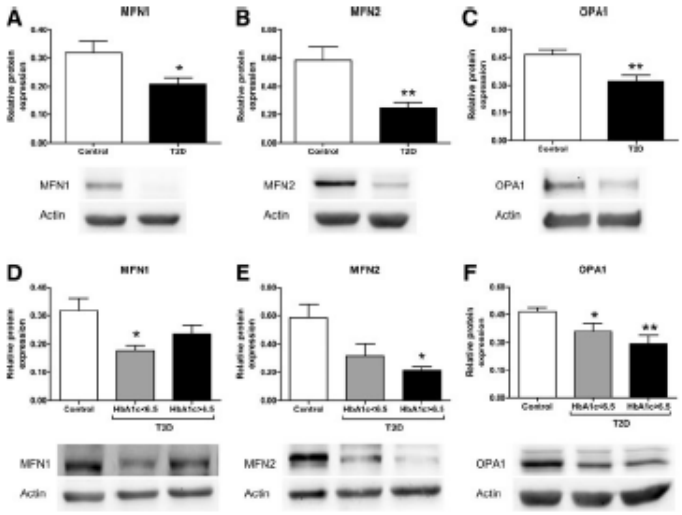

FIG. 2. Effect of T2D on mitochondrial fusion. $n = 15$ subjects per group. **(A)** Protein levels of MFN1 and representative WB images of MFN1 and actin in T2D and healthy subjects. **(B)** Protein levels of MFN2 and representative WB images of MFN2 and actin in T2D and healthy subjects. **(C)** Protein levels of OPA1 and representative WB images of OPA1 and actin in T2D and control subjects. Effects of HbA1c level on the protein expression of **(D)** MFN1, **(E)** MFN2, and **(F)** OPA1 in well-controlled T2D patients (HbA1c < 6.5%) and in T2D patients with poor glycemic control (HbA1c > 6.5%) compared with healthy subjects. $*p<0.05$ and $**p<0.01$ with regard to controls using Student's *t*-test or one-way ANOVA with Tukey's HSD *post hoc* test. MFN1, mitofusin 1; MFN2, mitofusin 2; OPA1, optic atrophy 1; WB, Western blot.

F4 ▶ leukocyte rolling velocity (Fig. 4A, $p<0.001$) and an increase in leukocyte rolling flux and adhesion (Fig. 4B, C, $p<0.001$) in T2D patients.

No significant differences were found in leukocyte rolling velocity between the two diabetic groups when separated by HbA1c levels below and above 6.5% (Fig. 4D). However, patients with higher levels of HbA1c showed higher leukocyte rolling flux than those showing better glycemic control ($p<0.05$) (Fig. 4E). Leukocyte adhesion to the endothelium was increased similarly in both diabetic groups (Fig. 4F).

Correlations

We explored potential correlations among fusion/fission proteins, anthropometric/biochemical parameters, oxidative stress determinations, and leukocyte–endothelium parameters. We found that HbA1c levels correlated negatively with the fusion proteins, MFN2 and OPA1 ($r=-0.415$, $p<0.05$; $r=-0.525$, $p<0.01$, respectively), and positively with FIS1 ($r=0.342$, $p<0.05$). Systolic blood pressure (SBP) was positively correlated with FIS1 protein levels ($r=0.704$, $p<0.01$). Interestingly, negative correlations were found between mitochondrial O_2 consumption and the fission proteins, FIS1 and DRP1 ($r=-0.571$, $p<0.01$; $r=-0.441$, $p<0.05$, respectively).

Leukocyte rolling velocity correlated positively with MFN1 ($r=0.502$, $p<0.01$) and OPA1 ($r=0.487$; $p<0.05$) and negatively with FIS1 expression ($r=-0.460$, $p<0.01$). Furthermore, a negative correlation was found between leukocyte adhesion and MFN1 ($r=-0.498$, $p<0.05$) and DRP1 ($r=-0.391$, $p<0.05$).

Hyperglycemia causes imbalances in the cellular redox state, inducing vascular complications during T2D. In previous studies, we have shown that mitochondrial dysfunction and ROS production are present in the leukocytes of T2D patients and are enhanced in patients with macro- and microvascular complications (2, 7). In the present study, we confirm that increased mitochondrial and total ROS production occurs in leukocytes of T2D patients and that reduced mitochondrial O_2 consumption is present specifically in those with poor glycemic control (HbA1c >6.5%), suggesting that leukocyte mitochondrial function is altered during long-term exposure to glucose. Indeed, it has been reported that mitochondrial respiration is inversely correlated with HbA1c levels in diabetic individuals.

Mitochondrial function and redox balance are closely related to mitochondrial dynamics. Defects in the fusion/fission machinery promote alterations in oxidative phosphorylation due to loss of respiratory complex activity, reduced membrane potential, and decreased O_2 consumption (9). Our results indicate that mitochondrial fusion is reduced in the leukocytes of T2D patients as MFN1, MFN2, and OPA1 protein levels are decreased. Intriguingly, MFN2 protein levels fell specifically in poorly controlled patients and OPA1 levels seemed to drop even further in this group. Moreover, we found a negative correlation between HbA1c and MFN2/OPA1 protein levels, which indicates that loss of glycemic control could inhibit mitochondrial fusion.

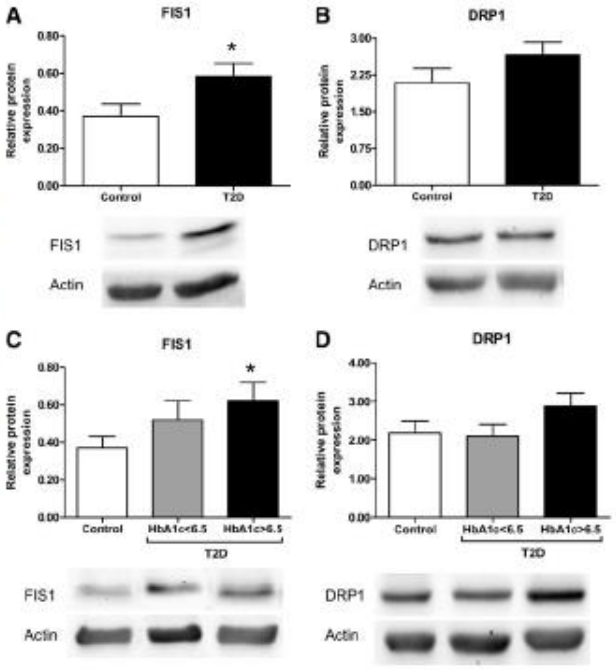

FIG. 3. Evaluation of the relative protein expression of mitochondrial fission markers in T2D patients and healthy subjects. $n = 15$ subjects per group. **(A)** Protein levels of FIS1 and representative WB images of FIS1 and actin in T2D and healthy subjects. **(B)** Protein levels of DRP1 and representative WB images of DRP1 and actin in T2D and healthy subjects. Effect of HbA1c levels on the protein expression of **(C)** FIS1 and **(D)** DRP1 in well-controlled T2D patients (HbA1c < 6.5%) and in T2D patients with poor glycemic control (HbA1c > 6.5%) compared with healthy subjects. $^{*}p < 0.05$ with regard to controls using Student's *t*-test or one-way ANOVA with Tukey's HSD *post hoc* test. DRP1, dynamin-related protein 1; FIS1, fission protein 1.

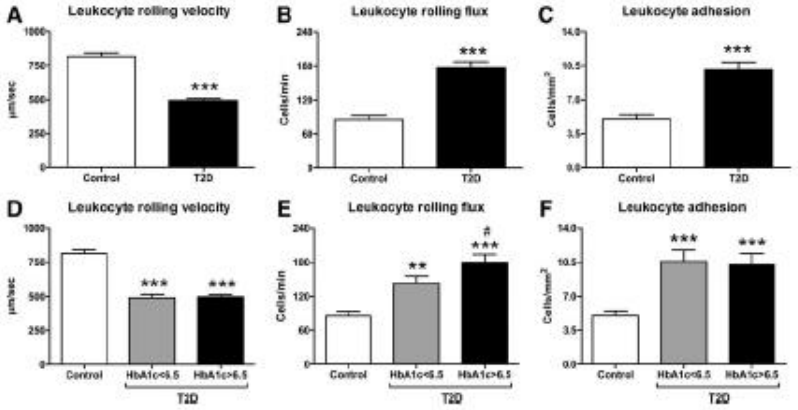

FIG. 4. Evaluation of leukocyte–endothelium interactions in T2D patients and healthy subjects. $n = 30$ subjects per group. **(A)** Leukocyte rolling velocity (measured as μm/s); **(B)** leukocyte rolling flux (expressed as cells/min); **(C)** leukocyte adhesion (measured as cells/mm^2). Effects of HbA1c levels on leukocyte rolling velocity **(D)**, rolling flux **(E)**, and adhesion **(F)** in well-controlled T2D patients (HbA1c <6.5%) and in T2D patients with poor glycemic control (HbA1c >6.5%) compared with healthy subjects. $^{**}p < 0.01$ and $^{***}p < 0.001$ with regard to controls and $^{\#}p < 0.05$ with regard to HbA1c <6.5% T2D patients using Student's *t*-test or one-way ANOVA with Tukey's HSD *post hoc* test.

Previous research has revealed that MFN2 protein and mRNA expression in the skeletal muscle of T2D patients is reduced and is related to insulin resistance (1). Besides its role in mitochondrial fusion and oxidative phosphorylation, MFN2 is involved in Ca^{2+} signaling, amplification of apoptotic signals, and the control of ER morphology. In addition, disturbances in MFN2 expression can also alter ER homeostasis and promote ER stress. In this sense, Ngoh *et al.* showed that MFN2 is essential to the proper temporal sequence of the ER stress response and that loss of Mfn2 causes upregulation of the proapoptotic factor, C/EBP homologous protein (CHOP) (4). Our present results are in accordance with these findings since we observed reduced levels of MFN2 in T2D patients with poor glycemic control, while in a previous cohort of T2D patients, the poorly controlled population displayed enhanced CHOP mRNA and protein expression levels (6). Furthermore, OPA1, the main orchestrator of inner mitochondrial membrane fusion, was reduced in parallel to HbA1c levels in our T2D population, with a strong negative correlation between OPA1 and HbA1c levels, thus suggesting that mitochondrial fusion is compromised during T2D, especially when patients are poorly controlled, and highlighting that glycemic control in T2D is crucial to maintain a healthy mitochondrial network.

Regarding the process of mitochondrial fission, we observed an increase of FIS1 protein levels in the leukocytes of T2D patients, again specifically in poorly controlled T2D individuals. DRP1 levels increase in the HbA1c >6.5% T2D group, although not significantly. These results indicate that in addition to the inhibition of mitochondrial fusion during T2D, mitochondrial fission is enhanced and chronic hyperglycemia worsens this situation. In this context, an increase in mitochondrial fission has been described in other types of cells under hyperglycemia, such as podocytes and endothelial cells.

We have previously reported that leukocyte–endothelial interactions in T2D patients are increased and that HbA1c levels, mitochondrial dysfunction, oxidative stress, and ER stress are positively correlated with these increases (2, 6, 7). The present study widens our perspective by revealing a direct relationship between enhanced leukocyte–endothelium interactions and altered mitochondrial dynamics, namely reduced mitochondrial fusion and increased fission. Since ER stress and mitochondrial fusion/fission alterations are closely related, we believe that these molecular mechanisms are disturbed in T2D, probably as a consequence of chronic hyperglycemia, as they are enhanced during poor glycemic control. Consequently, leukocytes interact more frequently with the endothelium, which is likely to be a consequence of an increase in adhesion molecule expression on their surface. In addition, we found that enhanced mitochondrial fission positively correlated with SBP, a cardiovascular risk factor, in our T2D population. We hypothesize that changes in mitochondrial dynamics related to T2D promote leukocyte recruitment to vascular walls, eventually favoring the onset of cardiovascular diseases (CVDs). Further research is needed to clarify the potential relationship between abnormal mitochondrial fusion/fission processes and cardiovascular complications of T2D such as myocardial ischemia or peripheral artery disease, among others.

Whether glycemic control influences mitochondrial dynamics is a question that has never been addressed before. Herein, we provide evidence that poorly controlled diabetes represses mitochondrial fusion and promotes mitochondrial fission. These disturbances are accompanied by mitochondrial dysfunction and oxidative stress, all of which influence leukocyte–endothelial interactions. Overall, our findings suggest that mitochondrial dysfunction and altered mitochondrial dynamics in leukocytes during T2D exacerbate leukocyte–endothelium contact. Furthermore, they point to the possibility that poor glycemic control of the disease enhances these processes and can accelerate the onset of CVD.

Notes

Subjects

Ninety-one T2D patients attending the Endocrinology and Nutrition Service of the University Hospital Doctor Peset (Valencia, Spain) and 78 voluntary controls adjusted by age and sex were enrolled in this study. T2D was diagnosed according to the American Diabetes Association's criteria. Subjects with any of the following conditions were excluded from the study: autoimmune disease; history of CVD (including ischemic heart disease, peripheral vascular disease, stroke, and chronic disease related to cardiovascular risk); presence of morbid obesity; or infectious, hematological, malignant, organic, or inflammatory disease; and insulin treatment. Diabetic patients were separated according to HbA1c levels below and above 6.5%. This cutoff point has been established in our hospital's Endocrinology Department based on the distribution of HbA1c levels for patients in our clinical setting (University Hospital Dr. Peset, Valencia, Spain). In accordance with the American Diabetes Association, 6.5% cutoff point is associated with an inflection point for microvascular complications of diabetes.

The study protocols were approved by the Ethics Committee of the University Hospital Doctor Peset and conducted according to the Helsinki Declaration. All participants underwent the process of informed consent required by these institutions.

Blood samples were collected in fasting conditions between 8 a.m. and 10 a.m. Subjects underwent an anthropometric and analytical assessment, in which height (m), weight (kg), BMI (kg/m^2), waist and hip circumference (cm), and systolic and diastolic blood pressure (SBP/DBP; mmHg) were measured.

Biochemical determinations

Venous blood was collected from the antecubital vein and centrifuged at 1500 *g* for 10 min at 4°C. By means of an enzymatic method, levels of glucose, total cholesterol, and triglycerides were determined in serum. HDL-c levels were obtained using a Beckman LX20 analyzer (Beckman Corp.) and LDL-c content was calculated with Friedewald's formula. Insulin levels were determined by immunochemiluminescence, and insulin resistance was estimated using HOMA-IR = [fasting insulin (μU/ml) × fasting glucose (mg/dl))]/405). The percentage of HbA1c was determined with an automatic glycohemoglobin analyzer (Arkray, Inc.) and hs-CRP levels were assessed by an immunonephelometric assay.

Cell isolation

Leukocytes were isolated from citrated blood samples that were incubated with dextran (3%) for 45 min. Supernatant was collected, placed over Ficoll-Hypaque (GE Healthcare), and spun at 650 *g* for 25 min at room temperature. Erythrocytes

remaining in the pellet were lysed with lysis buffer for 5 min at room temperature and centrifuged at 240 *g*. The leukocyte pellet was then washed and resuspended in Hanks' balanced salt solution (HBSS; Sigma Aldrich). Cells were counted with a Scepter 2.0 cell counter (Millipore Iberica).

Measurement of O_2 consumption and ROS production

Leukocyte suspensions were placed in a gastight chamber and O_2 consumption was measured with a Clark-type O_2 electrode (Rank Brothers) (6). Sodium cyanide (10^{-3} *M*) was used to evaluate whether or not O_2 consumption was mainly mitochondrial (95–99%). The rate of O_2 consumption was calculated as nmol/min per million cells and expressed as a percentage of the control.

ROS production was assessed by fluorometry using a fluorescence microscope (IX81; Olympus) coupled with the static cytometry software, ScanR (Olympus). Total ROS production was measured in leukocytes incubated for 30 min with the 2′,7′-dichlorodihydrofluorescein diacetate (DCFH-DA) fluorescent probe (5×10^{-6} *M*), and mitochondrial superoxide was detected with the fluorescent probe, MitoSOX (5×10^{-6} *M*, 30 min). Nuclei were visualized with Hoechst 33342. Measures of fluorescence are referred to % of control.

Western blot analysis

Leukocytes were lysed on ice for 15 min with cell lysis buffer (20 m*M* HEPES pH 7.5, 400 m*M* NaCl, 20% glycerol, 0.1 m*M* EDTA, 10 μ*M* Na_2MoO_4, 0.5% NP-40, 1 m*M* dithiothreitol), and protein extraction was performed in the presence of a protease inhibitor mixture (10 m*M* NaF, 1 m*M* $NaVO_3$, 10 m*M* PNP, 10 m*M* β-glycerolphosphate). Protein concentrations were determined by a BCA protein assay (Thermo Scientific) after 15 min of centrifugation. Protein samples (25 μg) were resolved on 4–20% Mini-Protean® TGX Stain-Free™ gels (Bio-Rad) and transferred onto nitrocellulose membranes. After blocking, membranes were incubated overnight with primary antibodies at 4°C. The primary antibodies used were anti-MFN1 (Millipore Iberica), anti-MFN2 (Millipore Iberica), anti-OPA1 (Millipore Iberica), anti-FIS1 (Millipore Iberica), anti-DRP1 (Abcam), and anti-actin (Sigma Aldrich). Blots were incubated with the secondary antibodies, horseradish peroxidase (HRP) goat anti-mouse (Thermo Scientific) and HRP goat anti-rabbit (Millipore Iberica), and were developed for 2 min with ECL plus reagent (GE Healthcare) or Supersignal West Femto (Thermo Scientific). Visualization was by means of a Fusion FX5 acquisition system (Vilbert Lourmat). The signals were analyzed and quantified by densitometry using BioID software (Vilbert Lourmat).

Leukocyte–endothelium interaction assay

Adhesion assays under flow conditions were carried out using a parallel plate flow chamber *in vitro* model as previously described (6). We employed coverslips with confluent human umbilical vein endothelial cell (HUVEC) monolayers to perform the adhesion assays. These coverslips were inserted in the bottom plate of the flow chamber so that a 5×25 mm portion of the endothelial cells was exposed, and the flow chamber was mounted on an inverted microscope (Nikon Eclipse TE 2000-S) connected to a camera. Leukocyte suspensions were drawn across the HUVEC monolayer at a flow rate of 0.36 ml/min. Real-time microscopic images of the flow-exposed monolayer were recorded for 5 min and examined. Leukocyte rolling velocity, flux, and adhesion were calculated as described elsewhere (6). Tumor necrosis factor alpha (10 ng/ml, 4 h) was used as a positive control for HUVECs and platelet-activating factor (1 μ*M*, 1 h) for leukocytes.

Data analysis

The data were collected and managed using SPSS 17.0. To compare controls and T2D patients, data were analyzed by unpaired Student's *t*-test. TG and hs-CRP were normalized by log transformation before analysis. Chi-square was employed to compare proportions. We also evaluated the T2D population divided by HbA1c percentages below and above 6.5% by means of one-way analysis of variance (ANOVA), followed by Tukey's honestly significant difference *post hoc* test. Correlations were calculated using Pearson's correlation coefficient. Values in Table 1 are reported as mean ± standard deviation for parametric data and median and 25th and 75th percentiles for nonparametric data. In graphs, data are expressed as mean ± standard error of the mean. In all tests, *p*-values <0.05 were considered to be significant.

Acknowledgments

The authors thank Brian Normanly (University of Valencia) for his editorial assistance. This study was financed by grants, PI13/01025, PI13/00073, PI15/01424 CIBERehd CB06/04/0071, PROMETEOII 2014/035, UGP-14-93, and UGP-14-95, and by the European Regional Development Fund (ERDF "A way to build Europe"). V.M.V. and M.R. are recipients of contracts from the Ministry of Health of the Valencian Regional Government and Carlos III Health Institute (CES10/030 and CP10/0360, respectively). N.D.-M. and S.L.-D. are recipients of a predoctoral fellowship from the Carlos III Health Institute (FI14/00125 and FI14/00350, respectively). C.B. is recipient of a postdoctoral contract from the Carlos III Health Institute (CD14/00043).

References

1. Bach D, Naon D, Pich S, Soriano FX, Vega N, Rieusset J, Laville M, Guillet C, Boirie Y, Wallberg-Henriksson H, Manco M, Calvani M, Castagneto M, Palacín M, Mingrone G, Zierath JR, Vidal H, and Zorzano A. Expression of Mfn2, the Charcot-Marie-Tooth neuropathy type 2A gene, in human skeletal muscle: effects of type 2 diabetes, obesity, weight loss, and the regulatory role of tumor necrosis factor α and interleukin-6. *Diabetes* 54: 2685–2693, 2005.
2. Hernandez-Mijares A, Rocha M, Rovira-Llopis S, Bañuls C, Bellod L, De Pablo C, Alvarez A, Roldan-Torres I, Sola-Izquierdo E, and Victor VM. Human leukocyte/endothelial cell interactions and mitochondrial dysfunction in type 2 diabetic patients and their association with silent myocardial ischemia. *Diabetes Care* 36: 1695–1702, 2013.
3. Montaigne D, Marechal X, Coisne A, Debry N, Modine T, Fayad G, Potelle C, El Arid JM, Mouton S, Sebti Y, Duez H, Preau S, Remy-Jouet I, Zerimech F, Koussa M, Richard V, Neviere R, Edme JL, Lefebvre P, and Staels B. Myocardial contractile dysfunction is associated with impaired mitochondrial function and dynamics in type 2 diabetic but not in obese patients. *Circulation* 130: 554–564, 2014.

Díaz-Morales et al., 2016

4. Ngoh GA, Papanicolaou KN, and Walsh K. Loss of mitofusin 2 promotes endoplasmic reticulum stress. *J Biol Chem* 287: 20321–20332, 2012.
5. Patti M-E and Corvera S. The role of mitochondria in the pathogenesis of type 2 diabetes. *Endocr Rev* 31: 364–395, 2010.
6. Rovira-Llopis S, Bañuls C, Apostolova N, Morillas C, Hernandez-Mijares A, Rocha M, and Victor VM. Is glycemic control modulating endoplasmic reticulum stress in leukocytes of type 2 diabetic patients? *Antioxid Redox Signal* 21: 1759–1765, 2014.
7. Rovira-Llopis S, Rocha M, Falcon R, de Pablo C, Alvarez A, Jover A, Hernandez-Mijares A, and Victor VM. Is myeloperoxidase a key component in the ROS-induced vascular damage related to nephropathy in type 2 diabetes? *Antioxid Redox Signal* 19: 1452–1458, 2013.
8. Shenouda SM, Widlansky ME, Chen K, Xu G, Holbrook M, Tabit CE, Hamburg NM, Frame AA, Caiano TL, Kluge MA, Duess MA, Levit A, Kim B, Hartman ML, Joseph L, Shirihai OS, and Vita JA. Altered mitochondrial dynamics contributes to endothelial dysfunction in diabetes mellitus. *Circulation* 124: 444–453, 2011.
9. Westermann B. Mitochondrial fusion and fission in cell life and death. *Nat Rev Mol Cell Biol* 11: 872–884, 2010.

Address correspondence to:
Dr. Victor M. Victor
Service of Endocrinology
FISABIO
University Hospital Doctor Peset
Avda Gaspar Aguilar 90
Valencia 46017
Spain

E-mail: victor.victor@uv.es

Date of first submission to ARS Central, March 26, 2016; date of acceptance, April 4, 2016.

Abbreviations Used

ANOVA = analysis of variance
BMI = body–mass index
CHOP = C/EBP homologous protein
CVD = cardiovascular diseases
DBP = diastolic blood pressure
DCFH-DA = dichlorodihydrofluorescein diacetate
DRP1 = dynamin-related protein 1
ER =
FIS1 = fission protein 1
HbA1c = glycated hemoglobin
HDL-c = high-density lipoprotein cholesterol
HOMA-IR = homeostasis model assessment of insulin resistance
HRP = horseradish peroxidase
hs-CRP = high-sensitive C-reactive protein
HSD = honestly significant difference
HUVEC = human umbilical vein endothelial cells
LDL-c = low-density lipoprotein cholesterol
MFN1 = mitofusin 1
MFN2 = mitofusin 2
OPA1 = optic atrophy 1
ROS = reactive oxygen species
SBP = systolic blood pressure
T2D = type 2 diabetes
WB = Western blot
WHR = waist-to-hip ratio

AU4

ARTÍCULO 9

Leucocyte-endothelial cell interactions of maraviroc, atazanavir, darunavir, raltegravir and rilpivirine: a comparison with abacavir

Orden S, De Pablo C, Calatayud S, Collado-Díaz V, Esplugues JV, Álvarez Á.

Antiviral Research 2016, en revisión

Leucocyte-endothelial cell interactions of maraviroc, atazanavir, darunavir, raltegravir and rilpivirine: a comparison with abacavir

Samuel ORDEN[1,2], Carmen DE PABLO[1], Sara CALATAYUD[1], Víctor COLLADO-DÍAZ[1,2], Juan V. ESPLUGUES[1,2] and Ángeles ÁLVAREZ[1,3,4*]

[1]Departamento de Farmacología and CIBERehd, Facultad de Medicina, Universidad de Valencia, Valencia, Spain.

[2]FISABIO-Fundación Hospital Universitario Dr. Peset, Valencia, Spain.

[3]Fundación General Universidad de Valencia, Valencia, Spain.

[4]Universidad Jaume I, Facultad de Ciencias de la Salud, Castellón de la Plana, Spain.

***Corresponding author details:**

Ángeles Álvarez. Departamento de Farmacología, Facultad de Medicina, Universidad de Valencia. Avda. Blasco Ibáñez 15-17, 46010 Valencia, Spain. Tel. 34-96-3864898. Fax. 34-96-3983879. angeles.alvarez@uv.es

Short running title: New anti-HIV drugs and leucocyte recruitment

Keywords: dfferent antiretrovirals, Rilpivirine, Abacavir, leucocyte-endothelium interactions, cardiovascular diseases.

ABSTRACT

Objectives: Cardiovascular (CV) toxicity associated with combined antiretroviral therapy (cART) has been attributed mainly to nucleoside reverse transcriptase inhibitors (specifically abacavir and didanosine), though particular drugs from other families (CCR5 antagonists, protease inhibitors, integrase strand transfer inhibitors or non-nucleoside reverse transcriptase inhibitors) may also produce this side effect as they are administered in combination. This study evaluates the actions of clinically relevant concentrations of maraviroc, atazanavir, darunavir, raltegravir and rilpivirine in the early phases of vascular responses (leucocyte-endothelium interactions) previously shown to be altered by abacavir.

Methods: The effects of the different drugs were analysed in vivo in rat mesenteric vessels using intravital microscopy and in vitro in human cells (interactions of leucocytes with HUVEC) by means of a flow chamber system. The expression of adhesion molecules in leucocytes and endothelial cells was studied by flow cytometry,

Results: Rilpivirine and abacavir increased rolling flux and adhesion of leucocytes in vivo and in vitro, but maraviroc, atazanavir, darunavir or raltegravir did not produce these effects. However, while abacavir induced emigration in rat venules, rilpivirine did not. Rilpivirine augmented the expression of CD11b, CD11c and CD18 on human neutrophils. Abacavir replicated these effects on CD11b and CD18 and also induced expression of these two molecules in human monocytes, while rilpivirine only increased that of CD11b. The action of rilpivirine was reversed by antibodies against Mac-1 (CD11b/CD18), gp150,95 (CD11c/CD18) or ICAM-1 (CD54).

Conclusions: Our results suggest that maraviroc, atazanavir, darunavir and raltegravir, and even rilpivirine, could be safer alternatives to abacavir in terms of their vascular side effects.

Total number of words in the synopsis: 255

1. INTRODUCTION

Current pharmacological treatment of the HIV infection, known as combined antiretroviral therapy (cART), is associated with toxic effects that determine the initial selection of treatment and/or subsequent changes in the therapy [1, 2]. cART involves the administration of at least three antiretroviral (ARV) drugs. Practically every recommended ARV combination consists of two nucleoside reverse transcriptase inhibitors (NRTIs), while the third component is a non-nucleoside reverse transcriptase inhibitor (NNRTI) or a protease inhibitor (PI) [2, 3]. In the most recent guidelines, the predominance of this third drug has been challenged by the arrival of new ARVs like the PI darunavir, the integrase strand transfer inhibitors (INSTI) raltegravir, elvitegravir and dolutegravir or the NNRTI rilpivirine [2, 3] which claim to have similar efficacy and virological suppression and a safer toxicological profile [2-5].

There is growing awareness of the association of some ARV with cardiovascular (CV) diseases, which is of concern given that this therapy is for life and that, as the HIV-infected population grows older, it will become increasingly at risk of developing such conditions. Clinical evidence has put the spotlight on NRTIs, in particular abacavir and didanosine, as the main culprits of CV toxicity [6], though a role for CCR5 antagonists, PIs, INSTIs or NNRTIs has not been ruled out [1, 7]. "The Data collection and Adverse events of anti-HIV Drugs study group" (D:A:D) reported in 2008 that current or recent (≤6 months) exposure to abacavir was associated with a two-fold increase in the risk of myocardial infarction, fact that was extended to didanosine, another NRTI analogue of purine [8]. A great controversy was generated since then because some studies confirmed this relationship [9-11], while others did not [12-14]. Despite the lack of a consensus, clinical guidelines now recommend limited use of ABC when there is a risk of CV disease [2, 3].

An increase in vascular permeability coupled with leucocyte infiltration is a hallmark of the inflammation that underlies vascular diseases and, indeed, the HIV-infection itself. This recruitment of white cells involves a sequential cascade of adhesive interactions between leucocytes and endothelial cells that begins with enhanced rolling and leads to the adhesion and

subsequent endothelial transmigration of these white cells in a process mediated by the adhesion molecules present on both cell populations [15]. Recent in vitro and in vivo data suggest that abacavir and didanosine induce such leucocyte-endothelium interactions [16, 17], and that the effect of abacavir is mediated by an interaction of Mac-1 with ICAM-1.

In this study, we have analysed the in vivo and in vitro vascular toxicity of darunavir, raltegravir and rilpivirine by evaluating their direct effects during the early phases of vascular responses (leucocyte rolling, adhesion and emigration) previously shown to be altered by abacavir [16, 17]. To provide a comprehensive profile we have included other important drugs used in cART, such as maraviroc, a CCR5 antagonist, and atazanavir, another PI.

2. MATERIALS AND METHODS

2.1. Intravital microscopy

Leucocyte-endothelial cell interactions were evaluated in fasted male Sprague-Dawley rats (200-250 g) following a standard experimental technique [17, 18]. In brief, rats were anaesthetised with sodium pentobarbital [65 mg/kg, intraperitoneally (i.p.)] and, following a midline abdominal incision, a segment of the midjejunum was exteriorized and placed on an optically clear viewing pedestal at 37ºC for tissue transillumination. The exposed mesentery was visualized using an orthostatic microscope (Nikon Optiphot-2, SMZ1, Nikon, Badhoevedor, The Netherlands) equipped with 20x objective lens (Nikon SLDW) and 10x eyepieces, during which time it was continuously superfused with bicarbonate buffer saline (BBS; pH 7.4, 37ºC, 2 mL/min). A video camera (Sony SSC-C350P; Sony, Koeln, Germany) mounted on the microscope projected images onto a computer. Single unbranched mesenteric venules were selected and their diameters (25 to 40 μm) measured online using a video caliper (Microcirculation Research Institute, Texas A&M University, College Station, TX). Haemodynamic parameters were analysed as previously described [17, 18]. Images of the vessels were captured digitally for playback analysis (final magnification of the computer screen: x

1300) of leucocyte parameters. Rolling flux was assessed by counting the number of leucocytes passing a reference point in the vessel per min. Leucocyte rolling velocity was defined as the time required for these cells to travel along 100 μm of the venule and was expressed as μm/s. A leucocyte was considered to have adhered to the endothelium if it remained stationary for a period equal to or exceeding 30 s, and the number of these leucocytes was expressed per 100 μm of vessel. Leucocyte emigration was evaluated as the total number of interstitial leucocytes per field. In some cases, the area of the mesentery selected for the experiment was excised, fixed with paraformaldehyde (4% in PBS, pH 7.4) and stained with hematoxylin and eosin. The preparation was subsequently observed under a clear field microscope (63x), and the infiltrated leucocytes were counted (number per 2.5 x 10^{-4} cm^2) and classified morphologically as PMN leucocytes, macrophages or lymphocytes by an observer who was unaware of the treatment in question. Animals were injected (2.5 mL, i.p.) with saline, vehicle (methanol or DMSO) or a solution containing one of the following ARV: maraviroc (2.5 μg/mL equivalent to 35 μg/kg), atazanavir (18 μg/mL, 250 μg/kg), darunavir (14 μg/mL, 190 μg/kg), raltegravir (2.5 μg/mL, 30 μg/kg) or rilpivirine (0.1-0.4 μg/mL, 1-5 μg/kg). The effects of these ARV drug solutions were compared with that of abacavir at 5 μg/mL, a clinically relevant concentration that has consistently been shown to induce leucocyte-endothelial cell interactions in vivo [17]. Maraviroc was dissolved in methanol, atazanavir, darunavir, raltegravir and rilpivirine in DMSO and abacavir in sterile water. The i.p. injection of drug solutions is a common practice in intravital microscopy [18-21], as it allows longer incubation periods than superfusion [22] and is thus more suited to lengthier time-course studies such as the present one. Images (5-min period) were recorded 4 h later and evaluated by an observer who was blind to the treatment. All doses were representative of plasma concentrations in patients [4, 23-27]. Care was taken at each stage of the experiment to avoid any suffering by the animals. Procedures followed Spanish law concerning the use of experimental animals and were approved by the Ethics Committee of the Faculty of Medicine of the University of Valencia (Spain).

2.2. Endothelial cell culture and leucocyte isolation

Human umbilical vein endothelial cells (HUVEC) were harvested from freshly obtained umbilical cords as previously described [28, 29] and passage 1 cells were subsequently employed in the experiments. Human peripheral blood polymorphonuclear (PMN) or mononuclear (PBMC) cells were isolated from whole blood drawn from healthy volunteers and anticoagulated with sodium citrate [16]. Leucocytes and HUVEC were treated independently (4 h, 37ºC) with medium, vehicle (methanol or DMSO), maraviroc (2.5 μg/mL), atazanavir (18 μg/mL), darunavir (14 μg/mL), raltegravir (2.5 μg/mL) or rilpivirine (0.1-0.4 μg/mL) and the effects compared with those of abacavir at 5 μg/mL, a clinically relevant concentration that has consistently been shown to induce leukocyte-endothelial cell interactions in vitro [16, 17]. The aforementioned concentrations were employed because they mimic clinically relevant plasma levels. The Medical Ethics Committee of the Hospital Clínico Universitario de Valencia approved the study, and the experiments were conducted in accordance with the Declaration of Helsinki after obtaining the written informed consent of each participant.

2.3. Dynamic adhesion assay under flow conditions

The characteristics of the parallel plate flow chamber model used in this study have been described previously [16, 30, 31]. In brief, coverslips [fibronectin (5 μg/mL)-coated] containing confluent HUVEC monolayers were inserted in the chamber (37ºC) and a portion (5 x 25 mm) was exposed to the flow. The chamber was mounted on an inverted microscope (Nikon Eclipse TE 2000-S, x40, Amstleveen, The Netherlands) with a video-camera (Sony Exware HAD, Koeln, Germany). PMN or PBMC were resuspended in Dulbecco's PBS with Ca^{2+} and Mg^{2+} [$DPBS^{+}$] buffer containing 20 mM HEPES and 0.1% human serum albumin (HSA) at 1 x 10^6 or 0.5 x 10^6 cells/mL, respectively, and were drawn across the monolayer (flow rate 0.36 mL/min, shear stress 0.7 dyne/cm^2). Images of a single field were recorded for 5 min and leucocyte parameters were determined. Rolling flux was calculated by counting the number of cells rolling

across 100 μm^2 of the monolayer during a 1-min period. The velocities of 20 consecutive leucocytes in the field of focus were determined by measuring the time required to travel 100 μm. Adhesion was determined after 5 min of perfusion by analysis of 5-10 high power (40x) fields. Leucocytes were considered to be adherent after 30 s of stable contact with the monolayer.

2.4. Flow cytometry: Expression of adhesion molecules

The expression of human leucocyte adhesion molecules was analysed in blood samples and that of endothelium molecules was quantified in confluent HUVEC. Blood samples (4 h, 37ºC) and endothelial cells were treated (4 h or 24 h, 37ºC) with the different ARV drugs and then incubated with saturating amounts of the antibodies (20 min, 4ºC, in darkness). Subsequently, the samples were fixed and identified in a flow cytometer (FACScalibur Flow Cytometer, BD, Madrid, Spain) [18]. Surface antigen expression [Fluorescein isothyocianate (FITC) or phycoerythrin (PE)-fluorescence] was analysed in granulocytes, monocytes and lymphocytes, which were identified by their specific features of size (forward-angle light scatter [FS]) and granularity (side-angle light scatter [SS]). HUVEC were also recognized by their FS and SS characteristics. Median fluorescence FITC or PE-intensity was employed as a marker of the expression of the respective epitope.

2.5. Functional role of adhesion molecules

This was assessed in both in vivo and in vitro settings by blocking the adhesion molecules with specific antibodies. For the in vivo experiments, antibodies were injected through the tail vein 30 minutes before rilpivirine administration, as previously described [32, 33], at doses that have been shown to block the in vivo function of the adhesion molecules analysed in the current study [2 mg/kg for WT-5 (antirat Mac-1, CD11b), and 1 mg/kg for WT-3 (antirat β_2-integrins, CD18) and for 1A29 (antirat ICAM-1, CD54)] or with control antibodies [2 mg/kg for IgA and

1 mg/kg for IgG1] [17]. To rule out a direct effect of the mAbs on circulating leucocytes, portal blood samples were obtained and their number evaluated after the intravital measurements. For the in vitro experiments, prior to treatment with rilpivirine, PMN and PBMC were pre-treated with anti-lymphocyte function-associated antigen-1 (CD11a-LFA-1, 10 µg/mL), anti-macrophage-1 antigen (CD11b-Mac-1, 20 µg/mL), anti-alpha-X integrin (CD11c-gp150,95, 10 µg/mL), anti-β_2 integrins (CD18, 10 µg/mL) or control antibodies (IgG1, 10 µg/mL) for 20 minutes at 4ºC in darkness. Prior to drug administration, HUVEC monolayers were pre-treated with anti-intercellular adhesion molecule-1 (ICAM-1-CD54, 20 µg/mL) or control antibodies (IgG1, 10 µg/mL) for 30 minutes at 37ºC. The antibodies were assayed at previously described doses [16].

2.6. Materials

Lysis solution, FITC and PE conjugated antibodies, blocking antibodies for in vivo experiments and blocking antibody against CD54 for in vitro experiments (BD Bioscience, Madrid, Spain); blocking antibodies against CD11a, CD11b and CD18 for in vitro experiments (Merck Millipore, Darmstadt, Germany), blocking antibody against CD11c for in vitro experiments (bioNova cientíca s.l., Madrid, Spain), Dulbecco's PBS with ($DPBS^+$) or without ($DPBS^-$) Ca^{2+} and Mg^{2+}, EGM-2 culture media and foetal bovine serum (Lonza, Barcelona, Spain); human serum albumin (HSA, albuminate 25%), RPMI1640 supplemented with 20 mM HEPES, HBSS, fibronectin, dextran and hematoxylin (Sigma Chemical Co, Madrid, Spain); Eosin (Panreac, Barcelona, Spain); Ficoll-Paque TM Plus (GE Healthcare, Valencia, Spain); coverslips (Nunc, Thermo Fisher Scientific, Madrid, Spain); PBS, collagenase, and trypsin (Gibco, Invitrogen, Barcelona, Spain); ARVs (Sequoia Research Products, Pangbourne, UK); Sprague-Dawley Rats (Charles River Laboratories, Barcelona, Spain) and pentobarbital (Guinama, Valencia, Spain).

2.7. Statistical analysis

One-way ANOVA with a Newman-Keuls post-test correction was employed for statistical analysis (mean ± S.E.M, $n \geq 4$, $p < 0.05$).

3. RESULTS

3.1. Leucocyte-endothelial cell interactions

In rat postcapillary venules in vivo, rilpivirine provoked a significant and dose-dependent decrease in leucocyte rolling velocity (Fig 1A) and an increase in rolling flux (Fig 1B) and adhesion (Fig 1C) to levels similar to those induced by abacavir at clinically relevant concentrations. However, while abacavir triggered emigration (Fig. 1D), rilpivirine had no effect on this parameter, even at high concentrations. This difference was reproduced when mesenterial leucocyte infiltration was measured by hematoxylin-eosin staining, which confirmed that rilpivirine had no significant effect (2.0±0.6 vs 0.8±0.1 leucocytes per field in DMSO-treated animals) (Fig 2H), while abacavir produced a significant increase in this parameter (15.1±4.1** vs 0.5±0.3 leucocytes per field in methanol-treated animals, $p<0.01$) (Fig 2I). None of the other agents analysed (maraviroc, atazanavir, darunavir or raltegravir) generated leucocyte-endothelial interactions (Fig 1 and 2). Systemic haemodynamic parameters were not modified by any of the compounds evaluated (data not shown).

In human cells in vitro, rilpivirine induced a decrease in rolling velocity (Fig 3A and 3B) and an increase in rolling flux (Fig 3C and 3D) and adhesion (Fig 3E and 3F) of both PMN and PBMC. These effects were reproduced with abacavir, while none of the other compounds induced any modification in said parameters.

3.2. Expression of adhesion molecules

Rilpivirine augmented the expression of CD11b, CD11c and CD18 on human neutrophils, as measured by flow cytometry. These effects were replicated by abacavir in CD11b and CD18;

however, while the latter drug also induced expression of these two molecules in human monocytes, rilpivirine only augmented that of CD11b (Fig 4). Neither rilpivirine nor abacavir affected the expression of CD11a, CD49d or CD62L (L-selectin) in neutrophils or monocytes (Table S1). Maraviroc, atazanavir, darunavir and raltegravir did not modify the expression of any of the adhesion molecules analysed on neutrophils or monocytes (Fig. 4 and Table S1). Finally, none of the agents evaluated had any effect on the adhesion molecules of lymphocytes (data not shown) or human endothelial cells (Table S2), while at 24 h only abacavir augmented the expression of ICAM-1 and VCAM-1 on endothelial cells (Table S2).

3.3. Role of adhesion molecules in rilpivirine-induced rolling and adhesion

The effects of rilpivirine on rolling and adhesion were not apparent in vivo in rat postcapillary venules when animals were pre-treated with antibodies against Mac-1 (CD11b), β_2 integrins (CD18) or ICAM-1 (CD54) (Fig 5). Neither haemodynamic parameters nor the systemic leucocyte count was affected by any of the antibodies employed (data not shown). The in vitro results confirmed these findings, as rilpivirine-induced PMN-endothelium interactions were avoided by blocking Mac-1 (CD11b), gp150,95 (CD11c), β_2 integrins (CD18) or their ligand ICAM-1 (CD54), but not by neutralizing LFA-1 (CD11a) (Fig 6A, 6C and 6E). Rilpivirine-induced PBMN-endothelium interactions were prevented by blocking the same adhesion molecules, but the reversal was only partial when CD11c was blocked (Fig 6B, 6D and 6F).

4. DISCUSSION

The attenuation of drug-induced side-effects has become a priority when selecting pharmacological treatment for HIV patients, with susceptibility to cardiovascular side effects being a factor of growing importance given the rising age of otherwise well-controlled patients. One of the more sound controversies in the area of HIV treatment has been the evidence for CV toxicity for abacavir. However, despite the lack of a consensus, clinical guidelines now

recommend limited use of ABC when there is a risk of CV disease [2, 3]. Previous studies in our laboratory have demonstrated that certain ARVs, in particular, abacavir and didanosine, induce leucocyte-endothelial cell interactions [16, 17]. The results in question were obtained employing the same experimental set-ups as we have used here which are procedures that have been instrumental in understanding the inflammatory cascade associated with vascular diseases and its pharmacological modulation - intravital microscopy in vivo and the flow chamber system *in vitro* [18, 22, 34-40].

There have been commercialized new antiretrovirals which claim to have safe CV profiles while maintain antiviral efficacy [2, 3]. In the present study, we have employed concentrations of maraviroc (2.5 µg/mL), atazanavir (18 µg/mL), darunavir (14 µg/mL), raltegravir (2.5 µg/mL), rilpivirine (0,1-0.4 µg/mL) or abacavir (5 µg/m/L) similar to or higher than those frequently reported in patients (0.2, 6.3, 7.1, 0.9, 0.6 or 3.9 µg/mL respectively) [4, 23-27]. Therefore, we assume that we are dealing with clinically relevant concentrations. We observed that maraviroc, atazanavir, darunavir and raltegravir did not induce leukocyte rolling, adhesion or emigration, which points to a better profile than that of abacavir. Although exhibiting none of the actions of abacavir on leucocyte emigration, rilpivirine, one of the former third drug more used, did induce significant effects on earlier steps of leucocyte recruitment in vivo. This difference between the two drugs is of particular relevance, as emigration is considered the definitive step in the vascular inflammatory cascade, while the preceding phases (rolling and adhesion) are reversible. Rilpivirine, but not maraviroc, atazanavir, darunavir or raltegravir, also induced human leucocyte (PMN or PBMC) rolling and adhesion in vitro and enhanced the expression of CD11b, CD11c and CD18 on human neutrophils, and only CD11b in monocytes. Nevertheless, abacavir reproduced this increment in the expression of only CD11b and CD18 in human neutrophils and monocytes. When the functional implication of adhesion molecules was evaluated, the rolling and adhesion induced by rilpivirine was reversed by pre-treatment, both in vitro and in vivo, with antibodies against CD11b, CD18 or ICAM-1 (CD54). Although an in

vivo analysis would have been interesting, the role of CD11c was evaluated in human cells only due to the lack of availability of a commercially-marketed rat-blocking antibody against this molecule (this molecule is responsible for rilpivirine-induced PMN and PBMC-endothelial interactions totally or partially, respectively). Our results suggest that both β_2-integrins - gp150,95 (CD11c/CD18) and Mac-1 (CD11b/CD18) - mediate these steps by interacting with their endothelial ligand ICAM-1 (CD54) constitutively expressed. On the other hand, the disparities in the effects of rilpivirine and abacavir on emigration may be a result of their differential actions on endothelial adhesion molecules (ICAM-1 and VCAM-1) [15]. Thus, while abacavir induced an increment on the expression of these molecules, rilpivirine did not. To our knowledge, our study is the first to analyse the vascular profile of rilpivirine, and our results complement preliminary clinical evidence which suggest that the adverse effects related with dyslipidemia are less common with rilpivirine, this drug produces minimal changes in total cholesterol, low-density lipoprotein-cholesterol, high density lipoprotein cholesterol and triglycerides in comparison with other antiretrovirals [41].

Interestingly, evidence is emerging supporting a role for the chemokine receptor CCR5 and its ligands CCL3 (MIP-1α), CCL4 (MIP-1β) and CCL5 (RANTES) in the initiation and progression of atherosclerosis [42]. Such data imply a potential use for CCR5 antagonists (such as maraviroc) as cardiovascular-protective drugs. Indeed, a previous study in mice has shown that maraviroc reduces ritonavir-induced atherogenesis and advanced plaque progression [43]. The results we have obtained with this compound are of no use for validating this hypothesis, since we have evaluated the direct proinflammatory properties of the compounds rather than how they modulate inflammation generated by other stimuli.

Warnings have been issued concerning the risk of cardiovascular toxicity with some protease inhibitors such as lopinavir and ritonavir [44-46]. However, in our experiments, we did not observe toxic vascular effects with atazanavir or darunavir, probably because the negative effects of PIs on CV risk are a result of dyslipidaemia. Furthermore, darunavir and atazanavir have been

shown to have more favourable lipid profiles than older PIs [47]; indeed, a previous study with human coronary artery endothelial cells has demonstrated that darunavir, unlike atazanavir and lopinavir, does not affect endothelial cell function, oxidative stress, inflammation or senescence markers [48].

Finally, there is very little available data regarding raltegravir. Two clinical studies have demonstrated that this compound does not have a significant impact on cardiovascular risk (assessed according to endothelial function) [49, 50], and one of them even suggested beneficial effects of raltegravir on monocyte activation (measured as sCD14) [49]. These studies are in keeping with our results.

5. CONCLUSIONS

Given that CV disease is the most prevalent cause of death among the normal-aged population, any hint that these new anti-HIV drugs are associated with CV disease is of relevance. Although our results should be interpreted with caution, they provide evidence that maraviroc, atazanavir, darunavir, raltegravir, and even rilpivirine, could be safer alternatives to abacavir due to the fact that they are less likely to induce vascular side effects.

ACKNOWLEDGEMENTS:

We thank Brian Normanly for English language editing and Nicole Roupain, Fernando Sabater and Dora Martí-Cabrera for providing well-characterized HUVEC.

Contribution: S.O. performed the research; C.d.P., SC and VCD helped perform the research, S.O. and A.A. analysed the data, A.A. conceived the study, and J.V.E. and A.A. designed the research and wrote the paper.

Funding section: This work was supported by Ministerio de Economía y Competitividad [grant number SAF2015-67678-R], CIBERehd [grant number G0071] and Generalitat Valenciana [grant numbers PROMETEOII/2014/035, ACOMP/2013/147 and ACOMP/2013/236]. S.O. was funded by Fundación FISABIO, C.d.P. by Ministerio de Ciencia e Innovación [FPI grant number BES-2008-004338], V.C.D. by Generalitat Valenciana (VALi+d grant number ACIF/2015/316) and A.A. by Ministerio de Ciencia e Innovación [Ramón y Cajal program RYC2005-002295 and I3 program].

TRANSPARENCY DECLARATIONS

JVE has received funds for speaking at symposia organized on behalf of Abbvie Farmaceutica S.L.U., Astra Zeneca and Gilead Sciences. None of the other authors have anything to declare.

REFERENCES

1. Triant VA. HIV infection and coronary heart disease: an intersection of epidemics. *J Infect Dis* 2012; **205 Suppl 3**: S355-S361.

2. Gunthard HF, Aberg JA, Eron JJ, et al. Antiretroviral treatment of adult HIV infection: 2014 recommendations of the International Antiviral Society-USA Panel. *JAMA* 2014; **312**: 410-25.

3. [GESIDA/National AIDS Plan: Consensus document on antiretroviral therapy in adults infected by the human immunodeficiency virus (Updated January 2015)]. *Enferm Infecc Microbiol Clin* 2015.

4. Martinez-Rebollar M, Munoz A, Perez I, et al. Pharmacokinetic study of dual therapy with raltegravir 400 mg twice daily and Darunavir/Ritonavir 800/100 mg once daily in HIV-1-infected patients. *Ther Drug Monit* 2013; **35**: 552-6.

5. Behrens G, Rijnders B, Nelson M, et al. Rilpivirine versus efavirenz with emtricitabine/tenofovir disoproxil fumarate in treatment-naive HIV-1-infected patients with HIV-1 RNA </=100,000 copies/mL: week 96 pooled ECHO/THRIVE subanalysis. *AIDS Patient Care STDS* 2014; **28**: 168-75.

6. Behrens GM, Reiss P. Abacavir and cardiovascular risk. *Curr Opin Infect Dis* 2010; **23**: 9-14.

7. Friis-Moller N, Reiss P, Sabin CA, et al. Class of antiretroviral drugs and the risk of myocardial infarction. *N Engl J Med* 2007; **356**: 1723-35.

8. Sabin CA, Worm SW, Weber R, et al. Use of nucleoside reverse transcriptase inhibitors and risk of myocardial infarction in HIV-infected patients enrolled in the D:A:D study: a multi-cohort collaboration. *Lancet* 2008; **371**: 1417-26.

9. Use of nucleoside reverse transcriptase inhibitors and risk of myocardial infarction in HIV-infected patients. *AIDS* 2008; **22**: F17-F24.

10. Worm SW, Sabin C, Weber R, et al. Risk of myocardial infarction in patients with HIV infection exposed to specific individual antiretroviral drugs from the 3 major drug classes: the data collection on adverse events of anti-HIV drugs (D:A:D) study. *J Infect Dis* 2010; **201**: 318-30.

11. Obel N, Farkas DK, Kronborg G, et al. Abacavir and risk of myocardial infarction in HIV-infected patients on highly active antiretroviral therapy: a population-based nationwide cohort study. *HIV Med* 2010; **11**: 130-6.

12. Brothers CH, Hernandez JE, Cutrell AG, et al. Risk of myocardial infarction and abacavir therapy: no increased risk across 52 GlaxoSmithKline-sponsored clinical trials in adult subjects. *J Acquir Immune Defic Syndr* 2009; **51**: 20-8.

13. Bedimo RJ, Westfall AO, Drechsler H, et al. Abacavir use and risk of acute myocardial infarction and cerebrovascular events in the highly active antiretroviral therapy era. *Clin Infect Dis* 2011; **53**: 84-91.

14. Ribaudo HJ, Benson CA, Zheng Y, et al. No risk of myocardial infarction associated with initial antiretroviral treatment containing abacavir: short and long-term results from ACTG A5001/ALLRT. *Clin Infect Dis* 2011; **52**: 929-40.

15. Ley K, Laudanna C, Cybulsky MI, et al. Getting to the site of inflammation: the leukocyte adhesion cascade updated. *Nat Rev Immunol* 2007; **7**: 678-89.

16. De Pablo C, Orden S, Apostolova N, et al. Abacavir and didanosine induce the interaction between human leukocytes and endothelial cells through Mac-1 upregulation. *AIDS* 2010; **24**: 1259-66.

17. De Pablo C, Orden S, Peris JE, et al. Profile of leukocyte-endothelial cell interactions induced in venules and arterioles by nucleoside reverse-transcriptase inhibitors in vivo. *J Infect Dis* 2013; **208**: 1448-53.

18. Alvarez A, Cerda-Nicolas M, Naim Abu NY, et al. Direct evidence of leukocyte adhesion in arterioles by angiotensin II. *Blood* 2004; **104**: 402-8.

19. Yamaki K, Lindbom L, Thorlacius H, et al. An approach for studies of mediator-induced leukocyte rolling in the undisturbed microcirculation of the rat mesentery. *Br J Pharmacol* 1998; **123**: 381-9.

20. Stalker TJ, Skvarka CB, Scalia R. A novel role for calpains in the endothelial dysfunction of hyperglycemia. *FASEB J* 2003; **17**: 1511-3.

21. Nabah YN, Mateo T, Cerda-Nicolas M, et al. L-NAME induces direct arteriolar leukocyte adhesion, which is mainly mediated by angiotensin-II. *Microcirculation* 2005; **12**: 443-53.

22. Hughes EL, Gavins FN. Troubleshooting methods: Using intravital microscopy in drug research. *J Pharmacol Toxicol Methods* 2010; **61**: 102-12.

23. Waters L, Jackson A, Else L, et al. Switching safely: pharmacokinetics, efficacy and safety of switching efavirenz to maraviroc twice-daily in patients on suppressive antiretroviral therapy. *Antivir Ther* 2015; **20**: 157-63.

24. Boffito M, Jackson A, Amara A, et al. Pharmacokinetics of once-daily darunavir-ritonavir and atazanavir-ritonavir over 72 hours following drug cessation. *Antimicrob Agents Chemother* 2011; **55**: 4218-23.

25. Blas-Garcia A, Polo M, Alegre F, et al. Lack of mitochondrial toxicity of darunavir, raltegravir and rilpivirine in neurons and hepatocytes: a comparison with efavirenz. *J Antimicrob Chemother* 2014; **69**: 2995-3000.

26. Usach I, Melis V, Peris JE. Non-nucleoside reverse transcriptase inhibitors: a review on pharmacokinetics, pharmacodynamics, safety and tolerability. *J Int AIDS Soc* 2013; **16**: 1-14.

27. Moyle G, Boffito M, Fletcher C, et al. Steady-state pharmacokinetics of abacavir in plasma and intracellular carbovir triphosphate following administration of abacavir at 600 milligrams once daily and 300 milligrams twice daily in human immunodeficiency virus-infected subjects. *Antimicrob Agents Chemother* 2009; **53**: 1532-8.

28. Ibiza S, Alvarez A, Romero W, et al. Gastrin induces the interaction between human mononuclear leukocytes and endothelial cells through the endothelial expression of P-selectin and VCAM-1. *Am J Physiol Cell Physiol* 2009; **297**: C1588-C1595.

29. Jaffe EA, Nachman RL, Becker CG, et al. Culture of human endothelial cells derived from umbilical veins. Identification by morphologic and immunologic criteria. *J Clin Invest* 1973; **52**: 2745-56.

30. De Pablo C, Orden S, Calatayud S, et al. Differential effects of Tenofovir/Emtricitabine and Abacavir/Lamivudine on human leukocyte recruitment. *Antivir Ther* 2012; **17**: 1615-9.

31. Cai YH, Alvarez A, Alcaide P, et al. Abrogation of functional selectin-ligand expression reduces migration of pathogenic CD8+ T cells into heart. *J Immunol* 2006; **176**: 6568-75.

32. Tamatani T, Kotani M, Miyasaka M. Characterization of the rat leukocyte integrin, CD11/CD18, by the use of LFA-1 subunit-specific monoclonal antibodies. *Eur J Immunol* 1991; **21**: 627-33.

33. Tamatani T, Miyasaka M. Identification of monoclonal antibodies reactive with the rat homolog of ICAM-1, and evidence for a differential involvement of ICAM-1 in the adherence of resting versus activated lymphocytes to high endothelial cells. *Int Immunol* 1990; **2**: 165-71.

34. Gavins FN. Intravital microscopy: new insights into cellular interactions. *Curr Opin Pharmacol* 2012; **12**: 601-7.

35. Goetz DJ, Greif DM, Shen J, et al. Cell-cell adhesive interactions in an in vitro flow chamber. *Methods Mol Biol* 1999; **96**: 137-45.

36. Gee DJ, Wright LK, Zimmermann J, et al. Dimethylsulfoxide exposure modulates HL-60 cell rolling interactions. *Biosci Rep* 2012; **32**: 375-82.

37. Victor VM, Rocha M, Banuls C, et al. Induction of Oxidative Stress and Human Leukocyte/Endothelial Cell Interactions in Polycystic Ovary Syndrome Patients with Insulin Resistance. *J Clin Endocrinol Metab* 2011; **96**: 3115-22.

38. Luu NT, Madden J, Calder PC, et al. Comparison of the pro-inflammatory potential of monocytes from healthy adults and those with peripheral arterial disease using an in vitro culture model. *Atherosclerosis* 2007; **193**: 259-68.

39. Gallego MJ, Zoja C, Morigi M, et al. Cyclosporine enhances leukocyte adhesion to vascular endothelium under physiologic flow conditions. *Am J Kidney Dis* 1996; **28**: 23-31.

40. Guba M, Steinbauer M, Buchner M, et al. Differential effects of short-term ace- and AT1-receptor inhibition on postischemic injury and leukocyte adherence in vivo and in vitro. *Shock* 2000; **13**: 190-6.

41. Tebas P, Sension M, Arribas J, et al. Lipid Levels and Changes in Body Fat Distribution in Treatment-Naive, HIV-1-Infected Adults Treated With Rilpivirine or Efavirenz for 96 Weeks in the ECHO and THRIVE Trials. *Clin Infect Dis* 2014; **59**: 425-34.

42. Jones KL, Maguire JJ, Davenport AP. Chemokine receptor CCR5: from AIDS to atherosclerosis. *Br J Pharmacol* 2011; **162**: 1453-69.

43. Cipriani S, Francisci D, Mencarelli A, et al. Efficacy of the CCR5 antagonist maraviroc in reducing early, ritonavir-induced atherogenesis and advanced plaque progression in mice. *Circulation* 2013; **127**: 2114-24.

44. Friis-Moller N, Thiebaut R, Reiss P, et al. Predicting the risk of cardiovascular disease in HIV-infected patients: the data collection on adverse effects of anti-HIV drugs study. *Eur J Cardiovasc Prev Rehabil* 2010; **17**: 491-501.

45. Friis-Moller N, Weber R, Reiss P, et al. Cardiovascular disease risk factors in HIV patients--association with antiretroviral therapy. Results from the DAD study. *AIDS* 2003; **17**: 1179-93.

46. Worm SW, Kamara DA, Reiss P, et al. Elevated triglycerides and risk of myocardial infarction in HIV-positive persons. *AIDS* 2011; **25**: 1497-504.

47. Overton ET, Arathoon E, Baraldi E, et al. Effect of darunavir on lipid profile in HIV-infected patients. *HIV Clin Trials* 2012; **13**: 256-70.

48. Auclair M, Afonso P, Capel E, et al. Impact of darunavir, atazanavir and lopinavir boosted with ritonavir on cultured human endothelial cells: beneficial effect of pravastatin. *Antivir Ther* 2014; **19**: 773-82.

49. Gupta SK, Mi D, Moe SM, et al. Effects of switching from efavirenz to raltegravir on endothelial function, bone mineral metabolism, inflammation, and renal function: a randomized, controlled trial. *J Acquir Immune Defic Syndr* 2013; **64**: 279-83.

50. Hatano H, Scherzer R, Wu Y, et al. A randomized controlled trial assessing the effects of raltegravir intensification on endothelial function in treated HIV infection. *J Acquir Immune Defic Syndr* 2012; **61**: 317-25.

Figure legends

Figure 1. Effects of antiretrovirals on leucocyte responses in rat mesenteric postcapillary venules. Animals were treated (i.p.) with maraviroc (MRV, 2.5 μg/mL), atazanavir (ATV, 18 μg/mL), darunavir (DRV, 14 μg/mL), raltegravir (RAL, 2.5 μg/mL), rilpivirine (RPV, 0.1-0.4 μg/mL), abacavir (ABC, 5 μg/mL), control or the corresponding vehicle (MRV in methanol; ATV, DRV, RAL and RPV in DMSO; ABC in sterile water). Responses of leucocyte rolling velocity (A), rolling flux (B), adhesion (C) and emigration (D) were quantified 4 hours later. Results are mean ± SEM, n=4-5. **p<0.01 vs. corresponding value in control-treated group (ANOVA followed by Newman-Keuls test).

Figure 2. Leucocyte infiltration in the mesentery of rats treated with antiretrovirals. Animals were treated (i.p.) with maraviroc (MRV, 2.5 μg/mL), atazanavir (ATV, 18 μg/mL), darunavir (DRV, 14 μg/mL), raltegravir (RAL, 2.5 μg/mL), rilpivirine (RPV, 0.1-0.4 μg/mL), abacavir (ABC, 5 μg/mL), control or the corresponding vehicle (MRV in methanol; ATV, DRV, RAL and RPV in DMSO and ABC in sterile water) during a 4-hour period. The mesentery selected for intravital experiments was excised, fixed with paraformaldehyde and stained with hematoxylin and eosin, and the number of infiltrated leucocytes (neutrophils, monocytes or lymphocytes) was counted in an area of $2.5x10^{-4}$ cm^2 in saline-, methanol-, DMSO-, MRV 5 μM-, ATV 25 μM-, DRV 5 μM-, RAL 5 μM-, RPV 1 μM- and ABC 10 μM-treated animals. Arrows denote examples of infiltrated neutrophils. Bar = 50 μm.

Figure 3. Effects of antiretrovirals on PMN-endothelial cell interactions and PBMC-endothelial cell interactions. Human umbilical vein endothelial cells (HUVEC) and leucocytes (PMN or PBMC) were incubated for 4 hours with maraviroc (MRV, 2.5 μg/mL), atazanavir (ATV, 18 μg/mL), darunavir (DRV, 14 μg/mL), raltegravir (RAL, 2.5 μg/mL),

rilpivirine (RPV, 0.1-0.4 µg/mL), abacavir (ABC, 5 µg/mL), control or the corresponding vehicle (MRV in methanol; ATV, DRV, RAL and RPV in DMSO and ABC in sterile water). After assembling the flow chamber, PMN rolling velocity (A), rolling flux (C) and adhesion (E) and PBMC rolling velocity (B), rolling flux (D) and adhesion (F) were quantified. Results are mean ± SEM, n=4-6. **p<0.01 vs. corresponding value in control-treated group (ANOVA followed by Newman-Keuls test).

Figure 4. Effects of antiretrovirals on the expression of CD11b, CD11c and CD18 on neutrophils and monocytes of human blood. Whole blood was treated with maraviroc (MRV, 2.5 µg/mL), atazanavir (ATV, 18 µg/mL), darunavir (DRV, 14 µg/mL), raltegravir (RAL, 2.5 µg/mL), rilpivirine (RPV, 0.1-0.4 µg/mL), abacavir (ABC, 5 µg/mL), control or the corresponding vehicle (MRV in methanol; ATV, DRV, RAL and RPV in DMSO and ABC in sterile water). 4 hours later, the blood was treated with CD11b mAb, CD11c mAb, CD18 mAb or the corresponding control mAb conjugated with FITC or PE. 30 minutes later, the samples were lysed with lysing solution and processed in the cytometer. Results are mean ± SEM, n=4. *p<0.05 or **p<0.01 vs. corresponding % value in DMSO-treated group (ANOVA followed by Newman-Keuls test).

Figure 5. Role of Mac-1 and ICAM-1 in rilpivirine-induced leucocyte-endothelium interactions in rat mesenteric postcapillary venules. Rats were treated (i.p.) with rilpivirine (RPV, 0.2 µg/mL), control or its vehicle (DMSO). Some animals were pre-treated (i.v.) with anti-CD11b mAb, anti-CD18 mAb, anti-ICAM-1 or the corresponding control mAbs 30 minutes before administration of RPV. 4 hours later, responses of leucocyte rolling velocity (A), rolling flux (B), adhesion (C) and emigration (D) were quantified. Results are mean ± SEM, n=4. **p<0.01 vs. corresponding value in DMSO-treated group and ++p<0.01 vs. corresponding value in RPV-treated group (ANOVA followed by Newman-Keuls test).

Figure 6. Role of Mac-1, gp150,95 and ICAM-1 on PMN-endothelial cell interactions and PBMC-endothelial cell interactions induced by rilpivirine. Human umbilical vein endothelial cells (HUVEC) and leucocytes (PMN or PBMC) were treated for 4 hours with rilpivirine (RPV, 0.2 µg/mL), control or its vehicle (DMSO). Some PMN or PMBC were pre-treated with anti-CD11a mAb, anti-CD11b mAb, anti-CD11c mAb or anti-CD18 mAb and, some HUVEC were pre-treated with anti-ICAM-1 mAb 30 minutes before treatment with RPV. After assembling the flow chamber, PMN rolling velocity (A), rolling flux (C) and adhesion (E) and PBMC rolling velocity (B), rolling flux (D) and adhesion (F) were quantified. Results are mean ± SEM, n=4-5. **$p<0.01$ vs. corresponding value in DMSO-treated group and $^{++}p<0.01$ vs. corresponding value in RPV-treated group (ANOVA followed by Newman-Keuls test).

Figure 1

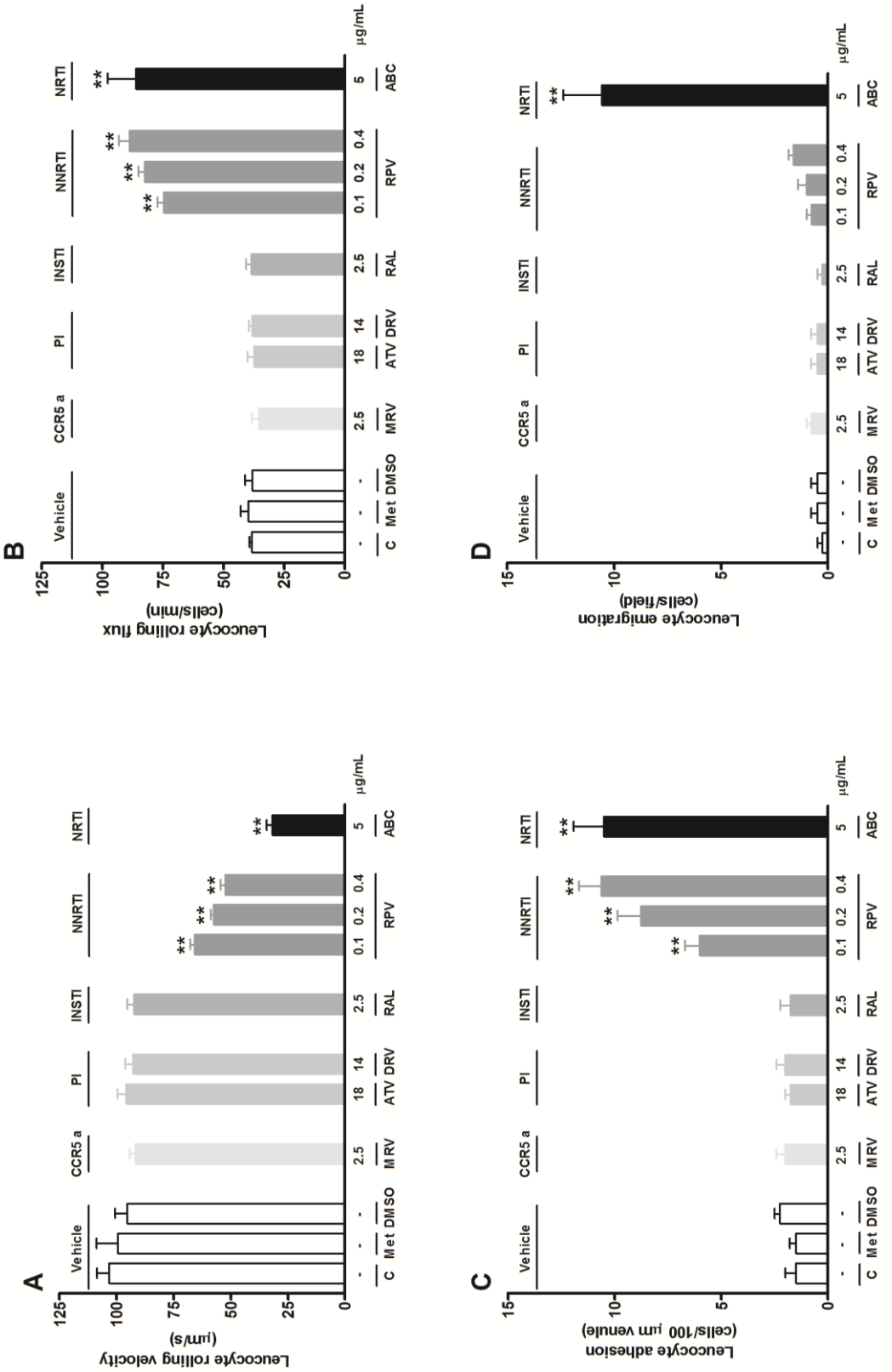
A
Leucocyte rolling velocity (μm/s)
B
Leucocyte rolling flux (cells/min)
C
Leucocyte adhesion (cells/100 μm venule)
D
Leucocyte emigration (cells/field)
Vehicle
CCR5 a
PI
INSTI
NNRTI
NRTI
C
Met
DMSO
MRV
ATV
DRV
RAL
RPV
ABC
μg/mL
**

Figure 2

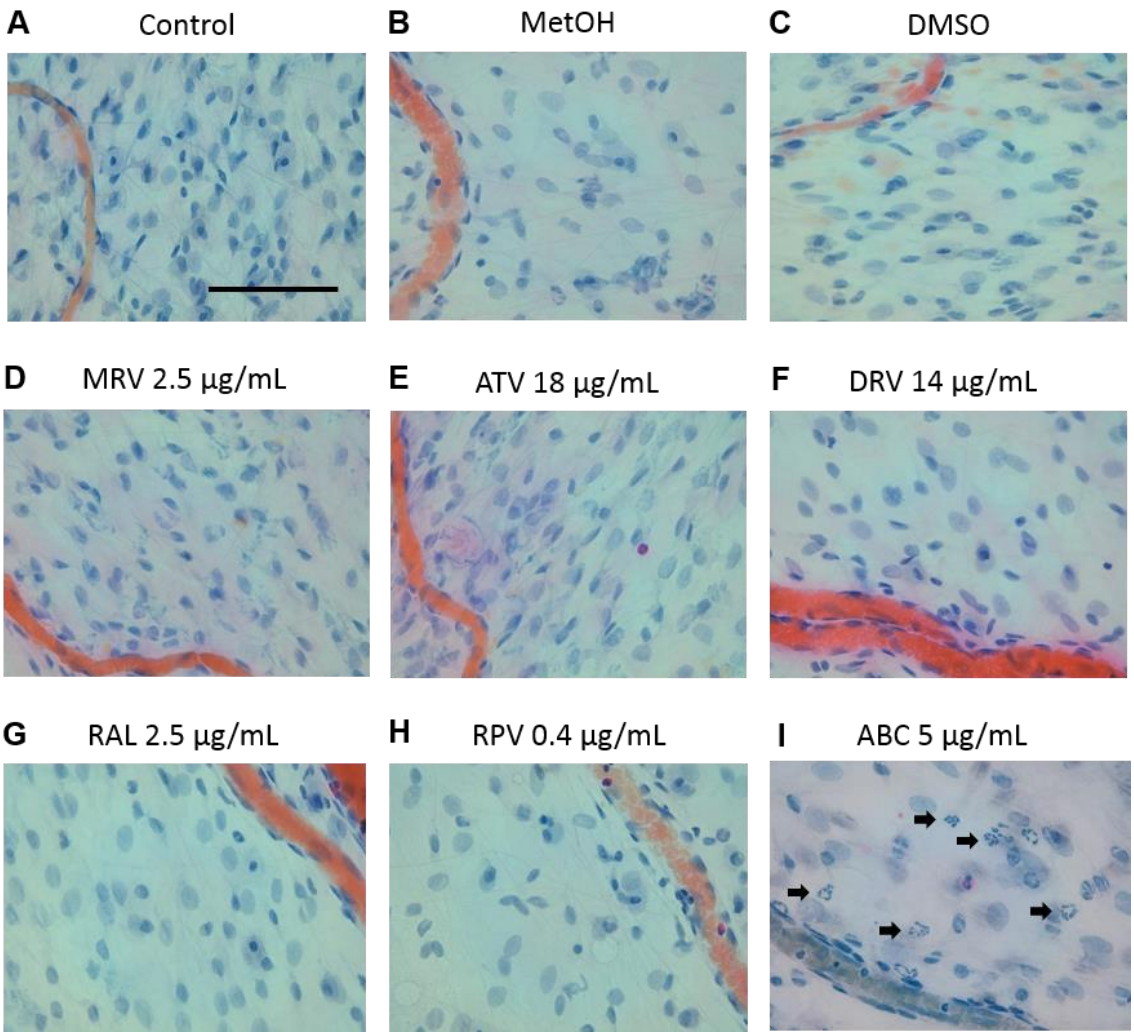
A
Control
B
MetOH
C
DMSO
D
MRV 2.5 µg/mL
E
ATV 18 µg/mL
F
DRV 14 µg/mL
G
RAL 2.5 µg/mL
H
RPV 0.4 µg/mL
I
ABC 5 µg/mL

Figure 3

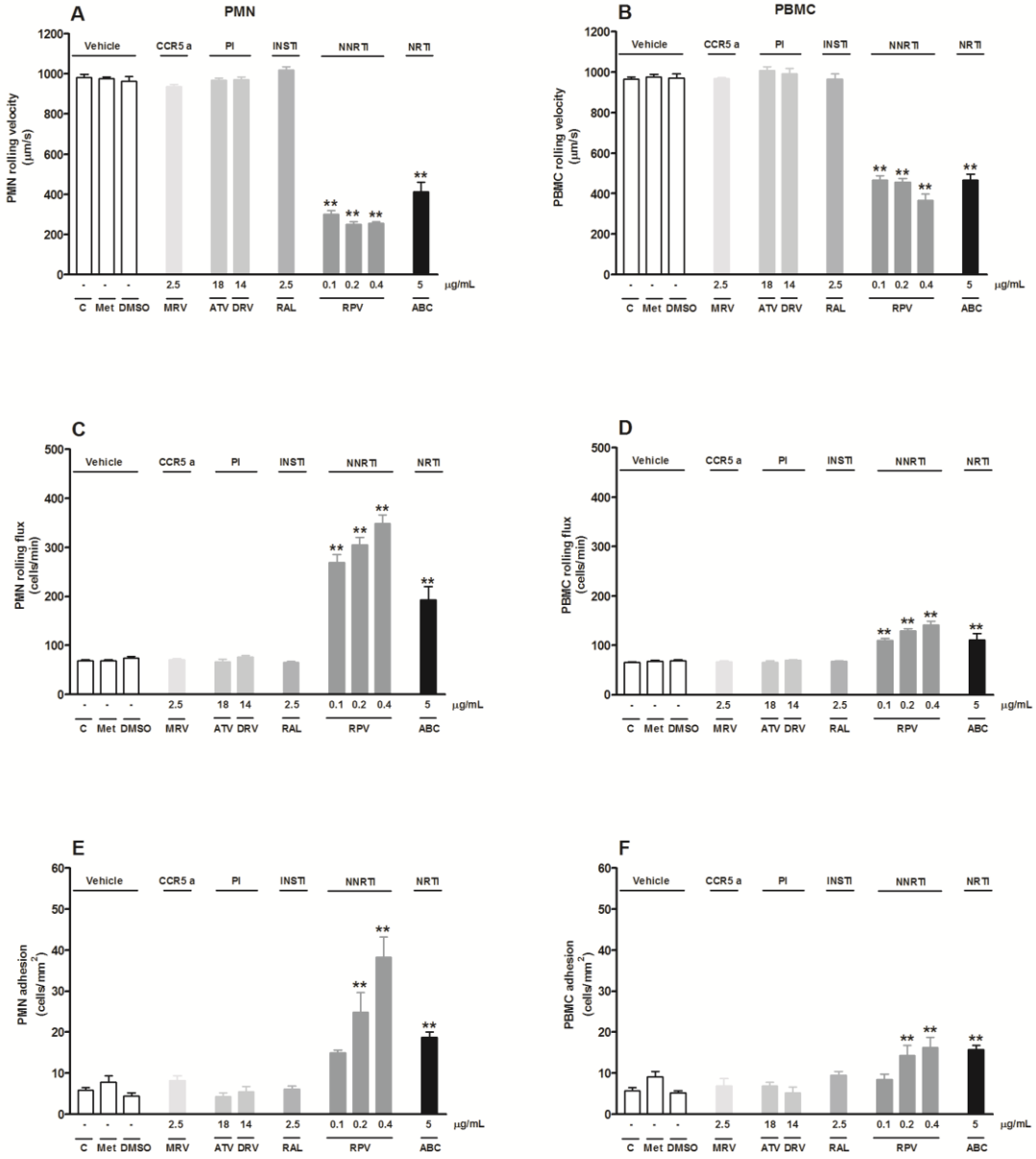
A
PMN
PMN rolling velocity (µm/s)
B
PBMC
PBMC rolling velocity (µm/s)
C
PMN rolling flux (cells/min)
D
PBMC rolling flux (cells/min)
E
PMN adhesion (cells/mm2)
F
PBMC adhesion (cells/mm2)
Vehicle
CCR5 a
PI
INSTI
NNRTI
NRTI
C
Met
DMSO
MRV
ATV
DRV
RAL
RPV
ABC
µg/mL

Figure 4

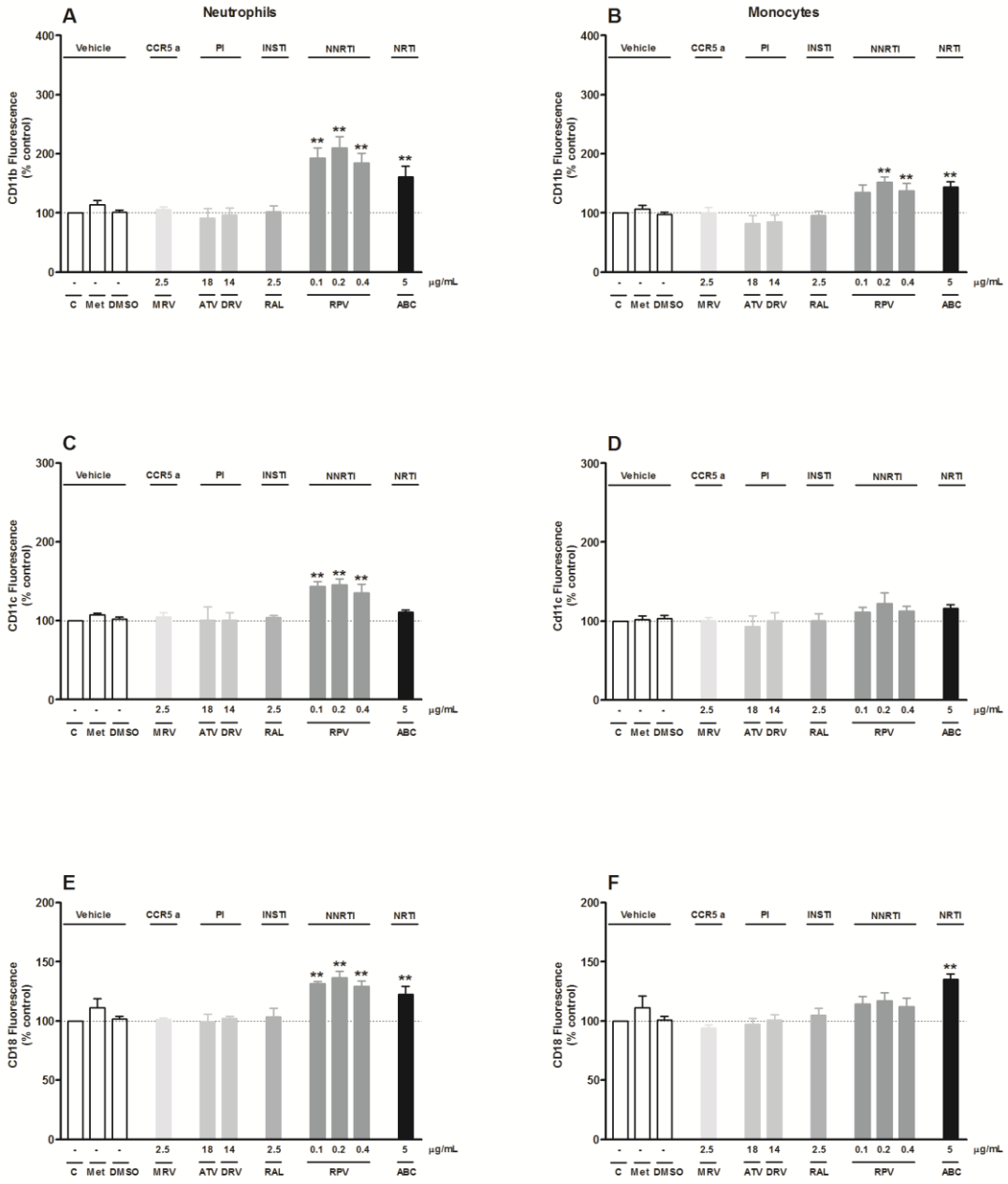
A
Neutrophils
B
Monocytes
C
D
E
F
CD11b Fluorescence (% control)
CD11c Fluorescence (% control)
Cd11c Fluorescence (% control)
CD18 Fluorescence (% control)
Vehicle
CCR5 a
PI
INSTI
NNRTI
NRTI
C
Met
DMSO
MRV
ATV
DRV
RAL
RPV
ABC
µg/mL

Figure 5

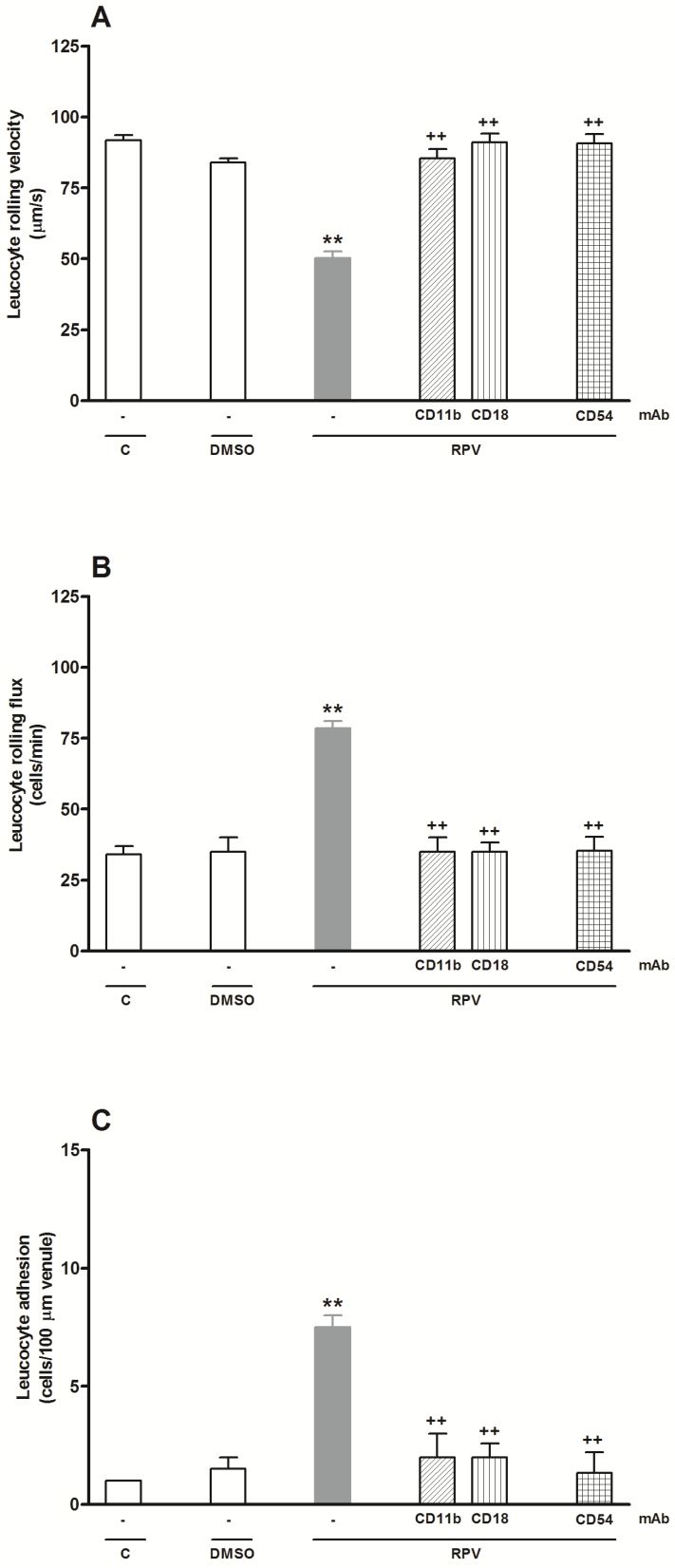
A
Leucocyte rolling velocity (μm/s)
125
100
75
50
25
0
**
++
++
++
-
-
-
CD11b
CD18
CD54
mAb
C
DMSO
RPV
B
Leucocyte rolling flux (cells/min)
125
100
75
50
25
0
**
++
++
++
-
-
-
CD11b
CD18
CD54
mAb
C
DMSO
RPV
C
Leucocyte adhesion (cells/100 μm venule)
15
10
5
0
**
++
++
++
-
-
-
CD11b
CD18
CD54
mAb
C
DMSO
RPV

Figure 6

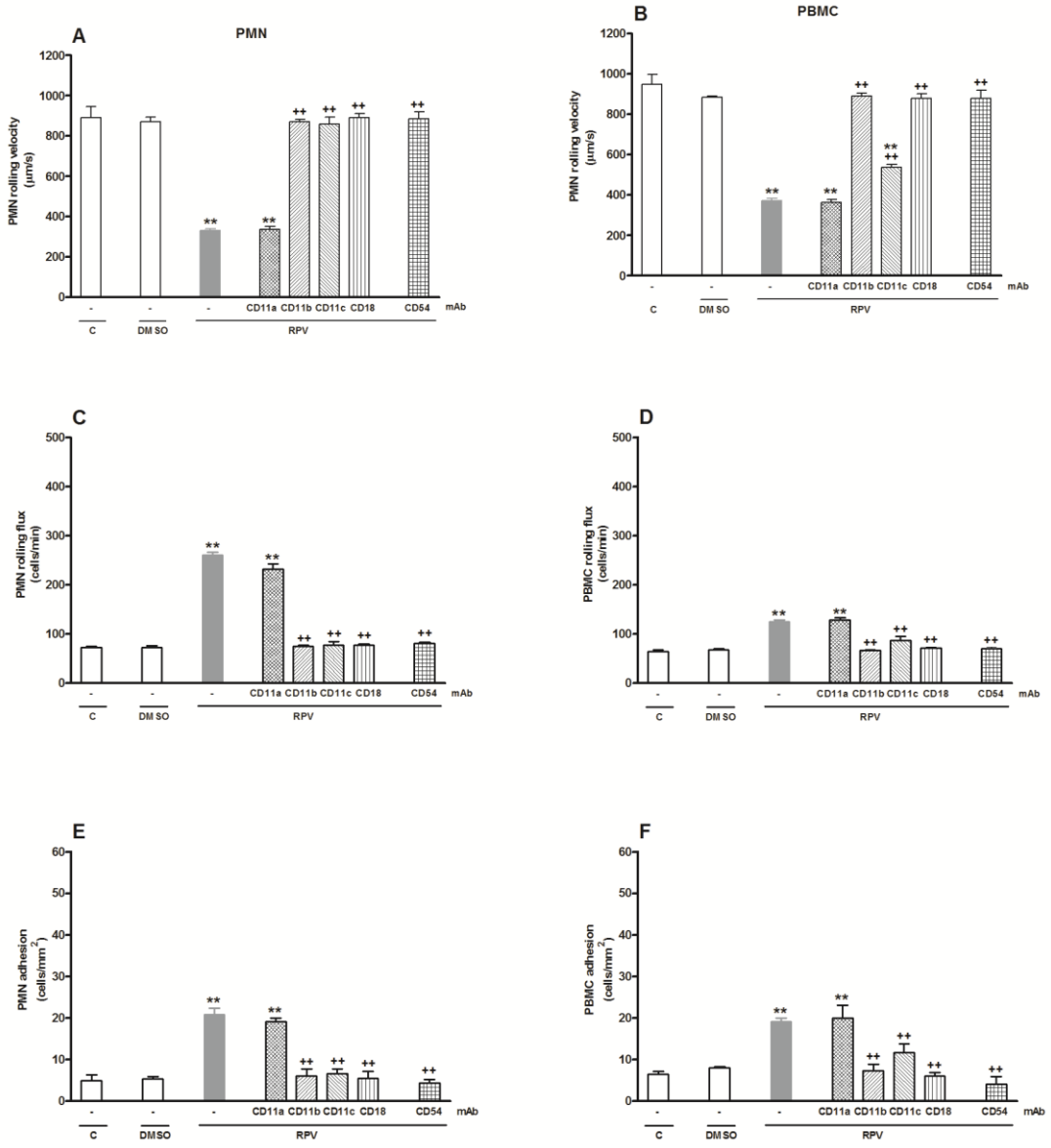
A
PMN
PMN rolling velocity (µm/s)
B
PBMC
PMN rolling velocity (µm/s)
C
PMN rolling flux (cells/min)
D
PBMC rolling flux (cells/min)
E
PMN adhesion (cells/mm2)
F
PBMC adhesion (cells/mm2)
-
-
-
CD11a CD11b CD11c CD18
CD54
mAb
C
DM SO
RPV

Supplemental Table 1. Effects of maraviroc, atazanavir, darunavir, raltegravir, rilpivirine and abacavir on the adhesion molecules expressed on neutrophils and monocytes.

	Treatment (µg/mL) / Adhesion molecules	Methanol	DMSO	MRV 2.5	ATV 18	DRV 14	RAL 2.5	RPV 0.1	RPV 0.2	RPV 0.4	ABC 5
NEUTROPHILS	CD11a	99.1±0.1	102.8±1.4	97.1±1.5	93.4±2.7	91.8±5.7	99.1±1.9	110.9±0.6	108.0±2.1	107.2±2.5	102.9±2.6
	CD49d	104.1±11.8	97.8±3.1	97.4±8.0	92.7±6.3	87.9±7.8	100.8±9.6	105.4±6.5	109.7±6.5	106.7±7.5	99.5±0.5
	CD62L	96.0±3.8	99.3±4.4	97.9±3.6	102.2±2.7	100.0±0.9	96.9±3.2	99.4±0.9	96.8±1.8	93.5±2.8	105.2±7.4
MONOCYTES	CD11a	106.0±0.5	104.7±5.3	98.9±8.1	91.5±4.5	91.4±4.9	101.3±2.2	11403±3.2	114.8±5.1	112.4±3.3	107.0±6.6
	CD49d	100.8±4.7	99.7±2.6	101.1±1.7	100.3±6.6	97.3±3.4	99.9±7.0	102.2±1.2	105.6±4.5	101.2±1.8	100.1±5.1
	CD62L	96.0±11.2	82.9±10.1	88.2±9.4	114.4±21.7	100.8±11.4	91.7±10.8	100.6±11.6	106.6±11.1	103.9±6.4	103.4±7.4

Whole blood was treated (4 h) with maraviroc (MRV, 2.5 µg/mL), atazanavir (ATV, 18 µg/mL), darunavir (DRV, 14 µg/mL), raltegravir (RAL, 2.5 µg/mL), rilpivirine (RPV, 0.1-0.4 µg/mL), abacavir (ABC, 5 µg/mL) or the corresponding vehicles (MRV in methanol; ATV, DRV, RAL and RPV in DMSO and ABC in sterile water). The expression of adhesion molecules was analysed by flow cytometry. Fluorescein isothyocianate (FITC)- or phycoeritrin (PE)-fluorescence values are expressed as a percentage of the mean fluorescence intensities of control cells (100%). Results are mean ± SEM of n=4-8.

Supplemental table 2. Effects of maraviroc, atazanavir, darunavir, raltegravir, rilpivirine and abacavir on the adhesion molecules expressed on HUVEC.

	Treatment (µg/mL) / Adhesion molecules	Methanol	DMSO	MRV 2.5	ATV 18	DRV 14	RAL 2.5	RPV 0.1	RPV 0.2	RPV 0.4	ABC 5
HUVEC 4h	ICAM-1	111.6±4.5	109.5±4.2	102.9±3.6	99.3±8.1	89.8±15.8	110.8±2.6	93.8±3.7	95.0±2.6	98.1±6.9	104.4±6.8
	VCAM-1	99.5±3.5	102.1±1.3	101.2±2.7	93.6±1.9	95.3±4.2	101.9±3.2	98.6±0.8	104.3±3.0	102.3±2.4	98.3±5.5
	E-Selectin	97.4 ±2.9	91.0±10.5	93.8±6.3	97.9±1.1	96.6±3.8	115.2±19.8	96.0±1.9	105.7±6.4	97.4±3.6	110.3±10.0
HUVEC 24h	ICAM-1	98.3±4.9	98.4±2.9	91.8±5.9	99.0±3.1	98.1±3.6	101.6±3.7	88.0±5.6	91.0±1.4	89.6±4.9	124.9±8.4**
	VCAM-1	100.0±3.8	98.3±2.7	98.7±4.5	99.8±3.4	98.2±3.0	98.9±3.8	99.9±8.1	102.0±9.3	105.1±10.7	121.8±8.6**
	E-Selectin	97.4±8.4	91.6±8.6	84.2±8.2	92.6±3.9	90.7±3.0	88.2±8.4	87.6±9.7	95.2±9.3	84.9±9.0	99.5±4.7

HUVEC were treated (4 h or 24 h) with maraviroc (MRV, 2.5 µg/mL), atazanavir (ATV, 18 µg/mL), darunavir (DRV, 14 µg/mL), raltegravir (RAL, 2.5 µg/mL), rilpivirine (RPV, 0.1-0.4 µg/mL), abacavir (ABC, 5 µg/mL) or the corresponding vehicles (MRV in methanol; ATV, DRV, RAL and RPV in DMSO and ABC in sterile water). The expression of adhesion molecules was analysed by flow cytometry. Fluorescein isothyocianate (FITC)- or phycoeritrin (PE)-fluorescence values are expressed as a percentage of the mean fluorescence intensities of control cells (100%). Results are mean ± SEM of n=3-5. **$p<0.01$ vs. corresponding value in control-treated group (ANOVA followed by Newman-Keuls test).